FINAL REPORT

Developing Tools for Ecological Forestry and Carbon Management in Longleaf Pine

SERDP Project RC-2115

AUGUST 2016

Dr. Lisa Samuelson
Auburn University

John Butnor
USDA Forest Service

Dr. Wendell Cropper Jr.
University of Florida

Dr. Carlos Gonzalez-Benecke
Oregon State University

Dr. Kurt Johnsen
USDA Forest Service

Dr. Tim Martin
University of Florida

SERDP
DOD ▪ EPA ▪ DOE

Page Intentionally Left Blank

Page Intentionally Left Blank

REPORT DOCUMENTATION PAGE

1. REPORT DATE (DD-MM-YYYY)	2. REPORT TYPE	3. DATES COVERED (From - To)
01/07/2016	Final	14-03-2011 - 14-09-2016

4. TITLE AND SUBTITLE

Developing Tools for Ecological Forestry and Carbon Management in Longleaf Pine

5a. CONTRACT NUMBER

W912HG-11-C-0008

5b. GRANT NUMBER

5c. PROGRAM ELEMENT NUMBER

6. AUTHOR(S)

Samuelson, Lisa J.
Butnor, John R.
Cropper, Wendell P., Jr.
Gonzalez-Benecke, Carlos A.
Johnsen, Kurt H.
Martin, Tim A.

5d. PROJECT NUMBER

RC-2115

5e. TASK NUMBER

5f. WORK UNIT NUMBER

7. PERFORMING ORGANIZATION NAME(S) AND ADDRESS(ES)

Auburn University
107 Samford Hall
Auburn, AL 36849-0001

8. PERFORMING ORGANIZATION REPORT NUMBER

9. SPONSORING/MONITORING AGENCY NAME(S) AND ADDRESS(ES)

Strategic Environmental Research and Development Program
4800 Mark Center Drive, Suite 17D03
Alexandria, VA 22350-3605

10. SPONSOR/MONITOR'S ACRONYM(S)

SERDP

11. SPONSOR/MONITOR'S REPORT NUMBER(S)

RC-2115

12. DISTRIBUTION/AVAILABILITY STATEMENT

Approved for public release: distribution is unlimited

13. SUPPLEMENTARY NOTES

14. ABSTRACT

Carbon density was measured in longleaf pine stands across the range to directly quantify ecosystem carbon pools and calibrate and validate longleaf pine carbon models. An even-aged longleaf pine model which enables simulation of scenarios for young planted stands being managed for transition toward uneven-aged structures with silvicultural tools such as thinning and prescribed fire was developed and linked to a modified single-tree-based longleaf pine model which enables simulation of older stands which are managed with silvicultural tools such as single tree or group selection harvests and prescribed fire.

15. SUBJECT TERMS

Forest carbon, carbon sequestration, forest management

16. SECURITY CLASSIFICATION OF:			17. LIMITATION OF ABSTRACT	18. NUMBER OF PAGES	19a. NAME OF RESPONSIBLE PERSON
a. REPORT	b. ABSTRACT	c. THIS PAGE			Lisa Samuelson
U	U	U	SAR		19b. TELEPHONE NUMBER (include area code) 334-844-1040

Page Intentionally Left Blank

Table of Contents

List of Tables

iii

List of Figures

v

List of Acronyms

AGC = aboveground carbon
BA = basal area (m^2 ha^{-1})
BA$_t$ = basal area for thinned stands (m^2 ha^{-1})
BA$_u$ = basal area of unthinned counterpart stand (m^2 ha^{-1})
BC = black carbon
BGC = belowground carbon
BPCA = Benzene Polycarboxylic Acid
Bt = bark thickness
C = carbon
CA = individual-tree crown area (m^2)
CI = competition index
CV = coefficient of variation
CW = individual tree crown width
CWD=Coarse woody debris
d = dbh threshold limit for merchantable product (cm)
Dq = quadratic mean diameter (cm)
d_t = top diameter outside bark (cm)
dbh, DBH = diameter outside bark at breast height (1.37 m) (cm)
dbh$_{IB}$ = diameter inside bark at breast height (cm)
DoD = Department of Defense
ε_r = relative dielectric value
FFC = forest floor carbon
Fm = fraction modern

FWD = fine woody debris
LLD = ground line diameter
GPR = ground penetrating radar
H = total height (m)
H_{dom} = mean height of dominant and codominant trees (m)
LAI = leaf area index
LLM-EA = longleaf pine model for even-aged stands
LLM-ST = longleaf pine model for single trees and uneven aged stands
MAE = mean absolute error
MRT = mean residence time
N = trees per hectare (trees ha^{-1})
n = number of observations
PHZ = plant hardiness zone
PyC = pyrogenic carbon, total bulk BPCA content * 2.27 correction factor to account for C lost during extraction (Glaser et al. 1998)
PyC_{OX} =,PyC oxidized with H_2O_2 + dilute HNO_3
PyC_R = PyC resistant to H_2O_2 + dilute HNO_3
QMD=quadratic mean diameter
R^2 = coefficient of determination
R_{IB} = ratio between merchantable stem volume inside bark to top diameter d_t divided by total stem volume inside bark up to 5.08 cm diameter limit outside-bark (m^3)
R_{OB} = ratio between merchantable stem volume outside bark to top diameter d_t divided by total stem volume outside bark up to 5.08 cm diameter limit outside-bark (m^3)
RMSE = root mean square error
SD = standard deviation
SD = stump diameter
SDI = Reineke's stand density index (trees ha^{-1})
SE = standard error
SI = site index, the H_{dom} at base age of 50 years (m)
SNA=specific needle are
SOC = soil organic carbon of bulk soil
SOC_R+PyC_{OX} = sum total of all soil carbon with either mineral or biochemical recalcitrance
SOC_{OX} = soil organic carbon not resistant to oxidation with H_2O_2 + dilute HNO_3
SOC_R = soil organic carbon resistant to oxidation with H_2O_2 + dilute HNO_3
t = top stem diameter outside bark merchantability limit (cm)
Tmin = average minimum temperature of plant hardiness zone (^0C).
TSF = time since last prescribed fire (years)
V_{IB} = individual-tree stem volume inside-bark (m^3)
V_{OB} = individual-tree stem volume outside-bark (m^3)
VIF = variance inflation factor
VOL_{m-IB} = merchantable stem volume inside-bark ($m^3\ ha^{-1}$)
VOL_{m-OB} = merchantable stem volume outside-bark ($m^3\ ha^{-1}$)
VOL_{IB} = total stem volume inside-bark ($m^3\ ha^{-1}$)
VOL_{OB} = total stem volume outside-bark ($m^3\ ha^{-1}$)
YSC = years since cut

Keywords

Aboveground
Age
Allometry
Basal area
Belowground
Below-stump
Biodiversity
Biomass
Carbon
Chronosequence
Coarse roots
Coarse woody debris
Decomposition
Density
Detritus
Duff
Eglin Air Force Base
Even-aged management
Fine roots
Fine woody debris
Forest floor
Forest management
Forest products
Ground cover
Ground penetrating radar
Growth and yield
Hardwoods
Harvesting
Height
Herbaceous cover
Kisatchie National Forest
Lateral roots
Litter
Longleaf pine
Marine Corps Base Camp Lejeune
Models
Necromass
Old-growth
Pinus palustris
Pyrogenic carbon
Prescribed fire
Savanna
Sequestration
Silviculture

Acknowledgements

Abstract

Objectives: The objective of this research was to develop the research knowledge necessary to create carbon management models that can be used to improve integrated natural resource management of longleaf pine. Specific objectives were to quantify carbon in ecosystem pools in longleaf pine forests located across the species' range, and develop longleaf pine carbon models that can be used to evaluate life-cycle carbon balance, forest structure and biodiversity, and yield of forest products in longleaf pine forests.

Technical Approach: Carbon density in above and belowground live and dead plant mass and in soils was measured in stands ranging in age from 5 to 118 years located across the range of longleaf pine at US Army Fort Benning, US Army Fort Polk/Kisatchie National Forest, Marine Corps Base Camp Lejeune and Eglin Air Force Base. Carbon in decaying longleaf pine tap roots was also measured. Field data were used to directly quantify ecosystem carbon and calibrate and validate the longleaf pine carbon models. The longleaf pine carbon model is driven by two linked forest carbon cycle models: an even-aged longleaf pine model (LLM-EA), which enables simulation of scenarios for young (0-70 years) planted stands being managed for transition toward uneven-aged structures with silvicultural tools such as thinning and prescribed fire, and a single-tree-based longleaf pine model (LLM-ST) which enables simulation of older (50 to > 200 years) stands which are managed with silvicultural tools such as single tree or group selection harvests and prescribed fire.

Results: Total soil carbon (C) stocks ranged from 44.1 to 98.1 ($\bar{x}$ = 77.0) Mg C ha^{-1} and no effect of stand age, biomass accumulation or geographical location on soil C stocks was detected. Variation in soil C concentration was largely dependent on depth. Pyrogenic C was a minor component of soil organic carbon (SOC) of bulk soil, comprising 5-7% of the total SOC stock and thus did not contribute substantially to long-term C accumulation in soil within the forest stand where it was produced. There was no enhanced accumulation or deposits of pyrogenic C with depth (to 1 m) and pyrogenic C declined in proportion with SOC, conversely the proportion of SOC resistant to oxidation in SOC increased with depth. The residence time of SOC in surface soils was hundreds of years and at depths > 50 cm residence time increased to thousands of years. Our results indicate that soils are not strong sinks for atmospheric CO_2 compared to C accumulation in biomass in longleaf pine forests. Measured ecosystem C stock (all pools except soil C) increased with stand age with a predicted asymptotic maximum of 119 Mg C ha^{-1}. At 100 years, ecosystem C was 69% of the predicted maximum. Ecosystem C was driven by increases in aboveground live tree C related to stand age and basal area. Live root C, the sum of below-stump C, ground penetrating radar measurement of lateral root C and live fine root C, was on average 32% of ecosystem C. Live understory C, forest floor C, down dead wood C and standing dead wood C were a small fraction of ecosystem C. Long-term accumulation of live tree C combined with the larger role of belowground accumulation of live lateral root C than in other forest types indicates a role of longleaf pine forests in balancing the more rapid C accumulation and C removal associated with more intensively managed forests. In addition, longleaf pine tap root necromass was found to contribute to long-term forest C sequestration.

Using the LLM-EA developed in this project to evaluate the effects of silvicultural management systems on C sequestration over a 300 year simulation period, we conclude that: i) site productivity was the major factor driving C sequestration in longleaf pine stands; ii) increasing rotation length increased C storage; iii) prescribed burning had a small effect on C sequestration; and iv) for medium quality sites, C sequestration of thinned 75-year rotation longleaf pine stands was similar than unthinned 25-year rotation slash pine stands. Our results support the use of unthinned, long rotation longleaf pine stands for C offset projects. In model simulations with the LLM-ST, we found no significant sensitivity to initial placement of trees in the stand lattice after a few decades of simulation and coefficients of variation for tree biomass were typically less than 10%, and this variation also includes stochastic mortality and recruitment processes. Sensitivity to fire return interval increased with longer simulation periods. Large increases in mean longleaf pine dbh, height, and basal area after 250 years with a ten year fire return time reflect a population with poorer recruitment of smaller individuals. Although the mean longleaf tree size was larger, the smaller population of trees resulted in decreased longleaf biomass and C accumulation. Hardwood biomass increased with the ten year fire return time as a consequence of reduced fire mortality and competition from longleaf pine trees. We examined a range of harvest intensities for both single tree and group selection harvests. The simulations indicate that a harvest return time of 20 years is not likely sustainable, particularly at the highest harvest intensities. With a target of 35 trees ha[1] removed every 20 years, longleaf pine aboveground biomass was reduced by 75% of the non-harvested stand. Hardwood dominance increases dramatically in this scenario, even with frequent fire management. Increasing the harvest return time to 80 years appears to be sustainable, with most stand characteristics similar to the range found in non-harvested stands.

Benefits: Allometric equation derived from comprehensive field measurements provide predictive equations for determining carbon in above and belowground biomass of longleaf pine trees across the range. Tap root decay functions allow prediction of residual carbon from previous harvests or known tree mortality. The LLM-ST model was extended to include carbon dynamics, coarse woody debris, and both single tree and group selection harvesting. Our integrated model framework allows simulation of the transition from longleaf pine plantations to old-growth savanna management regimes. The LLM-EA provides an important new tool for estimating C stocks for regional assessments and for guiding future longleaf pine management.

1. Objectives

The Statement of Need identified the need for basic and applied research that supports the transition of DoD forest management toward an ecological forestry model that will balance military mission support with the maintenance of native biodiversity, sustainable yield of forest products, and enhancement of forest carbon sequestration with a view toward offsetting facility carbon emissions. The overall goal of this project was to develop the research knowledge necessary to meet this need through the creation of a carbon management model that can be used to facilitate optimal allocation of resources to improve integrated natural resource management plans designed to restore native longleaf pine (*Pinus palustris* Mill.) ecosystems, protect the environment, manage carbon and maintain flexibility in mission training.

Technical Objectives

1. Develop a forest carbon cycle model that can be used to evaluate ecological forest management techniques in longleaf pine forests and in systems where restoration of longleaf pine ecosystems is the goal. The carbon model is driven by two linked pine forest carbon cycle models:
   a. An even-aged longleaf pine model (LLM-EA) which enables simulation of scenarios for young (0-70 years) planted stands being managed for transition toward uneven-aged structures with silvicultural tools such as thinning and prescribed fire.
   b. A single-tree-based longleaf pine model (LLM-ST) which enables simulation of older (50 to > 200 years) stands which are managed with silvicultural tools such as single tree or group selection harvests and prescribed fire.

2. Support calibration and validation of the LLM-EA and LLM-ST by:
   a. Quantifying carbon pools in longleaf pine ecosystems including carbon in above and belowground biomass, shrubs, the herbaceous layer (including wiregrass versus non-wiregrass systems), soils (including black carbon), litter, decomposing tap roots and standing and downed woody debris. Also, quantifying the pool of fire-derived carbon in soils in fire-adapted longleaf pine ecosystems.
   b. Developing allometric equations for longleaf pine trees in stands covering the native range including coastal and interior systems.
   c. Collecting data on four installations (Marine Corp Base Camp Lejeune, US Army Fort Benning, Eglin Air Force Base and US Army Fort Polk/Kisatchie National Forest) representing the range in longleaf distribution and both coastal and inland physiographies and in stands with a range of management histories.

3. Address biodiversity by simulating forest structural attributes important to wildlife habitat. The LLM-ST is spatially explicit and can model tree size and distribution, and the LLM-EA can generate diameter distributions and estimates of understory biomass. The models will simulate the processes that interact to provide the necessary conditions to sustain pine savanna biodiversity. Another key habitat attribute is coarse woody debris.

Both models will be able to produce explicit estimates of coarse woody debris through mortality and coarse wood detrital biomass.

4. As an initial guide for resource managers, prepare a suite of simulations demonstrating how land use practices and silvicultural prescriptions including prescribed burning influence the life-cycle carbon balance of longleaf pine ecosystems, biodiversity and sustained ecological yield of forest products over short (<10 years), intermediate (<50 years) and long-term horizons.

2. Background

Longleaf Pine Forest Carbon Sequestration

Prior to European settlement, longleaf pine forests were the largest temperate forest type in North America occupying between 24 and 36 million ha from the Gulf and Atlantic Coastal Plains from Virginia extending south into central Florida and north into the Piedmont and mountains of northern Alabama and Georgia (Frost 1993, Stout and Marion 1993, Landers et al. 1995). Land clearing for crops and pastures, logging, turpentine operations, and conversion to other southern pines (Brockway and Lewis 1997, Gilliam and Platt 1999) and the interruption of natural fire regimes brought about by forest fire protection policies implemented in the 1920's have reduced longleaf pine forests to 1.2 million ha, or 3 to 5% of its original range (Outcalt and Outcalt 1994). Longleaf pine ecosystems are among the most diverse in temperate North America and contain nearly two-thirds of all species in the southeastern U.S. that are declining, threatened or endangered. The loss of the longleaf pine ecosystem has led to a decrease in the abundance of 191 taxa of vascular plants and the listing of 30 endangered or threatened plant species (Hardin and White 1989, Walker 1993, Glitzenstein et al. 2001). The continued threat of longleaf ecosystem loss (Means and Grow 1985, Noss 1989, Noss et al. 1995) has resulted in increased interest in restoring this once vast ecosystem (Brockway and Lewis 1997), particularly on military installations. Because DoD is charged with maintaining or restoring remaining native ecosystem types and a key principle for military commanders is to adopt an ecosystem system-based management approach (www.dodbiodiversity.org), a decision support system is critical in balancing forest resource management objectives while providing realistic training conditions for troops and support of military training objectives.

Longleaf pine ecosystems on DoD military installations offer opportunities to sequester carbon and mitigate CO_2 emissions, primarily because longleaf pine is a long-lived tree species and DoD is focusing on restoration and protection of longleaf pine ecosystems for threatened and endangered species and other ecosystem services. Military installations can play a significant role in sequestering carbon due to differences in land use activities compared to surrounding urbanized areas (Zhao et al. 2010). However, carbon management must be balanced with other ecological services and in some cases managing for carbon can be detrimental to maintaining biodiversity and conservation of wildlife habitat (Putz and Redford 2009). To sustainably manage longleaf pine ecosystems for carbon sequestration and other ecosystem services requires modeling tools as well as information at the ecosystem level on how restoration and management practices, in

particular prescribed fire, impact carbon pools. Basic information on carbon in soils, above and belowground tree biomass, shrubs, herbaceous plants and detritus is needed.   A better understanding of the carbon cycle in longleaf pine ecosystems on DoD lands would improve integrated natural resource management plans designed to sustain a suite of ecosystem services including carbon cycle management, native biological diversity and ecological yield of forest products. Figure 2.1 is a conceptual model of the longleaf pine ecosystem carbon balance showing the pools, processes, mass transfers, and influences that were measured and modeled in this project.

Carbon sequestration in forests is a complex balance between uptake and storage of carbon in plant biomass, detritus, and forest product pools, and the emission of carbon by decay of detritus and product pools, as well as anthropogenic emissions associated with forest management activities. Sustainable forest management activities can increase sequestration of carbon in forest biomass and wood products (Johnsen et al. 2004). Approximately 12-16% of CO_2 emissions in the U.S. are offset by U.S. forests (U.S. EPA 2005) and forests in the Southeast and South-Central U.S. could offset up to 23% of regional emissions (Han et al. 2007). However, most assessments of carbon stocks in the U.S. are made in a rudimentary fashion. That is, tree carbon is estimated using standard inventory data applied to species or genera-level aboveground biomass equations deemed most appropriate from published literature. Biomass is then apportioned using standard root:shoot ratios and biomass is converted to carbon using an average value of 0.5. This approach is used because species and site specific data and functions are usually not available (for example see the U.S. Forest Service Carbon Online Estimator, http://ncasi.uml.edu/COLE/) and, though useful for making landscape-level estimates, does not provide the accuracy needed to explicitly manage forests for carbon sequestration. There is a great need for decision support tools for carbon management that encompass a wide variety of ecosystems and management scenarios (Birdsey et al. 2006), but the weakest link in most tree growth models and subsequently carbon models is the estimation of belowground biomass.

Even-Aged Longleaf Pine Ecosystem Carbon Balance Model
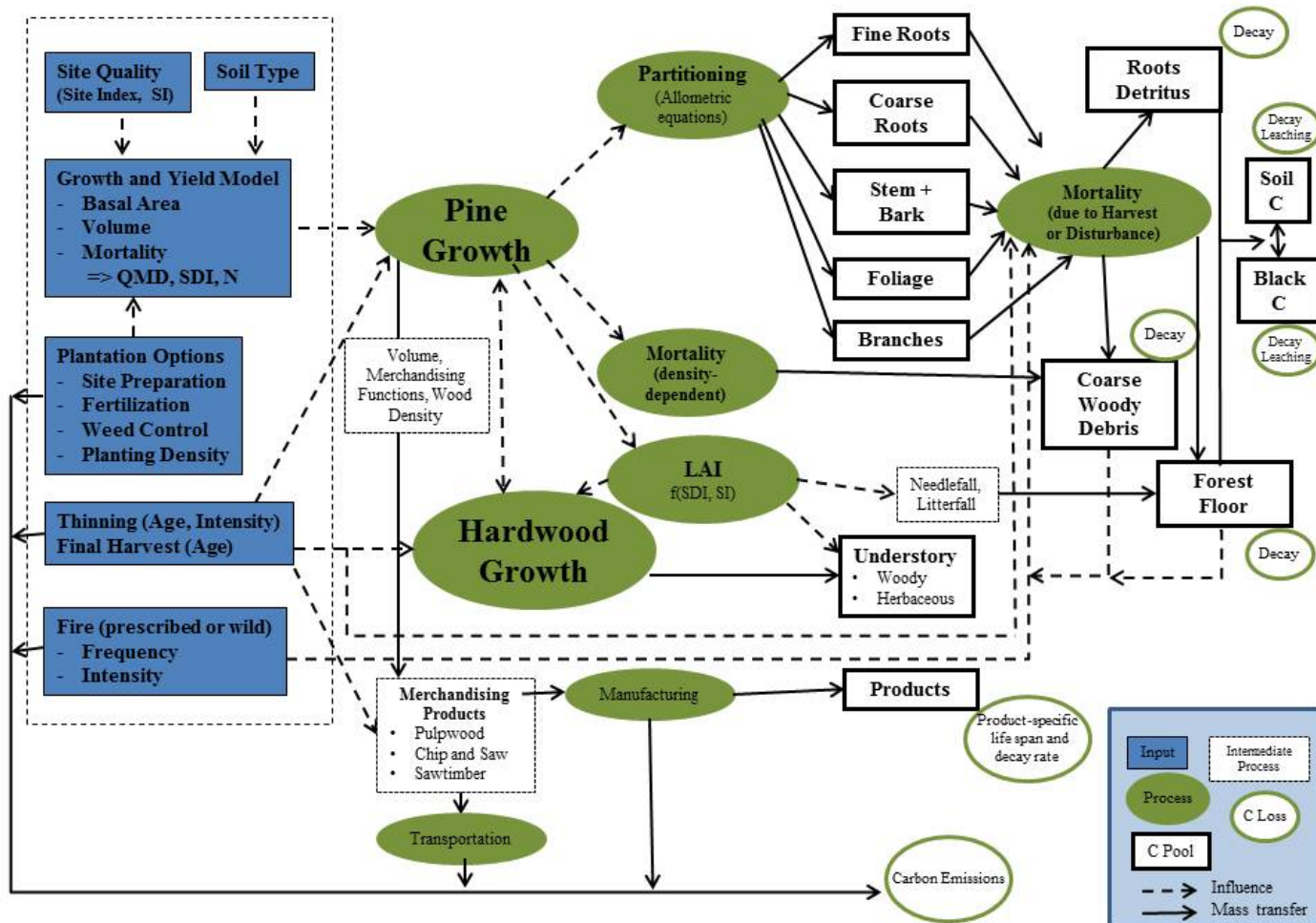
Figure 2.1. Conceptual model for the even-aged longleaf pine ecosystem carbon balance model showing the pools, processes, mass transfer functions, and influences measured and modeled in the project. The single-tree model is described in Chapter 16.

The investment trees make in roots is considerable. In temperate conifer forests (< 50 years old), root:shoot ratios average 0.2-0.3 but in moisture limited stands the root:shoot ratio may exceed 0.55 (Mokany et al. 2006), and in fire adapted ecosystems (e.g. scrub oak, eastern Florida) trees can allocate more than 80% of total biomass to roots (Stover et al. 2007, Seiler et al. 2009). In pine plantations, roots account for 15 to 45% of total stand biomass (Samuelson et al. 2004, Albaugh et al. 2006, King et al. 2007). Root carbon allocation varies with stand age, tree size, soil environment and management and represents a large uncertainty in current terrestrial carbon budgets. In addition, buried roots represent decay resistant structures. Some information is available on the root carbon pool in loblolly pine stands, but little science-based data exists for fire-adapted longleaf pine forests in the Southeast. Preliminary data collected by Kurt Johnsen and colleagues suggests that longleaf pine allocates more carbon to tap root biomass than other southern pines. However, little is known about belowground dynamics and carbon allocation in longleaf pine systems. Allometric equations relating diameter at breast height (DBH, dbh)) to the mass of the tap root or root ball directly underneath a tree are unavailable for longleaf pine, and distribution of lateral roots within this ecosystem is unknown. An objective of this project was to quantify root biomass of longleaf pine with a combination of below stump biomass excavation and lateral root surveys with ground-penetrating radar (GPR) to evaluate the size and variability of this pool and from these data develop the allometric equations needed to model belowground biomass. On soils suitable for radar studies, root biomass surveys with GPR provide valuable insight into belowground productivity in forest systems and have been useful in quantifying belowground biomass and spatial distribution of roots, and measuring root diameters (Butnor et al. 2001, Butnor et al. 2003, Barton and Montagu 2004, Cox et al. 2005, Stover et al. 2007, Samuelson et al. 2008). Ground penetrating radar permits intensive and extensive sampling far above that which is possible using conventional sampling with soil cores (Johnsen et al. 2004). It is important to note that surface-based GPR can only measure coarse lateral roots and not the tap root directly below individual trees or fine root biomass. Therefore, a complete picture of belowground allocation to roots requires the development of allometric equations to quantify the biomass associated with the tap root and measures of fine root biomass. Tap roots represent the largest component of root biomass, followed by lateral coarse roots and then fine roots and both coarse and fine roots are dynamic pools that respond to resource availability.

Following tree mortality, carbon in root necromass can persist for many years. Coarse root systems may require decades to decompose (Vaught 1989, Eberhardt et al. 2009, Weedon et al. 2009). Although not a long-term pool of *in-situ* carbon, root necromass can provide short to medium term storage pools. Very little work has been published examining the decomposition rates of root systems. In 60-year-old or younger loblolly pine, 50% of the root systems decayed within the first 10 years (Ludovici et al. 2002). Rapid rates of decomposition were associated with wetter sites in Monterey pine (Garrett et al. 2008). However, carbon contents in the vicinity of old tap roots can stay elevated for at least 50 years (Ludovici et al. 2002, Garrett et al. 2008, Palviainen et al. 2010). Sucre and Fox (2009) found that decomposing stumps accounted for 10% of total soil carbon in a mature hardwood forest. Longleaf pine root systems may be more resistant to decay than other tree species. Longleaf pine has been historically valued for its turpentine production (Gardner 1989). However, turpentine is only a small component of a range of compounds called collectively, oleoresins, that are produced by longleaf pine and other conifers (Vikstrom et al. 2005, Eberhardt et al. 2009). Components of oleoresin have been shown to increase the wood's

resistance to microbial decay and insect infestation (Hart and Shrimpton 1979, Klepzig et al. 1996, Nerg et al. 2004, Eberhardt et al. 2009). Additionally, as the volatile turpentine evaporates a physical barrier is created hindering access from foraging insects such as termites (Phillips and Croteau 1999). Tap roots of old longleaf pine have been observed to last intact for many decades, showing little visual evidence of decay and are harvested as a source of fatwood, "fat lighter" or "lighter wood". Despite the general acceptance that dead longleaf pine tap roots can persist for decades, there is no quantifiable scientific data available for carbon sequestration models.

Black carbon (BC) can constitute a major fraction of soil carbon (Schmidt and Noack 2000), especially on sites with frequent burns. Black carbon is a continuum of material ranging from partly charred plant material to char and charcoal to graphitic soot (Seiler and Crutzen 1980). The amount of BC in soils is variable and dependent on the intensity and frequency of burning. Worldwide, BC from biomass burning is estimated to be 50 to 270 Tg yr^{-1}, with more than 90% remaining in the soil (Kuhlbusch et al. 1996). Although highly resistant to decomposition, BC is not inactive. Black carbon can affect nutrient retention and cycling and plays a key role in a wide range of biogeochemical processes in soils (Schmidt and Noack 2000, Liang et al. 2006). Clearly, BC may be an important long-term carbon sequestration pool in longleaf pine forests and its quantity will be a function of past fire history and future fire management. In addition to finer particles of BC derived from the burning of fine-roots and above-ground biomass and necromass, large deposits of char and charcoal BC can be found belowground as the result of the smoldering of longleaf pine tap and coarse root channels.

Although there is great interest in increasing and maintaining longleaf pine forests throughout its former range for a variety of ecosystem services in addition to carbon sequestration, the process of establishing these forests requires significant time and resource investment (Figure 2.2). Modeling tools that facilitate evaluation of thinning and fire in terms of forest structure and carbon sequestration will be valuable assets for forest managers. Figure 2.2 depicts a commonly occurring forest restoration scenario in which newly-planted or already-existing even-aged longleaf pine stands are converted to uneven-aged or similarly structured stands through thinning, prescribed fire, and subsequent group selection or single-tree selection treatments.

Because of the radical differences in stand dynamics and structure in earlier and later phases of ecosystem development, we think a parsimonious modeling approach is to link an even-aged carbon longleaf pine model with a single-tree-based older stand longleaf pine model. The project investigators have extensive experience in quantifying management effects on the forest carbon cycle (Martin et al. 1997, Clark et al. 2001, Johnsen et al. 2004, Samuelson et al. 2004, Binford et al. 2006, Powell et al. 2008, Samuelson et al. 2009, McCarthy et al. 2009, Lavoie et al. 2010) and in the development of forest carbon models for southern pines (Cropper and Ewel 1987, Cropper and Gholz 1993, Cropper et al. 1998, Clark et al. 2004, Gonzalez-Benecke et al. 2010a). In this project we developed an even-aged longleaf pine model (LLM-EA) and modified an existing single-tree based longleaf pine model (LLM-ST) to represent the entire sequence of longleaf forest establishment and maintenance (Figure 2.2) and changes in all ecosystem carbon pools including belowground biomass. The overall goal of this project was to complete the development of the two models to simulate the range of management activities that occur on DoD bases across the longleaf pine range, including calibration and validation with extensive field measurements. While carbon sequestration assessments have been performed on several southern military bases,

none achieved the scope or generality that we proposed. For example, forest carbon sequestration at Camp Shelby was modeled from 1990 through 2040 under different hypothetical management scenarios, but carbon pools were not measured directly and all pools were not considered (Barker et al. 1995). Similarly, carbon stocks were assessed at US Army Fort Benning using remote sensing with no direct measurements (Zhao et al. 2010). Our work is unique in that we: (1) conducted thorough and direct measurements of carbon pools at four DoD installations chosen to cover the natural historic range of longleaf pine both longitudinally and along the coastal-interior axis, and (2) synthesized these measurements into a robust model that can be used by forest managers.
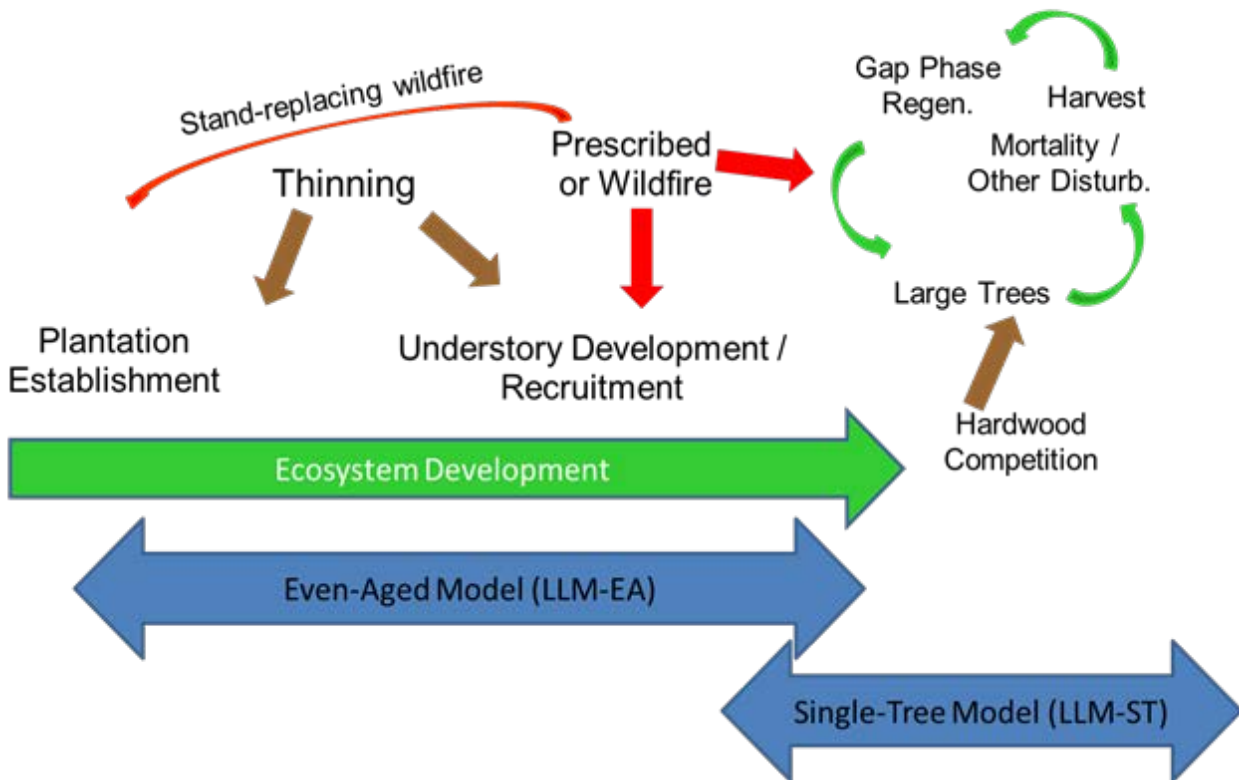
Figure 2.2. The process of establishing and sustaining longleaf pine forests and the two management models for estimating carbon sequestion.

3. General Technical Approach

LLM-EA Development

The DoD ecological forest management model that we developed is based on robust growth and carbon dynamics prediction models. The flexible modeling system for even-aged pine forest carbon sequestration combines growth and yield models with biometric equations to estimate fluxes and stocks of carbon (Gonzalez-Benecke et al. 2010a). The modeling system also tracks the fate of harvested carbon removed from the site and processed into forest products. The slash pine model was compared to data from eddy-covariance (Clark et al. 2004, Binford et al. 2006) and biometric net ecosystem exchange data (Bracho et al. unpublished) from long-term plantation eddy-covariance sites. Parameterization of the LLM-EA used the same model framework as the validated model previously described for slash pine plantations by Gonzalez-Benecke et al. (2010a). The new longleaf pine model used a similar platform; an integrated an even-aged longleaf pine growth and yield model based on the equations proposed by Yin et al. (1998) fitted to longleaf pine yield tables published by Baldwin and Saucier (1983) and Lohrey and Bailey (1977). Dominant height at any given age was estimated using the longleaf pine model reported by Boyer (1980, 1983). Thinning was simulated by fitting the thinning model of Pienaar (1995) to the thinned longleaf pine yield tables presented by Farrar (1979). Allometric equations for stand biomass components were obtained by fitting a general model to longleaf pine data and longleaf pine equations reported by Garbett (1977), Taras and Clark (1977), Edwards and McNab (1977) and Thomas et al. (1995) and using allometric data collected in this project. The improvement of the allometric functions in this model was a key element of this proposal. Stand leaf area index (LAI) was determined by using needle biomass and specific leaf area. Dynamics of understory biomass accumulation and litterfall biomass accumulation were assumed to follow the same dynamic as reported by Gonzalez-Benecke et al. (2010a) using LAI-dependent understory and annual litterfall models. Information about the relationship between longleaf stand LAI and litterfall and understory biomass gathered by this project were important components of the model. Decay rates were set as component-specific.

The effects of thinning on carbon fluxes of forest floor and understory biomass were also incorporated into the model. Reductions in LAI were set to be proportional to reductions in basal area due to thinning and therefore forest floor and understory biomass were affected due to their LAI-dependence. Logging slash from thinned trees was incorporated into flux calculations; thinning slash (root and crown biomass of extracted trees) was determined at each thinning and incorporated into the dead biomass pool. A routine for prescribed fire was incorporated into the model. The existing mortality and detritus models were used to generate estimates of fuel load, and data from the literature and from our own longleaf pine prescribed fire research and from new measurements in pre- and post-prescribed fire stands were used to parameterize the functions.

Final harvest logging residues are calculated by assuming a harvest efficiency of 87% of total volume (Bentley and Johnson 2004) and stem residues biomass calculated by using specific gravity values for bark and stem reported by Taras and Clark (1977). Final harvest slash (root and crown biomass of extracted trees) is determined at each rotation and also incorporated into the dead biomass pool. Calculations are also included to track the fate of carbon in harvested wood pools,

with literature values of conversion efficiencies and decay rates used to model decay in the product pools. Carbon emissions due to silvicultural activities (fertilization, harvest) and transportation to processing facilities are also simulated based on data from Markewitz (2006) and White et al. (2005).

Specific actions that enhanced the LLM-EA carbon balance model included the incorporation of improved allometric functions to estimate ecosystem carbon pools; incorporation of additional longleaf pine growth and yield functions; calibration of model functions with forest carbon pool and coarse root decomposition data collected from across the sampling range and from a range of management scenarios; and validation of the model against additional data held back from the calibration dataset.

Long-term longleaf pine growth data from the USDA Forest Service Palustris Experimental Forest in Louisiana and the USDA Forest Service Harrison Experimental Forest in Mississippi were used to revise growth and yield equations for longleaf pine. It is important to note that while the LLM-EA model uses the most up-to-date longleaf pine functions available its operation is not dependent on any particular function. The model framework is flexible and new functions can be incorporated as they become available, whether the functions are derived from our work or the work of others.

LLM-ST Development

The longleaf pine and hardwood population model used in this project is an explicit single-tree model (LLM-ST). The model represents an extension of our previous longleaf pine population (Cropper and Loudermilk 2006) and landscape (Loudermilk and Cropper 2007) modeling efforts that identified the need for a spatial demography approach to correctly represent longleaf pine forests. The framework uses a lattice-based approach, similar to cellular automata (Silvertown et al. 1992), where trees within cells (5 m x 5 m) interact with nearby cells (trees) based on adjacency and distance. The Python programming language (an open source, freely available tool) was used for model development. For model development, we chose a reasonably compact area (125 m x 125 m; 1.56 ha) using a torus shaped landscape, eliminating issues with edge effects. Spatial interactions included seed dispersal or rhizomatous spreading (fecundity), inter- and intra-species plant competition impacts on growth and mortality, as well as effects of tree density on leaf litter or fuel distribution. The model has a one year time step, with yearly probabilities for fire occurrence and pine seed masting events. The stochastic fire regime represents a natural longleaf pine forest. The model can be easily modified to include the time and extent of fires.

The LLM-ST is designed to simulate the critical interactions between fire, trees, and fuels (Figure 3.1). Both longleaf pines and hardwoods can exist in each cell. During the reproductive stage, up to ten trees of each type (20 total) can establish in an empty cell, with individual mortality incidences causing a natural thinning effect as the cell or trees within a cell age. Mortality for an individual tree can be from competition, fire, or other natural causes (background mortality). Masting is an important feature of longleaf pines, and is included as a stochastic element of the model based on data collected for over 40 years across the southeastern U.S. (Boyer 1998). Each

year has a 0.15 probability of being a mast year, where only adult and subadult trees produced 40-125 cones and 10-70 cones, respectively. During non-mast years, adults and subadults produced 1-40 cones and 1-20 cones, respectively. Juveniles do not produce any cones. We assumed all trees produced 32 seeds per cone [average value from (Boyer 1990)]. Seeds are dispersed based on distance from a focal cell with subadult or adult trees and whether it was a mast year or not. In mast years, seeds are dispersed three cells and two cells from the focal cell for adults and subadults, respectively. In non-mast year, seeds are dispersed two and one cell from the focal cell for adults and subadults, respectively. Germination rates are highly dependent on the ability of the large seeds to reach the soil bed, free from immediate competition (Myers 1990). With fire removing understory vegetation and accumulated necromass, fire frequency essentially drives germination probability. Therefore seed germination was a function of time since fire at time t and a maximum germination probability.

Growth is often modeled as function of potential growth with modifiers (Quicke et al. 1994). For the LLM-ST, longleaf pine height growth within a cell is asymptotic and a function of age (Age_{LP}). This potential growth is modified or suppressed based on the competitive environment (CI_{LP}) of adjacent trees.

$$Ht_{LP} = AHt_{LP} (1.0 - e^{-0.02\,Age_{LP}})(1.0 - CI_{LP})$$

The asymptotic height (AHt_{LP}) is the potential growth of the entire longleaf pine population being modeled and is determined by a stand's site index. Simulated age to height relationships were comparable to other studies (Platt et al. 1988, Greenberg and Simmons 1999) with similar asymptotic associations and dispersion characteristics (i.e., higher variation of height values as trees age). Furthermore, we implemented a 'dormant tag' for each newly established seedling to represent the commonly found grass stage. Each seedling remains in the grass stage for 1-10 years (average 5), while initiating height growth using the equation above. Thereafter, seedlings grow readily and usually reach a height of 1.5 m within the next four years. For simplicity, all trees within a cell grow or remain in the grass stage together (i.e., same height values within a cell).

Fire does not necessitate a season time step in the model. The model currently simulates only woody tree species composition. A task of this work was to incorporate gross understory biomass dynamics into LLM-ST. The LLM-EA uses relationships between overstory LAI and understory biomass to simulate changes in understory as the overstory develops or is thinned.
The LLM-ST implicitly accounts for vegetation release following fire. Mortality leads to reduced competition which leads to increased growth. One of our tasks was to extend the model to calculate tree and litter carbon, and carbon losses from fire. We interpret "vegetation release" as referring to changes in overstory productivity in response to reduced competition from understory or from other overstory trees that were killed by fire. This is separate from accounting for changes in understory productivity (in particular for wiregrass or bluestem grasses) and forest floor carbon pools after fire, which will be accounted for in both models. Therefore, both understory and overstory phenomena will be incorporated into the models.
Specific actions to enhance and improve the LLM-ST and to meet the needs for evaluating carbon sequestration included extending the LLM-ST to include ecosystem carbon pools above and belowground; improving decomposition functions from the root decomposition studies and carbon

losses from fires; simulating soil carbon and litter pools using first-order ordinary differential equations, with litter inputs derived from allometric equations, and turnover rates estimated from literature values; adding management (single or group tree harvest, prescribed fires) into the LLM-ST; and adding a connection between the final stages of the LLM-EA and LLM-ST. Tree density and size distribution data are important inputs. Key elements of the final model include the full integration of the LLM-EA and LLM-ST models and incorporation of the ability to "enter" the system at various stages of stand development.
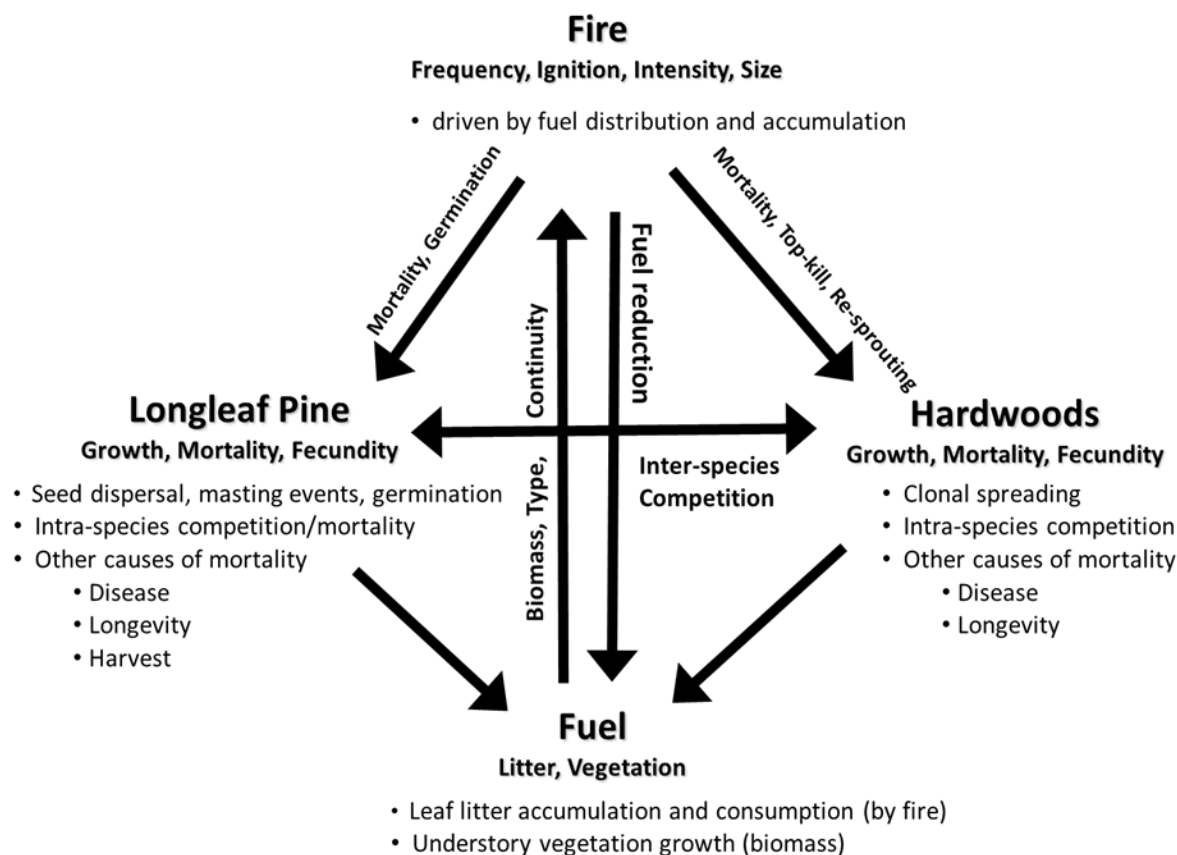
Figure 3.1. Important processes and state variables in the LLM-ST.

Data Collection

We collected field data needed to develop allometric equations, quantify carbon pools, and validate the models at four DoD bases chosen to represent the longleaf pine range: US Army Fort Benning

in Georgia; US Army Fort Polk/Kisatchie National Forest in Louisiana, Eglin Air Force Base in Florida; and Marine Corps Base Camp Lejeune, NC (Figure 3.2). The sites were selected based on representation of unique climate and soils zones for longleaf pine from Craul et al. (2005) and understory composition. Inventory data were used to select stands based on stand structure, management history, ground cover, and soil type (Figures 3.3-3.6).
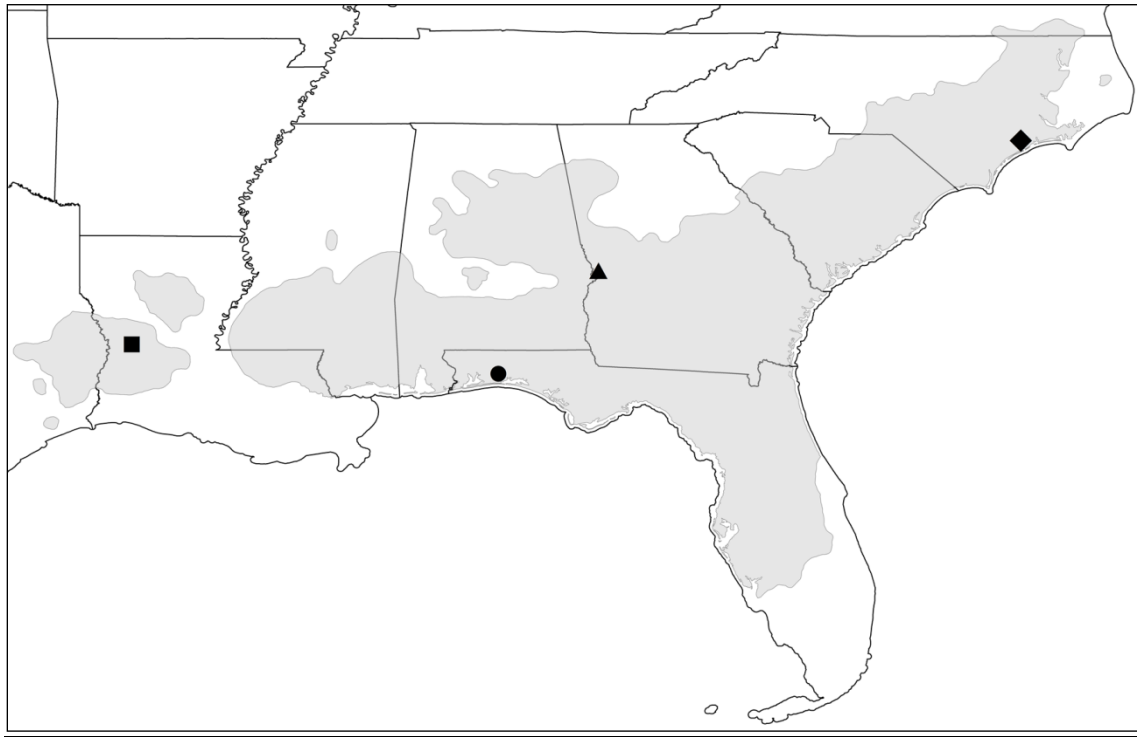
Figure 3.2. Map showing the location of DoD bases sampled in this project within the historical range of longleaf pine. Symbols denote Marine Corps Base Camp Lejeune (diamond), US Army Fort Benning (triangle), Eglin Air Force Base (circle), and US Army Fort Polk/Kisatchie National Forest (square).

US Army Fort Benning
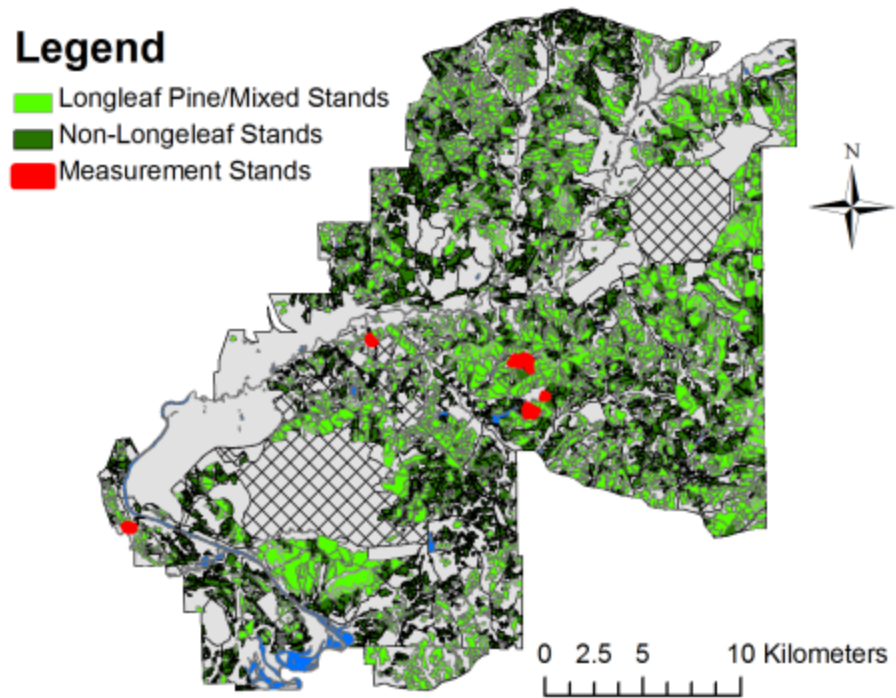
Figure 3.3. Location of stands sampled at US Army Fort Benning.

US Army Fort Polk/Kisatchie National Forest
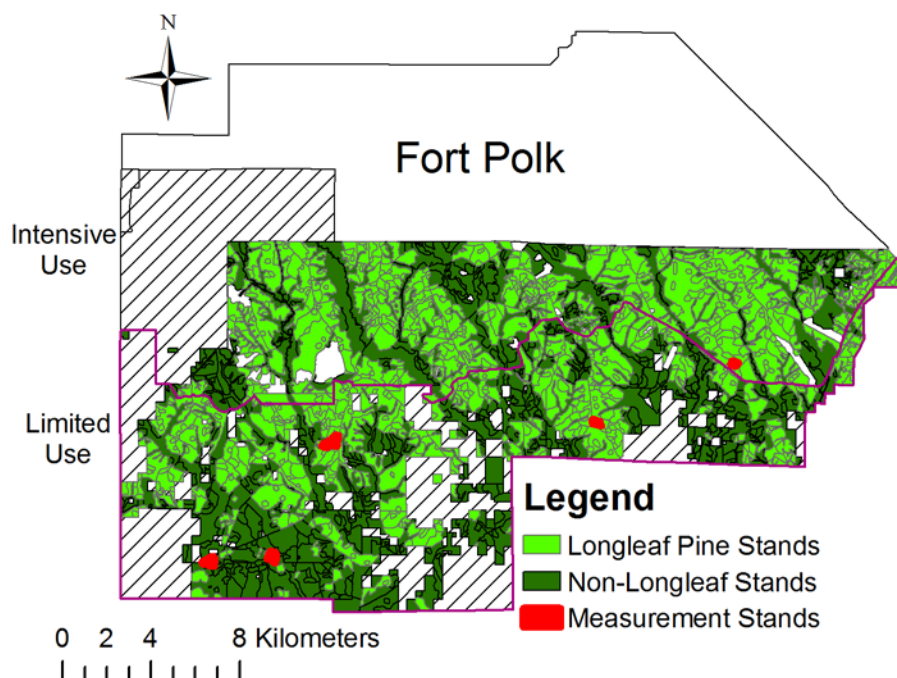
Figure 3.4. Location of stands sampled at US Army Fort Polk/Kisatchie National Forest.

Marine Corps Base Camp Lejeune
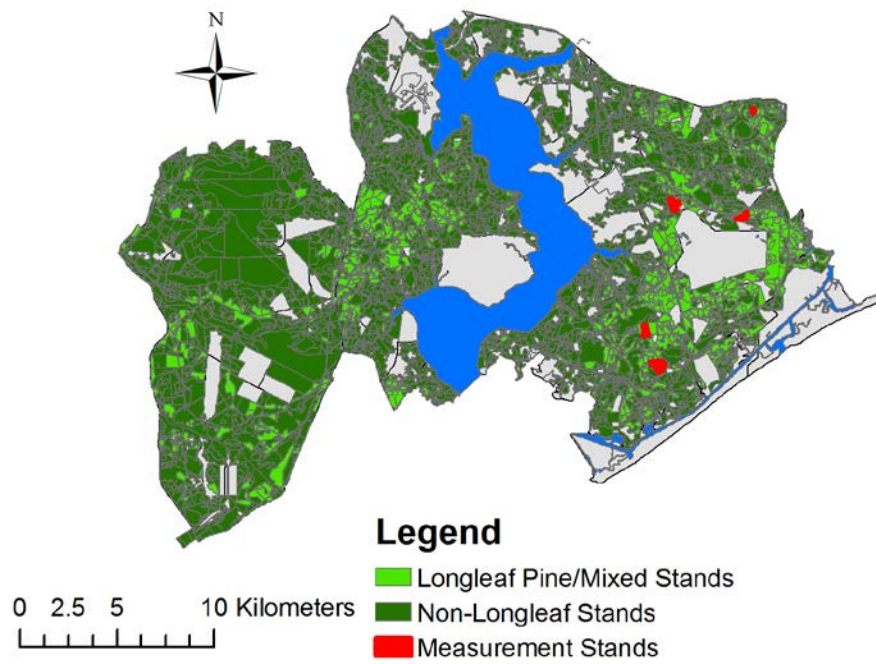
Figure 3.5. Location of stands sampled at Marine Corps Base Camp Lejeune.

Eglin Air Force Base
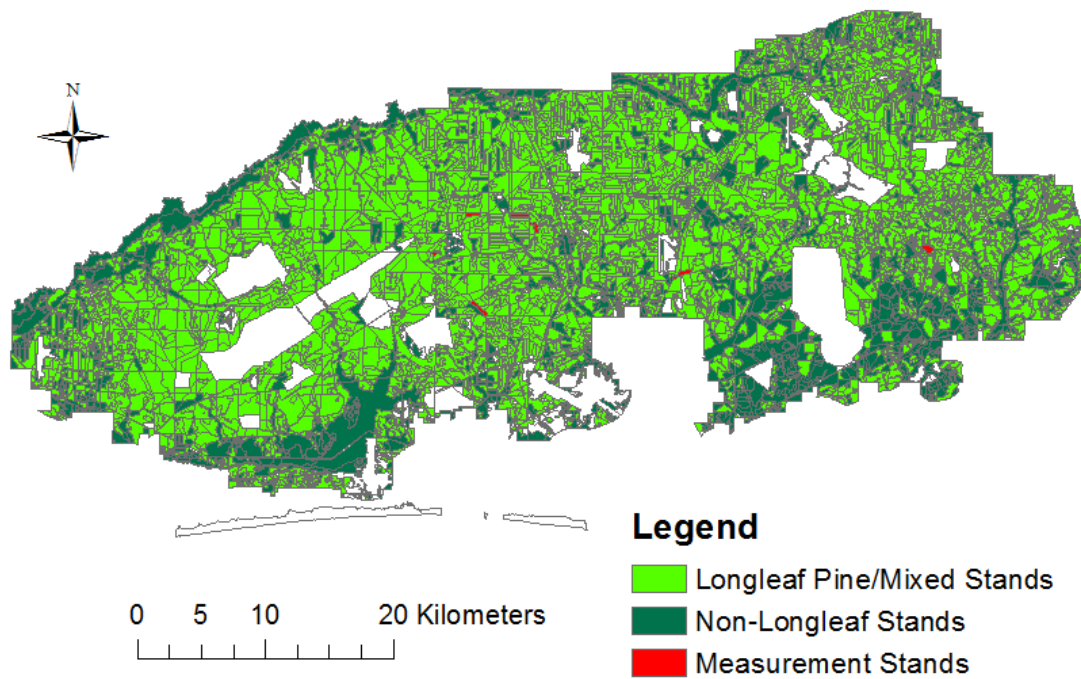
Figure 3.6. Location of stands sampled at Eglin Air Force Base.

4. Organization of this Report

To address Objective 2 (support calibration and validation of the models), Chapter 5 details carbon protocol measurement procedures and presents carbon stock data collected from four stands located at US Army Fort Benning. The carbon sampling protocols were also used in Chapter 7, which describes a synthesis of ecosystem carbon pool data and soil carbon collected across all sample sites to develop a comprehensive carbon chronosequence for longleaf pine. In Chapter 6, we describe the technical approach used to coordinate tap root pit excavations with ground penetrating radar to accurately estimate the carbon stored in longleaf pine root systems described in Chapter 7. Chapter 8 focuses on the outcome of our field research quantifying carbon retained in decaying tap roots of longleaf pine. The functions developed in Chapter 8 facilitate prediction of below-stump carbon of dead longleaf pine trees in carbon assessments. Chapter 9 provides more detailed analyses of soil carbon including soil carbon age and pyrogenic carbon.

To address Objective 1 (develop forest carbon cycle models), in Chapters 10-12 we describe the development of longleaf pine biometric functions critical for model development. To facilitate modeling of understory biomass in the LLM-EA (Objective 3), Chapter 13 explores the relationship between fire and understory development using data collected at the calibration sites. In Chapter 14, we use the LMM-EA to demonstrate how forest management and silvicultural prescriptions influence life-cycle carbon balance, forest structure and forest products (Objective 4). Chapter 15 provides additional detail on validation of the LLM-EA. In Chapter 16 the multi-model framework for the LLM-ST is described and new additions to the model are detailed and the model is used to simulate the effects of prescribed fire and harvesting to address Objectives 1, 3 and 4.

Conclusions and implications for future research and implementation are described in Chapter 17 and followed by Chapter 18 listing the literature cited and the Appendices in Chapter 19.

5. Field Sampling Methodologies and Ecosystem Carbon Stocks in Longleaf Pine Forests at US Army Fort Benning

[Contents of this chapter were extracted from Samuelson, L.J., T.A. Stokes, J. R. Butnor, K.H. Johnsen, C.A. Gonzalez-Benecke, P. Anderson, J. Jackson, L. Ferrari, T. A. Martin, and W. P. Cropper, Jr. 2014. Ecosystem carbon stocks in *Pinus palustris* Mill. forests. Canadian Journal of Forest Research 44: 476-486]

Introduction

Forests serve as a means for mitigating climate change by acting as sinks for atmospheric CO_2 and storing carbon (C) in plant biomass, detritus and forest soils. In the southeastern United States, forests contain 36% of Nation's sequestered C (Turner et al. 1995) and have the potential for greater sequestration with improved forest C management. Carbon accumulation in forest ecosystems is influenced by interactions among forest structure and development, site quality and species composition, and thus there is a need for C assessment in a wide variety of ecosystems under different management scenarios (Birdsey et al. 2006). The weakest link in most tree growth models and subsequently C models is the estimation of tree biomass, which is the main input for estimation of C stocks (Vashum and Jayakumar 2012). Most assessments of forest carbon stocks rely on standard inventory data and general aboveground biomass equations from the published literature. Belowground biomass can be included and is most often calculated using generalized component ratio equations (Jenkins et al. 2004). These approaches are used because species and site specific allometric functions are usually not available and, though useful for making landscape-level estimates, general functions do not provide the accuracy needed to explicitly manage forests for C sequestration.

Longleaf pine forests were once an important forest ecosystem in the southeastern United States, and there is increased interest in the restoration of longleaf pine forests for not only traditional forest products but also to provide a variety of ecosystem services and, more recently, as a species resistant to disturbances associated with climate change (Johnsen et al. 2009). Longleaf pine has been suggested as a species that can contribute to climate change mitigation, because of long rotations and long-term C storage combined with greater resistance to insects, diseases and wind damage, less energy inputs relative to the more intensively managed southern pines and tolerance of drought (Johnsen et al. 2009). Longleaf pine has generally been considered a slower growing southern pine, but its longevity (up to 400 years) offers opportunities to sequester C, particularly in C offset projects with longer (100 year) contracts.

Longleaf pine plantations and naturally regenerated ("natural" pine *sensu* Smith et al. 2009) stands typically have lower tree densities than that of other southern pines with understory competition and ground cover diversity controlled by prescribed fire. Thus, assessments of C storage using allometric equations developed for other southern pines or for pine species in general may be inappropriate. For example, Remucal et al. (2013) applied a hypothetical offset project on a longleaf pine site in Georgia. The accounting approach used standardized biomass equations and look up tables (Smith et al. 2006; Woodall et al. 2011). When compared to site specific longleaf pine equations, the standardized equations underestimated aboveground C by 36% and significantly underestimated emissions reductions, making the project economically nonviable. The hypothetical project highlighted conflicts between ecological restoration and climate benefits

from low-density semi-mature stands, typical of longleaf pine forests, and the need for better assessment of C stocks for effective C management in longleaf pine ecosystems.

The overall goal of this research was to improve our understanding of ecosystem C stocks in longleaf pine forests. Ecosystem C was defined as the summation of C in plants, detritus and soil. Specific objectives were to: (1) develop allometric equations for above and belowground biomass of longleaf pine trees, and (2) quantify C stocks in trees, ground cover vegetation, detritus and soil in five longleaf pine stands ranging in age from 5 to 87 years. Belowground C was measured using a unique combination of below-stump excavations, soil cores and ground penetrating radar (GPR).

Methods and Materials

Study area

The study was conducted at US Army Fort Benning Military installation (32.38° N, 84.88° W) which occupies portions of Chattahoochee and Muscogee Counties in Georgia and Russell County in Alabama. The installation covers 73,533 ha. Prior to becoming a military installation in 1918, land use was mainly farming and grazing with some remnant forest. Currently, 61,538 ha are forested, with approximately 9,300 ha in managed pure longleaf pine and 9,300 ha in managed mixed pine comprised of at least 25% longleaf pine. The terrain ranges from predominately rolling to areas with flat ridges and gentle slopes and elevations range from 58 to 225 m. The climate in the area is humid and mild. The 30 year (1982-2011) mean annual precipitation measured in Columbus, GA is 1180 mm and the 30 year mean annual temperature is 18.7°C, with an average January temperature of 8.5°C and average July temperature of 28.1°C (http://www.ncdc.noaa.gov/cdo-web/datasets/annual/stations/COOP_092166/detail).

Because the primary objective of the sampling was to obtain data from a wide range of tree sizes and not to develop relationships strictly with stand age, we chose to sample a larger number of ages rather than sampling in replicated stands from a smaller number of ages. Five longleaf pine stands were selected and were 5, 12, 21, 64, and 87 years of age (Table 5.1). All stands were located in Georgia with the exception of the 64-year-old stand which was located in Alabama. Stands were selected based on age and stand structure, similarities in soils and the degree of access permitted by the military.

The 12, 21 and 87-year-old stands were located in the Southeastern Mixed Forest Province Southern Appalachian Piedmont Section Ecoregion characterized by deep, infertile clayey soils that are highly eroded (Bailey 1995). The 5 and 64-year-old stands were located in the Southeastern Mixed Forest Province Coastal Plains Middle Section Ecoregion characterized by marine-deposited sediments ranging from sands and silt to chalk and clays. The soil series was a Nankin sandy clay loam (greater than 45% sand, less than 28% silt, and 20-35% clay) for the 5 and 12-year-old stands, a Troup sandy loam (greater than 52% sand, 7-20% clay, and the silt plus twice the clay fraction totals more than 30%) for the 21 and 87-year-old stands, and Troup Springhill Luverne sandy loam complex for the 64-year-old stand (Soil Survey Staff, 1999).

Table 5.1. Stand characteristics and range in diameter, height and tap root depth of longleaf pine trees selected for whole tree harvests.

Stand age (years)	Planting density (trees ha^{-1})	Burn history	Sample Size	DBH (cm)	Height (m)	Tap root depth (m)
5	1494	2007, 2010	10	3.8-7.2	0.6-3.4	0.2-1.4
12	1494	2002, 2005, 2008, 2010	10	2.9- 16.8	6.0-10.4	0.5-1.0
21	2235	1992, 1995, 1998, 2001, 2004*, 2005, 2006*, 2009, 2010*	10	3.2-16.2	4.5-14.4	0.9-1.8
64	Natural	1991, 1994*, 1999, 2002, 2003, 2008, 2010	3	22.8-36.9	16.1-23.5	1.1-1.5
87	Natural	1981, 1985*, 1990, 1992, 1994, 1998, 2001, 2004, 2006, 2008, 2010	3	34.3-48.6	27.3-29.9	1.6-3.1

Notes for Table 5.1: Ground line diameter (cm) was used for the 5-year-old stand. Burn records began in 1981. * Indicates wildfire. DBH is diameter at breast height.

The three youngest stands were planted, and the two oldest stands were naturally regenerated and had few other species at the time of sampling. The two youngest stands were planted with containerized seedlings and the 21-year-old was planted with bare root seedlings. No older planted stands were available for study. The 5 and 12-year-old stands were planted at a density of 1494 trees ha^{-1} and the 21-year-old stand was planted at a density of 2235 trees ha^{-1}. All planted longleaf pine in the 5-year-old stand was out of the grass stage. Prior to initiation of burn records in 1981, frequent fires were common as a result of live fire during military training. All stands were last burned in 2010 and since 2002 burned every 1-3 years (Table 5.1). The only stand with a record of a thinning was the 64-year-old stand in which a thinning was conducted in 2004 or 2005, with no other details available. There was no record of thinning in the 87-year-old stand.

In February 2012, a 1 ha circular main plot (56.4 m radius) with four 0.04 ha circular subplots (11.3 m radius) was installed in each stand following the protocol of Law et al. (2008). In each stand, one subplot was positioned at the center of the main plot and three subplots were positioned 35 m from the center of the main plot at 0°, 120°, and 240° from North.

Forest inventories

Forest inventories were conducted in the four subplots in each stand February 2012. Species, diameter at breast height (DBH) (in the 5-year-old stand ground line diameter, GLD) to the nearest

0.1 cm, and total height to the nearest 0.1 m were recorded. In the 5 and 12-year-old stands, tree height was measured using a telescoping height pole. In the older stands, tree heights were measured using a laser hypsometer (TruPulse 200, Laser Technology, Inc, Centennial, CO). All dead stems (snags) were measured provided the angle of the stem from true vertical was <45°.

In all stands, DBH, height of live trees and snags with DBH ≥10 cm, and GLD of all stumps were measured within the entire circular subplots (4 per stand). DBH and height of all live trees and snags with DBH < 10 cm and height ≥2 m were measured within a 5 m radius of subplot center. In addition, to account for all planted trees in the three plantations, DBH or GLD (5-year-old stand) and height of all planted trees in the subplot were measured.

Understory was defined as all woody species ≥ 1 and < 2 m in height. GLD and height of all understory woody plants were measured within five 1 m^2 circular sampling rings in each subplot located using the stratified-random polar coordinates method described by Gaiser (1951).

Longleaf pine C stocks

Longleaf pine trees representing the range in DBH and height distribution in each stand were selected for felling (Table 5.1). Ground line diameter was used to select trees in the 5-year-old stand. In June 2012, 10 longleaf pine trees per stand were felled in the 5, 12, and 21-year-old stands and three longleaf pine trees per stand were felled in the 64 and 87-year-old stands, for a total of 36 trees. All trees were cut at ground level. Entire trees were sampled in the 5 and 12-year-old stands. Given the large range in tree size in the 21-year-old stand, the six smallest trees were sampled and the four larger trees were subsampled. In the 64 and 87-year-old stands, all trees were subsampled, with the exception of the largest tree in the 87-year-old stand for which all biomass was sampled due to difficulties in determining branch location after felling, which caused substantial breakage.

Biomass was separated into foliage, branches, and main stem and oven-dried at 70°C until reaching a constant mass. To determine the dry weight of branches and foliage in subsampled trees, every branch from every whorl was cut adjacent to the stem and branch diameter was measured at the cut end in two directions using digital calipers. Green weights of entire branches were measured in the field using a digital scale (Intercomp CS200 Digital Hanging Scale, IntercompCo, Inc., Medina, MN). One branch was randomly selected from each whorl, separated into foliage and wood mass, and oven-dried. In 64 and 87-year-old trees, green weights of all branches were measured, but due to the large size of branches, dry weight was determined only on two branches randomly selected from each third of the canopy (six branches per tree). Stand specific relationships between branch green weight, branch diameter and oven dry weight of foliage and woody tissues were developed by pooling all sample branches per stand. These relationships were then used to predict individual tree foliage and branch dry weight from branch green weight.

In subsampled trees, the main stem was cut into 1.3 m sections and the green weight of each section was measured in the field. A disc which included wood and bark was cut from the base of every other section and the green and dry weights measured. Data were pooled by stand and stem dry

weight was predicted from green weights using relationships between green weight and the oven-dried weight of discs.

In July 2012, five of the ten longleaf pine trees harvested from each of the 5, 12, and 21-year-old stands were randomly selected for below-stump excavations. Below-stump biomass was sampled in all three trees from the two older stands (six total). The square area of the excavation pit ranged from the minimum set at 1 m^2 for the smallest tree to a set maximum of 4 m^2 for the largest tree. Pit size was limited to a maximum of 4 m^2 due to the time demanding nature of manual root excavations in large tree pits. The area of the stump was excluded from the pit area and length and width of the pit was measured beginning at the stump edges. Pit size for remaining trees was calculated from the linear relationship between tree basal area and pit size developed using the minimum and maximum set pit size and the corresponding tree basal area. The goal of the calculation was to come up with a method to objectively vary pit size (and therefore effort) for different size trees, and to keep pit size within the realm of field reality (e.g. no 10 cm diameter pits and no extremely large pits). Pits sizes ranged from 1.0-1.2 m^2 in the 5-year-old stand, 1.0-1.3 m^2 in the 12-year-old stand, 1.0-1.3 m^2 in the 21-year-old stand, 2.0-2.7 m^2 in the 64-year-old stand and 2.6-4.0 m^2 in the 87-year-old stand.

All coarse roots ≥5 mm were manually extracted from the pit to a 1 m depth and all lateral roots branching off the main tap root were cut at the pit wall. Soil to a 1 m depth was sieved using a 0.63 cm hardware cloth and all roots ≥5 mm in diameter were collected. The pit was then excavated around the entire tap root and the tap root was removed using a mini excavator if needed. The length of all tap roots was measured.

Carbon concentrations were measured in two stem samples per harvested tree, one at DBH and the other at the base of the live crown, and in two composite samples of foliage per sample tree and averaged by stand (Table 5.2). In two stumps per stand, C concentration was measured in one random sample from the tap root, one from a large (50-100 mm) lateral root and one from a small (10-50 mm) lateral root (Table 5.2). The mean of the small and large root sample was applied to all coarse roots (≥ 2 mm) extracted from the pits or detected by GPR. Carbon concentration was measured on a composite sample of fine roots (<2 mm) collected from each subplot and each stand had a total of four samples. Branch C concentration was assumed to be the same as stem. All tissue samples were analyzed for total C using a using a Flash EA 1112 series Thermo Finnigan NC soil analyzer (Milan, Italy).

Other species C stocks

Across all stands, a total of eight species other than longleaf pine were recorded in the overstory. Allometric equations from the literature were used to predict aboveground biomass from DBH and included: general oak and pine equations from Jenkins et al. (2004), a loblolly pine (*Pinus taeda* L.) equation from Naidu et al. (1998), and southern red oak (*Quercus falcata* Michx.), blackgum (*Nyssa sylvatica* Marsh.), sweetgum (*Liquidambar styraciflua* L.) equations from Phillips (1981). Carbon concentrations in all tissues of species other than longleaf pine were assumed to be 50% (Woodbury 2007). Tap root mass of other pine species was predicted using the allometric equation we developed for tap root biomass of longleaf pine because site characteristics such as depth to

the clay layer may have more influence on tap root development than species. For example, Gibson et al. (1985) found no differences in below-stump biomass among longleaf pine, loblolly pine and slash pine growing on the same site. We assumed that that GPR measurement of coarse roots captured all hardwood coarse root mass.

Table 5.2. Carbon concentrations (%) of plants in the ground cover layer (< 1 m in height) by growth form and C concentrations in longleaf pine (LLP) tissues, litter and duff in longleaf pine stands.

Component	Stand age (years)				
	5	12	21	64	87
Forbs	49.9±1.3	47.8±0.6	44.9±1.1	47.1±2.9	48.0±1.9
Graminoids	46.7±1.4	46.5±1.9	48.2±0.4	48.5±0.8	49.2±2.1
Legumes	47.2±1.1	45.7±4.0	48.2±2.1	51.5±1.6	47.1±2.3
Vines	50.0±0.06	49.1±1.0	49.9±1.3	48.1±1.0	49.8±0.7
LLP stem	51.6±0.4	51.6±0.1	51.0±0.4	51.2±0.2	53.9±0.5
LLP foliage	51.5±0.2	51.4±0.2	50.8±0.2	52.2±0.2	53.8±0.2
LLP coarse root	50.6±0.6	51.3±1.8	49.6±1.1	50.5±1.3	52.1±1.2
LLP fine root	40.3±4.1	44.7±1.0	43.4±1.3	43.4±2.7	37.5±1.9
Litter	48.3±0.5	50.5±1.1	50.6±0.2	51.2±0.5	51.4±0.3
Duff	43.9±1.9	41.3±7.0	49.0±2.9	21.7±7.5	54.8±1.3

Notes for Table 5.2: Values are means ± SEs. For the ground cover, litter and duff layers, SEs represent variation among subplots within a stand. For longleaf pine tissues, SEs represent variation among trees within a stand.

Understory and ground cover C stocks

For understory woody stems (between 1 and 2 m height), allometric equations derived from the 5-year-old stand were used to predict aboveground biomass for longleaf pine between 1 and 2 m in height. If available, species specific allometric relationships from Robertson and Ostertag (2009) were used to predict aboveground biomass of understory woody stems, otherwise a general equation was used (Robertson and Ostertag 2009).

Ground cover vegetation was defined as trees and shrubs <1 m in height, including longleaf grass stage seedlings (seven seedlings in the 64-year-old stand and two seedlings in the 87-year-old stand were found), and all herbaceous species. Within each 1 m² sample ring, all vascular plants were clipped at the root collar and bagged by category (shrubs/tree seedlings, vines, graminoids, legumes, forbs and ferns) and placed in an oven at 70° for 72 h and weighed. Only plants rooted inside the sample ring were included. Carbon concentrations were measured in the non-woody ground cover by category (vines, grass, legume, forbs) (Table 5.2). Two composite samples of each category were collected from each subplot and pooled by subplot. Since ferns were found on only one subplot in the 64-year-old stand the C concentration for ferns was assumed to be 50%.

Plot level root C stocks

Ground penetrating radar was used to augment the below-stump root mass estimates by accounting for lateral root biomass between trees and outside of the excavated pit area. At the center of each subplot, a square 100 m^2 GPR measurement plot was prepared by mowing and raking away all grass, woody brush and accumulated litter. A series of 21 parallel transect lines 10 m long and 0.5 m apart were established on each subplot and scanned with a SIR-3000 radar unit (Geophysical Survey Systems Inc. (GSSI), Salem, NH) equipped with either a 900 or 1500 MHz antenna. Post collection data processing was used to remove signal noise, and determine the location and relative size of roots using RADAN 7 software (GSSI, Salem, NH). Image analysis was applied to summarize processed data and quantify root biomass at 65 locations along each transect (1365 total per subplot) using an approach described by Butnor et al. (2012*a*) with SigmaScan Pro Image Analysis Software, (Systat Software, Point Richmond, CA). The relationship between GPR data and actual root mass was assessed at each stand using (25) 15 cm diameter validation root/soil cores which were scanned with GPR prior to collection, then dry sieved, washed, oven dried at 65°C to a constant weight (Butnor et al. 2012a). In addition to GPR calibration, the subplot cores were used to determine fine root mass. Roots were hand separated into categories of pine/non-pine, live/dead, and diameter class (<2 mm, 2 – 10 mm, > 10 mm). Dead roots varied from being undetectable to marginally detectable, so GPR data were scaled using live root mass. To integrate GPR data with longleaf pine below-stump estimates derived from inventory data, it was assumed that GPR cannot detect fine roots (< 2 mm diameter), tap roots or most decaying roots, and GPR has accounted for all lateral roots regardless of species (Butnor et al. 2012a). Because of the predominance of large overlapping roots in the excavation pits and potential underestimation by GPR of lateral roots in the pits, coarse root GPR C (tap root not included) was calculated using two different assumptions: (1) that GPR captured all lateral root mass in the excavation pit area (coarse root GPR = GPR – predicted longleaf pine lateral roots in pits), or (2) that GPR captured no lateral roots in the pits (coarse root GPR = GPR + predicted longleaf pine lateral roots in pits). The average of the two approaches was used in estimating ecosystem C.

Detritus C stocks

A total of 66, 14, 2, 12, and 14 stumps were tallied in the 5, 12, 21, 64 and 87-year-old stands, respectively. In the 5-year-old stand, the 66 stumps had an average top diameter of 31.7 cm. For these stumps, we assumed the trees were cut the year preceding planting. Initial tap root biomass was predicted from the ground line diameter relationship in Table 5.4, and residual tap root C after 5 years of decay was predicted using an exponential decay model and baseline decay rate of 0.15 (±25%) (Ludovici et al. 2002). The average C concentration measured for live tap roots was used. The C in residual stumps in the other stands was not estimated or included in ecosystem C because time since cutting was unknown. Residual tap root C likely contributed additional dead organic matter C in the older stands, but the degree to which would depend on knowledge of decay duration, tap root size, resin content and burning frequency.

A modified approach of the Planar Intersect Technique described by Harmon and Sexton (1996) was used for sampling coarse woody debris (≥7.6 cm diameter, CWD) and fine woody debris (≥2.5 cm and <7.6 cm diameter, FWD). In May 2012, CWD was measured along four 56.4 m transects

positioned 45°, 135°, 225°, and 315° from North in each subplot. The slope of each transect was recorded. Along the entire transect, CWD intersecting the transect plane up to a height of 2 m was recorded. Fine woody debris was sampled along a sub-section of each transect from 15 m to 37.6 m from plot center (22.6 m total). For each CWD intersection along the transect line, true diameter at the line intercept and one of 5 decay classes (Waddell 2002) were recorded. For FWD, the number of intersections was recorded.

The volume of logs per unit ground area for CWD from the line intercepts was calculated following Warren and Olson (1964) and Van Wagner (1968). We assumed all CWD was from longleaf pine trees. The volume of decaying CWD was converted to mass from the density of wood (0.5413 g cm^{-3}) reported for longleaf pine by Woodall and Monleon (2010) and applying a decay-class reduction factor (Waddell 2002). The volume of FWD per unit area from the line intercepts was calculated following Harmon and Sexton (1996) and the mass of FWD was calculated and corrected for slope following Parresol et al. (2006). Forest floor samples were collected from four 50 cm diameter PVC rings placed 2 m from subplot center at 0°, 90°, 180°, and 270° from North in each subplot in May 2012. All woody detritus ≥2.5 cm in diameter was discarded. Forest floor components were separated into: 1) duff, which consisted of the fermentation and humus layers combined and included the dark, partly decomposed organic material (unrecognizable plant forms) above the mineral soil, 2) litter on top of the duff and included recognizable plant parts such as leaves, flowers, and twigs < 0.6 cm in diameter, 3) very fine woody debris ≥0.6 cm and <2.5 cm in diameter, and 4) cones. Samples were pooled by subplot and component and oven-dried. Very fine woody debris was added to the FWD category.

Carbon concentrations were measured in litter and duff samples. Duff C concentration was ash corrected to remove the influence of any soil C in the sample. Because of low CWD and FWD in all stands and lack of range in decay classes, C concentration of CWD and FWD was assumed to be 50% (Prichard et al. 2000; Harmon et al. 2008).

Soil C

A 1.9 cm diameter push tube was used to collect samples at 2 m, 5 m, and 11 m from subplot center at 0°, 90°, 180°, and 270° from North (12 locations total per subplot) at 0.0-0.1 and 0.1-0.2 m depths (24 samples). A 10 cm diameter bucket auger was used to collect samples at 0.2-0.5 m and 0.5-1.0 m depths from two of the soil sampling locations (4 samples). Within each subplot, the subsamples were combined by depth. Soil was air dried for several weeks and passed through a 2 mm sieve to separate roots and rocks. Total soil carbon concentration was determined by dry combustion with detection by thermal conductivity (Flash EA 1112 Series C/N analyzer (ThermoFinnigian Instruments, Milan, Italy). Soil bulk density was measured at the same depths at one of the soil sampling locations in a subplot, randomly selected, using a 5.7 cm diameter core (0200 Soil Core Sampler, Soil Moisture Equipment Corp., Goleta, CA). Soil was oven-dried at 105°C for 96 hours and then passed through a #10 sieve and roots and rocks were extracted and weighed separately. The effect of root volume on bulk density was negligible. Rock volume was determined by water displacement. Soil bulk density was then calculated by soil mass (minus rock and root mass)/soil volume (minus rock volume) (Law et al. 2008). Total percent C concentration was converted to content and scaled to Mg·ha^{-1} using stand-level soil bulk density means by depth.

Statistical analyses

Because the majority of longleaf pine in the 5-year-old stand had not reached DBH and only GLD was measured, allometric regressions were developed for the 5-year-old stand separately. The 5-year-old trees were in the process of bolting from the grass stage and had little if any branching. Branch biomass was therefore not predicted for the 5-year-old trees and any branch biomass was pooled into stem biomass. Data from all other stands were combined to develop regressions. Models were selected based on R^2 values and analysis of residuals. Three measures of accuracy were used to evaluate the goodness-of-fit between the observed and predicted values for the above and belowground allometric functions: (i) root mean square error (RMSE); (ii) mean bias error (BIAS, the difference between mean observed and predicted values); and (iii) coefficient of determination (R^2). Because the chronosequences lacked true replication and stands varied in age, structure (basal area, density) and management history, differences between stands were not tested. Standard errors of the mean in tables and figures indicate variation among the four subplots within a stand.

Results

Stand structure

In the 5-year-old stand, the majority of longleaf pine tree (625 trees ha^{-1}) were still in the understory layer (< 2 m in height) and the understory layer in the 5-year-old stand was dominated by species other than longleaf pine (Table 5.3). In the 12-year-old stand, the majority (67%) of longleaf pine in the overstory layer was < 10 cm DBH (Table 5.3, Figure 5.1). The understory layer in the 12-year-old stand was also dominated by species other than longleaf pine. In stands older than five years, the majority of basal area in the overstory was longleaf pine. In the two oldest stands, there were cohorts of smaller longleaf pine in the < 10 cm DBH class. Compared to the younger stands, the two oldest stands were made up of fewer but larger trees up to 56 cm in DBH in the 64-year-old stand and 58 cm in the 87-year-old stand (Figure 5.1, Table 5.3). Total basal area in longleaf pine was 6.1, 20.9, 7.8, and 14.5 m^2 a^{-1} in the 12, 21, 64 and 87-year-old stands, respectively. The high basal area in the 21-year-old stand was due to the high planting density (2235 trees ha^{-1}).
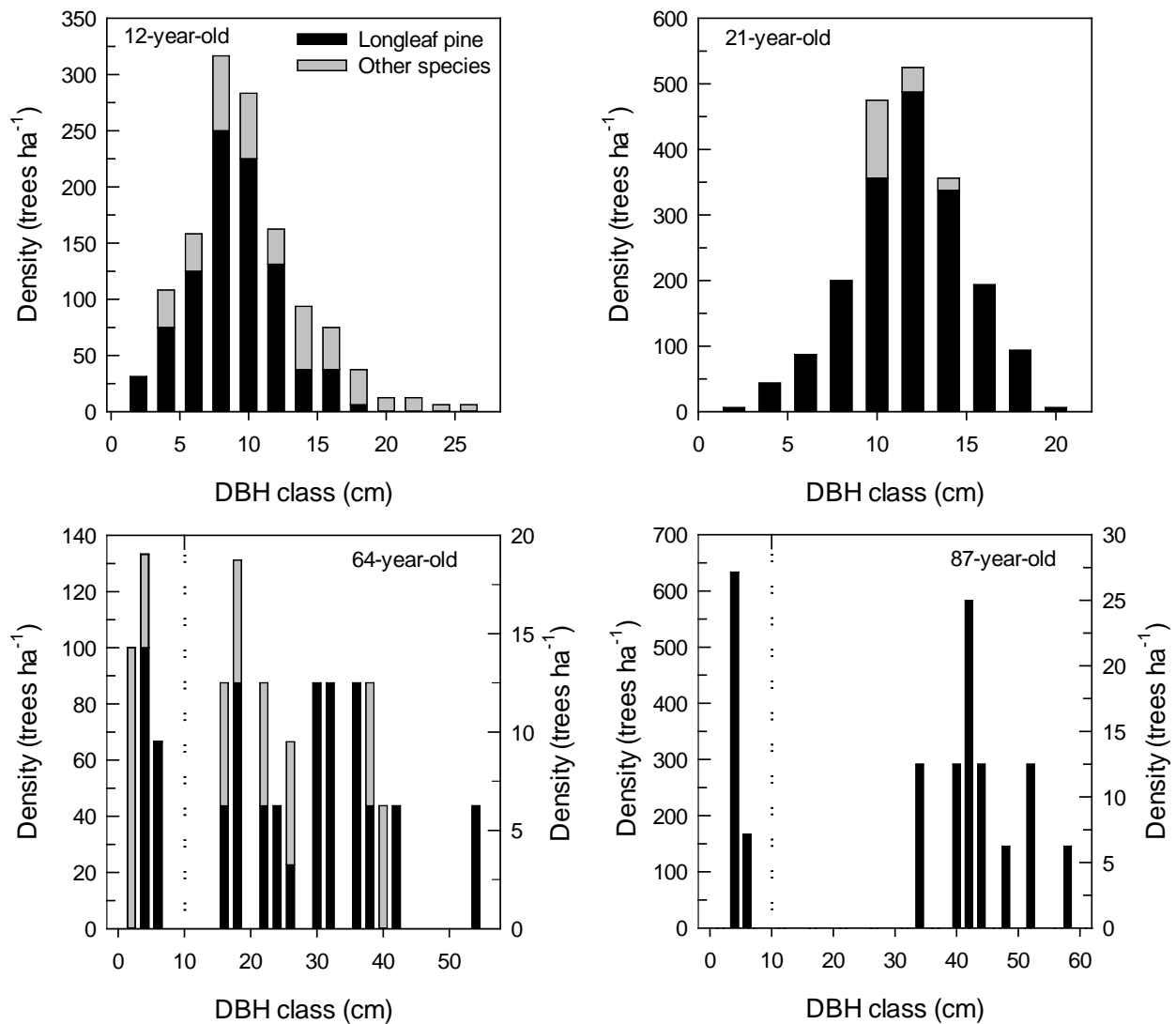
Figure 5.1. Density of trees by diameter class (DBH, diameter at breast height) for longleaf pine stands. For the 64 and 87-year-old stands, the right y-axis applies to all classes greater than 10 cm DBH.

Allometric models

The best models tested were linear relationships between natural log transformed biomass and the product of natural log transformed diameter squared and height. Because the models were logarithmic regressions, a correction ratio (ratio of the sample mean to the predicted values) was applied to correct for proportional BIAS (Snowdon 1991). Non-linear versions of the models were also evaluated, but resulted in no improvement in model performance (data not shown). For the combined stands, regressions for all longleaf pine tree components were highly significant ($P < 0.001$) with R^2 ranging from 0.91 to 0.99 (Table 5.4). Allometric relationships for 5-year-old trees were significant but model R^2 were lower, ranging from 0.84-0.96, most likely due to the smaller sample size and greater variability in tree size associated with bolting from the grass stage.

The model for aboveground biomass reported in this study produced BIAS and RMSE of -1.3% and 20.7 kg tree^{-1}, respectively. When applied to our data, the longleaf pine allometric equations from Taras and Clark (1977) for natural uneven-aged sawtimber in Alabama, Baldwin and Saucier (1983) for unthinned plantations in Texas and Louisiana, Gibson et al. (1985) for 25-year-old plantations in Louisiana, and Mitchell et al. (1999) for uneven-aged stands in Georgia produced larger BIAS (-18.8, -25.4, -28.9 and 28.3%, respectively) and larger RMSE (108.9, 145.0, 165.7 and 120.8 kg tree^{-1}, respectively). The equation of Mitchell et al. (1999) predicted negative aboveground biomass for trees with DBH of about 8 cm. The relationships between observed and predicted aboveground biomass using the five equations are shown in Figure 5.2. The model for below-stump biomass reported in this study produced BIAS and RMSE of 9.5% and 30.3 kg tree^{-1}, respectively. When applied to our data, the allometric equations from Gibson et al. (1985) produced smaller BIAS (-3.4%) but larger RMSE (35.2 kg tree^{-1}) (Figure 5.2).

Live plant C stocks

Carbon in longleaf pine trees was dominated by stem C followed by below-stump C (Figure 5.3). Foliage made up the least amount of within-tree C in all stands. Total live aboveground C ranged from 1.4 Mg C ha^{-1} in the 5-year-old stand to 78.4 Mg C ha^{-1} in the 87-year-old stand and in all stands except the youngest was dominated by wood plant C (Table 5.5). In the 5-year-old stand, the largest live aboveground C stock was ground cover C (Table 5.5, Figure 5.3).

Longleaf pine live below-stump C varied from 0.2 Mg C ha^{-1} in the youngest stand to 12.8 Mg C ha^{-1} in the 21-year-old stand (Table 5.5). Plot level measurements of lateral coarse root mass by GPR added from 2.2 to 7.1 Mg C ha^{-1}, depending on the stand (Table 5.5). Carbon allocated to fine roots added from 0.6 to 1.4 Mg C ha^{-1} to the total root C pool (Table 5.5). Pine fine root C was linearly related to pine basal area (Figure 5.4). A nonlinear regression between all fine roots and total basal area provided the best fit for all fine roots combined.

A non-linear relationship between live plant aboveground C and belowground C was observed (Figure 5.5). In both functions, which included a minimum or maximum estimate of lateral coarse root C from GPR, proportionally less total root C was observed with higher aboveground C.
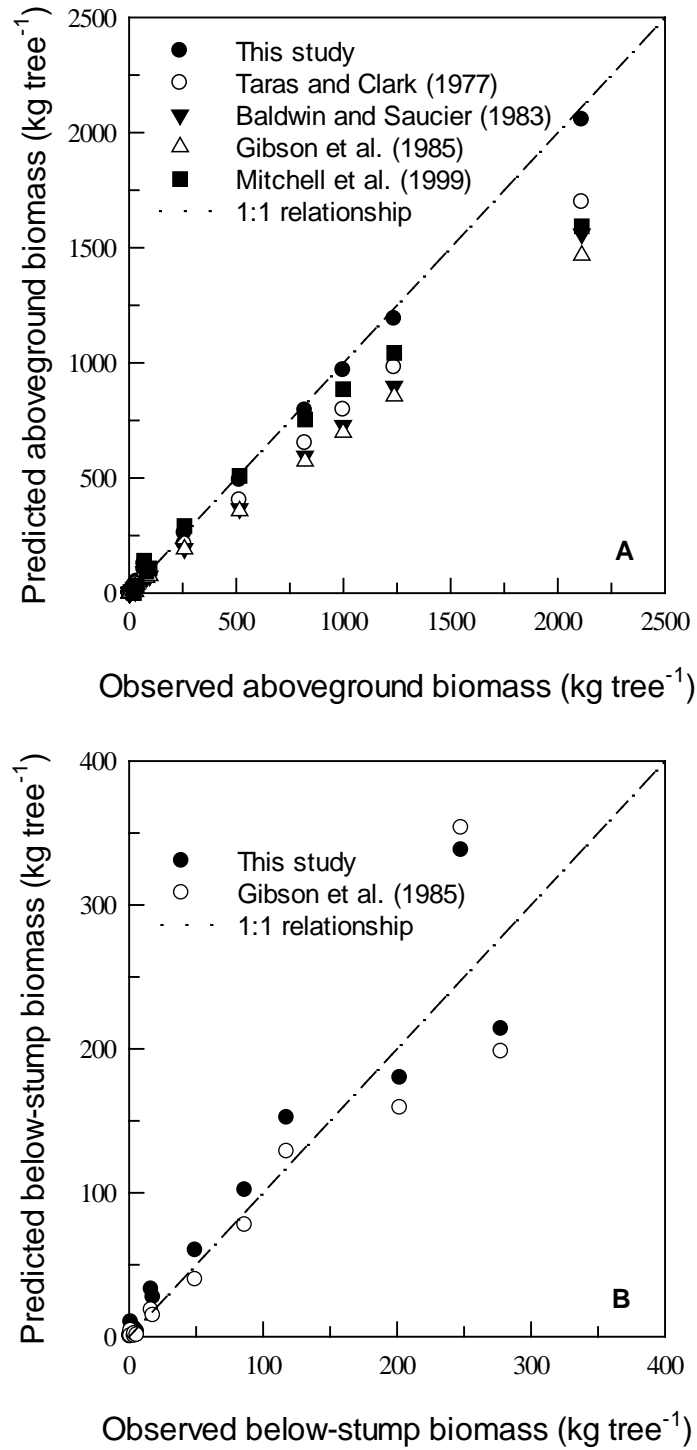
Figure 5.2. Observed versus predicted aboveground (A) and belowground (B) biomass using equations from this study and from other longleaf pine studies. The broken line represents the 1:1 relationship.

Table 5.3. Structure of sampled longleaf pine stands.

Stand age (years)	Size class (cm)	Species	Basal area ($m^2\,ha^{-1}$)	Density (trees ha^{-1})	DBH (cm)	Height (m)
5	DBH ≥ 10	LLP	0.0	0.0	-	-
		Other	0.0	0.0	-	-
	DBH <10	LLP	0.4	150	3.7	2.4
		Other	0.04	64	2.6	2.7
	Understory	LLP	-	625	-	<2
		Other	-	1,000	-	<2
12	DBH ≥ 10	LLP	3.4	300	12.3	9.1
		Other	4.4	219	15.6	10.5
	DBH <10	LLP	2.7	619	7.2	6.2
		Other	0.6	159	6.8	5.7
	Understory	LLP	-	625	-	<2
		Other	-	1,000	-	<2
21	DBH ≥ 10	LLP	18.6	1331	13.2	11.8
		Other	0.8	75	11.9	9.4
	DBH <10	LLP	2.3	481	7.6	8.7
		Other	0.6	95	9.3	8.0
	Understory	LLP	-	625	-	<2
		Other	-	1,000	-	<2
64	DBH ≥ 10	LLP	7.5	94	30.2	19.1
		Other	2.4	37	26.7	16.8
	DBH <10	LLP	0.3	159	4.8	3.3
		Other	0.05	127	2.2	2.3
	Understory	LLP	-	625	-	<2
		Other	-	1,000	-	<2
87	DBH ≥ 10	LLP	13.4	87	43.7	29.0
		Other	0.0	0.0	-	-
	DBH <10	LLP	1.1	764	4.1	3.8
		Other	0.0	0.0	-	-
	Understory	LLP	-	625	-	<2
		Other	-	1,000	-	<2

Notes for Table 5.3: Values are means of 4 subplots per stand. The two oldest stands were naturally regenerated and the others were planted. DBH, diameter at breast height; LLP, longleaf pine. The < 10 cm DBH class included only stems ≥1 cm DBH and ≥ 2 m in height. Understory is all woody plants from ≥1 to < 2 m in height. The 5-year-old stand understory also includes all planted longleaf < 2 m height.
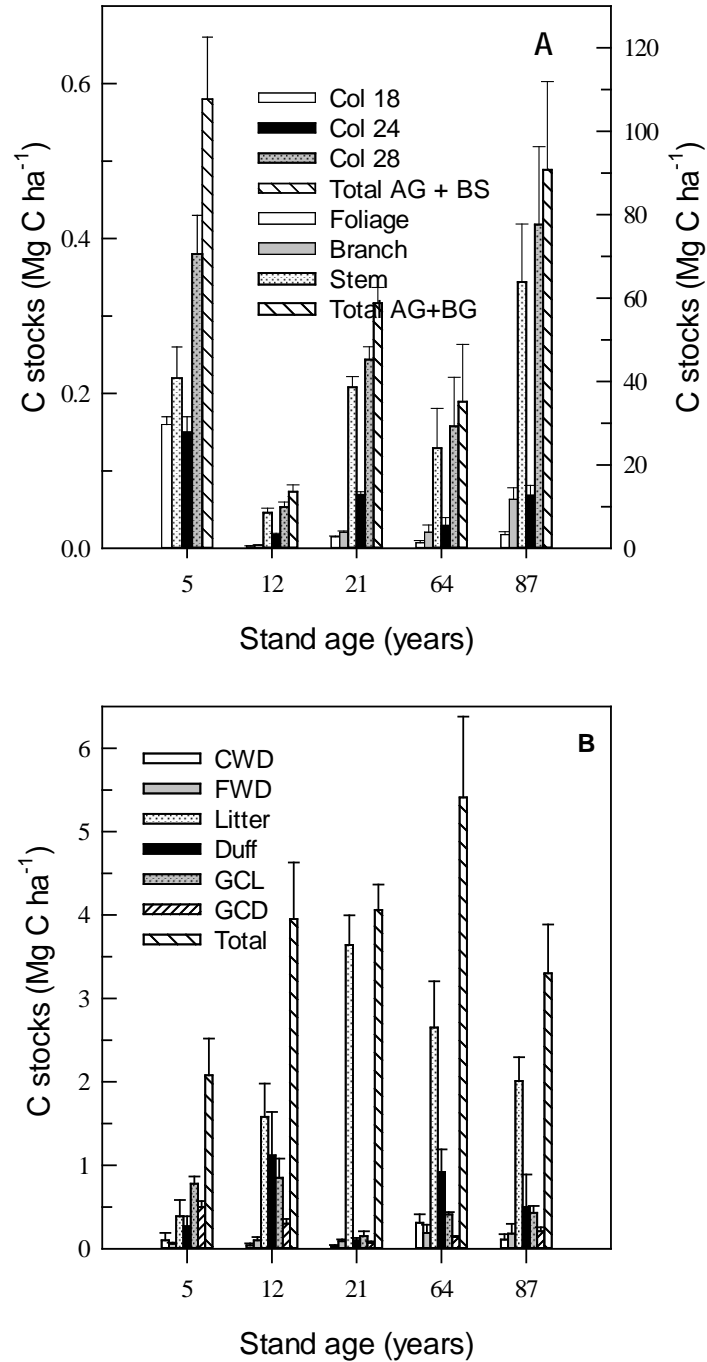
Figure 5.3. Carbon stocks in longleaf pine trees predicted using allometric equations developed from trees harvested from all stands (A) and C stocks in the forest floor and ground cover layer (B). For longleaf pine C stocks (A), the left y-axis applies to the 5-year-old stand and the right y-axis refers to all other stands. Values are means ± SEs. AG, aboveground; BS, Below-stump; CWD, coarse woody debris;, FWD, fine woody debris; GC$_L$, live ground cover; GC$_D$, dead ground cover.

33
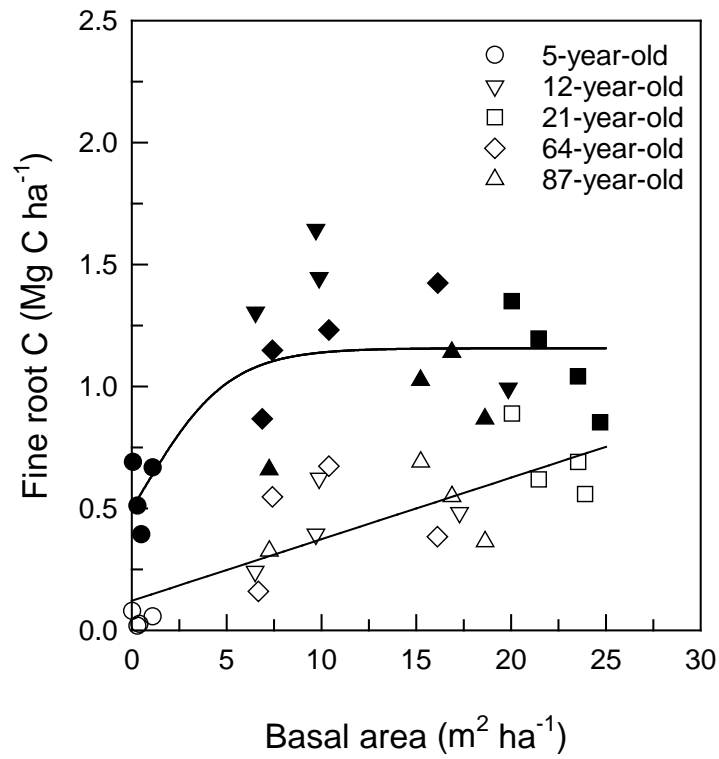
Figure 5.4. Relationship between pine-only fine root C or total fine root (all species) C and pine or total basal area in longleaf pine stands. Open symbols represent pine fine roots and solid symbols represent fine roots of all species. The linear equation for pine fine root C was $y = 0.122 + 0.025x$, $R^2 = 0.63$, $P < 0.001$, where x is pine basal area. The nonlinear equation for all fine root C was $y = 1.16/(1 + e^{(-((x-0.62)/2.24))})$, $R^2 = 0.50$, $P = 0.003$, where x is total basal area. Each point represents a subplot average.
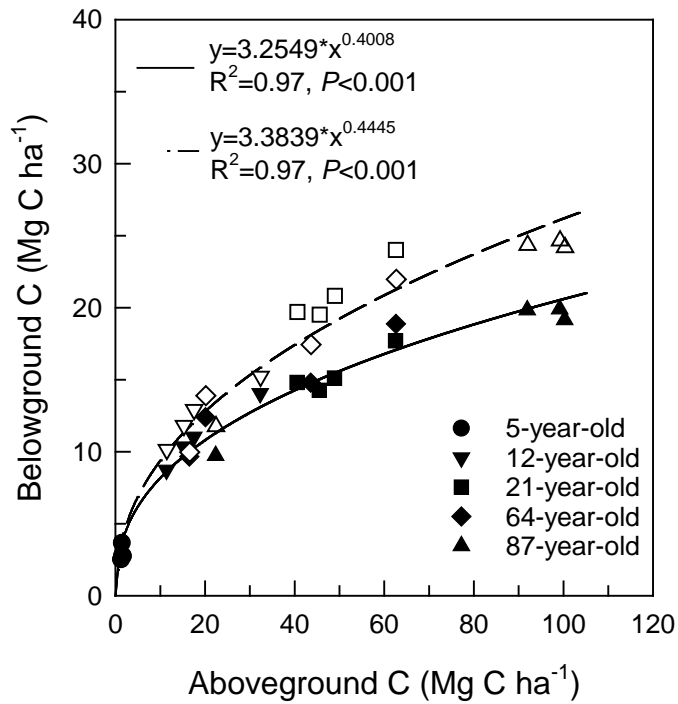
Figure 5.5. Relationship between total live aboveground and belowground (below-stump + GPR lateral coarse roots + fine roots) C stocks in longleaf pine stands. The two lines indicate the maximum (dashed line, open symbols) and minimum (solid line, closed symbols) belowground C based on calculation of GPR lateral root C.

Table 5.4. Regression equations between dry weight biomass and tree size for longleaf pine trees.

Stand age (years)	Dependent variable	n	B_0 (SE)	B_1 (SE)	CF	MSE	$P > F$	R^2
5	Foliage	10	-3.355±0.31	0.653 ±0.08	0.005	0.06	<0.001	0.89
	Branch	-	-	-	-	-	-	-
	Stem	10	-5.009 ±0.31	1.136 ±0.08	0.027	0.06	<0.001	0.96
	Total AG	10	-3.566 ±0.30	0.923 ±0.08	0.015	0.06	<0.001	0.94
	Below-stump	5	-4.267 ±0.83	0.879 ±0.22	0.025	0.24	0.027	0.84
12-87 pooled	Foliage	26	-5.403 ±0.30	0.888 ±0.04	-0.085	0.27	<0.001	0.95
	Branch	26	-7.319 ±0.26	1.176 ±0.04	-0.054	0.21	<0.001	0.98
	Stem	26	-3.730 ±0.16	0.991 ±0.02	0.074	0.08	<0.001	0.99
	Total AG	26	-3.571 ±0.15	0.997 ±0.02	0.058	0.07	<0.001	0.99
	Below-stump	16	-3.730 ±0.47	0.837 ±0.06	0.200	0.36	<0.001	0.93
	Lateral roots	16	-4.164±0.46	0.763±0.06	0.027	0.34	<0.001	0.93
	Tap root1	16	-4.706 ±0.38	0.911 ±0.05	0.001	0.23	<0.001	0.96
	Tap root2	16	-4.404±0.59	2.38±0.19	0.001	0.68	<0.001	0.91

Notes for Table 5.4: With the exception of Tap root2, the regressions were of the form: lnbiomass = CF + B_0 + $B_1 ln$(DBH^2*H) where CF is a correction factor. Ground line diameter (GLD) was used in regressions for the 5-year-old stand. Mass was measured in kg per tree; diameter at breast height (DBH) and GLD were measured in centimeters and height (H) was measured in meters. AG= aboveground biomass. Below-stump is tap root mass plus lateral coarse root ($\geq$5 mm diameter) mass within the excavation pit area. Lateral roots are roots $\geq$ 5 mm in diameter in the excavation pit area and not including tap roots. Tap root regression of the form lnbiomass = CF + B_0 + $B_1 ln$(GLD).

Table 5.5. Forest carbon stocks in longleaf pine stands.

Forest C Stock	Stand age (years)				
	5	12	21	64	87
Live aboveground	--------------------------------Mg C ha^{-1}--------------------------------				
LLP					
Overstory	0.17±0.06	9.90±1.22	45.28±3.04	29.27±11.76	77.45±18.86
Understory	0.21±0.02	0.0±0.0	0.0±0.0	0.0±0.0	0.18±0.18
Other woody species					
Overstory	0.01±0.01	8.00±5.51	3.90±1.80	5.42±2.26	0.0±0.0
Understory	0.23±0.17	0.33±0.13	0.005±0.005	0.58±0.35	0.36±0.21
Ground Cover	0.78±0.04	0.85±0.23	0.15±0.06	0.41±0.03	0.43±0.08
Live aboveground total	1.41±0.09	19.08±4.57	49.33±4.71	35.68±10.79	78.42±18.78
Live belowground[‖]					
LLP below-stump	0.15±0.02	3.25±0.36	12.83±0.76	5.45±1.94	12.66±2.43
Other pine tap root	0.0±0.0	1.30±0.93	0.37±0.07	1.12±0.52	0.0±0.0
Coarse roots (GPR)	2.22±0.19	5.89±0.43	3.94±0.47	7.14±0.51	5.62±0.48
Fine roots pine	0.05±0.01	0.44±0.08	0.69±0.07	0.44±0.11	0.46±0.07
Fine roots non-pine	0.52±0.06	0.91±0.16	0.42±0.06	0.73±0.11	0.46±0.06
Live belowground total	2.94±0.25	11.79±1.09	18.25±0.90	14.88±2.25	19.20±2.82
Dead organic matter					
Snags	0.0±0.0	0.06±0.05	0.27±0.18	0.73±0.73	0.0±0.0
CWD	0.11±0.09	0.04±0.02	0.03±0.01	0.31±0.10	0.11±0.06
FWD	0.06±0.01	0.10±0.04	0.09±0.02	0.19±0.10	0.18±0.12
Litter	0.39±0.19	1.58±0.40	3.64±0.36	2.65±0.55	2.01±0.29
Duff	0.27±0.12	1.12±0.52	0.10±0.03	0.93±0.27	0.50±0.39
Residual tap root	4.92±0.14	0.0±0.0	<0.001±<0.01	0.001±0.001	0.0±0.0
Dead organic matter total	6.25±0.46	3.19±0.90	4.261±0.45	4.95±0.55	3.00±0.63
Soil (1 m depth)	61.01±5.16	75.99±9.13	52.86±5.30	85.91±8.30	84.82±4.09
Ecosystem total	71.61±5.25	110.06±15.45	124.65±10.36	141.4±5.63	185.44±19.26

Notes for Table 5.5: Values are means ± SEs. CWD, coarse woody debris; FWD, fine woody debris; GPR, ground penetrating radar; LLP, longleaf pine. Overstory includes all trees ≥ 2 m height. †Understory includes all stems ≥ 1 and < 2 m height. The understory of the 5-year-old stand also includes all planted pine < 2 m in height. Ground cover is all plants < 1 m in height. Below-stump is tap root plus lateral coarse roots (≥5 mm diameter) in the excavation pit area. Coarse roots (GPR) is lateral coarse roots (≥ 2 mm in diameter) (no tap root) measured by GPR and an average of values assuming GPR accounted for all or none of the lateral coarse roots in the excavation pit area. Fine roots are < 2 mm in diameter. Residual tap root in the 5-year-old stand was from the previous stand harvested before planting and in the 21 and 64-year-old stands from pine snags recently dead. Residual tap root C for old stumps was not determined in stands older than 5 years of age.

Detritus and soil C

A total of 3 snags >10 cm DBH were tallied: 2 longleaf pine trees in the 21-year-old stand and 1 non-pine tree in the 64-year-old stand. Using allometric equations for longleaf pine and other species (see other species allometry described previously) and the tap root function in this paper and assuming no decay, snag C was 0.3 Mg C ha^{-1} and 0.7 Mg C ha^{-1} in the 21 and 64-year-old stand, respectively. In the 5-year-old stand, residual tap root C was the highest dead organic matter stock at 4.9 Mg Cha^{-1} (±25% boundary of 4.2 and 5.9 Mg C ha^{-1}).   In stands older than 5 years, the second largest aboveground C stock after woody plant C was litter C, which ranged from 1.6 Mg C ha^{-1} in the 12-year-old stand to 3.6 Mg C ha^{-1} in the 21-year-old stand (Table 5.5, Figure 5.3). The combined CWD and FWD pool contributed less than 1 Mg C·ha^{-1} in all stands and duff contributed 0.1 to 1.1 Mg C ha^{-1}. Total dead organic matter C ranged from 3.0 Mg C ha^{-1} in the oldest stand to 6.2 Mg C ha^{-1} in the 5-year-old stand. The range in soil C to a 1 m depth was from 52.9 Mg C ha^{-1} in the 21-year-old stand to 85.9 Mg C ha^{-1} in the 64-year-old stand (Table 5.5).

Ecosystem C stocks

The sum of all C stocks varied from 71.6 to 185.4 Mg C ha^{-1} (Table 5.5). From 42% to 85% of ecosystem C was in soil C, depending mainly on the contribution of woody plant C. Live woody plant C exceeded soil C (1 m depth) in the 21 and 87-year-old stands.

Discussion

The inclusion of height in longleaf pine allometric equations has been shown to better predict biomass accumulation in longleaf pine than DBH alone (Taras and Clark 1977; Baldwin and Saucier 1983) and this was the case for longleaf pine in this study. The 12-year-old and 64-year-old stands had similar basal area in longleaf pine but carbon stored in aboveground biomass of longleaf pine was 66% higher in the 64-year-old stand, because of greater tree height. Chojnacky et al. (2014) recently updated generalized biomass equations for North American trees and used a modified equation similar to Taras and Clark (1977) for longleaf pine, which would underestimate biomass in our stands. Comparisons of our allometric models with other reported functions suggest that local models that take into account local site effects and management history may be needed,

in the absence of general models that account for differences in stand structural development, climate and soils within the expansive range of longleaf pine.

Aboveground C stocks were dominated by live woody plant C in all stands except the youngest, in which C in the ground cover layer and in residual tap roots exceeded live woody plant C. Assessment of non-woody C stocks indicated that litter C greatly exceeded all other non-woody C pools in stands greater than 12 years of age and was highest in the 21-year-old stand, most likely because of the denser spacing and a high leaf area index. Litter and duff C pools are counted in some forest project protocols (www.climateactionreserve.org) and used in predicting first order fire effects (Reinhardt 2003), and although relatively small C pools in regularly burned longleaf pine forests, litter and duff influence soil C flux (Samuelson and Whitaker 2012) and plant diversity in the ground cover layer (Hiers et al. 2007).

Live woody plant C in longleaf pine was within the range reported for other southern pines when comparisons were made with stands of similar structure. For example, 28.5 Mg C ha^{-1} was reported for woody aboveground C in an even-aged, naturally regenerated 50-year-old longleaf pine stand in southern Alabama with 8 m^2 ha^{-1} basal area (Samuelson and Whitaker 2012), which is similar to the 64-year-old stand. In 18-year-old slash pine (*Pinus elliottii* Engelm.), basal area (21.0 m^2 ha^{-1}) and aboveground woody plant C (48 Mg C ha^{-1}) (Gholz and Fisher 1982) were similar to the 21-year-old longleaf pine stand. Maximum aboveground C accumulation in longleaf pine trees was 78 Mg C ha^{-1} in the 87-year-old stand. Lichstein et al. (2009) developed regional biomass chronosequences for many U.S. tree species and projected average stem biomass accumulation of 63 Mg C ha^{-1} in longleaf pine stands over 100 years. Similar biomass trajectories were projected for lodgepole pine (*Pinus contorta* Dougl. ex Loud var. *latifolia* Engelm.) and ponderosa pine (*Pinus ponderosa* Doug. ex Laws var. *scopulorum* Engelm.) (Lichstein et al. 2009). Both species possess a lifespan similar to longleaf pine and are associated with fire-frequent environments.

Lateral roots of longleaf pine are usually located in the upper 20 cm of soil, are commonly intermixed with roots of nearby trees and can extend considerable distances from their source (Hodgkins and Nichols, 1977). Hodgkins and Nichols (1977) found that longleaf pine lateral root length and spread was related to tree age and competitive position; lateral root spread averaged 5 m for dominant trees in a closed canopy, 7.4 m on edges and 9.3 m for isolated trees aged 30-33 years in southwest Alabama. In the present study, combining allometric equations to capture below-stump biomass with plot level lateral coarse root biomass estimates with GPR provided a more comprehensive estimate of total belowground biomass. This was particularly relevant in accounting for root mass in the gaps in the 64-year-old stand with low basal area. Considering the tendency for longleaf pine roots to spread widely, it is likely that roots have entered from outside the measurement plots as well as the reverse. Since the subplots were located on contiguous areas with the same stand history and density, the quantity of roots leaving and entering plots should be similar.

Surface-based GPR excels in detecting lateral roots, but is unable to delineate the mass of roots directly beneath a tree. In longleaf pine, tap roots and vertical sinker roots adjacent to trees comprise much of the belowground biomass and were not detected by GPR. In older stands where large diameter lateral roots overlap or are near the tap root, root mass may be underestimated. This

left some uncertainty as to the area in which GPR was capable of detecting all lateral roots. Presenting the maximum (all lateral roots near tree detected) and minimum (no lateral roots near tree detected) ability of GPR to detect lateral root mass around trees in the pit areas constrains this uncertainty: at maximum aboveground C (100 Mg C ha^{-1}) belowground C varied 20%.

Fine root C was a relatively small contribution to total root C, but high fine root turnover rates, estimated to range from one to three times standing biomass per year (West et al. 2004), make the fine root C pool a dynamic component in longleaf pine dominated ecosystems (Hendricks et al. 2006). While total basal area was dominated by overstory longleaf pine, on all but the 21-year-old stand non-pine fine roots (hardwoods, shrubs, herbaceous plants) comprised half or more of the fine root C pool. Pine fine root C ranged from 0.05 to 0.69 Mg C ha^{-1} across all sites and is in agreement with values of 0.20 to 0.65 Mg C ha^{-1} (calculated from standing biomass assuming 42% C content) reported by Carter et al. (2004) and Hendricks et al. (2006) for longleaf pine sites near Newton, Georgia. Separating fine roots into pine and non-pine classes revealed a linear relationship between pine fine roots and pine basal area, but the nonlinear relationship between total fine root C and total basal area indicates full site occupancy of fine roots at approximately 8 m^2 ha^{-1} basal area. Samuelson and Whitaker (2012) report a similar range in total fine root C, from 0.8 to 1.4 Mg C ha^{-1}, and no relationship between fine root mass and basal areas greater than 7 m^2 ha^{-1} in 50-year-old naturally regenerated longleaf pine stands.

In carbon accounting, belowground biomass is often predicted from a general root to shoot ratio such as 0.20 for softwood forests (Birdsey 1992; Brown et al. 1993). The belowground to aboveground C ratio was 0.20 or 0.25 in the 87-year-old stand, depending on how GPR lateral coarse root mass was calculated. Gholz and Fisher (1982) determined that the proportion of total coarse root mass to total aboveground wood mass generally decreased with increasing aboveground biomass in slash pine. For young loblolly pine plantations (7-18 years) with varying basal areas, total coarse root mass was 50% of stem mass (Albaugh et al. 2006). However, Van Lear and Kepeluck (1995) reported a coarse root to stem ratio of 0.30 for 48-year-old loblolly pine with average aboveground biomass of 144 Mg ha^{-1}. In the 5-year-old stand, live root C exceeded live aboveground C, but in other stands the relationship between belowground and aboveground C was not wholly dependent on stand age, as some subplots in older stands had low aboveground C. Given that tree age and size, stand density, soil conditions and management influence root to shoot ratios (King at al. 2007, Litton et al. 2003), it is difficult to separate age differences from variation in stand structure and site conditions. Longleaf pine has been purported to invest proportionately more growth in belowground root mass than other southern conifers due to the presence of a grass stage and enhanced early tap root development. However, Gibson et al. (1985) found no differences in belowground biomass allocation between 25-year-old longleaf pine compared to the same age loblolly pine and slash pine growing on the same sites.

Across all sites, soil C (measured down to 1 m) averaged 72 Mg C ha^{-1} and soil C dropped precipitously with depth (data not shown) on all sites. Although stand age could not be compared statistically, soil C represented the greatest ecosystem C stock in the 5, 12, and 64-year-old stands and was almost equal to total plant C pools in the 87-year-old stand. The anomaly occurred in the 21-year-old stand where soil C represented 42% of the total ecosystem C. Thus, no general trend in increasing soil C with stand age was observed, and soil C was likely more related to land use

history and soil type than stand age. Markewitz et al. (2002) reported no difference in soil C content on sandy soils up to 14 years after afforestation with longleaf pine on marginal agricultural lands on a 2-3 year fire interval, and soil C to a 50 cm depth was on average 23 Mg C ha^{-1} in plantations versus 42 Mg C ha^{-1} in natural longleaf pine stands that were never tilled. Butnor et al. (2012b) reported 60 Mg C ha^{-1} soil C (down to 30 cm) for coarse loamy soils in 50-year-old longleaf pine stands in Mississippi planted after clear-cutting a mature longleaf pine stand and regularly burned. Mean soil C (to a 1 m depth) reported by (Heath et al. 2001) for the longleaf- slash pine forest type group was 166 Mg C ha^{-1} and for the loblolly-shortleaf (*Pinus echinata* Mill.) forest type 75 Mg C ha^{-1}. Thus, soil C in longleaf pine stands in our study is comparable to other reports for southern pines.

In summary, ecosystem stocks excluding soil C ranged from 10.6 Mg C ha^{-1} to 100.6 Mg C ha^{-1} and including soil C ranged from 71.6 Mg C ha^{-1} to 185.4 Mg C ha^{-1}. Carbon accumulation in longleaf pine stands was similar to other *Pinus* ecosystems when comparisons were made to stands with similar structure. As observed for a lodgepole pine chronosequence, in which average maximum total ecosystem C (150 Mg C ha^{-1}) was attained at age 70 years, total ecosystem C was driven by live biomass C, related to stand basal area and density in addition to age, and soil C (Kashian et al. 2013). Although limited to one geographic area and pure, even-aged stands, the work reported here is the first comprehensive measurement of above and belowground C pools in longleaf pine forests across a range of stand ages and structures, site conditions and management histories. The U.S. Department of Agriculture Forest Service Forest Inventory and Analysis (FIA) database indicates approximately 1 million ha in natural longleaf pine forest with the majority (88%) less than 80 years in age and 0.4 million ha in plantation longleaf pine with 77% in the 0-20 year age class (Woudenberg et al. 2010). Therefore, this work is applicable to present-day and future longleaf pine forests. These results were combined with new C stock data collected at an additional three installations and combined with results from the next Chapter 6, used to assess ecosystem C stock across the range in Chapter 7.

6. The Use of Ground Penetrating Radar in the Assessment of Longleaf Pine Root Carbon Stocks

[Contents of this chapter were extracted from Butnor, J.R., L.J. Samuelson, T.A. Stokes, K.H. Johnsen, P.H. Anderson, and C.A. Gonzalez-Benecke. 2016. Surface-based GPR underestimates below-stump root biomass. Plant and Soil 402: 47-62]

Introduction

Roots are an important C stock in forest ecosystems and knowledge of root biomass is critical for accurate estimation of ecosystem C in longleaf pine forests. The most common way to estimate allocation to roots on a whole tree or stand-level is through the development and application of allometric relationships, where easily measured parameters such as tree diameter and height are related to difficult to measure parameters such as: stem, branch, foliar, below-stump, tap root, or lateral root biomass (Ter-Mikaelian and Korzukhin 1997, Drexhage and Colin 2001; Jenkins et al. 2003). Allometric equations are indispensable for modeling forest production and carbon allocation, though they may be site specific and, contingent on climate, soil drainage, or available nutrients and stand structure; however, such equations may also be modified by factors such as latitude, stand basal area and density, and site index (Gonzalez-Benecke et al. 2014a). Because it is difficult to conduct complete belowground harvests of a single tree with multiple nearby neighbors and overlapping lateral root systems, predefined pits or pits proportion to tree size are excavated at the base of the tree to capture the bulk of roots (Retzlaff et al. 2001; Samuelson et al. 2004; Albaugh et al. 2006; Samuelson et al. 2014). These allometric relationships do not account for roots beyond the excavation pit, which can be a significant omission in forests with widely dispersed individuals exploiting resources unevenly in large open gaps or competing with different size trees. Despite lower density, extensive roots are critical for accessing water and nutrient resources further from the tree (Stone and Kalisz 1991). For example, in mature longleaf pine (*Pinus palustris* Mill.) forests, roots have been reported to extend up to 9.3 m from the stem with total root lengths up to 12.2 m (Hodgkins and Nichols 1977), thus other approaches to augment models based on pit excavation are required.

For the past 15 years, ground penetrating radar (GPR) operated in frequencies between 400 and 2600 MHz has been evaluated and used as a tool to augment or replace destructive belowground sampling of lateral roots (Hruska et al. 1999; Butnor et al. 2001; Butnor et al. 2003; Barton and Montagu 2004; Stover et al. 2007; Butnor et al. 2012a; Guo et al. 2013a). To collect such data, a GPR antenna comprised of an electromagnetic transmitter and receiver is pulled along a transect propagating electromagnetic waves into the soil at specific intervals (usually 100-200 per m) and the receiver precisely records the time of arrival and amplitude of energy that reflects off of buried objects and returns to the surface (A-scan). With knowledge of soil dielectric properties, the A-scans may be combined to form a two-dimensional profile (distance X depth) to create a radagram (B-scan), showing hyperbolic reflections from roots at given depths and relative amplitude along a transect (Figure 6.1). Approaches that use signal amplitude and image analysis processing can be used to rapidly quantify GPR data and relate high amplitude area (number of pixels above an amplitude threshold) to total coarse root mass and be used to create root biomass maps. High amplitude area is calibrated using soil cores or small excavations, so that excavated coarse root

mass and area on an image file above some threshold may be correlated (Butnor et al. 2001; Butnor et al. 2003; Cox et al. 2005; Stover et al. 2007; Dannoura et al. 2008; Butnor et al. 2012a; Day et al. 2013; Guo et al. 2013b; Borden et al. 2014). Other approaches that use waveform (A-scan) geometry are able to extract data from individual or stacked waveforms to calculate root depth, diameter or make estimates of biomass from root
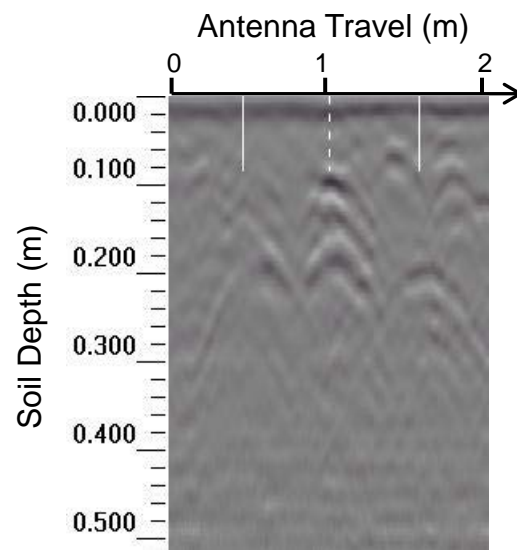
Figure 6.1. Sample radargram (B-scan) from a 25 year-old stand longleaf pine stand in North Carolina. Numerous longleaf pine roots were detected and appear as hyperbolic reflections. At a distance of 1 m (dashed line), a 15 cm diameter soil corer was used to verify coarse root mass to a depth of 0.5 m. Total dry coarse root mass of the core was 61.2 g with two larger roots (1.1 and 4.3 cm diameter) recovered between soil depths of 10 and 20 cm.

diameter (Barton and Montagu 2004; Dannoura et al. 2008; Hirano et al. 2009; Cui et al. 2011; Guo et al. 2013b). Root mapping may be achieved by algorithms that predict which roots are continuous or separate between adjacent scans. There have been many recent advances in geometric data interpretation, though the post-collection processing is still operator intensive and is often difficult to automate without some user guidance (Butnor et al. 2012a; Guo et al. 2013a).

For GPR root surveys to be successful they need to be conducted on suitable soils that are not prone to signal attenuation (Doolittle et al. 2007). Sandy soils with low dielectric values are ideal, while high clay, haline or wet soils are unsuited (Butnor et al. 2001; Daniels 2004; Doolittle et al. 2007). Variation in root water content (Hirano et al. 2009; Guo et al. 2013b) and root orientation relative to antenna travel may also limit accurate detection of root parameters (Tanikawa et al. 2013; Guo et al. 2015). Recently, Guo et al. (2015) proposed a novel method to correct for the effect of cross angle on amplitude area of a root reflection. As methods of GPR root surveys

advance, it is important to recognize and mitigate other limitations of surface-based antennas. The soil volume directly beneath and adjacent to a tree is a problematic environment for root detection with surface-based GPR antennas operated in reflection mode, as vertical root detection is limited. Roots need to be located belowground, not protruding the soil surface and covered with only some minimum amount of soil to detect single or multiple reflections of electromagnetic waves from the soil/root interfaces. The most readily interpretable, hyperbolic root reflections come from lateral roots crossed at 90 degrees by a GPR antenna, with adequate soil volume above and below the root (Butnor et al. 2001; Barton and Montagu 2004; Tanikawa et al. 2013; Guo et al. 2015). Even if a tap root were cut below the soil surface and covered with soil, its location and basal area would be detected, but its vertical extension into the soil profile would not. Large overlapping lateral roots originating from vertically orientated tap root would also be difficult to detect due to interference from reflections from the first root, closest to the surface. Based on past field observations, it was expected that GPR would underestimate below-stump (tap root + lateral) root mass of trees that develop tap roots, though the magnitude of the underestimation is unknown. The issue of partial detection of below-stump root mass was raised by Samuelson et al. (2014) working with mature longleaf pine. While integrating below-stump biomass data from longleaf pine pit excavations with lateral root data from GPR, the lack of insight into where the two methods overlap lead to the consideration and averaging of two options. It was assumed that tap roots were undetectable and either: 1) estimated total root mass = GPR root + excavated tap root or 2) estimated total root mass = GPR root + excavated tap root + excavated lateral root (Samuelson et al. 2014). The logic being that GPR detected all lateral roots adjacent to trees (1) or GPR detected none of the lateral roots adjacent to trees (2). If GPR detected all of the lateral roots adjacent to trees there would be overlap with pit excavations. This led to considerable uncertainty, as the bounds of these two scenarios were rather wide (Samuelson et al 2014). For the purpose of belowground biomass accounting the average of the two detection scenarios was used, since there were no direct comparisons between GPR and pit excavations to guide the calculation. This need not detract from the usefulness of GPR for detecting coarse lateral roots, but is an important complexity to consider when scaling these values to the level of a forest stand, since using GPR data alone could greatly underestimate belowground biomass of trees. Preliminary reports of cross-hole tomography with borehole radar are promising, but have not materialized as a practical approach or had the necessary research and development for application of the technology (Butnor et al. 2006; Butnor et al. 2012a).

We compared root mass estimated with GPR (1500 MHz) in a defined area at base of 33 longleaf pine trees ranging in DBH from 4.0 to 54.3 cm with excavated root mass to determine if tree size effects accuracy of root detection under field conditions. While it has been assumed that tap roots are not detectable with surface-based GPR, the detectability of lateral roots proximal to trees had not been quantified. Information on root detectability near trees is needed to better integrate whole tree biomass harvests with extensive GPR surveys further away from trees. This is particularly important for species that develop large tap roots (e.g. *Pinus* sp.) or have large overlapping lateral roots originating from the vertically orientated tap root. Once the relationship between tree size (DBH) and root detection was established for longleaf pine, it was applied to correct stand-level root mass estimates from 20 longleaf plots (Samuelson et al. 2014).

Materials and Methods

Study sites

The locations selected for study represent the east-west range of longleaf pine from Marine Corps Base Camp Lejeune, near Jacksonville, North Carolina on the Atlantic coast to the Kisatchie National Forest, near Leesville, in west-central Louisiana. A total of eight even-aged stands ranging in age from 8 to 83 years old were selected on soils suitable for GPR surveys (Table 6.2). The Louisiana soils were sandy loams and sandy clay loams that were suited to shallow surveys in the upper 50 cm above heavy clay horizons, while the coarse sands in the North Carolina were ideal for GPR (Doolittle et al. 2007). Within the eight stands, a wide variety of tree sizes were selected; DBH ranged from 4.0 to 54.3 cm and tree heights ranged from 2.3 to 30.4 m (Table 6.2).

Calibration of GPR with soil cores

At each stand, a set of 1 cm diameter aluminum rods were driven horizontally into undisturbed soil at depths of 10, 20, 30, 40 cm via an access trench (subsequently re-filled) in order to estimate soil dielectric value using a SIR-3000 radar unit (Geophysical Survey Systems Inc., Nashua, NH, USA) connected to a 1500 MHz antenna. The dielectric value varies with soil mineralogy and moisture content and was used to scale two-way travel time of reflected energy to predicted depth. Stand specific dielectric and range values are listed in Table 6.2. All GPR data were collected at 140 scans per m, 512 samples per scan, and 16 bits per sample with FIR (boxcar) collection filter and gain settings of -20, 15, 30. To directly compare image-based GPR indices with root biomass, a total of 25 locations in each stand were carefully marked, scanned with the 1500 MHz antenna and a 15 cm diameter core was used to collect roots to a depth of 50 cm. Within each stand, a subsample point was located at the center and three additional subsample points were located 35 m distant at 0, 120, 240 degrees from north following the protocol of Law et al. (2008). Soil cores were located 2 m away from each subsample point at 0, 90, 180, 270 degrees from north. The 16 cores (4 cores X 4 subplots) were chosen without regard to tree proximity, giving them similar distribution attributes to random soil core samples i.e. many soil cores with low to moderate root contents, very few with large root content. To develop regressions that relate GPR observations to biomass it was necessary to populate the calibration data with a full range of root biomass from low to high rather than to obtain a normal distribution which would not be achieved without a very large sample. An additional 9 cores were located by surveying for areas of low and high root mass a priori with GPR. In this manner, an additional 3 low root mass and 6 high root mass "radar-guided" core locations were selected. Roots were washed free of soil, classified as live or dead and separated into size classes (<2 mm, 2-10 mm, >10 mm. Roots were dried to constant mass at 65° C and weighed.

Table 6.1. Descriptive site and study tree parameters for the eight longleaf pine stands where GPR coarse root mass surveys were compared to excavation.

Year sampled	Location & stand age (years)	Origin	Soil texture	n	Mean DBH (cm)	DBH range (cm)	Mean height (m)	Height range (m)	Mean pit area (m^2)
	Louisiana								
2013	8	Planted	sandy loam	5	7.0	4.0 - 11.2	5.1	2.3 - 11.2	1.04
2013	18	Planted	sandy loam	4	12.8	4.6 - 23.4	9.8	4.4 - 13.2	1.20
2013	34	Planted	sandy clay loam	5	21.8	11.0 - 33.3	17.8	14.6 - 22.1	1.53
2013	60	Planted	sandy clay loam	3	36.8	31.7 - 42.8	23.1	21.9 - 24.8	2.30
2013	83	Planted	sandy clay loam	3	49.4	45.9 - 54.3	28.2	26.6 - 30.4	3.42
	North Carolina								
2014	15	Planted	sand	5	16.2	9.5 - 22.7	10.5	8.7 - 12.5	1.19
2014	25	Planted	sand	5	15.4	8.0 - 22.5	12.0	7.6 - 14.8	1.22
2014	79	Natural Regen.	sand	3	41.9	28.8 - 54.3	21.6	19.4 - 25.8	2.67

Radar data were processed and scaled to biomass using methods described by Butnor et al. (2012) and summarized with the following steps:

1. Post-collection processing of GSSI GPR radargrams (*.dzt) was performed with RADAN 7.0 software (Geophysical Survey Systems Inc., Nashua, NH, USA). All files received position correction and background removal to remove planar (horizontal) reflections from soil horizons and surfaces. Extra gain was applied radargrams on stands with particularly low amplitude if necessary.

2. Root location was spatially corrected using Kirchoff migration to reduce multiple reflections and help identify the geometry of a hyperbolic reflectors (Oppenheim and Schafer 1975; Berkhout 1981; Daniels 2004) The results were compared with the Hilbert transformation (Butnor et al. 2003; Stover et al. 2007), where the magnitude of the phase of the signal is transformed and reflectors may be revealed by reducing multiple reflections. In most cases the Hilbert transform alone was used, and at one stand the Hilbert transform was applied after migration and extra gain to resolve faint reflectors (Table 6.2).

3. Processed *.dzt files converted to 8-bit grayscale bitmap image files.

4. Images were analyzed with an intensity threshold to determine the relative proportion of the image populated with root reflections using SigmaScan Pro Image Analysis Software (Systat Software, Point Richmond, CA). The threshold range is highly dependent on root and soil properties and is manually determined intensity threshold range will by focusing on small roots (~1 cm diameter) and comparing resolution of different threshold values (0 is black, 255 is white), usually within the range of 60–200.

5. The entire radargram image is parsed into sections representative of a 15 cm soil core and the number of "high-amplitude" pixels above the threshold are tallied for each individual "virtual core", i.e. 15 m transect would be sectioned in 100 images, that would be tallied separately with SigmaScan.

6. The dry mass of live roots (g) in series of soil cores is compared with the number of high amplitude pixels or area using regression analysis. The resulting equation is applied to pixel tallies from virtual cores to estimate root mass at specific locations.

Below-stump root biomass estimation with GPR

A 4 m by 4 m square (16 m^2) centered on each sample tree was designated for GPR surveying prior to excavation. The surface was raked clear of litter and woody debris, then a series of 9 parallel lines, 4 m long, spaced 0.5 m apart were established with ground marking paint.

Table 6.2. System settings for the SIR-3000 radar unit equipped with a 1500 MHz antenna and post-collection data processing parameters.

Stand	Soil Water Con. (%)	Soil ε	Range (ns)	Post-Collection Filters					Image Analysis	
				Pos. Corr.	Back. Rem.	Mig.	Hilbert Trans.	Extra Gain	Amplitude Threshold	Correlation Coeff. (r) with soil cores
Louisiana										
8	18.0	8	14	✓	✓		✓		140	0.69
18	14.8	8	14	✓	✓		✓		136	0.89
34	11.5	7	14	✓	✓		✓		136	0.84
60	11.3	8	14	✓	✓		✓		140	0.85
83	26.6	10	18	✓	✓		✓		136	0.89
North Carolina										
15	5.8	7	14	✓	✓		✓		140	0.79
25	4.5	6	14	✓	✓	✓	✓	✓	136	0.77
79	4.3	5	14	✓	✓		✓		135	0.74

The transects were scanned with a 1500 MHz antenna connected to a SIR-3000 GPR unit using system settings presented in Table 6.2. As the center line (line 5) cannot go through the tree, the antenna was advanced to the base of the tree, then followed the circumference (to the right) and resuming a straight path on the other side of the tree.

The GPR data were processed as previously described, though prior to image analysis (steps 4-6), reflections from debris related to military exercises (shell casings, wire, metal foil) were parsed from the images. Unwanted reflections from metallic objects were readily identified, having either very high amplitude or "ringing" parallel reflections from throughout the profile. Less than 10% of each radargram was omitted. After image analysis was complete, the lowest denominator for spatial distribution was the amount of root mass predicted in a 15 cm^2 core to a depth of 50 cm expressed as g/m^2, kg/m^2 or Mg ha^{-1} depending on the relevant scale at hand. Along each transect a root mass value was calculated every 15 cm, resulting in 9 lines, 50 cm apart containing 28 observations each for a total of 252 observations per tree (16 m^2). These data were used to create a root biomass distribution map for the entire 16 m^2 area around each tree where the x, y coordinates are linked to root mass values. The data were summarized as the total amount of root mass predicted in the excavation area (1 to 4 m^2), that varied with tree size (described in the next section). The root mass data were also analyzed as a function of distance from the center of the tree, where the tree centered at (2 m, 2 m) was adjusted to the origin (0 m, 0 m) by subtracting 2 from both the x and y coordinates of all 252 observations. The distance between the center of the tree and the root mass estimate was calculated with the Pythagorean equation where:

$$x^2 + y^2 = distance\ to\ center\ of\ tree^2$$

In order to better understand the relationship between accuracy of GPR detection of lateral roots and tree proximity, 11 trees across the range of DBH were scanned with GPR at a distance of 0.5, 1 and 1.5 m from the outer edge of the tree and cored for verification. These 33 soil cores are separate from the cores used to calibrate GPR to provide some core-based validation of the GPR results within the excavation pit.

Harvest of below-stump coarse root biomass

After GPR surveying was complete, trees were felled and a square excavation area (pit) centered on the stump was designated. It had been common practice to sample below-stump root mass (lateral + tap root) in loblolly pine (*Pinus taeda* L.) by designating a fixed area e.g. 1 m^2 centered on the tree, and excavate the full extent of the tap root (Retzlaff et al. 2001; Samuelson et al. 2004; Albaugh et al. 2006). The standard 1 m^2 pit had previously been applied to trees as old as 18 years (Albaugh et al. 2006), but was considered too small for large trees in the present study (up to 83 years old). It was not feasible to excavate and follow the full extent of all roots in the field; hence a variable pit area proportional to tree size was used. The minimum pit area for the smallest trees was 1 m^2 (trees < ~10 cm DBH) and the maximum was 4 m^2. The specific area of each pit was calculated from the linear relationship between tree basal diameter (ground-level) to objectively link variable pit area with tree size (Samuelson et al. 2014). Pit area may also be approximated using DBH (cm) where: pit area (m^2) = 0.8322 e $^{0.0301 * DBH}$; R^2 =0.95, p < 0.001. Mean pit areas by stand are presented in Table 6.1.

We define below-stump coarse root mass as tap root mass (cut at ground-level) and all mass from lateral roots > 5 mm diameter within the excavation pit. Lateral coarse roots (> 5 mm) were excised from the tap root and cut cleanly at pit walls to a depth of 1 m. The excavated soil was sieved through hardware cloth (0.63 cm mesh) and all longleaf pine roots > 5 mm in diameter were collected. The entire tap root was removed either manually or with a mini-excavator. All roots were washed free of soil and dried to constant mass at 65° C.

Statistical Analysis

Root mass estimated by GPR within the excavation pit (1 – 4 m²) was compared to below-stump mass (tap root + lateral) and lateral root mass excavated from each of the 33 trees. Data were analyzed using SAS for Windows 9.4 (SAS Institute, Cary, NC). Regression analysis was used to predict the ratio of GPR root detection (coarse root mass estimated with GPR: excavated coarse root mass) in the excavation pit using tree DBH. As data were collected at two geographically distinct regions (western Louisiana and eastern North Carolina), the F-test for extra sum of squares was applied to determine if the regions had similar regression parameters and could be pooled. The resulting *p* value was > 0.1 for both below-stump and lateral root mass models so the Louisiana and North Carolina data were pooled. Specific regression models were selected based on analysis of residuals and R^2 values. Mixed model analysis was used to examine the relationship between tree DBH and allocation of root mass to tap roots within the excavated pit.

Results

The linear relationships between lateral coarse root mass collected via soil cores and GPR index (high amplitude area) had correlation coefficients (r) between 0.69 and 0.89 for each the eight stands (Table 6.2). These regressions were site specific, dependent on soil and root properties and soil moisture at the time of sampling. A total 14 cores were uninterpretable from high soil water content and 32 contained metallic debris from military training and were omitted from the analysis. Regression equations were developed using the remaining 156 core scans to predict the amount of root mass in each core (Figure 6.2). The 95% confidence interval largely included the 1:1 line, demonstrating the relative accuracy of GPR lateral root biomass estimates ($R^2 = 0.72$, $p < 0.0001$). The y-intercept (6.94 g root mass) of regression line did not pass through zero as a minimum amount of root mass was needed for detection (Figure 6.2).

To help visualize rooting density in the excavation pit as well as entire 16 m² area around a tree, root biomass maps from four trees ranging in DBH from 8 to 54.3 cm were presented as contour plots (Figure 6.3). The maps are not intended to reveal details of root architecture; rather detectability of roots near trees in stand-level surveys. These maps show that detection of roots with GPR near the base of the tree and within the area designated for excavation was suppressed. GPR underestimated below-stump root mass and the magnitude increased with tree size. For the examples in Figure 6.3: 64% of below-stump root mass was detected near the smallest tree (8.0 cm DBH), while only 5% was detected proximal to the largest tree (54.3 cm DBH).
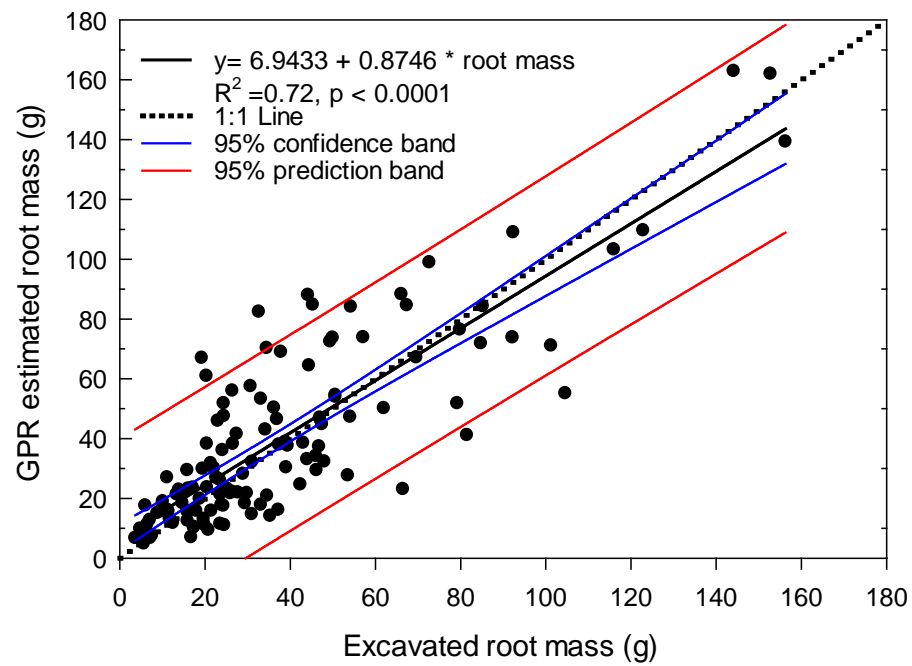
Figure 6.2. Comparison of excavated and GPR estimated root mass from 15 cm diameter soil cores to a depth of 50 cm. Dry root mass is presented as grams (g) per core.
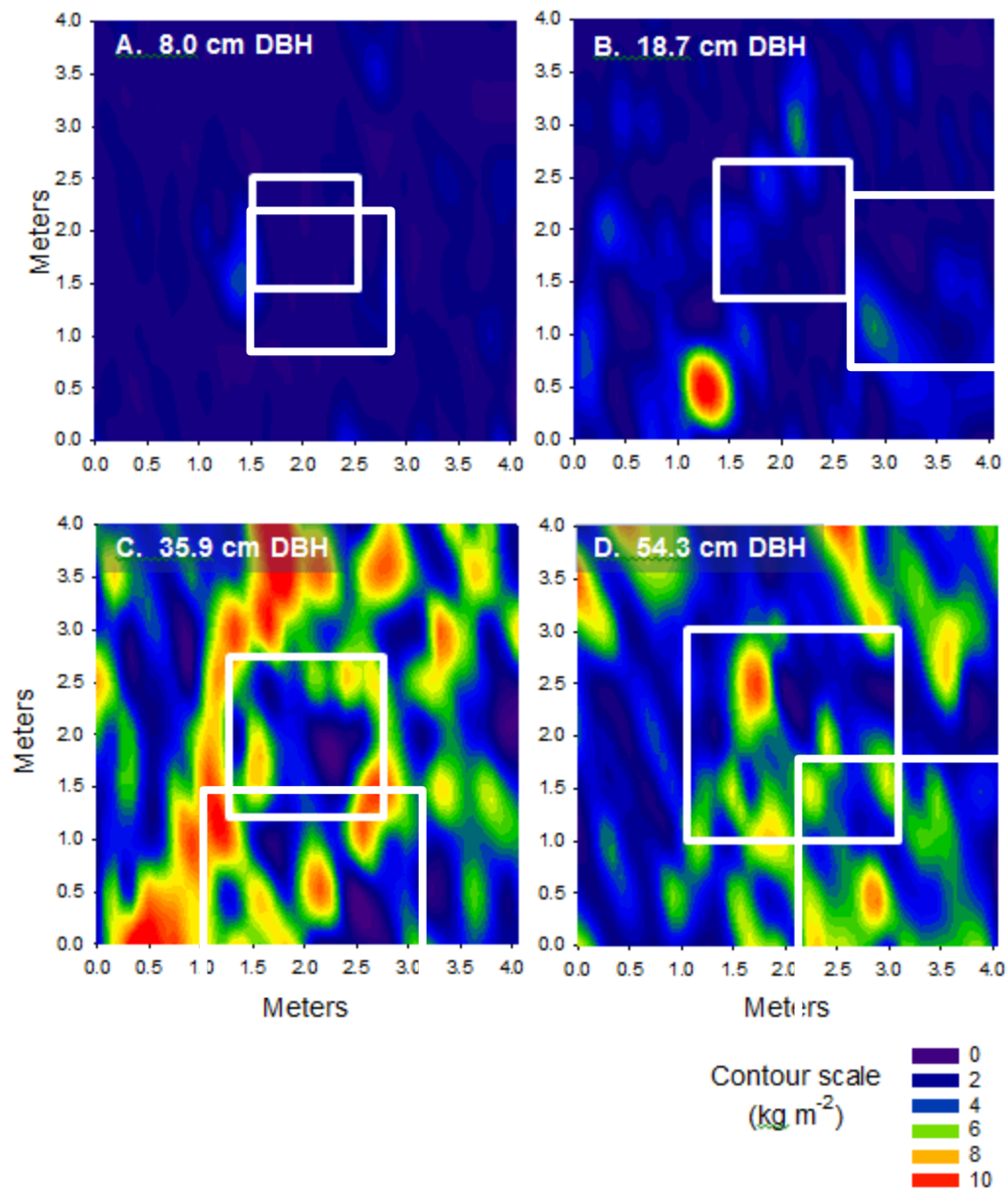
Figure 6.3. Root biomass maps (16 m^2) generated using GPR data from four trees representing the range of tree DBH analyzed A) 8.0 cm, B) 18.7 cm, C) 35.9 cm and D) 54.3 cm. The white outlines indicate the excavation area. Tree parameters are summarized in Table 6.3.

Table 6.3. Predicted and excavated root mass associated with root biomass maps.

DBH (cm)	Height (m)	Age (years)	Root detected with GPR in pit (kg)	Lateral root excavated (kg)	Tap root excavated (kg)	Below-stump excavated (kg)	Lateral roots detected (%)	Below-stump detected (%)
8.0	7.6	25	1.2	0.9	1.0	1.9	132	64
18.7	14.4	25	3.5	5.6	25.0	30.6	62	11
35.9	24.8	60	19.9	25.3	140.3	165.6	78	12
54.3	25.8	79	26.5	211.0	305.9	516.9	13	5

Due to the vertical orientation of the tap root, it was unlikely that GPR is detecting much of the tap root mass. If it is assumed that the tap root is undetectable and GPR results are compared with lateral roots excavated from the pits, the proportion detected increased markedly (Table 6.3).

The relationship between GPR root detection (GPR estimated/excavated root mass) in the excavation pits and tree DBH was analyzed using non-linear regression. Using data from all 33 trees, the portion of root mass in the pit detected by GPR and tree DBH were highly significant for both lateral root mass ($p < 0.0001$, $R^2=0.65$) and below-stump root mass ($p < 0.0001$, $R^2=0.77$) (Figure 6.4). GPR overestimated lateral coarse root mass on small longleaf pine trees (DBH <10 cm) and underestimated on trees >10 cm DBH (Figure 6.4.a). Less than 13% of the lateral coarse root mass of the two largest trees (both 54.3 cm DBH) was detected with GPR. Below-stump root mass was largely underestimated by GPR and the ratio of GPR estimated to excavated root mass decreased sharply with tree diameter (Figure 6.4.b). At diameters of >15 cm, less than 20% of below-stump mass was detectable with GPR.

Pooling all data from North Carolina and Louisiana (n=33), 67% of the root biomass in the pit was attributed to the tap root. Allocation of root mass to tap root in trees with DBH < 10 cm was significantly lower than the 10-20, 20-30, 30-40 cm DBH classes (F = 6.58, p= 0.0004). There were no significant differences between the other DBH classes. Allocation to tap root by DBH intervals is presented in Table 6.4. Even if it is assumed that GPR is not detecting tap roots that comprise the majority of below-stump root mass, laterals roots are still being underestimated proximal to trees (Figure 6.4) and this is at odds with the relative agreement between GPR estimates and excavated root mass from soil cores (Figure 6.2). Eleven of the 33 trees were surveyed with GPR at a distance of 0.5, 1 and 1.5 m from the outer edge of the stem and GPR estimates were compared to excavated root mass from soil cores (Figure 6.5). At a distance of 0.5 m from the tree, the proportion of roots detected declined with DBH, though the effect was not significant at 1.0 or 1.5 m (Figure 6.5). Despite being a small sample, this supports the supposition that GPR calibration equations developed away from trees will underestimate root mass near trees and this effect will lessen as the distance from the tree widens.

Root mass detected with GPR in the entire16 m^2 sample area was plotted as distance from tree to illustrate root distribution within and beyond the excavation pit (Figure 6.6.a). The data are not normally distributed as they were collected in parallel lines and expressed as the radius from the center of the tree (Figure 6.6.b). Data were averaged by DBH class (<10, 10-20, 20-30, 30-40, 40-50, >50 cm) resulting in 252 mass/distance observations per class (Figure 6.6.a). For comparison, mean lateral root mass recovered via pit excavation for each DBH interval was 1.10, 2.31, 6.64, 11.40, 41.30 and 41.02 kg m^{-2}, respectively. The smallest DBH class (<10 cm) shows a gradual increase in root mass closer to the tree and good agreement between GPR and excavated lateral root mass near the tree. The next two intervals (10-20 and 20-30 cm) show similar patterns, though root mass detected near the tree is 1.4 to 3.7 times lower than excavated root mass. Trees > 30 cm DBH show a marked increase in root detection between 2.5 and 1.5 m from the tree were they appear to be in close agreement, near the tree lateral root mass is underestimated between 3.1 and 11 times.
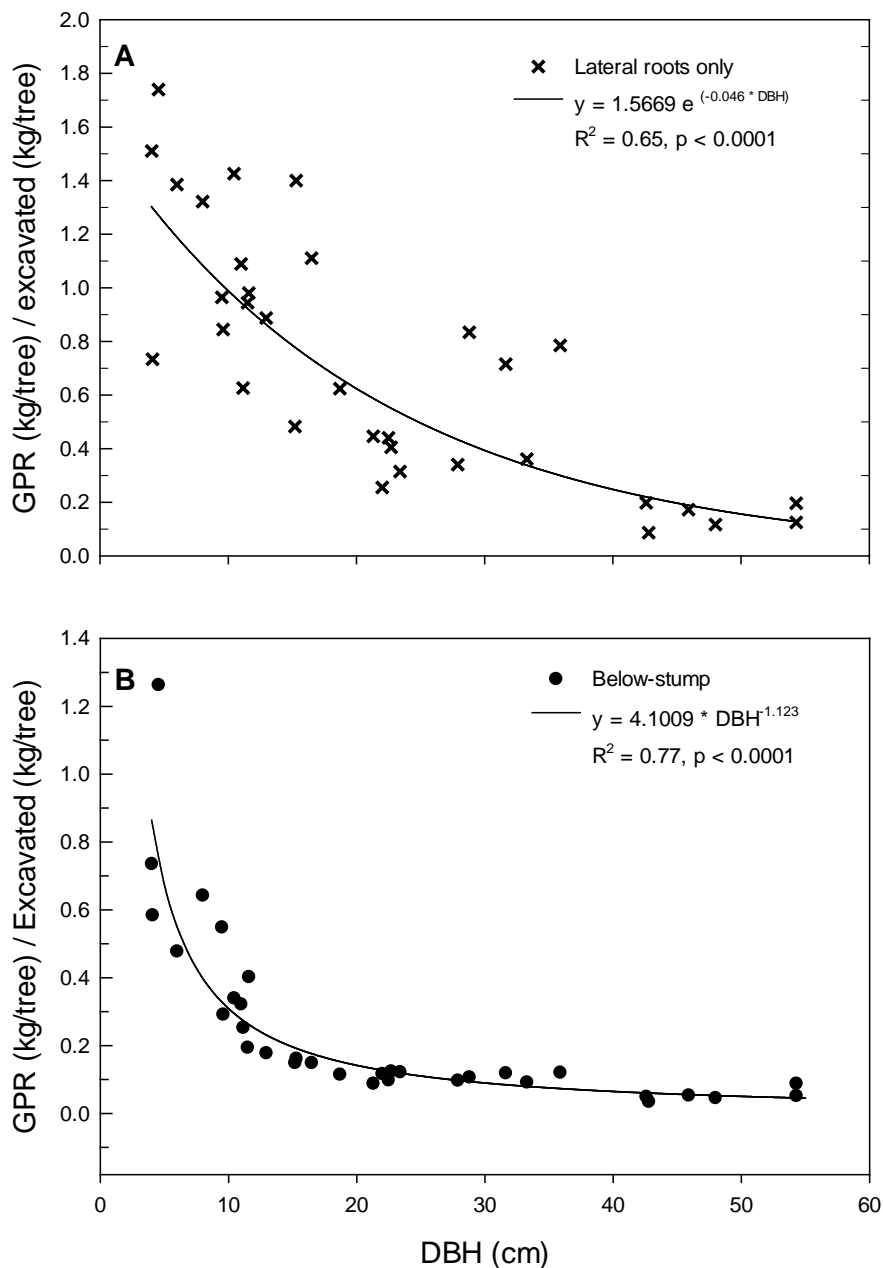
Figure 6.4. Regression analysis of GPR root detection in the excavation pit (mass estimated (kg/tree) / mass excavated (kg/tree)) with tree DBH for 33 longleaf pine trees in Louisiana and North Carolina. Separate regressions were made for lateral roots (A) and below-stump (tap + lateral roots) (B). Overestimation of lateral roots with GPR occurred adjacent to small longleaf pine (<10 cm dbh) followed by underestimation of lateral roots adjacent to larger trees (A). Below-stump (tap + lateral roots) mass was overestimated with GPR for one tree (4.6 cm dbh), followed by underestimation of lateral roots adjacent to remaining trees (B).

Table 6.4. Proportion of longleaf pine coarse root biomass attributed to the tap root compared with published values of several *Pinus* species. Age and DBH are denoted either as a mean or an age interval depending on the study.

Species	Location	n	Age (yrs)	DBH (cm)	Tap root:total root biomass (%)	Reference
Pinus palustris	Louisiana and North Carolina	7	13	< 10	46	Based on excavation data from present study, all data pooled by DBH
		10	19	10-20	75	
		7	31	20-30	72	
		3	66	30-40	81	
		4	78	40-50	67	
		2	81	50-60	57	
Pinus pinaster	S.W. France (maritime)	30		10-20	45	Augusto et al. (2015), tap root includes stump
		25		20-30	40	
		17		30-60	30	
Pinus pinea	Italy (coastal)	14	50-62	24-39	57	Cutini et al. (2013)
Pinus resinosa	Michigan (U.P.)	*	5	5	85	Calculated from: King et al. (2007), tap root includes stump 30 cm above ground line.
			8	6	90	
			12	10	80	
			17	14	68	
			32	17	82	
			22	18	89	*260 total trees harvested across all ages*
			55	25	64	
Pinus sylvestris	Finland (southern)	7	34	9-20	30	Calculated from: Vanninen et al. (1996), tap root includes stump.
		5	65	20-30	27	
		3	121	30-40	35	
		3	169	40-50	33	
Pinus taeda	South Carolina	15	48	30	55	Vanlear and Kapeluck (1995) *combination of harvest and modeling*
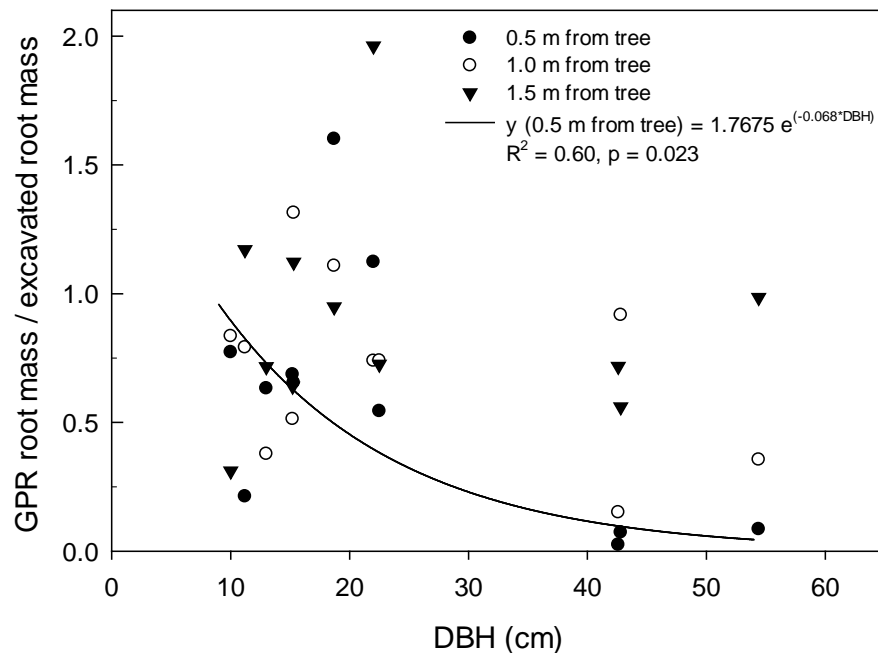
Figure 6.5. Regression of the proportion of roots detected with GPR (verified with soil cores) at distances of 0.5, 1.0 and 1.5 m from and tree DBH for 11 of the 33 sample trees.
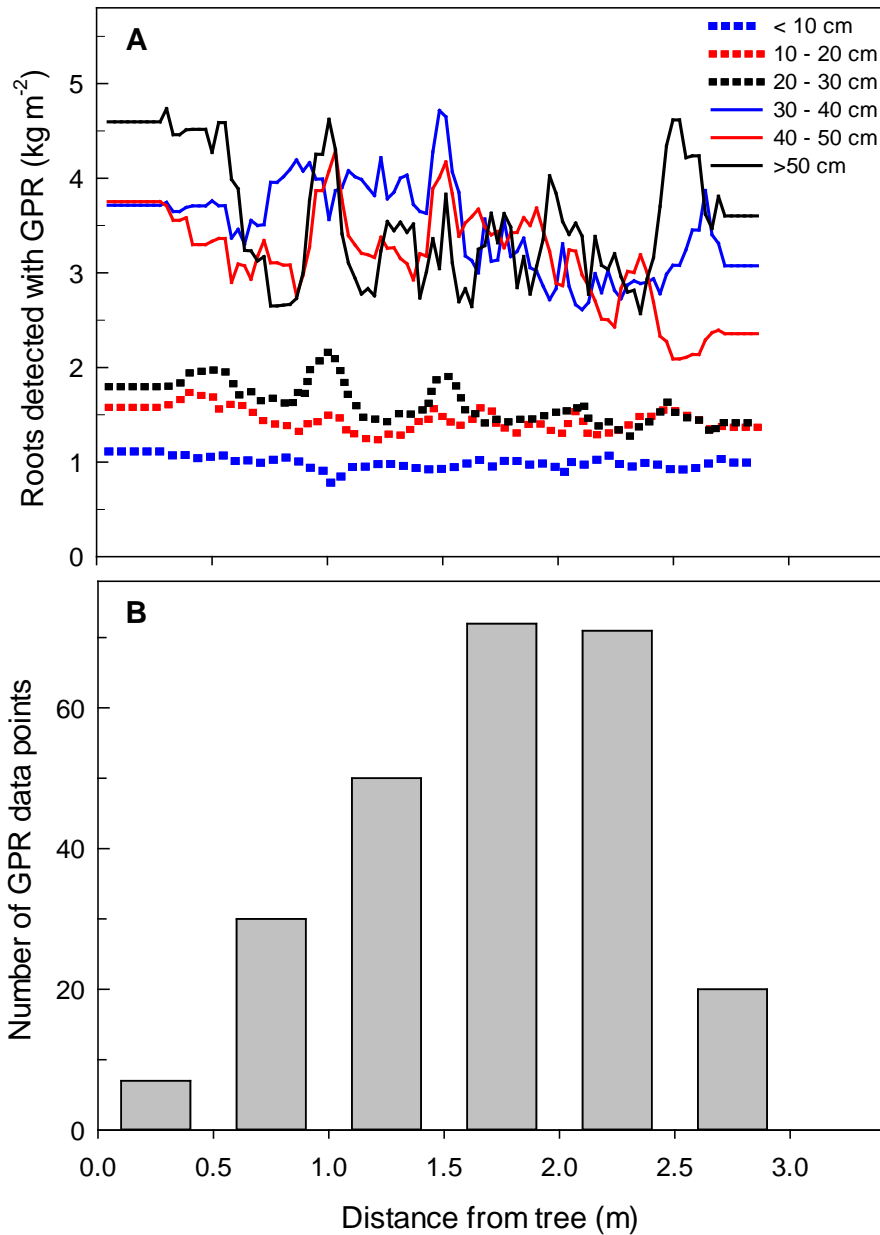
Figure 6.6. Root mass detected with GPR in the entire 16 m^2 sample area plotted as distance from tree (A). Data were averaged by DBH class (<10, 10-20, 20-30, 30-40, 40-50, >50 cm) resulting in 252 mass/distance observations per class. The data were smoothed using a running average filter with a sampling proportion of 0.05. The distribution of GPR data points as related to distance from tree are presented in inset B.

Discussion

Direct comparison between GPR estimates and excavated root mass at the base of trees demonstrated that GPR underestimates below-stump root mass and the degree of underestimation is related to tree size (DBH). This in opposition to comparisons between GPR estimates of lateral root mass and verification with soil cores (that were not proximal trees) which were in close agreement. The footprint of the antenna is an inverted cone, with some limited ability for side-scanning (Conyers and Goodman 1997), this may be a factor with small trees (<10 cm DBH) where there is adequate soil volume to coarse root mass near the base of the tree. The overestimation of lateral root mass observed on small trees may result from the tap root being detected as additional lateral roots, as radargrams did not show any deep reflections consistent with vertical tap roots.

Our findings contrast with those reported by Borden et al. (2014) who scanned a 20.25 m^2 area around 25 year old trees of five tree species in southern Ontario, Canada (12 trees total) with a 1000 MHz GPR antenna and compared the results to excavations to a depth of 1 m. When pooled across species, GPR estimates and excavation were within 1% of each other. When considered by species, GPR estimates by Borden et al. (2014) for *Juglans nigra* L. (n=2) and *Quercus rubra* L. (n=3) were in close agreement with excavation data, underestimates were reported for *Populus* sp. (32%, n=2) and *Thuja occidentalis* L. (16%, n=3) and overestimates for *Picea abies* L. Karst (24%, n=2). While underestimation of root mass is anticipated with deep or vertical roots, it was observed to a lesser degree by Borden et al. (2014). The authors explained that some of the detected biomass may be from false positives and that with the exception of *Populus* sp., these trees tended to have more readily detectable horizontal roots. Roots were not classified as horizontal and vertical (tap root), so further quantitative assessment is not possible. Key differences with the present study are: 1) the excavation area was 20.25 m^2 versus our variable 1-4 m^2 pits and the larger area may dilute any underestimates proximal to the tree, 2) pine species have a tendency for tap or sinker roots and thus root morphology of pine is very different than the species examined by Borden et al. (2014), and 3) use of a 1000 MHz center frequency antenna would afford deeper penetration, but have less ability to detect smaller roots (<1.5 cm) than the 1500 MHz antenna used in the present study.

Longleaf pine has some similarities in root morphology and below-stump allocation of biomass with the other major southern yellow pines (*Pinus taeda* L.; *Pinus elliottii* Engelm.; *Pinus echinata* Mill.) and other *Pinus* sp. that develop a tap root or a cluster of vertical roots beneath the tree. Tree root biomass harvests are conducted to develop allometric equations, though few published reports describe the percent allocation to lateral and tap roots. Data from the present study are compared to reported values for other *Pinus* sp. in Table 6.4. Over half of the root biomass in *P. palustris*, *Pinus pinea* L., *Pinus resinosa* Ait. and *P. taeda* are allocated to tap roots while approximately one third is allocated to tap roots in *Pinus pinaster* Ait. and *Pinus sylvestris* L. (Table 6.4). This is a considerable amount of coarse root mass that GPR is unlikely to detect, especially in mature trees, and thus needs to be explicitly accounted for when scaling GPR-based data to the stand level. With some parameterization, the equations in Figure 6.4 could be adapted for other *Pinus* sp. so that spatial analysis of root distribution GPR could be used in conjunction with below-stump allometry. It seems likely that GPR would underestimate coarse root mass proximal to mature trees of other genera; more so with deep, vertical rooting patterns and less with shallow rooting patterns.

Globally, temperate coniferous forests have an average root : shoot ratio of 0.18 with over 50% of the root mass located in the upper 30 cm of soil (Jackson et al. 1996), making it important to mitigate this potential for underestimation proximal to trees with GPR. An analysis by Robinson (2007) cites evidence that root biomass is widely underreported and could be as much as 68% greater on a global basis. It is possible that current estimates of belowground biomass in many forests are underrepresenting extensive roots further away from trees and wider adoption of GPR protocols could help mitigate this. Thus, GPR remains an important tool to estimate stand-level root biomass.

The need for the present study became apparent while conducting stand-level surveys of ecosystem C pools in longleaf stands in Georgia (Samuelson et al. 2014), Louisiana and North Carolina. Surveying root mass with GPR on the scale of hundreds or thousands of square meters per day necessitates wider transect spacing for expediency and may preclude gridding in multiple angles that would be applied in root architecture studies. While less detailed than close spaced gridded data collection (e.g. 25 cm grid, (Zenone et al. 2008); 10 cm grid (Borden et al. 2014)), a 10 by 10 m plot scanned at 0.5 m line spacing and mass estimates every 15 cm still affords over 1400 root mass observations in 100 m^2, which is rather comprehensive and would be prohibitive to sample otherwise via destructive methods. The single tree plots were sampled at the same density as stand-level surveys so they could be used to correct for near tree bias. While detectability of below-stump root mass by GPR within defined pit areas is highly predictable and the accuracy of GPR lateral root detections away from trees is very good, our study design is limited in determining were the two metrics intersect. With limited core validation in the present study, it can only be speculated that by 1.5 m away from large longleaf pine the underestimation by GPR is abated. This leaves some ambiguity, which would have been better addressed by making many more comparisons of GPR and soil cores at a finer scale (e.g. 0-4 m from tree at 0.25 m intervals).

In a study of 20 longleaf pine stands aged 5 to 87 years in Georgia, USA, Samuelson et al. (2014) estimated belowground live root C using a combination of allometry and GPR. They developed allometric equations with tree height and DBH to predict below-stump mass from the harvest of 21 trees using the same variable pit area method as the present study (1 - 4 m^2). Stand inventory data (tree height, DBH) from the 20 plots was used to estimate stand-level below-stump biomass that was expressed as Mg C ha^{-1} (root mass * carbon concentration). At the center of each plot a 100 m^2 subsample was surveyed with GPR to estimate stand-level lateral root C (Mg C ha^{-1}). As the potential for overlap or "double counting" of root mass between allometric modeling of below-stump mass and GPR lateral root surveys was unknown, stand-level live root C was calculated two ways: 1) estimated total root C = GPR lateral root C + tap root C (allometric modeling), and 2) estimated total root C = GPR root + tap root C (allometric modeling) + lateral root C (allometric modeling). This led to uncertainty when analyzing ratios of above- and belowground C allocation, at maximum aboveground C of 100 Mg C·ha^{-1}, belowground C varied by 20% (Samuelson et al. 2014). We recalculated the GPR estimates of lateral roots reported by Samuelson et al. (2004); Samuelson et al. (2014) using inventory data with the following steps:

1. Calculated the below-stump mass of each tree via allometric equations (Samuelson et al. 2014)

2. Determined the ratio of below-stump mass detected by GPR for that tree (Figure 6.4.b):

(GPR mass/excavated mass = $4.1009 \cdot DBH^{-1.123}$)

3. Calculated the amount of below-stump mass per tree that was estimated by both allometry and GPR per tree (overlap between methods)

4. Converted biomass to C content by multiplying by below-stump C concentration

5. Deducted this amount from the GPR stand-level estimate of lateral root C.

Using this approach we obtained stand-level estimates of lateral root C (detected with GPR) for each plot separate from estimates of stand-level below-stump C (allometric modeling) + fine root C. Lateral root C (detected with GPR) increased with aboveground C for the 20 longleaf pine plots and represented 34 % of the belowground C pool at maximum aboveground C (100 Mg C ha-1) compared with 66 % attributed to below-stump C + fine root C (allometric modeling) (Figure 6.7.a). Stand-level lateral root C (GPR) was then added to below-stump C + fine root C (allometric modeling) to obtain a corrected value for total belowground C (Figure 6.7.b). Since the tap root and large overlapping roots near the trunk of the tree make up the bulk of below-stump root C and are widely underestimated by GPR, it is logical that corrected belowground C estimate is closer to the assumption that GPR detected no lateral roots in the excavated pits (Figure 6.7.b). While GPR underestimates below-stump root mass, it does account for roots between and away from trees that would otherwise go unaccounted for using only allometric modeling based on excavation pits. Across the range of stand ages (5 to 87 years) analyzed by Samuelson et al. (2014), GPR accounted for 67 % of the belowground C in the youngest and 34 % in the oldest stand (Figure 6.7.a).

Conclusions

When using GPR-based data to scale coarse root mass to the stand level, it is critical to account for the portion of mass directly under and adjacent to trees that is not measureable by surface-based antennas. Although GPR can accurately measure lateral coarse root mass under suitable soil conditions, the proportion of below-stump mass detected with GPR declined sharply with tree diameter. We would expect similar below-stump mass underestimation with other species that develop large tap roots and associated proximal lateral roots, particularly in older stands with large trees. For example, many pine species allocate more than half of root mass to vertical tap roots or sinker roots. Thus, accurate scaling of GPR-based coarse root mass data to the stand level and subsequent estimation of root C stock requires integration with allometric modeling of below-stump mass. Results from this work were used to provide a more complete assessment of ecosystem C described in the following Chapter 7.
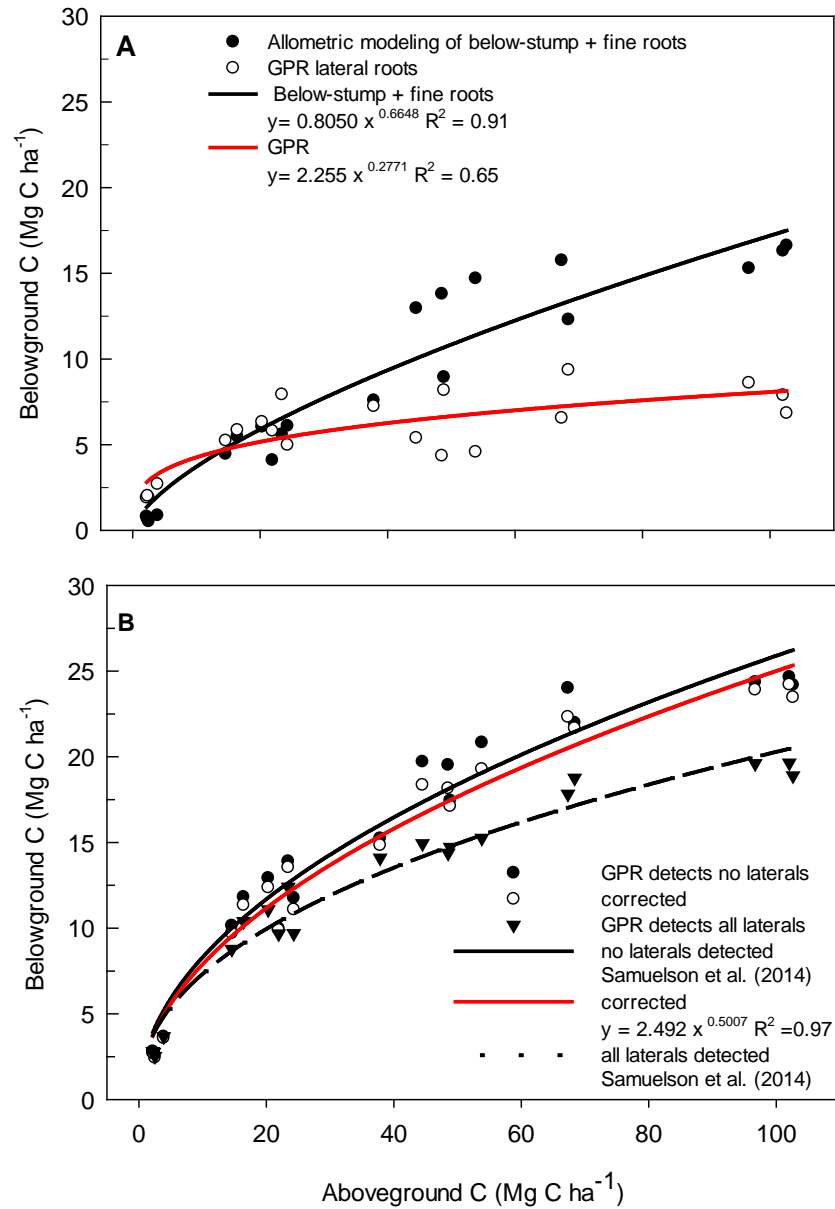
Figure 6.7. Comparison of above and belowground C from 20 plots of longleaf pine aged 5 to 87 years in Georgia (Samuelson et al. 2014) where lateral root C (GPR) is presented separate from below-stump C plus fine roots (allometric modelling) (A). Stand-level lateral root C (GPR) and below-stump mass plus fine roots (allometric modelling) were combined to calculate total root C (B). These data were originally reported by Samuelson et al. (2014) with assumptions of *no lateral roots are detected by GPR in the below-stump sample area* and *all lateral roots are detected by GPR in the below-stump sample area.* The lateral root (GPR) C data were corrected for below-stump underestimation using the approach and equation described in the present study.

7. Ecosystem Carbon Density and Allocation Across a Chronosequence of Longleaf Pine Forests

[Contents of this chapter were extracted from: L. J. Samuelson, T. A. Stokes, J.R. Butnor, K.H. Johnsen, C. A. Gonzalez-Benecke, T. A. Martin, W. P. Cropper, Jr., P.H. Anderson, M.R. Ramirez, and J. Lewis. 2016. Ecosystem carbon density and allocation across a chronosequence of longleaf pine forests in the southeastern USA. Submitted to Ecological Applications]

Introduction

This Chapter builds on the research described in Chapters 5 and 6 to quantify ecosystem C stocks in longleaf pine forests across the five installations and the range of longleaf pine. Forests can partially offset greenhouse gas emissions and contribute to climate change mitigation, mainly through increases in live biomass both above and belowground (Heath et al. 2011). The total carbon (C) stock, not including soil, in temperate forests in the conterminous USA was estimated as 43 billion Mg C in 2007 (Pan et al. 2011), and forests sequestered 790 million metric tons of CO_2 equivalent on 253 million ha of forestland in 2008 (Heath et al. 2011). More recent analysis of forest C stocks and stock change from 1990 to 2016 indicated that forest growth and expansion offset 15% of annual C emission from combustion of fossil fuels in the USA (Woodall et al. 2015*a*). Accurate estimates of total ecosystem C stocks are critical, because changes in C stocks may influence the balance between terrestrial and atmospheric C (Keith et al. 2010). Furthermore, total ecosystem C stocks can be used as a C carrying capacity baseline to evaluate the impact of changes in land use, forest management and forest health on C storage and climate change mitigation (Keith et al. 2010). In the Unites States, forest chronosequences have been used to define C storage potential of forests, with most estimating biomass and C sequestration using data from the Forest Inventory and Analyses National Program (FIA) and genus-level allometric equations from the literature (Lichstein et al. 2009, McKinley et al. 2011, Chojnacky et al. 2014), and fewer based on actual sampling of tree biomass and C concentrations (King et al. 2007, Kashian et al. 2013). However, the paucity of biomass chronosequences is a major source of inconsistencies among national estimates of C stocks (Williams et al. 2012). Keith et al. (2014) identify the need for chronosequences of known age and the assumption of space-for-time substitution to calibrate growth functions for prediction of carbon stocks at the site and landscape scales. Furthermore, lack of empirical information on belowground tree biomass has hampered accurate estimations of forest C stocks and subsequent understanding of forest C dynamics (McKinley et al. 2011, Russell et al. 2015).

Longleaf pine forests (*Pinus palustris* Mill.) were once a dominant forest type in the Coastal Plain of the southeastern USA and their restoration may serve as a pathway to increase the resilience of forests to changing climate, because of greater resistance to disturbance, disease and insects conferred by structurally diverse stands (Johnsen et al. 2009, Churchhill et al. 2013). While higher quality sites have greatest forest C carrying capacity, less productive sites, which are often planted with longleaf pine, may also be suitable for greenhouse gas mitigation projects (Hoover and Smith 2012). Reductions in terrestrial C stocks as a result of conversion of forest land to other uses, such as agriculture and urbanization, has increased the importance of climate change mitigation by

forest lands with typically lower C stocks (Birdsey and Pan 2015). Although longleaf pine forests are low density forests maintained by frequent fire, they can sequester comparable C over time relative to other plantation species in the southeastern United States. For example, Gonzalez-Benecke et al. (2015*a*), using a growth and yield based C model, reported similar average C stock between unthinned longleaf pine and unthinned slash pine stands on medium and high quality sites after a 75-year simulation, and higher average C stock in unthinned longleaf pine with a 75-year rotation length compared to three successive 25-year slash pine rotations. In addition, natural longleaf pine forests commonly experience only small scale disturbances, mimicked by uneven-aged management (Brockway et al. 2014), that may extend C storage depending on the harvest interval (Ryan et al. 2010). Because longleaf pine ecosystems provide a variety of economic goods and environmental services, they may be particularly well suited for applied long-term forest C management when benefits to biodiversity and resilience to wildfire and other disturbances are also considered (Schwenk et al. 2012, Martin et al. 2015). However, unlike other pines, little is known about the potential role of longleaf pine restoration across the landscape in offsetting greenhouse gas emissions (Susaeta et al. 2014).

In previous work described in Chapter 5, we quantified ecosystem C stocks in five different aged longleaf pine stands in Georgia (Samuelson et al. 2014). Here, we combine those data with comparable C data collected in 15 additional longleaf pine stands positioned across the native range of longleaf pine in Louisiana, North Carolina and Florida to assess C across a chronosequence spanning from five years of age to a mean canopy age of 118 years. Stands selected for sampling represent the current condition of the longleaf pine resource (Oswalt et al. 2012). We sampled aboveground and belowground biomass to develop robust allometric equations for longleaf pine and quantified C density in live tree biomass, live understory biomass, standing dead trees, down dead wood, the forest floor and soil to a 1 m depth. Our specific objectives were to: (1) quantify C density in longleaf pine forests representing ranges in age, forest structure, management, and site quality, (2) estimate above and belowground C accumulation trajectories for longleaf pine over time, and (3) determine what forest structural variables were related to ecosystem C stocks. We used the novel relationships presented in Chapter 6 to develop estimates of root C for longleaf pine.

Examples of old-growth forests are rare in the eastern United States (Lichstein et al. 2009). Mitchell et al. (2009) defined old longleaf pine forests as possessing trees > 50 cm dbh (diameter at 1.37 m), large standing and down dead wood pools, and patches of varying age classes, and suggested that old-growth characteristics begin to develop at 115-120 years of age. Because our chronosequence spanned the seedling grass stage to a mean canopy age of 118 years and many older stands consisted of trees ≥ 50 cm dbh, we hypothesized that live biomass C density would increase with age following a saturation function (e.g. Michaelis-Menton equation), as reported for forest chronosequences in temperate (Pregitzer and Euskirchen 2004) and *Pinus* dominated forests (Kashian et al. 2013). Due to the long residence time of mineral soil C and variability in soil C stabilization mechanisms across the landscape (Pregitzer and Euskirchen 2004), we also hypothesized that soil C content would not accrue with age.

Methods

Study sites

A total of 20 stands ranging in age from five to 118-years-old were sampled across the range of longleaf pine in Georgia (US Army Fort Benning at the Georgia-Alabama border, the 64-year-old stand was located in Alabama and the other four stands were in Georgia), Louisiana (Kisatchie National Forest), North Carolina (Marine Corps Base Camp Lejeune) and Florida (Eglin Air Force Base) (Figure 7.1, Table 7.1). Stands varied in density and tree size distributions (Figure 17.2) and were either planted or naturally regenerated (Table 7.1). With the exception of the 65-year-old stand, the eight stands older than 59 years contained some trees with dbh $\geq$ 50 cm (Figure 7.2). Georgia stands (5, 12, 21, 64 and 87 years of age) were sampled in 2012 (Samuelson et al. 2014). Stands in Louisiana (8, 18, 34, 60 and 83 years of age) were sampled in 2013, North Carolina stands (15, 25, 65 and 79 years of age) were sampled in 2014, and Florida stands (9, 19, 43, 50, 85 and 118 years of age) were sampled in 2015. Sampling was conducted from May through October of each sample year with the exception of Florida stands, which were sampled from February through June.

All Louisiana stands were planted but the planting density of the two oldest stands was unknown (Table 7.1). For all other sites, stands less than 60 years of age were planted and older stands were natural stands. For natural stands, stand age was based on the mean age of canopy trees and inventory records. All stands were dominated by one age class in the canopy, with the exception of the 118-year-old stand in Florida in which two cohorts were dominant, one approximately 150 years of age and a second approximately 75-years-old. Forest management records indicate one thinning in the 83-year-old stand in Louisiana and one in the 65-year-old stand in North Carolina, both five to seven years before sampling. Approximately 5 m^2 ha^{-1} of basal area was removed from the 83-year-old stand and 1 m^2 ha^{-1} was removed from the 65-year-old stand. Otherwise, there were no records of any other forest management activities besides prescribed fire. Stands were burned regularly and the majority of stands were burned 1-3 years prior to sampling, the exception being the 50-year-old stand which was burned five years before sampling and the 25-year-old stand which was burned four years before sampling.

Forest inventories

In all stands, a 1 ha circular main plot and four 400 m^2 circular subplots within the main plot were located as described in Samuelson et al. (2014). One subplot was centered on the center of the main plot and the center of the other three subplot centers was positioned 35 m from the center of the main plot at 0°, 120°, and 240° from north. Forest inventories were conducted in January or February of the designated sampling year. All live and standing dead trees $\geq$ 10 cm dbh were measured in each subplot. All live and standing dead trees $\geq$ 1 and < 10 cm dbh and $\geq$ 2 m height were measured within a 5 m radius of subplot centers. Species, dbh to the nearest 0.1 cm, and total height to the nearest 0.1 m were recorded. Height was measured using a telescoping height pole or laser hypsometer (TruPulse 200, Laser Technology, Inc, Centennial, Colorado, USA). Standing dead tree stems were measured provided the angle of the stem from true vertical was < 45°. The diameters of all stumps $\geq$ 10 cm at ground line were measured within the entire subplot.

Figure 7.1. Location of sampling sites within the historic range of longleaf pine (range map from U.S. Geological Survey 1999). Symbols denote: Marine Corps Base Camp Lejeune (triangle), US Army Fort Benning (triangle), Eglin Air Force Base (circle) and Fort Polk/ Kisatchie National Forest (square).
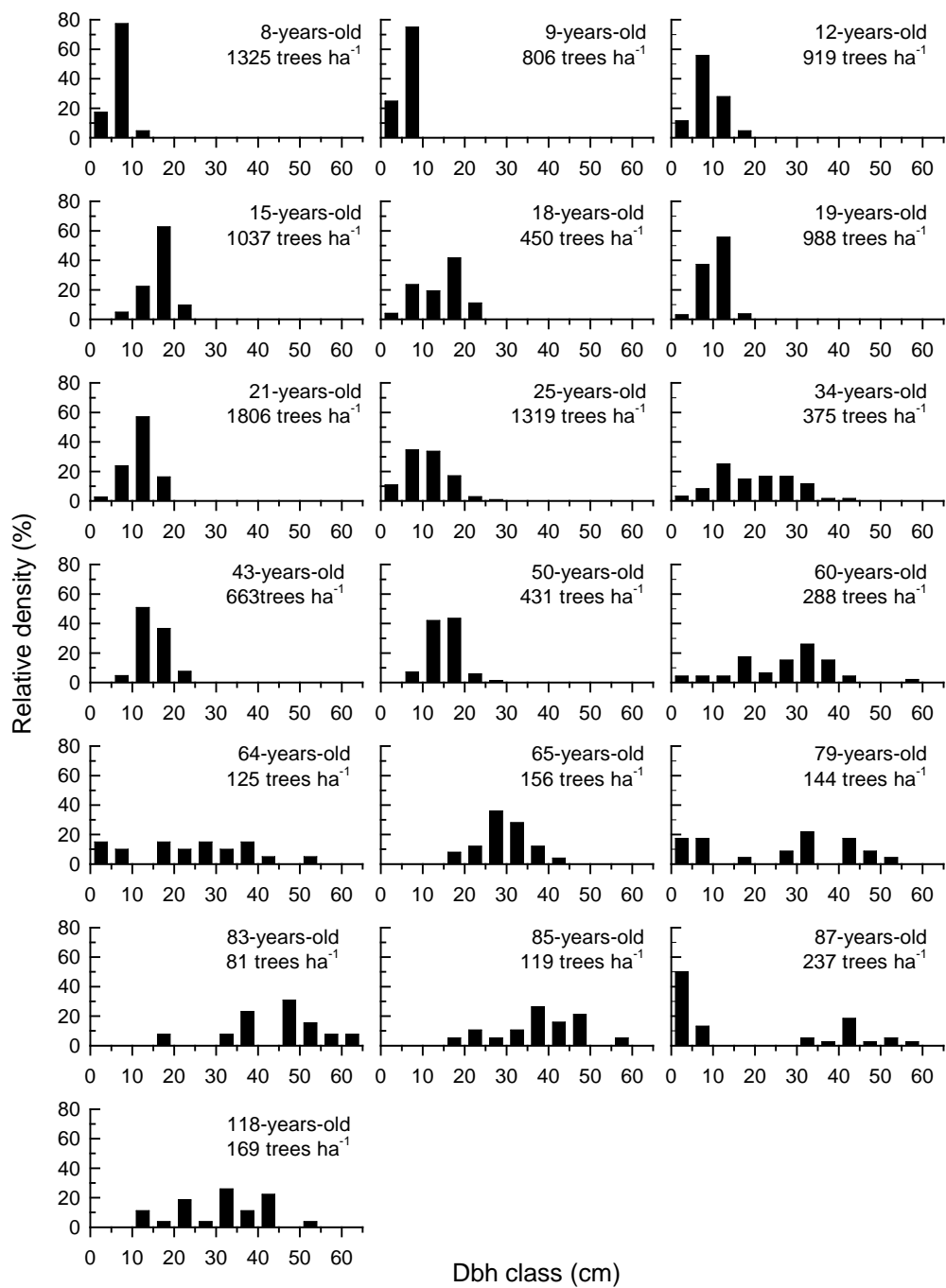
Figure 7.2. Diversity of forest structure in sampled longleaf pine stands.

Table 7.1. Location and characteristics of longleaf pine stands.

Stand age (years)	Latitude, longitude	Total basal area (m² ha⁻¹)	Longleaf pine basal area (m² ha⁻¹)	Site index (m)	Soil sand (%)	Planting density (trees/ha)	Mean dbh (cm)	Mean height (m)	Stump basal area (m² ha⁻¹)
5	32.400,-84.870	0.5	0.5	18.7	66.2	1494	-	-	35.0
8	30.944,-93.162	5.2	5.2	21.1	63.6	1976	10.8	6.5	21.1
9	30.580,-86.638	3.3	2.5	18.8	94.0	1494	-	-	2.1
12	32.373,-84.777	11.5	6.4	19.3	64.1	1494	12.3	9.1	7.1
15	34.589,-77.271	25.0	22.7	25.0	90.5	1482	16.8	10.3	8.6
18	30.943,-93.192	8.0	7.9	21.3	64.5	1976	17.0	11.2	11.9
19	30.607,-86.569	9.1	9.1	17.5	94.2	1494	12.2	9.4	0.1
21	32.391,-84.789	22.4	20.9	20.5	80.6	2235	13.2	11.8	0
25	34.645,-77.450	17.7	14.6	15.8	95.3	1729	14.9	11.3	0.2
34	30.991,-93.134	18.2	14.3	21.3	61.1	1235	21.8	16.7	4.1
43	30.609,-86.606	16.1	12.5	13.0	94.6	1890	15.2	11.7	0.7
50	30.601,-86.557	9.2	8.8	10.3	95.4	1890	15.8	10.2	0.6
60	30.997,-93.019	20.0	19.4	19.2	51.0	unknown	28.8	20.2	1.8
64	32.319,-85.008	10.2	7.8	15.7	70.8	natural	30.2	19.1	8.8
65	34.705,-77.252	11.6	10.8	15.4	76.7	natural	29.1	17.9	4.0
79	34.702,-77.303	11.2	11.2	12.6	89.8	natural	37.2	21.0	3.5
83	31.024,-92.944	13.8	13.5	21.4	49.3	unknown	44.2	25.2	11.5
85	30.583,-86.235	14.0	13.9	14.2	92.3	natural	39.2	22.5	0.9
87	32.366,-84.785	14.5	14.5	19.3	67.3	natural	43.7	29.0	10.6
118	30.537,-86.596	14.2	14.2	12.2	90.1	natural	31.2	19.9	0.2

Notes for Table 7.1: Mean dbh (diameter at 1.37 m) and mean height is for all trees ≥ 10 cm dbh.

In order to provide an old-growth reference, height and dbh of trees in a longleaf pine forest representative of old-growth known as the Wade Tract (30.758, -84.001) located near Thomasville, Georgia were measured in October 2014. The tract was previously described in detail (Noel et al. 1998, Platt et al. 1988, West et al. 1993) and contains many large trees 100-400 years of age. Plots were located in an area roughly 7 ha in size within the south-central portion of the 84 ha tract. Nine variable radius plots were sampled using a 10 basal area factor prism. All trees within each plot were longleaf pine. Plot centers were established by selecting a large presumably old-growth tree based on dbh and age relationships reported in Platt et al. (1989) and West et al. (1993). Plot center trees ranged in dbh from 46 to 70 cm with the majority greater than 60 cm dbh, suggesting an age range of 100 years to 396 years at sampling, and a median age of 248 years (West et al. 1993). Plot basal area and density ranged from 9 to 25 m^2 ha^{-1} and 38 to 395 tree ha^{-1}, respectively, and the corresponding means were 16 m^2 ha^{-1} and 102 trees ha^{-1}, respectively.

Longleaf pine biomass

A total of 117 longleaf pine trees representing the range in dbh and height in stands older than five years of age were selected for biomass sampling (Table 7.2). In addition to subsampling within the defined stands, two older isolated trees (188 years of age) in a tract with scattered old trees were harvested at Florida, for a total of 119 trees. The majority of planted pine in the 5-year-old stand was in the grass stage (an extended seedling stage in which shoot elongation is inhibited) and allometric equations based on ground-line diameter were used to predict aboveground and below-stump biomass previously reported by Samuelson et al. (2014). Tree biomass data collected in Georgia stands older than five years were combined with biomass data from the other sites to develop new allometric equations and biomass estimates for Georgia stands older than age 5 years.

For trees < 18 cm dbh, the aboveground biomass of the entire tree was collected and separated into foliage, branch and main stem components and oven-dried at 70°C for foliage and 105°C for woody tissues until reaching a constant mass. Trees larger than approximately 18 cm dbh (crown development greatly increased at a mean dbh of 18 cm and trees required substantially more time to sample) were subsampled following procedures described by Samuelson et al. (2014). Stand-specific relationships between branch green weight, branch diameter and oven dry weight of foliage mass and branch mass were developed to predict individual tree foliage and branch dry mass from total branch green weights, and all regressions were linear with a minimum R^2 of 0.84 for branch mass and 0.83 for foliage mass. Data were pooled by stand to develop regressions between green and oven-dried disk weights and tree stem mass was calculated by summing the predicted dry weights for each stem section.

Table 7.2. Characteristics of longleaf pine trees used to develop allometric equations.

Stand location	Age (years)	Dbh range (cm)	Height range (m)	Aboveground n	Below-stump n	Mean pit area (m^2)
Georgia	12	2.9-16.8	2.3-10.4	10	4	1.06
	21	3.2-16.2	4.5-14.4	9	3	1.08
	64	22.8-36.9	16.1-23.5	3	3	2.10
	87	34.3-48.6	27.3-29.9	3	3	3.16
Florida	9	2.4-9.5	2.1-6.4	5	5	1.05
	19	6.0-16.9	7.2-10.6	5	4	1.19
	43	10.9-21.5	10.3-14.7	5	5	1.35
	50	13.2-23.8	10.0-13.3	5	5	1.44
	85	30.3-49.9	20.3-22.9	5	5	3.03
	118	32.6-51.0	18.7-22.0	5	5	3.08
	188	34.5-47.2	14.3-14.5	2	2	3.28
Louisiana	8	3.3-11.1	2.3-8.0	10	5	1.04
	18	3.6-23.4	3.7-13.5	10	5	1.16
	34	11.0-33.3	9.6-22.1	10	5	1.53
	60	31.6-42.8	21.9-24.8	3	3	2.30
	83	45.9-54.3	26.6-30.4	3	3	3.42
North Carolina	15	6.4-22.7	6.9-16.5	10	5	1.25
	25	7.0-22.5	7.6-14.8	9	4	1.22
	65	21.0-39.4	13.2-23.0	4	4	2.04
	79	42.6-54.3	19.8-25.8	3	3	2.94

Notes for Table 7.2: dbh is diameter at 1.37 m height.

For below-stump sampling, depending on the site and tree size, all or a subset of harvested trees was randomly selected for excavations. Across all sites in stands older than 5 years a total of 81 trees were excavated (Table 7.2). The square area of the excavation pit ranged from the minimum set at 1 m^2 for the smallest diameter trees, a standard size for sampling *Pinus* plantations in the southern United States (Butnor et al. 2016), to a maximum of 4 m^2 for the largest diameter trees. Pit size was limited to a maximum of 4 m^2 due to the time demanding nature of manual excavations. The area of the stump was excluded from the pit area and length and width of the pit was measured beginning at the stump edges. Pit size for remaining trees was scaled with tree dbh approximated by: pit area (m^2) = 0.8322*e $^{0.0301*dbh}$ (Butnor et al. 2016) (Table 7.2).

All soil in the pit to a 1 m depth was sieved using a 5 mm hardware cloth and roots $\geq$ 5 mm in diameter were collected. Lateral roots branching off the main tap root were cut at the pit wall. The pit was then excavated around the entire tap root and the tap root was removed. When required, a mini excavator was used to dig and lift out the tap root. The length of all tap roots was measured. Tap roots were dried to a constant mass in a large walk-in-oven (Model LR-96B, LR Technologies, Los Angeles, California, USA).

Longleaf pine allometric models

For each biomass component (foliage, live branch, stem, tap root and lateral root mass in pits), model performance and fit were tested on two forms of allometric equations:

$$W = \beta_o dbh^{\beta_1}$$

$$W = \beta_o dbh^{\beta_1} height^{\beta_2}$$

(where W is biomass per tree and height is total tree height) using nonlinear regression techniques (MODEL procedure in SAS software, SAS version 9.3, SAS Institute, Cary, North Carolina, USA) and nonlinear seemingly unrelated regressions to account for the additivity among components of tree biomass and total tree biomass (Parresol 2001, Zhao et al. 2015). Models were selected based on analyses of residuals and goodness-of-fit parameters including *P* values, pseudo-R^2 (1-SS_{error}/$SS_{corrected\ total}$) and root mean square error (RMSE). The best models for all biomass components were based a multiplicative error structure (i.e. $lnW = ln\ \beta_o + \beta_1 lndbh + \varepsilon$ or $lnW = ln\ \beta_o + \beta_1 lndbh + \beta_2 lnheight + \varepsilon$) to stabilize heteroscedastic variance (Dong et al. 2015). Equations for foliage and branch biomass and tap root included only dbh and for stem mass and pit lateral root mass included dbh and height (Table 7.3). The correction factors for systematic bias introduced by anti-log transformation were calculated following Snowdon (1991) and applied to each component model. Scatter plots of residuals showed no evidence of bias for any of the final models. Allometric models were used to predict the aboveground and below-stump biomass of all longleaf pine trees $\geq$ 1 cm dbh and $\geq$ 2 m height tallied in the forest inventories.

Table 7.3. Regression models for longleaf pine tree biomass.

Biomass component	Variable	Coefficient	Estimate	Standard error	P	CF	Pseudo-R^2
Aboveground							0.97
Stem		β_0	0.018	0.001	<0.001	1.08	0.98
	dbh	β_1	2.098	0.069	<0.001		
	height	β_2	0.942	0.087	<0.001		
Foliage		β_3	0.024	0.002	<0.001	1.02	0.79
	dbh	β_4	1.966	0.041	<0.001		
Live branch		β_5	0.001	0.0001	<0.001	1.05	0.75
	dbh	β_6	3.215	0.044	<0.001		
Below-stump							0.89
Lateral root		β_7	0.015	0.003	<0.001	1.42	0.62
	dbh	β_8	2.779	0.2416	<0.001		
	height	β_9	-0.729	0.287	0.013		
Tap root		β_{10}	0.006	0.001	<0.001	1.05	0.88
	dbh	β_{11}	2.768	0.043	<0.001		

Notes for Table 7.3: Stem includes bark. The final model for aboveground mass was kg tree^{-1} = $\beta_0 dbh^{\beta_1} height^{\beta_2} CF_{stem} + \beta_3 dbh^{\beta_4} CF_{foliage} + \beta_5 dbh^{\beta_6} CF_{branch}$ where dbh is diameter at 1.37 m in centimeters, height is total height in meters, and CF is the correction factor for systematic bias introduced by anti-log transformation. The final model for below-stump biomass was kg tree^{-1} = $\beta_7 dbh^{\beta_8} height^{\beta_9} CF_{lateral\ root} + \beta_{10} dbh^{\beta_{11}} CF_{tap\ root}$.

Other tree species biomass

Allometric equations from the literature were used to predict aboveground biomass from dbh for species other than longleaf pine (Jenkins et al. 2003). Below-stump biomass of other pine species was predicted using the allometric equation developed in this work, because site may have more influence on tap root development than species (Gibson et al. 1986). We assumed that the ground penetrating radar (GPR) measurement of coarse roots (described under plot-level root biomass methods) captured all hardwood coarse root biomass.

Live understory biomass

The live understory was measured in Georgia, Louisiana and North Carolina stands but not Florida stands, because of prescribed burning prior to scheduled sampling. Live understory was considered the sum of woody stems ≥ 1 m and < 2 m height, and ground cover vegetation (all vegetation < 1 m in height). Procedures for sampling woody stems ≥ 1 m and < 2 m height and ground cover vegetation followed those described in Samuelson et al. (2014). Ground cover biomass, and ground line diameter and height of all woody stems ≥ 1 m and < 2 m height were measured within five (Georgia) or 10 (Louisiana and North Carolina) 1 m^2 circular sampling rings located in each subplot using the stratified random polar coordinates method (Gaiser 1951). Allometric equations published for the 5-year-old longleaf pine stand (Samuelson et al. 2014) were used to predict aboveground biomass for longleaf pine; otherwise, species specific or general allometric equations from were used to predict aboveground biomass of understory woody stems from ground line diameter (Robertson and Ostertag 2009). We assumed that GPR measurements accounted for coarse root mass of the understory. Ground cover biomass data were previously published by Samuelson et al. (2014) and Gonzalez-Benecke et al. (2015*b*).

Live understory C for FL stands was predicted from the nonlinear relationship between mean stand live understory C and total basal area (m^2 ha^{-1}) developed using data from the other sites. When the outlier for understory C from the 60-year-old stand in Louisiana was not included in the regression (*n* = 13), live understory C (Mg C ha^{-1}) was significantly and negatively related to total basal area (y = 2.0911*e$^{-0.0560totalbasalarea}$, R^2 = 0.40, *P* < 0.001) and similar to the model structure reported by Gonzalez-Benecke et al. (2015*b*). The high value (5 Mg C ha^{-1}) in the 60-year-old stand in Louisiana was due to dense patches of longleaf pine seedling regeneration recorded on two of the subplots.

Plot-level root biomass

Fine root biomass from manual coring and plot-level coarse root biomass estimated by GPR were measured at all sites except Florida. Ground penetrating radar cannot readily detect dead roots, fine roots or separate roots by species; hence GPR estimated root mass includes live coarse root biomass regardless of species (Butnor et al. 2003, Butnor et al. 2012*a*). A 100 m^2 measurement plot was located at the center of each subplot. Plots were prepared by cutting woody brush and herbaceous cover to the ground level and removing surface debris. Ground penetrating radar data were collected with a SIR-3000 radar unit (Geophysical Survey Systems Inc. (GSSI), Nashua, New Hampshire, USA) connected to 1500 MHz antenna along (21) 10 m transects spaced 50 cm m apart in each plot. Post-collection data processing and root mass quantification were previously described by Samuelson et al. (2014). Ground penetrating radar reliably detects belowground

lateral roots under suitable soil conditions, but the area directly beneath trees where tap roots and large overlapping lateral roots reside is largely underestimated by GPR (Butnor et al. 2016). There is overlap between below-stump biomass modeled with allometric equations and coarse root mass estimated with GPR. Butnor et al. (2016) determined that GPR detected 100% of below-stump biomass of longleaf pine trees < 3.5 cm dbh, therefore the amount of root mass estimated by allometric modeling of below-stump mass of trees ≥ 3.5 cm dbh was deducted from the GPR estimates to eliminate double counting of mass between methods. The GPR data previously used for Georgia stands (Samuelson et al. 2014) were reprocessed using the current protocol.

For live fine root (< 2 mm diameter) sampling, large diameter (15 cm) soil cores were collected 2 m from subplot center at 0°, 90°, 180°, and 270° from north in each subplot to a depth of 50 cm. Soils were dry sieved in the field. In the laboratory, live roots were washed and oven-dried at 65° C to a constant mass. Total live root mass C was considered the sum of below-stump C of pines ≥ 3.5 cm dbh, GPR detected lateral root C and fine root C. For smaller pines (< 3.5 cm dbh), GPR was assumed to account for below-stump C. The sum of fine root C and GPR lateral root C was predicted for Florida stands from the linear relationship between the sum of fine root C and GPR lateral root C (Mg C ha^{-1}) and below-stump C of trees ≥ 3.5 cm dbh (Mg C ha^{-1}) and site index (SI base age 50 years in meters) developed from the other 14 stands (y = 14.228 + 0.3806below-stump C - 0.53750SI; R^2 = 0.64; *P* = 0.002).

Detritus

Coarse woody debris (≥ 7.6 cm diameter) and fine woody debris (≥ 2.5 cm and < 7.6 cm diameter) were sampled following a modified approach of the planar intersect technique (Harmon and Sexton 1996) and sampling procedures described in detail by Samuelson et al. (2014). Briefly, four 56.4 m transects were positioned 45°, 135°, 225° and 315° from north in each subplot and the number, diameter at the line intercept, and decay class of coarse woody debris intersections to a 2 m height along the entire transect and the number of fine woody debris intersections along a 22.6 m subsection were recorded. Samples of the forest floor were collected at the time of inventory measurements from four 50 cm diameter rings placed 2 m from subplot centers at 0°, 90°, 180°, and 270° from north. All woody detritus ≥ 2.5 cm diameter was discarded from forest floor samples and the forest floor was considered the sum of three categories: 1) duff (dark, partly decomposed organic material) above the mineral soil, 2) litter on top of duff, including recognizable plant parts such as leaves, flowers, and twigs < 0.6 cm in diameter, and 3) very fine woody debris (≥ 0.6 cm and < 2.5 cm in diameter) (Smith et al. 2013). Samples were composited by category and subplot and oven-dried at 70°C until reaching a constant mass.

The basal area of decaying stumps was highest in the two youngest stands known to be previously occupied by pine plantations (35 and 21 m^2 ha^{-1} in the 5 and 8-year-old stands, respectively) and otherwise ranged from 0 to 12 m^2 ha^{-1} in older stands (Table 7.1). Carbon in decaying stumps was previously estimated for the 5-year-old stand (5 Mg C ha^{-1}) (Samuelson et al. 2014) and recalculated following Wang et al. (2012) (6 Mg C ha^{-1}) and likely represents the maximum C addition from decaying stumps in stands we sampled. Carbon in decaying stumps was not included in this new analysis, because the year of mortality was unknown for all stumps in all stands and

lack of information on stump decay rates across sites. Therefore, only coarse woody debris was considered in the down dead wood pool.

To estimate aboveground C in the standing dead wood pool (trees with dbh ≥ 1 cm and height ≥ 2 m), the amount of live tree C was estimated as previously described. The same decay-class reduction factors used for coarse woody debris were used for estimating the decay class of standing dead trees. In addition, the degree of retention of branches and twigs was also considered in determining the decay factor. No standing dead trees exhibited broken tops and all standing dead trees fell into decay class 1 (no change in mass). Based on the range of 3-12% in the ratio of foliage to total aboveground mass for hardwoods and 10-30% range for softwoods (Jenkins et al. 2003), 8% of aboveground biomass was subtracted from hardwood biomass and 20% subtracted from pine biomass to account for foliage loss in standing dead trees. We recognize that in some cases branch biomass in standing dead trees may be overestimated. Belowground C of standing dead trees was not estimated, since the number and sizes of dead trees were small, the exception being the 118-year-old stand in which three dead longleaf pine trees (20-32 cm dbh) and one dead oak tree (27 cm dbh) were tallied on one subplot. Based on the longleaf pine below-stump to shoot ratio for that stand (0.22) below-stump C of standing dead wood in longleaf pine was less than 1 Mg C ha^{-1} assuming no decomposition.

Plant and detritus C concentration

Carbon concentrations were measured in Georgia, North Carolina and Louisiana stands. Carbon concentration sampling protocols for plant tissues and litter and duff pools were described by Samuelson et al. (2014) and concentrations were determined by dry combustion with detection by thermal conductivity (Flash EA 1112 Series C/N analyzer (ThermoFinnigian Instruments, Milan, Italy). Ranges in C concentrations across stands within a site were similar and no significant effects of stand age on C concentrations were observed (data not shown). Therefore, values were averaged across all stands (Table 7.4) and the means used in calculating C density. The C concentrations of live trees and live woody stems ≥ 1 m and < 2 m height of species other than longleaf pine was assumed to be 50% (Woodbury 2007). To calculate ground cover C, ground cover was separated into graminoid, woody and "other" classes for C concentration measurements. The C concentration was measured by category on two composite samples from each subplot that were averaged by stand and then averaged across stands (Table 7.4). The C density was summed across categories. Because of low coarse, fine and very fine woody debris in all stands and the lack of range in decay classes, their C concentration was assumed to be 50% (Prichard et al. 2000, Harmon et al. 2008).

Table 7.4. Carbon concentrations in longleaf pine forests.

Component	Carbon concentration (%)
Longleaf pine	
Foliage	51.27 (0.25)
Stem wood	51.97 (0.31)
Coarse root	51.12 (0.24)
Fine root	43.59 (0.87)
Forest floor	
Litter	50.54 (0.41)
Duff	41.52 (2.14)
Groundcover	
Graminoid	47.38 (0.62)
Woody	50.36 (0.60)
Other	46.93 (0.52)

Notes for Table 7.4: Standard errors represent variation among the 20 stands.

Soil organic C and soil texture

In Georgia, Louisiana and North Carolina stands, soil samples were collected at 2 m, 5 m, and 11 m from each subplot center at 0°, 90°, 180°, and 270° from north (12 locations total per subplot) at 0-10 and 10-20 cm depths (24 samples) using a 19 mm diameter push tube. In Florida stands, samples were collected only at 5 m from each subplot center (a total of four locations per subplot). At all sites, a 10 cm diameter bucket auger was used to collect samples at 20-50 and 50-100 cm depths from two of the soil sampling locations in a subplot. Subsamples were composited by depth for each subplot. Soil was air dried and passed through a 2 mm sieve to separate roots and rocks. Total soil C concentration was determined by dry combustion with detection by thermal conductivity (Flash EA 1112 Series C/N analyzer (ThermoFinnigian Instruments, Milan, Italy). Soil bulk density was measured at the same depths at one randomly selected location in each subplot using a 57 mm diameter core (0200 Soil Core Sampler, Soil Moisture Equipment Corp., Goleta, California, USA) and determined as described by Samuelson et al. (2014). Average texture to a 100 cm depth was determined by averaging the results of particle size analysis using the hydrometer method (Bouyoucos 1962) of soil from the four depth intervals weighted by depth length.

Statistical analysis

The stand was the sample unit and values for each subplot were averaged by stand. All analyses were performed using SAS version 9.3 (SAS Institute, Cary, North Carolina, USA). Linear ($Y = \beta_1 x$), power ($Y = \beta_1 x^{\beta_2}$), saturation ($Y = \beta_1 x/(\beta_2+x)$), Chapman-Richards ($Y = \beta_1(1-e^{-\beta_2 x})$), and negative exponential ($Y = \beta_1 e^{-\beta_2 x}$) functions were tested to determine relationships between C pools and stand age. The best models selected based on plots of residuals, pseudo-R^2, RMSE and *P* values. Live tree C from the old-growth Wade tract was not included in model fitting. Relationships between C stocks and stand structure were examined by regressing the residuals of

the equations against total basal area and density using stepwise linear regression. Relationships between tap root depth and tree dbh, height, age and percent sand, silt and clay to a 100 cm depth were examined using linear and nonlinear regression.

Results

Ecosystem C, which included all pools except soil C, was best modeled with a saturation function (Figure 7.3a; Table 7.5). The predicted asymptotic maximum of the nonlinear equation for ecosystem C was 119 ($\pm$22) Mg C ha^{-1}, and the residuals of the nonlinear equation were positively related to basal area ($R^2 = 0.60$, $P < 0.001$). Live tree C (aboveground C of trees ≥ 1 cm dbh and ≥ 2 m height) was also best modeled with a saturation function with a predicted asymptotic maximum of 87 ($\pm$25) Mg C ha^{-1} (Figure 7.3b; Table 7.5). The residuals from the nonlinear equation were positively related to basal area ($R^2 = 0.58$, $P < 0.001$). Live understory C (sum of aboveground C of woody plants ≥ 1 m and < 2 m height and ground cover C) was not related to stand age and represented 14 to 24% of ecosystem C in stands younger than 10 years of age and on average 2% of ecosystem C in older stands (Figure 7.3c).

Live root C based on below-stump C (for pines of which the great majority was longleaf pine) or total live root C (the sum of below-stump, live fine root, and GPR lateral root C), was best modeled with a power function (Figure 7.4a; Table 7.5), and the residuals of the nonlinear equations were positively related to basal area in both cases ($R^2 > 0.70$, $P < 0.001$). Average total live root C was nearly double mean below-stump C, mainly due to the addition of lateral root C detected by GPR rather than fine root C. Fine root C contributed from < 1 to 2 Mg C ha^{-1} (data not shown). Total live root C was on average 32% of ecosystem C. The root to shoot ratio (R/S) declined nonlinearly with stand age and was best modeled with a power function (Figure 7.4b). Excluding the grass stage stand from the average, mean R/S based on total live root C to total live aboveground C was 0.52 and mean R/S based on longleaf pine below-stump C to longleaf pine aboveground C was 0.26. Tap root depth increased with increasing dbh, average percent sand in soil to a 100 cm depth and tree age, with 47% of the variation in tap root depth explained by dbh alone in the model and 76% explained with all three variables in the model (Figure 7.5; Table 7.5). Average percent sand in soil was 61%, 71%, 92%, 93% at the Louisiana, Georgia, North Carolina and Florida sites, respectively (Table 7.1).

Forest floor C was best modeled with a Chapman-Richards function (Figure 7.6a; Table 7.5), and residuals were positively related to basal area ($R^2 = 0.20$, $P = 0.049$). Maximum down dead wood was <1 Mg C ha^{-1} and unrelated to stand age or stand structure (Figure 7.6b). With the exception of the 118-year-old stand, standing dead C was less than 2 Mg C ha^{-1} (Figure 7.6c) and unrelated to stand age or structure. The total of forest floor C and standing and down dead wood C was on average 9% of ecosystem C.

Soil C to 100 cm was generally lower in Florida stands (32 to 58 Mg C ha^{-1}) and highest in Louisiana stands (79 to 98 Mg C ha^{-1}), and exceeded ecosystem C in stands less 20 years of age and in several older stands (Figure 7.7). No significant relationships between soil C and stand age or structure were observed, but soil C was significantly related to SI (soil C = 22.424 + 2.575SI, $R^2 = 0.25$, $P = 0.026$).

77

Table 7.5. Regression models for longleaf pine forests.

Dependent variable	Model form	β_1	β_2	β_3	β_4	Model P	Pseudo- R^2
Ecosystem C	S	119.165 (21.596)	31.326 (14.669)			<0.001	0.64
Live tree C	S	87.321 (24.765)	44.267 (28.247)			<0.001	0.57
Below-stump C	PWR	1.806 (0.900)	0.433 (0.122)			<0.001	0.48
Total root C	PWR	4.190 (1.186)	0.388 (0.070)			<0.001	0.69
Forest floor C	CR	4.462 (0.375)	0.0778 (0.025)			<0.001	0.43
Tap root depth	PWR	0.240 (0.179)	0.324 (0.080)	1.098 (0.164)	0.229 (0.062)	<0.001	0.76
Root/shoot							
Below-stump	PWR	2.335 (0.612)	-0.657 (0.103)			<0.001	0.64
Total root	PWR	3.568 (0.962)	-0.566 (0.101)			<0.001	0.58

Notes for Table 7.5: Abbreviations are: S, saturation function $y = \beta_1 age/(\beta_2 + age)$; PWR, power function $y = \beta_1 age^{\beta_2}$; CR, Chapman Richards function $y = \beta_1(1-exp^{\beta_2 age})$. The model for tap root depth was $y = \beta_1 dbh^{\beta_2} sand^{\beta_3} age^{\beta_4}$.
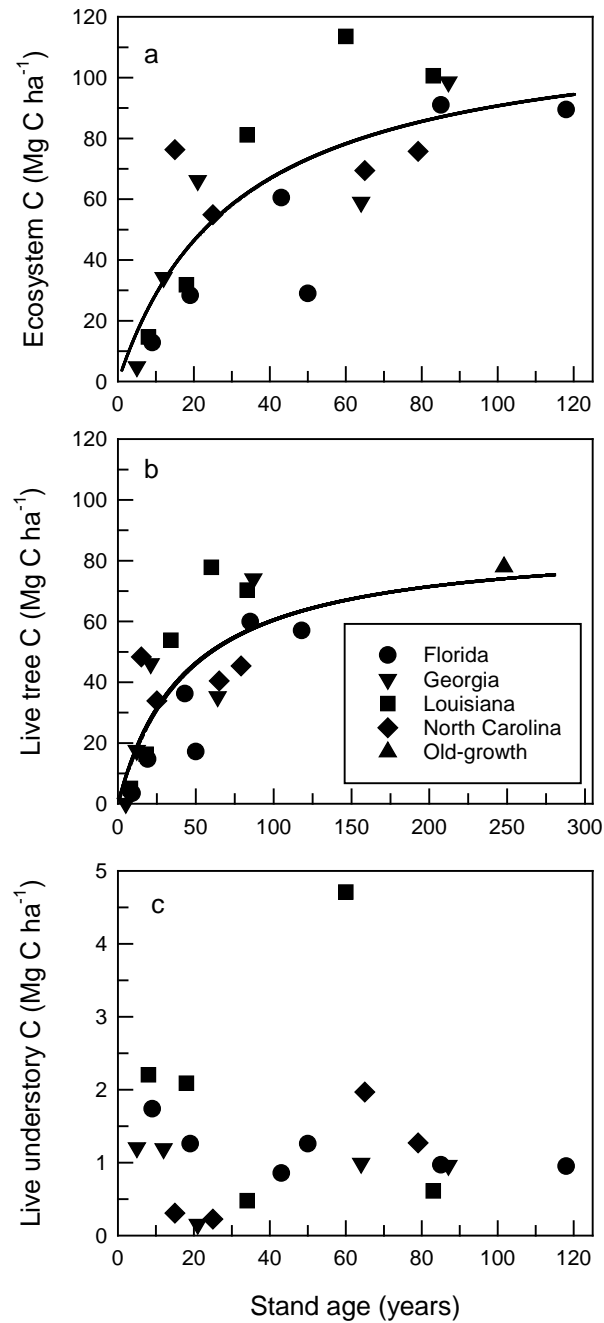
Figure 7.3. Ecosystem C of longleaf pine forests increases with stand age with 79% of the maximum accumulated by age 120 (a) and mainly driven by age-related increases in live tree C (b). Live tree C of an old-growth tract in Georgia was similar to the mean prediction. Live understory C was age-independent (c).
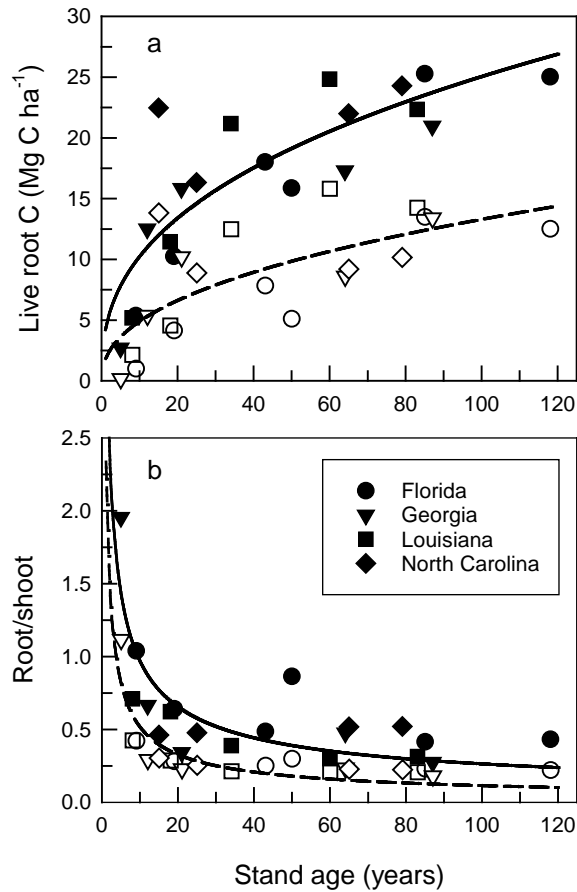
Figure 7.4. Live root C of longleaf pine forests increases with stand age (a) but nearly doubles when all live root C (ground penetrating radar detection of lateral root C, fine root C and below-stump C) are included (solid line) compared to below-stump C alone (dashed line). The root to shoot ratio declines with stand age (b), and the ratio of all live root C to live aboveground C (solid line) is higher than the ratio of below-stump C to aboveground C of only longleaf pine (dashed line).
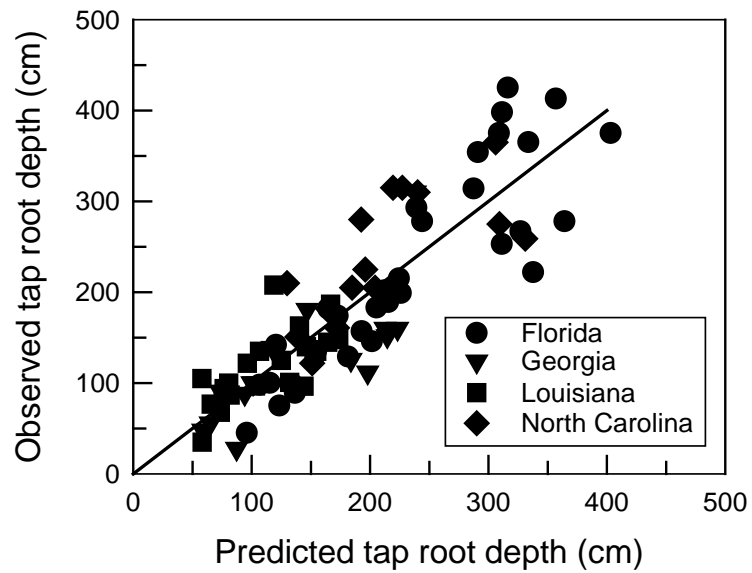
Figure 7.5. Diameter at breast height (1.37 m) and percent sand to a 1 m soil depth explained 76% of the variation in tap root depth in longleaf pine forests. The line represents the 1:1 relationship.
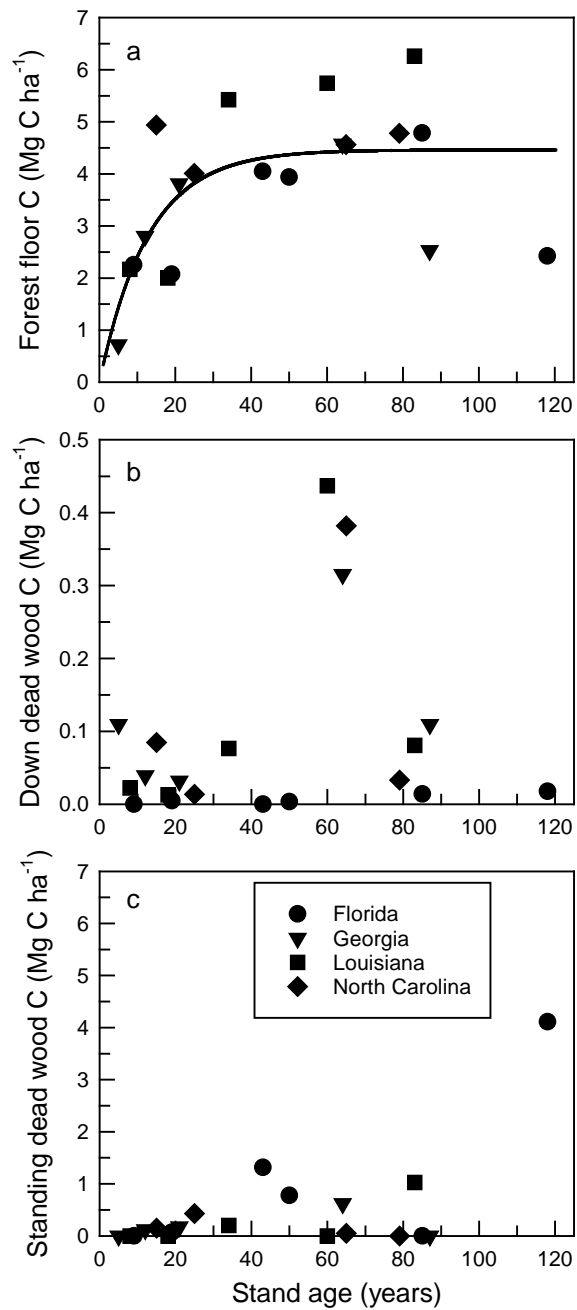
Figure 7.6. Forest floor C increases with stand age until around age 40 (a) whereas down dead wood C (b) and standing dead wood C (c) are age-independent in longleaf pine forests.
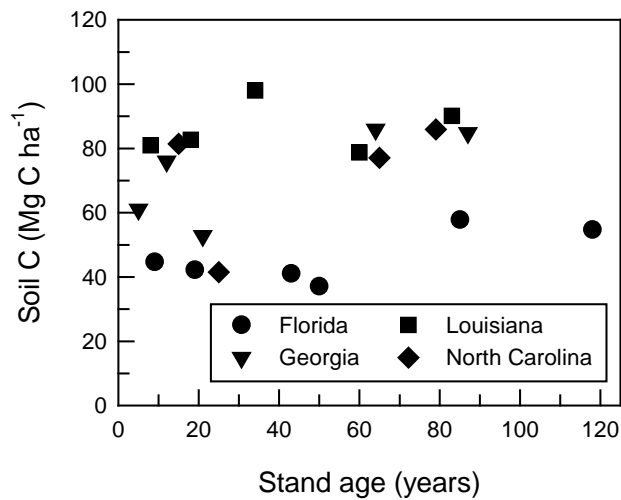
Figure 7.7. Soil C is not related to stand age in a longleaf pine chronosequence located across the species' range.

Discussion

Utilizing a chronosequence assumes that variation among stands is due only to age (Jenny 1941), but for longleaf pine ecosystems meeting this assumption was difficult to impossible, as longleaf forests are now restricted to about 3% of their historical importance and dominated by second growth and plantation stands (Oswalt et al. 2012). However, replicating the chronosequence across the landscape as we did strengthens the inference space if stands and sites are representative of the landscape (Kashian et al. 2013). Oswalt et al. (2012), in an assessment of the current status of longleaf pine forests sampled by the FIA program, reported that as of 2010, 58% of the longleaf pine forest-type consisted of stands ≤ 50 years of age and only 7% of the longleaf acreage was older than 80 years. Thirteen percent of natural stands were ≤ 25 years of age whereas 84% of planted stands were ≤ 25 years of age (Oswalt et al. 2012). In the East Coastal Plain and Piedmont, longleaf pine forests exhibit a bimodal age class structure with peaks in the 61-70 year age class and 0-10 year age class. Thus, our selection of stands represents the current status of longleaf pine forests.

Mean live tree C of longleaf pine (38 Mg C ha^{-1}) was similar to the regional mean live tree C (31 Mg C ha^{-1}) estimated for the longleaf/slash pine (*Pinus elliottii* var. *elliottii*) forest type by Smith et al. (2013). However, regional mean C density for standing and down dead wood, and forest floor pools in the longleaf/slash pine forest type estimated by Smith et al. (2013) were higher than observed in this study. Higher C density in detritus reported by Smith et al. (2013) could be a result of combining longleaf pine and slash pine into one forest type, variation in prescribed burning across the region, and the substantial uncertainty associated with modeling dead wood C and forest floor C at large scales (Coulston et al. 2015). The absence of age-related changes in

down dead wood and standing dead wood, attributes suggested as characterizing old-growth longleaf pine forests (Mitchell et al. 2009), is likely explained by several factors including the lack of legacy wood from previous stands (McGarvey et al. 2015), the stochastic nature of the dead wood C stock (Woodall et al. 2015*b*), and the combustion of dead wood from prescribed burning.

Carbon in living biomass of temperate forests increases hyperbolically with age and the older age classes (up to 200 years) contain two to 10 times as much living biomass C as the youngest age class (Pregitzer and Euskirchen 2004). Longleaf pine ecosystem C was driven by increases in aboveground live tree C related to age and basal area. Similarly, the majority of ecosystem C accumulation in *Pinus contorta*-dominated forests over 270 years was driven by accrual in live vegetation (Kashian et al. 2013), and C accumulation over 250 years in a sub-boreal *Picea* forest were also driven by gains in aboveground large-tree C (Bois et al. 2009). Ecosystem C accumulation over 300 years in *Pinus resinosa* forests was also mainly in response to age-related increases in aboveground live tree C (Powers et al. 2012). In most forest types in the United States, aboveground biomass stabilizes or even increases in late succession (Lichstein et al. 2009). In longleaf pine, predicted ecosystem C at 100 years was nearly four times greater than at 10 years of age and 69% of the modeled maximum, indicating that longleaf stands may continue to accumulate C during as well as beyond the first century. West et al. (1993) reported annual diameter increments in longleaf pine as old as 396 years on the Wade tract in Georgia that contrasted with the expected growth decline in old-growth trees.

Lichstein et al. (2009) estimated a late successional trajectory in aboveground biomass of longleaf pine forests using inventory data from the FIA database and allometric equations (Jenkins et al. 2003), and at a mean canopy age of 100 years live tree C was 50-63 Mg C ha^{-1} (assuming a 2:1 biomass to C ratio), depending on site water availability. Using our saturation function, predicted live tree C accumulation at 100 years was very similar (60 Mg C ha^{-1}) and the modeled asymptotic maximum for live tree C was 87 Mg C ha^{-1}. Martin et al. (2015) simulated live tree C accumulation in longleaf pine stands at US Army Fort Benning using the LANDIS-II Century succession extension model and at 100 years C accumulation was higher (74 Mg C ha^{-1}), most likely because their parameterization data were collected in one ecological region whereas our model and the trajectory by Lichstein et al. (2009) were derived from a wide range of stand ages, structures and site quality.

The Wade tract located in Georgia is recognized as one of the few remaining remnant old-growth tracts of longleaf and provides an opportunity for comparison of modeled maximum C accumulation based on secondary growth and plantations to a forest structure that is the goal of current restoration efforts (Gilliam et al. 2006). The modeled and observed (using biometric estimations) of live tree C for the Wade tract were similar (75 versus 78 Mg C ha^{-1}, respectively), and live tree C of the old-growth tract represented 87% of the modeled maximum, lending support for the selection of stands for our chronosequence. As observed for standing volume in other remnant old-growth pine ecosystems in the southern United States (Bragg 2002), the exceptional size of individuals at the Wade tract did not translate into exceptionally high C density due to the openness of stands and spatial heterogeneity of stocking.

Rooting depth is important to understanding plant productivity and biosphere-atmosphere interactions (Jackson et al. 1999). Reports of maximum rooting depth for mature pines in the southeastern United States include 480-500 cm for longleaf pine, 330-460 cm for *Pinus elliottii* var. *elliottii*, 330 cm for *Pinus echinata*, 400 cm for *Pinus clausa* , 400-610 cm for *Pinus taeda* (Stone and Kalisze 1991, Canadell et al. 1996) and 370-670 cm for 26 and 27 year-old *Pinus taeda*, *Pinus echinata*, *Pinus elliottii* var. *elliottii* and longleaf pine trees grown on the same sites (Gibson et al. 1986). Tap root depths of longleaf pine were therefore within the range of other pine species in the region and the deepest (420 cm) was found in the 118-year-old stand on the deep sandy soils of coastal Florida. Tap root depth was related to tree size and age and percent sand in soil, most likely because of the deeper infiltration depths typical of coastal soils (Schenk and Jackson 2002). Tap root depth in the 5-year-old grass stage stand was variable (16-142 cm), with some depths comparable to 6-year-old planted *Pinus taeda* (26 cm) and 5-year-old planted *Pinus echinata* (25 cm) (Harrington et al. 1989) but the majority deeper, presumably an outcome of preferential allocation of carbohydrates to root growth and storage rather than shoot growth in pines with a grass stage (Keeley and Zedler 1998).

The contribution of roots outside the excavation pits in longleaf pine forests was considerable. The percentage of land area covered by modeled below-stump C was at most 21% in the dense 21-year-old stand and otherwise ranged from 3% to 15%. Coarse roots detected by GPR outside of the excavation pits accounted for 95% of the plot area in stands >30 years of age and 88% of the plot area in stands < 30 years. Heyward (1933) excavated a lateral root of a mature longleaf pine and traced its linear extension to 15 m from the tap root with branching that increased its extension to 22 m, and Hough et al. (1965) report a lateral root spread of 17 m in mature longleaf pine. Linear lateral root spread was 8 m in 30-33 year old longleaf pine trees and 9 m in trees 115-125 years of age (Hodgkins and Nichols 1977). In their review on the maximum extent of tree roots, Stone and Kalisz (1991) conclude that many tree species are capable of producing far-reaching lateral roots in the absence of restrictive soil. While excavation pits offer the advantage of direct quantification of roots concentrated around the stem and may represent the majority of root biomass (Addo-Danso et al. 2016), pit excavations, by themselves, can underestimate root C in species with far-reaching lateral roots such as longleaf pine.

Total root C increased with stand age whereas the R/S decreased with stand age, as reported for a wide variety of forests (Mokany et al. 2006). Thus, root C carrying capacity appears to be lower than aboveground C carrying capacity. A power function and not the saturation model best fit belowground live root C which may be explained by sampling limitations, i.e. limiting the maximum pit size to 4 m^2, combined with the potential for continued lateral root extension in large, old longleaf pine trees. When based on only below-stump and aboveground C of longleaf pine, mean R/S excluding the grass stage (0.26) was comparable to the average 0.26 for gymnosperms (Cairns et al. 1997), 0.18 for temperate coniferous forests (Jackson et al. 1996), and 0.21 for the longleaf/slash pine forest type group (Smith et al. 2013). However, inclusion of all roots and live aboveground biomass increased mean R/S to 0.52. There have been other reports of high R/S in conifers. For example, Litton et al. (2003) observed a range in R/S from 0.21 to 0.68 in 13-year-old *Pinus contorta* var. *latifolia* forests varying in density. Mokany et al. (2006) report a maximum R/S of 0.50 for temperate conifer forests/plantations with a similar range in shoot mass (50-150 Mg ha^{-1}).

Conventional wisdom assumes that longleaf pine allocates more biomass to roots than other southern pines, presumably as an adaptation to drier sites (Hodgkins and Nichols 1977). Our data from pit excavations alone do not support this assumption. Examples of R/S values derived from pit excavations range from 0.31-0.35 in a six-year-old *Pinus taeda* plantation (Samuelson et al. 2004), 0.20 for 22-year-old *Pinus elliottii* var. *elliottii* trees (Howard 1973), and 0.26 for a 23-year-old *Pinus taeda* plantation (Miller et al. 2006). Gonzalez-Benecke et al. (2016) reported an asymptotic minimum of 0.23 (below-stump to woody shoot ratio) for 2- to 27-year-old *Pinus taeda*. However, Van Lear and Kepluck (1995) excavated the entire coarse root systems of three 48-year-old *Pinus taeda* trees and estimated a mean R/S of 0.25. In longleaf pine stands with trees similar in diameter to trees studied by Van Lear and Kepluck (1995) (stands greater than 50 years of age), mean R/S based on all live roots was 0.41, thus suggesting greater allocation to coarse roots in longleaf pine than in *Pinus taeda*, but considerable variation existed among stands. Lacking species comparisons on the same sites among stands of similar forest structure, it remains unclear if high R/S values observed in this study are a result of more intensive sampling, the more open nature of longleaf pine stands that may facilitate greater lateral root spread (Hodgkins and Nichols 1977), or proportionally greater allocation to far-reaching lateral roots in longleaf pine relative to other southern pines. In any case, this work supports the hypothesis of Robinson (2007) of a larger-than-suspected root C pool that may be ecosystem- and perhaps site-specific.

The quantity of soil C in managed pine forests in the southeastern United States is varied and dependent on soil mineralogy and land use history. Highly productive sites can retain large quantities of soil C as well as support stands with higher productivity, and soil C was related to SI in this study. *Pinus taeda* planted on former agricultural land in southwest Georgia contained 268 Mg C ha^{-1} in the upper 30 cm of soil (Johnsen et al. 2013) and a *Pinus taeda* plantation in the coastal plain of South Carolina contained 171 Mg C ha^{-1} in the upper 60 cm (Maier et al. 2012). Mean soil C in the present study was lower these values reported for highly productive sites, but was in the observed range for pine plantations on eroded soils where marginal farmland was converted to pine plantations (Garten 2002, Markewitz et al. 2002, Sartori et al. 2007, Butnor et al. 2012*b*). Soil C was unrelated to stand age in longleaf pine which was expected since the long-term rate of soil C accumulation is slow and changes in the terrestrial C sink are driven mainly by changes in vegetation biomass (Schlesinger 1990). Conversion from agricultural land to forest may lead to increased soil C, though the process is gradual and much of the accumulated C is in the near surface (Nave et al. 2013). In a meta-analysis of 39 studies in the USA, Nave et al. (2013) found that afforestation of agricultural land resulted in small reductions in soil C for the first 15 years followed by gradual increases in soil C compared to non-afforested baseline over time. Prescribed burning periodically reduces the forest floor and C in surface soils, exposing mineral soil, though it has little effect on mineral soil C (Binkley et al. 1992, Lavoie et al. 2010). Soil organic C in longleaf pine forests is explored in more detail in the following Chapter 8. In addition, the need for a better understanding of the contribution of decaying tap root C was identified by this work and new research related to decaying tap root C is described in Chapter 9.

8. Soil Organic Carbon

[Contents of this chapter were extracted from Butnor, J.R., L.J. Samuelson, K.H. Johnsen, P.H. Anderson, C.A. Gonzalez-Benecke C. Boot, M.F. Cotrufo, K.A. Heckman, J.A. Jackson, T.A. Stokes, C.W. Swanston, and S. Zarnoch. 2016. Vertical distribution and persistence of soil organic carbon in fire-adapted longleaf pine stands. In preparation for submission to Forest Ecology and Management]

Introduction

This Chapter expands on our soil C work described in Chapter 7 to better understand soil C dynamics in longleaf pine forests. A key component of forestry has become the responsible management of carbon (C) to ensure that site quality is maintained and to potentially sequester C (Johnsen et al. 2001). Aggrading forests can rapidly accumulate atmospheric C in biomass during the early stages of a rotation, though the persistence of this biomass is ephemeral, making soil the primary long-term C pool. Entry to and exit from soil C pools is slow, the amount of the biomass that enters the soil pool is almost equal to the amount respired on an annual basis (Oades 1988). Managed southern pine systems in the United States are strong sinks for atmospheric C in forest biomass, but increases in soil C have not been observed in stands aged <18 years (Markewitz et al. 2002, Johnson et al. 2003, Johnsen et al. 2013). Over a longer period of 30 years in a loblolly pine (*Pinus taeda)* plantation, Richter et al. (1999) reported that annual accretion of soil C (4 gm^2) was very low (<1%) compared to C in the forest floor (94 gm^2) and tree biomass (426 gm^2). They concluded that despite considerable C inputs to soil, rapid decomposition limited carbon sequestration in mineral soil. Stabilization of organic matter in soil is dependent on chemical composition, climate, moisture retention, soil minerology, pyogenic transformation as well as physical isolation from environmental fluctuations at depth (Oades 1988, Batjes 1996) leading to considerable variability in soil C quantity and residence time among and within sites and regions. In the Southern US, rapid turnover of soil C inputs from forests may be facilitated by coarse sands and low-activity clay mineralogy (Richter et al. 1999).

Longleaf pine (*Pinus palustris* Miller) forests in the southern United States, are being restored and actively managed via planting, thinning and prescribed fire to reduce fuel loads, improve biodiversity, enhance forest resilience (from stand disturbance), provide forest products, and increase C sequestration (Churchill et al. 2013). Longleaf pine exhibits slower growth rates after establishment than other southern pines (Schmidtling 1973), consequently it is seldom managed with intensive silvicultural practices. The stands are planted at lower densities and left for longer rotations, resulting in longer periods between disturbances. New research indicates that longleaf stumps persist in the environment much longer relative to other pine species (see Chapter 9). Longleaf pine are noted for high levels of oleoresin production and have elevated monoterpene levels in coarse roots that may suppress decomposition (Eberhardt et al. 2009). Longleaf pine occurs on a variety of soil types from coastal sands to eroded upland clay soils, but little is known about the quantity and persistence of soil C as well as the role of soil properties on the rate of soil C accumulation across its range.

Longleaf pine ecosystems existed for several thousand years as the dominant forest type across a vast area of the southeastern United States (~37 million ha) (Frost 1993, Schmidtling and Hipkins 1998). These ecosystems were maintained by frequent low intensity fires that suppressed

hardwood competition and supported a diverse assemblage of herbaceous cover in pine savannas. In the Kisatchie National Forest in Southwest Louisiana mean fire return from 1650-1905 was determined to be 2.2 years using fire scars and dendrochronology on remnant longleaf stands (Stambaugh et al. 2011). In the 19th and early 20th centuries the majority (>95%) of the longleaf forest was logged and converted to agriculture (Frost 2006), and poor management led to considerable losses of topsoil. Thus, most current longleaf pine sites experienced millennia of frequent low intensity fire, removal of forest cover including an interruption of fire while experiencing major soil degradation, and now have been returned to longleaf pine as plantations. The long history of frequent fire prior to settlement and use of fire restored systems produced pulses of pyrogenic C (PyC) sometimes referred to as "black carbon" into the soil. PyC can persist for millennia, thus it potentially can be an important avenue of soil C sequestration in terrestrial and marine systems (Jaffe et al. 2013). Prior studies reported that frequent burning in southern pine plantings typically does not impact mineral soil C, though PyC was not specifically quantified and only shallow soil depths of (< 20 cm) were analyzed (Binkley et al. 1992, Lavoie et al. 2010). Therefore, the actual quantity of PyC and its role in long-term storage in longleaf pine forests is unknown.

PyC found in soil is the result of incomplete combustion of biomass under low oxygen conditions. PyC is composed of a spectrum of carbon compounds; being a class rather than a specific material, the 'combustion continuum' has been reviewed elsewhere (Schmidt and Noack 2000, Masiello 2004, Preston and Schmidt 2006, Hammes et al. 2008). In brief, fire transforms these organic compounds into a spectrum of amorphous materials dominated by fused aromatic rings. This material ranges from partially burned woody material to char to pure graphite. PyC becomes more recalcitrant along the spectrum associated with aromatic condensation, persisting from hundreds to thousands of years (Hammes et al. 2008, Ascough et al. 2009). The PyC products have a range of biochemical stability, though in general PyC formed at low temperatures have higher O:C ratios and are more readily degraded than PyC formed at high temperatures (Inoue and Inoue 2009, Spokas 2010, Ascough et al. 2011). The amount of biomass converted to PyC is dependent on feedstock chemistry, combustion temperature and oxygenation. Preston and Schmidt (2006) estimated a conversion rate, of combusted organic matter, of 1-6 % in boreal systems, while others contend that the mean conversion rate is substantially higher e.g. 5-15% (Santin et al. 2016).

To better understand the composition of extant C soil pools and assess the potential of C sequestration of longleaf pine ecosystems, it is necessary to have quantitative data on vertical distribution of C within the soil profile, persistence of C in soil as well as overall stocks. Longleaf pine forests are characterized by longer rotations, fewer disturbances, high fire frequency and potentially more decay resistant roots than other southern pines which could affect soil C dynamics. Key questions include: Does stand age or stage of forest stand development affect the quantity of soil organic C (SOC)? What are the physical characteristics of soil (texture, density, minerology) that influence the C content of soil? How long does SOC persist in these systems? Considering the dependence of longleaf pine ecosystems on fire, is PyC accumulating? Where is it accumulating? Is the legacy of PyC storage found in deeper soils that was not reported in prior studies? Does is PyC substantially contribute to longer soil C residence time?

To address these questions we analyzed the vertical distribution and persistence of soil organic carbon in fire-adapted longleaf pine forests aged 5 to 87 years old to a depth of 1 m for which there

was detailed accounting of biomass C (Samuelson et al. 2014, Samuelson et al. 2016). A total of 14 stands were studied at 3 locations in western Louisiana (5), southwest Georgia (5) and coastal North Carolina (4). Bulk SOC was chemically fractionated into resistant and oxidizable pools, then radiocarbon techniques were applied to quantify persistence of those fractions. Benzene Polycarboxylic Acid (BPCA) markers were used to quantify and characterize PyC (Glaser et al. 1998). This allowed us to analyze the effect of forest stand development (age, stand characteristics, above and belowground biomass C) and soil properties (depth, bulk density, texture, extractable iron) on the vertical distribution and persistence of C in soil. Assessing SOC pools by resistance to oxidation, PyC content, and mean residence in longleaf pine stands across the southern US will provide quantitative data to understand the legacy of past land use, frequent forest fires and current forest management on soil C stocks in longleaf pine stands. Such quantification of soil C stocks will contribute to regional and national efforts to model C storage in soil and guide long-term management efforts.

Methods and Materials

Study areas

Sites selected for this study were part of a larger effort to produce robust allometric equations for biomass estimation, quantify C pools, and develop forest management decision models for biomass accumulation in longleaf pine systems (Samuelson et al. 2014, Gonzalez-Benecke et al. 2015a, Gonzalez-Benecke et al. 2015b, Samuelson et al. 2016). A chronosequence of 14 managed longleaf pine stands were selected for intensive sampling and characterization; they were located in three states across the east-west range of the species. The stands varied in age and basal area within each state and the soils varied between states (Table 8.1). The study sites were selected primarily on forest stand characteristics typical for each region and active management with cyclical prescribed burning. Five stands located on US Army Fort Benning (GA) were sampled in 2012. Five stands located on the Kisatchie National Forest in Vernon Parish, Louisiana (LA) were sampled in 2013. Four stands located on Marine Corps Base Camp Lejeune (NC) were sampled in 2014. Stand coordinates, soil type, drainage class, basal area, site index and date of last 3 prescribed fires are presented in Table 8.1. Stands in NC were typified by deep sands while those in GA and LA had greater clay and silt fractions. Detailed characterization of forest carbon stocks including overstory, understory, ground cover, tap roots, coarse roots, fine roots, dead snags, woody debris, litter and duff are presented by Samuelson et al. (2014), Samuelson et al. (2016). All of the stands were even-aged with a minor component of volunteer *Pinus taeda* or hardwood recruitment and actively managed with an approximate three year fire return cycle. Four of the older stands were naturally regenerated and the others were planted.

Table 8.1. Location and characteristics of longleaf pine stands sampled for soil carbon.

State	Annual rainfall[1] (mm)	Annual air temp[1] (C)	Stand Age (yrs)	Coordinates (Lat., Long.)	Soil series	Soil drainage class	Basal area (m² ha⁻¹)	SI (m)	Origin	Last three burns (year)
GA	1180	18.7	5	32.400, -84.870	Nankin sandy clay loam	WD	0.5	19	Planted	2003 2007 2010
			12	32.373, -84.777	Nankin sandy clay loam	WD	11.5	19	Planted	2005 2008 2010
			21	32.391, -84.789	Troup sandy loam	ED	22.4	20	Planted	2005 2009 2010
			64	32.319, -85.008	Troup-Springhill-Luverne complex	ED to WD	10.2	16	Natural	2003 2008 2010
			87	32.366, -84.785	Troup sandy loam	ED	14.5	19	Natural	2006 2008 2010
LA	1447	18.9	8	30.944, -93.162	Troup sandy loam	MWD	5.2	21	Planted	2006 2008 2011
			18	30.943, -93.192	Beauregard-Malbis complex	MWD	8.0	21	Planted	2006 2007 2011
			34	30.991, -93.134	Briley loamy fine sand	WD	18.2	21	Planted	2007 2009 2012
			60	30.997, -93.019	Malbis fine loamy sand	MWD	20.0	19	Planted	2008 2009 2011
			83	31.024, -92.944	Malbis fine loamy sand	MWD	13.8	21	Planted	2001 2007 2011
NC	1356	17.4	15	34.586, -77.270	Leon fine sand	PD	25.0	25	Planted	2005 2009 2013
			25	34.645, -77.450	Stallings loamy fine sand	PD	17.7	16	Planted	2008 2009 2010
			65	34.705, -77.252	Onslow loamy fine sand	MWD	11.6	15	Natural	2005 2009 2011
			79	34.702, -77.303	Malbis fine loamy sand	MWD	11.2	13	Natural	2007 2009 2012

WD=well drained, MWD=moderately well drained; ED=excessively drained; PD=poorly drained. SI = site index at base age 50.
[1] 30 yr mean (1982-2011) Columbus, GA, Leesville, LA and Jacksonville, NC; NOAA, National Centers for Environmental Information (http://www.ncdc.noaa.gov/cdo-web).

Soil collection

Within each stand, a one ha circular main plot (56.4 m radius) with four 0.04 ha circular subplots (11.3 m radius) were installed (Law et al. 2008). Within a main plot, one subplot was located at the center and three subplots were positioned 35 m from the center at 0°, 120°, and 240° from north. A 1.9 cm diameter push tube was used to collect soil samples for C and texture at 2 m, 5 m, and 11 m from subplot center at 0°, 90°, 180°, and 270° from north (12 locations total per subplot) at depths of 0-10 and 10–20 cm. A 10 cm diameter bucket auger was used to collect soil samples for C and texture at 20-50 and 50-100 cm from two of the soil sampling locations 2 m from the subplot center. Within each subplot, the subsamples were combined by depth resulting a in 224 samples (14 sites x 4 subplots x 4 depths), that were further combined in equal portions into composite sample by depth for each plot (14 sites x 4 depths) for a total of 56 samples. Soil samples for bulk density were collected at 0-10, 10-20, 20-50 and 50-100 cm at one location 2 m north of subplot center using a 5.7 cm diameter soil core (0200 Soil Core Sampler, Soil Moisture Equipment Corp., Goleta, California). Samples were collected during May and June from the GA stands in 2012, LA stands in 2013, and NC in 2014.

Chemical fractionation

Oxidation resistant soil organic C (SOC_R) was isolated from bulk soil organic C (SOC) via selective oxidation with 20% H_2O_2 and 0.33 $\underline{M}$ HNO_3 with a method originally used to isolate charcoal fractions from soil and litter, described by Kurth et al. (2006) and modified by (Ball et al. 2010). In this approach, organic matter and nonresistant soil organic carbon (SOC_{OX}) are digested and converted to CO_2, leaving the SOC_R fraction (e.g. Eusterhues et al. (2005)). One gram of soil was placed in a pre-weighed 240 ml canning jar and 20 mL of 30% (v/v) of reagent grade H_2O_2 in water and 10 ml of 1 $\underline{M}$ HNO_3 were added to the jar to achieve a concentration of 20% H_2O_2 and 0.33 $\underline{M}$ HNO_3. The mixture was left at room temperature for 30 minutes with occasional swirling, then covered with a watch glass and incubated in an oven at 80°C for 24 hrs. The watch glasses were then removed and the samples were left to dry uncovered at 80°C for another 24 hrs. After drying, the samples (jar plus soil) were weighed again, scraped free with a spatula and ground to a fine powder using a mortar and pestle. To avoid contamination, all glassware, mortars, pestles, and chemical spatulas were cleaned with a laboratory grade cleaner (Micro SD, International Products Corp, Burlington, NJ USA) and soaked overnight in a 1% hydrochloric acid bath (HCL), and then rinsed with deionized water. C concentration was determined by dry combustion with detection by thermal conductivity (Flash EA 1112 series CN analyzer, Thermo Finnigan Instruments, Milan, Italy).

Pyrogenic carbon (PyC) content

Benzene Polycarboxylic Acid (BPCA) marker quantification yields conservative, yet consistent estimates of PyC (Glaser et al. 1998, Wiedemeier et al. 2013). Samples of SOC and SOC_R (14 stands X 4 depths) were analyzed using high performance liquid chromatography equipped with a photo diode array detector (Wiedemeier et al. 2013) after a digestion process with concentrated HNO_3 described Boot et al. (2015). BPCA extraction and analyses were conducted at the EcoCore

Analytical Service facility in Fort Collins, CO (http://ecocore.nrel.colostate.edu/). BPCA content of SOC_{OX} was calculated as the difference between SOC and SOC_R. BPCAs are formed from the cleaving of condensed aromatic structures into single aromatic rings distinguished by a range of carboxylic acid moieties. More highly condensed ring structures have a greater proportion of B6CAs while structures with fewer fused rings have proportionally more B3CAs, providing insight into to the degree of biochemical stability (Glaser et al. 1998, Boot et al. 2015, Wiedemeier et al. 2015). Since the formation of BPCAs causes a net loss of C, there is not a 1:1 ratio between PyC and BPCA markers. Depending on the molecular structure of the PyC, BPCA contents are 2-5 times lower than actual PyC contents. A conservative correction factor of 2.27 was applied to bulk BPCA contents to estimate soil PyC stocks (Glaser et al. 1998).

Radiocarbon analysis (^{14}C)

Samples of SOC and SOC_R (14 stands X 4 depths) were prepared by combustion with CuO and Ag to produce CO_2 which was converted to graphite (Vogel et al. 1987) at Michigan Technological University, Houghton, Michigan, USA. Radiocarbon content was analyzed by accelerator mass spectrometry at the Center for Accelerator Mass Spectrometry (CAMS), Lawrence Livermore National Lab (LLNL), Livermore, California, USA. SOC_{OX} Δ ^{14}C levels were calculated as the difference between SOC and SOC_R $\Delta^{14}C$ values. Radiocarbon data are reported as fraction modern (Fm) which is the ratio of ^{14}C / ^{12}C in the sample to modern atmospheric ^{14}C / ^{12}C conditions circa 1950, prior to extensive aboveground testing of nuclear weapons (Stuiver and Polach 1977). Mean residence times (MRT) of SOC, SOC_{OX} and SOC_R were calculated using a time-dependent steady-state model (Trumbore 1993, Torn et al. 2009).

Soil texture, extractable Fe analysis and bulk density
Soil was air-dried for several weeks and passed through a 2 mm sieve to remove roots and rocks. Particle size (soil texture) analysis was performed by hydrometer method (Bouyoucos 1962). Fe was extracted from soil using Mehlich-3 extractant (Mehlich 1984) and analyzed with inductively coupled plasma spectrometry by Spectrum Analytic Inc. Washington Court House, Ohio, USA) (Mehlich 1984). Bulk density samples were oven-dried at 105 °C for 96 h and then passed through a 2 mm sieve, and roots and rocks were extracted and weighed separately. Rock volume was determined by water displacement. The effect of root volume on bulk density was negligible. Soil bulk density was then calculated by soil mass (minus rocks and roots) / soil volume (minus rock volume) (Law et al. 2008).

Statistical analysis

The approach taken was to first consider if forest stand development and biomass stocks were affecting accumulation of soil C among fractions, then analyze the vertical distribution, residence time and soil properties related to C retention. Stepwise multiple linear regression (0.25 s.l. level for entry, 0.05 s.l. for exit) was used to determine whether belowground C stocks to a depth of 1 m (SOC, SOC_R, SOC_{OX} and PyC) from 14 longleaf pine forests were dependent on any stand biomass parameters (C stocks, stand age, basal area) with Proc Reg (SAS Institute Inc. 2013) using SAS/STAT 9.4 software (SAS Institute, Cary, NC, USA).

The vertical distribution of C concentrations between states was analyzed with two-way analysis of variance. The effect of soil depth and state on soil C fractions, physical properties, fraction modern and mean residence time of C was analyzed with Proc Mixed (SAS Institute Inc. 2013) using the five stands per state as replicates. The repeated measures option was used with soil depth as the repeated factor, where soil was collected from several depths at a given forest stand. The depth intervals were uneven (0-10, 10-20, 20-50, 50-100 cm), so based on theoretical grounds of unequal spacing and comparison of the AICC between several option types, we decided to use spatial power covariance matrix. Mean separation analysis within states by depth was performed with the Bonferroni correction. This adjustment uses the pooled variance across states and depths from the overall analysis which may result in significances that are slightly different from those based on the individual standard errors alone. The Bonferroni method performed all six possible pairs of comparisons between the four depths and ensured an experiment-wise error rate of 0.05 for the set by using the alpha=0.05/6=0.0083 level for testing each pair. Differences in stocks of SOC, SOC_{OX}, SOC_R, and PyC in the upper 1 m of soil between states were analyzed with one-way analysis of variance Proc Mixed (SAS Institute Inc. 2013).

Stepwise linear multiple regression was applied to analyze the relationship between dependent concentrations of C fractions in soil (SOC, SOC_{OX}, SOC_R, and PyC) and independent soil properties (texture, depth, bulk density, Fe concentration) across the 14 longleaf pine with Proc Reg (SAS Institute Inc. 2013). Mean residence time of SOC_{OX} and SOC_R was also analyzed with stepwise linear multiple regression using the above soil properties with the addition of variables related to BPCA speciation (%B6CA, %B5CA, %B4CA, %B3CA, %B4CA/B6CA, and %B5CA/B6CA). Mean residence time of bulk soil (SOC) was similarly analyzed using soil, BPCA variables, plus the percent of SOC comprised of SOC_R and PyC.

Results

Stand age, biomass and soil C stocks

To analyze potential effects of forest stand biomass accumulation on soil C, it was necessary to scale soil C concentration same units as biomass C (Mg C ha^{-1}). C concentrations of SOC, SOC_R, SOC_{OX} and PyC were converted to Mg C ha^{-1} using soil bulk density and summed across all sample depths to yield a C stock (0-1 m) for each (Table 8.2). Stepwise multiple regression analysis was applied to determine if the soil C fractions were dependent on stand-level biomass C stocks (Mg C ha^{-1}) including: live aboveground C (all aboveground parts of living plants), live belowground C (all live roots), non-living C (standing dead trees, coarse woody debris, forest floor, etc.), live C (above + belowground C) and total C (live + dead C), as well as stand age and basal area. Despite wide ranges in biomass C stocks across the 14 stands (Table 8.2), there were no significant relationships ($p > 0.05$) between SOC, SOC_R, SOC_{OX} and PyC and any biomass parameter (C stocks, stand age, basal area). Stand age and biomass were dropped from further consideration and the sampling across ages was used for replication in subsequent analyses.

Carbon concentration and soil depth

SOC, SOC_{OX}, SOC_R and PyC contents of bulk soils were highest near the surface and declined with depth (Figure 8.1). While soil depth accounted for most of the variability in C concentration

(SOC: F=54.3, $p<0.0001$; SOC_{OX}: F=55.6, p<0.0001; SOC_R: F=22.1, $p<0.0001$; PyC: F=20.2, $p<0.0001$), state and the interaction between state and soil depth were also significant for all variables ($p<0.05$). The stands within a state were located in relatively close proximity and shared similar soil properties making comparison of soil C fractions by state useful (Table 8.3). LA and NC have very similar mean C concentrations among the fractions (SOC, SOC_{OX}, SOC_R and PyC) by depth and with only one exception the means were within the standard error at each depth (Table 8.3). All LA and NC soil C fraction concentrations were highest near the surface and declined with depth. The GA soils differed from LA and NC in several ways: SOC, SOC_{OX}, PyC concentrations were approximately half of that of LA and NC in the upper 20 cm, and SOC_R and PyC did not significantly decline with depth. To explore these differences further SOC_{OX}, SOC_R and PyC fractions were analyzed as a proportion of total SOC. As SOC declined with soil depth the proportion of SOC_R in SOC increased at the GA and NC stands, though there was no significant effect of depth on PyC/SOC (Table 8.4). Carbon concentrations were scaled to C stocks by incorporating soil bulk density and the length of the depth interval to calculate a sum total C stock in the upper 1 m of soil. There were no differences in SOC stocks between the states (F=1.55, $p=0.2560$), though SOC_R stocks in GA were nearly double those in LA and NC (F=22.24, p=0.0001), while LA had the highest SOC_{OX} (F=4.77, $p=0.0322$) and PyC stock (F=11.57, $p=0.0020$) (Table 8.5).

Table 8.2. Minimum, maximum, and mean for soil C stocks to a depth of 1 m and stand-level biomass C stocks from 14 longleaf pine forests.

C Stock	Minimum (Mg C ha^{-1})	Maximum (Mg C ha^{-1})	Mean (Mg C ha^{-1})
Soil			
SOC	41.5	98.1	77.0
SOC_{OX}	33.2	87.3	61.8
SOC_R	8.3	22.9	15.2
PyC	2.1	7.2	4.6
Biomass			
Live aboveground C	1.4	82.5	41.6
Live belowground C	2.7	24.8	17.1
Live C	4.1	107.4	58.7
Non-living C	0.8	7.4	4.2
Total C	4.9	113.6	63.0

PyC oxidative degradation

PyC resistant to oxidation with H_2O_2 and HNO_3 (PyC_R) was a relatively small proportion of PyC ($\bar{x}$ across depths: GA 9.2%, LA 7.8%, NC 13.5%) and is included in both the SOC_R and PyC fractions (Figure 8.2). Using the differences between least square means (two-way analysis of variance) PyC_R/PyC in the upper 10 cm of soil in NC was significantly higher than any other state/depth combination, though soil depth did not significantly affect PyC_R/PyC in GA or LA (Figure 8.2). This could indicate different formation conditions for PyC resulting in more resistant PyC_R in NC. The key finding is that the majority of PyC across all states is included in SOC_{OX} fraction and PyC_R accounts for only 2-5% of the C in the SOC_R fraction. This has important implications for radiocarbon as it was only possible to analyze SOC, SOC_R and calculate SOC_{OX} from the difference between SOC and SOC_R. PyC radiocarbon was not analyzed; after digestion, minute quantities of PyC were dissolved in 65% nitric acid, making it difficult to recover the amount needed for conversion to graphite.
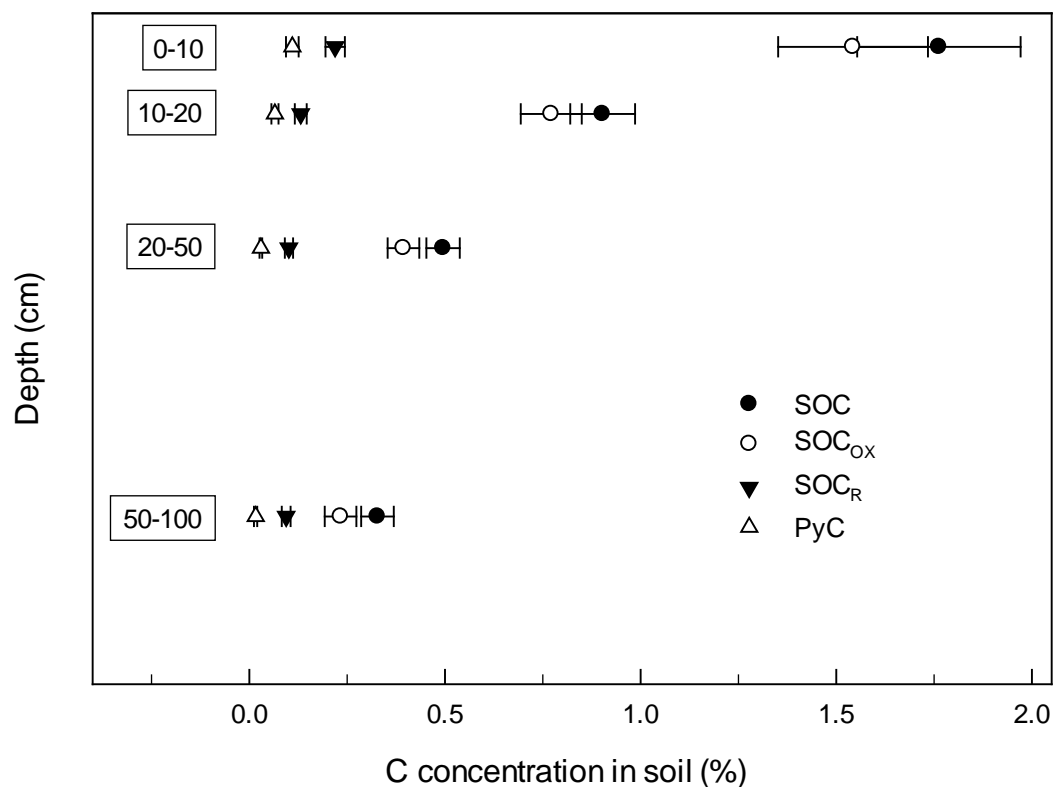
Figure 8.1. Concentration of SOC, SOC_{OX}, SOC_R and PyC in soil (+/- se.) from 14 longleaf pine stands in Georgia, Louisiana and North Carolina by sample depth.
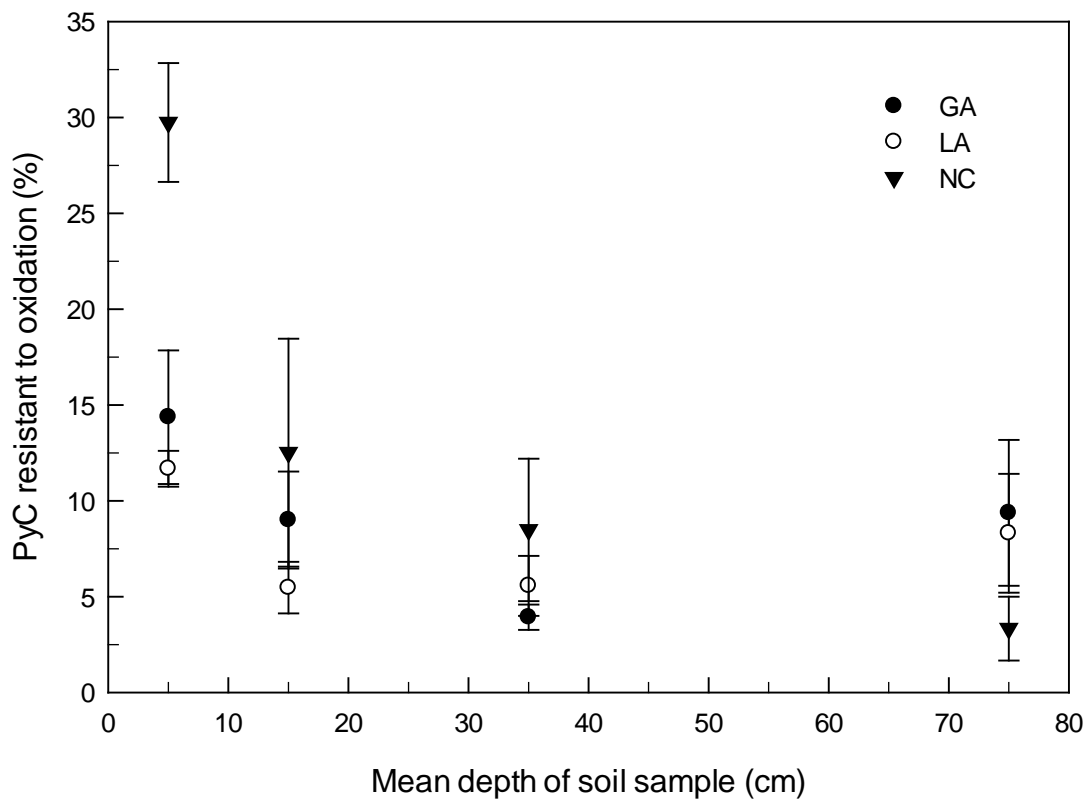
Figure 8.2. Percent of PyC resistant to oxidation with H_2O_2 and HNO_3 (+/- se.) from 14 longleaf pine stands in Georgia (n=5), Louisiana (n=5) and North Carolina (n=4) by depth.

Table 8.3. Concentration of mean SOC, SOC_{OX} SOC_R and PyC (+/- se.) by depth. Within each state, means followed by the same letter are not significantly different at the alpha = 0.05 level using the Bonferroni adjustment.

State	Depth (cm)	n	SOC (%)		SOC_{OX}		SOC_R (%)		PyC (%)	
GA	0 to 10	5	1.05 (0.05)	*a*	0.87 (0.03)	*a*	0.18 (0.02)	*a*	0.057 (0.009)	*a*
	10 to 20	5	0.68 (0.04)	*ab*	0.53 (0.04)	*ab*	0.15 (0.02)	*a*	0.037 (0.004)	*a*
	20 to 50	5	0.51 (0.05)	*ab*	0.37 (0.05)	*ab*	0.15 (0.01)	*a*	0.027 (0.005)	*a*
	50 to 100	5	0.35 (0.03)	*b*	0.21 (0.02)	*b*	0.14 (0.01)	*a*	0.013 (0.002)	*a*
LA	0 to 10	5	2.18 (0.33)	*a*	1.97 (0.30)	*a*	0.21 (0.03)	*a*	0.158 (0.019)	*a*
	10 to 20	5	1.05 (0.11)	*b*	0.95 (0.10)	*b*	0.10 (0.01)	*b*	0.095 (0.017)	*b*
	20 to 50	5	0.51 (0.04)	*bc*	0.44 (0.04)	*c*	0.07 (0.01)	*b*	0.038 (0.005)	*c*
	50 to 100	5	0.36 (0.12)	*c*	0.30 (0.11)	*c*	0.06 (0.01)	*b*	0.020 (0.011)	*c*
NC	0 to 10	4	2.13 (0.39)	*a*	1.85 (0.33)	*a*	0.28 (0.07)	*a*	0.117 (0.034)	*a*
	10 to 20	4	0.99 (0.22)	*b*	0.84 (0.19)	*b*	0.15 (0.04)	*b*	0.064 (0.010)	*ab*
	20 to 50	4	0.45 (0.14)	*bc*	0.37 (0.13)	*bc*	0.08 (0.02)	*b*	0.022 (0.008)	*b*
	50 to 100	4	0.26 (0.02)	*c*	0.18 (0.02)	*c*	0.08 (0.01)	*b*	0.014 (0.006)	*b*

Table 8.4. Ratio of C fractions in SOC by depth. Mean values reported with standard errors in parentheses. Within each state, means followed by the same letter are not significantly different at the alpha = 0.05 level using the Bonferroni adjustment.

State	Depth (cm)	n	$SOC_{OX}/SOC*100$ (%)		$SOC_R/SOC*100$ (%)		$PyC/SOC*100$ (%)	
GA	0 to 10	5	83.24 (1.38)	*a*	16.76 (1.38)	*a*	5.32 (0.68)	*a*
	10 to 20	5	77.94 (2.54)	*ab*	22.06 (2.54)	*ab*	5.47 (0.39)	*a*
	20 to 50	5	69.82 (4.50)	*b*	30.18 (4.50)	*b*	5.22 (0.48)	*a*
	50 to 100	5	59.12 (2.69)	*c*	40.88 (2.69)	*c*	3.65 (0.30)	*a*
LA	0 to 10	5	90.24 (0.44)	*a*	9.76 (0.44)	*a*	7.46 (0.50)	*a*
	10 to 20	5	90.71 (0.50)	*a*	9.29 (0.50)	*a*	8.97 (1.08)	*a*
	20 to 50	5	85.72 (0.86)	*a*	14.28 (0.86)	*a*	7.62 (1.20)	*a*
	50 to 100	5	80.82 (2.99)	*a*	19.18 (2.99)	*a*	4.53 (1.21)	*a*
NC	0 to 10	4	86.86 (1.77)	*a*	13.14 (1.77)	*a*	5.15 (1.10)	*a*
	10 to 20	4	84.92 (2.11)	*a*	15.08 (2.11)	*a*	7.20 (1.34)	*a*
	20 to 50	4	78.62 (3.68)	*a*	21.38 (3.68)	*a*	4.24 (0.77)	*a*
	50 to 100	4	68.40 (3.58)	*b*	31.60 (3.58)	*b*	5.34 (1.80)	*a*

Table 8.5. Soil stocks of SOC, SOC_{OX}, SOC_R, and PyC in the upper 1 m of soil. Mean values reported with standard errors in parentheses. Within each state, means followed by the same letter are not significantly different at the alpha = 0.05 level.

State	n	SOC (Mg ha^{-1})		SOC_{OX} (Mg ha^{-1})		SOC_R (Mg ha^{-1})		PyC (Mg ha^{-1})	
GA	5	72.12 (6.56)	*a*	51.22 (5.72)	*a*	20.90 (1.01)	*a*	3.54 (0.58)	*a*
LA	5	86.16 (3.54)	*a*	75.42 (3.43)	*b*	10.73 (0.40)	*b*	6.39 (0.40)	*b*
NC	4	71.48 (10.16)	*a*	57.93 (8.63)	*ab*	13.55 (1.92)	*b*	3.73 (0.37)	*a*

PyC BPCA ratios

In addition to total BPCA contents that were scaled to estimate PyC in soil, the approach also characterized the ring structure of PyC. Nitric acid digestion of aromatic rings in PyC form carboxylic acids (B3CA, B4CA, B5CA, B6CA) diagnostic of the number of rings in the original sample i.e. 3-6 rings. Relative recalcitrance of PyC may be inferred from the ratio carboxylic acid moieties (B5CA:B6CA) recovered post-digestion, where higher proportion of aromatic rings has greater biochemical stability. The ratio of B5CA to B6CA in SOC declined at deeper soil depths indicating a higher degree of aromatic condensation and biochemical stability at GA and LA, but not NC (Figure 8.3). The low concentration of BPCA in SOC_R precluded further analysis of that fraction (data not shown).

Radiocarbon

Bulk soil (SOC) and SOC_R were analyzed for radiocarbon and the difference between them was calculated to be the contribution of oxidizable SOC (SOC_{OX}). SOC_{OX} is primarily non-resistant SOC plus oxidizable (PyC_{OX}) and by definition is more degradable than SOC or SOC_R. Soil depth and state explained most of the variation in Fm for SOC, SOC_{OX}, and SOC_R, there were no significant state*depth interactions. Both soil depth (SOC: F=43.1, p<0.0001; SOC_{OX}: F=67.1, p<0.0001; and SOC_R: F=35.6, p<0.0001) and state (SOC: F=17.9, p=0.0055; SOC_{OX}: F=12.0, p<0.0001; and SOC_R: F=46.1, p<0.0001) affected Fm.). Soil was most ^{14}C depleted at depth, Fm declined with depth for all of the variables (Table 8.6). Fm predicted the age continuum as expected, the least resistant fraction was the youngest, the oxidation resistant fraction was the oldest, and the combination of the two was intermediate i.e: $SOC_{OX} < SOC < SOC_R$ (Table 8.6). Fm values of SOC_{OX} were similar between the states, though Fm of SOC_R in GA was much lower than LA or NC (Table 8.6). SOC is in a state of equilibrium where C is continually entering and leaving the soil, therefore a discrete "radiocarbon age" is not appropriate as it would be with an object of a specific age such as a tree ring, bone, char fragment etc. The Fm value was used to model MRT to give greater context to the radiocarbon data. SOC MRT ranged from 123 to 6226 depending on depth (Table 8.6). With our approach it was not possible to separate PyC from SOC and obtain discrete estimate of PyC MRT. As previously noted, the majority of PyC (GA 90.8 %,

LA 92.2 %, NC 86.5 %) was in the SOC$_{OX}$ fraction, it still remains the youngest fraction with similar MRT's across states (Table 8.6). SOC$_R$ is the oldest fraction, MRT values were similar for LA and NC; they were much older for the stands in GA averaging 22,626 years at the 50 to 100 cm depth interval (Table 8.6). These results illustrate the longevity of C that is retained in forest soil and though SOC$_R$ is a minority component of SOC, its MRT is a magnitude higher than the oxidizable fraction. Mean residence time of C may also be considered as a measure of annual turnover (Figure 8.4). The most rapid annual turnover rates (% C oxidized per year) were in the upper 10 cm of soil (GA 0.26 %, LA 0.52%, NC, 0.82 %), where rates from each state were significantly different from each other ($p < 0.05$).

Soil properties associated with C stabilization and retention

Soil physical properties of bulk density and texture are summarized by state and depth in Table 8.7. A wide range of soil texture combinations were observed; NC soils were typified by deep sandy soil, GA soils had gradual increase in clay with depth, and LA soils had a clay profile similar to GA, but also had 20-26% silt fraction throughout the profile. LA had the highest bulk density, while NC soils were the least dense. Fe has been shown to form stable associations with C, therefore extractable Fe (Mehlich-3) was included in the analysis (Table 8.7). Extractable Fe declined with depth at GA and LA, but remained stable throughout the profile in NC. Soils were acidic ranging from pH 4.28 to 5.04 (Table 8.7).

The dependence of SOC, SOC$_{OX}$, SOC$_R$ and PyC concentrations on soil depth, texture, bulk density and extractable Fe was analyzed with stepwise linear multiple regression. After examination of the residual vs predicted values, it was deemed necessary to log transform the soil C variables, summaries of regression analysis are presented in Table 8.8. Bias from log transformation was corrected using a method described by Snowdon (1991). Soil depth was the primary driver of the models as soil C across fractions was highest near the surface and declined with depth. Since soil texture, BD and Fe concentrations are all influenced by depth (Table 8.7), it was important leave depth in the model to not imply unwarranted causality to soil parameters that are themselves affected by depth. All of the model parameters had low variance inflation factors (<5) indicating that the parameters had minimal collinearity with each other and supported keeping depth in the model. Both Fe and clay can stabilize C in soil and are representative of absorptive capacity of the soil for C. Fe was positively associated with concentration of all soil C fractions, accounting for 10% of the variation in SOC$_R$ and 7% of the variation in PyC (Table 8.8). Clay content was positively associated with C concentration (or conversely negative association with sand) and accounted for 15% of the variation in SOC$_R$. Bulk density was also negatively associated with SOC$_{OX}$, and SOC$_R$ (Table 8.8).

Soil properties and soil C fractions associated with residence time of soil C

The dependence of SOC$_{OX}$ MRT and SOC$_R$ MRT concentrations on soil depth, texture, bulk density and extractable Fe was analyzed with stepwise linear multiple regression similar to the approach with C concentrations. In addition to the aforementioned parameters, SOC$_R$/SOC *100 (%) and PyC/SOC *100 (%) were included in stepwise selection process for SOC MRT to include the contribution of SOC$_R$ and PYC content to the overall model for SOC. To meet the assumption of homoscedasticity it was necessary to log transform all MRT values. Summaries of regression

analysis are presented in Table 8.8. Soil depth and bulk density were associated with increased residence time for both SOC_{OX} MRT and SOC_R MRT. SOC_R MRT was negatively associated with sand and silt, inferring a positive relationship with clay content (Table 8.8). As SOC MRT is the sum total of the contributions of SOC_{OX} MRT and SOC_R MRT, it was positively associated with depth and BD. SOC_R/SOC (%) contributed an additional 10% to the SOC MRT regression model ($R^2 = 0.88$) though PyC/SOC (%) was not retained in the model at the $p < 0.05$ level. Pooling data from all depths from the 14 longleaf pine stands, SOC_R/SOC increases with SOC MRT, while PyC/SOC declines with SOC MRT (Figure 8.5). These results indicate that SOC_R is driving long term stabilization of C in fire-adapted longleaf pine forests and not PyC.
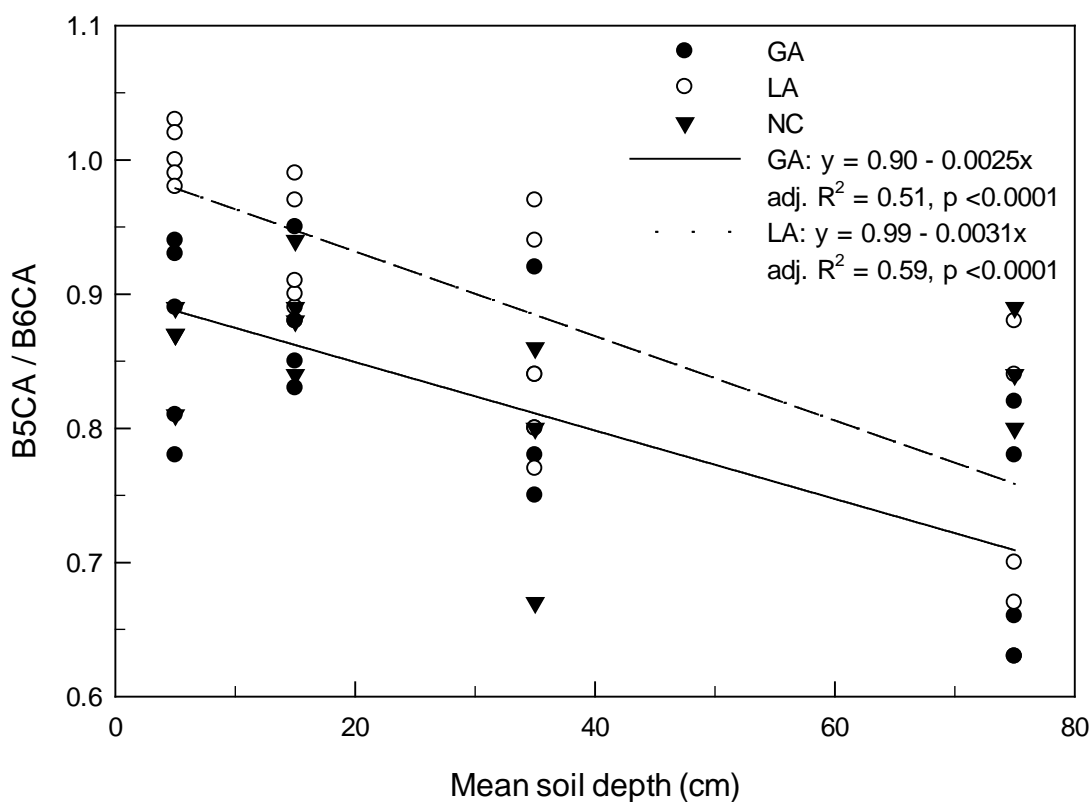
Figure 8.3. Linear regression analysis of B5CA/B6CA with soil depth. No significant relationship was observed at the NC sites.

Table 8.6. Fraction modern and modeled mean residence time of SOC, SOC_{OX} and SOC_R in soil by depth. Mean values reported with standard errors in parentheses. Within each state, means followed by the same letter are not significantly different at the alpha = 0.05 level using the Bonferroni adjustment.

State	Depth (cm)	n	SOC Fm		SOC_{OX} Fm		SOC_R Fm		$SOC^{[1]}$ MRT (years)		$SOC_{OX}{}^{[1]}$ MRT (years)		$SOC_R{}^{[1]}$ MRT (years)	
GA	0 to 10	5	0.97 (0.03)	a	1.03 (0.03)	a	0.66 (0.03)	a	541 (189)	a	274 (144)	a	4344 (581)	a
	10 to 20	5	0.90 (0.03)	a	1.01 (0.03)	ab	0.48 (0.03)	ab	1112 (209)	a	322 (90)	a	8882 (1016)	ab
	20 to 50	5	0.76 (0.06)	b	0.94 (0.02)	b	0.41 (0.05)	bc	2927 (1001)	b	743 (149)	b	12917 (2790)	bc
	50 to 100	5	0.58 (0.05)	c	0.86 (0.04)	b	0.28 (0.04)	c	6226 (1203)	c	1521 (417)	b	22626 (3973)	c
LA	0 to 10	5	1.03 (0.01)	a	1.06 (0.01)	a	0.88 (0.03)	a	200 (20)	a	144 (16)	a	1223 (243)	a
	10 to 20	5	0.98 (0.01)	a	0.99 (0.01)	ab	0.81 (0.02)	ab	452 (38)	a	360 (32)	b	1990 (272)	a
	20 to 50	5	0.89 (0.01)	a	0.94 (0.01)	b	0.63 (0.03)	bc	1090 (120)	b	687 (71)	b	4836 (610)	b
	50 to 100	5	0.67 (0.04)	b	0.75 (0.02)	c	0.51 (0.05)	c	4266 (702)	c	2802 (342)	c	8345 (1421)	b
NC	0 to 10	4	1.07 (<0.01)	a	1.12 (0.02)	a	0.87 (0.03)	a	123 (7)	a	63 (13)	a	1345 (338)	a
	10 to 20	4	1.01 (0.01)	ab	1.06 (0.01)	ab	0.75 (0.05)	ab	290 (66)	a	142 (12)	ab	2870 (681)	ab
	20 to 50	4	0.88 (0.06)	bc	0.97 (0.03)	bc	0.58 (0.09)	bc	1473 (731)	b	530 (208)	bc	7289 (2998)	bc
	50 to 100	4	0.75 (0.04)	c	0.89 (0.02)	c	0.54 (0.07)	c	2891 (725)	b	1102 (165)	c	7691 (2228)	c

[1]To meet assumption of homoscedasticity variables were log transformed for statistical analysis. Actual means and standard errors are presented.
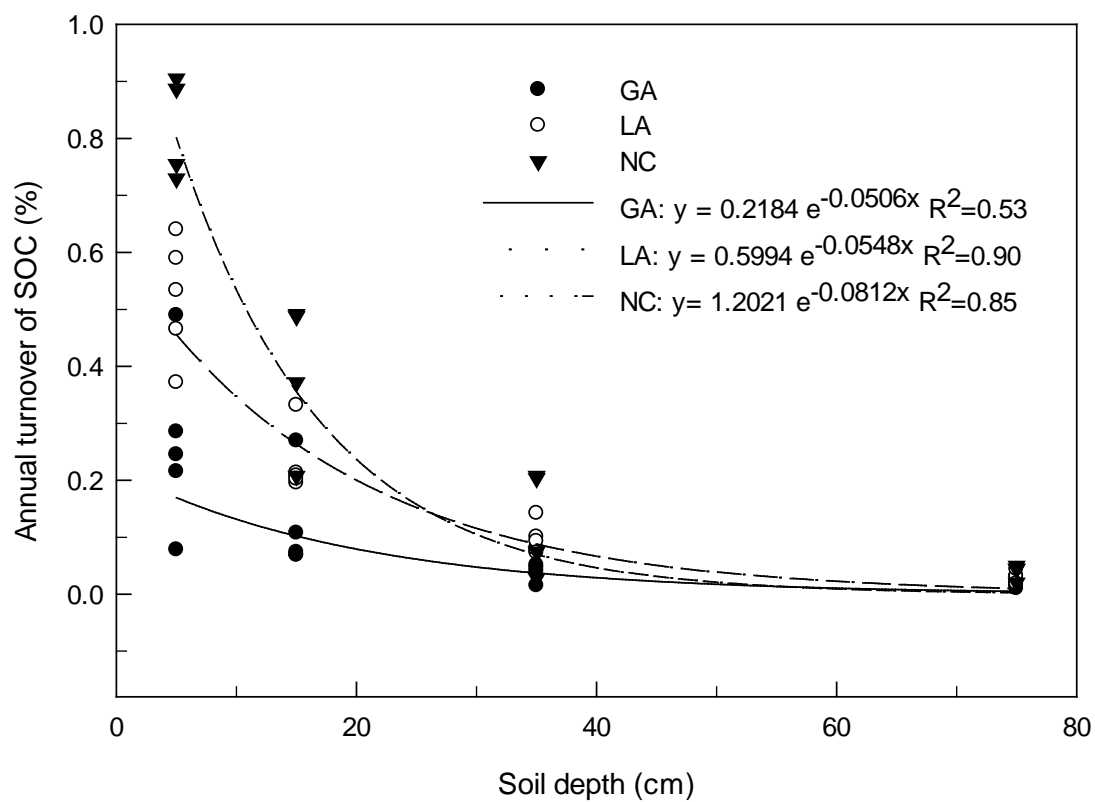
Figure 8.4. Annual turnover of SOC (%) from 14 longleaf pine stands in Georgia (n=5), Louisiana (n=5) and North Carolina (n=4) by depth.

Table 8.7. Soil physical properties plus pH and extractable Fe content by depth. Mean values reported with standard errors in parentheses. Within each state, means followed by the same letter are not significantly different at the alpha = 0.05 level using the Bonferroni adjustment.

State	Depth (cm)	n	Bulk Density (g cm^2)		Sand (%)		Silt (%)		Clay (%)		pH		Fe (ppm)	
GA	0 to 10	5	1.30 (0.10)	a	83.0 (0.6)	a	8.1 (0.4)	a	8.9 (0.4)	a	4.98 (0.09)	a	122.2 (11.5)	a
	10 to 20	5	1.55 (0.07)	b	79.5 (1.9)	b	8.0 (0.3)	a	12.5 (1.9)	b	4.97 (0.06)	a	94.3 (7.9)	b
	20 to 50	5	1.58 (0.05)	b	73.3 (1.8)	c	8.7 (0.6)	a	18.0 (2.2)	c	4.96 (0.09)	a	69.7 (7.3)	bc
	50 to 100	5	1.53 (0.03)	b	63.1 (4.5)	d	7.9 (0.4)	a	29.0 (4.8)	d	4.90 (0.08)	a	40.1 (2.4)	c
LA	0 to 10	5	1.44 (0.06)	a	67.0 (2.5)	a	25.9 (2.2)	a	7.1 (1.1)	a	5.01 (0.08)	a	152.4 (16.2)	a
	10 to 20	5	1.69 (0.06)	b	64.4 (2.8)	b	24.8 (2.4)	a	10.8 (1.9)	b	5.02 (0.06)	a	114.2 (15.8)	b
	20 to 50	5	1.64 (0.03)	ab	58.7 (3.8)	c	23.4 (2.2)	ab	17.9 (4.0)	c	5.04 (0.04)	a	65.0 (16.9)	c
	50 to 100	5	1.77 (0.05)	b	54.3 (3.3)	c	20.5 (2.6)	b	25.2 (3.7)	d	4.94 (0.03)	a	34.9 (4.5)	c
NC	0 to 10	4	1.09 (0.09)	a	91.2 (3.3)	a	5.8 (1.9)	a	3.0 (1.4)	a	4.28 (0.06)	a	96.7 (35.3)	a
	10 to 20	4	1.30 (0.04)	b	91.2 (3.5)	a	5.2 (1.9)	a	3.7 (1.7)	a	4.46 (0.08)	b	97.5 (37.5)	a
	20 to 50	4	1.36 (0.05)	b	88.8 (4.1)	a	5.3 (1.7)	a	5.8 (2.4)	a	4.80 (0.06)	c	74.9 (18.5)	a
	50 to 100	4	1.49 (0.04)	b	86.3 (4.2)	a	4.5 (1.3)	a	9.2 (2.9)	a	4.83(0.05)	c	93.9 (20.6)	a

Table 8.8. Linear regression model parameters and fit statistics of soil C fraction concentration and C mean residence time in longleaf pine stands in GA, LA and NC (n=56). All dependent variables were modeled with soil depth, BD, % sand, % silt, % clay, extractable fe (ppm). All models were highly significant $p < 0.0001$.

Dep. variable	Para-meters	Estimate	SE	VIF	p	Part. R^2	Model R^2	CF	RMSE
lnSOC	y0	-0.39876	0.2281	0	0.0865				
	Depth	-0.02126	0.00312	1.9756	<0.0001	0.6034	0.6784	1.1109	0.4391
	Fe	0.00485	0.00156	1.6200	0.0037	0.0412			
	Clay	0.01895	0.0082	1.7978	0.0249	0.0337			
lnSOC$_{OX}$	y0	2.41289	0.93445	0	0.00128				
	Depth	-0.02174	0.0032	1.8039	<0.0001	0.6280	0.7225	1.1104	0.4664
	Fe	0.00424	0.0016	1.5224	0.0126	0.0364			
	Sand	-0.01921	0.0060	1.7670	0.0024	0.0304			
	BD	-0.87857	0.3941	1.8413	0.0303	0.0276			
lnSOC$_R$	y0	-2.62703	0.8923	0	0.0049				
	Depth	-0.01067	0.0026	2.1423	0.0001	0.2641	0.6307	1.0546	0.3455
	Clay	0.05224	0.0101	4.3693	<0.0001	0.1492			
	Fe	0.00543	0.0013	1.7579	0.0001	0.1047			
	BD	-0.91864	0.2958	1.8900	0.0032	0.0771			
	Sand	0.01415	0.0065	3.7728	0.0346	0.0356			
lnPyC	y0	-2.12723	0.6167	0	0.0011				
	Depth	-0.02423	0.0042	1.7127	<0.0001	0.5456	0.6506	1.1332	0.6333
	Fe	0.00728	0.0022	1.5222	0.0019	0.0734			
	Sand	-0.01438	0.0067	1.1904	0.0366	0.0316			
lnSOC$_{OX}$ MRT	y0	2.29411	0.5110	0	<0.0001				
	Depth	0.02914	0.0029	1.2221	<0.0001	0.6981	0.7987	1.0866	0.5252
	BD	1.85970	0.3615	1.2221	<0.0001	0.1005			
lnSOC$_R$ MRT	y0	9.46139	1.47316	0	<0.0001				
	Depth	0.01101	0.0043	1.8398	0.0127	0.4178	0.6068	1.1523	0.6307
	Sand	-0.02934	0.0118	3.7801	0.0160	0.0806			
	Silt	-0.07884	0.0169	3.15890	<0.0001	0.0690			
	BD	1.22079	0.5393	1.8862	0.0279	0.0395			
LnSOC* MRT	y0	2.40683	0.4802	0	<0.0001				
	Depth	0.01962	0.0034	2.1037	<0.0001	0.7115	0.8792	0.9869	0.4526
	SOC$_R$/ SOC%	0.05624	0.0076	1.7244	<0.0001	0.0960			
	BD	1.76659	0.3211	1.2982	<0.0001	0.0717			
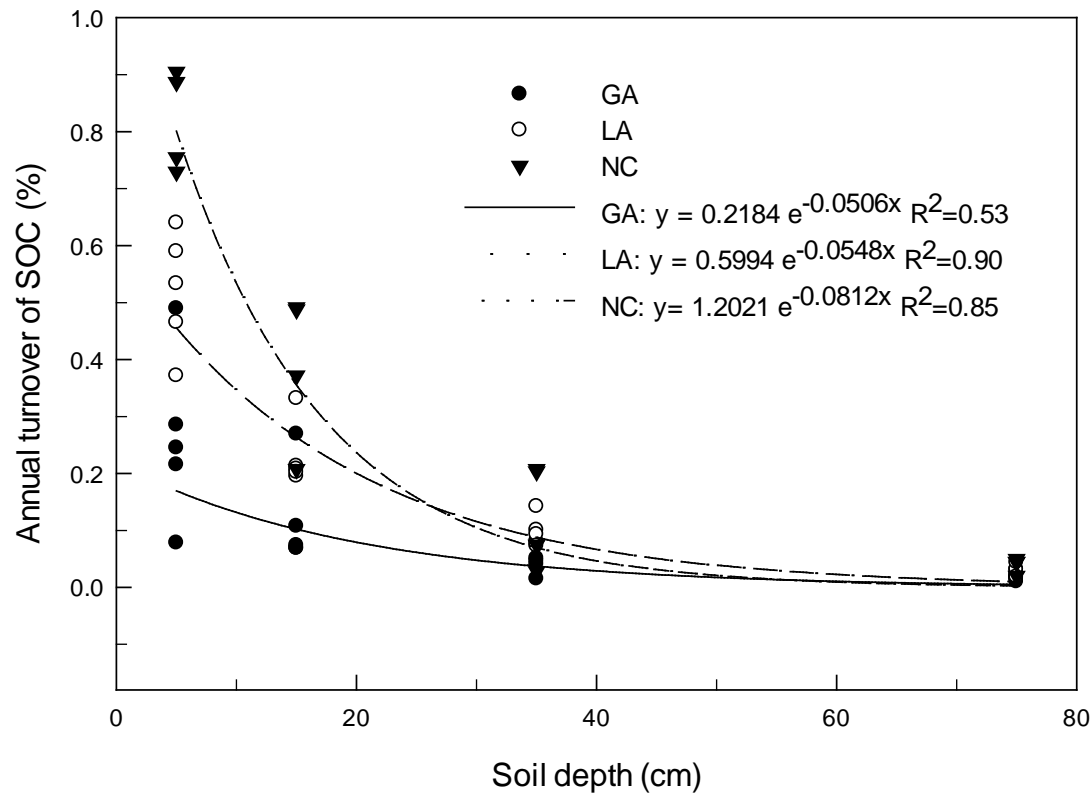
Figure 8.5. Annual turnover of SOC (%) from 14 longleaf pine stands in Georgia (n=5), Louisiana (n=5) and North Carolina (n=4) by depth.

Discussion

The present study found no effect of stand age or biomass accumulation on any soil C parameter using a chronosequence approach. These results are similar to other reports from southern pine plantations where little (Richter et al. 1999) or no increase in soil C was detectable over time (Markewitz et al. 2002, Johnson et al. 2003, Johnsen et al. 2013). Though rarely available, the use of archived soils e.g. (Richter et al. 1999, Hammes et al. 2008) provides a more powerful means of detecting change over time than chronosequence point-in-time collections (Richter et al. 2007). Across forest types, even large ecosystem disturbances from harvesting generally have little to no long-term effect of harvesting on soil C (Johnson et al. 2002). Regardless of whether the effect of age and related biomass accumulation on soil C retention is neutral or very low in longleaf pine ecosystems, the soils are not a strong sink for atmospheric CO_2.

Concentrations of SOC and all of the representative fractions (SOC_{OX}, SOC_R and PyC) declined with soil depth. Decomposition is more rapid at shallow depths and C that remains at deeper depths is older and more resistant to oxidation. While depth explained most of the variation in each

fraction, clay and extractable Fe were positively associated with C retention and negatively associated with bulk density. Fe and clay stabilize C via mineral association in forms that may persist for thousands of years (Eusterhues et al. 2005). C is moving from biomass pools to soil, but the capacity to stabilize and retain that C is limited. Richter et al. (1999) described a similar situation in a loblolly pine plantation at the Calhoun Experimental Forest where C retention in soil was not source limited, but rather storage limited in coarse soils with little absorptive capacity for C.

PyC can play important roles in soil carbon sequestration and stabilization, as well as enhancing fertility by enhancing soil nutrient retention and cation exchange capacity in soil (Glaser et al. 2001, Liang et al. 2006). Considering that frequent low intensity fires are central to longleaf pine management, we expected PyC to contribute to long-term sequestration, however the results did not support that hypothesis. PyC represented 5-7% of SOC and the majority of PyC was in the least persistent SOC_{OX} fraction with residence times one tenth that of SOC_R. Possible explanations for this observation include rapid degradation of PyC under environmental conditions and offsite transport of PyC.

While pyrogenic transformation of C can lead to biochemical stability for millennia, PyC is not immune to decomposition. Hammes et al. (2008) demonstrated after the cessation of grassland fires in a Russia Steppe in 1900, the stocks of PyC in soil declined by 25% over the next century and the turnover time was 293 years. Several studies have documented factors affecting PyC decomposition rates under laboratory and field conditions e.g. Cheng et al. (2006), Liang et al. (2008), Nguyen and Lehmann (2009), Zimmerman (2010), Foereid et al. (2011). The potential recalcitrance of PyC that does remain on site in forest soil is highly dependent on feedstock, temperature and aeration during formation, environmental conditions favoring decomposition, binding with soil minerals as well as physical protection after formation, i.e. charcoal left on the surface is susceptible to re-ignition in subsequent fires. Longleaf pine stands are commonly treated with dormant season prescribed fires in late winter to early spring to minimize tree injury and prevent damaging canopy fires. Consequently, these prescribed fires are intentionally of low intensity. In general, low temperature combustion yields PyC with less aromatic condensation e.g. Soucemarianadin et al. (2013), that is more susceptible to decomposition than PyC formed at higher combustion temperatures (Nguyen and Lehmann 2009, Zimmerman 2010). Soucemarianadin et al. (2015) found that early-season fires in boreal black spruce forests produce pyrogenic carbon with low intrinsic recalcitrance and this phenomenon may be occurring in longleaf pine forests. The majority of fires in longleaf pine stands are not stand replacing events and result in very different than combustion conditions and pyrogenic emissions than wildfires in the western United States (Campbell et al. 2007).

Most newly formed PyC is concentrated in the lightest fraction on the soil surface and is susceptible to rapid offsite transport via surface flow and leaching following precipitation unless it mixed with mineral soil. The material may be biochemically stable and sequestered from the atmosphere, but much of it may be removed and ultimately deposited in marine systems instead of the point of production (Masiello and Druffel 1998, Jaffe et al. 2013). In longleaf pine stands in the southeastern US, there is little mixing of PyC with mineral soil, combined with 1000 to 1500 mm annual precipitation, hence PyC would be expected to receive minimal protection. Decomposition and offsite transport are both reasonable mechanisms to explain why less PyC is

retained in forest soils than would be expected from PyC production estimates. Little to no research has been conducted to distill the contribution of the two. To better assess the contribution of each mechanism, new research where high frequency sampling of soil surfaces, soil, surface flow and ground water is required.

Key Results and Conclusions

Total soil C stocks in 14 longleaf pine stands ranged from 44.1 to 98.1 ($\bar{x}$ = 77.0) Mg C ha^{-1}, though no effect of stand age, biomass accumulation or geographical location was detected. Variation in soil C concentration was largely dependent on depth, though positive association with clay and extractable Fe content were found. PyC is minor component of SOC, comprising 5-7% of the total SOC stock. The majority of PyC was in the oxidizable fraction, which was found to have a residence time almost a magnitude lower than the resistant fraction. This indicates that PyC is not contributing substantially to long-term C accumulation in soil within the forest stand where it was produced. There was no enhanced accumulation or deposits of PyC with depth (to 1 m), PyC declined in proportion with SOC, conversely the proportion of SOC_R in SOC increased with depth. The residence time of SOC in surface soils was hundreds of years and at depths > 50 cm residence time increased to thousands of years. Despite the flow of C from biomass in the form of decay products, litter fall, root turnover and pulses of PyC, the soils are retaining little of the new C, which may be rapidly oxidized, lost to the atmosphere from periodic fires or in the case of PyC may be transported out of the system. These results combined with results from Chapter 7, indicate that soils are not strong sinks for atmospheric CO_2 compared to C accumulation in biomass in longleaf pine forests.

9. Tap Root Decomposition

[Contents of this chapter were extracted from Anderson, P.H., K.H. Johnsen, J.R. Butnor, C.A. Gonzalez-Benecke, and L.J. Samuelson. 2016. Modeling longleaf pine tap root decomposition across the southeastern US. In preparation for submission to Forest Ecology and Management]

Introduction

The research described in this chapter is part of the large effort described in previous chapters to quantify ecosystem C stocks in longleaf pine plantations and natural stands to help guide forest management across the southeastern US. Storage of belowground C in living root biomass is an important component of total forest C and can be difficult to estimate. However, after a root system dies, either due to harvesting or naturally, its C does not immediately disappear. It slowly decomposes in necromass over decades and decay rates may vary with species and climate. These decaying root systems play an important role in soil nutrient dynamics, C cycling, and thus forest productivity. Differences in wood chemistry, decay processes and climate control the rate of decay, though our understanding of residual root necromass in longleaf pine stands is very limited. More is known about fine root turnover (Pregitzer 2002) than the decomposition of long-lived coarse roots and tap roots. The decomposition of coarse roots in middle latitudes is more dependent on temperature than the decomposition rates of fine roots (Zhang and Wang 2015). Previous studies of loblolly pine (*Pinus taeda*) in the southeastern US (Ludovici et al. 2002, Mobley et al. 2012) demonstrated that lateral and tap roots can persist over long periods of time.

Our goal was to develop an equation to model longleaf pine coarse root decomposition over time that can be incorporated into carbon sequestration models for longleaf pine. Toward this end, we sampled root necromass from stumps across a range of: 1) tree age at the time of cut; and 2) time since tree harvest. Stumps were selected across the range of longleaf pine in North Carolina, Georgia, Florida, and Louisiana.

Methods and Materials

Study sites

A total of 37 stumps were identified and removed across the natural range of longleaf pine from North Carolina to Louisiana (Figure 9.1). Tree age (Age) defined as age of the tree when cut ranged from 14 to 260 years. Years since cut (YSC) was defined as the number of years since the tree was harvested and varied from 5 to 70 years (Figure 9.2). Stump location, Age, and YSC were identified with the help of on-site land managers and land use records. Trees that died naturally were not selected for this study and all of the stumps used were cut either for production harvest or research. For each site an average low air temperature value (Tmin) was assigned using the USDA plant hardiness zone map (PHZ) (Table 9.1).

Stump collection

After identifying stumps, underbrush and leaf litter were removed. A square pit 1 m from stump edge was then laid out. For stumps rotten at ground line the remaining bark ring was used to calculate stump diameter (SD). Remaining lateral roots were hand excavated and sorted by depth (0-10, 10-20, 20-30, 30-50, and 50-100 cm). Few lateral roots were found below 30 cm. A small backhoe was then used to loosen soil and remove the tap root. Tap roots were taken to lab to be cleaned, cut at a marked ground level for DS and by depth (0-10, 10-20, 20-30, 30-50, 50-100 cm and every 50 cm below 100). All woody components were dried at 65^0 C to a constant mass and weighed. Samples were then ground using a chipper. Subsamples were taken from the chipped material and ground using a Wiley mill. Wood C and N concentrations were determined by dry combustion with detection by thermal conductivity (Flash EA 1112 series CN analyzer, Thermo Finnigan Instruments, Milan, Italy). To correct for mineral soil contamination, loss on ignition was performed on all samples.
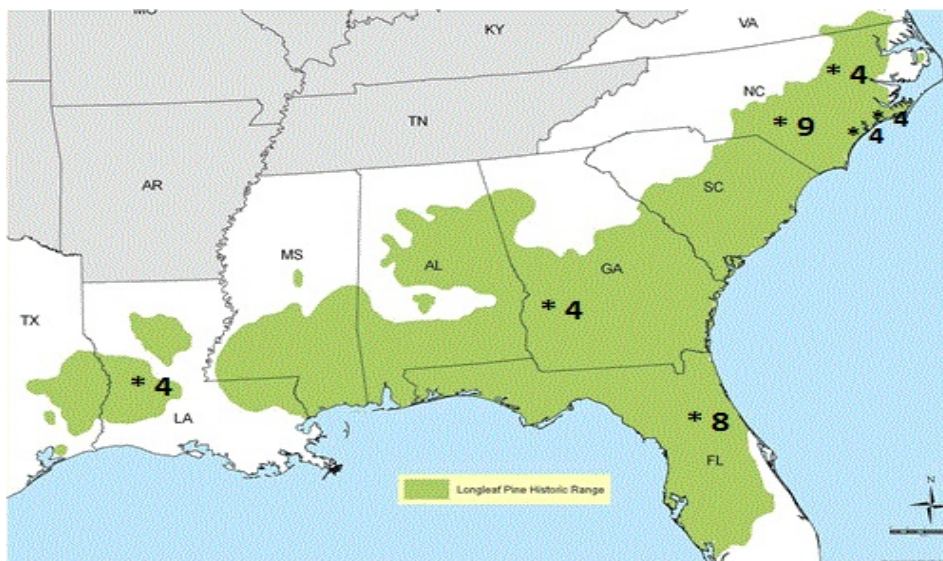
Figure 9.1. Map of longleaf pine range in the southeastern US. Asterisks represent sites where decaying tap roots were removed and the number removed from each site is indicated

Total Soil C, N,

For each stump two transects were run to the closest living trees. In sites that were planted, this distance was consistent but in older stands this distance was variable. Two samples were taken at a distance 0.5 m from the stump before excavation. Two samples were also taken 0.5 meters from the nearest living trees and two from the mid-point between the stump and living tree. Soil samples were collected at 5 depths (0-10, 10-20, 20-30, 30-50, 50-100). Soil was air-dried to a constant weight and passed through a 2 mm sieve to remove roots and rocks. Total soil C and N concentrations were determined by dry combustion with detection by thermal conductivity as above.

Table 9.1. Site descriptions for excavated longleaf tap roots. Site name, State, County, number of tap roots removed from each site, age of the tree when cut (AGE), years since cut (YSC), USDA plant hardiness zone (PHZ), and corresponding average low temperature (Tmin, ^{0}C) as per PHZ.

Site	State	County	# of Tap roots	AGE	YSC	PHZ	Tmin
Marine Corps Base Camp Lejeune	NC	Onslow	4	61	18	8A	13.5
Croatan NF	NC	Carteret	4	52	29	8A	14.1
Duke Forest	NC	Durham	2	64	10	7B	7.7
Duke Forest	NC	Durham	2	54	20	7B	7.7
US Army Fort Benning	GA	Chattahoochie	4	14	7	8A	14.4
Kisatchie National Forest	LA	Rapides	4	61	15	8B	18.3
Sandhills Gamelands	NC	Richmond	4	65	14	8A	10.6
Sandhills Gamelands	NC	Richmond	4	45	30	8A	10.6
Sandhills Gamelands	NC	Richmond	1	260	70	8A	10.3
University of Florida	FL	Alachua	4	75	5	9A	20.9
University of Florida	FL	Alachua	4	65	15	9A	20.9

Modeling and statistics

The following model was initially used to estimate root decay rate as a function of time since cut (Yavitt and Fahey 1982):

$$RW_t = RW_i \cdot exp(-k \cdot YSC) + \varepsilon_1$$

Where RW_t is the root mass remaining at time t, RW_i is the initial root mass, k is the decomposition rate (year^{-1}), and YSC is years since cut, and ε_1 is the error term, with $\varepsilon_1 \sim NID(0, s_1^2)$. This model assumes that decomposition is proportional to the amount of mass remaining and remaining root mass could be predicted only as a function of years since cut. As xylem structure changes as tree ages, k may also depend on tree age, so we also fitted an equation were k was a linear function of tree age (k = a1 + a2·AGE):

$$RW_t = RW_i \cdot exp((a1 + a2 \cdot AGE) \cdot YSC) + \varepsilon_2$$

where a1 and a2 are curve fit parameters, and ε_2 is the error term, with $\varepsilon_2 \sim N(0, s_2^2)$. These nonlinear models were fit using the PROC NLIN procedure (SAS Institute Inc. 2013). Separate mass models were fit to the lateral root wood (LR), tap root wood (TR), and total coarse roots (CR, lateral + tap). Additionally, necromass loss, root C, and root N content were initially estimated as follows:

$$RW_t = exp(b1 + b2 \cdot YSC) + \varepsilon_3$$

where b1 and b2 are curve fit parameters, and ε_3 is the error term, with $\varepsilon_3 \sim N(0, s_3^2)$. In addition to YSC, other variables were included as covariates in the above model to improve the mass loss equation. The variables considered were AGE, SD and Tmin. Similar to Gonzalez-Benecke et al. (2014), to test which variables should be included in the final model, a logarithm transformation was carried out and stepwise procedure was used on the resulting linear model with a threshold significance value of 0.15 as variable selection criteria and the variance inflation factor (VIF) was monitored to detect multicollinearity between explanatory variables. All variables included in the model with VIF larger than 5 were discarded, as suggested by Neter et al. (1996).

Three measures of accuracy were used to evaluate the goodness-of-fit between observed and predicted values for each variable based on the model evaluation dataset: (i) root mean square error (RMSE); (ii) mean bias error (Bias); and (iii) coefficient of determination (R^2). The residuals were examined by plotting them over the predicted and dependent variables for each model. All statistical analyses were performed using SAS 9.3 (SAS Inc., Cary, NC, USA).

Position differences of soil C and N concentrations by soil depth were analyzed using Proc GLM (SAS Institute Inc. 2013). Means separation by position was performed by the Tukey's procedure.

Results

Root necromass, C, N

Age of tree and YSC ranged from 14- 260 and 7- 70 years, respectively. To determine the age of the 260-year-old tree from the Sandhills Gamelands, tissue samples from the center of the stump were radio carbon dated with a result of 260 ± 30 years (National Ocean Science Accelerator Mass Spectrometry Lab, NOAA, Woods Hole, MA). All root necromass components decreased with depth. Tap root length ranged from 60 cm (US Army Fort Benning) to 340 cm (Kisatchie National Forest). Lateral root necromass ranged from 0 to 66% of total necromass with a mean of 19.2%. Lateral root necromass ranged from 0 to 68.1 kg while tap root necromass ranged from 8.6 to 125.2 kg. Total root C concentration ranged from 42.5 to 57.8% with a mean of 53.2%. Total root N ranged from 0.05 to 0.27% with a mean of 0.11%.

Soil C and N

Soil C, and N decreased with depth for at all positions excluding stump N between 30 and 50 cm. Soil C at the stump was significantly greater than the midpoint (between stump and living tree) at all levels except the 30 -50 cm depth. Stump soil C was also significantly greater than the living tree at 0 – 10 cm depth, and there was no significant difference between soil C at the midpoint and the living tree at all depths (Figure 9.2A). Stump soil N was significantly higher than the midpoint at 0-10 cm and both midpoint and living tree at 10-20 cm depth (Figure 9.2B).

Modeling

The total, lateral and tap root decay model using AGE and YSC had a k = 0.0578, -0.120, and 0.038 (R^2 =0.90, 0.45, 0.83) respectively. The necromass remaining, C, and N models all used SD, YSC and Tmin as independent variables. The lateral root model had an R^2 of 0.60, 0.59, and, 0.40 and the tap root model had an R^2 of 0.80, 0.79, and 0.34 for necromass remaining, C, and N respectively. The total (lateral + tap root) model had an R^2 of 0.85 for necromass remaining and R^2=0.87 and 0.54 for C and N (Tables 9.2, 9.3, 9.4).
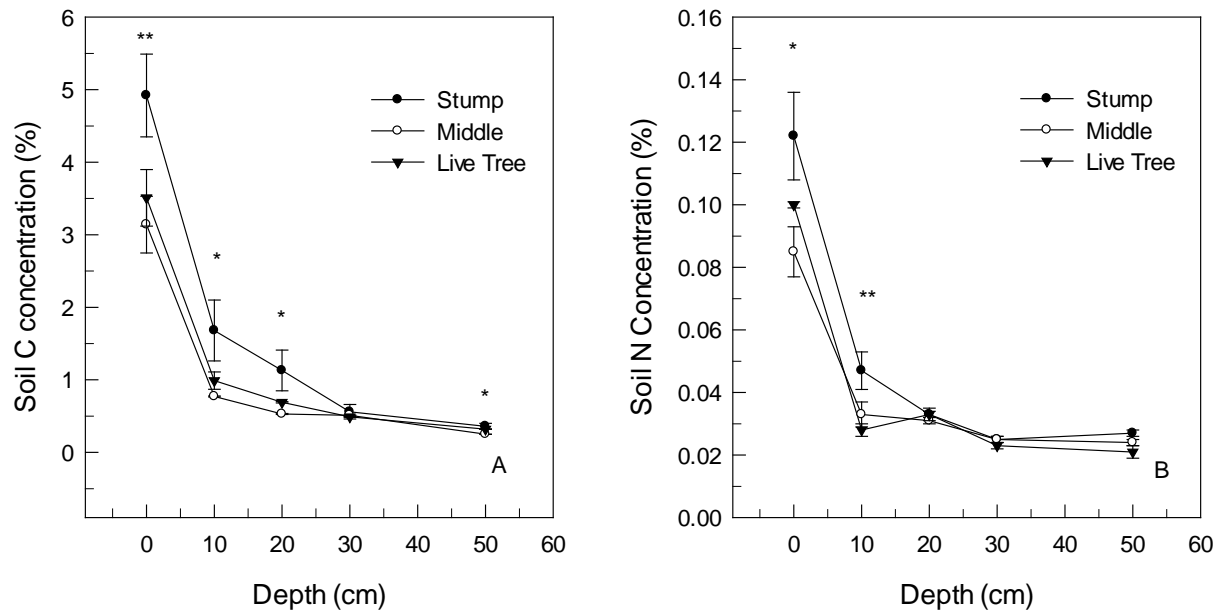
Figure 9.2. Mean soil carbon (A) and nitrogen (B) percentage by depth by position. Stump and live tree samples were taken 50 cm from the stem. The middle position was halfway between stems. * Represents significant difference between stump and middle position samples (p < 0.05). ** Represents significant difference between stump and live tree position samples (p <0.005).

Table 9.2. Parameter estimates and fit statistics of the selected functions to estimate decay rate for coarse roots of longleaf pine trees growing in southeastern U.S. CR_{Decay} is the fraction of initial mass of coarse roots (tap + laterals) after cut; CR_B is the necromass of the coarse roots (tap + laterals; kg) after tree cut; CR_C is the carbon content of the coarse roots (tap + laterals; kg) after tree cut; CR_N is the nitrogen content of the coarse roots (tap + laterals; kg) after tree cut; Age is age when tree was cut (years); YSC is years since cut (years); SD is stump diameter over bark (cm); Tmin is average minimum temperature of the plant hardiness zone (^{0}C).

Variable	Model	Parameter	Parameter Estimate	SE	R^2	RMSE	CV %
CR_{Decay}	$=\exp^{((a1\ +\ a2*AGE)*YSC)}$	a_1	-0.05780	0.00615	0.897	0.167	35.2
		a_2	0.00013	0.00005			
CR_B	$=\exp^{(b1+b2*\ln(YSC)+b3*\ln(SD+b4*\ln(Tmin))}$	b_1	-7.20281	0.82537	0.851	0.361	9.3
		b_2	-0.45562	0.11540			
		b_3	2.39777	0.20848			
		b_4	1.21002	0.19977			
CR_C	$=\exp^{(c1+c2*\ln(YSC)+c3(SD)\ +\ c4*\ln(Tmin))}$	c_1	-8.15494	0.80458	0.872	0.344	10.5
		c_2	-0.48931	0.11030			
		c_3	2.59934	0.19913			
		c_4	1.09425	0.20103			
CR_N	$=\exp^{(d1+d2*\ln(YSC)+d3*\ln(SD))}$	d_1	-8.12023	0.98222	0.536	0.525	16.8
		d_2	-0.75289	0.15555			
		d_3	1.84877	0.29651			

Table 9.3. Parameter estimates and fit statistics of the selected functions to estimate decay rate for lateral roots of longleaf pine trees growing in southeastern U.S. Notation: LR_{Decay} is the fraction of initial mass of lateral roots after cut; LR_B is the necromass of the lateral roots (kg) after tree cut; LR_C is the carbon content of the lateral roots (kg) after tree cut; LR_N is the nitrogen content of the lateral roots (kg) after tree cut; Age is age when tree was cut (years); YSC is years since cut (years); SD is stump diameter over bark (cm); Tmin is average minimum temperature of plant hardiness zone (^{0}C).

Variable	Model	Parameter	Parameter Estimate	SE	R^2	RMSE	CV %
LR_{Decay}	$=\exp^{((a1 + a2*AGE)*YSC)}$	a_1	-0.11970	0.02260	0.45	0.314	47.4
		a_2	0.000366	0.00012			
LR_B	$=\exp^{(b1+b2*\ln(YSC)+b3*\ln(SD+b4*\ln(Tmin))}$	b_1	-18.16572	3.54689	0.599	1.388	37.4
		b_2	-0.70000	0.26265			
		b_3	4.53677	0.77900			
		b_4	1.75683	0.53065			
LR_C	$=\exp^{(c1+c2*\ln(YSC)+c3(SD) + c4*\ln(Tmin))}$	c_1	-20.67174	3.53778	0.587	1.387	53.1
		c_2	-0.02359	0.01067			
		c_3	4.44656	0.78341			
		c_4	2.04335	0.50794			
LR_N	$=\exp^{(d1+d2*\ln(YSC)+d3*\ln(SD))}$	d_1	-17.06214	3.84098	0.404	1.813	23.7
		d_2	-1.23034	0.32889			
		d_3	4.06652	1.03927			

Table 9.4. Parameter estimates and fit statistics of the selected functions to estimate decay rate for tap roots of longleaf pine trees growing in southeastern U.S. Notation: TR_{Decay} is the fraction of initial mass of tap roots after cut; TR_B is the necromass of the tap roots (kg) after tree cut; TR_C is the carbon content of the tap roots (kg) after tree cut; TR_N is the nitrogen content of the tap roots (kg) after tree cut; Age is age when tree was cut (years); YSC is years since cut (years); SD is stump diameter over bark (cm); Tmin is average minimum temperature of plant hardiness zone (^{0}C).

Variable	Model	Parameter	Parameter Estimate	SE	R^2	RMSE	CV %
TR_{Decay}	$=\exp^{((a1 + a2*AGE)*YSC)}$	a_1	-0.0376	0.00556	0.834	0.270	56.9
		a_2					
TR_B	$=\exp^{(b1+b2*\ln(YSC)+b3*\ln(SD+b4*\ln(Tmin))}$	b_1	-5.72755	0.86935	0.799	1.074	10.2
		b_2	-0.37384	0.12155			
		b_3	2.03429	0.21959			
		b_4	1.05985	0.21042			
TR_C	$=\exp^{(c1+c2*\ln(YSC)+c3(SD) + c4*\ln(Tmin))}$	c_1	-7.34874	0.91437	0.794	1.079	12.5
		c_2	-0.01406	0.00511			
		c_3	2.09437	0.21038			
		c_4	1.07287	0.21901			
TR_N	$=\exp^{(d1+d2*\ln(YSC)+d3*\ln(SD))}$	d_1	-6.32135	0.9257	0.347	1.130	14.6
		d_2	-0.53357	0.1466			
		d_3	1.17716	0.27945			

Discussion

Storage of belowground C is an important component of total forest C. However, belowground C changes temporally due to forest growth and tree mortality (natural and via harvesting) and these changes are critical for modeling C in forests under varying management regimes. Decomposition and belowground C can also change spatially across the range of a species. Stump diameter, YSC, and Tmin explained 85, 60, and 80% of the variation in the total, lateral, and tap root necromass remaining.

The rapid decay of fine roots and soluble carbon has been reported in studies from various species and climates. It is generally thought that conifers have a slower decomposition rate and therefore

are a potential sink for C storage (Silver and Miya 2001). Old longleaf stumps are valued for producing "lighter wood" which is sold commercially. Longleaf pine also played an important role in the naval stores industry (Grissino-Mayer et al. 2001). The increased levels of monoterpine production in longleaf pine compared to other southern pine species has been attributed as the source of slow decomposition rates, but the evidence is observational. Eberhardt et al. (2009) showed that monoterpines persist for long periods in heartwood and sapwood of longleaf pine tap roots.

Ludovici et al. (2002) examined the decay rate of roots of 50-year-old loblolly pine in the North Carolina Piedmont and found a loss of 50% necromass after 10 years and that less than 5% of coarse root necromass persisted 60 years after harvest. Our total model (lateral + tap root, k=-0.578 year^{-1}) estimated that 54% of necromass remained after 10 years and 17% was still present after 60 years. When the total necromass model was separated by component, we found that the rapid decrease in lateral root (k=-0.12 year^{-1}) was driving the total root model. In 10 years, 26% of lateral root remained and after 60 years only 8% remained (Figure 9.3.). On the other hand, the tap root had a much lower decomposition rate (k= -0.0376 year^{-1}) and constitutes the majority (80%) of initial necromass. While both the longleaf and loblolly pine models show similar decay rates in the early years after cutting (at 10 years 59% and 64%, respectively), the longleaf pine model indicated that its tap root persisted longer relative to loblolly pine. After 60 years, 30% of longleaf pine tap root remained compared to 5% of loblolly pine. One hundred years after cutting, we estimate that 25% of longleaf tap root necromass remains (Figure 9.3). Although these are not direct species comparisons, we did set the parameters for longleaf pine estimations to share the same PHZ and initial tree size. Thus, it appears that longleaf pine course root systems exhibit substantially lower decomposition rates than loblolly pine. To put this in more context, our tap root model predicts that a longleaf pine with a diameter of 60 cm would still have 18 and 14.6 kg of C in its root system 60 and 100 years after harvest, respectively. Thus, this necromass pool could be a significant contributor to carbon sequestration.

In Norway, a study of aboveground stumps reported decomposition rates of 0.048, 0.052 and 0.068 year^{-1} for Scots pine (*Pinus sylvestris*), Norway spruce (*Picea abies*) and birch (*Betula* sp.), respectively (Shorohova et al. 2008). In Sweden, a model using SD and YSC for Norway spruce (*Picea abies*) reported a decay rate of 0.046 annually for tap and lateral root systems. Based on this rate, the time required for the loss of 50% and 95% of the wood is 15 and 64 years, respectively (Melin et al. 2009). However, these composition rates occurred under far colder conditions (>12^{0}C) than in our study which would greatly reduce decomposition rates.

Decomposing root systems provide many benefits to forests including providing a favorable soil matrix (root channels) for live root development because of decreased soil density and increased water and nutrient availability. Loblolly pine trees growing in natural stands in close proximity to old stumps showed an increase in productivity of 28% compared to controls (Van Lear et al. 2000). Increases in soil N and C in the area surrounding decomposing stumps has been shown in loblolly pine in South Carolina (Van Lear et al. 2000), and a mixed oak maple stand in the Appalachians of Virginia (Sucre and Fox 2009). In our study, soil N concentrations adjacent to the stumps were 30% higher than the midpoint at the 0-10 and 10-20 depths, indicating that decaying stumps have important implications for soil fertility. Soil C concentrations were higher at the stump compared to midpoint between trees at all depths excluding the 30 – 50 cm depth. Soil C at the 0-10 cm

depth was 36% and 29% higher at the stump compared to the midpoint between the stump and the living tree. At the 10 – 20, 20 – 30 and 50 – 100 cm depths, soil C at the stump was 54, 53, and 30% greater than the midpoint between the living trees. These higher soil C concentrations associated with the area surrounding the stumps also have implications for soil C sequestration, meaning that not only is C stored within the decaying stump but decaying stumps also contribute C to the surrounding soil matrix.
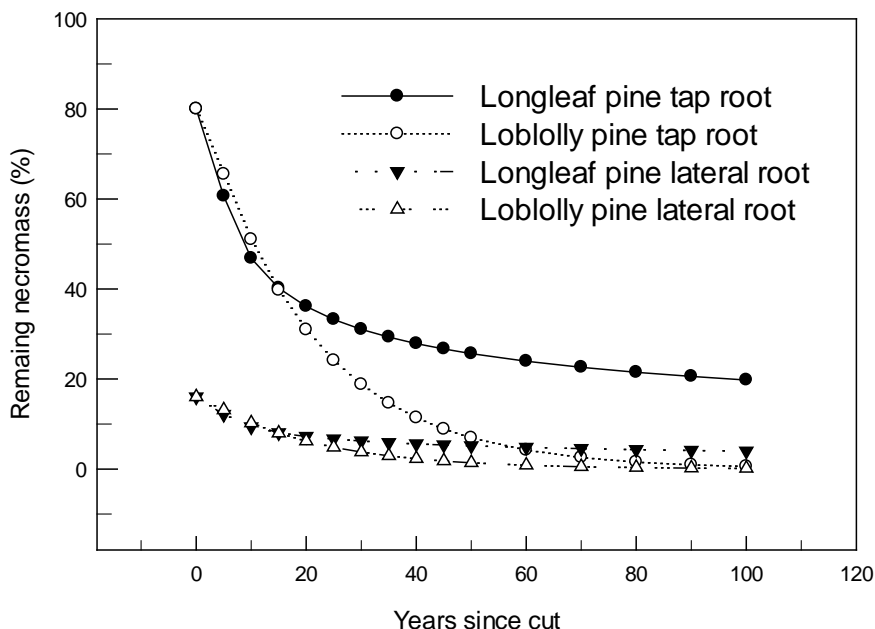
Figure 9.3. Predicted necromass of longleaf and loblolly pine by years since cut for Duke University Forest, Durham, NC by tap root and lateral components. Assumes an average low temperature of 7.7 ^{0}C, stump diameter of 60 cm and 50-years-old at time of harvest. Initial necromass of tap root set to 80% and lateral at 20%. The loblolly pine model was derived using the equation from Ludovici et al. (2002).

This study illustrated several important points. First, the approach was novel in that it utilized a chronosequence across a large range of longleaf pine. The models were rigorous and our results have a broader inference space than a chronosequence in a more narrow geographic area. Where data are available on YSC and SD, predictions of remaining necromass, C, and N can be made using the Tmin variable, easily accessed from the USDA plant hardiness zone map. When YSC and SD are known, and SD is often measured in C assessments (Law et al. 2008), the models can predict the quantity of C retained in necromass in the years following harvest and provide land managers throughout the Southeast with more accurate estimates of C sequestration in longleaf pine forests. Our results indicate that longleaf pine tap roots may be more resistant to decomposition than loblolly pine, most likely because of chemical variation (terpenes) in wood between the two species. Tap root persistence provides a conduit for root infiltration, an increase in soil C and N adjacent to the decaying stumps, and long term root channels, all of which may increase the productivity of remaining trees and enhance seedling recruitment. Lastly, persistence of tap root necromass contributes to long-term forest C sequestration.

119

10. Longleaf Pine Diameter, Height and Volume Functions for Carbon Modeling

[Contents of this chapter were extracted from: C.A. Gonzalez-Benecke, S.A. Gezan, T.A. Martin, W.P. Cropper Jr., L.J. Samuelson, and D.J. Leduc. 2014. Individual tree diameter, height, and volume functions for longleaf pine. Forest Science 60: 43-56.]

Introduction

Accurate estimates of tree height (H, m), stem diameter outside bark at 1.37 m height (dbh, cm) and stem volume (V, m^3) are central to our ability to understand and predict forest C stocks and dynamics from allometric equations described in Chapter 7. Measures of H and V are needed for estimating site productivity, stand vertical structure, and stand and tree-level growth and yield (Staudhammer and LeMay 2000, Temesgen et al. 2007, Weiskittel et al. 2011). Bark thickness (bt, cm) and therefore diameter inside bark (dbh$_{IB}$, cm) and V inside bark (V$_{IB}$, m^3) are also important tree attributes, useful for bark and wood production quantification (Feduccia and Mann 1975, Tiarks and Haywood 1992). Functions to estimate merchantable stem volume from the stump to any top diameter are useful tools to estimate volume breakdown functions when threshold merchantable limits are known (Burkhart 1977, Amateis et al. 1986).

Often local functions to estimate H, bt and dbh$_{IB}$ rely on dbh as the explanatory variable (Weiskittel et al. 2011), and functions to estimate V also rely on dbh and H as explanatory variables (Harrison and Borders 1996). These models are widely used but limited to certain stand characteristics, particularly those from which the data originate. However, inclusion of additional stand variables in these models related to stand age, density and/or productivity often improves the relationships, resulting in general models that provide more accurate predictions (Larsen and Hann 1987, Huang and Titus 1994, Staudhammer and LeMay 2000, Leduc and Goelz, 2009 and 2010). In addition, general models allow for better conditions for inter- and extrapolation and they can provide a sound biological interpretation of the relationships under study.

Few local models have been produced that predict H, dbh$_{IB}$ and V (Baldwin and Saucier 1983, Farrar 1987, Quicke and Meldahl 1992), and only one general model has been reported to predict H (Leduc and Goelz 2010) in longleaf pine trees. Therefore, the objective of this study was to develop a set of local and general models to predict H, dbh$_{IB}$, V$_{OB}$ and V$_{IB}$, as well as functions to determine merchantable stem volume ratio (R) (both, outside and inside bark) from the stump to any top diameter. To our knowledge, this is the first comprehensive individual-tree-level set of equations for longleaf pine trees that includes local and general models that can be applied to longleaf pine trees over a large geographical area and across a wide range of ages and stand characteristics. Functions to estimate V$_{OB}$, V$_{IB}$ and R were used to determine stand-level parameters in order to develop a comprehensive stand-level growth and yield model for the species (Gonzalez-Benecke et al. 2012b).

Materials and Methods

Data description

The dataset used to estimate the parameters for individual tree equations for longleaf pine originates from 229 permanent plots measured and maintained by the U.S. Forest Service's Laboratory at Pineville, LA (Goelz and Leduc 2001). The data were collected from permanent operational plots in a combination of seven studies exploring the effects of spacing and thinning on longleaf pine plantations distributed throughout the Western Gulf Coastal Plain, U.S., from Santa Rosa County in Florida to Jasper County in Texas, and represent the current range of longleaf pine in the Western Gulf Coastal Plain (Goelz and Leduc 2001).

On 25,695 trees, dbh and H were measured to the nearest 2.54 mm and 3.05 cm, respectively. Tree stem V was determined from 9,690 standing trees by measuring diameter outside bark and height to the diameter at 5.08 cm diameter taper steps along the bole from the stump to the point on the stem where diameter was 5.08 cm. On a subset of 2,484 trees, bt was measured at 1.37 m height in two opposite directions, and the average was used for diameter inside bark determinations. Associated with the individual tree-level assessments, basal area (BA, m^2 ha^{-1}), number of trees per hectare (N, ha^{-1}), mean dominant height (H_{dom}, m), defined as the mean of the top 25th percentile tree height, and site index (SI, m), defined as the H_{dom} at a reference age of 50 years, were determined for each plot. Site Index was not directly determined in 79 plots (those plots were not measured at age 50 years), here, SI was predicted using the equation reported by Gonzalez-Benecke et al. (2012). For all trees with H measurement a form factor F = H/dbh (m cm^{-1}) was calculated. In order to eliminate broken and malformed individuals, trees with F less than 0.54 m cm^{-1} and greater than 13.5 m cm^{-1} were excluded from further analyses. Trees with H less than 2.2 m and dbh less than 3 cm were also discarded from the dataset for diameter-height analysis. From the complete dataset, 30 plots were randomly selected and removed to use for model evaluation and the rest (i.e. 237 plots) were used for model fitting. The model evaluation dataset contained 3,163 trees for the dbh vs. H relationship, 1,254 trees for V modeling, and 264 trees for dbh_{IB} modeling. A second independent source of evaluation data (described below) included stands planted outside the geographic range of the data used for model development. In August, 2012, 20 plots were measured in five stands at the US Army Fort Benning in Georgia. Selected stands were 5, 11, 21, 64 and 87 years of age. The 5, 11 and 22- year-old stands were planted and the 64 and 87-year-old stands were natural. Within each stand, dbh, H and CW were directly determined on four 0.4 ha plots. Details of tree and stand characteristics of the fitting dataset and of both evaluation datasets are shown in Table 10.1. General relationships between dbh and H and V outside bark (V_{OB}, m^3) are shown in Figure 10.1.

Model description

The following model proposed by Curtis et al. (1981) and Parresol (1992) was used to estimate total tree height:

$$(H - 1.37) = e^{a_1 + a_2 \cdot dbh^{a_3}} + \varepsilon_1 \tag{1}$$

where a_1 to a_3 are curve fit parameters and ε_1 is the error term, with $\varepsilon_1 \sim N(0, \sigma_1^2)$. This tree-height static local model is commonly fitted considering a fixed power a_3 of -1.0 (Quicke and Meldahl 1992), but in some cases other values can produce better fits (Curtis 1967, Larsen and Hann 1987, Wang and Hann 1988, Zhao et al. 2006).

In addition to dbh, several stand-level variables were included as covariates in the above model to improve the local height-diameter equation, resulting in a general height-diameter equation. . The variables considered corresponded to Age, N, BA, H_{dom}, SI, SDI and Dq. These variables were selected as they represent different aspects of the stand, such as stocking, productivity and competition, which could affect the height-diameter relationships. A model was fitted considering all potential variables and a simplified version was also evaluated that did not considered SI or H_{dom}, as these are not always available. Similar to Crecente-Campo et al. (2010), to test which stand-level variables should be included in the final general model, a logarithm transformation was carried out and stepwise procedure was used on the resulting linear model with a threshold significance value of 0.15 as variable selection criteria and the variance inflation factor (VIF) was monitored to detect multicollinearity between explanatory variables. All variables included in the model with VIF larger than 5 were discarded, as suggested by Neter et al. (1996). The final non-linear forms of the models finally selected to estimate H were:

$$H - 1.37 = e^{(a_1 + a_2 \cdot dbh^{a_3} + Age^{a_4} + BA^{a_5})} + \varepsilon_2 \qquad [2]$$

$$H - 1.37 = e^{(a_1 + a_2 \cdot dbh^{a_3} + Age^{a_4} + BA^{a_5} + SI^{a_6})} + \varepsilon_3 \qquad [3]$$

where Age is the stand age (yr.), BA is the basal area (m^2 ha^{-1}), SI is the site index at age 50 years (m), a_1 to a_6 are curve fit parameters and ε_2 and ε_3 are the error terms, with $\sigma_i \sim N(0, \sigma_i^2)$.

Table 10.1. Summary of individual-tree and stand-level characteristics for planted longleaf pine in Western Gulf Coastal Plain U.S.

Variable	Model development dataset (n = 199)				Model evaluation dataset (n = 30)				Model evaluation dataset (US Army Fort Benning) (n = 20)			
	Mean	SD	Min.	Max.	Mean	SD	Min.	Max.	Mean	SD	Min.	Max.
Age	37.6	15.6	4	73	39.4	16.8	8	73	17.9	14.9	5.0	87.0
dbh	24.6	10.3	3.6	61	25.1	10.2	3.6	57.4	13.0	12.3	0.6	57.4
H	19.6	6.1	2.4	33.3	20	6.2	3	33.9	9.8	7.6	1.5	32.4
dbh_{IB}	15.8	7.9	2.3	44.5	17.9	8.3	3.3	39.9	n.a.	n.a.	n.a.	n.a.
bt	13.8	5.3	2.5	40.6	15.2	5	5.1	34.3	n.a.	n.a.	n.a.	n.a.
V_{OB}	0.5	0.4	0	2.8	0.5	0.4	0	2.1	0.8	1.0	0.0	2.9
N	453	170	175	934	626	448	99	2,145	1396	589	50	2150
BA	14	6.8	3.8	33.1	25.7	12.3	0.4	57.6	14.3	9.0	0.4	24.2
SDI	294	109	97	589	504	230	22	1,160	376	235	19	642
H_{dom}	19.8	4.3	10.8	27.6	22.1	6	2.4	32.2	10.5	5.2	3.1	32.4
SI	28.6	2.7	19.6	34	25.4	1.8	21.4	29.2	25.4	4.1	18.2	33.9

Notes for Table 10.1: Age: stand age (yr.); dbh: diameter at 1.37 m height (cm); H: tree height (m); dbh_{IB}: diameter at 1.37 m height inside bark (cm); bt: bark thickness at 1.37 m height (mm); V_{OB}: stem volume outside bark (m^3); N: trees per hectare (ha^{-1}); BA: stand basal area ($m^2 \ ha^{-1}$); H_{dom}: average height of dominant and codominant trees (m); SI: site index at base age of 50 years (m); SD: standard deviation; n: number of plots.
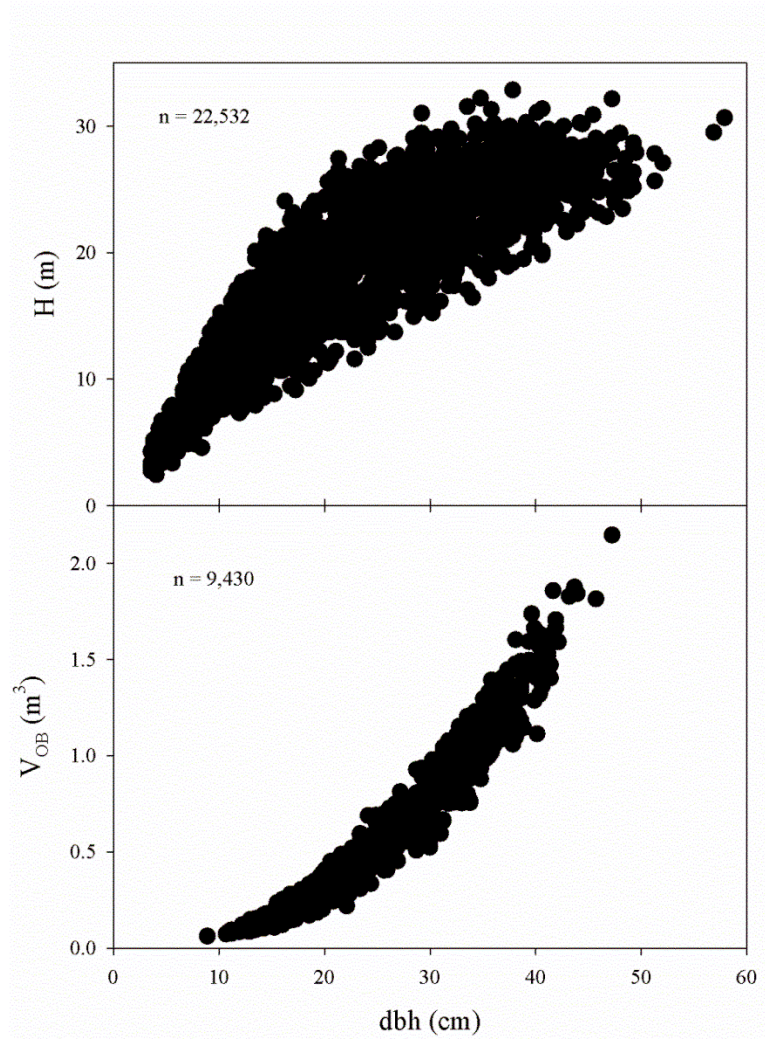
Figure 10.1. Relationships between stem diameter outside bark at 1.37 m height (dbh, cm) and total tree height (H) and stem volume outside bark (V_{OB}, m^3) using the model fitting dataset.

Functions to estimate dbh_{IB} and V_{OB} were fitted using dbh as an independent variable using the following models:

$$dbh_{IB} = b_1 + b_2 \cdot (dbh) + \varepsilon_4 \qquad [4]$$

$$V_{OB} = c_1 \cdot dbh^{c_2} + \varepsilon_5 \qquad [5]$$

If H is known, an alternative model to determine V_{OB} was also fitted:

$$V_{OB} = c_1 \cdot dbh^{c_2} \cdot H^{c_3} + \varepsilon_6 \qquad [6]$$

where b_1, b_2, c_1, c_2 and c_3 are curve fit parameters and ε_4, ε_5 and ε_6 are the error terms, with $\sigma_i \sim N(0, \sigma_i^2)$.

Following the same procedure of linear log-transformation and variable selection criteria used for dbh-H models, general models that include stand-level variables were also fitted for equations 4 to 6. The model finally selected to estimate dbh_{IB} was:

$$dbh_{IB} = b_1 + b_2 \cdot dbh + b_3 \cdot Age + \varepsilon_7 \qquad [7]$$

If H_{dom} and SI are also known, the alternative general model finally selected was:

$$dbh_{IB} = b_1 + b_2 \cdot dbh + b_3 \cdot Age + b_4 \cdot BA + b_5 \cdot SI + \varepsilon_8 \qquad [8]$$

where b_1 to b_5 are curve fit parameters and ε_7, and ε_8 are the error terms, with $\sigma_i \sim N(0, \sigma_i^2)$.

As diameter inside bark was not measured directly at each step along the bole where diameter outside bark was measured, we used the equation reported by Cao and Pepper (1986) that predicts diameter inside bark at any stem height, from outside diameter, outside and inside dbh, relative height and total height, for planted longleaf pines. Stem volume inside-bark (V_{IB}, m^3) was determined in the same way as V_{OB}. Similarly to V_{OB}, local and general functions to estimate V_{IB} were fitted using dbh and dbh and H as independent variables.

The models finally selected to estimate V (both, outside and inside-bark) were:

$$V_{OB} \text{ or } V_{IB} = c_1 \cdot (dbh^{c_2}) \cdot (Age^{c_3}) \cdot (N^{c_4}) \cdot (BA^{c_5}) + \varepsilon_9 \qquad [9]$$

$$V_{OB} \text{ or } V_{IB} = d_1 \cdot (dbh^{d_2}) \cdot (H^{d_3}) \cdot (Age^{d_4}) \cdot (BA^{d_5}) + \varepsilon_{10} \qquad [10]$$

If H_{dom} and SI are also known, the alternative general models finally selected were:

$$V_{OB} \text{ or } V_{IB} = c_1 \cdot (dbh^{c_2}) \cdot (N^{c_3}) \cdot (BA^{c_4}) \cdot (H_{dom}{}^{c_5}) \cdot (SI^{c_6}) + \varepsilon_{11} \qquad [11]$$

$$V_{OB} \text{ or } V_{IB} = d_1 \cdot (dbh^{d_2}) \cdot (H^{d_3}) \cdot (N^{d_4}) \cdot (BA^{d_5}) \cdot (H_{dom}{}^{d_6}) + \varepsilon_{12} \qquad [12]$$

where c_1 to c_6 and d_1 to d_6 are curve fit parameters and ε_9 to ε_{12} are the error terms, with $\sigma_i \sim N(0, \sigma_i^2)$.

A model to estimate merchantable stem volume (both outside and inside bark) from the stump to any top diameter was fitted following the method of Burkhart (1977), where a function that predicts the ratio of merchantable stem volume (both outside and inside bark) divided by total stem volume was determined as follows:

$$R = 1 + e_1 \cdot \left(\frac{d_t^{e_2}}{dbh^{e_3}}\right) + \varepsilon_{13} \tag{13}$$

where R is the ratio between merchantable stem volume (inside or outside bark) to top diameter outside bark (d_t, cm) and total stem volume up to 5.08 cm top limit, e_1, e_2 and e_3, are curve fit parameters and ε_{13} is the error term, with $\varepsilon_{13} \sim N(0, \sigma_{13}^2)$. Average stump height was considered to be 20 cm.

Model evaluation

All statistical analyses were performed with SAS 9.3 (SAS Inc., Cary, NC, USA). The predictive ability of equations 1 to 6 (including general models for equations 3 to 5) was evaluated by comparing predictions to data from the trees in the evaluation dataset. The models that estimate H (eq. 1, 4 and 5) and V_{OB} (eq. 7, 8, 11, 12, 13 and 14) were also evaluated against an independent dataset consisting on five stands located in US Army Fort Benning. The stands had age of 5, 11, 21, 64 and 87 years-old. In each stand, four 0.04 ha inventory plots were measured, recording H and dbh in all trees. In a subset of 11 trees (5 from the 21-year-old stand, 3 from the 64 year-old stand and 3 from the 87 year-old stand), stem volume over bark was directly measured by destructive harvesting the trees and measuring bole diameter over bark at 2 m steps from stump to a minimum diameter of 5 cm (this measurement is part of biomass sampling for a project on Developing Tools for Ecological Forestry and Carbon Management in longleaf pine that is being carried out at the site: http://clpe.auburn.edu/index.html). The three younger stands were planted and the two older stands were naturally regenerated.

Four measures of accuracy were used to evaluate the goodness-of-fit between observed and predicted values for each variable based on the model evaluation dataset: (i) mean absolute error (MAE); (ii) root mean square error (RMSE); (iii) mean bias error (Bias); and (iv) coefficient of determination (R^2) (Fox 1981, Loague and Green 1991, Kobayashi and Salam 2000).

Using the same dataset for model evaluation, the equations were also compared against other models reported in the literature for longleaf pine trees. These corresponded to: (i) diameter-height equations reported by Quicke and Meldahl (1992) and Leduc and Goelz (2010); (ii) diameter inside bark at breast height equation reported by Farrar (1987); (iii) total stem volume equations reported by Baldwin and Saucier (1983); and (iv) merchantable stem volume from the stump to any top diameter equation reported by Saucier et al. (1981).

Results

The model parameter estimates for the planted longleaf pine trees growing in Western Gulf Coastal Plain U.S. are reported in Tables 10.2 and 10.3. The index 1 was used in these models as they are all local equations (i.e. do not consider stand-level variables). All parameter estimates were significant at $P < 0.001$.

Model fitting

The model that estimates H using dbh as the only dependent variable (H1) has a coefficient of variation (CV, RMSE as a percentage of observed mean value) of 14.9% (Table 10.2). When stand parameters Age, N, BA, H_{dom} and SI were included into the model (H3), N and H_{dom} were not significant into the final model that minimized the sum of squares of equation 2, having a CV of 7.6% (Table 10.3). As an alternative model we fitted the equation without SI and H_{dom} (H2): this model had a RMSE 1.36% larger than the model that included SI, but 40% smaller than the model that only used dbh as predictor. The parameters Age, BA and SI had a positive effect on H (positive value of parameter estimates): as the value of those parameters increased, the height of the tree was larger for any given tree dbh. In all cases multicollinearity between explanatory variables was small (VIF < 5).

The model that estimates dbh_{IB} as a function of dbh ($dbh_{IB}1$) had a CV, RMSE and R^2 of about 3.53%, 0.53 and 0.995, respectively. When stand parameters Age, N, BA, H_{dom} and SI were included into the model ($dbh_{IB}3$), Age, BA, H_{dom} and SI were significant, but as H_{dom} presented a VIF of 25.7, it was dropped from the final model (data not shown). The final general model to estimate dbh_{IB} only slightly improved the fit, having RMSE and CV of about 3.2% and 0.51, respectively. An alternative model was fitted assuming that H_{dom} and SI are unknown. This optional model ($dbh_{IB}2$) presented similar CV, RMSE and R^2 than the whole models described previously. In all cases, the multicollinearity between explanatory variables was small (VIF < 5).

Two different local models were fitted to estimate V (both, outside and inside-bark): using dbh (eq. 7) or using dbh and H (eq. 8) as independent variables. Including H highly improved the fit of the model: the former model that used only dbh ($V_{OB}1$) had a CV and RMSE of about 14.9% and 0.08, respectively, while the model that used dbh and H ($V_{OB}4$) had a CV and RMSE of about 8.1% and 0.04 (Table 10.2). For the models that depended on dbh, when stand parameters Age, N, BA, H_{dom} and SI were included, all variables were significant in the final model but as Age produced a VIF of 16.4 (data not shown), it was dropped from the final model. The final general model, which included N, BA, H_{dom} and SI as explanatory variables ($V_{OB}3$), had CV and RMSE of about 10.4% and 0.05, respectively (Table 10.3). An alternative model was fitted assuming that H_{dom} and SI are unknown: the resulting model ($V_{OB}2$) was dependent, besides dbh, on Age, N and BA and had both a CV and RMSE 14% smaller than the reduced model. For $V_{OB}2$, the parameters for Age and N had a positive effect on V [positive value of parameter estimate]: trees of the same dbh will have a greater V_{OB} if they are older or they are growing in stands with larger tree density.

Table 10.2. Parameter estimates and fit statistics of the Western Gulf Coastal Plain U.S. planted longleaf pine trees equations.

	Model	Parameter	Parameter Estimate	SE	n	R^2	RMSE	CV
H1	$H - 1.37 = a_1 + a_2 \cdot dbh^{a_3}$	a_1	3.773937	0.019028	22,532	0.977	2.92	14.88
		a_2	-7.844121	0.194658				
		a_3	-0.710479	0.015122				
$dbh_{IB}1$	$dbh_{IB} = b_1 + b_2 \cdot dbh$	b_1	-0.869346	0.027399	2,173	0.995	0.53	3.30
		b_2	0.897180	0.001320				
$V_{OB}1$	$V_{OB} = c_1 \cdot dbh^{d_2}$	c_1	0.000457	0.000009	9,430	0.986	0.08	14.94
		c_2	2.187608	0.005386				
$V_{IB}1$	$V_{IB} = c_1 \cdot dbh^{d_2}$	c_1	0.000264	0.000005	9,430	0.986	0.06	11.18
		c_2	2.260839	0.005491				
$V_{OB}4$	$V_{OB} = d_1 \cdot dbh^{d_2} \cdot H^{d_3}$	d_1	0.000054	0.000001	9,430	0.996	0.04	8.04
		d_2	1.842136	0.003652				
		d_3	1.070207	0.007229				
$V_{IB}4$	$V_{IB} = d_1 \cdot dbh^{d_2} \cdot H^{d_3}$	d_1	0.000031	0.000001	9,430	0.996	0.03	6.13
		d_3	1.917270	0.003781				
		d_2	1.072289	0.007467				
R_{OB}	$R_{OB} = 1 - e_1 \cdot \left(\dfrac{d_t^{e_2}}{dbh^{e_3}}\right)$	e_1	0.532609	0.003100	35,571	0.996	0.04	6.28
		e_2	3.997480	0.007351				
		e_3	3.808041	0.007641				
R_{IB}	$R_{IB} = 1 - e_1 \cdot \left(\dfrac{d_t^{e_2}}{dbh^{e_3}}\right)$	e_1	0.551688	0.003183	35,571	0.995	0.05	6.20
		e_2	3.975042	0.007266				
		e_3	3.792207	0.007554				

Notes or Table 10.2: H: total tree height (m); dbh: diameter outside-bark at 1.37 m height (cm); dbh_{IB}: diameter inside-bark at 1.37 m height (cm); V_{OB}: stem volume outside-bark up to 5.08 cm diameter limit (m^3); V_{IB}: total stem volume inside-bark up to 5.08 cm diameter limit (m^3); R_{OB}: ratio between merchantable stem volume outside bark to top diameter d_t divided by total stem volume outside bark up to 5.08 cm diameter limit outside-bark; R_{IB}: ratio between merchantable stem volume inside bark to top diameter d_t divided by total stem volume inside bark up to 5.08 cm diameter limit outside-bark; d_t: top diameter outside bark (cm); SE: standard error; n: number of observations; R^2: coefficient of determination; RMSE: root mean square error; CV: coefficient of variation (100·RMSE/mean). For all parameter estimates: P < 0.001.

Table 10.3. Parameter estimates and fit statistics of the Western Gulf Coastal Plain planted longleaf pine trees equations including stand variables.

Model		Parameter	Parameter estimate	SE	n	VIF	R^2	RMSE	CV
H2	$H - 1.37 = e^{(a_1 + a_2 \cdot dbh^{a_3} + \cdot Age^{a_4} + BA^{a_5})}$	a_1	0.059425	0.009450	22,532	-	0.992	1.762	8.97
		a_2	-10.803775	0.298591		2.55			
		a_3	-1.127503	0.014269		4.95			
		a_4	0.150532	0.000942		3.43			
		a_5	0.121239	0.000832		2.61			
H3	$H - 1.37 = e^{(a_1 + a_2 \cdot dbh^{a_3} + \cdot Age^{a_4} + BA^{a_5} + SI^{a_6})}$	a_1	-2.573981	0.015599	22,532	-	0.994	1.495	7.61
		a_2	-13.977064	0.350413		2.42			
		a_3	-1.266507	0.012507		3.49			
		a_4	0.185690	0.000724		1			
		a_5	0.078576	0.001010		1.58			
		a_6	0.283800	0.001563		1.46			
$dbh_{IB}2$	$dbh_{IB} = b_1 + b_2 \cdot dbh + b_3 \cdot Age$	b_1	-1.089962	0.034429	2,173	-	0.996	0.519	3.23
		b_2	0.886879	0.001639		1.61			
		b_3	0.014879	0.001460		1.61			
$dbh_{IB}3$	$dbh_{IB} = b_1 + b_2 \cdot dbh + b_3 \cdot Age + b_4 \cdot BA + b_5 \cdot SI$	b_1	-2.150585	0.170537	2,173	-	0.996	0.514	3.20
		b_2	0.886310	0.001642		1.65			
		b_3	0.022423	0.002441		4.59			
		b_4	-0.005599	0.003249		3.61			
		b_5	0.032070	0.005073		1.36			
$V_{OB}2$	$V_{OB} = c_1 \cdot (dbh^{c_2}) \cdot (Age^{c_3}) \cdot (N^{c_4}) \cdot (BA^{c_5})$	c_1	0.000078	0.000003	9,430	-	0.990	0.066	12.78
		c_2	2.099555	0.006652		1.86			
		c_3	0.540248	0.009501		3.92			
		c_4	0.085189	0.004088		2.89			
		c_5	-0.145425	0.004398		4.80			
$V_{OB}3$	$V_{OB} = c_1 \cdot (dbh^{c_2}) \cdot (N^{c_3}) \cdot (BA^{c_4}) \cdot (H_{dom}^{c_5}) \cdot (SI^{c_6})$	c_1	0.000031	0.000001	9,430	-	0.993	0.054	10.40
		c_2	2.078588	0.005352		1.84			
		c_3	0.065959	0.003444		3.17			
		c_4	-0.108270	0.003745		4.52			
		c_5	1.085691	0.013359		2.88			
		c_6	-0.127886	0.015951		1.71			

Model		Parameter	Parameter estimate	SE	n	VIF	R^2	RMSE	CV
$V_{IB}2$	$V_{IB} = c_1 \cdot (dbh^{c_2}) \cdot (Age^{c_3}) \cdot (N^{c_4}) \cdot (BA^{c_5})$	c_1	0.000045	0.000002	9,430	-	0.990	0.050	9.61
		c_2	2.173753	0.006798		1.86			
		c_3	0.541315	0.009676		3.92			
		c_4	0.084559	0.004127		2.89			
		c_5	-0.145635	0.004456		4.80			
$V_{IB}3$	$V_{IB} = c_1 \cdot (dbh^{c_2}) \cdot (N^{c_3}) \cdot (BA^{c_4}) \cdot (H_{dom}^{c_5}) \cdot (SI^{c_6})$	c_1	0.000018	0.000001	9,430	-	0.993	0.04	7.85
		c_2	2.151768	0.005495		1.84			
		c_3	0.065305	0.003492		3.17			
		c_4	-0.108915	0.003819		4.52			
		c_5	1.095234	0.013734		2.88			
		c_6	-0.136949	0.016283		1.71			
$V_{OB}5$	$V_{OB} = d_1 \cdot (dbh^{d_2}) \cdot (H^{d_3}) \cdot (Age^{d_4}) \cdot (BA^{d_5})$	d_1	0.000046	0.000001	9,430	-	0.996	0.04	7.82
		d_2	1.856293	0.004046		1.74			
		d_3	1.012445	0.007939		2.31			
		d_4	0.101381	0.005997					
		d_5	-0.030956	0.001454		1.74			
$V_{OB}6$	$V_{OB} = d_1 \cdot (dbh^{d_2}) \cdot (H^{d_3}) \cdot (N^{d_4}) \cdot (BA^{d_5}) \cdot (H_{dom}^{d_6})$	d_1	0.000056	0.000002	9,430	-	0.996	0.04	7.85
		d_2	1.851051	0.004908		1.73			
		d_3	1.046938	0.012733		2.23			
		d_4	-0.021418	0.002519		1.06			
		d_5	-0.003044	0.002522					
		d_6	0.041285	0.014362		1.51			
$V_{IB}5$	$V_{IB} = d_1 \cdot (dbh^{d_2}) \cdot (H^{d_3}) \cdot (Age^{d_4}) \cdot (BA^{d_5})$	d_1	0.000026	0.000001	9,430	-	0.996	0.03	5.98
		d_2	1.931795	0.004190		1.74			
		d_3	0.105677	0.006205		2.31			
		d_4	-0.032210	0.001500					
		d_5	1.013361	0.008168		1.74			
$V_{IB}6$	$V_{IB} = d_1 \cdot (dbh^{d_2}) \cdot (H^{d_3}) \cdot (N^{d_4}) \cdot (BA^{d_5}) \cdot (H_{dom}^{d_6})$	d_1	0.000032	0.000001	9,430	-	0.996	0.03	6.00
		d_2	1.926111	0.005073		1.73			
		d_3	1.048862	0.013118		2.23			
		d_4	-0.022558	0.002589		1.06			
		d_5	-0.002865	0.002605					
		d_6	0.042822	0.014821		1.15			

Notes for Table 10.3: H: total tree height (m); dbh: diameter outside-bark at 1.37 m height (cm); bt: bark thickness (mm); dbh_{IB}: diameter inside-bark at 1.37 m height (cm); V_{OB}: stem volume outside-bark up to 5.08 cm diameter limit (m^3); V_{IB}: total stem volume inside-bark up to 5.08 cm diameter limit (m^3); Age: tree age (years); BA: stand basal area (m^2 ha^{-1}); N: trees per hectare (ha^{-1}); H_{dom}: average height of dominant and codominant trees (m); SI: stand site index (m); SE: standard error; n: number of observations; VIF: variance inflation factor; R^2: coefficient of determination; RMSE: root mean square error; CV: coefficient of variation (100·RMSE/mean). For all parameter estimates: $P < 0.001$.

Only the parameter for BA had a negative sign. Trees of the same dbh, age and growing in stands with the same N will have smaller V_{OB} if they are growing in stands with larger BA. This effect should be related to changes in tapering and crown length in those stands.

In the case of the model to estimate V that depended on dbh and H, stand parameters had little effect on model fitting even if they were statistically significant. The model that minimized the sum of squares included, besides dbh and H, stand Age, N, H_{dom} and SI, but H_{dom} was dropped due to their high VIF (18.5 respectively, data not shown); however, this new model had little impact on model fit, reducing both CV and RMSE by less than 1% ($V_{OB}6$). The parameter N had a negative value on $V_{OB}6$ model, implying that trees of the same dbh and H will have a smaller V if they are growing in stands with larger N. This effect should be related with changes in tapering and crown length in those stands. An alternative model was also fitted assuming that H_{dom} and SI are unknown ($V_{OB}5$). The resulting model was dependent on Age and BA in addition to dbh and H. In the case of V_{IB} models, the fit was always slightly better than V_{OB} models with the same set of predicting variables. In all cases VIF < 5 (Table 10.3).

The models that estimate the ratio of merchantable stem volume (both outside and inside bark) to top diameter outside bark d_t divided by total stem volume up to 5.08 cm diameter limit outside-bark (eq. 8) had a CV, RMSE and R^2 of about 6.2%, 0.048 and 0.996, respectively (Table 10.2).

Model validation

The relationship between predicted and observed values of H using the general model, that only depended on dbh (Model H1; Figure 10.2), showed a tendency to underestimate the results for trees with H larger than about 25 m. When stand parameters stand Age, BA and SI were included in the model the relationship between observed and predicted values improved considerably (Model H3; Figure 10.2) and there was no noticeable trend in residuals against observed values. All model performance tests showed that H estimations improved their agreement with measured values when stand parameters were included in the general model (Table 10.4). For example, MAE and RMSE were reduced from 11.9 and 14.6% (Model H1) to 4.9 and 6.5% (Model H3), respectively, and R^2 was increased from 0.784 to 0.957, respectively.

There was good agreement between predicted and observed values for dbh$_{IB}$ (Figure 10.3), with no noticeable trend in residuals against observed values (Figure 10.3). For dbh$_{IB}$ models, there was not model performance improvement when stand parameters were included.

There was good agreement between predicted and observed values for V (Figure 10.4, only V$_{OB}$ shown), with no noticeable trend in residuals against observed values. In the case of the model that used dbh as explanatory variable (Figure 10.4), when stand parameters were included, the final local model, showed a better agreement (Figure 10.4) with reduced dispersion of residuals (Figure 10.4). On the other hand, the model that used only dbh and H as explanatory variables (Figure 10.4) showed better agreement than the model that used only dbh (Figure 10.4). Performance tests showed that V estimations that use dbh as explanatory variable were improved when stand parameters were included in the general model (Table 10.4).
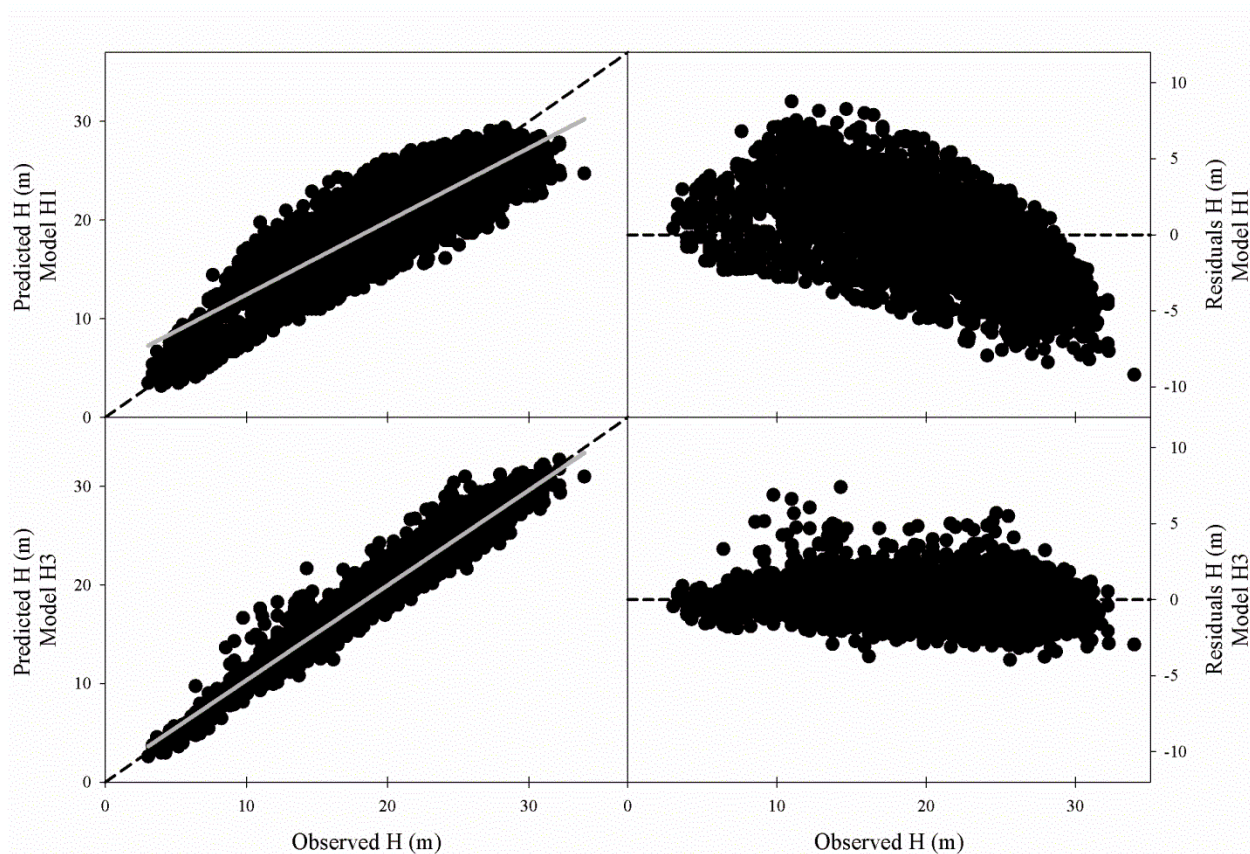
Figure 10.2. Observed versus predicted height (H) using the Model H1 that used dbh as an explanatory variable or Model H3 that used dbh, age, BA, N and SI. The relationships between the residuals versus observed values using Model H1 and Model H3 are also shown. The gray line in the left panels represents the linear fit between observed and predicted values.
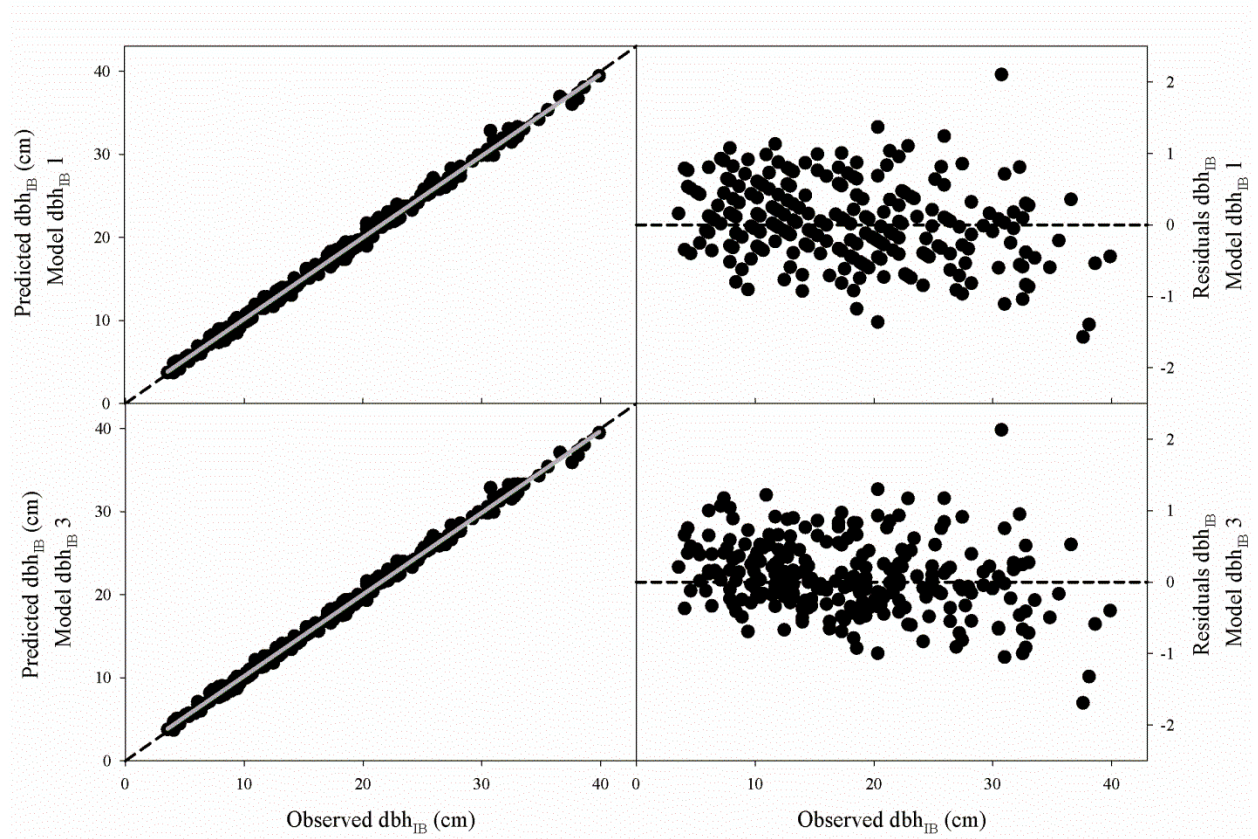
Figure 10.3. Observed versus predicted diameter at breast height inside bark (dbh$_{ib}$) using Model dbh$_{IB}$1 that used dbh as explanatory variable and Model dbh$_{IB}$3 that used dbh and H$_{dom}$. The relationships between residuals versus observed values using Model dbh$_{IB}$1 and Model dbh$_{IB}$3 are also shown The gray line in the left panels represents the linear fit between observed and predicted values.
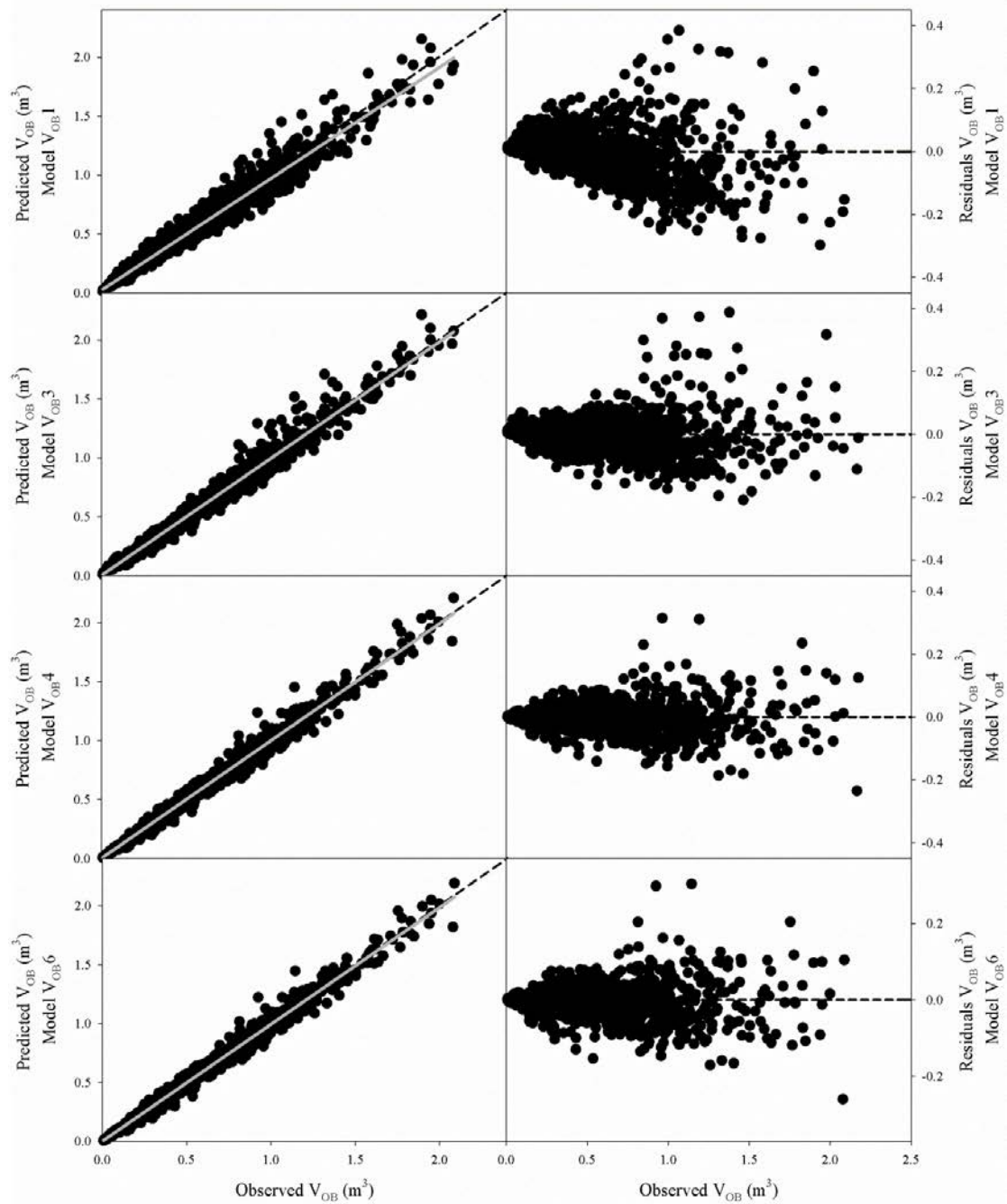
Figure. 10.4. Observed versus predicted values for stem volume outside bark (V_{OB}) using Model $V_{OB}1$ that used dbh as explanatory variable, Model $V_{OB}4$ that used dbh and H, Model $V_{OB}3$ that used dbh, N, H_{dom} and SI, and Model $V_{OB}6$ that used dbh, H, N, H_{dom} and SI. Relationships between residuals and observed values are shown. The gray lines in the left panels represent the linear fit between observed and predicted values.

Table 10.4. Summary of model evaluation statistics for H, dbh$_{IB}$, V$_{OB}$, V$_{IB}$, dbh, R$_{OB}$ and R$_{IB}$ estimations.

Dependent Variable	Model	Explanatory Variables	$\overline{O}$	$\overline{P}$	n	MAE	RMSE	Bias	R^2
H	H1	dbh	20.03	19.89	3,163	2.374 (11.9)	2.915 (14.6)	-0.132 (-0.7)	0.784
	H2	dbh, Age, BA	20.03	20.32	3,163	1.459 (7.3)	1.849 (9.2)	0.295 (1.5)	0.915
	H3	dbh, Age, BA, SI	20.03	19.99	3,163	0.99 (4.9)	1.297 (6.5)	-0.033 (-0.2)	0.957
dbh$_{IB}$	dbh$_{IB}$1	dbh	17.95	17.97	263	0.432 (2.4)	0.551 (3.1)	0.023 (0.1)	0.996
	dbh$_{IB}$2	dbh, Age	17.95	18.01	263	0.397 (2.2)	0.517 (2.9)	0.054 (0.3)	0.996
	dbh$_{IB}$3	dbh, Age, BA, SI	17.95	18.02	263	0.395 (2.2)	0.514 (2.9)	0.067 (0.4)	0.996
V$_{OB}$	V$_{OB}$1	dbh	0.544	0.536	1,254	0.054 (9.9)	0.076 (14.0)	-0.008 (-1.4)	0.963
	V$_{OB}$2	dbh, Age, N, BA	0.544	0.54	1,254	0.046 (8.5)	0.068 (12.4)	-0.004 (-0.8)	0.970
	V$_{OB}$3	dbh, N, BA, H$_{dom}$, SI	0.544	0.541	1,254	0.038 (7.0)	0.057 (10.5)	-0.003 (-0.6)	0.979
	V$_{OB}$4	dbh, H	0.544	0.543	1,254	0.029 (5.3)	0.045 (8.2)	-0.001 (-0.2)	0.987
	V$_{OB}$5	dbh, H, Age, BA	0.544	0.542	1,254	0.028 (5.1)	0.042 (7.8)	-0.002 (-0.4)	0.988
	V$_{OB}$6	dbh, H, N, BA, H$_{dom}$	0.544	0.541	1,254	0.028 (5.2)	0.043 (7.9)	-0.003 (-0.5)	0.988
V$_{IB}$	V$_{IB}$1	dbh	0.401	0.395	1,254	0.04 (10.0)	0.057 (14.2)	-0.005 (-1.3)	0.964
	V$_{IB}$2	dbh, Age, N, BA	0.401	0.398	1,254	0.034 (8.6)	0.051 (12.7)	-0.003 (-0.7)	0.971
	V$_{IB}$3	dbh, N, BA, H$_{dom}$, SI	0.401	0.398	1,254	0.029 (7.1)	0.044 (10.9)	-0.002 (-0.6)	0.979
	V$_{IB}$4	dbh, H	0.401	0.399	1,254	0.022 (5.5)	0.034 (8.5)	-0.002 (-0.5)	0.987
	V$_{IB}$5	dbh, H, Age, BA	0.401	0.398	1,254	0.021 (5.3)	0.032 (8.1)	-0.003 (-0.7)	0.988
	V$_{IB}$6	dbh, H, N, BA, H$_{dom}$	0.401	0.399	1,254	0.022 (5.4)	0.033 (8.2)	-0.002 (-0.5)	0.988
R$_{OB}$ d_t=10.16	R$_{OB}$	dbh, d_t	0.933	0.927	1,199	0.015 (1.6)	0.033 (3.5)	-0.005 (-0.6)	0.931
R$_{IB}$ d_t=10.16	R$_{IB}$	dbh, d_t	0.938	0.932	1,199	0.014 (1.5)	0.032 (3.4)	-0.006 (-0.7)	0.931
R$_{OB}$ d_t=15.24	R$_{OB}$	dbh, d_t	0.836	0.834	1,050	0.028 (3.4)	0.045 (5.3)	-0.003 (-0.3)	0.934
R$_{IB}$ d_t=15.24	R$_{IB}$	dbh, d_t	0.828	0.826	1,050	0.029 (3.5)	0.045 (5.5)	-0.002 (-0.3)	0.934

Notes for Table 10.4: H: total tree height (m); dbh: diameter outside-bark at 1.37 m height (cm); dbh$_{IB}$: diameter inside-bark at 1.37 m height (cm); V$_{OB}$: total stem volume outside-bark up to 5.08 cm diameter limit (m^3); V$_{IB}$: total stem volume inside-bark up to 5.08 cm diameter limit (m^3); R$_{OB}$: ratio between merchantable stem volume outside bark to top diameter d_t divided by total stem volume outside bark up to 5.08 cm diameter limit outside-bark; R$_{IB}$: ratio between merchantable stem volume inside bark to top diameter d_t divided by total stem volume inside bark up to 5.08 cm diameter limit outside-bark; d_t: top diameter outside bark (cm); Age: tree age (years); BA: stand basal area (m^2 ha^{-1}); N: trees per hectare (ha^{-1}); H$_{dom}$: average height of dominant and codominant trees (m); SI: stand site index (m); $\overline{O}$: mean observed value; $\overline{P}$: mean predicted value; n: number of observations; MAE: mean absolute error; RMSE: root of mean square error; Bias: absolute bias estimator; R^2: coefficient of determination. Values in parenthesis are percentage relative to observed mean. Note: MAE, RMSE and Bias are presented in the same units as dependent variable.

For example, Bias was reduced from 1.4% (Model $V_{OB}1$) to 0.6% (Model $V_{OB}3$) underestimations, and MAE and RMSE were reduced from 9.9 and 14.0% (Model $V_{OB}1$) to 7.0 and 10.5% (Model $V_{OB}3$), respectively. In the case of V estimations that use dbh and H as explanatory variables, the improvement in model performance was marginal when stand parameters were included (MAE and RMSE were reduced from 5.3 and 8.2% (Model $V_{OB}4$) to 5.2 and 7.9% (Model $V_{OB}6$), respectively). Estimated and observed values were highly correlated, with R^2 values greater than 0.96.

For the two examples of d_t used (d_t = 10.16 cm, Figure 10.5; d_t = 15.24 cm, Figure 10.5), there was good agreement between predicted and observed R_{OB} (Figure 10.5) and merchantable volume outside-bark (V_{m-OB}; Figure 10.5). There was more data dispersion for small R_{OB} (Figure 105), that correspond with trees with dbh closer to d_t (Figure 10.5), but the magnitude of that error (m^3) was negligible when V_{m-OB} was calculated (Figure 10.5). There was no noticeable trend of residuals with observed values (data not shown). All model performance tests showed that estimations of R (both, outside and inside bark) agreed well with measured values (Table 10.4). For the two d_t used, MAE and RMSE ranged between 1.5 to 3.5%, and 3.4 to 5.5% of the observed values, respectively. The Bias ranged between 0.3 to 0.7% under-estimations. Estimated and observed values were highly correlated, with R^2 values greater than 0.93.

Comparison against reported equations for longleaf pine

When tested on the dataset used for model evaluation, predicted values of the models proposed in this study for H, dbh_{IB}, V_{OB} and R_{OB} are within the range of variation of the estimations using other published longleaf pine equations. The effects of tree age on H, dbh_{IB}, V_{OB} and R_{OB} estimations for several models for longleaf pine trees are presented in Figure 10.6.

Across four age classes (< 20, 21-40, 41-60 and 61-73 years), the models reported in this study predicted dbh_{IB} and V_{OB} consistently, with no clear trend to over- or under-estimate, with Bias less than 6% and RMSE less than 16% (Figure 10.6). However, for all models, there was a general trend to reduce RMSE% as trees aged (right panels in Figure 10.6). In the case of H estimations for trees younger than 20 years-old using the model that used only dbh as explanatory variable (H1, Figure 10.6), Bias and RMSE averaged about 16% and 27%, respectively. For that age range, H estimations with the models reported by Quicke and Meldahl (1992) (H4, for naturally regenerated longleaf pine trees, only use dbh as explanatory variable) and Leduc and Goelz (2010) (H5, for planted longleaf pine trees, use dbh, H_{dom} and quadratic mean diameter as explanatory variable) had Bias of about 22.1 and 7.7%, respectively. On the other hand, the model reported in this study that included stand parameters (H3, uses dbh, N, BA and SI as explanatory variables) had a Bias of 2.4%. In the age class 41-60 years all models showed Bias ranging between -4.2 to -0.2%. For the age class 61-73 years, the model reported by Leduc and Goelz (2010) had smaller RMSE than all other models. Across all age classes, H3 had smaller Bias than all other models (Figure 10.6).
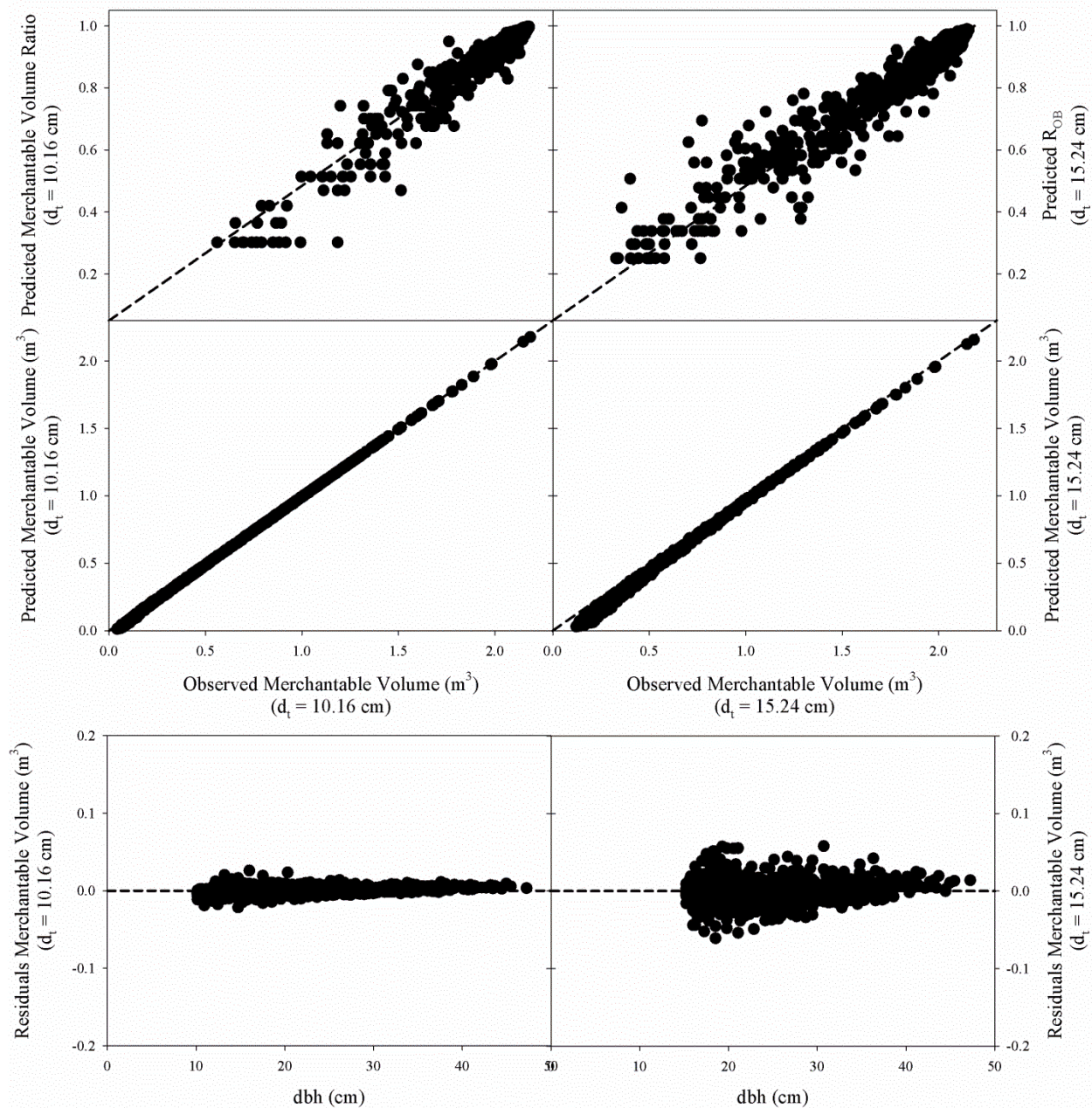
Figure 10.5. Observed versus predicted values, and residuals versus observed values for merchantable volume outside bark ratio (R_{OB}) and merchantable volume outside bark ($V_{m\text{-}OB}$), and residuals of $V_{m\text{-}OB}$ versus observed dbh. Two examples of merchantable volume outside bark are shown using $d_t = 10.16$ and $d_t = 15.24$ cm.

137
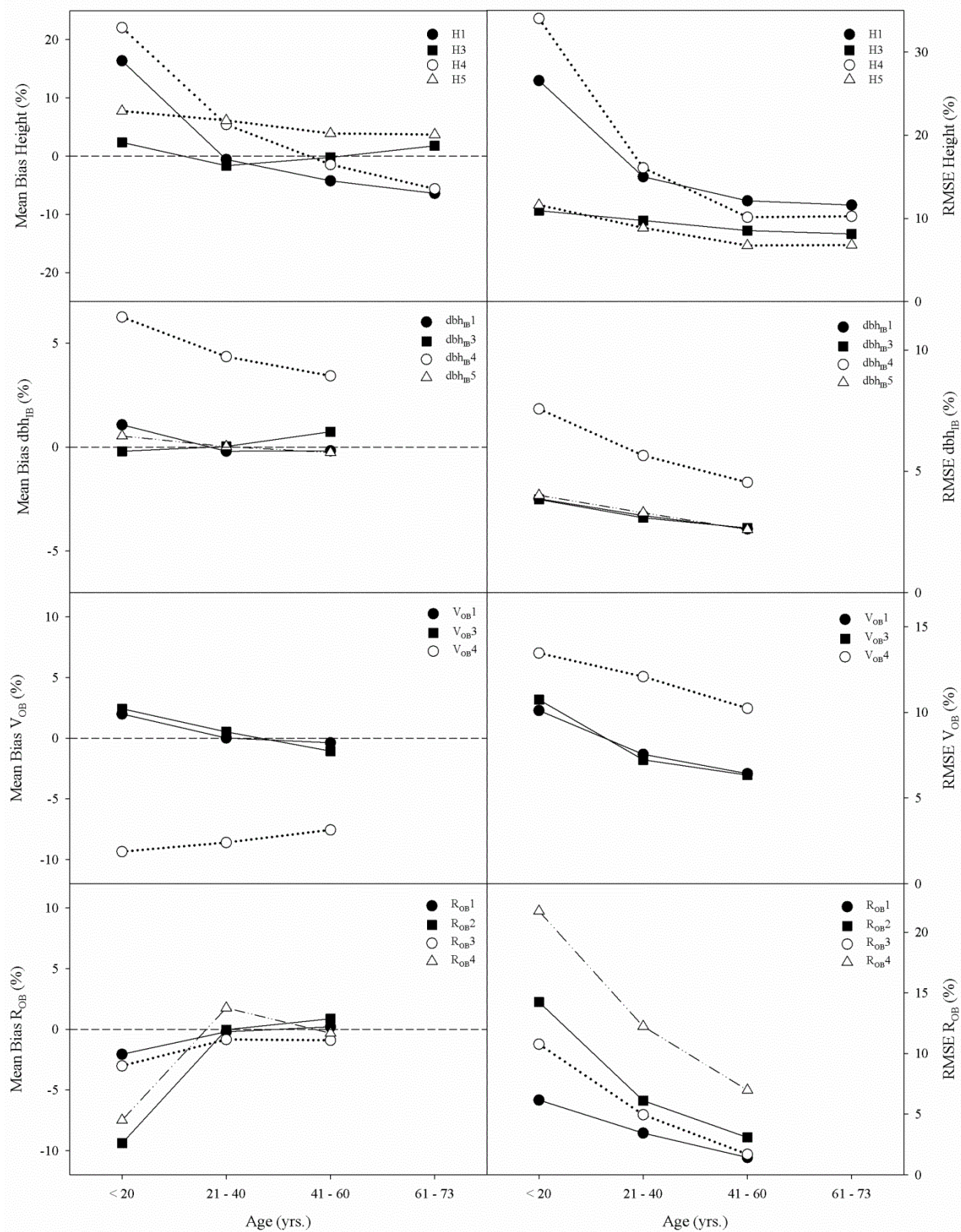
Figure 10.6. Mean Bias and RMSE presented as percentages of the mean for the models reported in this study and in the literature for predicted total tree height (H), diameter at breast height inside bark (dbh$_{ib}$), stem volume outside bark (V$_{OB}$), and stem volume ratio outside bark (R$_{OB}$) of longleaf pine trees across four stand age classes: < 20, 21-40, 41-60 and 61-73 years. The H models are: current report general model (H1), current report local model (H3), Quicke and Meldahl (1992) (H4) and Leduc and Goelz (2010) (H5). The dbh$_{ib}$ models are: current report general model (dbh$_{IB}$1), current report local model (dbh$_{IB}$3), Farrar (1987) (dbh$_{IB}$4, assuming a live crown ratio smaller than 36%) and Farrar (1987) (D$_{IB}$5, assuming a live crown ratio greater than 50%). For VOB the models are: current report general model (V$_{OB}$1), current report local model (V$_{OB}$3) and Baldwin and Saucier (1983) (V$_{OB}$4). For R$_{OB}$ the models are: current report using dt = 10.16 cm (R$_{OB}$1), current report using dt = 15.24 cm (R$_{OB}$2), Saucier et al. (1981) using dt = 10.16 cm (R$_{OB}$3) and Saucier et al. (1981) using dt = 15.24 cm (R$_{OB}$4).

For dbh$_{IB}$ estimations, the models reported in this study, across all age classes, ranged in Bias between -0.2 to 1.1% (dbh$_{IB}$1) and -0.2 to 0.7% (dbh$_{IB}$3), while the model reported by Farrar (1987) predicted well if a live crown ratio larger than 50% was assumed with Bias ranging between -0.3 to 0.5%. If a live crown ratio lower than 36% was assumed, the Bias of the model of Farrar (1987) increased, ranging between 2.1 and 3.4%.

In the case of V$_{OB}$, across age classes, the model reported by Saucier et al. (1981) underestimated by about 8.5% and had an average RMSE of 11.9%, while the model reported in this study that used dbh^2·H (V$_{OB}$1 and V$_{OB}$3), had a Bias and RMSE between -1.1 to 2.4%, and 6.3 and 10.7%, respectively. For merchantable volume ratio outside-bark, the models tended to underestimate for trees younger than 20 years-old (Figure 10.6). For example, for dt = 10.16 cm, the model reported in this study and the model reported by Baldwin and Saucier (1983) had a Bias of about -2.1% (R$_{OB}$1) and -3.0% (R$_{OB}$3), respectively. For dt = 15.24 cm, the Bias was about -9.4% (R$_{OB}$2) and -7.5% (R$_{OB}$4), respectively; but for older trees the Bias is drastically reduced being always lower than 1.9% (Figure 10.6). For R$_{OB}$ estimations, RMSE of the model reported in this study were always smaller than the model of Baldwin and Saucier (1983) (Figure 10.6). Similar responses to V$_{OB}$ and R$_{OB}$ were observed for inside bark estimations (data not shown).

Model validation using external data

When models to estimate H and V$_{OB}$ were evaluated using trees measured outside the geographical range of the model development dataset (US Army Fort Benning), across stand age, there was no difference between observed and predicted values for H and V$_{OB}$ for any of the predicting models reported (P > 0.11). For H estimations, the model that only depended on dbh (local model H1; Figure 10.7) showed a tendency to overestimate H (only in 87-year-old stands the model underestimated by 7%), with errors ranging between 13 and 30% underestimations. When stand parameters Age and BA were included in the general model H2, the relationship between observed and predicted values, across all ages, was improved compared with model H1 (Figure 10.7), but there was still significant differences between observed and predicted values

(those differences ranged between 17% underestimations for 5-year old stands to 1.8% overestimations for 87-year-old stands). When SI was incorporated into the model (general model H3), there were no differences between observed and predicted values for any stand (age) (Figure 10.7). Similar results were observed for residuals distribution (Figure 10.7). For all models, larger differences were found at the 64-year-old naturally regenerated stand, maybe due to its low productivity (average SI of 19.6 m), lower to the minimum values observed in fitting dataset (SI for other stands ranged between 22.4 and 33.9 m). As V_{OB} was measured only on 11 trees at US Army Fort Benning, no model validation within stand age was carried out, and as was stated previously, there was no difference between observed and predicted values for any of the models to predict V_{OB}.

Discussion

The set of prediction equations for longleaf pine trees reported in this study provides useful tools for the study and management of this species. General and local models are presented for H, dbh_{IB}, V_{OB} and V_{IB} estimations. The user should decide which model to use depending on data availability and level of accuracy desired.

The model selected for H estimations was compared against linear and non-linear equations reported elsewhere (Curtis 1967, Arabatzis and Burhart 1992, Huang et al. 1992, Staudhammer and LeMay 2000, Temesgen et al. 2007, Leduc and Goelz 2010, Bi et al. 2012). The final model selected showed similar predictive ability to models reported in the literature (data not shown), but at the same time allowed for the incorporation of stand-level parameters selected by a statistical procedure that included VIF discrimination. Similar to our study, other authors such as Staudhammer and LeMay (2000), Temesgen et al. (2007) and Leduc and Goelz (2010) also included stand parameters into their final models and concluded that measures of stand density and development should be included into dbh-H models in order to improve accuracy of H predictions. We also provide the option to include measures of stand productivity (i.e. SI), which produced more accurate predictions. Leduc and Goelz (2010) used a similar approach by including H_{dom} in their model to estimate H. These authors also included quadratic mean diameter in their model, a direct combination of N and BA. In our case, the inclusion of stand-level parameters highly improved the accuracy of the model, essentially eliminating bias for trees with H larger than about 25 m.

The equation for dbh_{IB}, and, hence, the estimations of bark thickness (as bark thickness can be determined as the difference between dbh and dbh_{IB}), showed little improvement from the inclusion of stand-level parameters. Similar results were reported for *Pinus taeda* (loblolly pine) trees, where bark thickness was linearly correlated with dbh but not associated to stand density (Feduccia and Mann 1975) or stand age (Johnson and Wood 1987). Also for loblolly pine trees, Tiarks and Haywood (1992) reported no effect of weed control and fertilization on the relationship between bark thickness and dbh. For longleaf pine, Farrar (1987) also reported equations that linearly correlated dbh_{IB} with dbh for trees with different live crown ratio classes. Those equations performed well but relied on additional measurements (total tree height and height to the live crown base to estimate live crown ratio) that are not always available.
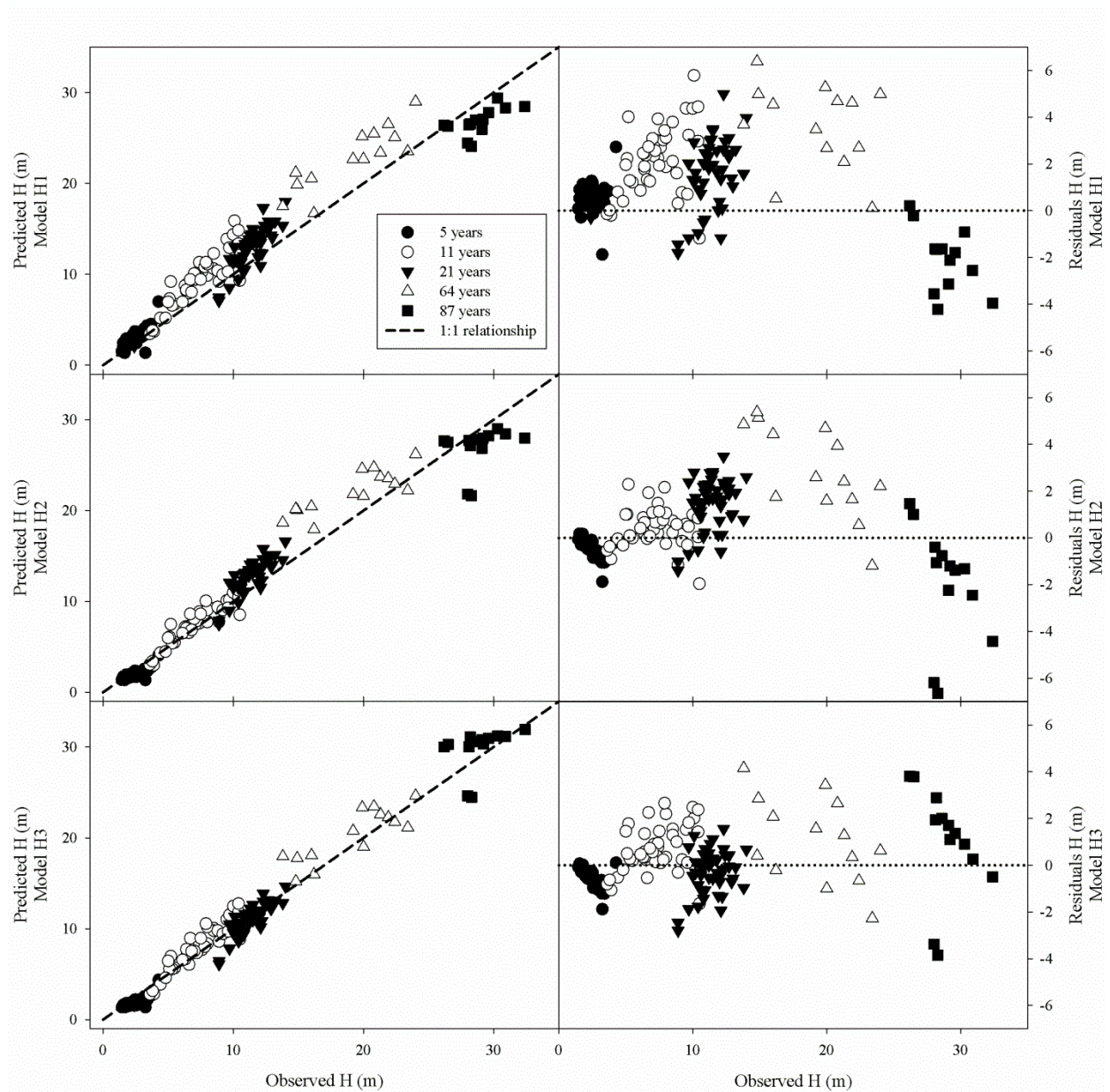
Figure 10.7. Observed versus predicted values and residuals versus observed values of height (H) using local model H1, general model H2, and general model H3.

Furthermore, the reported model performed better than the models presented in this study when live crown ratio was assumed to be larger than 50%, a value that is generally associated with smaller trees (Farrar 1987). Stem volume is a key parameter for forest owners, managers and researchers. Different types of analyses, such as economics, restoration ecology planning or carbon sequestration accounting, are directly or indirectly dependent on estimation of stem growth, so equations for accurate determinations of V are critical. We present a set of equations for both outside and inside bark V estimations that can be improved if H measurements are available. The best model used dbh and H as the independent variables and showed almost no improvement if stand-level parameters were included. On the other hand, the model that used only dbh as explanatory predictor was improved when stand Age and BA were included, reducing Bias to the same magnitude as the model with dbh and H. This result implies that differences in stem tapering that affect the relationship between dbh and H can be successfully addressed by the inclusion of stand parameters without the need of direct measurements of H.

Another option to determine V when H is unknown is to estimate H using a dbh-H equation and then use the estimated H in one of the functions that use dbh and H to determine V. When we tested this approach, better results were obtained based on models that relied only on dbh and stand parameters (data not shown). Therefore, in the case of H unknown, we recommend using models V2 or V3 instead of models V4 to V6 with estimated H.

It is important to note that the parameter value of the power of dbh (c_2, d_2) in equations 5 to 12 had a value slightly different than 2, a value generally used to correlate dbh with V (Baldwin and Saucier 1983; Van Deusen et al. 1981). Interestingly, the value of parameters c_2 was reduced from about 2.188 ($V_{OB}1$) to 2.099 ($V_{OB}2$) and 2.078 ($V_{OB}3$) when stand-level parameters were incorporated into the equation. When H was included in the model, instead of using $dbh^2 \cdot H$ we determined that the power of dbh and H, instead of 2.0 and 1.0, should be 1.917 and 1.072, respectively, for the local model $V_{OB}4$, and 1.853 (dbh) and 1.012 (H), and 1.851 (dbh) and 1.047 (H), for the general models $V_{OB}5$ and $V_{OB}6$, respectively. This implies that models that rely on dbh^2 or $dbh^2 \cdot H$ should be revised and future models for this species should determine the correct power of dbh and H.

The approach presented by Burkhart (1977) to estimate stem volume ratio to any top diameter was adequate for our dataset. Similar to the model of Saucier et al. (1981), when the equations presented in this study were tested for trees younger than 20 years (top limit diameter close to dbh), results showed a tendency to underestimate the merchantable volume ratio. Nevertheless, for trees older than 20 years, the bias was negligible. Hence, the equations presented in this study are a valuable tool for foresters who need to estimate merchantable volume to any stem diameter limit.

The models reported in this study performed well for the dataset used for evaluation. When the equations to estimate H and V_{OB} were tested in a dataset obtained in stands located outside the geographical zone of the data used for model development (US Army Fort Benning), the results support the robustness of the models. When stand parameters were included in the models, there were no differences between observed and predicted values for H for any stand age tested, even in naturally-regenerated stands (64 and 87-year-old stands). Due to costs constrains, our validation of V_{OB} with data from US Army Fort Benning was carried out only on 11 trees with ages ranging

between 21 and 87 years. This small dataset does not allow us to properly validate V_{OB} within stand ages, but in any case, across stand ages, there were no differences between observed and predicted V_{OB}. This suggests that the models are a robust alternative for H and V_{OB} estimations on planted stands (and perhaps naturally-regenerated as well) across a wide range of ages. Even though we strongly recommend using the equations within the range of data used to fit, the results presented in this validation study provide a valuable alternative to available models and are intended as a tool to support present and future longleaf pine management decisions.

11. Estimating Longleaf Pine Tree Diameter and Stem Volume from Tree Height, Crown Area and Stand-Level Parameters

[Contents of this chapter were extracted from: C.A. Gonzalez-Benecke, S.A. Gezan, L.J. Samuelson, W.P. Cropper Jr., D.J. Leduc, and T.A. Martin. 2014. Estimating *Pinus palustris* tree diameter and stem volume from tree height, crown area and stand-level parameters. Journal of Forestry Research 25: 43-52]

Introduction

This Chapter builds on the tree-level modeling described in Chapter 10 by further developing models described in Chapter 10 and inclusion of stand-level parameters. Forests are a significant proportion of the terrestrial biosphere and are important not only economically, but also for the ecosystem services associated with forested landscapes (Thompson et al. 2011; Goldstein et al. 2012). One important ecosystem service is carbon sequestration (McKinley et al. 2011). Forest biomes are a significant sink for sequestration of atmospheric CO2 with a potentially important role in climate change mitigation (Luyssaert et al. 2008; Fahey et al. 2010). A standard method for assessing forest productivity and carbon sequestration in pine dominated forests has been the use of growth and yield models (e.g. Gonzalez-Benecke et al. 2010a, 2011). These models are typically applicable to closed canopy forests, but may be more difficult to apply to savannas and woodlands, particularly those with un-even aged tree populations.

Individual tree biomass, stem volume and carbon content can be estimated with field measurements of stem diameter and height coupled with the application of allometric equations. The equations used for field-based tree biomass estimation typically include height and diameter as independent prediction variables (Satoo and Madgwick 1982). However, direct field measurement of a large number of individual trees is an expensive and time-consuming process. LiDAR (light detection and ranging) is a technique well suited to characterizing trees and other measurements through remote sensing (Lefsky et al. 2002; Roberts et al. 2005; Andersen et al. 2006; Popescu 2007; Dean et al. 2009; Lee et al. 2009, 2010). In addition, satellite interferometry (Ulander et al. 1995) may also be used to characterize tree height profiles.

Given a good algorithm for individual tree detection (Lee et al. 2010; Kaartinen et al. 2012; Li et al. 2012), remote sensing techniques, such as LiDAR, can be used to provide accurate tree height and crown area estimates (Nelson et al. 1988; Nakai et al. 2010), and individual tree diameter in some cases (Popescu 2007; Dalponte et al. 2011). Here, LiDAR estimation of tree height can efficiently feed equations used to calculate biomass of a large number of trees.

Longleaf pine savannas in the southern Coastal Plain are fire-dependent ecosystems characterized by large canopy gaps (Jose et al. 2006). Remote sensing-based methods for individual tree volume estimates are particularly useful for savannas or woodlands that are far from canopy closure. Estimates of savanna biomass have included direct harvesting (Menaut and Cesar 1979) or measurements of individual tree diameters and heights applied to allometric equations (Chen et al. 2003; Sawadogo et al. 2010).

The objective of this study was to develop models to predict longleaf pine tree diameter at breast height (dbh, cm) and merchantable volume (V, m3). Our models are applicable to direct estimates of stem volume or forest carbon sequestration or as a component of individual-tree-based models of longleaf pine savannas (Drake and Weishampel 2001; Loudermilk et al. 2011) where tree height is the principal state variable that can be derived from remote sensing or obtained from field measurements.

Materials and Methods

Data description

We used a dataset consisting of 127 permanent plots measured and maintained by the U.S. Forest Service's Laboratory at Pineville, LA (Goelz and Leduc 2001). Data were collected from regularly remeasured permanent plots in a combination of seven studies exploring the effects of spacing and thinning on longleaf plantations distributed through the Western Gulf Coastal Plain, U.S., from Santa Rosa County in Florida to Jasper County in Texas, representing a large portion of the current range of longleaf pine in the southern Coastal Plain (Goelz and Leduc 2001; Leduc and Goelz 2009).

Total tree height (H, m), dbh, living crown width (CW, m) and V were measured on 3,420 trees. CW was measured in two opposite directions, and living crown area (CA, m^2) was determined assuming tree crown shape as an ellipse. Tree stem volume outside bark (V$_{OB}$, m^3) was determined by measuring diameter outside bark and its height at 5.08 cm diameter taper steps along the bole from the stump to the 5.08 cm top. Tree stem volume inside bark (V$_{IB}$, m^3) was determined after estimating diameter inside bark at each diameter taper steps using an equation reported by Gonzalez-Benecke et al. (2014b). Stand-level variables including basal area (BA, m^2 ha^{-1}), number of trees per hectare (N, ha^{-1}) and dominant height (H$_{dom}$, m) were determined for each plot to be used as additional independent variables in prediction equations. Site index (SI, m), defined as the H$_{dom}$ at a reference age of 50 years, was calculated using an equation reported by Gonzalez-Benecke et al. (2012b). In order to eliminate broken and malformed individuals, trees with form factor F = H/dbh (m cm^{-1}) less than 0.54 m cm^{-1} and trees with F greater than 13.5 m cm^{-1} were excluded. Hence, a total of 44 trees were discarded from further analysis.

From the whole dataset, 20 plots (16% of total) were randomly selected and removed to be used for model validation and the rest (i.e. 107 plots) were used for model fitting. The model validation and fitting datasets contained 425 and 2,951 trees, respectively. In order to test the robustness of the models, an independent second source of validation data, that included stands planted outside the geographic range of the data was used. This dataset contains 469 trees measured in four stands on US Army Fort Benning. Selected stands had ages of 12, 21, 64 and 87 years. The 12 year-old and 21 year-old stands corresponded to plantations and the 64 year-old and 87 year-old stands were naturally regenerated. In each stand, four 0.04 ha inventory plots were measured and H and dbh recorded for all 469 trees (the total number of trees measured per each stand was 149, 292, 15 and 13, respectively) and CW was recorded in 120 trees (all trees were measured in the 64 and 87 year-old stand and trees in younger stands were subsampled and included 44 and 48 trees for ages 12 and 21 year-old stands). In a subset of 11 trees (5 from the 21 year-old stand, three from the 64

year-old stand and three from the 87-year-old stand), stem volume over bark was directly measured by destructive harvesting the trees and measuring bole diameter over bark at 2 m steps from stump to a minimum diameter of 5 cm. Stand-level variables BA, N, H_{dom} and SI were also calculated for each plot. Details of tree and stand characteristics of the three datasets are shown in Table 11.1. General relationships between dbh and H, CA, dbh and V_{OB} are shown in Figure 11.1.

Model description

Data from permanent plots with repeated measures, such as the one used in this study, often suffer from within-plot and temporal correlation (Gregoire et al. 1995). In order to address this potential problem of autocorrelation, linear mixed models were fitted to the data by including in the model a random effect of plot (to model spatial correlation) and by specifying an autoregressive error structure (to model temporal correlation). The models fitted to estimate dbh and V corresponded to a modified version of the model proposed by Nakai et al. (2010), as shown below:

$$\ln(dbh) = a_1 + a_2 \cdot \ln(H - 1.37) + a_3 \cdot \ln(CA) + p_{j1} + \varepsilon_1 \qquad [1]$$

$$\ln(V) = b_1 + b_2 \cdot \ln(H) + b_3 \cdot \ln(CA) + p_{j2} + \varepsilon_2 \qquad [2]$$

where a_1 to a_3 and b_1 to b_3 are curve fit parameters. The random effects p_{j1} and p_{j2} are effects associated to the jth plot, with $p_{ji} \sim N(0, \sigma_{pi}^2)$ where σ_{pi}^2 corresponds to the variance between plot effects for the dbh and the V models. The error terms ε_1 and ε_2 were modeled assuming and autoregressive error structure of order one, with $\varepsilon_i \sim N(0, \sigma_i^2 \cdot \rho_i^d)$, where σ_i^2 is the residual variance, ρ_i is the year-to-year temporal correlation and d is the lag (in years) between consecutive measurements.

In addition to the explanatory variables H and CA, stand-level variables were included as covariates into the model in order to improve the general equation. The general model used was:

$$\ln(dbh) = a_1 + a_2 \cdot \ln(H - 1.37) + a_3 \cdot \ln(CA) + a_4 \cdot \ln(N) + a_5 \cdot \ln(H_{dom}) + a_6 \cdot \ln(SI) + p_{j3} + \varepsilon_3 \qquad [3]$$

$$\ln(V) = b_1 + b_2 \cdot \ln(H) + b_3 \cdot \ln(CA) + b_4 \cdot \ln(N) + b_5 \cdot \ln(H_{dom}) + b_6 \cdot \ln(SI) + p_{j4} + \varepsilon_4 \qquad [4]$$

where a_1 to a_6 and b_1 to b_6 are curve fit parameters, and as before, p_{j3} and p_{j4} are the random plot effect terms associated to plot measurements, and ε_3 and ε_4 were modeled using an autoregressive error structure of order one as indicated earlier.

Stand age was not included as a stand-level covariate as it was highly correlated with H_{dom}. Also, BA was not included as its calculation depends on dbh values, which are assumed to be unknown. For the same reason other stand parameters that depend directly on BA, as do stand density index and quadratic mean diameter, were not considered in the general model. For comparison, we also fitted the models presented in eq. 1 and 2 without CA as a predicting variable, resulting in local models for dbh and V that only rely on H as the predictive variable.

146

Model validation

The predictive ability of the equations previously described, including the reduced local model without CA, was compared against the data from the plots selected from the validation database. The models were also evaluated against the data from the four stands on US Army Fort Benning. In all cases, four measures of accuracy were used to evaluate the goodness-of-fit between observed and predicted (simulated) values for each variable from the model validation dataset. These were: (1) mean absolute error (MAE); (2) root mean square error (RMSE); (3) mean bias error (Bias); and (4) coefficient of determination (R^2) (Fox 1981; Loague and Green 1991; Kobayashi and Salam 2000).

All statistics were obtained using SAS 9.3 (SAS Inc., Cary, NC, USA). The procedure MIXED was used in order to model spatial and temporal correlations, and statistical comparison of fitted models was done using a likelihood ratio test. The variance inflation factor (VIF) was calculated to detect multicollinearity between predicting variables, discarding all variables included in the model with VIF larger than 5 (Neter et al. 1996).

Results

Model Fitting

The covariance structure estimated from the analysis indicated a significant spatial and temporal correlation for all dbh, V_{OB} and V_{IB} models. The year-to-year residual correlation values ranged from 0.85 to 0.99 where the largest values were obtained, as expected, for dbh (Table 11.2). The average relative magnitudes of the plot variance components (in relation to the error component) showed moderate levels of the spatial component but important changes across models. The largest relative plot components were found on models that did not depend on CA or any stand-level variable (i.e. models dbh1, $V_{OB}1$ and $V_{IB}1$), reflecting the effect of these extra factors on explaining additional between plot variability.

The prediction equations and parameter estimates for planted longleaf pine trees are presented in Table 11.3. All parameter estimates were significant at $p < 0.001$. Parameter estimates for intercepts in all equations (a_1, b_1 and c_1) include the correction proposed by Snowdon (1991) for logarithm transformation of the response variable.

Table 11.1. Summary of individual-tree and stand-level characteristics for measured longleaf pine.

Variable	Model development dataset (n = 2,951)				Model validation dataset inside geographical range (n = 425)				Model validation dataset outside geographical range (US Army Fort Benning) (n = 469)			
	Mean	SD	Min.	Max.	Mean	SD	Min.	Max.	Mean	SD	Min.	Max.
Age	31.9	8.2	20.0	45.0	31.6	7.9	20.0	45.0	28.7	25.5	12	87
dbh	21.3	8.3	4.1	46.5	21.1	7.7	4.3	40.4	16.1	12.1	2.5	57.4
H	18.5	4.2	4.3	27.4	18.4	4.1	4.6	25.9	12.4	7.0	2.4	32.4
CW	3.9	1.8	0.6	11.0	3.8	1.6	0.6	9.3	3.6	268	0.8	15.0
CA	14.4	13.6	0.3	94.3	13.3	11.1	0.3	67.9	15.0	28.2	0.4	175.0
V_{OB}	0.45	0.37	0.00	2.01	0.43	0.32	0.00	1.33	0.82	0.97	0.03	2.95
N	923	495	49	2,056	899	506	204	2,145	819	795	50	2,150
BA	24.7	6.9	6.7	47.6	25.1	6.2	11.9	39.6	14.2	6.3	4.5	24.2
H_{dom}	20.7	3.0	14.9	26.9	20.5	2.9	15.5	26.4	18.3	8.5	8.7	32.4
SI	27.0	2.2	21.3	33.6	26.8	2.4	21.5	33.3	22.2	3.3	13.5	27.4

Notes for Table 11.1: Age: stand age (yr.); dbh: average diameter at 1.37 m height (cm); H: average tree height (m); bt: bark thickness at 1.37 m height (mm); V_{OB}: average stem volume outside bark (m^3); N: trees per hectare (ha^{-1}); BA: stand basal area (m^2 ha^{-1}); H_{dom}: average height of dominant and codominant trees (m); SI: site index at base age of 50 years (m); SD: standard deviation; n: number of trees. At US Army Fort Benning, n = 120 for CA and n = 11 for V_{OB}.

Table 11.2. Variance components and correlation estimates from fitted models of dbh and stem volume predicted from tree height and stand characteristics for planted longleaf pine trees (n = 2,951).

Model		Covariance Component	Parameter Estimate	SE	P-value
dbh1	$\ln(\text{dbh}) = a_1 + a_2 \cdot \ln(\text{H} - 1.37)$	σ_p^2	0.031549	0.004655	< 0.001
		ρ	0.988316	0.000776	< 0.001
		σ^2	0.037139	0.001473	< 0.001
dbh2	$\ln(\text{dbh}) = a_1 + a_2 \cdot \ln(\text{H} - 1.37) + a_3 \cdot \ln(\text{CA})$	σ_p^2	0.002741	0.000635	< 0.001
		ρ	0.905937	0.008053	< 0.001
		σ^2	0.013623	0.000463	< 0.001
dbh3	$\ln(\text{dbh}) = a_1 + a_2 \cdot \ln(\text{H} - 1.37) + a_3 \cdot \ln(\text{CA}) + a_4 \cdot \ln(\text{N}) + a_5 \cdot \ln(\text{H}_{\text{dom}}) + a_6 \cdot \ln(\text{SI})$	σ_p^2	0.007011	0.001860	< 0.001
		ρ	0.954079	0.005971	< 0.001
		σ^2	0.015963	0.000818	< 0.001
$\text{V}_{\text{OB}}1$	$\ln(\text{V}_{\text{OB}}) = b_1 + b_2 \cdot \ln(\text{H})$	σ_p^2	0.094202	0.014834	< 0.001
		ρ	0.974914	0.001870	< 0.001
		σ^2	0.125801	0.005271	< 0.001
$\text{V}_{\text{OB}}2$	$\ln(\text{V}_{\text{OB}}) = b_1 + b_2 \cdot \ln(\text{H}) + b_3 \cdot \ln(\text{CA})$	σ_p^2	0.006006	0.001363	< 0.001
		ρ	0.849064	0.011258	< 0.001
		σ^2	0.050265	0.001521	< 0.001
$\text{V}_{\text{OB}}3$	$\ln(\text{V}_{\text{OB}}) = b_1 + b_2 \cdot \ln(\text{H}) + b_3 \cdot \ln(\text{CA}) + b_4 \cdot \ln(\text{N}) + b_5 \cdot \ln(\text{H}_{\text{dom}}) + b_6 \cdot \ln(\text{SI})$	σ_p^2	0.002819	0.000975	0.002
		ρ	0.875927	0.009473	< 0.001
		σ^2	0.049234	0.001584	< 0.001
$\text{V}_{\text{IB}}1$	$\ln(\text{V}_{\text{IB}}) = b_1 + b_2 \cdot \ln(\text{H})$	σ_p^2	0.108387	0.017007	< 0.001
		ρ	0.976026	0.001762	< 0.001
		σ^2	0.141412	0.005899	< 0.001
$\text{V}_{\text{IB}}2$	$\ln(\text{V}_{\text{IB}}) = b_1 + b_2 \cdot \ln(\text{H}) + b_3 \cdot \ln(\text{CA})$	σ_p^2	0.006982	0.001592	< 0.001
		ρ	0.852428	0.011022	< 0.001
		σ^2	0.055810	0.001698	< 0.001
$\text{V}_{\text{IB}}3$	$\ln(\text{V}_{\text{IB}}) = b_1 + b_2 \cdot \ln(\text{H}) + b_3 \cdot \ln(\text{CA}) + b_4 \cdot \ln(\text{N}) + b_5 \cdot \ln(\text{H}_{\text{dom}}) + b_6 \cdot \ln(\text{SI})$	σ_p^2	0.003301	0.001141	0.002
		ρ	0.879683	0.009257	< 0.001
		σ^2	0.055202	0.001793	< 0.001

Table 11.3. Parameter estimates and fit statistics of equations for predicting dbh and stem volume from height and stand characteristics for planted longleaf pine trees (n = 2,951).

	Model	Parameter	Parameter Estimate	SE	R^2	RMSE	CV (%)
dbh1	$\ln(dbh) = a_1 + a_2 \cdot \ln(H - 1.37)$	a_{1*}	0.403079	0.032711	0.771	3.93	18.39
		a_2	0.970048	0.009821			
dbh2	$\ln(dbh) = a_1 + a_2 \cdot \ln(H - 1.37) + a_3 \cdot \ln(CA)$	a_{1*}	0.342191	0.027786	0.901	2.59	12.11
		a_2	0.804174	0.011660			
		a_3	0.185289	0.003761			
dbh3	$\ln(dbh) = a_1 + a_2 \cdot \ln(H - 1.37) + a_3 \cdot \ln(CA) + a_4 \cdot \ln(N)$ $+ a_5 \cdot \ln(H_{dom}) + a_6 \cdot \ln(SI)$	a_{1*}	0.288848	0.204670	0.916	2.38	11.11
		a_2	0.930729	0.015051			
		a_3	0.132246	0.004031			
		a_4	-0.065363	0.005838			
		a_5	-0.337178	0.026633			
		a_6	0.393273	0.058204			
$V_{OB}1$	$\ln(V_{OB}) = b_1 + b_2 \cdot \ln(H)$	b_{1*}	-9.944543	0.078449	0.784	0.17	38.21
		b_2	3.123691	0.024536			
$V_{OB}2$	$\ln(V_{OB}) = b_1 + b_2 \cdot \ln(H) + b_3 \cdot \ln(CA)$	b_{1*}	-9.686492	0.062915	0.909	0.11	24.84
		b_2	2.661325	0.025422			
		b_3	0.372844	0.007370			
$V_{OB}3$	$\ln(V_{OB}) = b_1 + b_2 \cdot \ln(H) + b_3 \cdot \ln(CA) + b_4 \cdot \ln(N) + b_5 \cdot \ln(H_{dom}) +$ $b_6 \cdot \ln(SI)$	b_{1*}	-6.480444	0.308427	0.919	0.10	23.38
		b_2	2.953958	0.031336			
		b_3	0.327533	0.008107			
		b_4	-0.092607	0.011486			
		b_5	-0.820639	0.053347			
		b_6	-0.259927	0.087629			
$V_{IB}1$	$\ln(V_{IB}) = b_1 + b_2 \cdot \ln(H)$	b_{1*}	-10.531556	0.082652	0.768	0.14	41.48
		b_2	3.216861	0.025772			
$V_{IB}2$	$\ln(V_{IB}) = b_1 + b_2 \cdot \ln(H) + b_3 \cdot \ln(CA)$	b_{1*}	-10.270262	0.066367	0.902	0.09	27.02
		b_2	2.729643	0.026808			
		b_3	0.395527	0.007778			
$V_{IB}3$	$\ln(V_{IB}) = b_1 + b_2 \cdot \ln(H) + b_3 \cdot \ln(CA) + b_4 \cdot \ln(N) + b_5 \cdot \ln(H_{dom}) +$ $b_6 \cdot \ln(SI)$	b_{1*}	-6.960066	0.328228	0.913	0.08	25.43
		b_2	3.025198	0.033191			
		b_3	0.346722	0.008570			
		b_4	-0.100300	0.012157			
		b_5	-0.833450	0.056431			
		b_6	-0.264805	0.093337			

Notes for Table 11.2: dbh: diameter outside-bark at 1.37 m height (cm); H: total tree height (m); VOB: stem volume outside -bark up to 5.08 cm diameter limit (m^3); VIB: Stem volume inside-bark up to 5.08 cm diameter limit (m^3); N: trees per hectare (ha^{-1}); Hdom: average height of dominant and codominant trees (m); SI: site index at base age of 50 years. (m).

Notes for Table 11.3: dbh: diameter outside-bark at 1.37 m height (cm); H: total tree height (m); V_{OB}: stem volume outside -bark up to 5.08 cm diameter limit (m^3); V_{IB}: Stem volume inside-bark up to 5.08 cm diameter limit (m^3); N: trees per hectare (ha^{-1}); H_{dom}: average height of dominant and codominant trees (m); SI: site index at base age of 50 years. (m); SE: standard error; R^2: coefficient of determination; RMSE; root mean square error; CV: coefficient of variation ($100 \cdot RMSE/mean$). For all parameter estimates: P-value < 0.001. Parameters estimates for a_1 and b_1 include the correction proposed by Snowdon (1991).

The model that estimates dbh using H as the only dependent variable (local model dbh1) had a coefficient of variation (CV, RMSE as a percentage of observed mean value) of 18.4% and R^2 of 0.77 (Table 11.3). When CA was included into the model (local model dbh2), the fit of the model was improved considerably reducing CV to 12.1% and increasing R^2 to 0.90. When stand parameters N, H_{dom} and SI were also included into the model (general model dbh3) all variables were significant in the final model (equation 3). This final general model showed little improvement when compared with the local model dbh2 (CV of 11.1% and R^2 of 0.92 (Table 11.3). The parameter SI had a positive effect on dbh (positive value of parameter estimate): as site productivity increased, trees had larger dbh for any given H and CA. Contrary, the parameters N and H_{dom} had a negative effect on dbh (negative value of parameter estimates): in stands with higher stand density or in older stands, trees had smaller dbh for any given fixed value of H, CA and SI. In all cases multicollinearity between explanatory variables was small (VIF < 3.37; data not shown).

The models that estimate V_{OB} and V_{IB} using H as the only independent variable (local models $V_{OB}1$ and $V_{IB}1$, respectively) had an R^2 of 0.78 and 0.77, respectively (Table 11.3). The fit of both models improved when CA was included (local models $V_{OB}2$ and $V_{IB}2$), reducing CV by about 38% compared to models $V_{OB}1$ and $V_{IB}1$, and increasing R^2 to 0.91 and 0.92, respectively. Similar to the dbh3 model, all stand-level variables were significant in the final general model (equation 4). These final general models $V_{OB}3$ and $V_{IB}3$ showed little improvement when compared with local models $V_{OB}2$ and $V_{IB}2$ (Table 11.3). The parameters N, H_{dom} and SI had a negative effect on V_{OB} and V_{IB}: as stand density and site productivity increased, likely due to tapering changes, trees had smaller V for any given fixed value of H and CA. In all cases multicollinearity between explanatory variables was small (VIF < 3.54; data not shown).

Model validation

The relationship between predicted and observed values of V_{OB} and dbh using the local models, that only depends on H (local models $V_{OB}1$ and dbh1; Figure 11.2 a and b, respectively), showed a tendency to underestimate trees with V_{OB} and dbh larger than about 1 m^3 and 30 cm, respectively. When CA was included in the local models the relationship between observed and predicted values improved considerably (local models $V_{OB}2$ and dbh2; Figure 11.2 c and d, respectively) and there was no important departure in residuals.
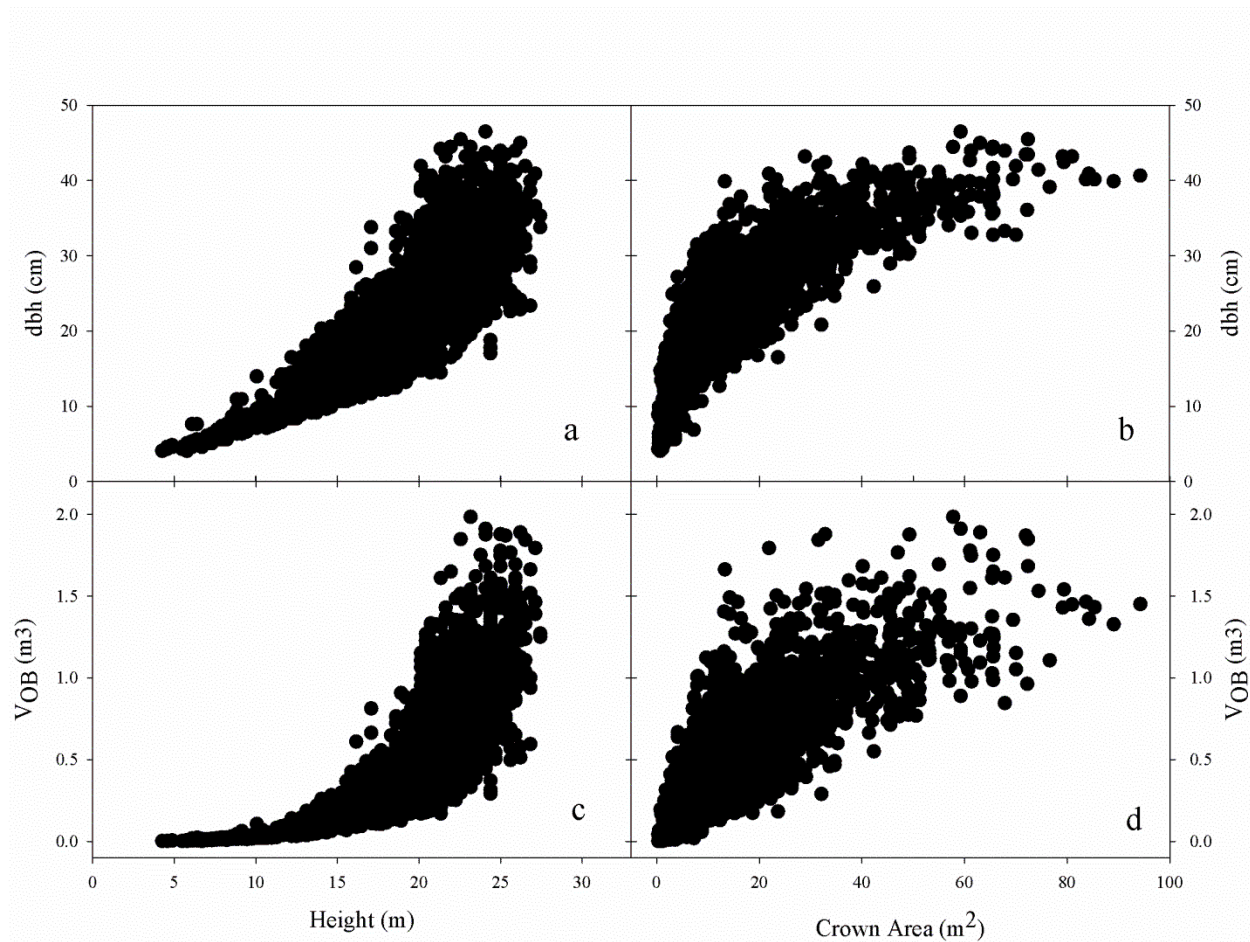
Figure 11.1. Relationships between total tree height (H) and crown area (CA) with stem diameter outside bark at 1.37 m height (dbh) (a, b) and stem volume outside bark (V_{OB}) (c, d) for the model development dataset.
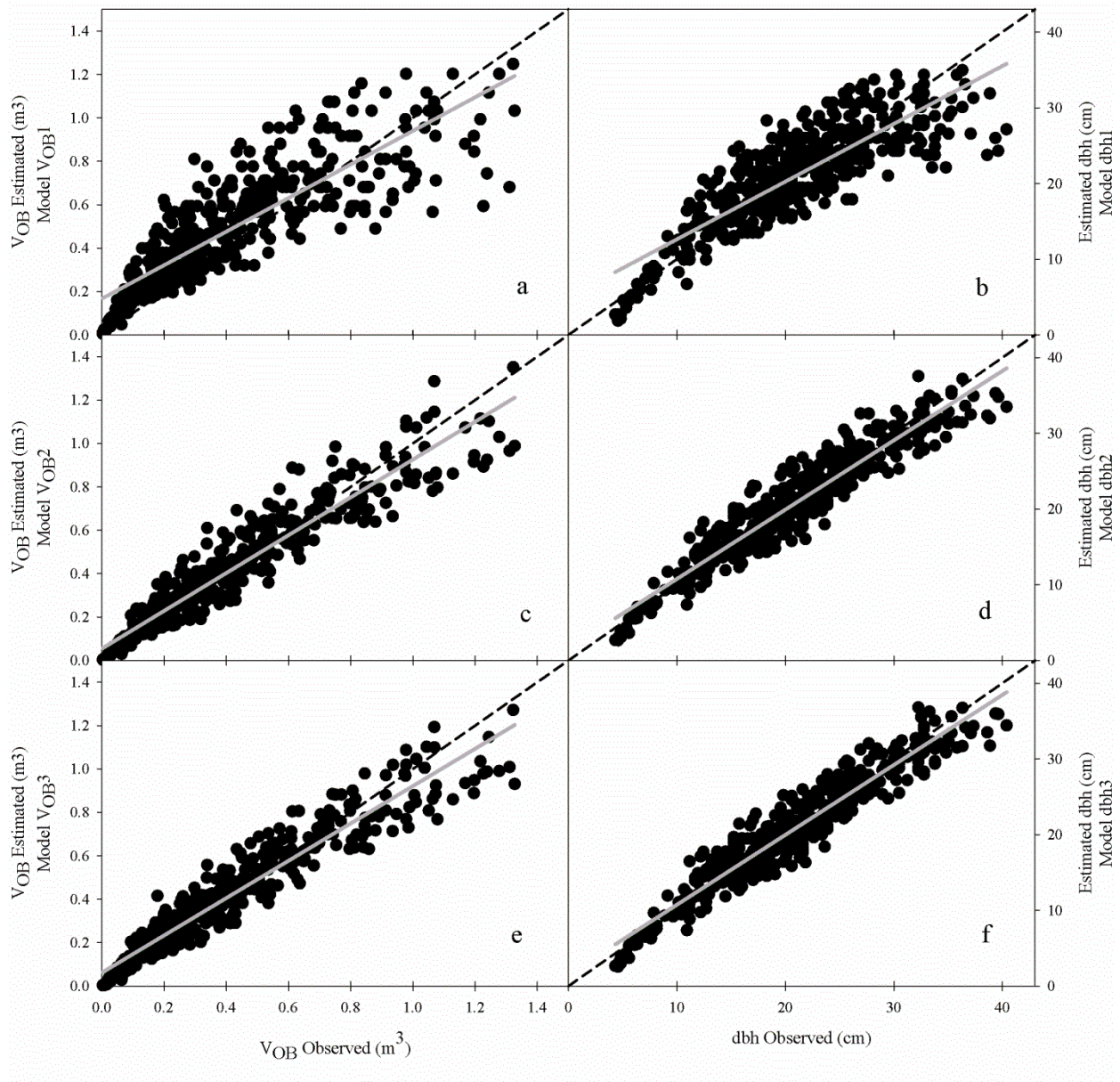
Figure 11.2. Examples of validation of stem volume outside bark (V_{OB}) (a, c, e) and stem diameter outside bark at 1.37 m height (dbh) (b, d, f) models using data inside the geographical range of fitting plots. Observed versus predicted (simulated) values for V_{OB} and dbh using local model $V_{OB}1$ (a) and dbh1 (b) (only use H as independent variable), local model $V_{OB}2$ (c) and dbh2 (d) (use H and CA as independent variables), and general model $V_{OB}3$ (e) and dbh3 (f) (use H, CA, N, H_{dom} and SI as independent variables). Gray lines represent linear regression fits.

153

When stand parameters N, H_{dom} and SI were also included into the local models $V_{OB}2$ and dbh2, the relationship between observed and predicted values resulted in little improvement (general models $V_{OB}3$ and dbh3; Figure 11.2 e and f, respectively).

All model performance tests showed that agreement between dbh and V observed and estimated values improved when CA was included in the local model (Table 11.4). For example, using the validation dataset, MAE and RMSE for dbh estimations were reduced from 15 and 20% (local model dbh1) to about 9 and 11% (local model dbh2), respectively; and R^2 increased from 0.71 to 0.90. In the case of VOB estimations, MAE and RMSE were reduced from 33 and 43% (local model $V_{OB}1$) to 16 and 24% (local model $V_{OB}2$), respectively; and R^2 increased from 0.70 to 0.90. Bias was highly reduced when CA was included into the local model to estimate V_{OB} (from 15% overestimations to 0.8% underestimations). Performance tests showed that dbh, V_{OB} and V_{IB} estimations that used H and CA as explanatory variables with little improved when stand parameters were added in the general models (Table 11.4).

Model validation using external data

When models to estimate dbh and V_{OB} were evaluated using trees measured outside the geographical range of the model development dataset (i.e. US Army Fort Benning), across stand ages, there was no difference between observed and predicted values for any of the predicting models reported (p > 0.21, paired t-test). For dbh estimations, the model that only depended on H (local model dbh1; Table 11.4; Figure 11.3a) showed a tendency to underestimate dbh, with larger absolute errors as tree dbh increased. Similar to previous results, when CA was included the relationship between observed and estimated values improved considerably (local model dbh2; Table 11.4; Figure 11.3c). As before, there was little improvement when stand parameters N, H_{dom} and SI were included in the local model dbh2 (general model dbh3; Table 11.4; Figure 11.3e). Figure 11.3 b, d and f show plot of residuals (as a proportion of observed values) versus observed dbh; here, CA reduced residuals dispersion but stand-level parameters resulted in an increase in Bias for younger stands.

For dbh estimations, when CA was included, Bias was reduced from 4.2 to 1.8% over-estimations. For VOB estimations, the Bias reduction was from 15.3 to 5.7% underestimation when CA was included (Table 11.4). As only 11 trees were measured for V_{OB} at US Army Fort Benning, the model validation was only carried out for means differences, and as stated previously, there was no difference between mean observed and predicted values for any of the models to predict V_{OB}.

Table 11.4. Summary of model validation statistics for dbh, V_{OB} and V_{IB}, estimations using validation datasets inside (n = 425) and outside the geographical range (US Army Fort Benning; n = 120 for dbh; n = 11 for V_{OB}) of model development plots.

Validation Dataset	Model	Independent Variables	$\overline{O}$	$\overline{P}$	MAE	RMSE	Bias	R^2
Inside geographical range	dbh1	H	21.15	21.06	3.16 (15.0)	4.16 (19.7)	-0.08 (-0.4)	0.708
	dbh2	H, CA	21.15	20.94	1.90 (9.0)	2.44 (11.5)	-0.20 (-1.0)	0.900
	dbh3	H, CA, N, H_{dom}, SI	21.15	21.01	1.83 (8.6)	2.31 (10.9)	-0.14 (-0.7)	0.910
	V_{OB}1	H	0.428	0.493	0.139 (32.6)	0.185 (43.3)	0.065 (15.3)	0.702
	V_{OB}2	H, CA	0.428	0.424	0.070 (16.4)	0.104 (24.3)	-0.003 (-0.8)	0.896
	V_{OB}3	H, CA, N, H_{dom}, SI	0.428	0.427	0.066 (15.5)	0.097 (22.6)	-0.001 (-0.2)	0.913
	V_{IB}1	H	0.312	0.363	0.109 (34.9)	0.145 (46.7)	0.051 (16.5)	0.684
	V_{IB}2	H, CA	0.312	0.310	0.054 (17.4)	0.082 (26.3)	-0.002 (-0.7)	0.890
	V_{IB}3	H, CA, N, H_{dom}, SI	0.312	0.311	0.052 (16.5)	0.076 (24.5)	0.000 (-0.1)	0.908
Outside geographical range	dbh1	H	16.80	17.51	3.27 (19.5)	4.51 (26.9)	0.71 (4.2)	0.920
	dbh2	H, CA	16.80	17.10	2.05 (12.2)	3.36 (20.0)	0.30 (1.8)	0.929
	dbh3	H, CA, N, H_{dom}, SI	16.80	18.10	3.17 (18.8)	4.00 (23.8)	1.30 (7.8)	0.916
	V_{OB}1	H	0.824	0.698	0.193 (23.4)	0.327 (39.7)	-0.126 (-15.3)	0.947
	V_{OB}2	H, CA	0.824	0.777	0.251 (30.5)	0.381 (46.3)	-0.047 (-5.7)	0.846
	V_{OB}3	H, CA, N, H_{dom}, SI	0.824	0.780	0.219 (26.6)	0.328 (39.8)	-0.044 (-5.3)	0.877

Notes for Table 11.4: dbh: diameter outside-bark at 1.37 m height (cm); H: total tree height (m); V_{OB}: stem volume outside-bark up to 5.08 cm diameter limit (m^3); V_{IB}: Stem volume inside-bark up to 5.08 cm diameter limit (m^3); N: trees per hectare (ha^{-1}); H_{dom}: average height of dominant and codominant trees (m); SI: stand site index (m); $\overline{O}$: mean observed value; $\overline{P}$: mean predicted value; n: number of observations; MAE: mean absolute error; RMSE: root of mean square error; Bias: absolute bias estimator; R^2: coefficient of determination. Values in parenthesis are percentage relative to observed mean. MAE, RMSE and Bias are presented in the same units as dependent variable.
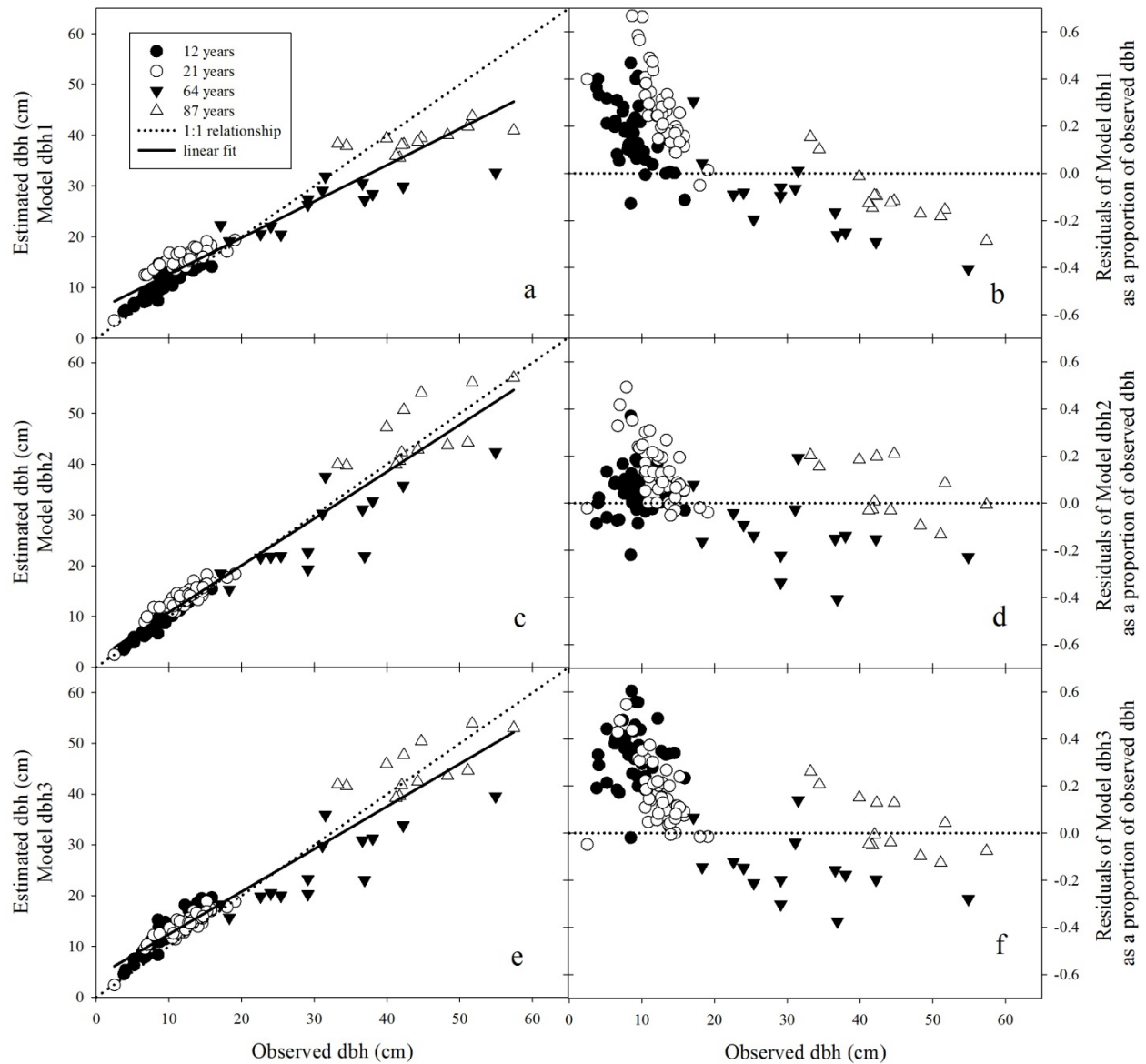
Figure 11.3. Validation of stem diameter outside bark at 1.37 m height (dbh) models using data outside geographical range of fitting plots (US Army Fort Benning), for stands of different ages. Observed versus predicted (simulated) values (a, c and e) and residuals (predicted-observed) versus observed values (b, d and f) of dbh using model dbh1 (a, b) (only use H as independent variable), local model dbh2 (c, d) (use H and CA as independent variables), and general model dbh3 (e, f) (use H, CA, N, H_{dom} and SI as independent variables).

157

Discussion

The prediction equations for longleaf pine trees reported in this study represent useful tools for the study and management of this species. We anticipate that the main use of the equations reported here will be for cases when stem diameter is unknown, and tree height and crown width measurements are available, as is the case when data are obtained though remote sensing. General and local models are presented for dbh, V_{OB} and V_{IB} estimations. The user should decide which model to use depending on data availability (stand and tree-level) and the desired accuracy.

The inclusion of CA into the models greatly improved the accuracy of the predictions. As longleaf pine trees age they continue growing in diameter and volume and also develop larger crowns, but older trees tend to plateau in height. When H and CA are known, small improvements were found when additional stand parameters were included, implying that CA implicitly incorporates the effects of stand stocking and productivity on the allometric relationships of longleaf pine trees.

The additional elements incorporated to model spatial and temporal correlations resulted in improved fittings, where, for all variables and models, significant spatial components were noted, and, as expected, their relative importance decreased as other explanatory variables were included. In addition, important year-to-year correlations were detected reflecting the non-independent nature of the data.

The observed relationship between dbh and H for longleaf pine trees indicated that dbh continues growing when H reached its asymptote (see Figure 11.1a) and dbh estimations for known large H values had low accuracy (see Tables 11.1 and 11.2). Similar observations have been reported for other pine species, such as *Pinus sylvestris* (Kalliovirta and Tokola 2005) and *Pinus radiata* (Bi et al. 2012). The final model selected for dbh estimations showed similar fitting to non-linear models proposed by Bi et al. (2012), or a linear model (after root-square transformation) proposed by Kalliovirta and Tokola (2005). The inclusion of CA into the models to estimate dbh and V greatly improved the accuracy of the predictions. Similar results were reported for *Pinus densiflora* and *Cryptomeria japonica* by Nakai et al. (2010) and for *Pinus sylvestris*, *Picea abies* and *Betula pendula* by Kalliovirta and Tokola (2005).

As with our study, the stand parameters included in the models reported by Kalliovirta and Tokola (2005) for *Pinus sylvestris* resulted in only small improvements in model performance. In our general models, stand variables related to density (N) and site quality (H_{dom} and SI) were significant in the final model selected but only marginally improved model fitting.

When the equations to estimate dbh and V_{OB} were tested using a dataset obtained in stands located outside the geographical zone of the data used for model fitting (i.e. US Army Fort Benning), the results support the robustness of the models that included CA, even in naturally-regenerated stands. When stand parameters were included into the general models, there was minimal further improvement in dbh prediction for any stand age tested. Due to cost constrains, our validation of V_{OB} with data collection from US Army Fort Benning was carried out only on 11 trees with ages ranging from 21 to 87 years.

Our results suggest that the fitted models are a robust tool for dbh and V_{OB} estimations when H and CA measurements are available on planted stands (and perhaps naturally-regenerated as well)

with non-overlapping crowns across a wide range of ages. One alternative for dbh and V estimation from H measurements consists of determining dbh by solving the inverse of an equation fitted for H estimations from known dbh, and determining V by solving an individual tree-level equation fitted for V estimations from dbh^2 or $dbh^2 \cdot H$, where dbh was previously solved from H. This option is not recommended. For comparison purposes we estimated dbh and V_{OB} using local and general equations reported by Gonzalez-Benecke et al. (2014b). These estimates had similar Bias but, as expected, larger MAE and RMSE (data not shown). Even though in the general model stand-level parameters improved the fitting, the estimates still showed a considerable Bias for trees with dbh larger than about 40 cm (data not shown). Therefore, we do not recommend the use of this alternative estimation methodology. The same previous analysis applies to allometric equations to estimate biomass from dbh^2 or $dbh^2 \cdot H$.

Forestry and forest ecology studies often produce estimates of the standing biomass or of carbon stocks and how these variables change over time. These estimates are relevant to assessments of economic value as well as non-market benefits such as carbon sequestration. Climate change mitigation through reduced loss of stored carbon (Putz et al. 2008) and provision of other ecosystem services (Tallis and Polasky 2009) are important applications that require accurate stand estimations. Traditional estimates using allometric equations require time consuming measurements of large numbers of individual trees. Our models provide a straight-forward method of estimating tree diameter, volume and later biomass without necessarily resorting to ground-based measurements.

An ideal example of potential model applicability is in situations where LiDAR data have been collected for longleaf pine forests with no overlapping crowns (Loudermilk et al. 2011). In this case, a typical application of the model would be for estimation of stand-level volume and/or biomass. LiDAR techniques are now well developed for tree-level H and CA indirect measurements (Nilsson 1996; Popescu et al. 2003; Popescu and Wynne 2004; Popescu 2007; Li et al. 2012). After applying equations 1 and 2, the dbh and V can be determined for each tree. To determine biomass, allometric equations, such as those reported by Baldwin and Saucier (1983), can be applied, as dbh and H, the independent variables of the biomass equations, would be known. After applying the appropriate scaling factor, stand-level basal area, volume and stand- level biomass can be easily determined.

In conclusion, the models reported in this study performed well for both independent validation datasets within and outside of the geographical range of the fitting dataset. The equations presented here provide a valuable tool for supporting present and future longleaf pine research and management decisions, and for facilitating the use of remote sensing data for quantifying longleaf pine stand structure and function. The models reported here were used in the following Chapter 12 as well as the C simulation modeling described in Chapter 14.

12. Modeling Survival, Yield, Volume Partitioning and their Response to Thinning for Longleaf Pine Plantations

[Contents of this chapter were extracted from: C.A. Gonzalez-Benecke, S.A. Gezan, D.J. Leduc, T.A. Martin, W.P. Cropper Jr., and L.J. Samuelson. 2012. Modeling survival, yield, volume partitioning and their response to thinning for longleaf pine (*Pinus palustris* Mill.) plantations. Forests 3: 1104-1132].

Introduction

In order to improve stand management planning, researchers, managers and landowners need reliable information about stand dynamics and development. While a number of long-term data sets exist for longleaf pine, these data for the most part have not been summarized in a comprehensive manner. As forest management decisions are based on information about current and future resource conditions, forest growth and yield modeling plays an important role by quantifying and summarizing relationships observed in field studies, and by providing stand projections under alternative management scenarios. Whole-stand-level growth and yield models predict future yields as a function of previous stand-level attributes such as age, stand density and site quality (Avery and Burkhart 2002).

A number of models have been produced that predict elements of longleaf pine plantation stand dynamics (Farrar 1973; Lorey and Bailey 1977; Boyer 1980; Brooks and Jack 2006; VanderShaaf 2010). To our knowledge, however, no comprehensive stand-level growth and yield system has been produced for longleaf plantations that includes growth for thinned stands and merchantable volume estimations, and that can be applied to planted stands across a wide range of ages.

The objective of this study was to develop a stand-level growth and yield model system for thinned and unthinned longleaf pine plantations, using a long-term (>40 years) dataset measured and maintained by the U.S. Forest Service. A system of equations was developed to summarize the dynamics observed in the extensive, long-term dataset, and to provide a tool to predict and project stand growth and yield, including merchantable volume breakdown functions.

Materials and Methods

Data description

The dataset used to estimate growth and yield parameters comes from 267 permanent plots measured and maintained by the U.S. Forest Service's Laboratory at Pineville, LA (Goelz and Leduc 2001). The data were collected from regularly remeasured plots in a combination of seven studies exploring the effects of spacing and thinning on longleaf plantations distributed through the Western Gulf Coastal Plain from Santa Rosa County in Florida to Jasper County in Texas (Figure 12.1) and representing its current range in the Western Gulf Coastal Plain (Goelz and Leduc 2001; Leduc and Goelz 2009). Plantations were established on both old field and cutover sites. Soil texture for plots were primarily silt loams, very fine sandy loams, or fine sandy loams, characteristic of the U.S. Upper Coastal Plain. Most plots were burned regularly by prescribed burns or wild fires. Each plot was measured for ~40 years at ~five-year intervals, averaging eight

measurements per plot. Plots were rectangular and ranged in size from 0.04 to 0.1 ha (Lorey and Bailey, 1977).

Figure 12.1. Location of 267 permanent plots measured within the Western Gulf Coastal Plain and longleaf pine natural distribution range.

For each tree, stem diameter outside bark at 1.37 m height (dbh, cm) was measured to the nearest 0.25 cm and total tree height (H, m) was measured to the nearest 0.3 m on a subsample of 4 to 15 trees per plot. Using the model proposed by Quicke and Meldahl (1992) that relates H to the inverse of dbh, individual plot by measurement time regressions were determined (P < 0.0001) to estimate H in all trees without H measurement (MAE% = 4.3%; RMSE% = 5.6%; Bias% = −0.4%; R^2 = 0.97). Mean dominant height (H_{dom}, m) was determined for each plot at every measurement time as the mean of the top 25th percentile tree height. Site index (SI, m) was defined as Hdom at a reference age of 50 years after planting. As several plots were not measured at exactly age 50 years, SI was assessed using Hdom at index age plus/minus one year if necessary (i.e., 49 and 51 years).

From the complete dataset, 30 plots were randomly selected and removed to use for model evaluation and the rest (i.e., 237 plots) for model fitting. A total of 81 plots were thinned to constant basal area levels at five-year intervals; however, only pre-thinning measurements were considered on those plots. Summary statistics of individual trees and stand characteristics of both sub-datasets are shown in Table 12.1.

For all trees with H measurement (28,083 observations) a form factor $F = H/dbh$ (m cm^{-1}) was calculated. In order to eliminate broken and malformed individuals, trees with F less than 0.54 m cm^{-1} and trees with F greater than 13.5 m·cm^{-1} were discarded for Hdom determination (5.4% of H observations). Plots with less than four trees with H measured were also not considered for Hdom fitting (7.9% of total plots).

The distribution of total observations (used for model fitting and model evaluation) by age, SI and surviving trees (N, ha^{-1}) is shown in Table 12.2. Only 2% of plots had $N > 2000$ ha^{-1}, while 28% of data points had $N < 500$ ha^{-1}. About 29% of data had N between 1000 and 1500 ha^{-1}. Most stands (52%) had SI between 25 and 28 m, and only 4% of data had $SI < 22$ m. About 22% of stands had $SI > 28$ m. In term of age distribution, about 20% of data had age < 20 years and 9% had age > 60 years.

Model description: survival and yield models for unthinned stands

Data from all unthinned plots and from thinned plots prior to thinning were used to estimate survival, H$_{dom}$, stand basal area and stand volume (inside and outside bark) parameters.

Following the guide curve method to produce an anamorphic model (Clutter et al. 1983), a dominant height function was fitted based on the Chapman-Richards function using the following expression:

$$H_{dom} = a_0 \cdot SI \cdot (1 - e^{(a_1 \cdot Age)})^{a_2} + \varepsilon_1 \tag{1}$$

where Age is the stand age (years), a_0, a_1 and a_2 are curve fit parameters and ε_1 is the error term, with $\varepsilon_1 \sim N(0, \sigma_1^2)$. For the selected site index age of 50 years, the model can be re-written as:

$$H_{dom} = SI \cdot \left(\frac{1 - e^{(a_1 \cdot Age)}}{1 - e^{(a_1 \cdot 50)}}\right)^{a_2} + \varepsilon_1 \tag{2}$$

This equation can be inverted to determine SI if stand age and H$_{dom}$ are known. This anamorphic model has the assumption that the shape of the height-age curve is independent of SI, and differences between any two curves are proportional to the ratio of their SI's [13].

Table 12.1. Summary statistics and stand characteristics for 267 permanent longleaf pine plots measured (thinned and unthinned).

Variable	Model fitting dataset (237 plots)					Model evaluation dataset (30 plots)				
	Mean	SD	Minimum	Maximum	n	Mean	SD	Minimum	Maximum	n
Age	35.9	15.7	7.0	73.0	725	36.8	16.3	7.0	73.0	140
dbh	21.6	8.3	6.8	44.1	725	21.6	7.8	6.8	42.4	140
H	18.6	5.3	5.3	30.1	725	19.3	5.8	5.4	30.5	140
N	865	504	99	2849	725	982	548	198	2422	140
BA	27.0	11.3	6.6	62.9	725	31.5	13.1	6.8	65.9	140
Dq	22.6	8.4	7.0	44.3	725	22.6	8.0	7.1	42.8	140
SDI	566	222	129	1222	725	655	250	144	1287	140
H_{dom}	20.6	5.6	6.7	32.0	725	21.5	6.1	6.4	32.8	140
SI	25.8	1.9	19.6	30.8	173 *	26.4	1.6	22.1	29.3	21 *
VOL_{OB}	274.6	141.2	46.7	688.6	725	320.7	161.4	55.0	701.3	140

Notes for Table 12.1: Age: stand age (year); dbh: arithmetic mean diameter outside bark at breast height (cm); H: total height (m); N: trees per hectare (trees ha^{-1}); BA: basal area (m^2 ha^{-1}); Dq: quadratic mean diameter (cm); SDI: Reineke's stand density index (trees ha^{-1}); H_{dom}: height of dominant and codominant trees (m); SI: site index (m); VOL_{OB}: total stem volume outside-bark (m^3 ha^{-1}); SD: standard deviation; n: number of plot-level observations; * SI reported only for plots measured at age 50 years.

Table 12.2. Distribution of observations by age, site index and surviving density for 267 permanent longleaf pine plots measured (thinned and unthinned).

Surviving Density Class (ha^{-1})	Stand Age Class (years)				
	7–20	20–40	40–60	60–73	Total
99–500	8	66	105	61	240
500–1000	51	112	91	17	271
1000–1500	69	153	27	-	249
1500–2000	36	49	2	-	87
2000–2849	10	8	-	-	18
Site Index Class (m) *					
19–22	4	45	12	4	35
22–25	46	78	46	21	191
25–28	49	217	132	49	447
28–31	75	78	35	4	192
Total	174	388	225	78	865

Notes for Table 12.2: *SI reported for plots not measured at age 50 years was estimated with model presented in this study.

A negative-exponential survival model that includes H_{dom} was used to estimate survival using a modified version of the model proposed by Dieguez-Aranda et al. (2005 and 2006) and Zhao et al. (2007):

$$N_j = N_i \cdot e^{\left[\left(b_1 + b_2 \cdot H_{dom_i}{}^{b_3}\right) \cdot \left(Age_j^{b_4} - Age_i^{b_4}\right)\right]} + \varepsilon_2 \qquad (3)$$

where N_j is the number of trees ha^{-1} at age j (yr.), N_i is the number of trees ha^{-1} at age i (yr.) ($i < j$), H_{dom_i} is the dominant height (m) at age i (yr.), b_1 to b_4 are curve fit parameters and ε_2 is the error term, with $\varepsilon_2 \sim N(0, \sigma_2{}^2)$. Several models proposed by Dieguez-Aranda et al. (2005 and 2006), Zhao et al. (2007) and Burkhart and Tome (2012) were also tested, but the model that we selected showed the best fit. After model testing, similar to Zhao et al. (2007), the parameters b_1 and b_3 were set equals to 0 and 1, respectively, due to no improvement in predictive ability and convergence difficulties. The final model to estimate H_{dom} was:

$$N_j = N_i \cdot e^{\left[\left(b_1 \cdot H_{dom_i}\right) \cdot \left(Age_j^{b_2} - Age_i^{b_2}\right)\right]} + \varepsilon_2 \qquad (4)$$

The following generic equation, proposed by Borders (1989), was initially used to predict basal area:

$$\ln(BA) = c_1 + c_2 \cdot \ln(N) + c_3 \cdot \ln(H_{dom}) + c_4 \cdot \ln(SI) + c_5 \cdot \left(\frac{1}{Age}\right) +$$
$$c_6 \cdot \ln(N/Age) + c_7 \cdot \ln(H_{dom}/Age) + \varepsilon_3 \qquad (5)$$

where BA is the stand basal area ($m^2 \cdot ha^{-1}$), N is the survival (trees ha^{-1}), c_1 to c_7 are curve fit parameters and ε_3 is the error term, with $\varepsilon_3 \sim N(0, \sigma_3^2)$. After step-wise procedure and variance inflation factor (VIF) analysis, parameters non-significant and/or with high multicollinearity were discarded, resulting in the following final model to estimate BA:

$$\ln(BA) = c_1 + c_2 \cdot \ln(N) + c_3 \cdot \ln(H_{dom}) \, \varepsilon_3 \tag{6}$$

The equations reported by Gonzalez-Benecke et al. (2014b), which depend on the individual dbh and stand parameters N, H_{dom} and SI, were used to estimate individual tree volume outside and inside bark for each living tree in the dataset. After aggregating all individual tree volumes within each plot, stand volume outside and inside bark was determined for each plot. This information at the plot level was used to fit a model for stand volume prediction, which was initially based in the following generic model proposed by Borders (1989) and Pienaar (1995):

$$\ln(VOL) = d_1 + d_2 \cdot \ln(N) + d_3 \cdot \ln(BA) + d_4 \cdot \ln(SI) + d_5 \cdot \ln(H_{dom}) + d_6 \cdot (1/Age) + d_7 \cdot \ln(N/Age) + d_8 \cdot \ln(H_{dom}/Age) + d_9 \cdot \ln(BA/Age) + \varepsilon_4 \tag{7}$$

where VOL is the stand stem volume outside or inside bark ($m^3 \cdot ha^{-1}$), d_1 to d_9 are curve fit parameters and ε_4 is the error term, with $\varepsilon_4 \sim N(0, \sigma_4^2)$. Similar to BA, after the step-wise procedure and VIF analysis, parameters non-significant and/or with high multicollinearity were discarded, resulting in the following final model to estimate VOL:

$$\ln(VOL) = d_1 + d_2 \cdot \ln(N) + d_3 \cdot \ln(BA) + d_4 \cdot \ln(BA/Age) + d_5 \cdot \ln(SI) + \varepsilon_4 \tag{8}$$

Model description: basal area growth model for thinned stands

As the effects of thinning on survival and H_{dom} are small for southern pines (Westfall and Burkhart 2001; Sharma et al. 2006), we only modeled the response in BA growth after thinning. Several models, presented in Burkhart and Tome (2012), were also tested in order to simulate BA growth after thinning, but the methodology reported by Pienaar (1979, 1995) was selected. Following Pienaar (1979), BA projection for thinned stands (BA_t, $m^2 \cdot ha^{-1}$) was determined by using a competition index (CI) and the basal area of an unthinned counterpart stand (BA_u, $m^2 \cdot ha^{-1}$), assuming that BA_t can be expressed as a proportion of the basal area of an unthinned stand of the same age, H_{dom} and number of surviving trees (*i.e.*, an unthinned counterpart) that change over time.

The CI is the rate of competition decline, a measure of the relative degree of competition affecting tree size in the thinned compared to the unthinned stands, and it was determined as follows:

$$CI = \frac{(BA_u - BA_t)}{BA_u} \tag{9}$$

From Equation 7, when BA_t equals BA_u with the same number of trees, the CI is zero. Similarly, when BA_t is less than BA_u (that is the general case in operational thinnings), the CI is larger than zero, but approaching zero as stand ages, as BA_t will converge to BA_u (Pienaar 1995). As the permanent plots of thinned stands do not have an unthinned counterpart, projections of BA_u over

time were estimated using Equations 2, 4 and 5. The BA growth response after thinning was determined indirectly by projecting the time trend of CI, assuming an asymptotic trajectory towards a value of zero. Thus, reflecting that the thinned stand, which has the same age, H_{dom} and number of trees as the unthinned counterpart, will approach, over time, the unthinned stand in terms of total BA (Pienaar 1979). The projected CI after thinning was estimated using a modified version of the model proposed by Pienaar (1979), including the effect of stand age on the rate of competition decline:

$$CI_j = CI_i \cdot e^{\left[\left(\frac{f_1}{Age_j}\right)\cdot(Age_j - Age_i)\right]} + \varepsilon_5 \tag{10}$$

where CI_i and CI_j are the competition index at age i and j (yr.) ($i < j$), respectively, and f_1 is the curve fit parameters and ε_5 is the error term, with $\varepsilon_5 \sim N(0, \sigma_5^2)$. The exponential of the coefficient term, $\frac{f_1}{Age_j}$, corresponds to the annual decline rate of the CI as the stand ages after thinning.

After combining Equations 5 and 6, BA of a thinned stand is estimated using the projected CI as:

$$BA_{t_j} = BA_{u_j} \cdot (1 - CI_j) \tag{11}$$

where BA_{t_j} and BA_{u_j} are the projected BA ($m^2 \cdot ha^{-1}$) in the thinned and unthinned counterpart stands at age j (yr.), respectively.

Model description: merchantable volume

For each tree in the fitting dataset, merchantable stem volume (both outside and inside bark), from the stump to any top diameter, was estimated using the equations reported by Gonzalez-Benecke et al. (2014b) for a range of combinations of threshold dbh values (d, from 5.08 to 40.64 cm) and top diameter limit values (t, from 5.08 to 45.72 cm) that incremented at steps of 5.08 cm. Finally, for each plot, merchantable stem volume per hectare for each combination of d and t was calculated based on all living trees within each plot.

The merchantable volume yield breakdown at the stand-level function was determined following Amateis et al. (1986), where total volume yield outside or inside bark (*i.e.*, VOL_{OB} and VOL_{IB}, $m^3 \cdot ha^{-1}$) was proportionally assigned to product classes defined by two variables: top stem diameter outside bark merchantability limit (t, cm) and a dbh threshold limit (d, cm):

$$VOL_m = VOL \cdot e^{\left[m1 \cdot \left(\frac{t}{Dq}\right)^{m_2} + m_3 \cdot (N^{m_4}) \cdot \left(\frac{d}{Dq}\right)^{m_5}\right]} \tag{12}$$

where VOL_m is merchantable volume per hectare ($m^3 \cdot ha^{-1}$) for trees with dbh larger than d cm, to a top diameter of t cm outside bark, VOL is the total volume per hectare ($m^3 \cdot ha^{-1}$), Dq is the quadratic mean diameter (cm), N the survival (trees ha^{-1}), and m_1 to m_5 are curve fit parameters.

Model evaluation

The predictive ability of the fitted models for N (Equation 4), H$_{dom}$ (Equation 2), BA of unthinned stands (Equation 6), VOL of unthinned stands (Equation 8) and BA of thinned stands (Equation 11) was assessed with the 30 plot evaluation dataset. In the case of VOL$_m$ (Equation 12), two combinations of d and t were selected to evaluate this model. The selected values of d and t correspond to the threshold values used to estimate breakdown volume yield for other southern pine species (Harrison and Borders 1996; Pienaar et al. 1996; Yin et al. 1998), corresponding to chip-and-saw (d = 21.6 cm; t = 10.2 cm) and sawtimber (d = 29.2 cm; t = 20.3 cm) products.

Four measures of accuracy were used to evaluate the goodness-of-fit between observed and predicted (simulated) values for each variable originated from the dataset obtained in the model evaluation: (i) mean absolute error (MAE); (ii) root mean square error (RMSE); (iii) mean bias error (Bias); and (iv) coefficient of determination (R^2) (Fox 1981; Willmott et al. 1986; Loague and Green 1991; Kaboyashi and Salam 2000). For BA and VOL, the statistics MAE, RMSE and Bias were back-transformed from logarithmic values.

The system of equations was also compared against other models reported in the literature for longleaf pine plantations using the same model evaluation dataset indicated above. The models compared were: (i) survival equations reported by Lohrey and Bailey (1977), Brooks and Jack (2006) and Lauer and Kush (2011), (ii) dominant height equations reported by Farrar (1973) and Brooks and Jack (2006), and (iii) VOL$_{OB}$ equations reported by Lohrey and Bailey (1977) and Brooks and Jack (2006). The breakdown volume outside bark yield function was also compared against the functions reported for *Pinus taeda* (Harrison and Borders 1996) and *Pinus elliottii* (Pienaar et al. 1996) across different Dq and stand densities, and for three product classes (sawtimber: d = 29.2 cm and t = 20.3 cm; chip-and-saw: d = 21.6 cm and t = 11.2 cm; pulpwood: d = 11.4 cm and t = 5.1 cm), assuming stands with VOL$_{OB}$ of 100 m$^3 \cdot$ha^{-1}. This value of VOL$_{OB}$ was selected to facilitate percent comparisons. The results of the breakdown volume yield function are independent of the value assumed.

An overall evaluation of the model was carried out for unthinned plots of the validation dataset. On each plot, for known initial stand age, N and SI, stand BA and VOL$_{OB}$ were estimated on the same ages where they were originally measured by using the final equations fitted to estimate N, H$_{dom}$, BA and VOL$_{OB}$. The same four measures of accuracy described previously were used to assess the agreement between observed and predicted values.

All of the summary, model fitting and model evaluation statistics were obtained using SAS 9.3 (SAS Inc., Cary, NC, USA) (SAS 2011). When multiple linear regressions were carried out, the variance inflation factor (VIF) was monitored to detect multicollinearity between predicting variables, discarding all variables included in the model with VIF larger than 5, as suggested by Neter et al. (1996). In the case of BA and VOL fitting, where multiple linear regressions were carried out, step-wise procedure was used with a threshold significance value of 0.15 as variable selection criteria to enter and to stay Neter et al. (1996). For these responses, a logarithm transformation was preferred as it allows controlling for heterogeneity of variances, approximate to normality and uses the linear model framework to select among the large set of, potentially collinear, predicting variables.

Model application example

167

The system of equations developed was used to predict stand growth of unthinned and thinned (3 thinnings, removing 33% of living trees at ages 30, 40 and 50 years) longleaf pine stands growing at sites with two different SI's: 20 and 30 m. The initial planting density used was 1400 trees ha^{-1}, the survival after the first year was assumed to be 95%, and the simulation length was 70 years. Here it was assumed that the percentage of removed trees was the same as the percentage removal of BA during thinning.

Results

Model fitting

The parameter estimates for the growth and yield predictive and projective equations (Equations 2, 4, 6, 8, 10 and 12) for longleaf pine plantations growing in Western Gulf Coastal Plain U.S. are reported in Table 12.3. All parameter estimates were significant at $P < 0.05$. Non-linear versions of the models presented in Equation 6 (BA) and 8 (VOL) were also evaluated, but these resulted in no improvement in model performance (data not shown), therefore, natural logarithm-transformed response variables were used. Parameter estimates for the intercept in Equations 6 (c_1) and 8 (d_1) include the correction proposed by Snowdon (1991). The correction factor proposed by Baskerville (1972) was also evaluated, but it presented lower bias reduction (data not shown).

Parameter estimates for the model that projects dominant height (Equation 2) are shown in Table 12.3. For SI of 20 m, the model projects dominant height of 5.4 and 22.6 m at age 10 and 70 years, respectively. If SI increased to 29 m, the model projects dominant height of 7.9 and 32.8 m at age 10 and 70 years, respectively. For all 194 plots where SI was measured, the mean observed and predicted SI was 25.84 and 25.88 m, respectively.

The survival model (Equation 4) was dependent on stand age and H_{dom}. The performance of the N model for the range of SI present on the dataset used for model fitting (*i.e.*, between 20 and 29 m, see Tables 12.1 and 12.2) and using a planting density of 1500 trees ha^{-1} showed little mortality and only small differences in survival at age 10 years (between 1450 and 1429 trees ha^{-1}, for SI 20 and 29 m, respectively). At age 70 years, however, the model estimated large differences in survival across SI's (between 493 and 300 trees ha^{-1}, for SI = 20 and 29 m, respectively).

After applying the step-wise procedure and checking variance inflation factors (VIF), the final selected model that predicts BA (Equation 6) was only dependent on N and H_{dom} (Table 12.3). Although the variables 1/Age, ln(N)/Age and ln(H_{dom})/Age were significant after the step-wise variable selection procedure ($P < 0.001$, data not shown), their VIF's were high with values of 296, 173 and 35, respectively (data not shown). Therefore, these variables were discarded from the model and the goodness-of-fit of the final model was lower than the full model, having a CV of 3.6% and a R^2 of 0.944. Partial R^2 of H_{dom} and N were 0.579 and 0.366, respectively (data not shown).

The final model that predicts stand volume (Equation 8), after the step-wise variable selection procedure and VIF checking, was dependent on N, BA, ln(BA)/Age and SI (Table 12.2). The variable H_{dom} was discarded from the final model, even though they were selected after step-wise variable selection procedure ($P < 0.001$, data not shown), due to its high multicollinearity (VIF =

42.3, data not shown). The final models that predict stand V_{OB} and V_{IB} had a CV of about 1% and R^2 greater than 0.99. Stand BA explained most of the variability in V_{OB} and V_{IB}, with partial R^2 of about 0.912 and 0.867, respectively. Stand density presented partial R^2 of about 0.079 and 0.121, for V_{OB} and V_{IB}, respectively. Even though SI and ln(BA)/Age were significant, both explained less than 0.1% of changes in stand volume (data not shown).

The model that projects the time trend of CI after thinning (Equation 10) was dependent on stand age (Table 12.3). The exponential of the coefficient for a 36 year-old stand (mean values of stand age reported in Table 12.1), represents an average annual decline rate of the CI as the stand ages after thinning of 4.3%.

Parameter estimates for merchantable volume yield breakdown function (Equation 12) for both, outside (VOLm-OB, m^3 ha^{-1}) and inside (VOLm-IB, m^3 ha^{-1}) bark total volume yield, are shown in Table 12.3. The models had a CV of about 11% and an approximate R^2 of 0.99 for both outside and inside bark volume yield breakdown estimates.

There was a good agreement between predicted and observed values of N (Figure 12.2a), Hdom (Figure 12.2c) and BA (Figure 12.2e). The slope and the intercept of the relationship between predicted and observed values were not statistically different from one (P = 0.32) and zero (P = 0.14), respectively.

If residuals are expressed as a percentage of the observed value, maximum absolute residuals observed represent about 17% and 16% of observed N and H_{dom}, respectively. Residuals for predicting the BA model were larger, with maximum residuals of about 30% of observed BA but centered around zero. There was no noticeable trend in residuals with observed values (Figure 12.2b for N; Figure 12.2d for H_{dom} and Figure 12.2e for BA) or stand age (data not shown).

Table 12.3. Parameter estimates and fit statistics of Western Gulf Coastal Plain U.S. longleaf pine plantation growth and yield equations.

Model	n	Parameter	Parameter estimate	Approx. SE	Approx. P > F	VIF	R^2	RMSE	CV%
$H_{dom} = SI \cdot \left(\dfrac{1 - e^{(a_1 \cdot Age)}}{1 - e^{(a_1 \cdot 50)}}\right)^{a_2}$	600	a_1	-0.0362307	0.0016031	<0.0001	n.a.	0.998	0.974	4.7
		a_2	1.2833052	0.0455901	<0.0001	n.a.			
$N_j = N_i \cdot e^{\left[(b_1 \cdot H_{dom_i}) \cdot (Age_j^{b_2} - Age_i^{b_2})\right]}$	620	b_1	-0.0014438	0.0006709	0.0324	n.a.	0.997	53.835	6.9
		b_2	0.8684429	0.0999107	<0.0001	n.a.			
$\ln(BA) = c_1 + c_2 \cdot \ln(N) + c_3 \cdot \ln(H_{dom})$	771	c_1*	-5.2620359	0.0790110	<0.0001	0	0.946	1.154	4.7
		c_2	0.4805023	0.0075357	<0.0001	1.02			
		c_3	1.7683088	0.0187287	<0.0001	1.02			
$\ln(VOL_{OB}) = d_1 + d_2 \cdot \ln(N) + d_3 \cdot \ln(BA) + d_4 \cdot [\ln(BA)]/Age + d_5 \cdot \ln(SI)$	771	d_1*	3.1110579	0.0809271	<0.0001	0	0.997	1.109	0.72
		d_2	-0.1406022	0.0045948	<0.0001	4.41			
		d_3	1.1826310	0.0040024	<0.0001	2.48			
		d_4	-2.4435259	0.0989071	<0.0001	4.02			
		d_5	-0.0782880	0.0265719	0.0033	1.49			
$\ln(VOL_{IB}) = d_1 + d_2 \cdot \ln(N) + d_3 \cdot \ln(BA) + d_4 \cdot [\ln(BA)]/Age + d_5 \cdot \ln(SI)$	771	d_1*	3.0888853	0.1026120	<0.0001	0	0.996	1.050	0.96
		d_2	-0.1943861	0.0058271	<0.0001	4.41			
		d_3	1.2580580	0.0050738	<0.0001	2.48			
		d_4	-3.1281571	0.1254092	<0.0001	4.02			
		d_5	-0.098259	0.0336921	0.0037	1.49			
$CI_j = CI_i \cdot e^{\left[\left(\frac{f_1}{Age_j}\right) \cdot (Age_j - Age_i)\right]}$	331	f_1	-1.2779203	0.2365130	<0.0001	n.a.	0.815	0.0589	200.8

Model	n	Parameter	Estimate	SE	p	VIF	R²	SE	CV
$\text{VOL}_{m-OB} = \text{VOL}_{OB} \cdot e^{\left[g_1 \cdot \left(\frac{t}{\text{Dq}}\right)^{g_2} + g_3 \cdot (N^{g_4}) \cdot \left(\frac{d}{\text{Dq}}\right)^{g_5}\right]}$	21541	g_1	-1.0385828	0.0026438	<0.0001	n.a.	0.990	0.0702	11.1
		g_2	4.2526170	0.0147436	<0.0001	n.a.			
		g_3	-0.6266850	0.0596972	<0.0001	n.a.			
		g_4	-0.1246646	0.0185442	<0.0001	n.a.			
		g_5	9.1649608	0.1878172	<0.0001	n.a.			
$\text{VOL}_{m-IB} = \text{VOL}_{IB} \cdot e^{\left[g_1 \cdot \left(\frac{t}{\text{Dq}}\right)^{g_2} + g_3 \cdot (N^{g_4}) \cdot \left(\frac{d}{\text{Dq}}\right)^{g_5}\right]}$	21541	g_1	-1.0537628	0.0027184	<0.0001	n.a.	0.990	0.0708	11.2
		g_2	4.2527499	0.0148697	<0.0001	n.a.			
		g_3	-0.6545719	0.0641831	<0.0001	n.a.			
		g_4	-0.1365633	0.0191092	<0.0001	n.a.			
		g_5	9.3108306	0.1971518	<0.0001	n.a.			

H_{dom}: average total height (m) of dominant and codominant trees; SI: site index (m); N_j: trees per hectare at stand age "j" years; N_i: trees per hectare (ha^{-1}) at stand age "i" years (i < j); H_{dom}: average total height (m) of dominant and codominant trees at stand age "i" years; ln(BA): natural logarithm of basal area of unthinned stands [ln(m^2 ha^{-1})]; ln(VOL): natural logarithm of total stem volume [ln(m^3 ha^{-1})]; CI_j: competition index at stand age 'j' years; CI_i: competition index at stand age 'i' years (i < j); OB: outside bark; IB: inside bark; VOL$_m$: merchantable stem volume (m^3 ha^{-1}); VOL is total stem volume (m^3 ha^{-1}); t: top diameter (outside bark) merchantability limit (cm); Dq: quadratic mean diameter (cm); d: dbh threshold limit (cm); n: number of observations used for model fitting; SE: standard error; VIF: variance inflation factor; R^2: coefficient of determination; CV: coefficient of variation (100·RMSE/mean). * Parameters estimates for c_1 and d_1 include the correction proposed by Snowdon (1991).
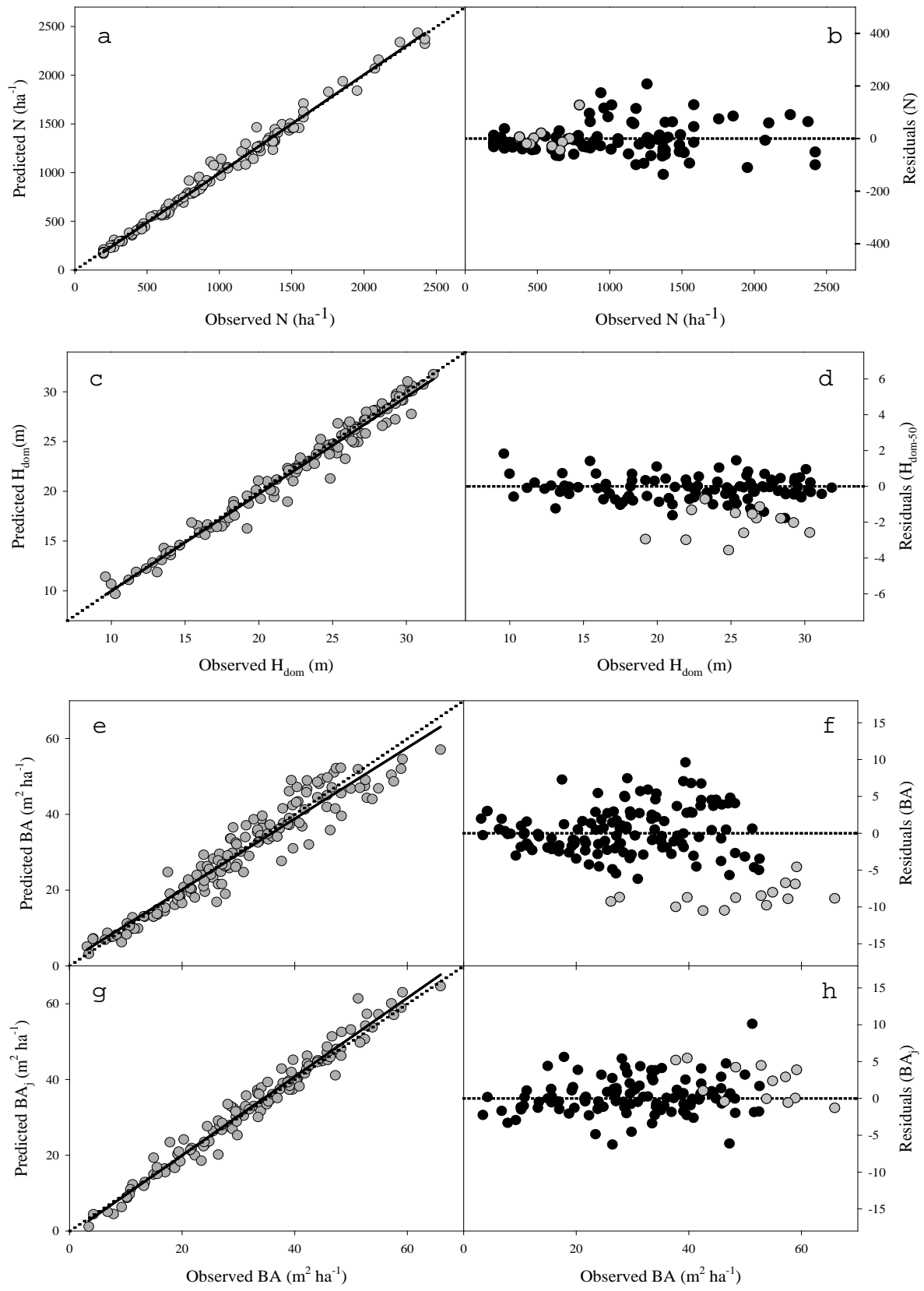
Figure 12.2. Validation of dominant height (H_{dom}) (a, b), surviving trees per hectare (N) (c, d) and basal area for unthinned stands (BA) (e to h) models based on 30 plots from the dataset used for model evaluation. Observed *versus* predicted (simulated) values (a, c, e and g) and residuals (predicted-observed) *versus* stand age (years) relationship of Hdom (b) and N (d), and residuals *versus* observed values of predicting (f) and projecting (h) BA. Solid line represents linear fit between observed and predicted values and dotted lines for plots (a, c, e and g) correspond to the 1-to-1 relationship. Residuals are presented as a proportion of observed values.

A growth model to project, or update, BA (BA_j) when some stand measurements are available, including current BA (BA_i), along with current (i) and future (j) Age, N and H_{dom}, was derived from the fitted BA model (Equation 5), and is expressed as:

$$BA_j = BA_i \cdot \left(\frac{N_j}{N_i}\right)^{0.4452486} \cdot \left(\frac{H_{dom_j}}{H_{dom_i}}\right)^{1.6516307} \tag{13}$$

As expected, this projecting growth model improved the estimations of BA, reducing the residuals as compared with BA predicting model (Figure 12.2g,h).

There was good agreement between predicted and observed values for VOL outside and inside bark (Figure 12.3a,c). In both cases, the intercept of those relationships was not statistically different from zero ($P > 0.16$). The slopes of the relationship between predicted and observed values (1.006 and 1.011, for VOL_{OB} and VOL_{IB}, respectively) were statistically different to one ($P < 0.02$). There was a good agreement between predicted and observed values of BA_t (Figure 12.3e). The intercept and slope were not different from zero ($P = 0.18$) and one ($P = 0.12$), respectively. If residuals are expressed as a percentage of observed value, maximum residuals observed in Figure 12.3 represent about 15% and 17% of observed VOL_{OB} and VOL_{IB}, respectively. There was no noticeable trend in residuals with observed values (Figure 12.3b for VOL_{OB}; Figure 12.3d for VOL_{IB} and Figure 12.3e for BA_t) or stand age (data not shown).

For the two combinations of t and d tested, there was good agreement between predicted and observed VOL_m (Figure 12.3g, i). For the two examples shown in Figure 12.3, the slope and intercept of those relationships were not different from one ($P > 0.41$) and zero ($P > 0.36$), respectively. For all variables listed above, there was no noticeable trend of residuals with observed values. Only for sawtimber VOL_m larger than about 500 $m^3 \cdot ha^{-1}$ (Figure 12.3i, j), there was a small tendency to increase residuals as VOL_m increased, but the magnitude of that overestimation was less than 5% of observed values.

Table 12.4. Summary of model evaluation statistics for N, H_{dom}, BA, BA_t, VOL, and VOL_m estimations based on 30 plots.

Variable	$\overline{O}$	$\overline{P}$	n	MAE	RMSE	Bias	R^2
N	938	929	120	40.3 (4.3)	53.1 (5.7)	−9.46 (−1.0)	0.991
H_{dom}	23.0	22.8	111	0.6 (2.7)	0.8 (3.6)	−0.20 (−0.9)	0.978
BA	31.5	30.8	140	3.1 (10.0)	4.2 (13.5)	−0.65 (−2.1)	0.898
BA_j	33.1	33.3	120	1.9 (5.8)	2.6 (7.8)	0.45 (1.4)	0.970
VOL_{OB}	340.4	341.1	115	11.9 (3.5)	16.4 (4.8)	0.61 (0.2)	0.990
VOL_{IB}	269.8	270.9	115	12.3 (4.6)	17.2 (6.4)	1.06 (0.4)	0.984
BA_t	28.5	27.9	52	0.9 (3.1)	1.1 (3.8)	−0.65 (−2.3)	0.984
$VOL_{m\text{-}OB\text{-}t=10,\,d=20}$	137.1	138.3	70	2.5 (1.9)	4.0 (1.9)	1.25 (0.9)	0.999
$VOL_{m\text{-}IB\text{-}t=10,\,d=20}$	109.9	110.8	70	1.9 (1.7)	3.0 (1.7)	0.94 (0.9)	0.999
$VOL_{m\text{-}OB\text{-}t=20,\,d=30}$	140.4	141.5	20	7.9 (5.6)	9.0 (5.6)	1.14 (0.8)	0.998
$VOL_{m\text{-}IB\text{-}t=20,\,d=30}$	115.0	114.4	20	6.3 (5.5)	7.2 (5.5)	−0.63 (−0.5)	0.998

Notes for Table 12.4: N: trees per hectare (ha^{-1}); H_{dom}: average total height of dominant and codominant trees (m); BA: predicted basal area of unthinned stands ($m^2\ ha^{-1}$); BA_j: projected basal area of unthinned stands ($m^2\ ha^{-1}$); VOL: total stem volume ($m^3\ ha^{-1}$); BA_t: basal area of thinned stands ($m^2\ ha^{-1}$); VOL_m: merchantable stem volume for trees d cm and above to a t cm top diameter limit ($m^3\ ha^{-1}$); $\overline{O}$: mean observed value; $\overline{P}$: mean predicted value; n: number of observations; MAE: mean absolute error; RMSE: root of mean square error; Bias: absolute bias; R^2: coefficient of determination. OB: outside bark; IB: inside bark; t: top diameter (outside bark) merchantability limit (cm); d: dbh threshold limit (cm). Values in parenthesis are percentage relative to observed mean.

All model performance tests showed that N, H_{dom}, BA, BA_t, VOL and VOL_m estimations agreed well with measured values (Table 12.4). For all estimations, MAE and RMSE ranged between 2.4% to 10.3%, and 3.4% to 13.4% of the observed values, respectively. In all cases, BA estimations presented the larger differences between the observed and predicted values. The Bias ranged between 1.9% under-estimations for projected BA and 1.4% over-estimations for BA_t, with no clear tendency to over- or under-estimate. Estimated and observed values were highly correlated, with R^2 values greater than 0.91. The performance of the BA model that included the variables with high collinearity was also tested, showing lower MAE and RMSE than the final model (8.8, 12.6%, respectively) and larger absolute Bias (−3.3%) (data not shown).

When tested on the dataset used for model evaluation, predicted values of the models proposed in this study for N, H_{dom} and VOL_{OB} are within the range of variation of the estimations using other published growth and yield models. The effects of stand age on survival, H_{dom}, and VOL_{OB} were predicted using several models for longleaf pine (Figure 12.4). Across three stand age classes (<25, 25–49 and 50–75 years), the models predict stand growth consistently, with no clear trend to over- or under-estimate. For example, N and H_{dom} estimations of all models performed adequately with Bias less than 10% (Figure 12.4a) and RMSE less than 15% with no apparent trend to change across stand age classes (Figure 12.4b).

175

Figure 12.3 Validation of total stem volume outside (VOL$_{OB}$) (a, b) and inside (VOL$_{IB}$) (c, d) bark, BA after thinning (BA$_t$) (e, f) and merchantable volume breakdown (VOL$_m$) (g to j) models based

on 30 pots from the model evaluation dataset. Observed *versus* predicted (simulated) values (a, c, e, g, i) and residuals (predicted-observed) *versus* observed values of VOL_{OB} (b) VOL_{IB} (d), BA_t (f) and VOL_m (h, j). Two examples of VOL_m outside bark are shown: using $d = 10.16$ cm and $t = 20.32$ cm (g, h) and $d = 20.32$ cm and $t = 30.48$ cm (i, j). Solid line represents linear fit between observed and predicted values and dotted lines for plots a, c, e, g and i correspond to the 1-to-1 relationship. Residuals are presented as a proportion of observed values.

The estimates of VOL_{OB} were similar for all models for age less than 25 years, but for older stands the model reported by Brooks and Jack (2006) over-estimated VOL_{OB} by around 70 $m^3 \cdot ha^{-1}$, while the model reported by Lohrey and Bailey (1977) over-estimated VOL_{OB} by about 50 and 10 $m^3 \cdot ha^{-1}$ for stand age between 25–49 and 50–75 years, respectively.

Similarly, the model presented in this study under-predicted VOL_{OB} by about 30 $m^3 \cdot ha^{-1}$ (or around 7%) for older stands (Figure 12.4e). The RMSE of VOL_{OB} estimations for the models reported in literature increased with stand age, averaging about 85 $m^3 \cdot ha^{-1}$ at age class 25–75 years, whereas the model presented in this study had an error of about 19 m^3 ha^{-1} at age class 25–49 years, and 42 $m^3 \cdot ha^{-1}$ at age class 50–75 years (Figure 12.4f).

All model performance tests showed that N, H_{dom}, BA, BA_t, VOL and VOL_m estimations agreed well with measured values (Table 12.4). For all estimations, MAE and RMSE ranged between 2.4% to 10.3%, and 3.4% to 13.4% of the observed values, respectively. In all cases, BA estimations presented the larger differences between the observed and predicted values. The Bias ranged between 1.9% under-estimations for projected BA and 1.4% over-estimations for BA_t, with no clear tendency to over- or under-estimate. Estimated and observed values were highly correlated, with R^2 values greater than 0.91. The performance of the BA model that included the variables with high collinearity was also tested, showing lower MAE and RMSE than the final model (8.8, 12.6%, respectively) and larger absolute Bias (-3.3%) (data not shown).

When tested on the dataset used for model evaluation, predicted values of the models proposed in this study for N, H_{dom} and VOL_{OB} are within the range of variation of the estimations using other published growth and yield models. The effects of stand age on survival, H_{dom}, and VOL_{OB} were predicted using several models for longleaf pine (Figure 12.4). Across three stand age classes (<25, 25–49 and 50–75 years), the models predict stand growth consistently, with no clear trend to over- or under-estimate. For example, N and H_{dom} estimations of all models performed adequately with Bias less than 10% (Figure 12.4a) and RMSE less than 15% with no apparent trend to change across stand age classes (Figure 12.4b). The estimates of VOL_{OB} were similar for all models for age less than 25 years, but for older stands the model reported by Brooks and Jack (2006) over-estimated VOL_{OB} by around 70 m^3 ha^{-1}, while the model reported by Lohrey and Bailey (1977) over-estimated VOL_{OB} by about 50 and 10 $m^3 \cdot ha^{-1}$ for stand age between 25–49 and 50–75 years, respectively.
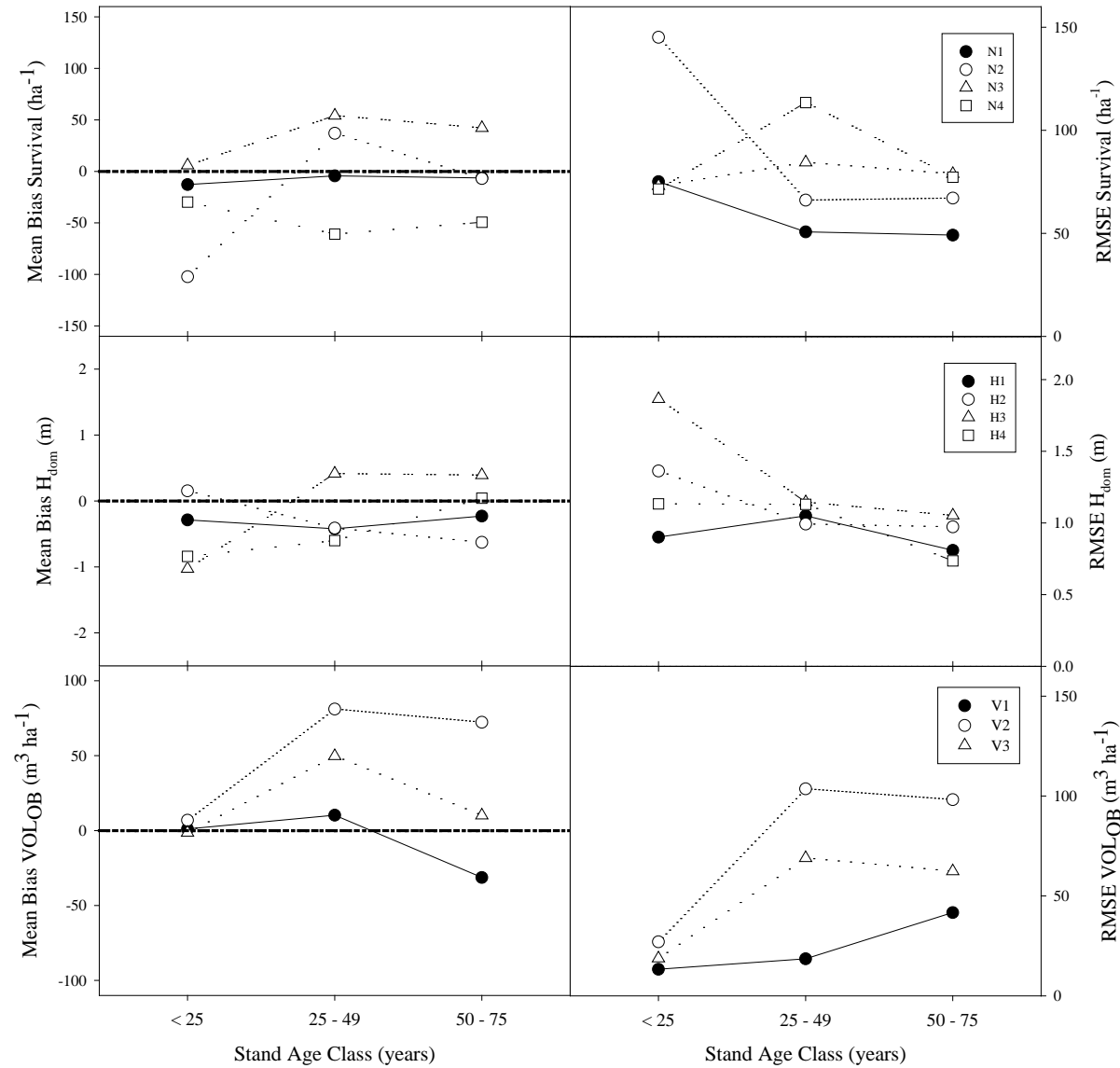
Figure 12.4. Mean bias and RMSE of the models presented in this study and reported in literature to predict survival (a, b), H_{dom} (c, d) and VOL_{OB} (e, f) of longleaf pine plantations across four stand age classes: <25, 25–49 and 50–75 years The survival models are: current report (N1), Brooks and Jack (2006) (N2), Lohrey and Bailey (1977) (N3), and Lauer and Kush (2011) (N4). The H_{dom} models are: current report (H1), Brooks and Jack (2006) (H2), Farrar (1973) using SI and base age 25 years (H3) and using SI and base age 50 years (H4). The VOL_{OB} models are: current report (V1), Brooks and Jack (2006) (V2) and Lohrey and Bailey (1977) (V3).
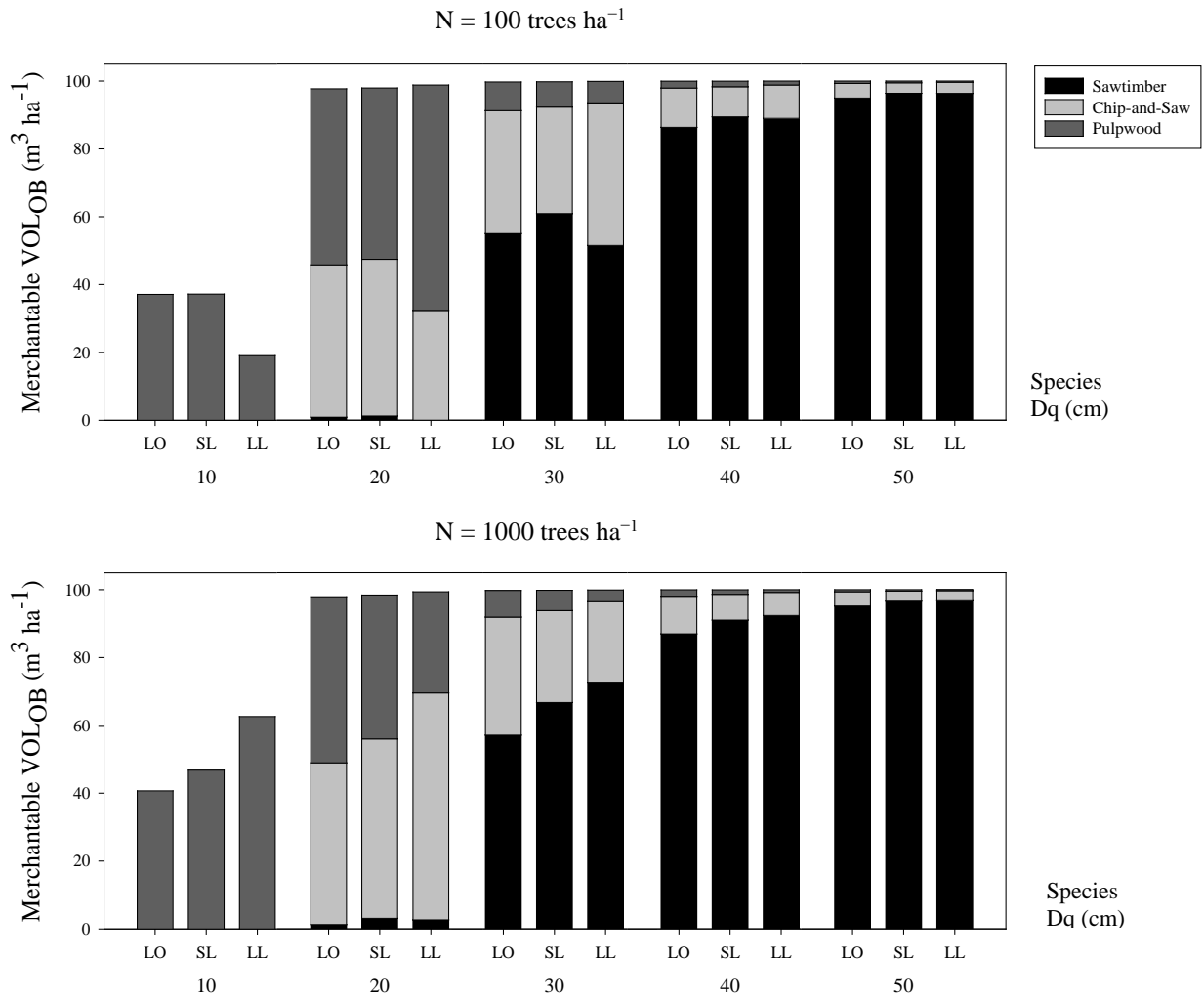
Figure 12.5. Comparison of merchantable volume yield breakdown functions published for *P. taeda* (LO, Harrison and Borders, 1996), *P. elliottii* (SL, Pienaar et al., 1996) and *P. palustris* (LL, this study). Effect of Dq (from 10 to 50 cm) and stand density [N = 100 trees ha^{-1}, upper panel (a); N = 1000 trees ha^{-1}, lower panel (b)] on volume yield breakdown for three product classes (sawtimber: d = 29.2 cm and t = 20.3 cm; chip-and-saw: d = 21.6 cm and t = 11.4 cm; pulpwood: d = 11.4 cm and t = 5.1 cm), assuming a VOL$_{OB}$ of 100 m^3·ha^{-1}.

179

Table 12.5. Summary of overall model evaluation statistics for N, H_{dom}, BA and VOL_{OB} estimations using different reference age for SI for different simulation lengths.

Variable	Simulation length (years)	$\overline{O}$	$\overline{P}$	n	MAE (%)	RMSE (%)	Bias (%)	R^2
N	0–20	818.5	818.3	339	8.3%	12.4%	0.0%	0.959
	21–40	541.1	560.9	172	21.3%	30.5%	3.5%	0.884
	All	20.9	20.9	339	11.6%	17.6%	0.9%	0.934
H_{dom}	0–20	27.2	27.2	172	3.3%	4.2%	−0.1%	0.960
	21–40	23.0	23.0	511	1.7%	2.1%	0.0%	0.948
	All	36.1	34.9	172	2.6%	3.4%	−0.1%	0.974
BA	0–20	30.6	29.7	511	9.8%	13.1%	−2.7%	0.887
	21–40	273.9	273.0	339	15.9%	19.1%	−3.5%	0.747
	All	333.6	320.1	511	12.2%	16.2%	−3.0%	0.837
VOL_{OB}	0–20	818.5	818.3	339	10.4%	13.6%	−0.3%	0.895
	21–40	541.1	560.9	172	19.6%	23.2%	−8.7%	0.557
	All	20.9	20.9	339	13.2%	18.3%	−4.2%	0.839

Notes for Table 12.5: N: trees per hectare (ha^{-1}); H_{dom}: average total height of dominant and codominant trees (m); BA: stand basal area ($m^2 \cdot ha^{-1}$); VOL_{OB}: total stem volume outside bark ($m^3 \cdot ha^{-1}$); $\overline{O}$: mean observed value; $\overline{P}$: mean predicted value; n: number of observations; MAE: mean absolute error (m); RMSE: root of mean square error (m); Bias: absolute bias (m); R^2: coefficient of determination. Values of MAE, RSME and Bias are percentage relative to observed mean.

Similarly, the model presented in this study under-predicted VOL_{OB} by about 30 $m^3 \cdot ha^{-1}$ (or around 7%) for older stands (Figure 12.4e). The RMSE of VOL_{OB} estimations for the models reported in literature increased with stand age, averaging about 85 $m^3 \cdot ha^{-1}$ at age class 25–75 years, whereas the model presented in this study had an error of about 19 m^3 ha^{-1} at age class 25–49 years, and 42 m^3 ha^{-1} at age class 50–75 years (Figure 12.4f).

Examples of merchantable yield breakdown function of VOL_{OB} estimations for *P. taeda* (Harrison and Borders 1996), *P. elliottii* (Pienaar et al. 1996) and *P. palustris* (this study) are presented in Figure 12.5, showing, notably, similar results across species.

For example, for sawtimber, defined as stem volume of trees with dbh larger than 29.2 cm outside bark (threshold dbh limit) to a top diameter of 20.3 cm outside bark (merchantability limit), when Dq was smaller than 20 cm there was no sawtimber volume production, but when Dq was 30 cm, sawtimber yield was about 55, 61 and 52% (N = 100 trees ha^{-1}) or 57, 67 and 73% (N = 1000 trees ha^{-1}) for *P. taeda*, *P. elliottii* and *P. palustris*, respectively (Figure 12.5a,b). In the case of chip-and-saw yield, when Dq was 10 cm, all models predicted no volume production for that product, which has a threshold dbh limit of 21.6 cm. Independent of N, when Dq was larger than 50 cm, sawtimber yield was larger than 95% of VOL_{OB} and the production of chip-and-saw (Figure 12.5c,d) and pulpwood (Figure 12.5e,f) declined when the stands reached Dq larger than the

merchantability limit for sawtimber. Overall, the merchantable yield breakdown functions presented in this study showed the expected behavior of product partitioning as Dq and N changed.

The overall test of the model indicated that, if only initial (*i.e.*, current) stand age, N and SI (reported at first measurement) are known, estimations of H_{dom}, BA and VOL_{OB} were not affected, in relative terms, by simulation length (Figure 12.6d,f,h). On the other hand, projections of N were sensitive to the length of the simulation (Figure 12.6b), with errors getting larger as simulation length increased. In all cases residuals were centered on zero. For all stand parameters simulated, there was no noticeable trend of residuals with observed values, and the slope and intercept of the relationships between observed and predicted values were not different from one ($P > 0.24$) and zero ($P > 0.42$), respectively.

If initial stand age, N and SI are known, the overall test of the model system indicated that projections of N, H_{dom} and predictions of BA and VOL_{OB} for less than ~40 years simulation length presented a bias that ranged between −7% and 10% (Table 12.5). Across simulation lengths, the overall bias of the model system for N, H_{dom}, BA and VOL_{OB} were over-estimations of about 6 trees ha^{-1} and under-estimations of about 0.2 m, 0.9 m^2·ha^{-1} and 13.4 m^3 ha^{-1}, respectively. The overall MAE and RMSE of the model system were about 12 and 18% for N, 3 and 3% for H_{dom}, 12 and 16% for BA and 13 and 18% for VOL_{OB}, respectively. The R^2 decreased as simulation length increased. The overall R^2 across simulation lengths were about 0.93, 0.97, 0.84 and 0.84, for N, H_{dom}, BA and VOL_{OB}, respectively. A trend of increasing error with simulation length was observed for Bias, MAE and RMSE (Table 12.5). Nevertheless, it is important to note that the number of observations decreases as the simulation length gets larger (Table 12.5), and therefore, the evaluation statistics on simulation lengths ~40 years can be affected by the unbalanced sampling size and specific characteristics of the sampled plots for evaluations.

An example of model behavior for a hypothetical longleaf stands planted with 1400 trees ha^{-1} is shown in Figure 12.7. The unthinned stands growing on a site with SI = 20 m reached at age 70 years a survival of about 46% of initial planting density, H_{dom} of 22.6 m, BA of 28.5 m^2 ha^{-1}, SDI of 571 trees ha^{-1} and VOL_{OB} of 338 m^3 ha^{-1}. When SI was 30 m instead, at the same age the survival was 31% and H_{dom} was 33.8 m. The unthinned stand reached a maximum BA of about 48.1 m^2·ha^{-1} at age 58 years, and SDI peaked at about 870 trees ha^{-1} at age 49 years and VOL_{OB} was still increasing, reaching about 610 m^3 ha^{-1} at age 70 years When a scenario of three thinnings was applied to both stands, at age 70 years the number of surviving trees was about 181 and 122 trees ha^{-1} and Dq was increased from 24.6 and 38.3 cm (unthinned), to 30.2 and 47.2 cm, for SI of 20 and 30 m, respectively. The harvested volume from thinnings was about 171 and 331 m^3 ha^{-1}, and the final yield was 162 and 293 m^3·ha^{-1} for SI of 20 and 30 m, respectively.
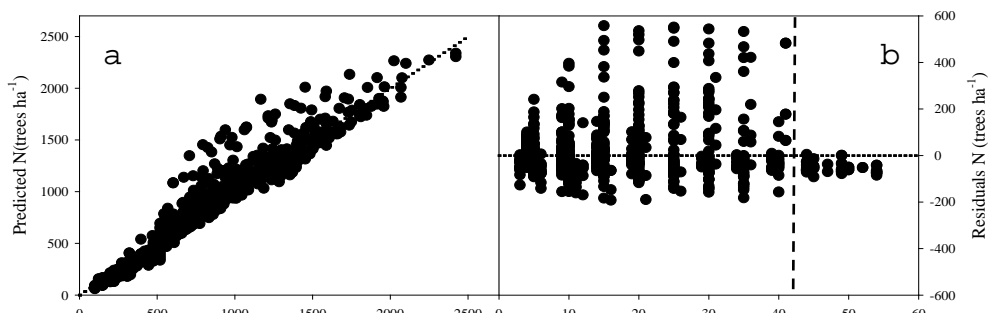
Figure 12.6. Overall simulation validation of survival (N) (a, b), dominant height (H_{dom}) (c, d), basal area (BA) (e, f) and stem volume outside bark (VOL_{OB}) (g, h) predictions. Observed *versus* predicted (simulated) values (a, c, e, g) and residuals (predicted-observed) *versus* simulation length (years) (b, d, f, h) relationships for unthinned stands if initial age, N and SI are known, using the models to estimate N, H_{dom}, BA and VOL_{OB} for all unthinned plots in the dataset based only on knowing the initial stand age, N and SI.
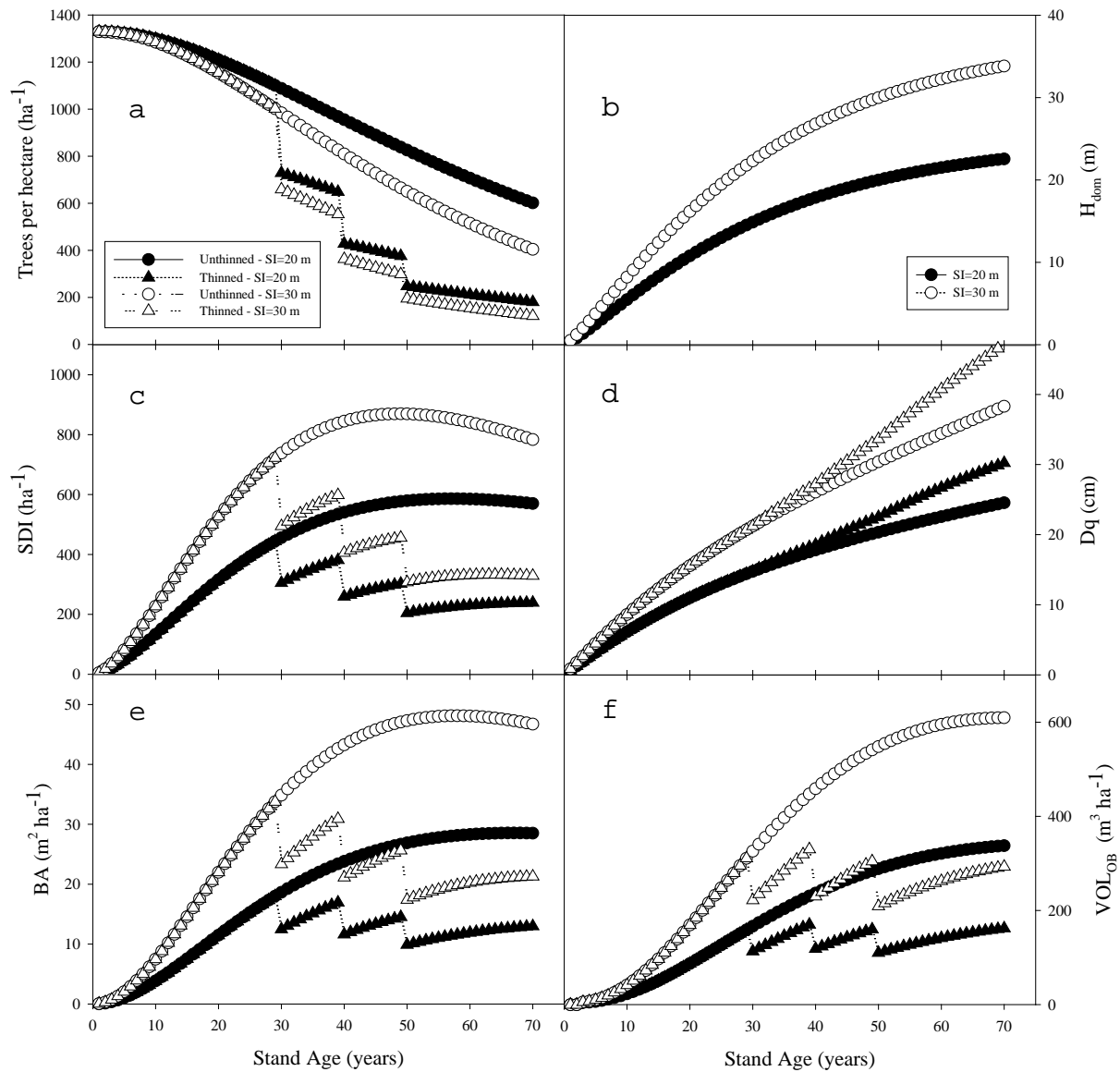
Figure 12.7 Example of model outputs. Simulation of survival (N, trees ha^{-1}): (a) dominant height (H$_{dom}$, m); (b) stand density index (SDI, trees ha^{-1}); (c) quadratic mean diameter (Dq, cm); (d) basal area (BA, m^2·ha^{-1}); (e) and stem volume outside bark (VOL$_{OB}$, m^3·ha^{-1}); (f) of unthinned (circle) and thinned (triangle) longleaf pine stands growing in sites with two different SI (20 m: black filled; 30 m: white filled).

Discussion

Bringing existing longleaf pine stands under management and restoring longleaf pine stands from degraded or otherwise converted forest stands is a priority for a number of land management entities in the southeastern U.S. (Johnson and Gjerstad 2006; Outcalt and Brockway 2010). Managers undertaking these tasks must have information about the response of growth and stand structure under alternative silvicultural scenarios. Growth and yield systems which incorporate long-term data from stands on a variety of sites and under a range of management regimes provide one of the best tools for exploring the possible outcomes of proposed management regimes. While a number of models predicting elements of longleaf pine plantation stand dynamics have been produced (Farrar 1973; Lohrey and Bailey 1977; Boyer 1980; Brooks and Jack 2006; VanderShaaf 2010), this study represents, to our knowledge, the first comprehensive stand-level growth and yield model for longleaf pine plantations, including stand growth and merchantable volume estimations, that can be applied to plantations across a wide range of ages (from 7 to 73 years) and site quality (SI ranging from 20 to 29 m).

All choices of model structure involve compromise. Whole-stand-level models, like the ones presented here, provide reliable predictions of stand variables, such as BA and N; on the other hand, they do not provide the level of detail that individual-tree-level models produce, which allow for more flexibility in modeling silvicultural practices. However, individual-tree models typically are unreliable in the prediction of cumulated stand information and often have issues with propagation of errors. In this study, we opted to fit a stand-level model to be used as a baseline, and in future work, we will consider incorporating individual-tree-level information.

Site index is the most widely used measure of forest productivity, particularly in plantations. Base age selection for SI can have significant implications for the accuracy of estimations, as bias increases as the stand age is further from the base age (Weiskittel et al. 2011). For this study we decided to set SI at age 50 year, a widely used reference age in the region (Farrar 1973; Lohrey and Bailey 1977; Lauer and Kush 2011). The H_{dom} model reported in this study, which behaved well for a wide range of stand ages, performed similar or slightly better than the models reported by Farrar (1973) and Brooks and Jack (2006). However, larger bias using the Brooks and Jack (2006) model could be a result of applying their equation out of the age range and geographic zone of inference, as it was fitted using stands located in southwest Georgia between the ages of two and 19 years. Dominant height is a major component of yield prediction systems for southern pine plantations. The anamorphic model obtained by this study seems suitable for H_{dom} estimations in the Western Gulf Coastal Plain, U.S.

In relation to the survival equations, the best model fitted was dependent on stand age and dominant height (a measure of site quality). Other models also incorporate the effect of site quality on survival, such as the models reported by Lauer and Kush (2011) and Farrar and Matney (1994) for naturally-regenerated longleaf pine stands, or the models reported for related southern pine species *P. elliottii* (Pienaar and Rheney 1993) and *P. taeda* (Clutter et al. 1984; Harrison and Borders, 1996). A model that was only dependent on stand age, similar to that reported by Brooks and Jack (2006) or Pienaar et al. (1996), was also fitted, but even though the resulting equation did perform well across all stands included in this study, the final model selected had a slightly better fit (data not shown) and at the same time allows the inclusion of the effect of site quality (reflected

in H_{dom}) on resource competition. The larger the SI (and hence H_{dom}), the larger the mortality rate after canopy closure. This process of accelerated self-thinning has been well documented for southern pines (Bailey et al. 1985; Dean and Jokela 1992; Zhao et al. 2007; Samuelson et al. 2008; Jokela et al. 2010). For example, 25-year-old *P. elliottii* and *P. taeda* stands in fertilized plots (with higher SI) had a cumulative mortality of about 59% and 43%, respectively, while non-fertilized plots showed lower mortality of about 43% and 22%, respectively (Jokela et al. 2010). Murphy and Farrar (1988) reported that models that include H_{dom} performed better than models that rely only on stand age to project survival, especially on prepared sites.

Other models that included SI (Diéguez-Aranda et al. 2005 and 2006; Zhao et al. 2007; Burkhart and Tomé 2012) were also tested, but H_{dom} was selected due to better predictive ability. An attempt was made to model survival as a two-step modeling approach (Zhao et al. 2007), including an equation to predict the probability of survival of all trees in the stand over a measurement interval, but no improvement was observed. The model presented in this study performed similar to, or slightly better, than other reported models to estimate future survival, but performance can be influenced by the fact that even though the validation plots were independent of the plots used for model fitting they were located in the same geographic region. Nevertheless, the model of Lohrey and Bailey (1977) was fitted with a subset of the same dataset used for this study, but perhaps the lower range of ages and N in their dataset influenced the results presented here. On the other hand, the model of Lauer and Kush (2011) performed well across different combinations of stand density and productivity in this study. Residual analysis for each model did not indicate any unusual trends, even though the stands cover a wide range of productivity, planting density and age. The models obtained by this study appear suitable for survival estimations within the Western Gulf Coastal Plain U.S.

The model that predicts BA for unthinned stands was only dependent on N and H_{dom}. Other models reported for southern pine species include other simple or composite variables such as SI, Age, N/Age and H_{dom}/Age as well. In this study, all of these variables were significant and could be included in the model, but the high multicollinearity between variables indicated the need to drop them from the final model. Therefore, it was decided to discard those variables, obtaining a simpler model to predict BA for unthinned longleaf pine stands with similar goodness-of-fit which avoided over-fitting problems. Widely used models for other southern pines (Harrison and Borders 1996; Pienaar et al. 1996) and for longleaf pine (Lauer and Kush 2011) include other stand variables to predict BA, but the existing publications contain no information regarding multicollinearity. The model that projected BA reported in this study had the same structure of the model reported by Brooks and Jack (2006).

In the case of thinned stands, the use of the approach proposed by Pienaar (1979, 1995), that uses CI and the basal area of the unthinned counterpart, fitted the available data well and allowed the estimation of BA growth after thinning. Modified versions of the model were also evaluated, which included H_{dom} or SI as dependent variables to modify the rate of decline of CI as stands age after thinning, but none of those variables were significant in the model (data not shown) and the final model that estimated the decline of CI as stand age after thinning was only dependent on stand age. For 25- and 50-year-old stands, the mean value of the annual rate of decline of the CI as the stand ages after thinning was 6.2% and 3.1%, respectively, reflecting the impact of stand age on the rate of decline of CI after thinning. The rate of decline in CI at age 50 years is lower than values

reported for other southern pine species. For example, Pienaar (1995) and Harrison and Borders (1996) reported values of 9.3% and 7.6% for *P. elliottii* and *P. taeda*, respectively. The dataset used in this study included plots thinned at ages ranging from 17 to 63 years, and measured, on average, for about 20 years. The slope of the relationship between observed and predicted BA after thinning was not different from 1, supporting the robustness of the model that projects BA growth for thinned stands.

The models that predict VOL (outside and inside bark) did not depend on stand age or N, and were similar or slightly better than other models reported for longleaf plantations (Lohrey and Bailey 1977; Brooks and Jack 2006) or naturally-regenerated stands (Lauer and Kush 2011). In this study, variables that showed high levels of multicollinearity were dropped to obtain a parsimonious final model that was only dependent on BA and H_{dom} and provided good prediction ability. The residuals of this model showed a tendency toward under-estimation for observed VOL_{OB} greater than 600 m^3 ha^{-1}, a condition which is rare in longleaf plantations which typically include multiple thinnings (Lohrey and Bailey 1977; Beers and Bailey 1985; Farrar and Boyer 1991; Jack et al. 2006). Nevertheless, the maximum residual found was less than 8% of the observed value, with residuals centered near zero at different age classes. For the dataset used for validation, the models reported by Brooks and Jack (2006) and Lohrey and Bailey (1977) showed very good prediction ability only for stands up to 25 years of age. This may be explained by the fact that the former was developed for stands younger than 20 years of age and the latter included a reduced range of ages and site quality as compared with the dataset used in the present study. This indicates that the new data used here expanded the ability to accurately predict stand volume if compared with the model of Lohrey and Bailey (1977).

One of the most important contributions of the system of equations presented in this study, in contrast to other longleaf models published, is the inclusion of the merchantable volume yield breakdown model. Similar to *P. elliottii* and *P. taeda*, it is now possible to estimate the merchantable volume for different combinations of threshold dbh and top diameter for longleaf pine stands by using equation 8. Although the model presented in this study made similar predictions to some models currently used for *P. elliottii* and *P. taeda*, differences in diameter distribution between species could explain the disagreements observed in merchantable volume yield breakdown, especially in chip-and-saw and pulpwood products.

The overall evaluation, where N, H_{dom}, BA and VOL_{OB} were calculated for all unthinned plots using the system of equations shown in Table 12.3 starting with a known initial age, N and SI (reported at first measurement), demonstrates the robustness of the model. As was expected, errors tended to increase as the length of simulations increased, but overall, the residuals centered on zero. Even though the number of observations was not balanced across simulation length classes, a fact that may explain the bias found for simulation lengths greater than 40 years, the results indicate that we can expect accurate estimations for simulation lengths of up to 40 years. Therefore, it is recommended that users update their stand inventories at least every 30–40 years in order to improve the predictions from the models presented here.

Despite the fact that the model system performed very well for the dataset used for validation, the functioning of the model outside the geographical range of the fitting data is uncertain. We strongly recommend using this system of equations only within the range of data used to fit the equations

(see Tables 12.1 and 12.2). In addition, the model does not include the effects of genetics, site preparation, weed control and fertilization. Nevertheless, the system presented here provides an important new tool that is used in Chapter 14 for supporting present and future longleaf pine management decisions. Future research expanding the area of inference and including the effects of genetically improved material and intensive silvicultural management is needed to improve the predictive ability of the model and to address 21st century forest management approaches.

13. Predicting Understory Plant Biomass Dynamics of Prescribed Burned Longleaf Pine Stands

Introduction

Longleaf pine (*Pinus palustris* Mill.) forests harbor a diverse community of plant species in the ground cover layer, with as many as 40 species per square meter (Peet and Allard 1993). Therefore models of longleaf pine C dynamics must include understory dynamics. This Chapter develops understory predictive equations that are used in the LLM-EA simulation described in Chapter 14. High plant diversity of the ground cover layer is maintained by frequent fire and an open discontinuous tree canopy (Glitzenstein et al. 1995). Prescribed burning is an important management tool in longleaf forests, with recommended burning frequencies of at least once per 10 years but ideally, in many cases, every two to four years (Chapman 1932; Glitzenstein et al. 2003; Loudermilk et al. 2011). The benefits of periodic prescribed fire in longleaf pine ecosystems include not only restoration of diverse native plant communities, but also seedbed preparation for longleaf seed germination and control of fuel quantity and quality, which affects fire intensity (Brockway et al. 2006; Harrington 2011) and thus plant community structure (Hiers et al. 2007). Without frequent fire, longleaf ecosystems become susceptible to woody plant encroachment and may transition to hardwood dominated forests (Quaterman and Keever 1962, Hartnett and Krofta 1989).

Ground cover biomass has been shown to be linearly related to ground cover species richness and proportional to stand productivity in longleaf pine-wiregrass systems (Kirkman et al. 2001). Similarly, Brockway and Lewis (1997) demonstrated that recurrent fire over four decades increased ground cover diversity and the standing biomass of grasses and all forbs relative to less frequent burn intervals in a flatwoods longleaf pine-wiregrass ecosystem (Brockway and Lewis 1997). In addition, the contribution of the ground cover layer to annual net primary productivity may be significant (Mitchell et al. 1999) and important in assessment of carbon stocks in low density stands (Samuelson et al. 2014). While fire volatilizes carbon, the immediate loss of plant carbon may not constitute a long-term loss in carbon stocks because of understory growth following fire.

Relationships between the forest understory and overstory offer a useful framework to understand the impact of forest management on species and community distribution and productivity. Management activities such as thinning and prescribed burning will alter those relationships. For example, thinning will reduce the number of trees and hence the basal area and leaf area index of the overstory, thereby altering the environment for ground cover species, and fire will directly affect the composition and biomass of the ground cover layer. Longleaf pine has wide ecological amplitude (Figure 13.1) and ground cover biomass across the species range varies not only with fire interval and stand structure but also soils, climate, management history and native vegetation (Hiers et al. 2003; Scott and Burgan 2005). However, models for prediction of ground cover biomass, and hence fuel load, are scarce and only provide coarse scale estimates (Scott and Burgan

2005; Ottmar et al. 2009) or are restricted on accuracy and geographical extrapolation (Parresol et al. 2012).

In this study we analyzed the dynamics of ground cover understory biomass of longleaf pine stands with varying stand structure and fire management history in stands located in Georgia, Louisiana and North Carolina (Figure 13.1). The objectives of the study were: 1) develop models to estimate ground cover biomass for unburned and burned longleaf pine stands, 2) develop models to estimate ground cover biomass partitioning into woody and herbaceous plants, and 3) assess the impact of stand density and prescribed fire frequency on ground cover biomass dynamics.
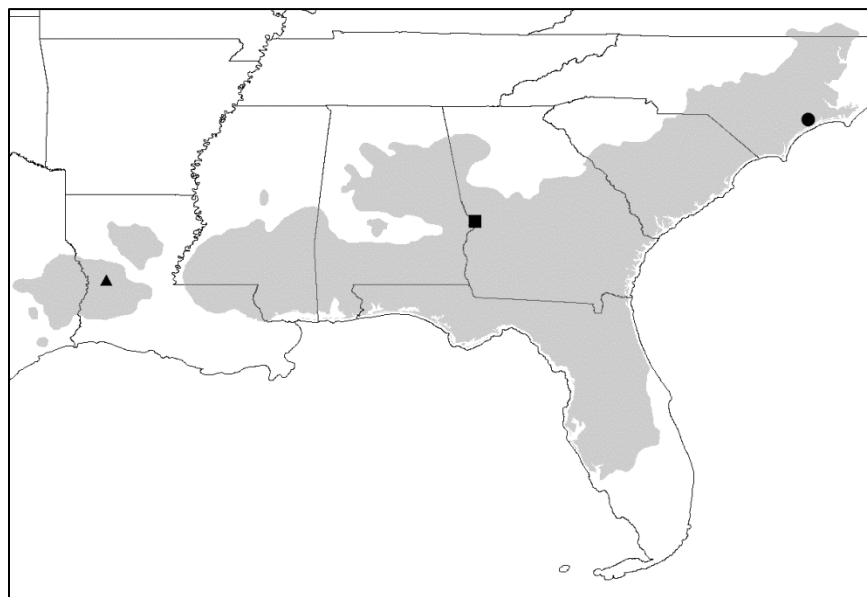
Figure 13.1. Location of the sampling sites in US Army Fort Polk/Kisatchie National Forest in Louisiana (triangle), US Army Fort Benning in Georgia (square), and Marine Corps Base Camp Lejeune in North Carolina (circle) within the species natural distribution range (shaded area).

Materials and Methods

Ground cover biomass for unburned stands

Ground cover biomass (GC_B) in all cases is defined as all live and dead plants < 1 m in height. Because the majority of reports in the literature are for burned longleaf pine stands, we included

data from two other southern pine species, loblolly pine (*Pinus taeda* L.), and slash pine (*Pinus elliottii* Engelm.), in modeling the dynamics of GC_B under unburned conditions (Bracho et al. 2012; Clark et al. 2004; Gholz and Fisher 1982; Haywood and Grelen 2000; Kush et al. 1999; Neary et al. 1990; Subedi 2013; Vogel et al. 1990). In all reports GC_B was measured using clip plots (0.2 m^2 to 4.0 m^2) located randomly within a stand. The number of clip plots ranged between 4 and 20 for each site.

For the stands without periodic prescribed burning, GC_B was correlated to overstory basal area (BA, m^2 ha^{-1}) and stand age (years). After testing several equations, the model selected was:

$$GC_B = a_1 \cdot \exp^{(-a_2 \cdot BA)} + \varepsilon_1 \qquad\qquad [1]$$

where a_1 and a_2 are curve fit parameter estimates, exp is base of natural logarithm and ε_1 is the error term, with $\varepsilon_1 \sim N(0, \sigma_1^2)$. Stand age was not a significant factor in the model.

Ground cover biomass for burned stands

In order to estimate GC_B for longleaf pine stands subjected to periodic prescribed burning, a biomass consumption recovery function was fitted using data from the Fire and Environmental Research Applications Team (FERA, http://depts.washington.edu/nwfire/dps/). The dataset consisted of B_{GC} sampled in seven stands in the sandhills and eight stands in the flatwoods (a et al. 2000 and 2003). In addition, two plots from one experimental site in Alabama (Kush et al. 1999) and two plots from one experimental site in Louisiana (Haywood 2011) were included into the dataset. Stands ranged in time since last prescribed fire (TSF) from 1 to 23 years and in pine BA from 1.5 to 24.6 m^2 ha^{-1}. For each report, all data were expressed as a fraction of the GC_B of the unburned condition. For stands reported by Ottmar et al. (2000 and 2003a), the average GC_B at TSF=20 years was assumed to be the unburned condition that had a value=1. Assuming an asymptotic response within the range of fire intervals under consideration, a sigmoidal model was fit to data of GC_B recovery after fire (recGC_B, the proportion of ground cover biomass on burned stands relative to initial unburned biomass), and TSF:

$$recGC_B = \frac{1}{1+b_1 \cdot \exp^{(-b_2 \cdot TSF)}} + \varepsilon_2 \qquad\qquad [2]$$

where b_1 and b_2 are curve fit parameter estimates, exp is base of natural logarithm and ε_2 is the error term, with $\varepsilon_2 \sim N(0, \sigma_2^2)$.

For stands with periodic prescribed burning, the partitioning of GC_B into herbaceous and woody components was analyzed using data collected from longleaf pine stands located on US Army Fort Benning Georgia (GA), US Army Fort Polk/Kisatchie National Forest Louisiana (LA) and Marine Corps Base Camp Lejeune North Carolina (NC) (Figure 13.1). Data were collected from five stands in GA in 2012, 14 stands in LA in 2013, and 9 stands in NC in 2014.

Stands encompassed a range in soil drainage classes (https://soilseries.sc.egov.usda.gov/), age, forest structure and TSF at the time of sampling. The herbaceous layer in GA stands was dominated by graminoids such as *Andropogon* spp. and *Schizachyrium scoparium* (Michx.) Nash, herbaceous species such as *Desmodium* spp., and *Lespedeza* spp., and composites such as *Eupatorium* spp., and *Solidago* spp. (Knapp et al. 2011). In LA stands, ground cover was dominated by *Schizachyrium* spp., *Panicum* spp., and *Dichanthelium* spp. (Haywood and Harris, 1999). The herbaceous ground layer in NC stands consisted of *Aristida* spp., *Andropogon* spp., *Schizachyrium* spp., *Panicum* spp,, *Dichanthelium* spp.), and *Rhynchospora* spp. (Knapp et al. 2008). Woody ground cover (< 1 m in height) in GA stands was dominated by *Ilex glabra*, *Rubus cuneifolius* and *Quercus* spp. (Dale et al. 2002). In LA stands, woody ground cover was dominated by *Ilex vomitoria*, *Vaccinium* spp., *Myrica cerifera* and *Gaylussacia* spp. (Scott, 2014). The woody ground cover in NC stands was dominated by *Ilex* spp. and *Cyanococcus* spp. (Hu, 2012). All stands were even-aged and planted, with the exception of the 64 and 87-year-old stands in GA and the 65 and 79-year-old stands in NC which were even-aged but naturally regenerated. Data from GA were previously reported by Samuelson et al. (2014). Stands ranged in age from 5 to 87 years, in BA from 0.1 to 31.5 m^2 ha^{-1} and in TSF from 1 to 4 years. In each stand, ground cover samples were collected over the last week of May and first week of June from five to ten 1 m^2 sample rings in each of four 0.04 ha circular subplots established in a stand, following Samuelson et al. (2014). All vascular plants (including dead and living shrubs and herbaceous plants) < 1 m in height were clipped at the root collar. Biomass was oven-dried at 70°C for 72 hours and weighed and classified as GC_{B-LW} (living woody plants including vines), GC_{B-LH} (living forbs, ferns, graminoids and legumes), and GC_{B-Dead} (all dead material pooled).

Models to estimate GC_B partitioning into woody and herbaceous ground cover biomass were fitted using the ratios of living herbaceous to GC_B (LHp: GC_{B-LH} / GC_B) and living woody to total GC_B (LWp: GC_{B-LW} / GC_B). The proportion of dead ground cover to GC_B (Dp: GC_{B-Dead} / GC_B) was calculated as Dp = 1 - LHp - LWp. The variables considered as possible covariates were TSF, BA, SI (site index at base age 50 years) and stand age. In order to test which variables should be included in the final model, a logarithmic transformation of the response variable was carried out and a stepwise procedure was used. A threshold significance value of 0.15 and 0.05 was used for variable selection criteria for a variable to enter and stay, respectively; and the variance inflation factor (VIF) was monitored to detect multicollinearity among explanatory variables. Variables included in the model with VIF larger than 5 were discarded, as suggested by Neter et al. (1996). After testing several non-linear equations, the models selected were:

$$LHp = c_1 \cdot (TSF^{c_2}) \cdot (BA^{c_3}) \cdot (age^{c_4}) + \varepsilon_3 \qquad [3]$$

where c_1 to c_4 are curve fit parameter estimates and ε_3 is the error term, with $\varepsilon_3 \sim N(0, \sigma_3^2)$.

$$LWp = \frac{1}{1 + d_1 \cdot \exp^{(d_2 \cdot \ln(TSF) + d_3 \cdot \ln(BA))}} + \varepsilon_4 \qquad [4]$$

where d_1 to d_3 are curve fit parameter estimates and ε_4 is the error term, with $\varepsilon_4 \sim N(0, \sigma_4^2)$.

Comparison against published models

The results from the combination of equations to predict GC_{B-LH} (equations 1, 2 and 3) and GC_{B-LW} (equations 1, 2 and 4) were compared against the models reported by Parresol et al. (2012). The authors presented equations to estimate separately ground cover living biomass in seedlings, shrubs and vines (grouped as GC_{B-LW}), as well as grasses and forbs (grouped as GC_{B-LH}).

Model fitting and evaluation

All statistical analyses were performed using non-linear model fitting in SAS 9.3 (SAS Inc., Cary, NC, USA). The predictive ability of equations 1, 3 and 4 was evaluated by using leave-one-out cross-validation (Neter et al. 1996). An overall validation of the models was also carried out using data shown in Table 13.2. For each stand, of known TSF, BA and stand age, we used equations 1 to 4 to estimate ground cover biomass. Estimated GC_{B-Dead} was computed as the difference between estimated GC_B and estimated $(GC_{B-LW} + GC_{B-LH})$. We recognize that there is a lack of independency for the overall validation, as data used for validation was also used to fit the models to estimate LHp and LWp, but the estimations of GC_B, $recGC_B$, that are the basis to estimate GC_{B-LW}, GC_{B-LH} and GC_{B-Dead}, are completely independent and provide a robust basis for validation.

Three measures of accuracy were used to evaluate the "goodness of fit" between observed and predicted (simulated) values for each variable from the dataset obtained in the model validation: (i) Root mean square error (RMSE); (ii) Mean bias error (Bias); and (iii) coefficient of determination (R^2). As non-linear model fitting was carried out, an empirical R^2 (Myers 2000) was determined as:

$$R^2 = 1 - \frac{SSE/df_e}{SST/df_t} \qquad [5]$$

where SSE and SST are the sum of squares of residuals and total, respectively, and df_e and df_t are the degrees of freedom of error and total, respectively. Paired t-tests were conducted to compare estimates against reported models.

Modelling the effect of prescribed burning on GC_B

The effect of prescribed burning on GC_B was computed using the consumption standards reported by Reinhardt (2003) and Ottmar et al. (2006), where consumption factors of 0.93 and 0.85 were assumed for herbaceous and woody ground cover, respectively. The growth and yield model reported by Gonzalez-Benecke et al. (2012b) was used to simulate stand dynamics in BA. Initial parameters assumed were: Age = 40 years; SI = 23 m, stand density = 250 trees ha^{-1}; BA = 16.5 m^2 ha^{-1}. Four burning frequencies were tested: 1, 3, 5 and unburned. The model was run for 10 years.

Results

Model fitting

The model parameter estimates for the selected functions to estimate ground cover biomass, ground cover biomass recovery after fire, ratio of living herbaceous to total GC_B and ratio of living woody to total GC_B are reported in Table 13.1. All parameter estimates were significant at $P < 0.05$, and all models showed $R^2 > 0.83$. The model selected to predict LHp depended on TSF, BA and stand age. On average, as TSF and BA increased, LHp decreased (negative sign of parameter estimates for TSF and BA). Older stands with the same TSF and BA had larger LHp (positive sign of parameter estimates for stand age).   The model selected to predict LWp depended only on stand BA and TSF. On average, as TSF and BA increased, LWp decreased.

Figure 13.2 shows the relationships between BA and GC_B for southern pine stands without periodic prescribed burning. As BA increased, GC_B of unburned stands decreased, and, on average, GC_B was 6 Mg ha^{-1} after the first year (BA < 1 m^2 ha^{-1}) and 2.4 Mg ha^{-1} at a BA of 20 m^2 ha^{-1}.
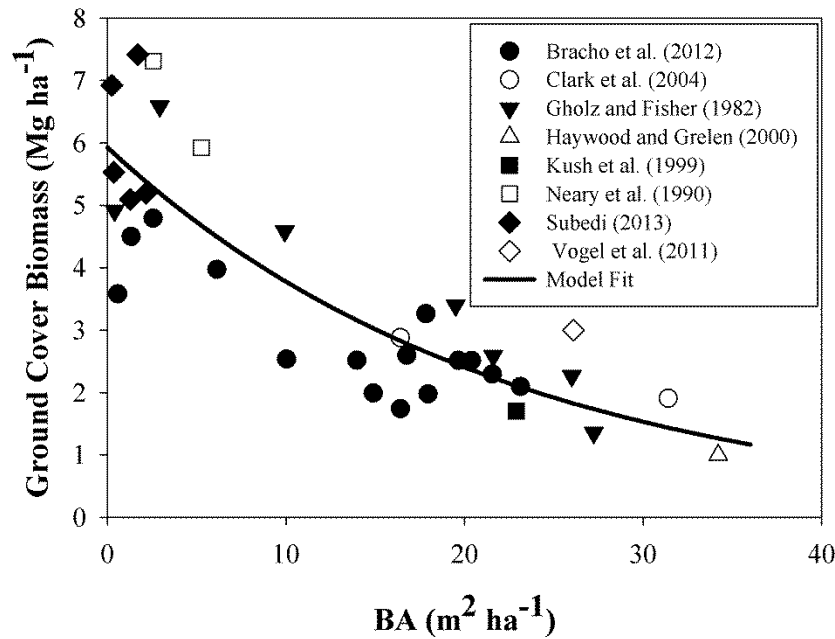
Figure 13.2. Relationship between overstory basal area (BA) and ground cover biomass (GC_B) for southern pine stands without periodic prescribed burning.

Table 13.1. Parameter estimates and fit statistics of the selected functions to estimate GC_B, $recGC_B$, LHp and LWp for longleaf pine stands growing in southeastern U.S.

Variable	Model	Parameter	Parameter Estimate	SE	n	R^2	RMSE	CV%
GC_B	$= a_1 \cdot \exp^{(-a_2 \cdot BA)}$	a_1	5.9272	0.3288	35	0.942	0.986	26.8
		a_2	0.0451	0.0061				
$recGC_B$	$= \dfrac{1}{1 + b_1 \cdot \exp^{(-b_2 \cdot TSF)}}$	b_1	14.2946	8.5931	14	0.967	0.131	20.1
		b_2	1.2124	0.2615				
LHp	$= c_1 \cdot (TSF^{c_2}) \cdot (BA^{c_3}) \cdot (age^{c_4})$	c_1	0.3416	0.1399	28	0.832	0.139	49.4
		c_2	-1.1361	0.2376				
		c_3	-0.4461	0.1604				
		c_4	0.4316	0.1748				
LWp	$= \dfrac{1}{1 + d_1 \cdot \exp^{(d_2 \cdot \ln(TSF) + d_3 \cdot \ln(BA))}}$	d_1	118.6	12.7600	28	0.850	0.175	50.4
		d_2	-2.4413	0.6345				
		d_3	-0.8725	0.3541				

Notes for Table 13.1: GC_B is the biomass of the ground cover vegetation (Mg ha^{-1}); $recB_{GC-W}$ is the recovery rate after fire of woody dominated ground cover biomass (unitless); LHp is the ratio of living herbaceous to GC_B; LWp is the ratio of living woody to GC_B; Age is stand age (years); BA is stand basal area (m^2 ha^{-1}); TSF is time since last prescribed fire (years); SE is standard error, n is number of observations; R^2 is coefficient of correlation; RMSE is root of mean square error ;CV% coefficient of variation (percentage).

Figure 13.3 shows the mean values of fractional GC_B for varying TSF for the 28 stands in GA, LA and NC. The proportion of woody and herbaceous ground cover biomass changed depending on the number of years since last fire. For example, on average, one year after prescribed fire (TSF=1), living herbaceous and living woody ground cover biomass represented 25% and 45% of GC_B, respectively. Four years after prescribed fire (TSF=4), living herbaceous and living woody ground cover biomass represented 79% and 10% of GC_B, respectively (Figure 13.4).
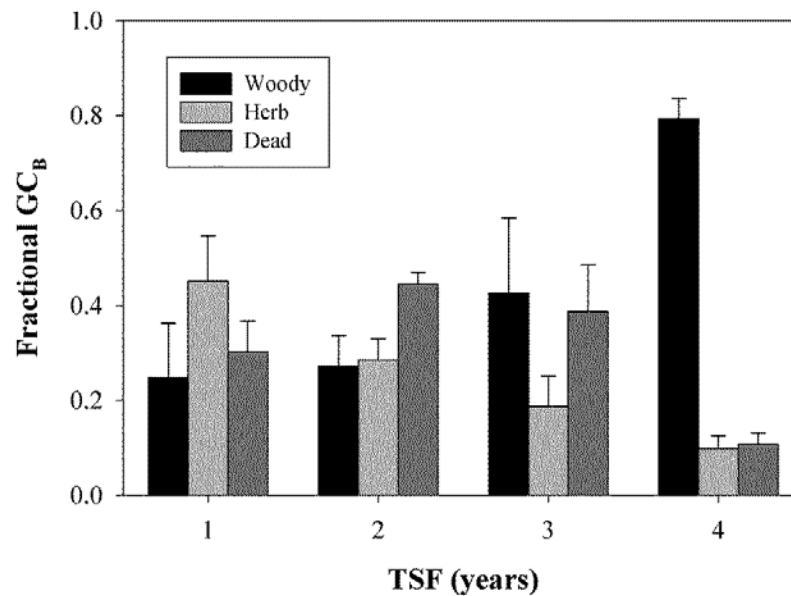
Figure 13.3. Fractional ground cover biomass (GC_B) in woody, herbaceous and dead pools in response to time since last prescribed fire (TSF).

Initially, we fit the model for $recGC_B$ separately for each type of site (not shown). After pooling all data, a single model was finally selected due to no further improvement using separate models. Figure 13.4 shows the relationship between TSF and $recGC_B$ for all sites. On average, after one and four years since prescribed fire, ground cover recovered 19 and 90% of the pre-fire biomass, respectively.
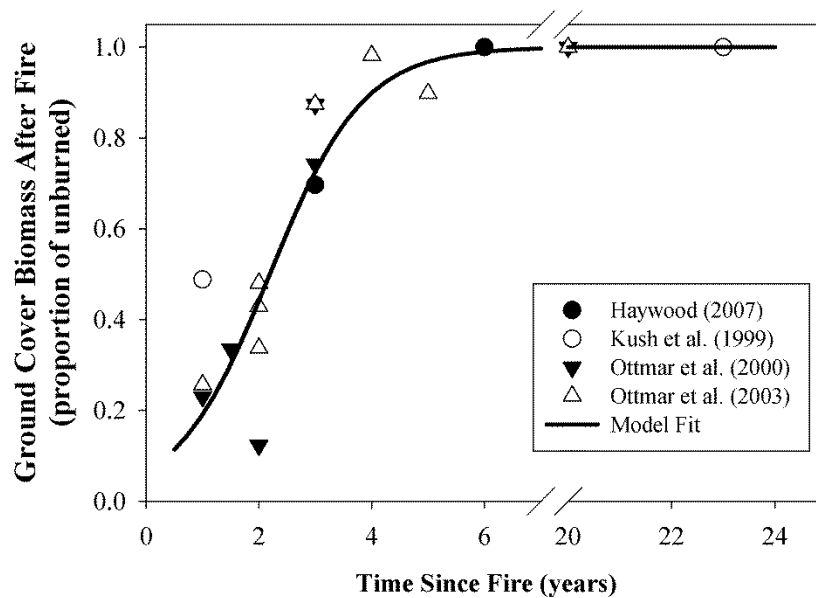
Figure 13.4. Model fit to estimate ground cover biomass recovery from time since last prescribed fire (TSF) after fire as a proportion of initial biomass.

Model validation

Figure 13.5 shows the dynamics of observed and predicted LHp and LWp for TSF ranging between 1 and 4 years. There was a good correlation between observed and predicted LHp and LWp across all stands. As TSF increased, LHp decreased and LWp increased. The models captured most of the variability observed at different TSF. The inclusion of BA and stand age as co-variables allowed the models to capture more variability of LHp (Figure 13.5a) and LWp (Figure 13.5b) for any given value of TSF, thus improving the agreement between observed and predicted values.

There was a good agreement between observed and predicted values of ground cover biomass for the 28 stands measured in GA, LA and NC. Even though predicted and observed values were moderately correlated for GC_{B-LW} and GC_{B-LH}, bias was smaller than 13%. Larger error, but high correlation, was observed for GC_{B-Dead} estimations, with a mean absolute bias of about 0.13 Mg ha^{-1} (Table 13.2).
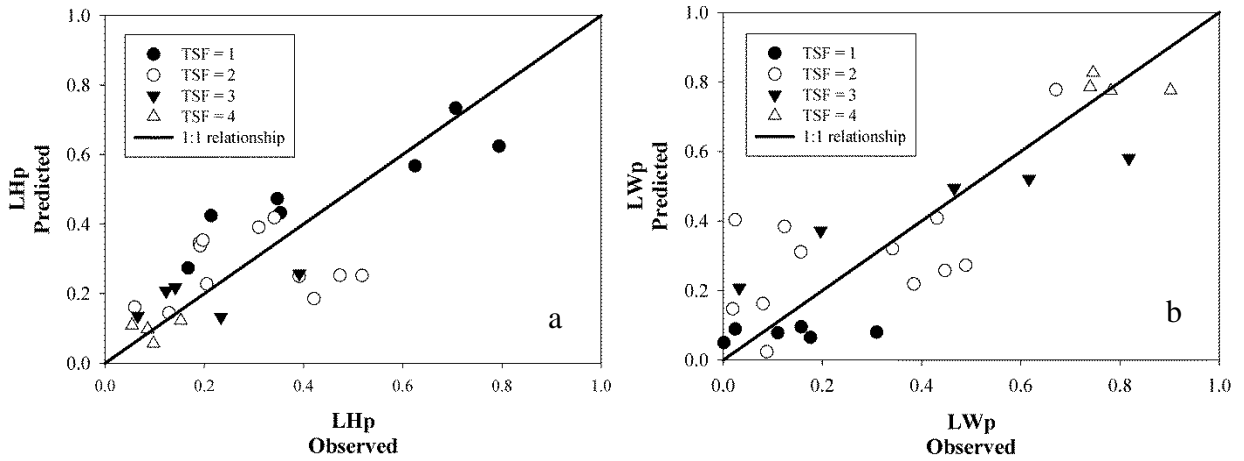
Figure 13.5. Relationship between observed and predicted a) ratio of living herbaceous (LHp) and b) ratio of living woody (LWp) to total ground cover biomass for different time since last prescribed fire (TSF) for longleaf pine stands in Georgia, Louisiana and North Carolina.

Table 13.2. Summary of model evaluation statistics for unburned southern pines and burned longleaf pine stands in Georgia, Louisiana and North Carolina.

Type of Validation	Variable	$\bar{P}$	$\bar{O}$	n	RMSE	Bias	R^2
leave-one-out cross-validation	GC$_B$ *	4.05	4.02	27	1.07 (26.6)	-0.03 (-0.7)	0.63
	GC$_{B\text{-}LW}$	0.30	0.28	28	0.21 (75.1)	-0.018 (-6.4)	0.81
	GC$_{B\text{-}LH}$	0.35	0.35	28	0.19 (53.7)	-0.0006 (-0.2)	0.59
Overall	GC$_B$ [†]	1.63	1.39	28	0.60 (43.3)	0.24 (17.1)	0.65
	GC$_{B\text{-}LW}$ [‡]	0.58	0.51	28	0.40 (78.7)	0.07 (13.0)	0.48
	GC$_{B\text{-}LH}$ [§]	0.39	0.35	28	0.21 (60.4)	0.04 (12.3)	0.46
	GC$_{B\text{-}Dead}$ [‡]	0.66	0.53	28	0.32 (60.0)	0.13 (24.3)	0.71

Notes for Table 13.2: GC$_B$ is the total biomass of the ground cover vegetation (Mg ha^{-1}); GC$_{B\text{-}LW}$ is the biomass of living woody ground cover vegetation (Mg ha^{-1}); GC$_{B\text{-}LH}$ is the biomass of living herbaceous ground cover vegetation (Mg ha^{-1}); GC$_{B\text{-}Dead}$ is the biomass of dead ground cover vegetation (Mg ha^{-1}); $\bar{P}$ is the mean predicted value; $\bar{O}$ is the mean observed value; n is the number of observations; RMSE is the root of mean square error; Bias is the bias estimator; R^2 is the coefficient of determination. Values in parenthesis correspond to percentage to mean observed value. *: Using data for unburned southern pine stands shown in Table 13.1; [†]: Using functions 1 and 2; [‡]: Using functions 1, 2 and 3; [§]: Using functions 1, 2 and 4; [‡]: computed as the difference between estimated GC$_B$ and estimated (GC$_{B\text{-}LW}$ + GC$_{B\text{-}LH}$).

When calculations of ground cover biomass were based only on known BA, stand age and TSF (overall validation), there was good correlation between observed and predicted values for the 28 stands measured in GA, LA and NC (Figure 13.6). In all cases, the intercept of the relationship between observed and predicted values was not different from zero (P>0.29). The slope of that relationship was not different from 1 only for GC_{B-LW} (P=0.10) and GC_{B-LH} (P=0.08). Paired t-tests indicated no difference between observed and predicted values for GC_{B-LW} (P=0.13) and GC_{B-LH} (P=0.15), but differences for GC_B (P=0.01) and GC_{B-Dead} (P=0.02). For GC_B, GC_{B-LH} and GC_{B-Dead}, residuals were centered on zero, but for GC_{B-LW} the estimations were sensitive to TSF (Figure 13.6d).

Comparison against reported functions

Figure 13.7 shows the comparison between observed (black bars) and predicted living ground cover biomass using the models reported in this study (light gray bar) and the models reported by Parresol et al. (2012) (dark gray bar). There was a good agreement between observed and predicted values using the models reported in this study for stands with TSF<4 years. It is interesting to note that for our dataset, the estimates of GC_{B-LW} using the model of Parresol et al. (2012) were practically insensitive to changes in TSF (Figure 13.7a). Even though there was moderate correlation (R^2=0.37) between observed and predicted GC_{B-LW} using the model of Parresol et al. (2012), the estimates were underestimated by 37% (P=0.001). For GC_{B-LH} the correlation was nill (R^2=0.00), but there was no difference between observed and predicted values (P=0.25), possibly because overestimation when TSF≤2 was compensated with underestimation when TSF>2.

Effect of fire frequency and BA on ground cover biomass

The interactive effect of fire frequency and BA on herbaceous and woody ground cover biomass is shown in Figure 13.8. While TSF has little impact on GC_{B-LH}, BA has a major effect, reducing GC_{B-LH} as BA increased, from about 0.3-0.4 Mg ha^{-1} for a stand with BA=10 m^2 ha^{-1}, to around 0.1-0.2 Mg ha^{-1} for a stand with BA=35 m^2 ha^{-1}. On the other hand, an opposite effect was observed for GC_{B-LW}, where BA has little impact when TSF<3 and TSF has a major effect, reducing GC_{B-LW} as fire frequency increased (smaller TSF). For example, independent of BA, when TSF=1 GC_{B-LW} ranged between 0 to 0.5 Mg ha^{-1}; when TSF=2, GC_{B-LW} ranged between 0.5 to 1.0 Mg ha^{-1}. When TSF≥3 there was an interactive effect; both TSF and BA affected ground cover biomass. For example, for TSF=3, when BA was increased from 5 to 35 m^2 ha^{-1}, GC_{B-LW} was reduced from about 1.5 to around 1.0 Mg ha^{-1}. For TSF=5, when BA was increased from 5 to 35 m^2 ha^{-1}, GC_{B-LW} was reduced from about 3.0 to around 1.0 Mg ha^{-1}.
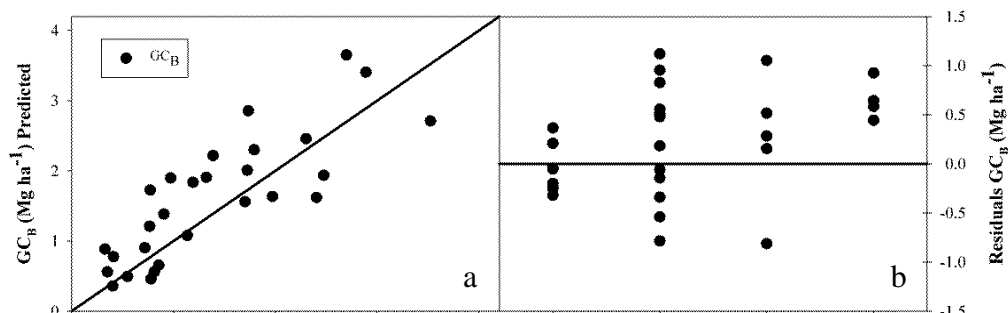
Figure 13.6. Overall simulation validation of total ground cover biomass (GC_B) (a, b), living woody biomass (GC_{B-LW}) (c, d), living herbaceous biomass (GC_{B-LH}) (e, f) and dead ground cover biomass (GC_{B-Dead}) (g, h), for longleaf pine stands in Georgia, Louisiana and North Carolina. Observed versus predicted (simulated) values (a, c, e, d) and residuals (predicted-observed) versus

time since last prescribed fire (TSF) (b, d, f, h). Solid line represents the 1-to-1 relationship. All calculations were based on known BA, stand age and TSF.
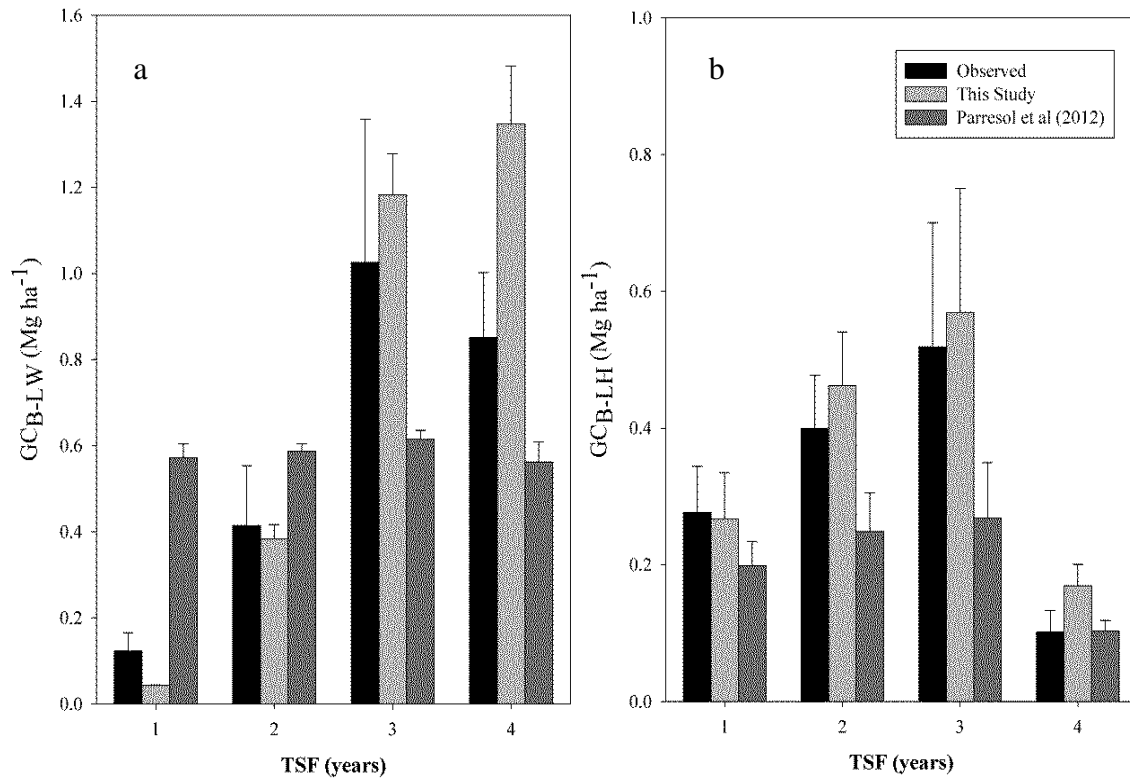
Figure 13.7. Comparison between mean observed (black bars) and predicted (gray bars) living woody (GC$_{B-LW}$, left panel) and herbaceous (GC$_{B-LH}$, right panel) ground cover biomass after last prescribed fire (TSF) for longleaf pine stands in Georgia, Louisiana and North Carolina.
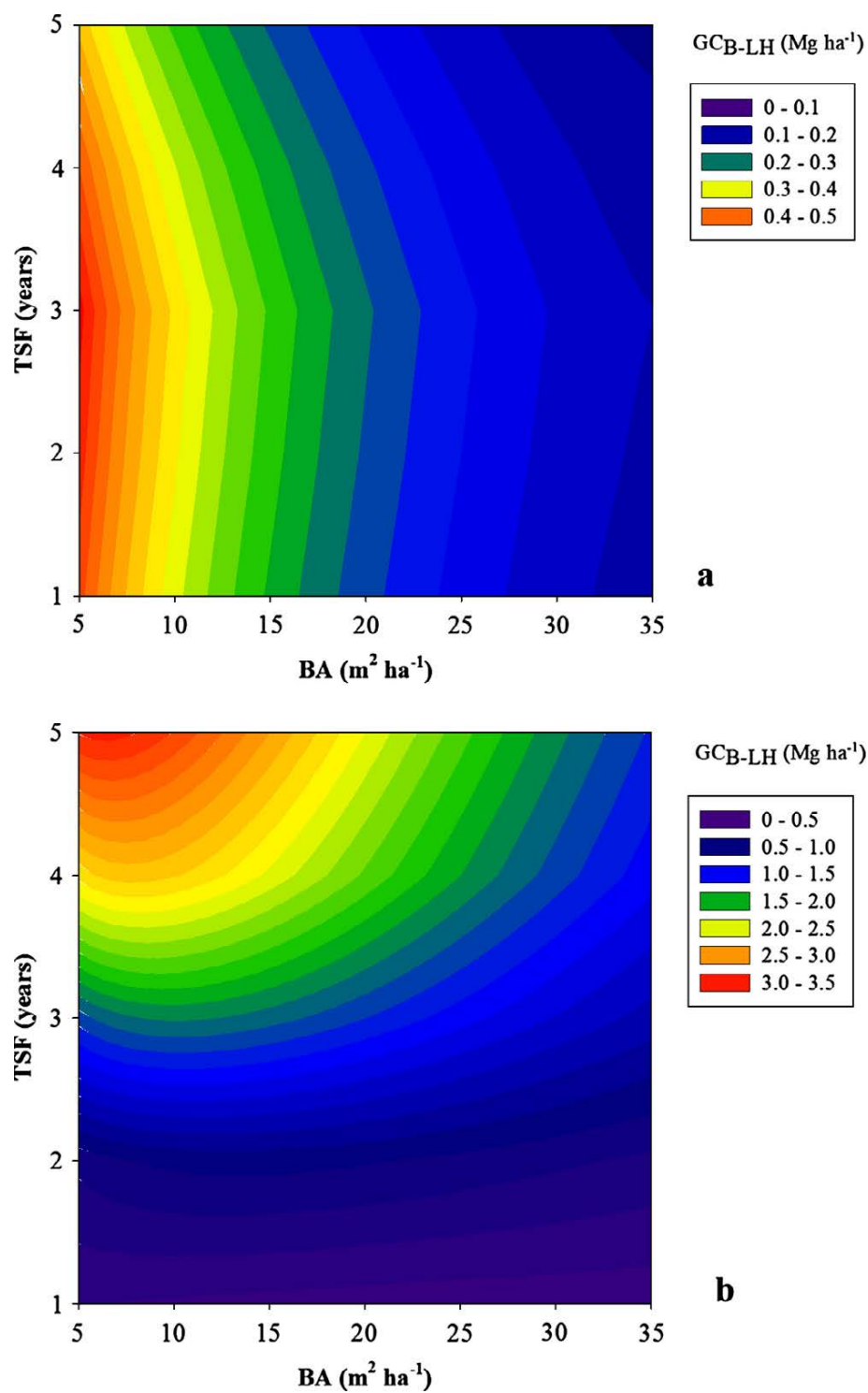
Figure 13.8. Effect of basal area (BA) and prescribed burning frequency (TSF) on a) living herbaceous (GC$_{B-LH}$) and b) living woody (GC$_{B-LW}$) ground cover biomass.

Modeling prescribed burning effect on ground cover biomass

Figure 13.9 shows the predicted dynamics of ground cover biomass for 40 to 50-year-old longleaf pine stands growing with different regimes of prescribed burning. Woody biomass was the component of ground cover most affected by prescribed burning. Assuming the stand was burned every year (rough= 1 year), GC_{B-LW} had a mean value of around 0.06 Mg ha^{-1} and GC_{B-LH} was maintained at about 0.24 Mg ha^{-1}. If the modeled stand was burned every 3 years (rough= 3 years), GC_{B-LW} reached around 1.1 Mg ha^{-1} at the time of the prescribed burning and GC_{B-LH} was maintained at about 0.25 Mg ha^{-1}. When the modeled stand was burned every 5 years (rough= 5 years), GC_B was similar to an unburned stand (around 2.4 Mg ha^{-1}), reaching GC_{B-LW} a mean value of around 1.9 Mg ha^{-1} at the time of the prescribed burning and maintaining GC_{B-LH} at about 0.24 Mg ha^{-1}.
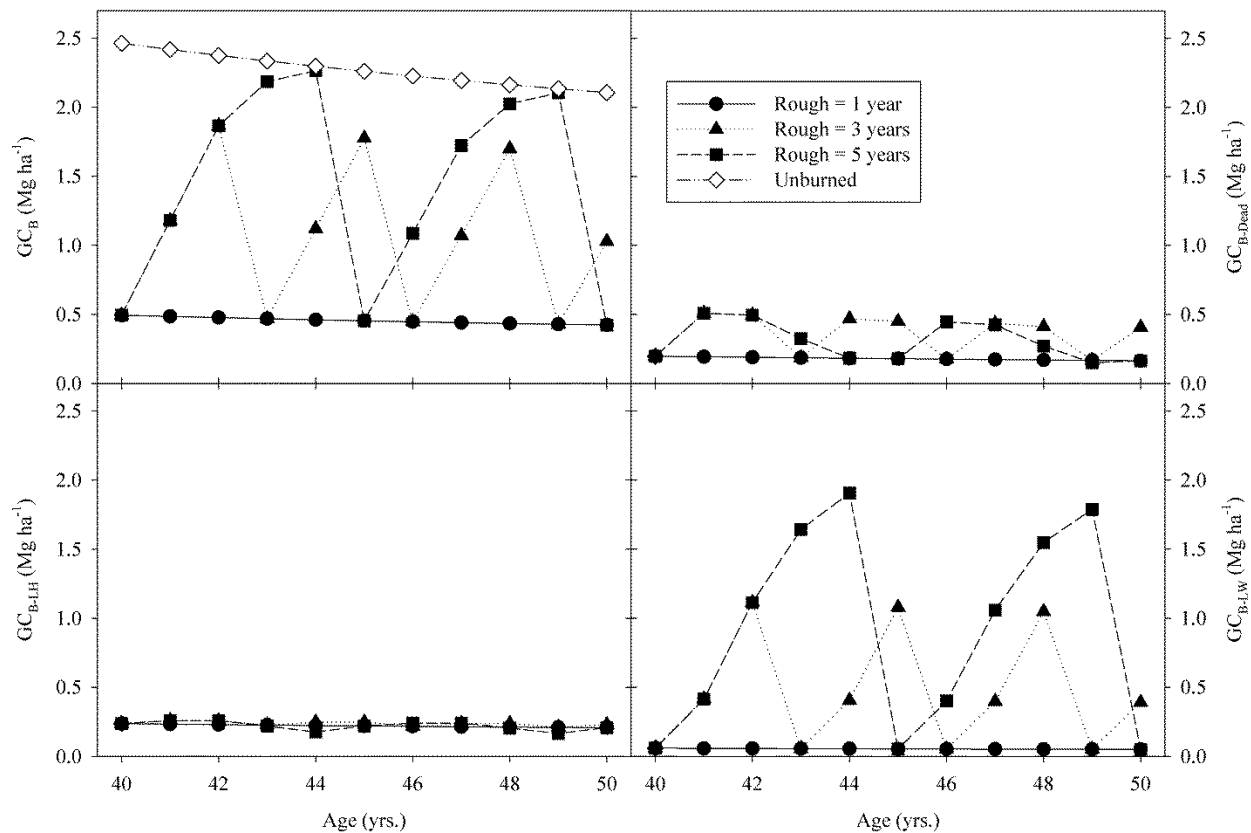
Figure 13.9. Simulated effect of prescribed burning frequency on a) total (GC_B), b) dead (GC_{B-Dead}), c) living herbaceous (GC_{B-LH}) and d) living woody (GC_{B-LW}) ground cover biomass. Prescribed burning was initiated at age 40 years with a frequency of 1 (filled circle), 3 (filled triangle), or 5 (filled square) years. In (a) GC_B for unburned stands is also shown (open diamond).

Discussion

Prescribed burning is the most important tool for managing understory density and species composition, and ground cover native plant diversity in longleaf pine forests (Brockway et al. 2006; Knapp et al. 2009; Haywood 2005). In general, prescribed burning will stimulate graminoid and forb abundance and reduce the growth of hardwood sprouts (Lewis and Harshbarger 1976; White et al. 1991; Heuberger and Putz 2003). The density of the ground cover layer is not only important for plant biodiversity conservation, but also for prescribed fire planning (Hiers et al. 2003; Wright 2013), wildlife habitat (Glitzenstein et al. 1995; Means 2006) and livestock management (Greene 1935; Wahlenberg et al. 1939). In addition, it is important to assess the impact of frequent prescribed fires on carbon dynamics to better understand the role of longleaf pine forests in forest carbon sequestration.

Our study focused on ground cover biomass rather than percentage cover, the most common reported metric of ground cover abundance and horizontal fuel continuity (Abrahamson and Abrahamson 1996; Brockway and Lewis 1997; Brockway and Outcalt 2005; Harrington 2011; Haywood 2011; Wright 2013). Ground cover biomass can reflect differences in community dominance and diversity (Guo and Rundel 1997; Chiaruccie et al. 1999) and has been shown to be positively related to ground cover species richness in some longleaf pine systems (Brockway and Lewis 1997; Kirkman et al. 2001).

We developed the models in this paper to estimate ground cover biomass for longleaf pine forests under varying stand age, basal area and fire management histories and, similar to Fernandes et al. (2006) and Parresol et al. (2012), we focused on models which used input information obtainable from simple inventories. The set of equations presented in this study provide a practical tool for researchers and land managers so they can analyze the impacts of varying management activities (thinning and burning frequency) on the dynamics of herbaceous and woody ground cover biomass. Our models are applicable for estimating fuel loading for fire simulation systems (Hiers et al. 2003; Ottmar et al. 2009; Wright 2013), to study interactions between wildlife habitat and prescribed fire (Means and Campbell 1982; Provencher et al. 2002), to study interactions between livestock (as pinewood cattle) and fire (Augustine and Milchunas, 2009; Albin 2014), and to account for biomass and carbon emissions for carbon balance models (Gonzalez-Benecke et al. 2010a, 2015a).

Our estimates of ground cover biomass of burned longleaf pine stands are within the range reported by other authors. For example, Parresol et al. (2012) reported mean values for woody and herbaceous ground cover biomass of about 0.56 and 0.21 Mg ha^{-1}, respectively, for stands growing in South Carolina with a burning frequency between 1 to 5 years. Our overall mean values were 0.58 and 0.35 Mg ha^{-1}, respectively. For stands growing in South Carolina, Glitzenstein et al. (2003) reported mean values for GC_{B-LW} of about 0.2, 0.4 and 0.8 Mg ha^{-1}, for stands with TSF of 1, 2 and 3 years, respectively. For the same TSF, our overall mean values were 0.15, 0.4 and 1.0 Mg ha^{-1}, respectively. The same authors also reported mean GC_{B-LH} of 0.45, 0.35 and 0.20 Mg ha^{-1} for stands with TSF of 1, 2 and 3 years, respectively. Kirkman et al. (2001) reported a range in GC_{B-LH} between 0.12 and 0.35 Mg ha^{-1} the year following a burn for longleaf pine on sites ranging from xeric to wet-mesic. Haywood et al. (1998) reported GC_{B-LH} of 0.78 Mg ha^{-1} for a 34-

year-old stand growing in Louisiana with TSF=3 years. Our overall mean values were 0.3, 0.4 and 0.5 Mg ha^{-1}, for stands with TSF=1, 2 and 3 years, respectively.

The model selected to estimate GC_B was similar to that reported by Gonzalez-Benecke et al. (2010a), but used BA as an independent variable rather than leaf area index, in order to incorporate more published data into the dataset and expand the applicability of the model, as leaf area index is not a common metric reported for longleaf pine stands. Most longleaf pine stands are managed with frequent prescribed fire (Samuelson et al. 2014), so specific information on ground cover dynamics in unburned longleaf pine stands was not readily available. Of the existing reports, only understory percentage cover (Brockway and Lewis 1997; Brockway et al. 2005); hardwood density and height (Haywood et al. 2001) or herbaceous biomass (Haywood 2012a, 2012b) were documented, rather than total ground cover biomass. In order to increase our sample size, we decided to include data from other southern pine stands (slash pine and loblolly pine), assuming that the general relationship between BA and GC_B holds for the three species. The model predicts a reduction in GC_B as pine overstory BA increases, which was expected since BA is coupled to dynamics in leaf area index and therefore to available light in the understory (Dougherty et al. 1995; Gonzalez-Benecke et al. 2012a).

When data were expressed as a fraction of unburned conditions, a unique sigmoidal response of ground cover biomass recovery following fire was determined. Our model predicts that on average, ground cover biomass returned to initial unburned conditions 4 to 5 years following the last burn. Lavoie et al. (2010) reported that the initial ground cover biomass was attained within three years following fire in longleaf pine flatwoods in North Florida. Hough (1982) reported that ground cover returned to pre-fire levels 6-8 years following a prescribed burn in natural slash/longleaf pine stands in Georgia and North Florida. Is important to note that the relationship shown in Figure 13.2 represents the mean value of the recovery rate of ground cover biomass after fire, and site-to-site variability can be expected.

Frequent prescribed fire reduces the amount of woody ground cover biomass (Waldrop et al. 1987; Haywood 2005), and in general, fire intervals of two to four years are recommended to properly control the woody midstory (Wade and Lunsford 1989;). Our model to estimate GC_{B-LW} is in agreement with those findings, having high sensitivity to fire frequency, and GC_{B-LW} declined as TSF decreased. On the other hand, our model to estimate GC_{B-LH} was insensitive to TSF, with GC_{B-LH} ranging between 0.1 to 0.5 Mg ha^{-1} depending on BA. Glitzenstein et al. (1995) reported GC_{B-LH} between 0.20 and 0.45 Mg ha^{-1} for stands with TSF between 1 and 3 years. Brockway and Lewis (1997) reported for a 39-year-old longleaf stand in Georgia with TSF ranging between 1 and 3 years, an average GC_{B-LH} between 0.2 and 0.6 Mg ha^{-1}.

Even though our model predictions agreed with mean observed values, there are sources of variation not included in our study, such as variation in soils and drainage as well as weather (principally rainfall) both spatially and temporally, that could improve these estimates. Future targeted research incorporating plant physiology and climate and soil attributes, and their interactions under varying management and fire regimes, would improve our understanding of

understory-overstory relationships and allow inferences to include behavior under a changing climate future.

Burning season and intensity are important factors that are also considered in fire management planning (Knapp et al. 2009). Our models do not include those effects and we assumed that our equations describe the average responses under varying conditions. Palik et al. (2002) concluded that in order to maintain understory biodiversity in longleaf pine systems burning frequency is more critical than burning season. Similar results were reported by Streng et al. (1993) who did not observe a change in biomass or percent cover of grasses and forbs in response to season of burn. Furthermore, fire frequency, fuel loading, and overstory canopy cover can confound the role of burning season (Haywood 2005; Knapp et al. 2009).

Conclusions

We developed a novel set of functions to simulate ground cover biomass dynamics in response to timing of prescribed burning longleaf pine stands in southeastern U.S. The models incorporate the effects of burning frequency, stand age and basal area. Woody understory ground cover was highly reduced as fire frequency increased, and was also affected by stand basal area when time since the last burn was longer than two years. Herbaceous understory ground cover was little affected by burning frequency, but sensitive to basal area. The set of equations is a useful tool that can be incorporated into fire management models (Ottmar et al. 2009) as well as growth and yield (Gonzalez-Benecke et al. 2012b) and carbon balance models (Gonzalez-Benecke et al. 2015a). Coupled with a model that simulates the dynamics of basal area under different thinning schemes, this set of equations allows analysis of the impacts of fire management regimes on ground cover biomass and diversity under varying stand age, basal area and productivity conditions. The equations were used in the following Chapter 14.

14. Modeling the Effects of Forest Management on Longleaf Pine Forest Carbon Stocks with the LLM-EA

[Contents of this chapter were extracted from: C.A. Gonzalez-Benecke, L.J. Samuelson, T.A. Martin, W.P. Cropper, Jr., T.A. Stokes, J. R. Butnor, K.H. Johnsen, and P.H. Anderson. 2015. Modeling the effects of forest management on *in situ* and *ex situ* longleaf pine forest carbon stocks. Forest Ecology and Management 355: 24-36]

Introduction

Here in Chapter 14, we use the equations and results described in Chapters 10-13 to parameterize the LLM-EA and to simulate C stocks in longleaf pine over time in response to forest management and site index. We also compare results of simulations to those with slash pine.

Atmospheric carbon dioxide (CO_2) mitigation requires an approach that combines increasing terrestrial carbon (C) storage with CO_2 emission reductions (Sundquist et al. 2008). Forests and forest management play an important role in the mitigation of atmospheric CO_2 through the fixation of atmospheric CO_2 into plant tissue (Sedjo, 1989 and 1997; Nabuurs, 2007). In the United States (U.S.), forests represent over 90% of the terrestrial C sink, which is equivalent to 12 to 16% of annual U.S. greenhouse gas (GHG) emissions (U.S. EPA, 2005). Southeastern U.S. forests contain 36% of the C sequestered in the contiguous U.S. (Turner et al. 1995), and these forests have the potential to sequester even more C via improved sustainable forest management (Johnsen et al. 2014).

Longleaf pine (*Pinus palustris* Mill.) was once a dominant forest type in the southeastern U.S., ranging from Virginia to Florida and Texas, but, due to logging and conversion to agriculture and other forest types, only about 1.2 million ha of longleaf pine forest remain (Frost, 2006). As part of the effort to restore longleaf pine ecosystems, longleaf pine is being planted in even-aged plantations. Currently there are approximately 0.4 million ha of longleaf pine plantations (Woudenberg et al. 2010). Longleaf pine is considered a slower growing species than loblolly (*Pinus taeda* L.) and slash (*Pinus elliottii* Engelm.) pines, the two other major commercial southern pines, but its relative longevity offers opportunities to sequester C in offset projects with longer contracts (Samuelson et al. 2014).

Longleaf pine planted for ecosystem restoration is often established at lower tree densities than other southern pines, and this often results in a more abundant and diverse ground cover community that is typically managed with prescribed fire. Prescribed burning is an important management tool in longleaf forests, with recommended burning frequencies of at every two to four years (Chapman, 1932; Glitzenstein et al. 1995, 2003; Loudermilk et al. 2011). Prescribed burning is mainly used to control competing vegetation, favoring pine regeneration and increasing diversity and productivity of herbaceous plants (Haywood, 2007). Without frequent fire, longleaf forests typically succeed into hardwood dominated forests (Quarterman and Keever, 1962;

Hartnett and Krofta, 1989; Mitchell et al. 2006). Thus, the role of frequent prescribed fire in carbon dynamics is important to assess. Fire volatilizes carbon, but may not represent a significant loss over a long rotation due to rapid recovery of biomass following fires.

The goal of this study was to develop a model that can be used to analyze the effects of silviculture on C budgets in longleaf pine plantations in the southeastern U.S. To simulate *in situ* C pools, we developed a hybrid model that integrates a growth and yield model for longleaf pine (Gonzalez-Benecke et al. 2012a) with allometric and biometric equations determined for the species (Baldwin and Saucier, 1983; Gonzalez-Benecke et al. 2014b; Samuelson et al. 2014). To estimate *ex situ* C pool dynamics, the model used the outputs of merchantable products from the growth and yield model and current values of forest product conversion efficiencies and forest product decay rates (Gonzalez-Benecke et al. 2010a and 2011). The model also simulated the C emissions of transportation and silvicultural activities of the various tested scenarios (Markewitz, 2006). Considering current and potential new management schemes, we used to the model to determine: (1) the degree to which site index and different management regimes, incorporating longer rotations and thinning, maximize accumulation of C *in situ* and *ex situ* pools; (2) how much prescribed burning reduces time-averaged C stocks; and (3) if C accumulation over longer rotations is comparable to slash pine, a more intensively managed southern pine species.

Materials and methods

All models used to estimate stand growth and biomass dynamics were based on longleaf pine datasets. Forest floor decay rate and *ex-situ* forest products functions were derived from slash pine publications. Emissions of transportation and silvicultural activities were assumed to be species independent, so we used the standards reported for loblolly pine.

Models

Growth and yield models were combined with allometric and biometric equations to estimate C fluxes and stocks. We used a longleaf pine growth and yield model reported by Gonzalez-Benecke et al. (2012a). The model predicts stand growth in basal area (BA, m^2 ha^{-1}), total volume (V, m^3 ha^{-1}), dominant height (Hd, m), quadratic mean diameter (QMD, cm) and number of surviving trees (Nha, trees ha^{-1}), using as inputs site index (SI, m), and number of trees at planting (PD, trees ha^{-1}).The reference age for SI of longleaf pine was 50 years. The model can also simulate thinnings, where the user defines a thinning scheme that can be described by timing and intensity (by defining age and removal percentage), or by target BA (by defining target maximum BA that triggers the thinning and residual BA after thinning). From the original set of equations reported by Gonzalez-Benecke et al. (2012a), the function to estimate survival was modified to include Reineke's stand density index (SDI, trees ha^{-1}) as a covariate. The new model showed better fit and prediction accuracy than the model reported Gonzalez-Benecke et al. (2012a), especially for mature and thinned stands. Table 14.1 presents a list of functions used for growth and yield modeling.

Table 14.1. Equations used for growth and yield modeling and understory biomass determinations for longleaf pine stands in southeastern U.S.

Parameter	Equation	Ref.
H_{dom}	$= SI \cdot \left(\dfrac{1-e^{(-0.0369815 \cdot Age)}}{1-e^{(-0.0369815 \cdot 50)}}\right)^{1.2928702}$	1
BA	$= \exp(-4.6484039 + 0.4452486 \cdot \ln(Nha) + 1.6526307 \cdot \ln(H_{dom}))$	1
CI	$= 1 - \dfrac{BA_{at}}{BA_U}$	1
CI_2	$= CI_1 \times \exp\left(\left(\dfrac{-1.5476196}{AGE_j}\right) \cdot (AGE_j - AGE_i)\right)$	1
BA_{t_2}	$= BA_{U_2} \cdot (1 - CI_2)$	1
V_{IB}	$= \exp(3.0888853 - 0.1943861 \cdot \ln(Nha) + 1.2580580 \cdot \ln(BA)$ $- 3.1281571 \cdot \dfrac{\ln(BA)}{AGE} - 0.098259 \cdot \ln(SI))$	1
$V_{d,t}$	$= V_{IB} \cdot \exp\left(-1.0537628(\frac{t}{QMD})^{4.2527499} - 0.6545719 \cdot\right.$ $\left. Nha^{-0.1365633(\frac{d}{QMD})^{9.3108306}}\right)$	1
H	$= 1.37 + \exp(0.05942 - 10.80378 \cdot dbh^{-1.1275} + AGE^{0.15053} + BA^{0.12124})$	2
GC_B	$= 5.9272 \cdot \exp^{(-0.04511 \cdot BA)}$	3
recGCB	$= \dfrac{1}{1 + 14.2946 \cdot \exp^{(-1.2124 \cdot TSF)}}$	3
LHp	$= 0.3416 \cdot (TSF^{-1.1361}) \cdot (BA^{-0.4461}) \cdot (AGE^{0.4316})$	3
LWp	$= \dfrac{1}{1 + 118.60 \cdot \exp^{(-2.4413 \cdot \ln(TSF) + -0.8725 \cdot \ln(BA))}}$	3

Notes for Table 14.1: H_{dom} is dominant height (m); SI is site index (m); BA is stand basal area (m^2 ha^{-1}); Nha is surviving trees per ha (ha^{-1}); CI is competition index at thinning Age; BA_{at} is basal area after thinning (m^2 ha^{-1}) ; BA_U is basal area in the unthinned counterpart (m^2 ha^{-1}) ; CI_2 is competition index at AGE 2; CI_1 is competition index at AGE 1; BA_{t2} is the basal area in the thinned stand at AGE 2 (m^2 ha^{-1}); BA_{U2} is the basal area in the unthinned counterpart at AGE 2 (m^2 ha^{-1}); V_{IB} is total inside bark stem volume (m^3 ha^{-1}); $V_{d,t}$ is merchantable volume (m^3 ha^{-1}) of trees with dbh $\geq$ d cm to a merchantable diameter t cm outside bark; QMD is quadratic mean diameter (cm); H is total height (m); GC_B is the biomass of the ground cover vegetation (Mg ha^{-1}); $recB_{GC-W}$ is the recovery rate after fire of woody dominated ground cover biomass (unitless); LHp is the ratio of living herbaceous to GC_B; LWp is the ratio of living woody to GC_B; TSF is the number of years after prescribed fire (years). (1): Gonzalez-Benecke et al. (2012a); (2): Gonzalez-Benecke et al. (2014b); (3): Gonzalez-Benecke et al. (2015b).

Using the data reported by Gonzalez-Benecke et al. (2012b), we fit new models to estimate survival of planted longleaf pine trees. The dataset consisted of 267 plots regularly remeasured and maintained by the U.S. Forest Service's Laboratory at Pineville, LA. Each plot was measured for ~40 years at ~five-year intervals, averaging eight measurements per plot. Plantation ages ranged between 7 and 73 years; BA ranged between 6.6 and 55.9 m^2 ha^{-1}; and SI ranged between 19.6 and 30.8 m (Gonzalez-Benecke et al. 2012b). A negative-exponential survival model that includes H_{dom} and SDI was used to estimate survival using a modified version of the model proposed by Zhao et al. (2007) and Gonzalez-Benecke et al. (2012b):

$$\text{Nha}_2 = \text{Nha}_1 \cdot e^{\left[\left(a_1 \cdot \frac{H_{dom_i}}{100} + a_2 \cdot \text{SDIr}_i\right) \cdot \left(\text{Age}_2^{a_3} - \text{Age}_1^{a_4}\right)\right]} + \varepsilon_1 \qquad [1]$$

where Nha_j is the number of trees ha^{-1} at age j (yr), Nha_i is the number of trees ha^{-1} at age i (yr) ($i < j$), H_{dom_i} is the dominant height (m) at age i (yr), SDIr_i is the relative SDI at age i (yr), a_1 to a_4 are curve fit parameter estimates, SDIr is the SDI relative to a maximum observed of 1111 trees ha^{-1} (Gonzalez-Benecke et al. 2012b) and ε_1 is the error term, with $\varepsilon_1 \sim N(0, \sigma_1^2)$.

At each age, allometric equations were used to estimate aboveground and belowground biomass. For belowground biomass we used the model reported by Samuelson et al. (2014). For aboveground biomass, we fitted new models to the data reported by Baldwin and Saucier (1983). We had access to the raw dataset that consisted of 111 trees sampled in 10 unthinned stands in Louisiana and Texas, with age ranging between 10 and 44 years, and dbh ranging between 2.8 and 52.3 cm (Baldwin and Saucier, 1983). The dataset included tree-level attributes, including dbh (cm), height (m) and dry weight (kg) of each tree aboveground tree component: living foliage, living branches, stemwood, stembark, stem outside bark (stem, the sum of stemwood and stembark), and the whole-tree aboveground biomass (TAGB, the sum of all components). The models selected to estimate aboveground biomass were:

$$\text{TAGB, branch, stem, stemwood, stembark} = b_1 \cdot (\text{dbh}^{b_2}) \cdot (\text{Height}^{b_3}) + \varepsilon_2 \qquad [2]$$

$$\text{Foliage} = b_1 \cdot (\text{dbh}^{b_2}) \cdot (\text{Height}^{b_3}) \cdot (\text{Age}^{b_4}) + \varepsilon_2 \qquad [3]$$

where b_1 to b_4 are curve fit parameter estimates and ε_2 is the error term, with $\varepsilon_2 \sim N(0, \sigma_2^2)$. At each age, stand biomass was calculated by multiplying Nha, estimated by the growth and yield model, by the individual-tree biomass estimated with the fitted functions, using QMD as a surrogate of dbh and the mean height estimated using the model shown in Table 14.1 (reported by Gonzalez-Benecke et al. 2014b).

At each age, mean yearly projected LAI of the longleaf pine overstory was estimated as the product between foliage biomass and the specific needle area (SNA, m^2 kg^{-1}). Using data collected by Samuelson et al. (2012, 2014 and unpublished), Samuelson and Stokes (2012) and Gonzalez-Benecke et al. (2010b), the relationship between age and SNA was determined by fitting the following model:

$$\text{SNA} = c_1 + c_2 \cdot e^{(-c_3 \cdot \text{AGE})} + \varepsilon_3 \qquad [4]$$

where c_1 to c_3 are curve fit parameter and ε_3 is the error term, with $\varepsilon_3 \sim N(0, \sigma_3^2)$.

Annual needlefall (NF, Mg ha^{-1} year^{-1}) was assumed to correspond to half of foliage biomass of the previous year. The needlefall/litterfall ratio model reported by Gonzalez-Benecke et al. (2012a) was used to estimate current year litterfall (LF, Mg ha^{-1} year^{-1}). A decay rate of 15 and 12%/year mass loss was assumed for foliage and coarse woody debris (CWD), respectively (Gholz et al. 1985 and 1986; Radtke et al. 2009).

Standing dead trees estimated from mortality equations were incorporated into the dead component of total biomass. Similar to Gonzalez-Benecke et al. (2010a and 2011), we assumed that, due to the effects of resource competition on suppressed and weak trees, mortality occurs in diameter classes below the median and the diameter class of dying trees corresponds to percentile 25th (D_{25}, cm). A model similar to that reported by Pienaar et al. (1996) was fit to the data used to obtain the growth and yield model published by Gonzalez-Benecke et al. (2012b) (Table 14.1). Biomass of dying trees was computed in the same way as standing biomass, but D_{25} at the previous year was used instead of QMD in order to estimate individual tree biomass.

The effect of thinning on C pools in forest floor and understory biomass was also incorporated into the model. At the time of thinning, reductions in longleaf pine foliage biomass were set to be proportional to reductions in BA due to thinning and therefore forest floor and understory biomass were affected due to their functional dependence on BA and foliage biomass. At thinning and final harvest (clear-cut), logging residues (root and crown biomass plus stem residues) from harvested tress were also included in the stock calculations and allocated to the dead biomass pool. We assumed that thinning was from below and the diameter class of thinned trees corresponded to the 35th percentile (D_{35}, cm). A decay rate of 15, 12 and 10%/year mass loss was assumed for foliage, CWD and lateral roots (Gholz et al. 1985 and 1986; Radtke et al. 2009; Wang et al. 2012). For tap root decomposition we used the model reported by Anderson et al. (2014). Stem residues were obtained by assuming a harvest efficiency of 87% of V (Bentley and Johnson, 2004; Beltley and Harper, 2007).

Using the data reported by Gonzalez-Benecke et al. (2012b), a modified version of the models proposed by Harrison and Borders (1996) was used to estimate D_{25} and D_{35} as follow:

$$D_{25}, D_{35} = d_1 \cdot Nha^{d_2} \cdot BA^{d_3} \cdot SI^{d_4} + \varepsilon_4 \qquad [5]$$

where d_1 to d_4 are curve fit parameter estimates and ε_4 is the error term, with $\varepsilon_4 \sim N(0, \sigma_4^2)$.

The dynamics of aboveground ground cover biomass, defined as the biomass of all live and dead plants < 1 m in height, was determined using the models reported by Gonzalez-Benecke et al. (2015b), that include functions to estimate total ground cover biomass, fractional recovery after fire and partitioning to living herbaceous, living woody and dead ground cover biomass. The effect of prescribed burning on biomass dynamics of ground cover, forest floor, CWD and standing dead trees was computed using the consumption standards reported by Reinhardt (2003), Ottmar et al. (2003b) and Prichard et al. (2007). Table 14.2 presents a summary of consumption factors used.

Carbon mass (Mg C ha^{-1}) was calculated using the C content reported by Samuelson et al. (2014) for longleaf pine and understory biomass components.

Table 14.2. Fuel consumption factors.

Component	Consumption Factor
Needles	0.950 (1)
Branches	0.784 (3)
CWD	0.200 (1)
Standing Dead Trees	0.040 (3)
Herbaceous Ground Cover	0.927 (2)
Woody Ground Cover	0.850 (1)
Harvest Residues	0.800 (1)

Sources: (1) Reinhardt (2003); (2) Ottmar et al. (2003b); (3) Prichard et al. (2007)

Model validation

There are few published reports of longleaf pine biomass accumulation. Model results were validated against published data of aboveground biomass accumulation in live longleaf pine trees reported by Johnsen et al. (2014). The authors reported aboveground biomass for a study installed in 1961 at the Harrison Experimental Forest in Saucier, Mississippi (Schmidtling, 1986). Initial parameters of the model, such as Nha and SI were set equal to those values reported in each plot used for validation. The study plots were measured at age 9, 12, 25, 39 and 46 years. The plots had SI ranging from 20.4 to 27.6 m. Validation of the growth and yield model was carried out in Gonzalez-Benecke et al. (2012b), and bias was shown to be less than 10% for Nha, H$_{dom}$, BA and V$_{IB}$ estimations.

Ex situ wood products pools

Similar to Gonzalez-Benecke et al. (2010a and 2011), harvested roundwood (from thinnings or clear-cuts) was assigned to three main product classes depending on stem DBH and merchantable diameter; sawtimber (ST), chip-and-saw (CNS) and pulpwood (PW) using the model reported by Gonzalez-Benecke et al. (2012b) (Table 14.1). Harvest efficiency of 87% of V was assumed (Bentley and Johnson, 2004; Beltley and Harper, 2007). Merchantable volume inside bark was calculated for each stand age and product volume was transformed to biomass (Mg ha^{-1}) by multiplying by an average whole-tree basic specific gravity (SG) of 0.585 (n=9, SE=0.012). This value of SG was obtained from trees sampled for biomass measurements, with dbh ranging between 8 and 49 cm (Samuelson et al. 2014). A C content of 50% was used to calculate C mass of each product type (Johnsen et al. 2014). Industrial conversion efficiencies of 65, 65 and 58% were assigned to ST, CNS and PW, respectively (Gonzalez-Benecke et al. 2010a and 2011). All the product-types were divided into four life span categories according to the classification proposed by Liski et al. (2001) and Gundimeda (2001) and adapted to southern pine utilization patterns in the SE United States (Birdsey, 1996; Harmon et al. 1996; Row and Phelps, 1991 and

1996; Skog and Nicholson, 1998). Table 14.3 presents a summary of wood products characteristics used to estimate *ex situ* C pool.

Table 14.3. Wood products characteristics.

Product	Product Proportion by life span category (%)				Conversion Efficiency (%)	Product Class Diameter (cm)	
	Long	Medium-long	Medium-short	Short		d	t
	(50)	(16)	(4)	(1)			
ST	50	25	0	25	65	30	20
CNS	25	25	0	50	65	20	15
PW	0	0	33	67	58	15	5

Notes for Table 14.3: ST : Sawtimber; CNS : Chip and Saw; PW: Pulpwood; d : minimum DBH; t : Merchantable diameter. Values in parenthesis indicate average life span for class (years).

Carbon emissions of transportation and silvicultural activities

Carbon emitted by silvicultural activities was determined from Markewitz (2006) and Chapagain (2012). The C emission estimates include fuel and lubricant consumption of machinery, and emissions associated with prescribed burning and manufacture of fertilizer and herbicide. Similar to Gonzalez-Benecke et al. (2010a and 2011), C emitted in transportation of raw material from the forest to the mill was estimated according to White et al. (2005), assuming an average distance of 100 km from forest to mill, load per logging truck of 24 m^3 and fuel economy of diesel logging truck of 2.6 km l^{-1}. Details of C emissions are presented in Table 14.4.

Table 14.4. Carbon emissions in silvicultural activities and product transportation to mill gate.

Activity	Description	C use (Mg C ha^{-1})
Site Preparation	Raking or spot piling + Weed control (application + product) + Bedding	0.357 (1)
Banded Weed Control	Banded Herbicide (backpack application + product)	0.091 (1) (*)
Initial fertilization (age 5)	120 kg·ha^{-1} diamonium phosphate + 210 kg·ha^{-1} urea	0.350 (1)
Prescribed Burning	Manual burning by torch drip	0.017 (2)
Thinning	Commercial thinning	0.233 (2)
Final harvest	Clear cutting at rotation age	0.233 (2)
Transportation	Average for 24 m^3 load capacity	0.0026 (3) (**)

Notes for Table 14.4: Sources: (1) Makewitz (2006); (2) White et al. (2005); (3) Chapagain (2012). (*) Carbon use in fertilization includes production, packing, transportation and application; (**) Carbon use for transportation is expressed in Mg C used per 24 m^3 transported.

Silvicultural management scenarios

To analyze the effect of silvicultural management and rotation length on C sequestration, C dynamics were simulated under four different scenarios for standard conditions of longleaf pine plantations. Initial parameters used were: SI=23 m and Nha=1500 trees ha^{-1}. First year survival of 75% was assumed. Clearcut harvest age was set at 75 years. We assumed prescribed burning each 3 years, starting at age 5 years, and burning residues after clearcut. Based on different management regimes reported for longleaf pine (Kush et al. 2006; Shaw and Long, 2007; Lauer and Kush, 2011), we defined the following three scenarios:

1. U: No thinning.
2. T1: Thinning when the stand reaches a target BA of 26 m^2 ha^{-1} with a residual BA of 18 m^2 ha^{-1}.
3. T2: Thinning when the stand reaches a target SDI of 610 trees ha^{-1} with a residual SDI of 330 trees ha^{-1}. The SDI thresholds selected corresponds to 55 and 30% of maximum SDI of 1111 trees ha^{-1} reported by Gonzalez-Benecke et al. (2012b).

Tree density and BA were highly dynamic (Figure 14.1) over a 75 year simulation for the three scenarios selected under standard site quality and management conditions.

Sensitivity analyses

A sensitivity analysis was conducted to determine the effects of changes in key parameters on total C balance. The effect of site quality was assessed by evaluating the model under contrasting SI of 16 and 30 m, which corresponds to the full range of site quality observed in longleaf pine plantations in the southeastern U.S. (Lauer and Kush, 2011; Gonzalez-Benecke et al. 2012b). Initial stand density effect was evaluated by running the model with contrasting planting densities of 750 and 2250 trees ha^{-1}. Rotation length effects were assessed by evaluating the model under the thinned and unthinned scenarios for 50 and 100 years. Prescribed burning effects were evaluated by running the model under different burning regimes: frequencies of 0 (unburned), 1, 3 and 5 years. Average product life span was evaluated by changing the proportion of products in different life span classes. In the case of ST and CNS, the proportion of products in the long life classes (50 years) were changed by 25% (step up and down), distributing the residual proportion in equal parts to the rest of the life span classes. Sensitivity analyses to industrial conversion efficiencies were not considered due to their low impact on *ex situ* C stocks (Gonzalez-Benecke et al. 2010a and 2011).
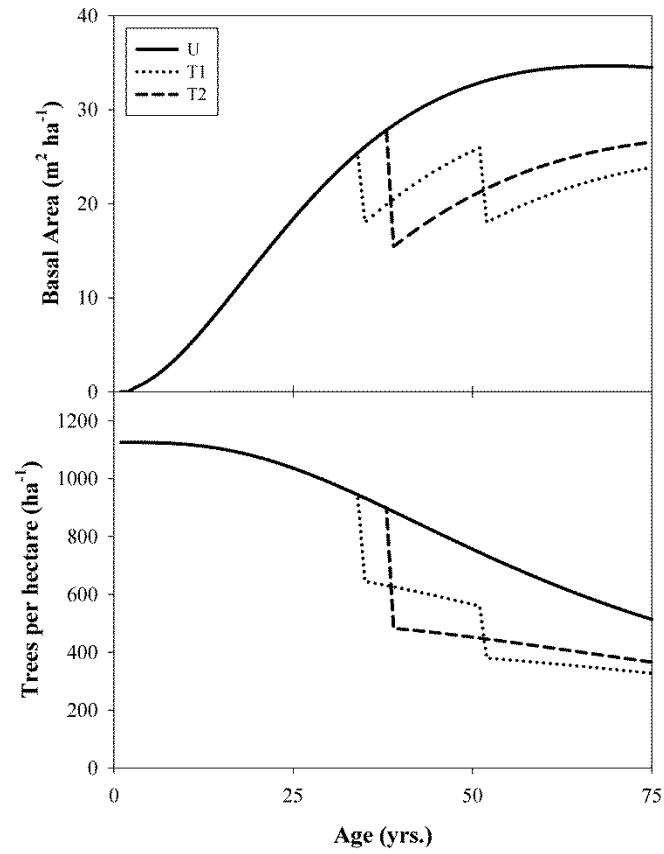
Figure 14.1. Dynamics of basal area (a) and density (b) for the silvicultural management scenarios tested (U=unthinned; T1: thinning using target BA; T2: thinning using target SDI).

Comparison between longleaf and slash pine C stocks

We also compared estimates of longleaf pine C stocks with those of slash pine, an important commercial southern pine species, using a previously reported model for slash pine (Gonzalez-Benecke et al. 2010a) that was updated with relationships used to estimate LAI, litterfall and forest floor accumulation (Gonzalez-Benecke et al. 2012a). Initial planting density was set equal for both species (i.e. 1500 trees ha^{-1}). In order to make appropriate comparisons of site productivity and taking in consideration that the reference age for SI was different for each species (50 years for longleaf and 25 years for slash pine), we defined comparable SI that represent similar site qualities. For longleaf pine stands, observed SI (base age 50 years) ranges between 16 and 29 m (Lauer and Kush, 2011; Gonzalez-Benecke et al. 2012b). For slash pine, observed SI (base age 25 years) ranges between 15 and 28 m (Pienaar, 1996; Jokela et al. 2010). Therefore, we compared the species growing on sites with low, medium and high SI, corresponding to 16 and 15 m, 23 and 22 m, and 28 and 28 m, for longleaf and slash pine, respectively. We defined the categories of low, medium and high SI based on the observed range of SI for each species across the southeastern U.S. A similar SI does not mean both species are growing at the same geographic point but rather indicates a site with low, medium or high productivity within the species' range.

The comparative analysis was carried out for unthinned stands with rotation length of 75 years for both species (LL75, for longleaf pine; SL75, for slash pine), including alternative scenarios with rotation length of 25 years for slash pine (SL25) and thinning using a target BA of 26 m^2 ha^{-1} with a residual BA of 18 m^2 ha^{-1} and rotation length of 75 years for longleaf pine (LL75T). First year survival of 75 and 90% was assumed for longleaf and slash pine, respectively. For longleaf pine stands, prescribed burning every three years was included, beginning at age 5 years. For slash pine stands, no prescribed burning between planting and clearcut was assumed. We recognize that lack of prescribed fire in slash pine plantations over a 75 year period may increase the risk of wildfire, but the slash pine model does not to date include a prescribed fire option. For both species, we assumed burning of residues after clearcut harvest.

Model

Average C stock was defined as: Average C stock = Total C *in situ* (C stored in living longleaf pine trees + understory + forest floor + CWD + standing dead trees) + Total C *ex situ* (C stored in wood products ST + CNS + PW), averaged for all yearly values from the first ~300 years of management, stopping the simulation at the end of the rotation closest to the 300 year endpoint (not stopping the simulations midway into a rotation). For the scenarios with rotation length of 50, 75 and 100 years, the number of rotations simulated was 6, 4 and 3, respectively. This simulation length was chosen to be sufficiently long to approach steady state values for *ex situ* pools, while remaining within plausible bounds for consideration of future forest management scenarios. Reported values of the C emissions due to silvicultural activities, including transportation of supplies, was estimated as the mean value of the sum of all emissions during each rotation.

Statistical analysis

Three measures of accuracy were used to evaluate the "goodness of fit" between observed and predicted (simulated) values for each variable from the dataset obtained in the model validation: (i) Root mean square error (RMSE); (ii) Mean bias error (bias); and (iii) coefficient of determination (R^2). As non-linear model fitting was carried out, an empirical R^2 (Myers, 2000) was determined as:

$$R^2 = 1 - \frac{SSE/df_e}{SST/df_t} \qquad [6]$$

where SSE and SST are the sum of squares of residuals and total, respectively, and df_e and df_t are the degrees of freedom of error and total, respectively.

Results

The model parameter estimates for the selected functions to project survival, and estimate D_{25}, D_{35}, aboveground biomass and SNA for longleaf pine trees growing in the southeastern U.S. are reported in Table 14.5. All parameter estimates were significant at $P < 0.05$.

The survival model was dependent on stand age, H_{dom} and SDI. The performance of the Nha model for the range of SI present on the dataset used for model fitting (i.e., between 20 and 30 m, see Gonzalez-Benecke et al. 2012b; Table 14.1) and using a planting density of 1500 trees ha^{-1} showed little mortality and only small differences in survival at age 10 years (between 1423 and 1417 trees ha^{-1}, for SI 20 and 29 m, respectively; data not shown). At age 70 years, however, the model estimated large differences in survival across SI's (between 707 and 506 trees ha^{-1}, for SI = 20 and 30 m, respectively; data not shown). For D_{25} and D_{35}, the parameter estimate for Nha had a negative value on the models, implying that trees growing in stands with the same productivity will have a smaller D_{25} and D_{35} if the stands have larger tree density. The parameter estimate for age was significant only for foliage biomass. This age parameter had a negative value, implying that for the same size, older trees will have less foliage biomass. More data are needed to better evaluate the modeled trend.

Average SNA for seedlings (Figure 14.2) was about 4.1 m^2 kg^{-1}, and decreased to values of about 2.8 m^2 kg^{-1} as trees reached ages of 80 to 90 years. Stands 20 years old and younger had the largest variation in SNA.

Table 14.5. Parameter estimates and fit statistics of the selected functions to estimate survival, D_{25}, D_{35}, aboveground biomass and SNA for longleaf pine trees growing in southeastern U.S.

Trait	Model	Parameter	Parameter Estimate	SE	R^2	RMSE	CV %
N_j	$= N_i \cdot exp\left[\left(a_1\frac{H_{dom_i}}{100}+a_2\cdot SDIr_i\right)\cdot(AGE_j^{a_3}-AGE_i^{a_4})\right]$	a_1	0.00872	0.00352	0.997	45.12	6.7
		a_2	-0.01173	0.00463			
		a_3	1.25434	0.09715			
D_{25}	$= d_1 \cdot Nha^{d_2} \cdot BA^{d_3} \cdot SI^{d_4}$	d_1	94.5255	17.1452	0.987	2.18	12.4
		d_2	-0.6347	0.0075			
		d_3	0.5396	0.0117			
		d_4	0.00998	0.0024			
D_{35}	$= d_1 \cdot Nha^{d_2} \cdot BA^{d_3} \cdot SI^{d_4}$	d_1	67.7105	7.9660	0.995	1.58	8.1
		d_2	-0.582	0.00483			
		d_3	0.514	0.00755			
		d_4	0.260	0.0417			
TAGB	$= b_1 \cdot(dbh^{b_2}) \cdot (H^{b_3})$	b_1	0.0335	0.0094	0.994	40.43	11.0
		b_2	2.1535	0.0358			
		b_3	0.6903	0.0871			
Foliage	$= b_1 \cdot(dbh^{b_2}) \cdot (H^{b_3}) \cdot (AGE^{b_4})$	b_1	1.1846	0.6948	0.935	5.08	34.9
		b_2	2.3160	0.1313			
		b_3	-1.1735	0.2167			
		b_4	-0.4295	0.1381			
Branch	$= b_1 \cdot(dbh^{b_2}) \cdot (H^{b_3})$	b_1	0.00215	0.0023	0.946	24.61	41.3
		b_2	3.8375	0.1556			
		b_3	-0.9431	0.2982			
Stem	$= b_1 \cdot(dbh^{b_2}) \cdot (H^{b_3})$	b_1	0.0138	0.0034	0.996	27.99	8.9
		b_2	1.8044	0.0301			
		b_3	1.2912	0.0782			
Stemwood	$= b_1 \cdot(dbh^{b_2}) \cdot (H^{b_3})$	b_1	0.0099	0.0027	0.995	27.00	9.6
		b_2	1.8134	0.0327			
		b_3	1.3520	0.0846			
Stembark	$= b_1 \cdot(dbh^{b_2}) \cdot (H^{b_3})$	b_1	0.00932	0.0048	0.977	6.76	20.0
		b_2	1.7326	0.0663			
		b_3	0.7885	0.1706			
SNA	$= c_0 + c_1 \cdot e^{(-c_2\cdot AGE)}$	c_0	2.8172	0.2437	0.411	0.50	14.5
		c_1	1.3218	0.2246			
		c_2	0.0366	0.0188			

Notes for Table 14.5: N_j is surviving trees per ha at AGE j; N_i is surviving trees per ha at AGE i (i<j); AGE is stand age (years); H_{domi} is dominant height at AGE i (m); $SDIr_i$ is the relative SDI at age i; Age is stand age (years); D_{25} is the 25th percentile of the diameter distribution (cm); Nha is surviving trees per ha (ha^{-1}); BA is stand basal area (m^2·ha^{-1}); SI is site index (m); D_{35} is the 35th percentile of the diameter distribution (cm); TAGB is total above-ground biomass (kg tree^{-1}); dbh is stem diameter at breast height (cm); H is total height (m); Foliage is foliage biomass (kg tree^{-1}); Branch is branch biomass (kg tree^{-1}); Stem is stemwood + stembark biomass (kg tree^{-1}); Stemwood is stemwood biomass (kg tree^{-1}); Stembark is stembark biomass (kg tree^{-1}); SNA is projected specific needle area (m^2 kg^{-1}).
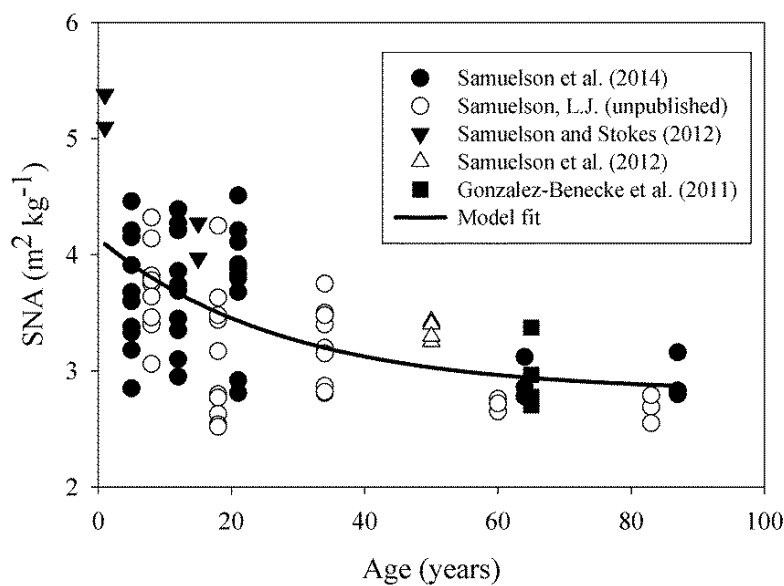
Figure 14.2. Model fit to estimate specific needle area (SNA) from stand age.

Model validation

There was good agreement between observed and predicted values for plots used for validation of BA, H_{dom}, Nha, QMD and AGB. Estimated and observed values were highly correlated, with R^2 values greater than 0.61. Even though, bias was less than 13% for most of the variables tested, larger differences were observed for survival estimations (Table 14.6). This disagreement can be explained by increased mortality in three plots at age 12 years, where Nha was reduced from about 938 to 492 trees ha^{-1}. If those three plots were discarded, bias of Nha, QMD and AGB estimation could be reduced to 10.6%, -11.0% and 9.2%, respectively. Another source of variation between observed and predicted AGB could be attributed to the functions used by Johnsen et al. (2014), who utilized a model that depended only on dbh, fitted from naturally-regenerated trees sampled in one site in Florida, with dbh ranging between 19 and 31 cm.

Table 14.6. Summary of model evaluation statistics.

Variable	$\bar{P}$	$\bar{O}$	n	MAE	RMSE	bias	R^2
BA	18.1	18.3	80	4.1 (22.5)	4.9 (27.1)	-0.11 (-0.6)	0.93
Nha	777.2	662.1	80	125.0 (18.9)	181.3 (27.4)	115.10 (17.4)	0.61
H_{dom}	15.3	15.7	80	1.1 (7.0)	1.3 (8.5)	-0.47 (-3.0)	0.99
QMD	16.5	19.1	80	2.7 (14.3)	3.3 (17.2)	-2.53 (-13.2)	0.96
AGB	107.5	94.3	80	25.2 (26.1)	35.2 (36.5)	10.89 (11.3)	0.97

Notes for Table 14.6: BA is basal area (m^2 ha^{-1}); Nha is trees per hectare (ha^{-1}); H_{dom} is dominant height (m); QMD is quadratic mean diameter (cm); AGB is above-ground biomass (Mg ha^{-1}); $\bar{P}$ is the mean predicted value; $\bar{O}$ is the mean observed value; n is the number of observations; MAE is the mean absolute error; RMSE is the root of mean square error; bias is the bias estimator; R^2 is coefficient of determination. Values in parenthesis correspond to percentage to mean observed value.

Silvicultural management effects on C sequestration

During the 300 year simulation period unthinned stands stored 26% more C than thinned stands harvested at age 75 years, and the two regimes that included thinning showed similar C sequestration. Average C stock, which corresponded to the average across the 300 year simulation period of total C *in situ* (living longleaf pine + understory + forest floor + CWD + standing dead trees + dead coarse roots) plus total C *ex situ* (C in wood products ST + CNS + PW), averaged 102, 80 and 82 Mg C ha^{-1} for U, T1 and T2, respectively (Figure 14.3). *In situ* C stock accounted for between 79 and 83% of the average C stock across silvicultural regimes. The relative impact on C sequestration for ST and CNS was similar, ranging between 8 and 10% of the average C stock. Due to frequent prescribed burning, the forest floor + understory components averaged ~2.5 Mg C ha^{-1} (about 2% of gross C stock). Standing dead trees + CWD + dead coarse roots accounted for about 9 to 13% of the average C stock. The magnitude of emissions associated with silvicultural activities (including transportation) was between 2 and 4% of the average stock C stock.

At their respective rotation ages, *in situ* C stocks were 151, 105 and 115 Mg C ha^{-1} for the U, T1 and T2 scenarios, respectively (Figure 14.4). From that total, the C stock in living longleaf pine and the understory was 141, 95 and 106 Mg C ha^{-1} for the same silvicultural regimes, respectively (data not shown). Total wood products C stock increased each rotation from 63, 48 and 51 Mg C ha^{-1} during the first rotation, up to 73, 57 and 60 Mg C ha^{-1} at the end of the rotation at 300 year endpoint, for the U, T1 and T2 scenarios, respectively. In general, after ~200 years, C flux in the wood products converged to stable values, reaching quasi-equilibrium minimum and maximum values (Figure 14.4).
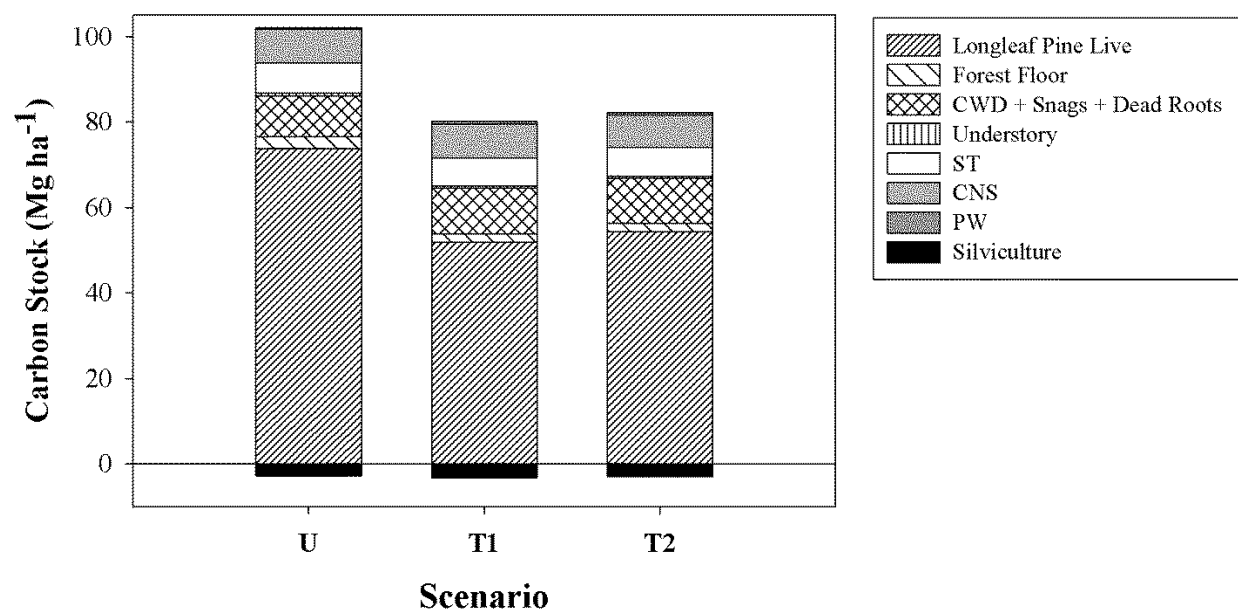
Figure 14.3. Carbon stocks for longleaf pine plantations for a 300-year simulation period under different silvicultural scenarios (U: unthinned; T1: thinning using target BA; T2: thinning using target SDI; CWD: coarse woody debris; ST: sawtimber; CNS: chip-and-saw; PW: pulpwood).
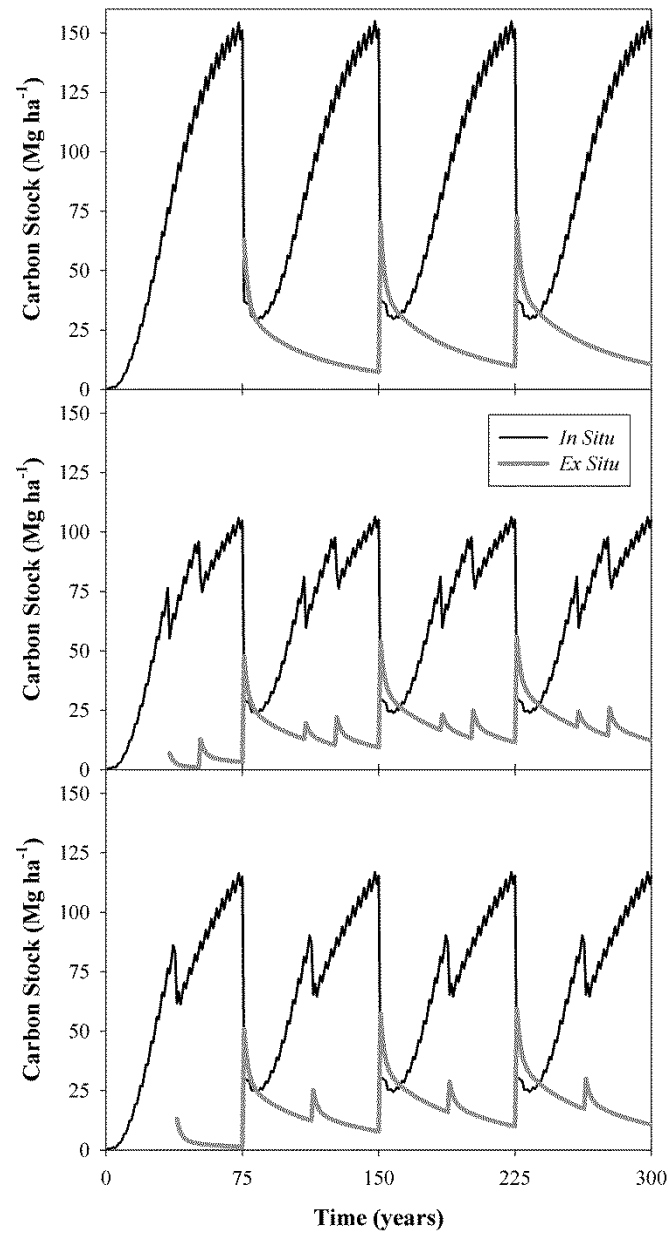
Figure 14.4. Annual carbon stocks for longleaf pine plantations under different silvicultural scenarios for a 300-year simulation period (U: unthinned; T1: thinning using target BA; T2: thinning using target SDI).

Prescribed burning effect on forest floor and ground cover C sequestration

Figure 14.5 shows the dynamics of forest floor and ground cover C stock for longleaf pine stands growing under the U scenario with and without prescribed burning every 3 years. Prescribed burning had a large impact on forest floor C sequestration: at age 75 years, maximum C stock accumulation in the forest floor was 28 and 8 Mg C ha^{-1}, for unburned and burned scenarios, respectively (Figure 14.5a). When averaged across the rotation, C stock accumulation in the forest floor was 15 and 3 Mg C ha^{-1} for the same scenarios, respectively. The impact of prescribed burning on ground cover C stock was smaller. At age 75 years the maximum C stock in ground cover was similar for the unburned and burned scenarios, between 1.5 and 1.4 Mg C ha^{-1}, for the same scenarios, respectively, and averaged across the rotation was 1.7 and 1.0 Mg C ha^{-1} for the same scenarios, respectively (Figure 14.5b). It should be noted that the impacts of fire suppression would be a transition to a very different forest type.
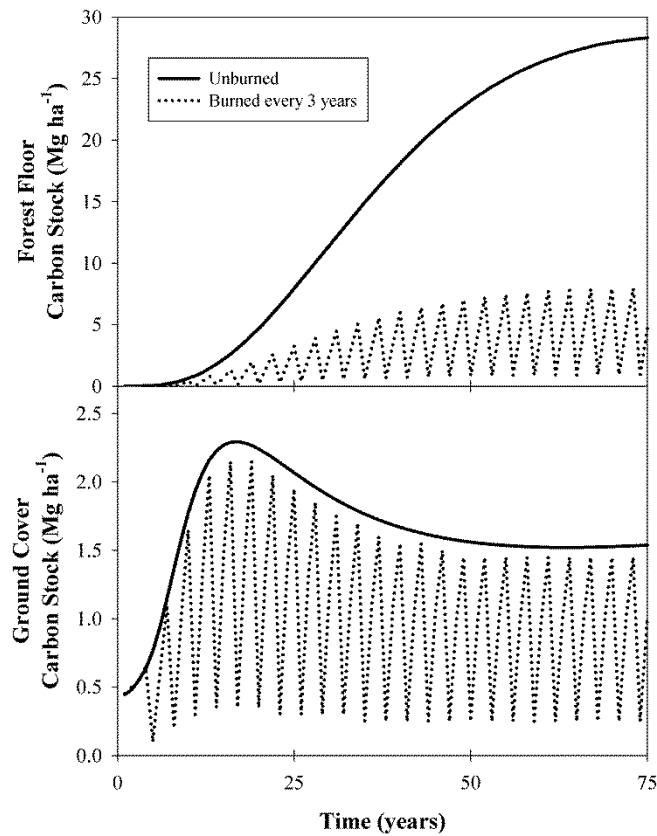
Figure 14.5. Effect of prescribed burning on a) forest floor and b) ground cover C stock. Prescribed burning was initiated at age 5 years with a frequency of 3 years.

Table 14.7. Sensitivity of average carbon stock for selected parameters under different silvicultural scenarios over a 300-year simulation period.

Parameter	Value	U		T1		T2	
		Mg C ha^{-1}	Δ%	Mg C ha^{-1}	Δ%	Mg C ha^{-1}	Δ%
Average C stock (Mg C ha^{-1})		102.0		80.0		82.2	
Site Index (m)	16	39.7	-61	39.7	-50	39.7	-50
(Default=23)	30	194.4	91	130.1	63	133.4	68
Planting density (trees ha^{-1})	750	85.1	-17	77.5	-3	85.1	7
(Default=1500)	2250	112.4	10	79.8	0	88.2	11
Rotation length (years)	50	72.0	-29	63.3	-21	62.4	-21
(Default=75)	100	115.0	13	89.9	12	93.5	18
Prescribed Fire Interval	0	117.1	15	94.2	18	95.7	21
(years)	1	98.4	-4	76.0	-5	78.0	-2
(Default=3)	5	104.6	3	82.8	4	84.3	6
ST percentage in	25	99.7	-2	77.9	-3	80.1	1
long lifespan class (%)	75	104.2	2	82.0	3	84.4	7
(Default=50)							
CNS percentage in long	0	97.8	-4	75.8	-5	78.3	-1
lifespan class (%)	50	106.1	4	84.1	5	86.2	9
(Default=25)							
PW percentage in medium-	0	101.8	0	79.8	0	82.0	4
short lifespan class (%)	67	102.1	0	80.2	0	82.5	4
(Default=33)							

Notes for Table 14.7: Average carbon stock (Mg C ha^{-1}) is the average of a ~300 year simulation period and Δ% is the percentage deviation from default parameter values used (site index = 23 m; planting density = 1500 trees ha^{-1}; rotation length = 75 years; Prescribed fire interval: 3 years; ST in long life class = 50%; CNS in long life class = 25%; PW in medium-short life class = 33%).

The effect of planting density on average C stocks was small for thinned scenarios (T1 and T2). For the unthinned scenario, reducing the initial planting density decreased average C stocks up to 17%, and increasing the planting density enhanced average C stocks by about 10%. The effect of planting density was largely reflected in *in situ* rather than *ex situ* C pools. By lowering planting density from 1500 trees ha^{-1} to 750 trees ha^{-1}, the average C stock decreased 17 and 3 Mg C ha^{-1} for the U and T1 management systems, respectively (Table 14.7). This reduction was explained principally by a decrease in the *in situ* C stocks of 17 and 3.7 Mg C ha^{-1} for the same silvicultural regimes. For the T2 scenario, there was an increase in average C stock of 2.9 Mg C ha^{-1}, possibly explained by the absence of thinnings due to low SDI that never reached the threshold for thinning. The effects on *ex situ* C stocks were substantially smaller, producing positive and negative variations smaller than 1.2 Mg C ha^{-1}, across all planting densities and management systems tested.

Rotation length had a larger impact than planting density on average C stock. Shortening the rotation length from 75 years to 50 years reduced the average C stock 30, 17 and 20 Mg C ha^{-1} for the U, T1 and T2 management systems, respectively. When the rotation age was extended from 75 years to 100 years the magnitude of the effect was smaller: average C stocks increased 13, 10 and 11 Mg C ha^{-1} for the same management systems, respectively. Similar to planting density, the effect of rotation length was largely reflected in *in situ* rather than *ex situ* C pools. By shortening rotation length to 50 years, *in situ* C stock decreased 27, 14 and 17 Mg C ha^{-1} for the U, T1 and T2 management systems, respectively. Conversely, extending rotation length to 100 years, *in situ* C stock increased 15, 12 and 13 Mg C ha^{-1} for the same management systems, respectively (Table 14.7).

If prescribed burning was implemented, changing the fire cycle interval between 1, 3 and 5 years produced little effect on C stock (Table 14.7). On average, across management systems tested, C sequestered in forest floor + CWD + understory was 9, 13 and 15 Mg C ha^{-1} for burning cycle lengths of 1, 3 and 5 years, respectively. When prescribed burning was suppressed, C sequestered in forest floor + CWD + understory averaged 27 Mg C ha^{-1}, across all management systems tested.

Variations in average life span of wood products had little effect on average C stock, where paper products life span had the smaller effect on C storage (Table 14.7). Modifying average life span of ST by changing the product proportion in the long-lived class (half-life 50 years, Table 14.2), affected average C stocks by reductions of 2.3 to increments of 2.2 Mg C ha^{-1}, across all management systems tested. The impact of the CNS half-life on average C stocks was more important than ST, affecting average C stocks by reductions of 4.2 to increments of 4.1 Mg C ha^{-1}, across all management systems tested. The impact of the PW half-life on average C stocks was very small (less than 0.3 Mg C ha^{-1}), across all management systems tested (Table 14.7).

Comparison of C sequestration between longleaf and slash pine stands

Under the default parameters used for simulations in unthinned stands harvested at age 75 years, average C stock of slash pine (SL75) stands was greater than of longleaf pine (LL75) stands. For scenarios of low, medium and high SI, average C stock of SL75 was 72, 138 and 207 Mg C ha^{-1}, respectively. For LL75, average C stock was 41, 106 and 172 Mg C ha^{-1}, for the same SI scenarios, respectively (Figure 14.6). The peak current annual increment in average C stock of SL75 was 3.7,

7.1 and 10.5 Mg C ha^{-1} year^{-1} at age 13, 11 and 10 years, for SI low, medium and high, respectively. On the other hand, LL75 peaked 1.4, 3.4 and 5.5 Mg C ha^{-1} year^{-1} at age 36, 30 and 28 years, for the same SI's (data not shown; see arrows in Figure 14.6). Current annual increment in average C stock of LL75 was larger than SL75 at about the same age when LL75 peaked (data not shown). When the species were compared using a rotation length of 25 years for slash pine (SL25), similar to operational rotations for industrial plantations in southeastern U.S (Gonzalez-Benecke et al. 2010a), average C stock of SL25 was lower than of LL75, and was 33, 80 and 142 Mg C ha^{-1} for SI of low, medium and high, respectively (Figure 14.6). For thinned longleaf pine stands (LL75T) average C stock was 41, 77 and 109 Mg C ha^{-1}, for scenarios of SI low, medium and high, respectively (Figure 14.6). It is important to note that for the low SI scenario, LL75 and LL75T showed the same results, as the stands never reached the target BA of 26 m^2 ha^{-1} that triggered thinning. For high quality sites, average C stock of SL25 (142 Mg C ha^{-1}) was larger to that of thinned longleaf pine. Nevertheless, for sites of medium site quality, average C stock of SL25 (80 Mg C ha^{-1}) was similar to that of LL75T (77 Mg C ha^{-1}). These differences can be explained by analyzing the dynamics of average C stock showed in upper panel of Figure 14.6. For the first 75 years (one rotation for SL75, LL75 and LL75T; 3 rotations for SL25), SL75 sequestered more C than LL75 for SI scenarios of low and medium, and more than LL75T for all SI scenarios. Only at the end of the rotation on high quality sites did LL75 attain a similar average C stock of the SL75. On the other hand, SL25 sequestered more C than LL75 only during first 25 years (ending age for first rotation for SL25), but after that time, LL75 sequestered more C than SL25. When compared SL25 with LL75T for medium SI, after 25 years (first rotation of SL25) there were periods of alternation that ultimately compensated for similar average C sequestration.
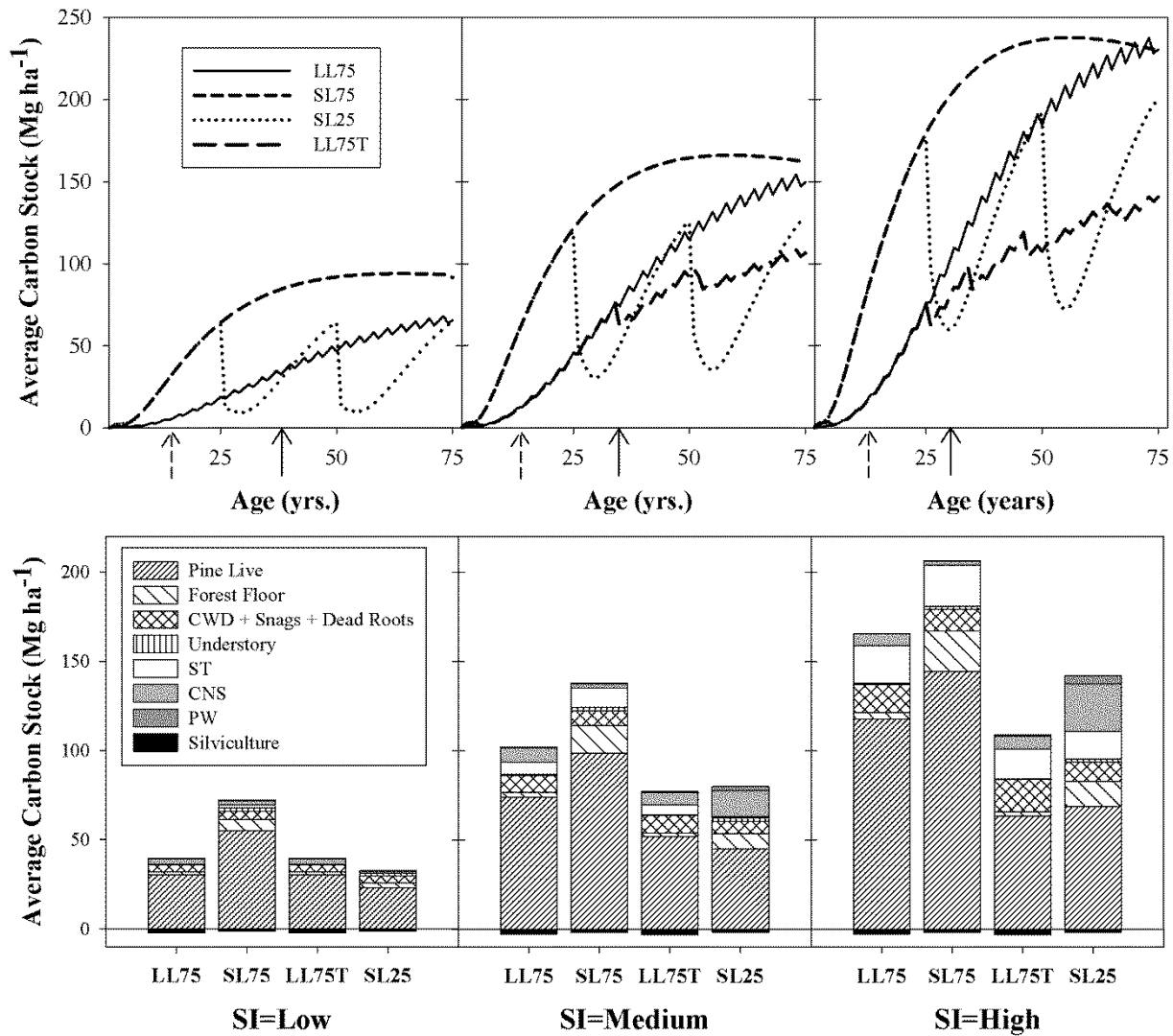
Figure 14.6. Average C stock for unthinned 75 year rotation longleaf (LL75) and slash (SL75), thinned 75 year rotation longleaf (LL75T) and unthinned 25 year rotation slash (SL25) pine plantations growing under three different site qualities (site index low, medium and high). Upper panel shows the dynamics of average C stock for the first 75 years. Arrows indicate year when current annual increment in average C stock peaked for SL75 (dashed) and LL75 (solid). Lower panel shows average C stock for a 300-year simulation period (4 rotations of 75 years for LL75, SL75 and LL75T, and 12 rotations of 25 years for SL25) (CWD: coarse woody debris; ST: sawtimber; CNS: chip-and-saw; PW: pulpwood).

Discussion

Longleaf pine forests are characterized by longer tree longevity and longer rotations relative to other southern pines, and thus may offer opportunities for long-term C storage, but longleaf pine forests are typically of lower density with slower growth rates. Accurate determinations of C stocks and the understanding of factors controlling C dynamics are important for C offset projects and the development of sustainable management systems for longleaf pine. To validate the model we used data from a long-term experiment using plots with contrasting productivity, with SI covering the range observed for the species. The good agreement between observed and predicted values supported the robustness of the model and its utility for assessing the effects of forest management activities on stand dynamics and C sequestration for planted longleaf pine in the southeastern U.S.

When compared with reported values of Johnsen et al. (2014), our estimates of BA and H_{dom} were highly correlated and closely estimated, but aboveground biomass estimates, even though they were highly correlated, had a larger bias, suggesting discrepancies between the allometric functions used. The authors reported aboveground biomass using a model that depended only on dbh, fitted from naturally-regenerated trees sampled in one site in Florida, with dbh ranging between 19 and 31 cm (Garbett 1977). Even though our functions cover a wider range of age and tree size, further work is needed to validate the functions on other sites and expand the limits of applicability. Work is underway to create general biomass functions for the species. Our estimations are also within the range reported for the species with stands of similar structure. For thinned stands simulated (T1 and T2), at age 75 years total *in situ* C stock was about 100-110 Mg C ha^{-1}. For a thinned 87 year-old naturally regenerated stand in Georgia (BA=13.4 m^2 ha^{-1}; SI=19 m), Samuelson et al. (2014) reported *in situ* C stock of 101 Mg C ha^{-1}. For 50 year-old even-aged naturally regenerated stands thinned to BA ranging between 7 and 36 m^2 ha^{-1} (average SI = 21 m), Samuelson and Whitaker (2012) reported *in situ* C stock (not including ground cover and dead trees) of about 45 to 153 Mg C ha^{-1}, respectively. For stands of the same age, SI and BA range, our model predicts *in situ* C stock (not including ground cover and dead trees) between 52 and 181 Mg C ha^{-1} (data not shown).

Site quality was the major factor controlling C sequestration in longleaf pine stands, but the magnitude of the response interacted with rotation length and thinning regime. Similar responses have been reported elsewhere for other pine species (Balboa-Murrias et al. 2006; Gonzalez-Benecke et al. 2010a and 2011). When comparing sites with average productivity (e.g. SI = 23 m) and high productivity (e.g. SI = 30 m) under the U scenario, average C stock increased about 92 Mg C ha^{-1}. Under thinned scenarios average C stock increased only 50 Mg C ha^{-1}. The productivity of longleaf pine stands can be augmented by silvicultural management (including genetic improvement, seedling culture, site preparation and nutrient and competition management) (Haywood 2005, 2011 and 2012; Johnsen et al. 2013; Jose et al. 2003; Loveless et al. 1989; Nelson et al. 1985; Ramsey et al. 2003). For example, at age 40 years, plots that received site preparation and fertilization at age 1 year accumulated about 50 Mg C ha^{-1} more aboveground biomass than control plots (Johnsen et al. 2014). The amount of C sequestered in *ex situ* C pool was similar across management regimes for each site quality tested (about 3, 15 and 33 Mg C ha^{-1} for SI= 16, 23 and 30 m, respectively). The development and application of techniques that increase productivity should increase C storage of future plantations, increasing not only *in situ* but also

ex situ C, by extending the proportion of trees producing valuable product grades that have a longer life span.

Even though at rotation age unthinned and thinned stands reached C storage in forest products of about 100 and 70 Mg C ha^{-1}, respectively (data not shown), the amount of *ex situ* C stored in long-lived products (i.e. sawtimber) was less than 45% and most of the C was sequestered in medium to short lived products. Nevertheless, the proportion of *ex situ* C stored in long-lived products increased as rotation length increased. For example, for average productivity sites (SI= 23 m), that proportion was 10% for stands harvested at age 50 years, and 65% for stands harvested at age 100 yrs (data not shown). On average, the *ex situ* C pool represented about 18% of average C sequestration. For slash pine, and loblolly pine stands, Gonzalez-Benecke et al. (2010a and 2011) reported that *ex situ* C pool accounted for 31% and 34% of average C sequestration, respectively. For longleaf pine forests, the *ex situ* C pool is not as important as for slash pine and loblolly pine, as the slower growth rate of longleaf pine reduces the potential of C sequestration in longer-lived forest products like sawtimber.

Prescribed burning reduced average C stock by about 16-19% and most of that reduction was observed in the forest floor. For unthinned and unburned stands, C sequestered in the forest floor was about 28 Mg C ha^{-1} at age 75 years. This value is within the range of reported values for mature slash pine and loblolly pine stands. Binkley et al. (1992) reported for a 30 year old mixed loblolly-longleaf stand with a BA of 32 m^2 ha^{-1}, forest floor biomass of about 38, 18 and 25 Mg ha^{-1} in stands unburned, burned every 2 years and burned every 4 years, respectively. We modified SI and planting density to get similar BA at the same age as Binkley et al. (1992), obtaining forest floor biomass of 37, 8 and 20 Mg ha^{-1} for the same burning scenarios, respectively (data not shown). Prescribed burning reduced C stored in the forest floor to average values of 0.2, 2.7 and 4.7 Mg C ha^{-1} for burning frequencies of 1, 3 and 5 years, respectively. For 64 and 87 year-old stands, Samuelson et al. (2014) reported C stock in dead organic matter between 3 and 5 Mg C ha^{-1} for stands burned every 2-3 years. Samuelson and Whitaker (2012) reported litter C stock of about 4.1 to 9.0 Mg C ha^{-1}, respectively. For stands of the same structure our model predicts values between 2.6 and 9.4 Mg C ha^{-1} (data not shown).

Preliminary results from longleaf pine sites at US Army Fort Benning show that black C makes up less than 5% of soil C and considering the slow turnover of black C, the new inputs from decades of prescribed burning into the soil are small (Butnor et al. 2014). While not dismissing the contribution of char from forest floor burning, in longleaf pine systems the contribution of char is likely small relative to western pine ecosystems with longer fire return intervals and different climatic conditions (Deluca and Aplet 2008).

Our model predicts little effect of burning frequencies on C stored in ground cover. For unburned stands (thinned and unthinned), the mean C stock in ground cover was 1.8 Mg C ha^{-1}, while on stands burned at frequencies of 1 to 5 years, the average C stock in ground cover was between 0.3 to 0.9 Mg C ha^{-1}. These values are in agreement with reported data for ground cover C stock on longleaf pine stands. For example, for 64 and 87 year-old stands burned every 2-3 years, Samuelson et al. (2014) reported about 0.6 Mg C ha^{-1} stored in ground cover. Brockway and Lewis (1997) reported, for a frequently burned 39 year- old stand, average C stock in herbaceous ground

cover between 0.1 to 0.3 Mg C ha^{-1}. Due to the low amount of ground cover biomass in longleaf stands, the benefit of prescribed burning on restoring or maintaining the diversity of herbaceous ground cover is not counteracted by the small reductions in C sequestration in ground cover.

The use of longer rotations has been suggested as one of the four major strategies to achieve increased C sequestration (Canadell and Raupach 2008). On a regional basis, longer harvesting cycles maintains a higher mean C storage, even in a highly dynamic forest system (Cropper and Ewel 1987). For longleaf pine, we estimated an average C stock increment of 13 and 10 Mg C ha^{-1} when rotation length was increased from 75 to 100 years, and an average C stock reduction of 30 and 19 Mg C ha^{-1} when rotation length was reduced from 75 to 50 years, on unthinned and thinned stands, respectively. A similar response was observed for other southern pine species (Gonzalez-Benecke et al. 2010a and 2011). The results of Liski et al. (2001) also support these results. They concluded that longer rotations increase C sequestration for *Pinus sylvestris* L. in Finland, with an approximate 12 Mg C ha^{-1} increase in average C stock when rotation length was increased from 60 to 90 years.

The magnitude of the emissions associated with silvicultural management activities was low (between 2 to 4% of gross C stock), but since this emitted C comes from fossil fuels it should be noticed that after 25 to 50 rotations (between 1875 and 3750 years in future), the decrease of fossil C pool resulting from silvicultural activities across all that time would be of the same magnitude of total C stocks, thus leading to a null average C stock. Although it is unlikely that site conditions and management plans can be projected so far into the future it is reasonable to conclude that longleaf pine plantations would more efficiently contribute to long-term C sequestration if the energy necessary for silvicultural practices were to come from renewable energy sources.

There is currently great interest in uneven aged silvicultural systems to manage older longleaf pine stands (Guldin 2006; Mitchell et al. 2006; Brockway et al. 2014). The model developed in this study may have limited applications to stands that are managed with individual tree or group selection in order to restore or maintain an uneven aged structure. Models of these more complex longleaf stands should incorporate spatial relationships, including competition effects, and regeneration processes (e.g. Loudermilk et al. 2011). It is possible that management approaches, similar to the Stoddard-Neel approach (Jack 2006), could result in greater stocks of stored carbon as well as better provision of wildlife habitat, plant diversity, and other ecosystem services, but this remains to be tested

At age 75 years, unthinned slash pine and longleaf pine reached a similar average C stock on medium and high quality sites. Similar results have been reported when comparing productivity of longleaf pine and other southern pine species. For example, Schmidtling (1986) reported that at age 9 years growth of slash pine was greater than longleaf pine, but the two species were of similar size after age 25 years. Johnsen et al. (2014) reported similar biomass of loblolly and longleaf pine stands at age 40 years. Even though unthinned slash pine and longleaf pine reached similar average C stocks at age 75 years, on average, across all rotations, slash pine sequestered more C due to longer periods with greater growth. In contrast, when unthinned longleaf pine with 75 year rotation length was compared with three slash pine rotations of 25 years, longleaf pine sequestered more C. The periods of low C sequestration after slash pine's harvest, with even negative C fluxes for

several years (Bracho et al. 2012), explains this last result. In contrast, for medium quality sites, C sequestration was similar between thinned 75-year rotation longleaf pine and unthinned 25-year rotation slash pine.

The following Chapter 15 describes additional validation of the LLM-EA using C stock data collected at Eglin Air Force Base, Marine Corps Base Camp Lejeune and US Army Fort Polk/Kisatchie National Forest. These C stock data were previously described in Chapter 7.

15. Additional LLM-EA Validation

LLM-EA Model Validation

In addition to the LLM-EA validation described in Chapter 14, validation of LLM-EA model was also carried out by comparing model outputs against data collected on eight stands for: (i) aboveground C accumulation in live longleaf pine biomass (AGC, Mg C ha^{-1}); (ii) belowground C accumulation in live longleaf pine biomass (BGC, Mg C ha^{-1}); and (iii) C accumulation in forest floor (FFC; Mg C ha^{-1}). For each site value, the reported initial stand characteristics such as planting density (PD), site index (SI) and burning management cycle (years since last burn, YSB) were used as model inputs. The LLM-EA model was run from planting until the age when each stand was measured. A summary of the data used for C accumulation validations is given in Table 15.1 and in Chapter 7.

Table 15.1. Stand characteristics of longleaf pine stands used for model validation.

Site	Stand age (years)	SI (m)	YSB (years)	PD (trees ha^{-1})	BA (m^2 ha^{-1})	Density (trees ha^{-1})	AGC (Mg C ha^{-1})	BGC (Mg C ha^{-1})	FFC (Mg C ha^{-1})
FL	9	19	3	1494	2.5	806	3.4	1.0	1.9
	19	18	1	1494	9.1	988	14.7	4.1	1.9
	43	13	2	1890	12.5	663	36.2	7.8	2.7
	50	10	5	1890	8.8	431	17.1	5.1	3.6
LA	8	21	1	1976	5.2	1325	5.1	2.1	1.2
	18	21	4	1976	7.9	450	16.3	4.5	1.6
	34	21	2	1235	14.3	375	53.8	12.5	2.4
NC	25	16	1	1729	14.6	1319	33.9	8.9	3.0

Notes for Table 15.1: FL: Eglin Air Force Base; LA: Kisatchie National Forest; NC: Marine Corps Base Camp Lejeune; site index (SI); years since burn (YSB); planting density (PD); basal area (BD); live aboveground C in longleaf pine (AGC); live belowground C in longleaf pine (BGC); forest floor C (FFC).

Results

Table 15.2 shows the summary LLM-EA model validation. There was good agreement between observed and predicted values of AGC, BGC and FFC for the 8 stands measured in FL, LA and NC. Predicted and observed values were highly correlated ($R^2 > 0.76$), and bias ranged between -3 and -21%. Smaller error, but lower correlation, was observed for FFC estimations, with a mean absolute bias of about -0.3 Mg ha^{-1}. On the other hand, larger error, but larger correlation was observed for AGC and BGC estimations, with a mean absolute bias of about -4.7 and -0.8 Mg ha^{-1}, respectively (Table 15.2).

Table 15.2. Summary of model evaluation statistics for aboveground C (AGC), belowground C (BGC) and forest floor C (FFC) estimations for longleaf pine stands.

Variable	$\overline{O}$	$\overline{P}$	n	RMSE	Bias	R^2

AGC	22.6	17.8	8	7.8 (34.5)	-4.7 (-21.0)	0.86
BGC	5.7	4.9	8	1.5 (26.0)	-0.8 (-14.1)	0.88
FFC	2.3	2.0	8	0.6 (27.6)	-0.3 (-13.4)	0.76

Figure 15.1 shows the relationship between observed and predicted AGC, BGC and FFC. There was very good correlation between observed and predicted AGC, BGC and FFC across all stands, and the intercept and slope of those relationships were not significantly different from 0 (P>0.24) and 1 (P>0.23), respectively, for all variables tested. After the additional validation, the LLM-EA was then linked to the LLM-ST and both models are available in Excel format at http://carboncenter.ifas.ufl.edu/models.shtml. Development of the LLM-ST by this project is described in detail the following Chapter 16.
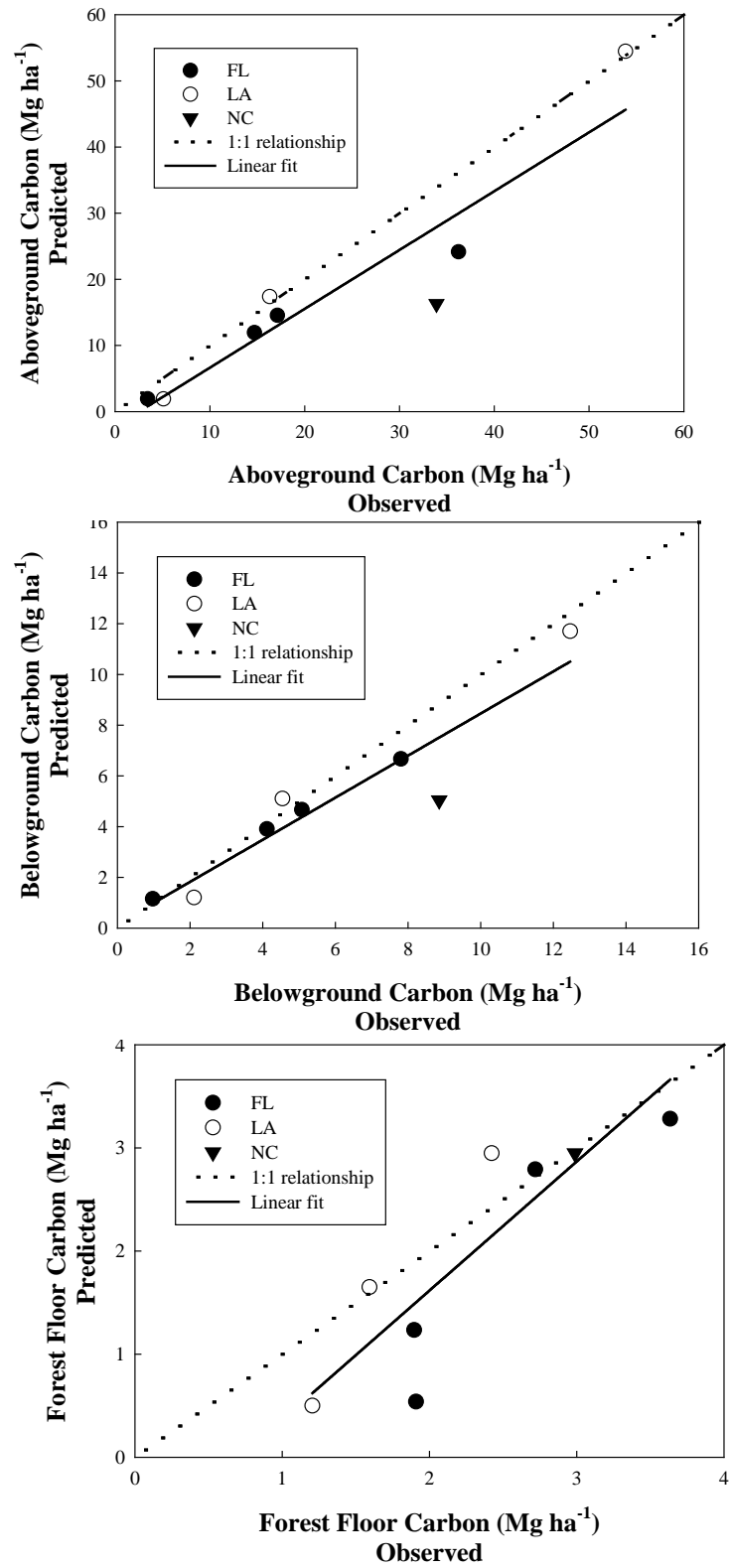
Figure 15.1. Observed versus predicted aboveground, belowground and forest floor C using the LLM-EA.

16. Simulating the Effects of Prescribed Fire and Harvesting Using the LLM-ST

Modeling Framework

An overall goal of this project was to modify a single-tree-based longleaf pine model (LLM-ST) which enables simulation of older (50 to > 200 years) stands which are managed with silvicultural tools such as single tree or group selection harvests and prescribed fire. The LLM-ST is spatially explicit and can model tree size and distribution, and the LLM-EA can generate diameter distributions and estimates of understory biomass. The models were enhanced to simulate the processes that interact to provide the necessary conditions to sustain pine savanna biodiversity. Another key habitat attribute is coarse woody debris. Both models were improved to produce explicit estimates of coarse woody debris through mortality and coarse wood detrital biomass. As an initial guide for resource managers, we prepared a suite of simulations demonstrating how land use practices and silvicultural prescriptions including prescribed burning influence the life-cycle carbon balance of longleaf pine ecosystems, biodiversity and sustained ecological yield of forest products.

Longleaf pine modeling has generally been used to address questions related to less intensively managed, uneven-aged savanna ecosystems. One simulation approach that has been used is population modeling. Tree population models include processes of reproduction, growth, and survival. Demographic parameters are often functions of size and not age (Caswell 2001). It can be difficult to find size-specific demographic parameters for long-lived species, but some models have been developed (Platt et al. 1988, Cropper and Loudermilk 2006). Although these models may include density dependence (Cropper and Loudermilk 2006), they are not spatially explicit, do not capture local competition effects with hardwoods, and simplify responses to fire. Another modeling approach is to use existing forest landscape models to address spatial interactions between longleaf pines, hardwood species and fire. Loudermilk and Cropper (2007) used the LANDIS model to link spatially explicit fire dynamics to the longleaf population dynamics. These model analyses led to the identification of the needs for a finer resolution spatial demography model to better represent the key ecological processes.

With the understanding that many important processes in a longleaf pine savanna are local interactions between individual trees another modeling framework was developed and described in Loudermilk et al. (2011). This longleaf pine model (LLM-ST) is a spatially explicit single tree model that includes longleaf pine, hardwoods, wiregrass, and fire. The spatial structure of this model is represented by a lattice of cells where trees within cells (5 m x 5m) interact with trees in adjacent cells based on distance and size of the adjacent trees. In order to provide reasonable computation time, the domain of the model is 1.56 ha (25 x 25 cells). With spatial competition modeling, edge effects are a potential concern. To address this issue the model uses periodic boundary conditions (a torus shaped landscape with no edges). The principal tree attribute in LLM-ST affecting competitive interactions, mortality risk, and seed production is height, following the approach of Drake and Weishampel (2001). This modeling approach has been demonstrated to provide a good fit to the horizontal and vertical distributions of trees in longleaf savannas (Drake and Weishampel 2001, Loudermilk et al. 2011).

Spatial interactions in LLM-ST include seed dispersal, rhizomatous spread of hardwoods, inter- and intra-specific influences on neighboring trees, and tree effects on leaf litter and fuel accumulation. Height and distance based competition influences tree growth and mortality risk (Loudermilk et al. 2011). The model uses an annual time step, with a stochastic fire event and a separate stochastic seed masting event possible in each year. Generally longleaf pines produce a spike of seed production (mast crop), often synchronized over large areas, every five to 10 years (Mitchell et al. 2006). In this scheme the mean fire frequency is a model parameter. The best conditions for seedling establishment (assuming open gaps are available) occur when fires and masting years coincide.

Longleaf pine forests are complex systems with multiple species interactions and frequent fire disturbances Figure 16.1). Both longleaf trees and hardwood trees can exist in each cell of the LLM-ST. Empty cells can have up to 20 trees established as new recruits. Seeds are dispersed based on distance from adult trees and mast year status. Fire is critical to establish conditions suitable for longleaf pine germination. After germination, each longleaf seedling remains in the grass stage for one to 10 years with a mean residence time of five years in the grass stage. Site quality (simulated as an asymptotic height parameter) is an important determinate of tree height, which in turn is critical for determining the strength of competition between adjacent trees (Drake and Weishampel 2001, Loudermilk et al. 2011).
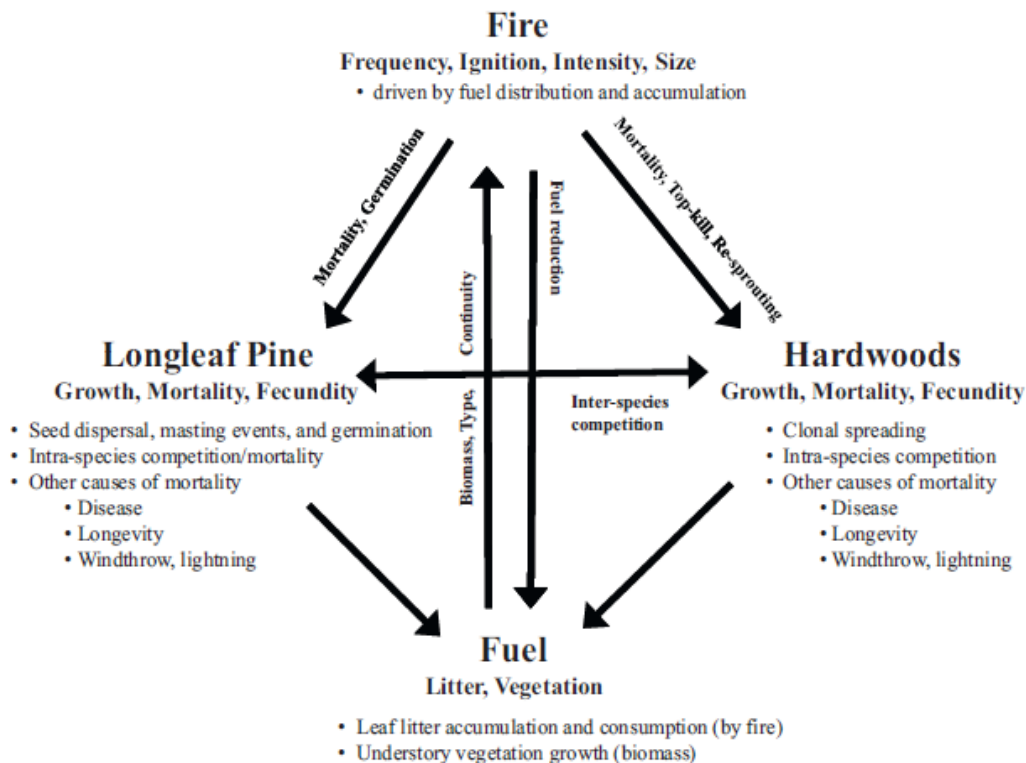
Figure 16.1 Important processes in the LLM-ST from Loudermilk et al. (2011).

When the LLM-ST is run for periods of 250 years or more, it appears to be in a quasi-steady state condition with minor stochastic variation in stand structure. At this point, the distribution of tree diameters typically follows a "J" shaped curve Figure 16.2) that is expected for uneven-aged longleaf pine forests (Johnson and Gjerstad 2007). One significant difference between model outputs and the real world is that the model tree counts are exact for any particular run. The smallest pine germinants are difficult to count under field conditions. The stochastic nature of the model requires multiple runs to characterize sensitivity analyses or responses to simulated management regimes.
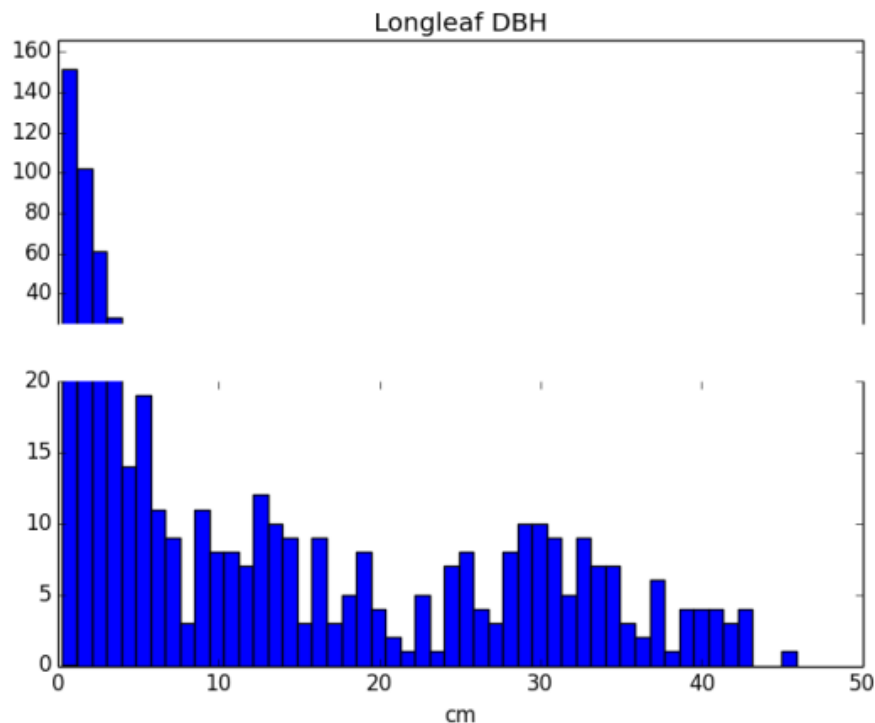
Figure 16.2 Simulated diameter distribution in a 1.56 ha area after 250 years for a longleaf pine savanna managed with a mean fire return time of four years.

Although these modeling approaches address many of the basic ecological issues that are important in longleaf pine restoration, they provide little capability to address management issues such as carbon storage or harvesting. Currently, many of the longleaf forests established in the southeastern United States can be characterized as even-aged or plantation forests (Gonzalez-Benecke et al. 2015). Management concerns in these forests can include prescribed fire, thinning or other harvesting techniques, and climate change mitigation through carbon sequestration.

When management goals include restoration of longleaf pine savannas or adoption of uneven-aged management, a plantation model alone is insufficient. In order to address a full suite of longleaf pine management scenarios, we have coupled an even-aged stand model (Gonzalez-Benecke et al. 2015) with the LLM-ST. The plantation model integrates a growth and yield model with longleaf specific allometric equations to simulate variable planting density, thinning, prescribed fire, and biomass dynamics. In this framework, we use an Artificial Neural Network model (ANN) to generate an individual tree list consistent with the even-aged stand characteristics that can then be used as a starting point for LLM-ST simulations. We extended the LLM-ST model to account for carbon stocks in the forest, as well as allowing single tree or group selection harvests with in the forest. We use an Excel interface to run each model and allow user selection of management options (models online at: http://carboncenter.ifas.ufl.edu/ models.shtml).

Artificial Neural Network models are an efficient machine learning technique that are relatively less constrained by statistical assumptions concerning the independent variables or predictors (Mehrotra et al. 2000). These models have widespread applications, including forest modeling (Shoemaker and Cropper 2010). The ANN in our model framework uses stand-level characteristics simulated by the even-aged model (e.g. site index, age, dominant height, density, quadratic mean diameter, and basal area) to help construct a list of individual trees, each with a diameter, height, and age consistent with the stand. The ANN bins the trees into 25 diameter classes between a dbh of 0 and 66 cm. A more detailed description of the approach can be found in Leduc et al. (2001). The neural network model simulated tree size distributions with fit indices for the thinned and unthinned stand models of 0.84 and 0.93 respectively.

Asymptotic height parameter

Much of the variation in forest tree growth rates can be attributed to site-level characteristics such as soil nutrient supply, topography, and water balance (Skovsgaard and Vanclay 2008). An important index of site quality in even-aged stands is site index (SI). The SI can be defined as an expected height of dominate and codominant trees at a defined base age since stand establishment (Nyland 2002). For even-aged longleaf pine stands, site quality is a major influence on tree productivity (Gonzalez-Benecke et al. 2015).

The concept of site index doesn't translate well to old growth longleaf pine savannas. It seems likely that site quality variation is also an important influence on maximum tree height in older longleaf savannas. Loudermilk et al. (2011) reported that the mean longleaf height (trees greater than 10 m in height) at the relatively xeric Ordway-Swisher Biological Station was 8.2 m less than at the more mesic Ichauway preserve. These differences were apparent using either airborne LIDAR data collection or ground based height measurements (Loudermilk et al. 2011).

The paucity of data on old growth longleaf pine stands with similar management and disturbance histories makes it difficult to predict the response surface of height to site quality for old growth stands. In order to incorporate this key relationship into the LLM-ST model, we have assumed that the SI of the even-aged plantation would be the best predictor of the key asymptotic height parameter (Loudermilk et al. 2011) for old growth stands on the same site.

In order to estimate asymptotic height we used a function from Lauer and Kush (2010) that predicts height at a given age as a function of the age at which trees reach a height of 4.5 ft (1.37 m) and of the SI. This equation approaches a height asymptote as age increases for any given SI. Data including more than 310,000 observations from longleaf stands measured in the this project (US Army Fort Benning, Marine Corps Base Camp Lejeune, Eglin Air Force Base) and from the Flomaton or E. A. Hauss Old Growth Longleaf Natural Area that was clear-cut in 2008 (data from John Kush), the Escambia Experimental Forest in Alabama (data from the U.S. Forest Service), the Palustris Experimental Forest in Louisiana (data from the U.S. Forest Service), the Harrison Experimental Forest in Mississippi (data from the U.S. Forest Service) and from Platt et al. (1988) indicated that maximum longleaf height should be expected by age 75 to 100 years of age Figure 16.3). Much of the variation in height at a given age can be attributed to site quality differences and disturbance history.
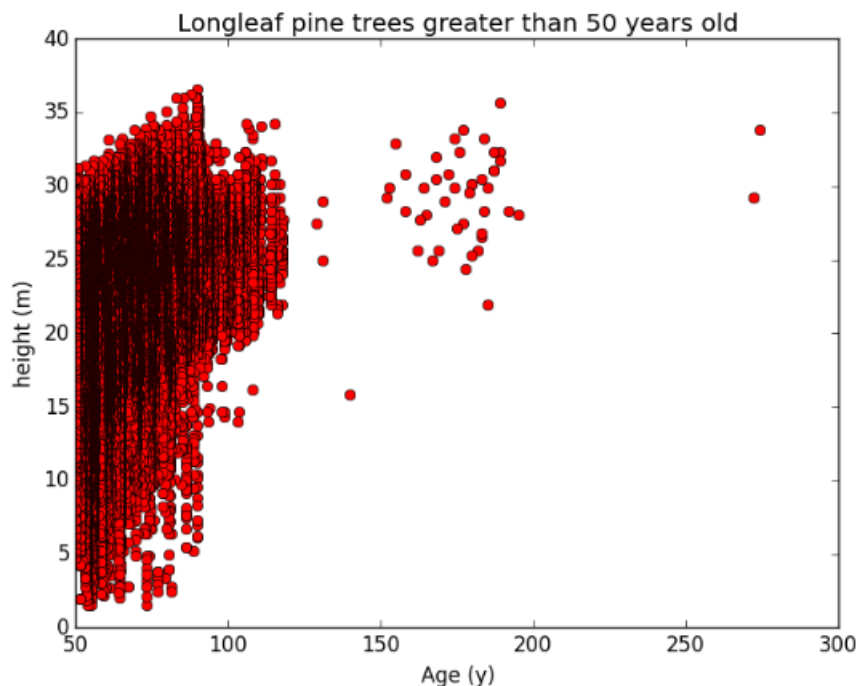
Figure 16.3 Longleaf pine height and age for trees greater than 50 years old.

This pattern of asymptotic growth at approximately 100 years can also be observed in Lauer and Kush (2010) using plot average height-age trajectories from 10 to 120 years. McCaskill and Jose (2012) reported that mean stand growth reached a plateau at approximately 80 to 90 years in a Florida chronosequence. The fitted Lauer and Kush (2010) equation predicts longleaf height increases slowly beyond 100 years of age. To calculate the asymptotic height parameter used as an input to LLM-ST, we used the Lauer and Kush (2010) equation with an input age of 300 years.

Carbon calculations

The original LLM-ST model used tree height as the key variable reflecting relative competitive strength (Loudermilk et al. 2011). In order to extend the model to estimate carbon dynamics in longleaf savannas, it was necessary to calculate stem diameters as well as heights. The following equation (Gonzalez-Benecke et al. 2014) was used to calculate dbh for all trees between 1.37 m height and the asymptotic height:

$$\ln(dbh) = -0.65364 + 1.30284 * \ln(ht - 1.37)$$

Where ht is the tree height in m, and dbh is in cm. Any tree reaching the maximum height can continue to grow in diameter until it reaches the maximum diameter. For these simulations, the maximum diameter was assumed to be 120 cm. Diameter growth for trees of maximum height was assumed to be a function of the competition index for the focal tree. In practice, this calculation was never used because no tree reached the asymptotic height maximum.

Aboveground biomass of longleaf pine trees was calculated as a function of diameter and height using the following equations (Gonzalez-Benecke et al. 2015):

$$\ln(stem) = -3.5379 + 0.9479 * \ln(ht * dbh^2)$$
$$\ln(branch) = -6.7721 + 1.0787 * \ln(ht * dbh^2)$$
$$\ln(foliage) = -4.9964 + 0.7871 * \ln(ht * dbh^2)$$

Where stem, branch, and foliage biomass are calculated in kg dry weight. Equations for belowground longleaf pine carbon were taken from Samuelson et al. (2014). Allometric equations for hardwood biomass were taken from Jenkins et al. (2003). As was the case with the simulated longleaf pine trees, it was necessary to calculate dbh from tree height in order to apply these equations. An equation was fit (C. Gonzalez-Benecke, personal communication) using data collected in longleaf pine stands at Marine Corps Base Camp Lejune and US Army Fort Benning and US Army Fort Polk/Kisatchie National Forest to predict hardwood dbh from the simulated height Figure 16.4)
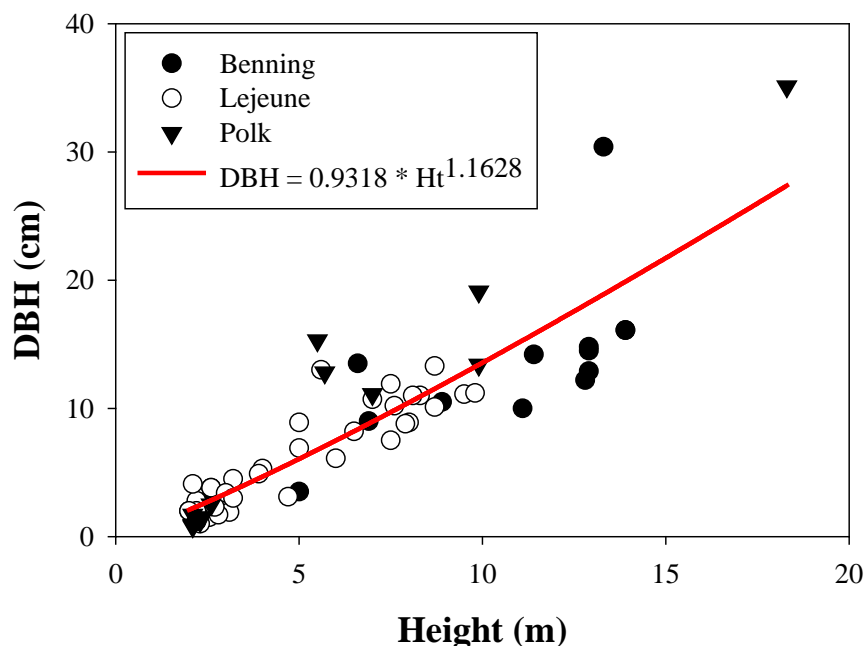
Figure 16.4. Hardwood dbh versus height relationship. The best fit equation is plotted with the data ($R^2 = 0.79$).

The aboveground biomass for hardwood trees was then calculated with this equation for mixed hardwoods from Jenkins et al. (2003):

$$\ln(biomass) = -2.4800 + 2.4835 * \ln(dbh)$$

Where biomass is calculated in kg dry weight. Stand level estimates of longleaf pine and hardwood storage were then calculated by assuming that 50% of the dry weight was comprised of carbon and summing these values for each tree.

Coarse woody debris

Forest ecosystems are dynamic systems that experience a range of disturbance frequencies and intensities. These disturbances, as well as individual tree mortality events, contribute to the pool of dead tree mass in the forest. Coarse woody debris (CWD) is an important structural feature of forested ecosystems and is associated with numerous ecosystem services (Harmon et al. 1986, Schmid et al. 2016). We extended the original LLM-ST to include CWD production, decomposition, and consumption in fire events. The model is based on assuming that all of the stem and branch biomass of dead trees is transferred to the CWD pool. Carbon is approximated as half of the dry weight, but it should be noted that carbon content changes during the course of decomposition in ways that cannot currently be specified as a function for our sites. Decay of CWD occurs through the process of consumption by fires and by biologically mediated

decomposition. We assumed a 0.2 rate of CWD consumption by fires and a decomposition rate of 0.14 per year (Gonzalez-Benecke et al. 2015).

The dynamics of the CWD pool Figure 16.5) is dependent on the stochastic nature of mortality interacting with fire events. The interaction is complicated by fire acting both as one of the agents of mortality and as a process that reduces the CWD standing stock. Some of the major uncertainties include the tree mortality and recruitment rates, the fire consumption rate, termite effects, and interaction of fire with the forest floor microclimate (Hanula et al. 2012).

Harvesting

Harvesting trees to promote restoration goals or to provide revenue is an important management tool in longleaf pine stands (Alavalapati et al. 2002, Gagnon et al. 2003, Johnson and Gjerstad 2007). In order to accommodate a range of harvest management goals, we implemented a single tree and group selection harvest simulation. In each case the user specifies the frequency (return time) and intensity of harvest. Only trees greater than or equal to 10 cm diameter are removed in a harvest event. Outputs from the simulated harvests include the number of trees and stem wood mass removed.

Group selection within the grid of cells Figure 16.6) can range from 0.04 to 0.3025 ha (2.5 to 19% of the 1.56 ha area). Because the gaps are selected as a range of cells to be harvested, the gaps must be selected from this list of sizes: 0.04, 0.0625, 0.09, 0.1225, 0.16, 0.2025, 0.25, and 0.3025.
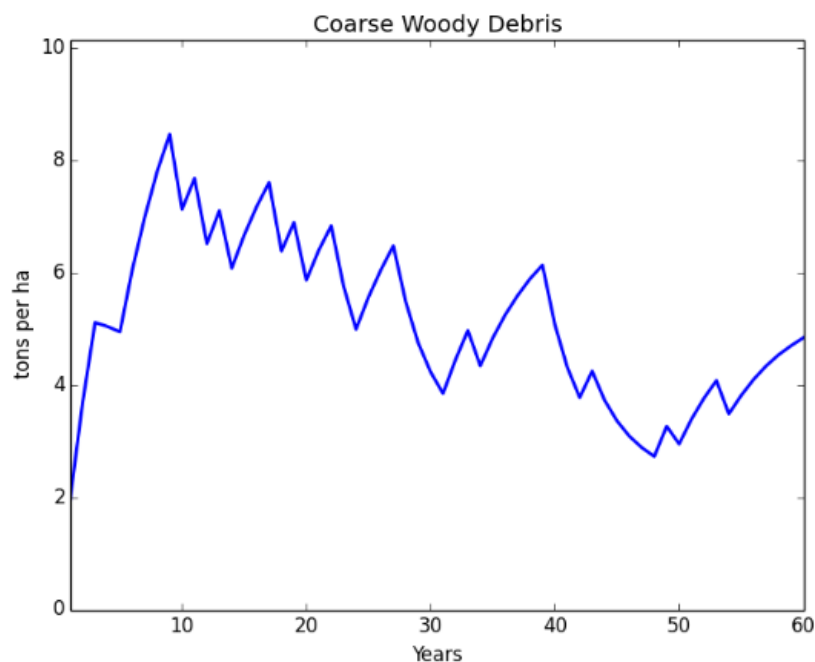
Figure 16.5. Representative simulation of coarse woody debris using the extended LLM-ST model.

For each harvest event, a random location is selected to be the upper left corner of the harvested area. Each longleaf pine greater than 10 cm diameter is removed from all of the cells in the harvest block. This approach can lead to a variable number of trees harvested, depending on the local stand density.

With single tree harvest, the user specifies the harvesting frequency and the target number of trees to be removed. It should be noted that the stand development is stochastic and a target number of harvested trees might not be consistent with maintaining a longleaf pine forest with high non-timber values. The user interface limits the range of the number of target tree harvested to 10-129, equivalent to between 6 and 83 trees per ha removed. Trees for harvest are randomly selected, but if the harvest target is not met, then the harvest loop will be stopped after 700 iterations.

Model evaluation

The modeling framework is based on the idea of converting an even-aged stand to an old growth longleaf pine savanna. Although the individual models have been compared to measured data (Loudermilk et al. 2011, Gonzalez-Benecke et al. 2015), there is no direct comparison possible for the full range of simulated stand development. Somewhat surprisingly, the LLM-ST model has a tendency to converge on similar stand structures (an open low density savanna) after about 10 decades of frequent fire management (Figure 16.7).

Figure 16.6. Randomly selected cells for group selection harvest. The stand is connected at the edges to form periodic boundary conditions (toroidal).
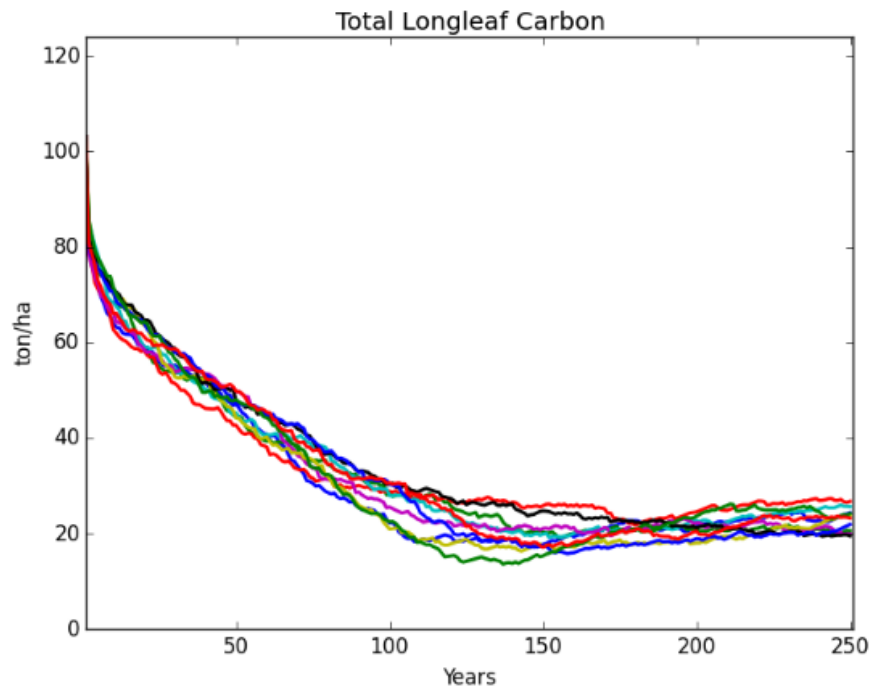
Figure 16.7. Stand level longleaf carbon simulation starting from an even-aged plantation under a fire return time of 3 years. Ten runs of the stochastic model are plotted.

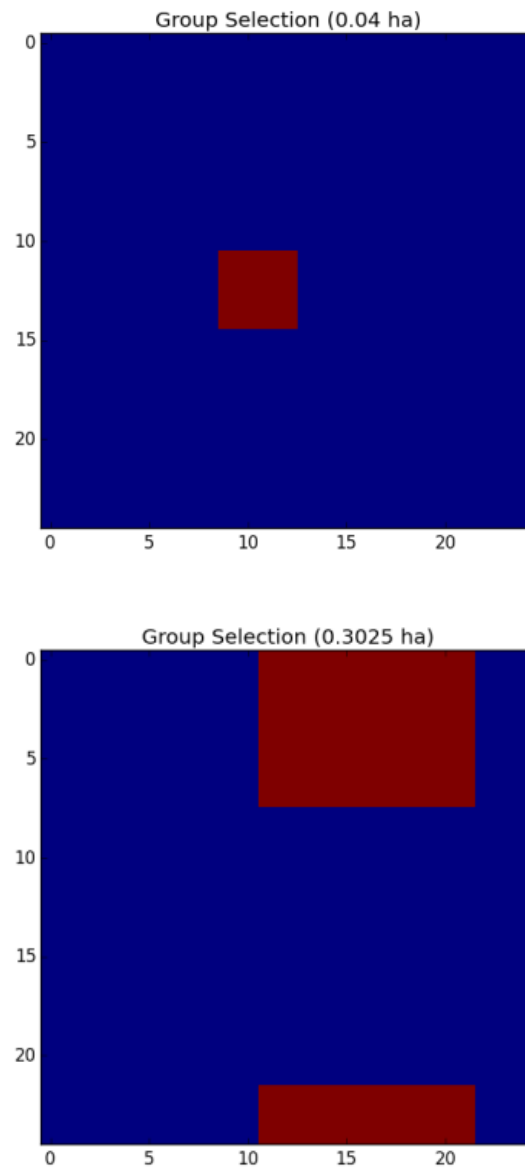One of the largest model uncertainties concerns the long-term rates of mortality and recruitment of longleaf pine under this fire regime. The size-specific longleaf survivorship was largely derived from the work of Platt et al. (1988). These data are limited by relatively short observation times for individuals in a long-lived species. Similarly, the recruitment parameters are difficult to estimate in the field and largely represent values that balance the simulated mortality.

Longleaf stands simulated over 250 years had characteristics generally similar to published values compiled for uneven-aged old growth longleaf pine savannas in Montane and Coastal Plain stands (Varner et al.. 2003) for (e.g. mean dbh = 20.2 cm, maximum dbh = 44.1 cm; mean height = 14.2 m, maximum = 31.6 m; mean age = 65.6 years, maximum = 310 years). One area of possible concern with this comparison is the maximum dbh of the oldest longleaf pines. The simulated value of 44.1 cm is substantially lower than old growth values between 82 and 106.5 cm reported for coastal plain old growth stands (Varner et al. 2003). Investigation of this mismatch led to the discovery that the simulated longleaf pines never reached the asymptotic height, and therefore diameters were determined by the allometric relation between height and dbh, and were not calculated by the function for diameter growth at maximum height.

The harvesting simulations are also difficult to evaluate in a stochastic simulation framework. Both the single tree and group selection methods rely on a random selection of trees to be harvested. For the single tree harvest, there is no consideration of the distance between selected trees. In both

cases, tree selection is independent for each subsequent harvest. For larger group selections there is a reasonable chance of overlap of previous harvest areas.

Sensitivity Analysis Results

Sensitivity analysis is one type of analysis to diagnose how models outputs would be affected by initial parameters or how sensitive or responsive those outputs would be to changes in parameter values. Sensitivity analysis of stochastic models can be more difficult than with a strictly deterministic model, particularly with more complex models (Prowse et al. 2016). We used multiple runs of the LLM-ST with the same initial tree list. Trees in this list are randomly assigned x,y coordinates at the start of the simulation. Multiple runs of the model allowed us to evaluate the sensitivity of the model to tree placement.

Additional sensitivity analyses to the LLM included mean fire return times ranging between 2 and 10 years. Fire return time is generally considered to be a key variable controlling the dominant species and forest structure of longleaf pine savannas, and in an earlier version of the LLM-ST (Loudermilk et al. 2011). Although we initially chose 2, 3, and 4 years, later on we also added 10 years due to lack of variance sensitivity to relatively frequent fire return times.

Each set of simulation conditions was run 15 times consecutively to better evaluate the sensitivity of the stochastic model. That is, for each of the fire intervals evaluated, we ran the simulation 15 times and obtained a total of 60 simulation results. Then, we merged these four sets of 15 simulation results separately, and calculated the mean of selected response variables, including dbh, height, age, wiregrass, basal area, CWD, and stand carbon stocks. dbh, stand carbon stocks, and CWD were not calculated in the original version of the LLM-ST (Loudermilk et al. 2011). The sensitivity of these parameters to fire interval is evaluated here for the first time.

Since the simulation results for the years 3 and 4 yielded similar estimates, we dropped the year 3, and only used year 2, 4, and 10. As a final step, we evaluated the effect of varying simulation length. Initially, we chose a simulation length of 50 years. However, after observing relatively small sensitivity, and recognizing that these long-lived trees were still heavily included by the initial stand after 50 years, we extended the simulation length from 50 years to 250 years. We used two different software packages, the Python programming language (v. 2.5.6, Python Software Foundation) and RStudio integrated development environment (Version 0.99.486 – © 2009-2015 RStudio, Inc.), to visualize the simulation results. First, we ran the models by using Python, and then we used RStudio to calculate the mean values for output variables.

Fire return interval is an important management consideration in longleaf pine savannas. A useful simulation model for these forests should model how the forest structure responds to altered fire regimes. Figures 16.8 and 16.9 show longleaf pine mean dbh is affected by fire return times for simulation periods of 50 years and 250 years. The sensitivity of longleaf pine dbh distribution to fire return time is not large when we have the fire return times ranging between 2 and 10 years. However, we found a significant difference when we extended the simulation length from 50 years to 250 years (Figure 16.9). In addition, the longleaf pine mean dbh is 21.1 cm when we simulate a fire return time for 2 years and 31.7 cm with fire return times of 10 years. This pattern might be

the result of suppressed longleaf recruitment due to increased competition from hardwoods released from fire control. This hypothesis is supported by the dbh distribution from a single representative run (Figure 16.10).

50 year

250 year

Figure. 16.8. Mean simulated longleaf pine diameter at breast height after 50 years of post-plantation management. Results are for fire return times of 2, 4, and 10 years.
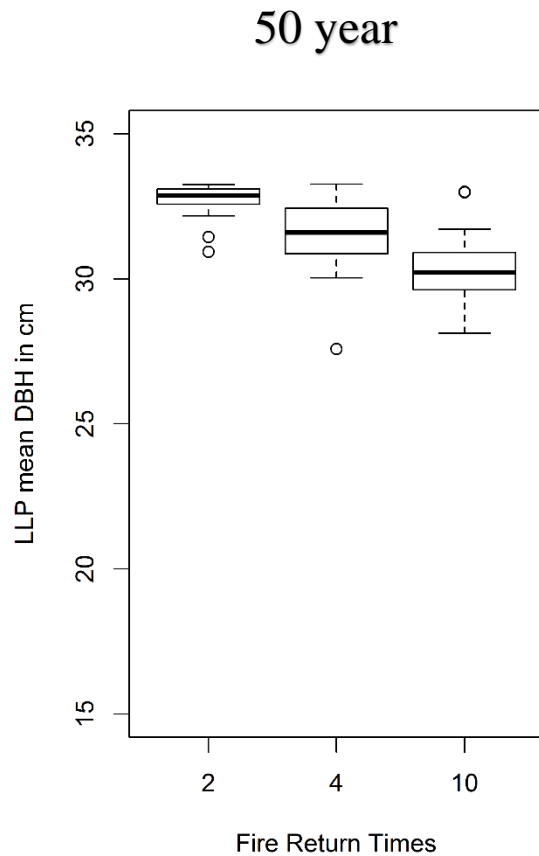
Figure.16.9. Mean simulated longleaf pine diameter at breast height after 250 years of post-plantation management. Results are for fire return times of 2, 4, and 10 years.
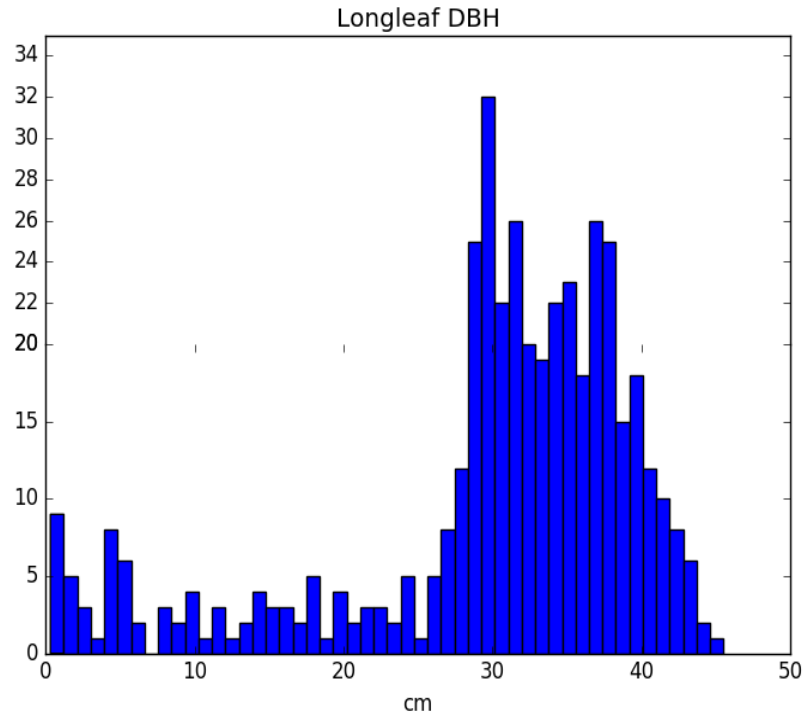
Figure 16.10 Frequency within a simulated longleaf pine stand of diameter at breast height with a fire return time of 10 years.

Figures 16.11 and 16.12 show that longleaf pine mean height is affected by the fire return times for simulation periods of 50 years and 250 years. In Figure 16.11 the variation is not significantly different to the fire return times ranging between 2 and 10 years. On the other hand, in Figure 16.12 the difference is significant when we extended the simulation length from 50 years to 250 years. Figure 16.12 also shows that longleaf pine mean height is 15.7 meters when we simulate a fire return time for 2 years and 26.4 meters with a fire return times of 10 years. These results show that fire return times affect longleaf pine recruitment at 250 years. Similar to mean dbh results, mortality rate goes up while the recruitment rate goes down for the mean height when the fire return time increases from 2 years to 10 years.

Figures 16.13 and 16.14 show that longleaf pine mean basal area is affected by the fire return times for simulation periods of 50 years and 250 years. We estimate in Figure 16.13 that the change is not significantly different to the fire return times between 2 and 10 years. In Figure 16.14, we observed a larger difference compared to Figure 16.9 and 16.12 for 2-year and 10-year intervals when we extended the simulation length from 50 years to 250 years. Figure 16.14 also shows that longleaf pine mean basal area is 8.49 m^2 ha^{-1} when the fire return time is 2 years and 22.06 m^2 ha^{-1} with fire return times at 10 years. These results demonstrate that fire return times affect mortality and recruitment at 250 years. Similar to mean dbh and mean height results, mortality rate increases, while the recruitment rate decreases for the mean basal area when fire return time is increased from 2 years to 10 years.
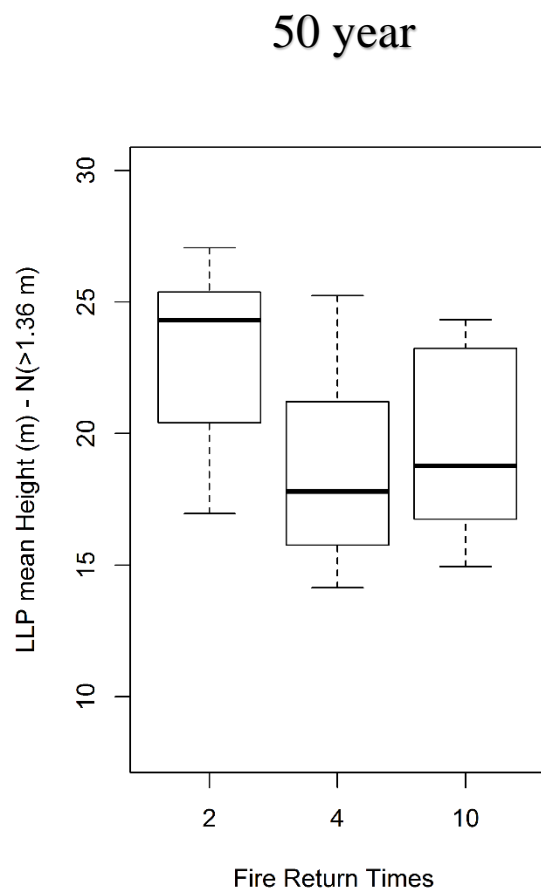
50 year

250 year

Figure. 16.11. Mean simulated longleaf pine height after 50 years of post-plantation management. Results are for fire return times of 2, 4, and 10 years.

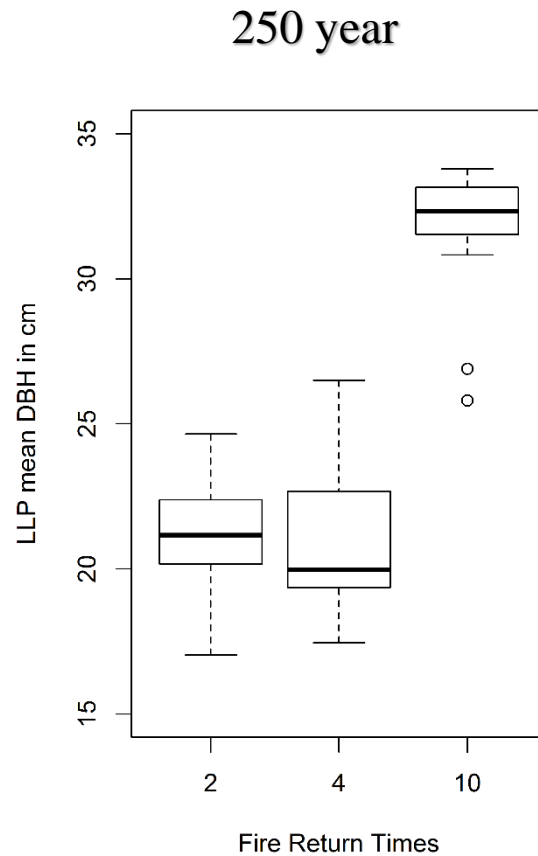Figure. 16.12. Mean simulated longleaf pine height after 250 years of post-plantation management. Results are for fire return times of 2, 4, and 10 years.

50 year

250 year

Figure. 16.13. Mean simulated longleaf pine stand basal area after 50 years of post-plantation management. Results are for fire return times of 2, 4, and 10 years.

Figure. 16.14. Mean simulated longleaf pine stand basal area after 250 years of post-plantation management. Results are for fire return times of 2, 4, and 10 years.

Longleaf pine mean CWD is influenced by fire return times in 50 years and 250 years (Figures 16.15 and 16.16). Fire return times between 2 and 10 years do not change the mean stock of CWD dramatically (Figure 16.15). One of the processes that influence the standing crop of CWD is tree mortality. Although mature longleaf pines generally experience low mortality rates (Platt et al. 1988), mature trees have a small chance of fire-induced mortality. The other main process affecting the response of CWD to fire is the fraction of the CWD that is consumed by fire (20% per fire event). Decreasing fire frequency eventually leads to decreased loss and increased CWD standing stock (Figure 16.15). However, in Figure 16.15 we observe a significant difference compared to Figure 16.16 for 2-year and 10-year intervals when we extended the simulation length from 50 years to 250 years. Coarse woody debris is 1.77 ton ha^{-1} when we simulate a fire return time for 2 years and 0.66 ton ha^{-1} when fire return times are at 10 years. Coarse woody debris is 1.769 ton

ha^{-1} when we setup fire return time for 2 years and 0.665 ton ha^{-1} when fire return times at 10 years. This pattern is likely to be the result of decreased longleaf pine CWD production due to the suppression of regeneration and the long-term decrease in the longleaf pine population as hardwoods become more dominant.

50 year

250 year

Figure 16.15. Mean simulated longleaf pine stand coarse woody debris mass after 50 years of post-plantation management. Results are for fire return times of 2, 4, and 10 years.
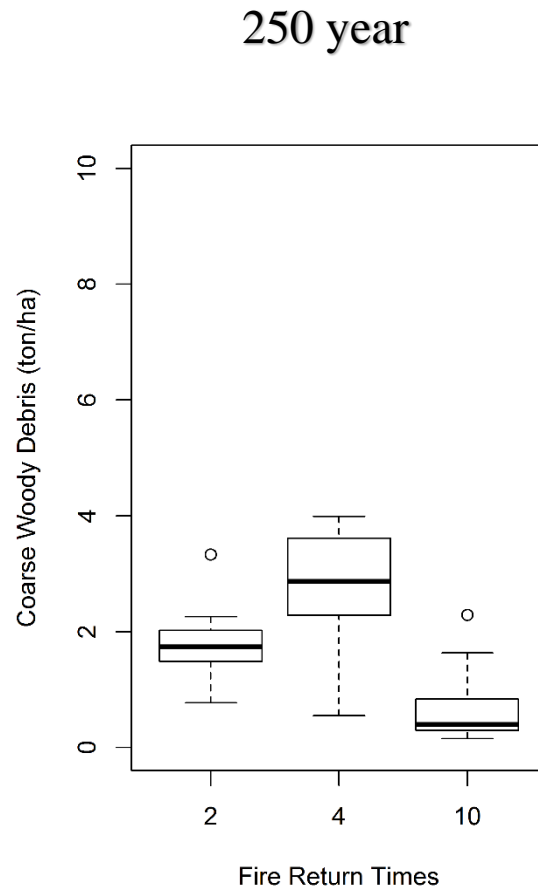
Figure 16.16. Mean simulated longleaf pine stand coarse woody debris mass after 250 years of post-plantation management. Results are for fire return times of 2, 4, and 10 years.

Figure 16.17 and 16.18 show that total carbon stock for longleaf pine decreases in the length-extended simulations. This is likely to be a direct result of the long-term decrease in the longleaf pine population. On the other hand, total carbon stock for hardwood increases in the simulations at 250 years, particularly for the fire return times at 10 years, compared to the simulations at 50 years (Figure 16.19 and 16.20). We can infer that this increase stems from hardwood dominance in the long-term.
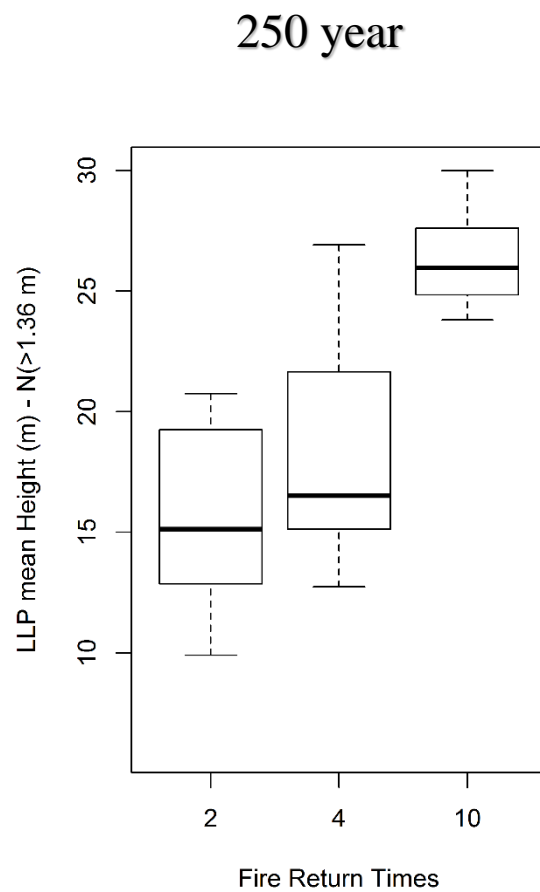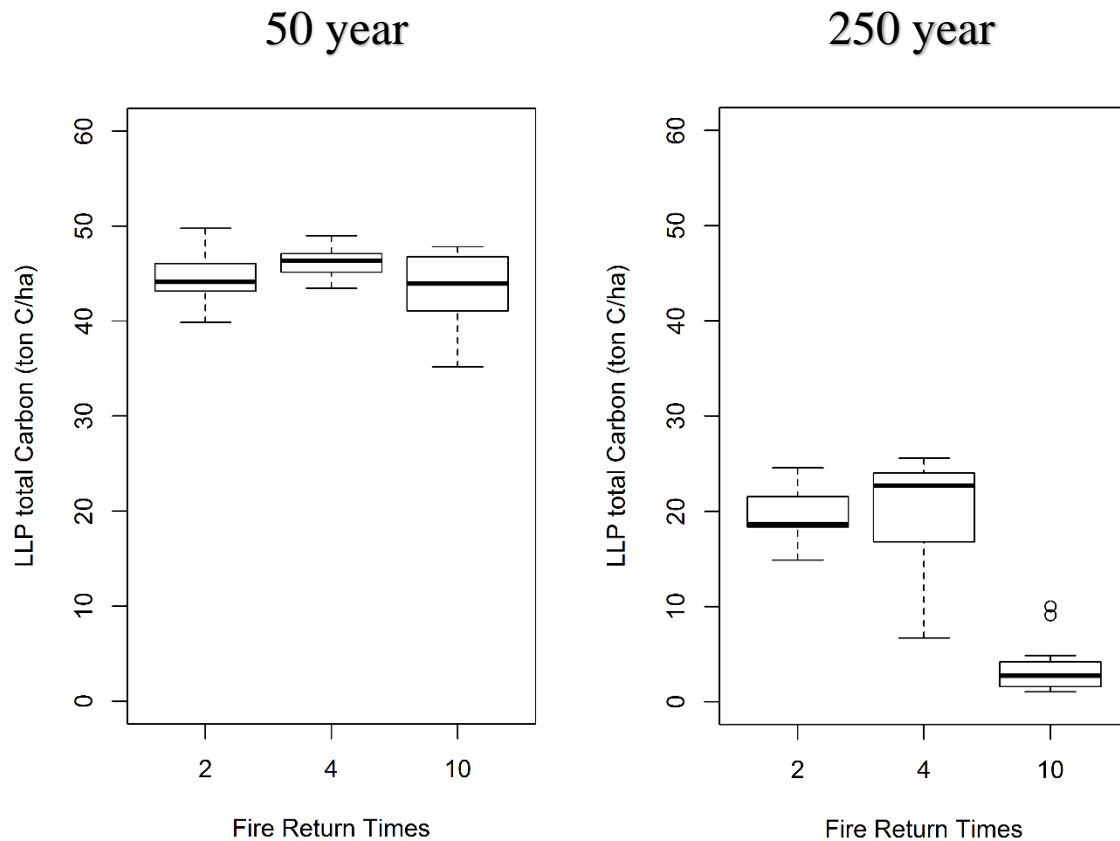

Figure 16.17. Mean simulated longleaf pine stand living carbon mass after 50 years of post-plantation management. Results are for fire return times of 2, 4, and 10 years.

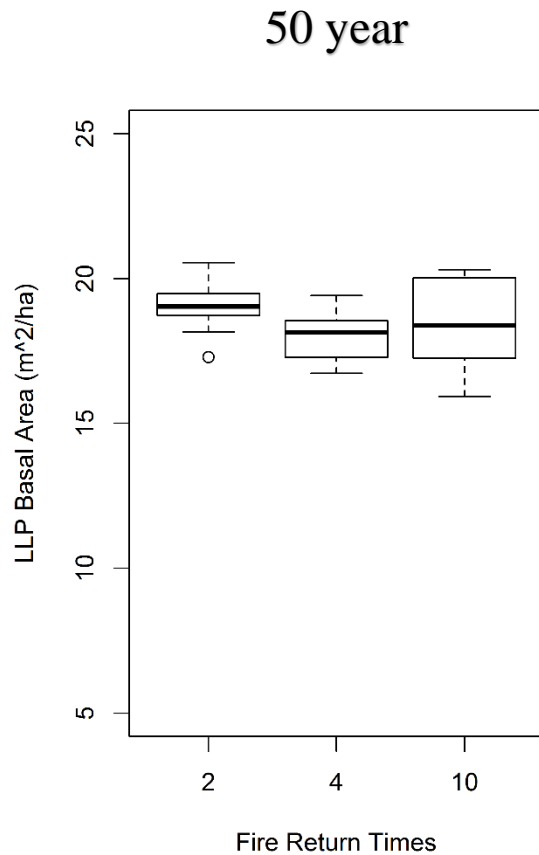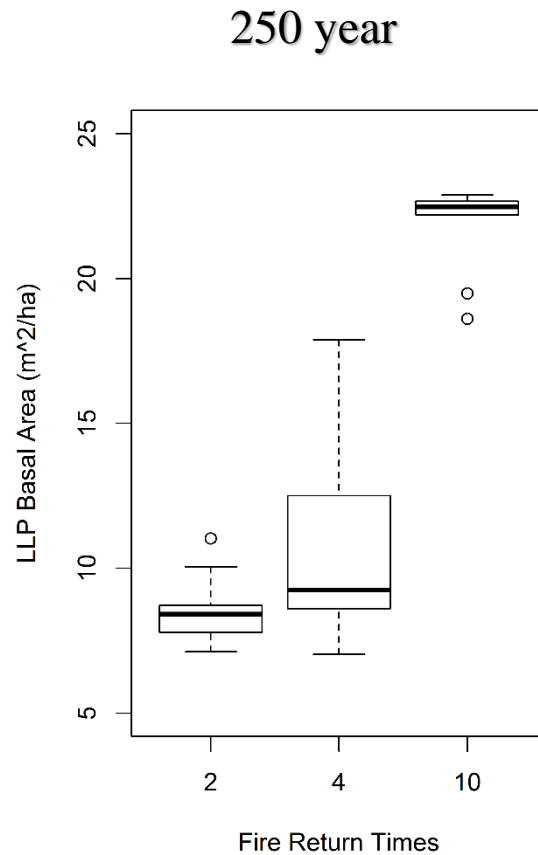Figure 16.18. Mean simulated longleaf pine stand living carbon mass after 250 years of post-plantation management. Results are for fire return times of 2, 4, and 10 years.
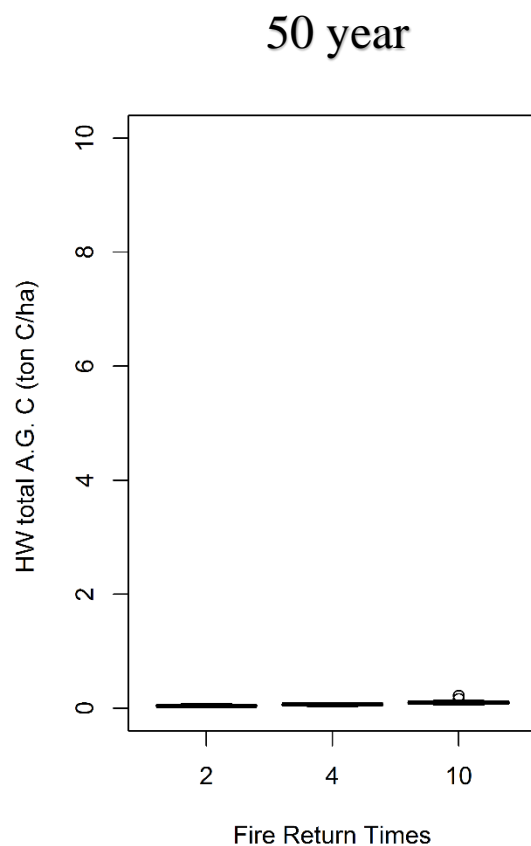
50 year

250 year

Figure 16.19. Mean simulated hardwood living above-ground carbon mass after 50 years of post-plantation management. Results are for fire return times of 2, 4, and 10 years.
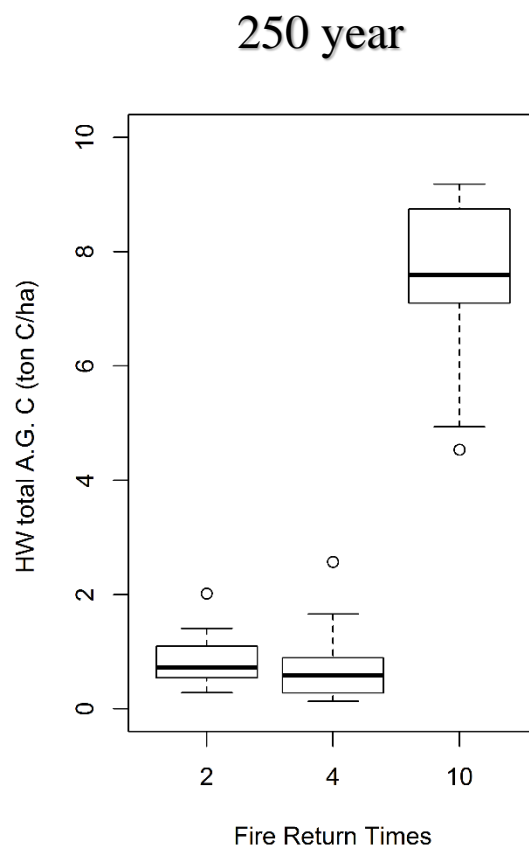
Figure 16.20. Mean simulated hardwood living above-ground carbon mass after 250 years of post-plantation management. Results are for fire return times of 2, 4, and 10 years.

Overall, Figure 16.21 shows that the total carbon for longleaf pine and hardwood combined is 44.54 ton C ha^{-1} when we setup fire return time for 2 years and 43.53 ton ha^{-1} with fire return times at 10 years. Total carbon for longleaf pine and hardwood becomes 20.65 ton C ha^{-1} when we setup the fire return time for 2 years and 11.15 ton ha^{-1} with fire return times at 10 years when we extended the simulation length to 250 years (Figure 16.22). Yet, these results show that hardwood does not influence the total carbon stocks for short-term, whereas hardwood has a small effect in the long-term due to increase in the hardwood population.
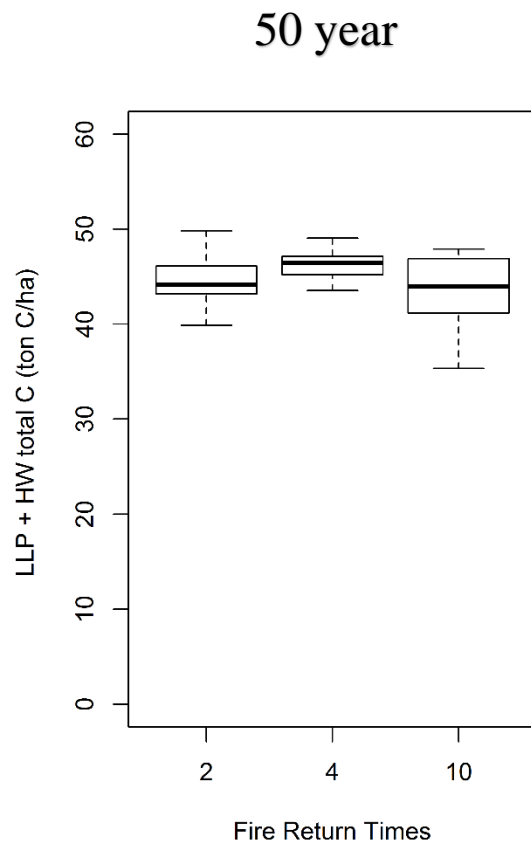
50 year

250 year
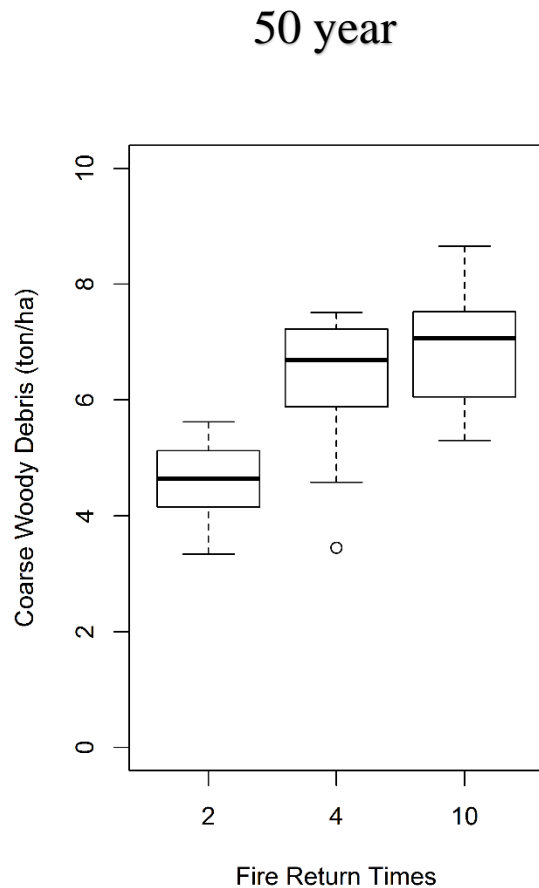
Figure 16.21. Mean simulated hardwood and longleaf pine carbon mass after 50 years of post-plantation management. Results are for fire return times of 2, 4, and 10 years.
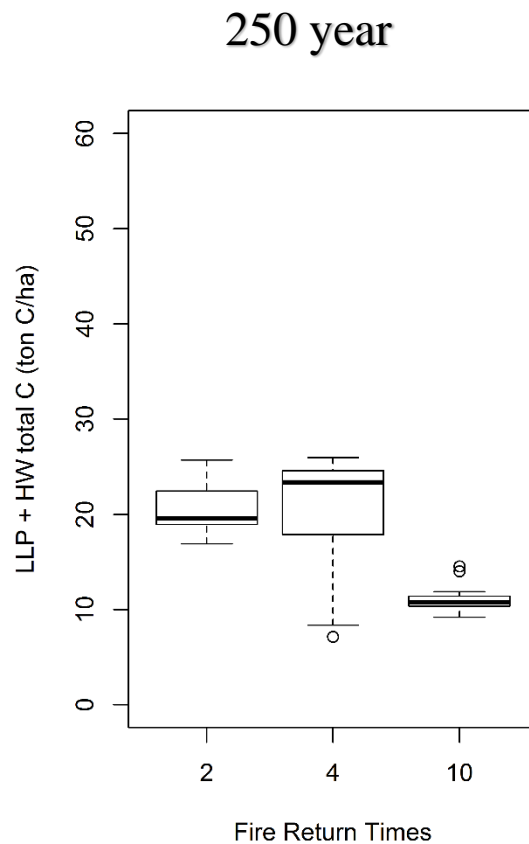
Figure 16.22 Mean simulated hardwood and longleaf pine carbon mass after 250 years of post-plantation management. Results are for fire return times of 2, 4, and 10 years.

Harvesting Simulation Results

There are many possible forest management regimes that can be used to optimize revenue (Silver et al. 2015), protect biodiversity (Brockway and Outcalt 2015), or enhance ecosystem services. It is not likely possible to optimize for all of these objectives simultaneously (Lutz et al. 2015). One consideration for long-term forest management is the concept of sustainable forestry. If the recruitment and competition release following harvest leads to growth greater than or equal to the

biomass removed, the harvest regime can be considered sustainable over some defined time period. We will examine this first by assessing the recovery following a single harvest event.

The simulated single tree harvest scheme randomly selects trees greater than 10 cm dbh in the stand at a set target intensity (16–35 trees ha^{-1} to be removed) and at a set time interval between harvests. Much of the dynamics of the response to a harvest event occurs in a few decades following the harvest. Comparing the temporal response from 10 to 40 years following a single harvest allows a qualitative assessment of stand recovery.

Tree biomass and carbon storage are of interest both in terms of timber products and in terms of habitat quality. Aboveground longleaf pine carbon 40 years after harvest with the removal of 16 trees per ha is not different from the no harvest run (Figure 16.23). Larger harvest rates are associated with reduced aboveground C standing stock. There is a general downward trend, independent of harvest intensity that is associated with the transition of plantation to a less dense pine savanna.
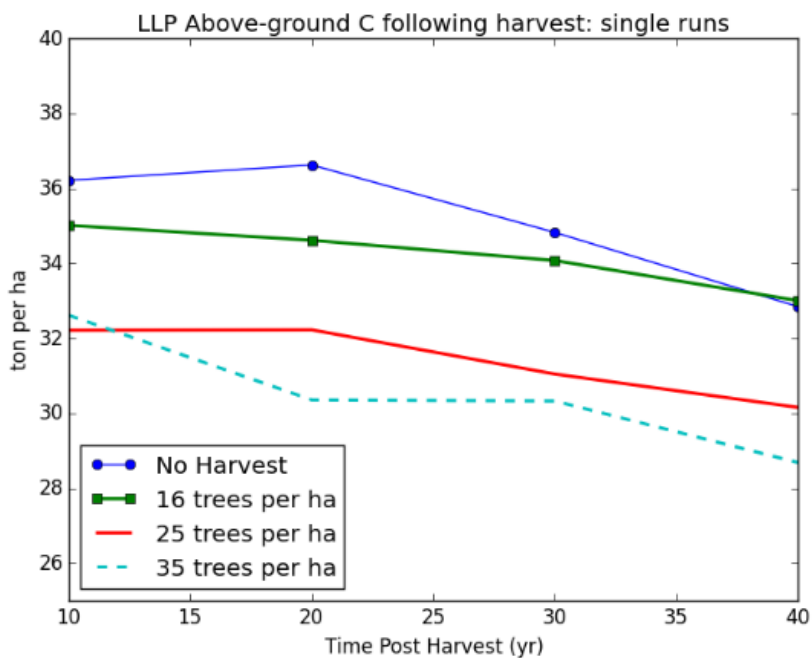
Figure 16.23. Longleaf pine aboveground carbon following single harvest events with tree removals ranging from 16 to 35 trees ha^{-1}.

At the time of 40 years post-harvest, the difference of aboveground longleaf pine standing crop between control and the 35 tree per ha harvest intensity is similar to the difference at 10 years. This implies that caution should be used in applying this harvest intensity with short return times. An alternative to single tree selection is group selection that might provide better longleaf pine regeneration and stand recovery (Gagnon et al. 2003).

The group selection harvest scenarios ranged from 0.04 to 0.2025 ha in area, and led to reductions in longleaf pine aboveground carbon similar to the single tree harvest scenarios

(Figure 16.24). Based on these individual simulations the 0.04 ha harvest area has reached longleaf pine biomass similar to the non-harvested forest after 40 years. Comparing the slopes of the group selections with the non-harvest simulation (Figure 16.24) supports that idea that longleaf pine recruitment was enhanced following gap creation. This response is insufficient to return 0.09 and 0.2025 ha harvest scenarios to control biomass standing pools by 40 years following harvest.
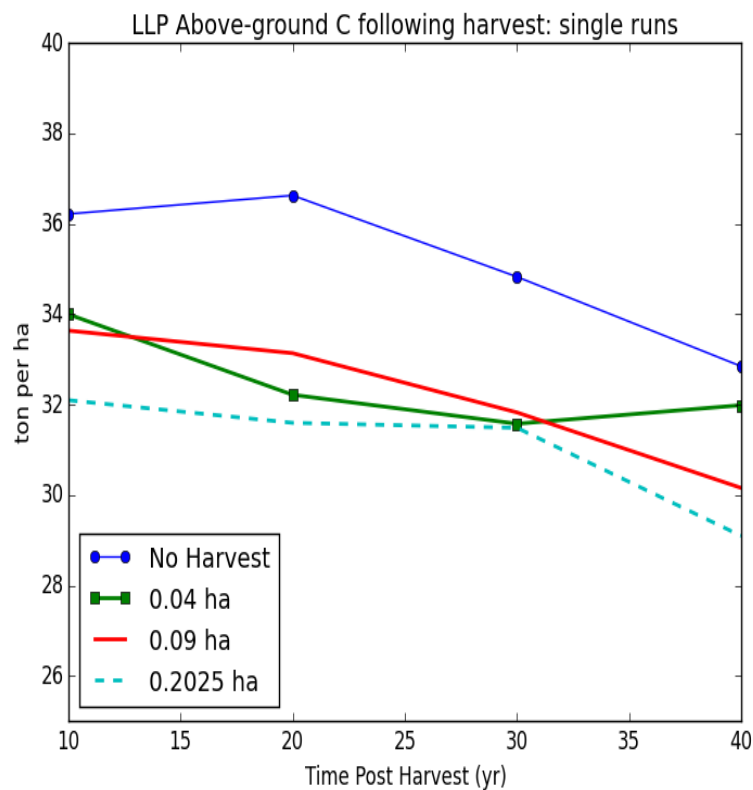
Figure. 16.24. Longleaf pine aboveground carbon following group selection harvest events with tree removals ranging from areas of 0.04 to 0.2025 ha.

Biomass or carbon stocks are not the only considerations for evaluating post-harvest recovery. Stand structure may also be important in terms of habitat quality and aesthetics. One measure of stand structure for a longleaf pine savanna is basal area. Recovery of basal area following harvest was different from the response patterns of above ground carbon stocks. The 0.04 ha group selection had greater basal area 20 to 40 years following the harvest event (Figure 16.25). The largest gap area harvest had linearly increasing basal area until 40 years following harvest. These trends can be attributed to enhanced recruitment and increased growth of the remaining trees due to competitive release.
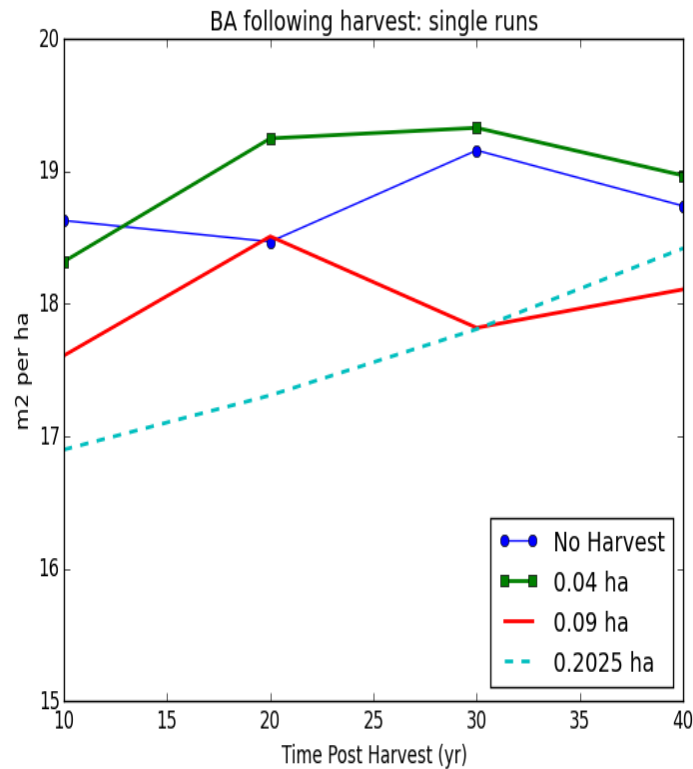
Figure 16.25. Longleaf pine basal area (BA) following group selection harvest events with tree removals ranging from areas of 0.04 to 0.2025 ha.

The harvest regime can be defined as the intensity of harvest (number and size of trees harvested) and the time interval between harvests. Several aspects of the simulated harvest regime include stochastic components. Each run of the model starts with the trees randomly assigned locations within the grid. Mortality and recruitment events are stochastic processes that alter the forest structure and composition (longleaf versus hardwood). Additionally, the areas selected for group harvest and the trees selected in the individual selection simulations are chosen randomly. In order to better understand the dynamics of forest response to harvesting, each harvest treatment is simulated 15 times and we report means at stand ages of 50 years and 250 years after plantation management is converted to old growth management. To characterize the forest attributes following harvests we use longleaf pine dbh, height, and basal area. Carbon storage and biomass are represented by mean CWD mass and living longleaf pine total carbon standing crop. Finally, we also report mean hardwood carbon standing crops.

Stand structure for the 50 year simulations is highly influenced by the initial conditions of the plantation at the start of the simulation. After 250 years of simulation without harvest, the longleaf pine stand has attributes similar to an old growth savanna (see Model Framework section). It is useful to examine these endpoints because human managers generally focus on relatively short-term time spans that might not adequately represent long-term sustainability.

256

The most intense single-tree selection simulated harvest regime (a target of 35 trees ha^{-1} every 20 years) results in relatively low standing carbon stock (Figure 16.26). It is questionable if this type of harvest would be sustainable in the real world that includes insect pests, wildfires, and extreme climate events. One reason that the drop off in longleaf carbon is not even more severe is that it becomes increasingly difficult to find the target number of trees greater than 10 cm dbh (Figure 16.27), resulting in smaller removals, and therefore reductions in stand carbon, as the simulation progresses.
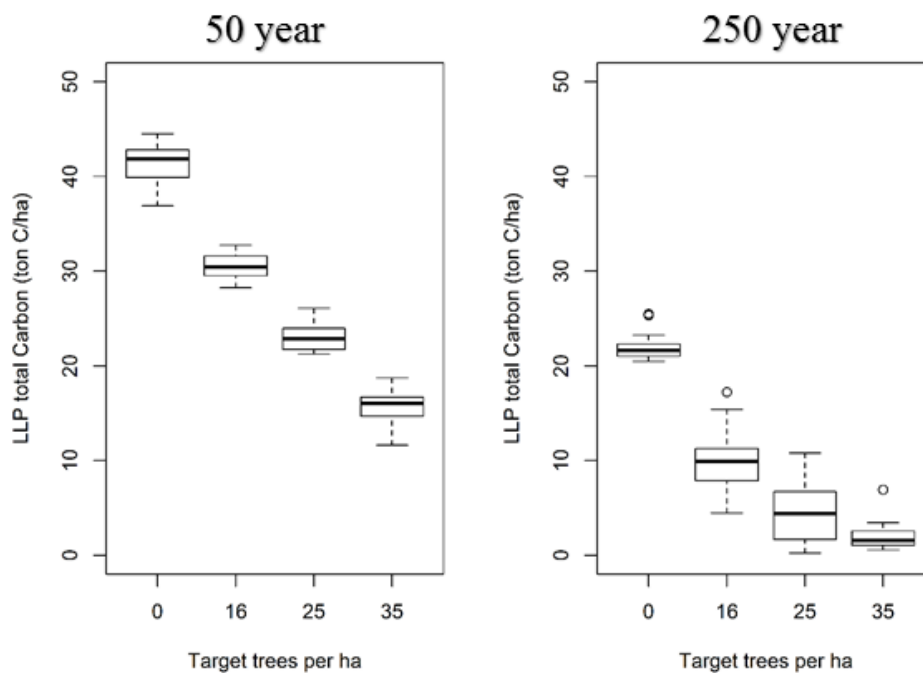
Figure 16.26. Mean longleaf pine stand carbon stock from 15 simulations at 50 and 250 years from plantation conversion with harvest return times of 20 years.
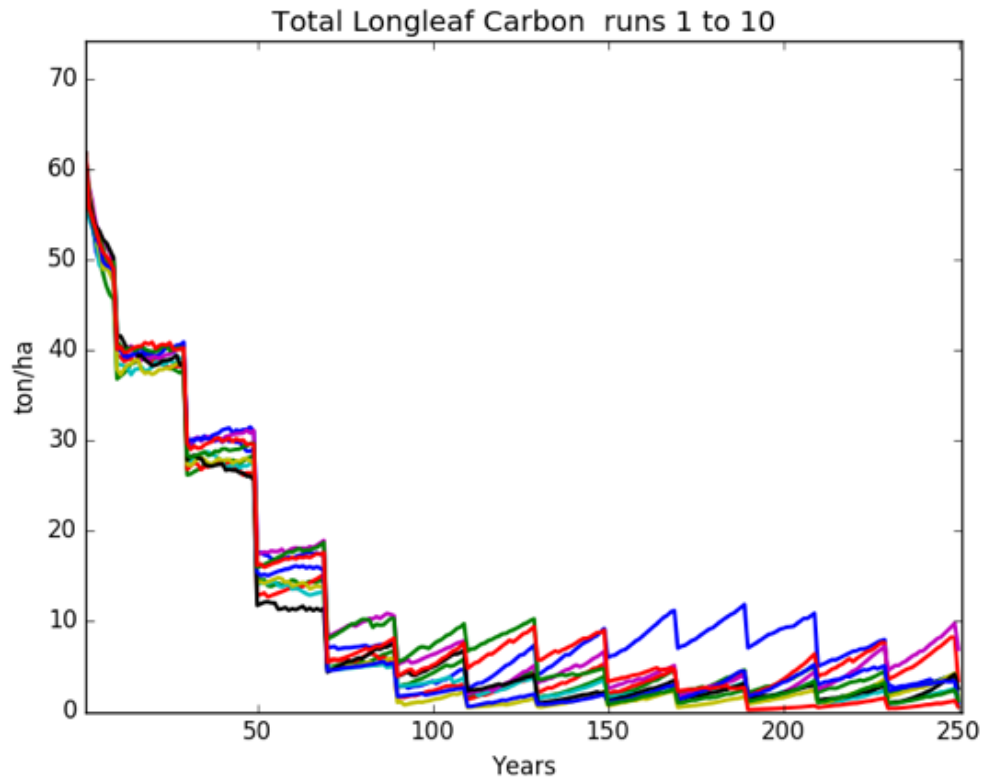
Figure 16.27. Total stand longleaf pine carbon with a harvest target of 35 trees per harvest every 20 years.

Although the mean dbh for a harvest target of 35 trees ha^{-1} every 20 years is above 10 cm by the end of the simulation period, the mean is highly sensitive to a few very large trees in the harvestable size class at the end of the simulation (Figure 16.28). The algorithm used to select trees will exit before reaching the selected target if trees of 10 cm dbh are rare in the stand. Interpretations of trends in mean height (Figure 16.29) and diameter could be complicated by an increasing number of longleaf recruits established following harvest. In order to address this issue we present only data for trees greater than 1.36 m height.

Standing biomass carbon and stand basal area (Figure 16.30) provide a better indication of the stand response to harvesting than mean dbh and height trends. There is a strong tendency for decreased basal area with the most intense harvest regimes. It is not surprising that these trends are similar to the reductions in standing stock of longleaf pine stand carbon since basal area is highly correlated with tree biomass. Given these trends, it would be risky to assume that any of these simulated harvest intensities at a return time of 20 years would be sustainable over periods of many decades.
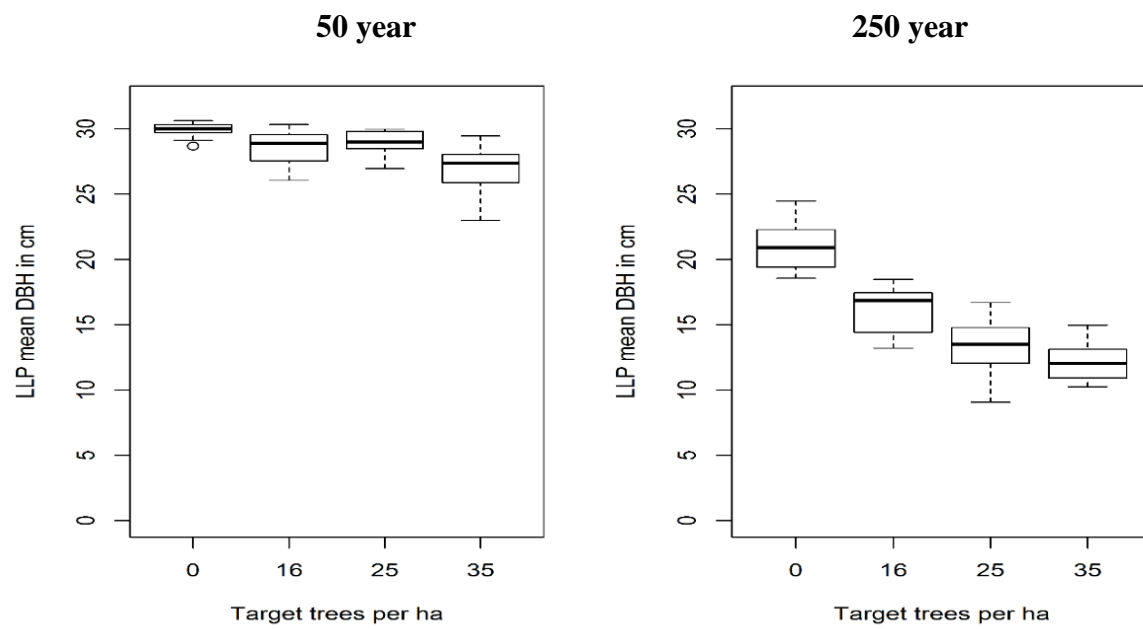
Figure 16.28. Longleaf pine mean dbh for a range of single tree harvesting intensities with harvest return times of 20 years.
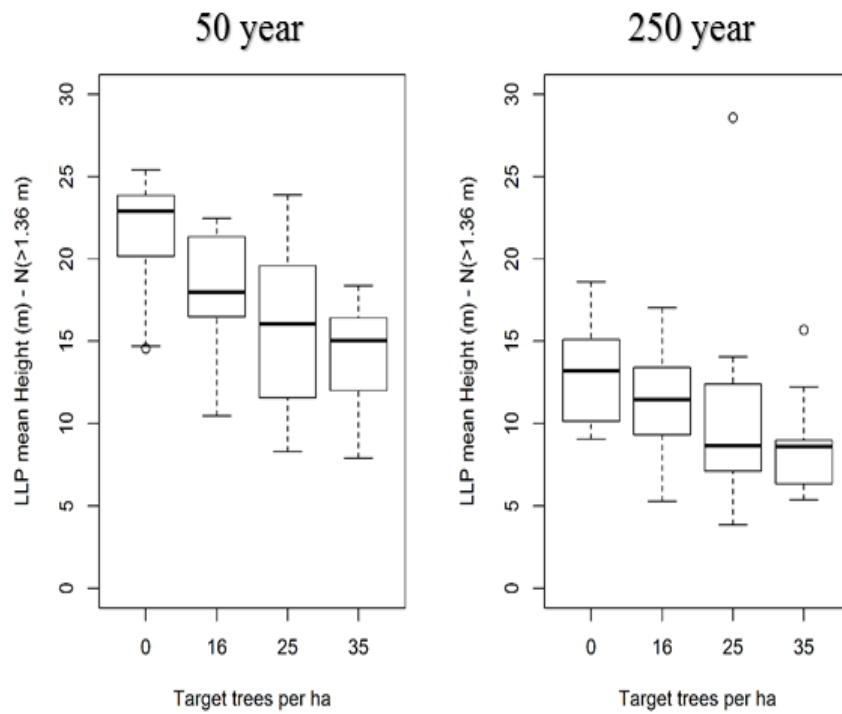
Figure 16.29. Longleaf pine mean height for a range of single tree harvesting intensities with harvest return times of 20 years.
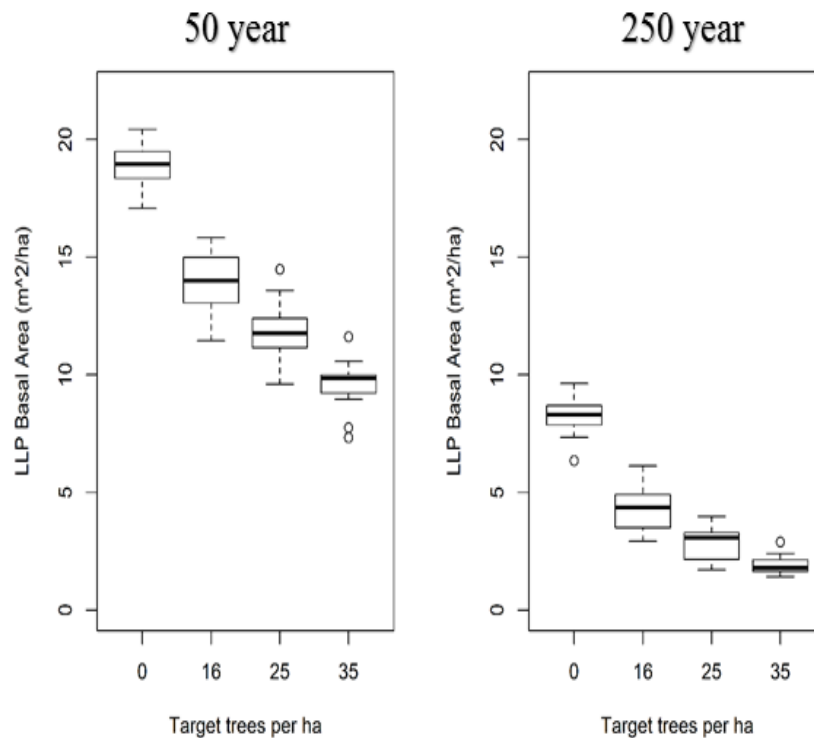
Figure 16.30. Longleaf pine mean stand basal area for a range of single tree harvesting intensities with harvest return times of 20 years.

Although these forests are dominated by longleaf pine, other considerations for evaluating responses to harvest include effects on the hardwood community and the detrital pool. These variables are likely related to habitat quality in longleaf pine savannas (Hanula et al. 2012, Hiers et al. 2014). The major source of coarse woody debris (CWD) in longleaf pine savannas is longleaf tree mortality. It is not surprising the trend of CWD standing stock is decreasing with increased harvest intensity (Figure 16.31). This pool does not include inputs from trees removed in the harvest.

Although oaks and other hardwoods are important parts of longleaf pine savanna biodiversity, they also represent a problem for sustainable management. Given long-term fire suppression, longleaf pine forests will transition to hardwood dominated forests (Hartnett and Krofta 1989, Kush 2016). This process occurs, in part, due to the suppression of longleaf pine regeneration by competing hardwoods. Similarly, an intense harvest regime can release hardwoods for competition and lead to increasing hardwood dominance over long periods (Figure 16.32). The simulated transition to increasing hardwood dominance is relatively slow because we have imposed a savanna fire regime with a return time of three years. With longer fire return times, we would expect hardwood dominance to increase much faster.
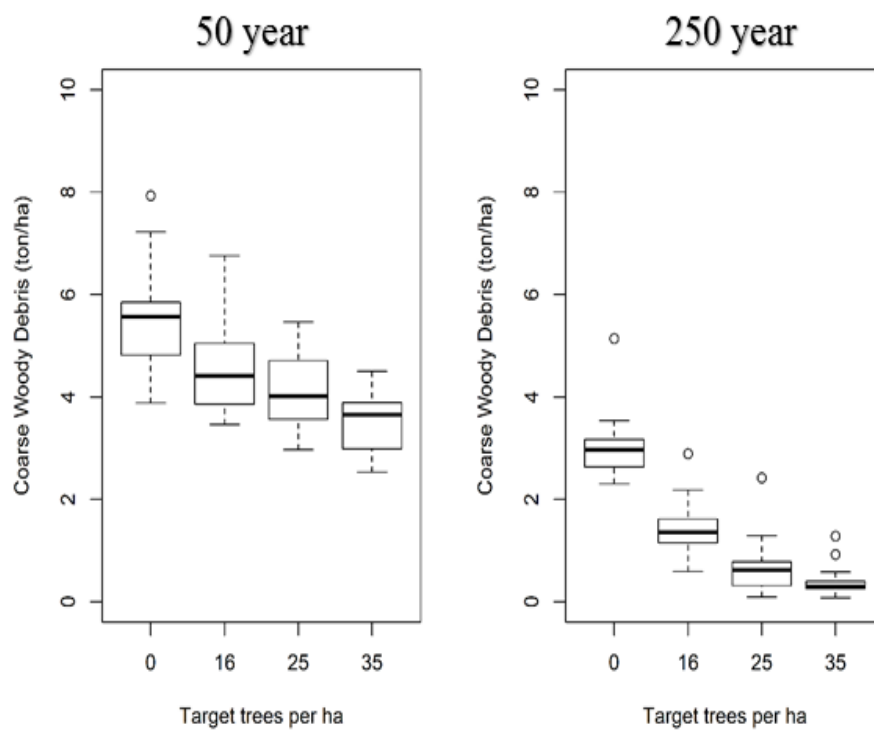
Figure 16.31. Coarse woody debris standing stock for a range of single tree harvesting intensities with harvest return times of 20 years.
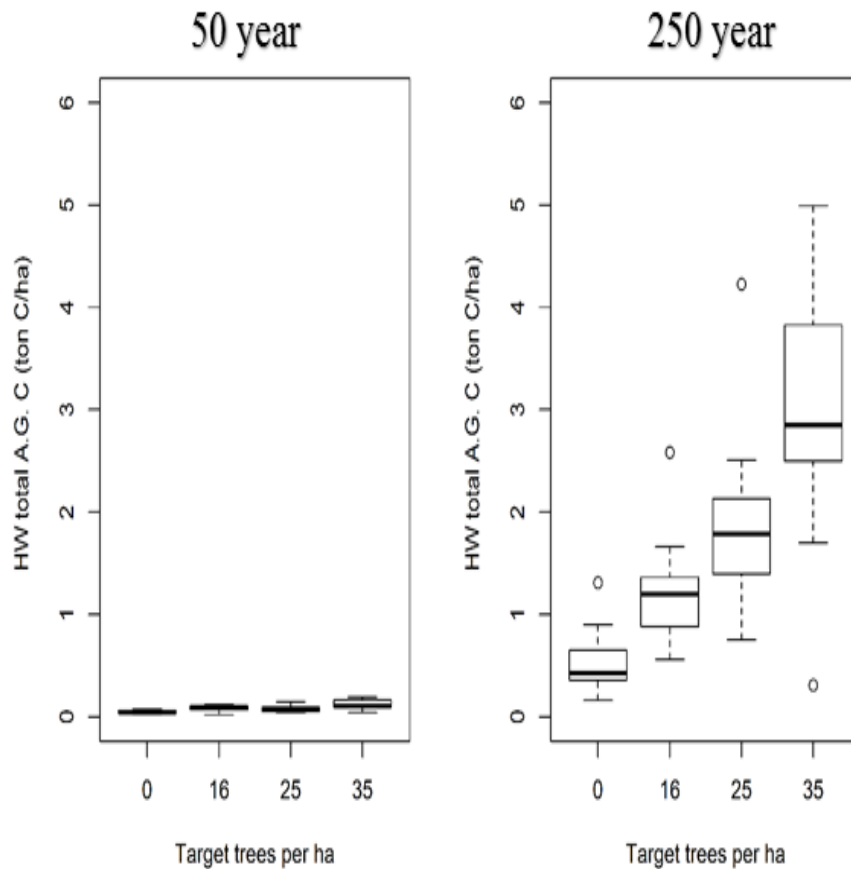
Figure 16.32. Hardwood above-ground biomass for a range of single tree harvesting intensities with harvest return times of 20 years.

A sustainable harvest regime with repeated harvest events should lead to a dynamic quasi steady-state with sufficient recovery of biomass to permit the harvest regime to continue indefinitely. Removing 35 trees (> 10 cm dbh) every 80 years seems to result in this type of equilibrium (Figure 16.33). With a harvest return time of 80 years, the stand retains structural characteristics similar to the unharvested savanna in terms of longleaf age, height, and DBH distributions (Figure 16.34). Additionally, other stand characteristics such as the CWD pool (Figure 16.35), the hardwood aboveground mass (Figure 16.36), and the wiregrass biomass (Figure 16.37) are consistent with a sustainable harvest regime that potentially conserves important aspects of habitat quality and biodiversity. The aboveground wiregrass biomass is highly variable because it reset to zero following the frequent fire events.
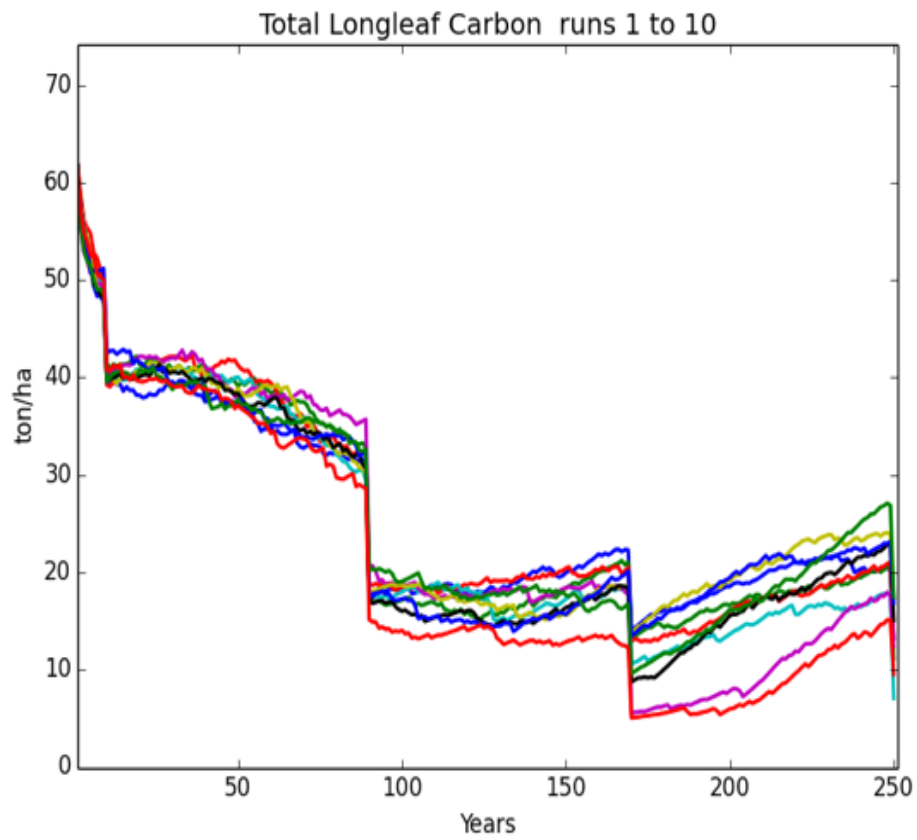
Figure 16.33. Total stand longleaf pine carbon with a harvest target of 35 trees per ha^{-1} every 80 years.
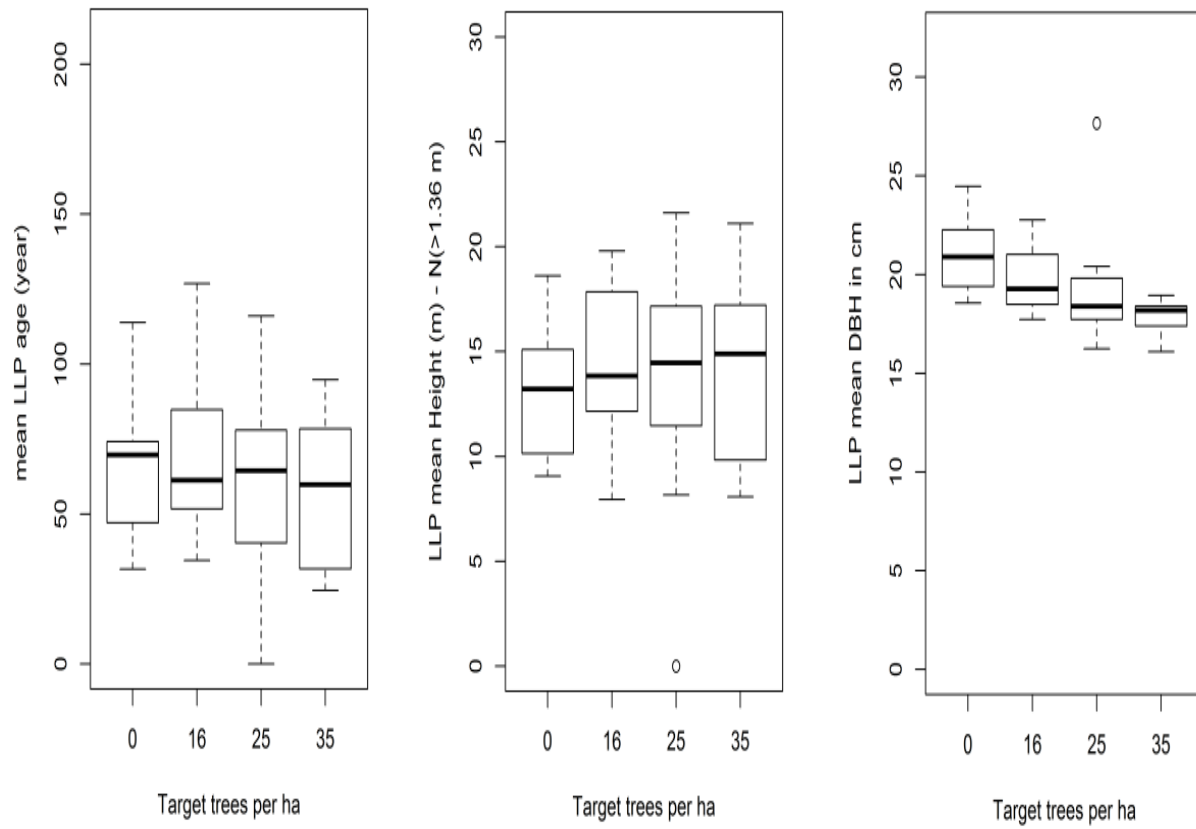
Figure 16.34. Longleaf pine stand structural characteristics with a harvest return time of 80 years.
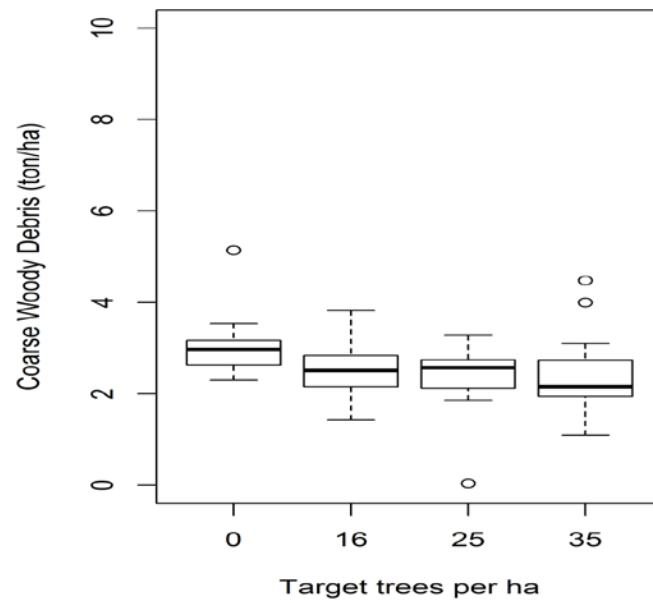
Figure 16.35. Coarse woody debris standing stock for a range of single tree harvesting intensities with harvest return times of 80 years.
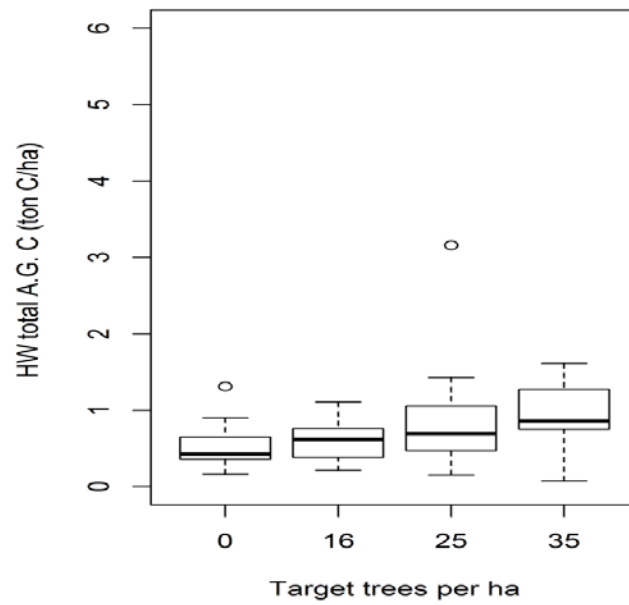
Figure 16.36. Hardwood aboveground biomass for a range of single tree harvesting intensities with harvest return times of 80 years.
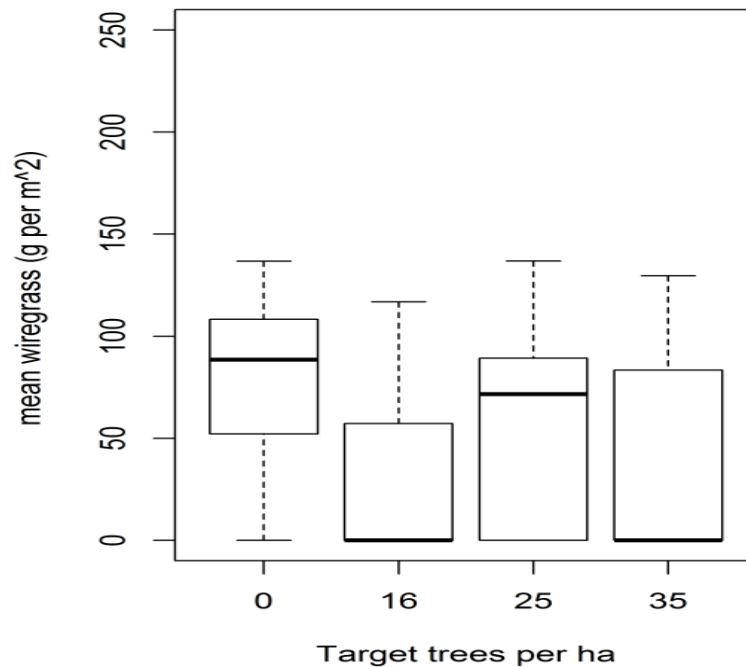
Figure 16.37. Mean wiregrass biomass for harvesting intensities of 16 to 35 trees ha^{-1}.

The harvest regime simulations at a return time of every 20 years do not clearly support a classification of sustainable for any of the modeled harvest intensities. Even the highest single tree harvest intensity (35 trees ha^{-1}) was generally consistent with sustainable timber production with a harvest return time of 80 years. The 40 year post-harvest trajectories (Figures 16.23 – 16.25) are also consistent with relative stability of this system. These results should be used with caution if applied to non-virtual forests. As with any simulation model, the results are a function of the assumptions used to assign parameter values and the structure of the model (equations).

It is useful to also examine the responses to a harvest regime intermediate between return times of 20 and 80 years. Qualitatively, a harvest return time of 40 years seems consistent with sustainable harvesting (Figure 16.38). Although stable, this management regime comes with a cost of lower standing stock of stand longleaf pine carbon (mean difference of 13.64 ton ha^{-1}; Figure 16.39). When a 40 year harvest return time is simulated with the group selection system, biomass is maintained closer to the no harvest simulation (Figure 16.40). The mean standing pool of longleaf pine carbon is reduced from the no harvest 22.01 ton ha^{-1} to 20.44, 19.91, and 16.32 ton ha^{-1} for harvest areas of 0.04 ha, 0.09 ha and 0.2025 ha, respectively. It would be wise to follow an adaptive management approach and carefully evaluate stand recovery before implementing a 40 year return time harvest regime for longleaf pine forests intended to preserve ecosystem services as well as provide revenue from timber harvests.
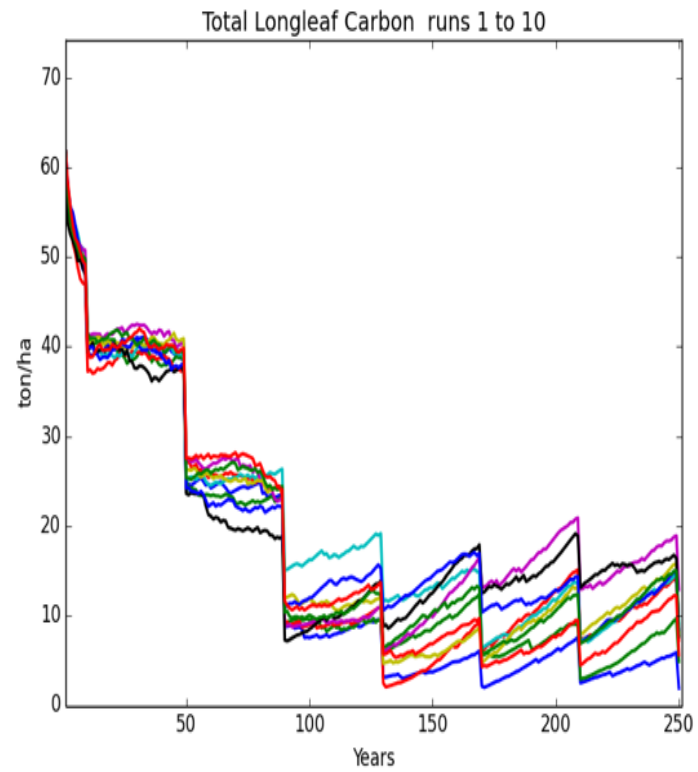
Figure 16.38. Total stand longleaf pine carbon with a harvest regime of 35 trees ha^{-1} targeted for removal every 40 years.
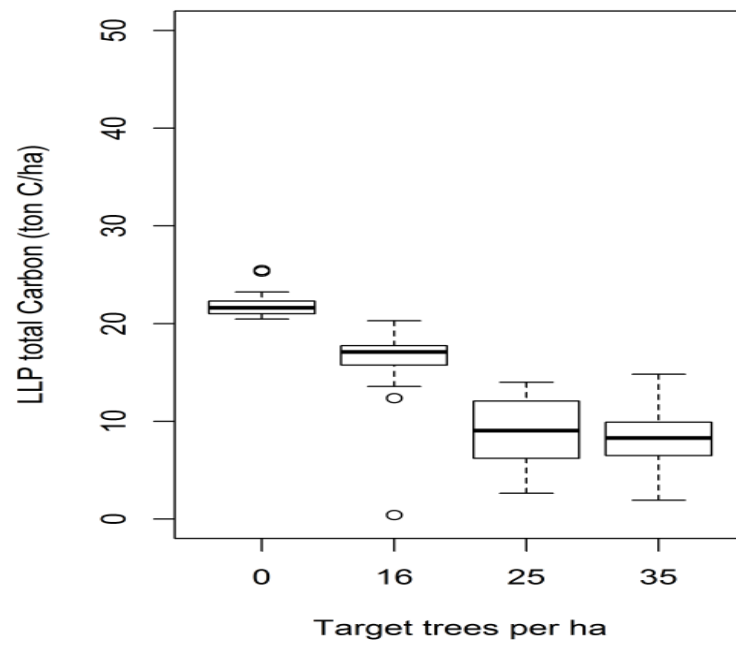
Figure 16.39. Total stand longleaf pine carbon with a harvest regime of 16 to 35 trees ha^{-1} targeted for removal every 40 years.
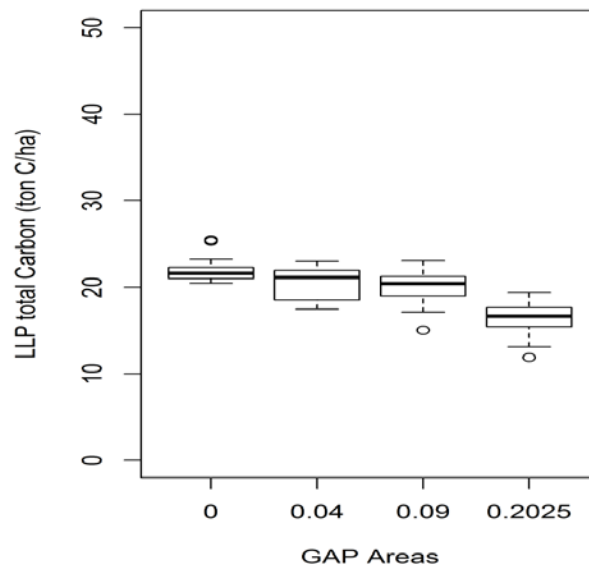
Figure 16.40. Total stand longleaf pine carbon with group selection harvest regimes of 0.04 to 0.2025 ha harvested every 40 years.

Table 16.1. Carbon storage patterns for harvesting scenarios with harvest return times of 20, 40, and 80 years.

Harvest Target	Mean aboveground LLP carbon (ton C ha^{-1})	Mean harvest (15 runs) from year 100 to year 244 (ton C ha^{-1} for one harvest)	Trees per harvest (1.56 ha) from year 100 to 244 (15 runs)
No Harvest	26.69 (4.11)	0.00	0
16 trees per ha every 20 years	16.24 (5.22)	2.08(0.73); 7 in 145 years.	11-25
16 trees every 40 years	20.89 (4.69)	2.52 (0.77); 3 in 145 years	25
16 trees every 80 years	25.10 (5.10)	2.47 (0.72); 1 in 145 years.	25
35 trees every 20 years	7.09 (3.74)	2.07 (0.93)	2-55
35 trees per ha every 40 years	14.40 (5.73)	3.76 (1.12)	15-55
35 trees per ha every 80 years	20.76 (7.46)	5.54 (1.15)	55
	N = 2175; 15 runs with 145 LLP aboveground C values selected from years 100-244		

It has long been understood that longer rotation lengths in managed forests increase the mean standing biomass crop of the trees (Cropper and Ewel 1987). A long-term increase in standing stock of carbon on a site represents sequestration of atmospheric carbon in the forest. In terms of a regular harvest regime, this could be interpreted as avoided emissions when considering the less intensive harvest regimes. Using this framework, the 35 tree ha^{-1} harvest intensity with a frequency of one harvest every 80 years, sequesters 13 tons C ha^{-1} more than harvests occurring every 20 years (Table 16.1). The standing stock of aboveground longleaf pine carbon is approximately the same for a harvest target of 16 trees ha^{-1} every 80 years and the no harvest scenario. It should be noted that all of these scenarios include frequent prescribed fires. The simulations, and our experience with longleaf pine savannas, indicate that carbon lost to fires is quickly recovered.

The mean biomass removed per harvest (associated with the potential economic return from timber sold) tends to be smaller for more frequent harvests (Table 16.1). Assuming that the model correctly projects the long-term dynamics of the harvest regimes, a harvest of 35 trees ha^{-1} every 80 years would maintain longleaf pine aboveground C at levels similar to the no harvest scenario. Increasing the harvest frequency to every 20 years would result in a mean decrease of about 19 tons C ha^{-1}. Even at one harvest per 40 years a substantial amount of C is removed from the site. The mean aboveground carbon in Table 16.1 represents the amount removed from harvest coupled with the amount of regrowth. This balance is perhaps the best measure of sustainability that the model can provide. These results should be evaluated in the context of multiple management objectives, with the understanding that tradeoffs between the objectives must exist in an optimal management plan.

Simulated harvest scenarios are based on an assumption of no damage to the remaining trees and no disruption of recruitment in the gaps left by harvest. We examined a range of harvest intensities for both single tree and group selection harvests. The simulations indicate that a harvest return time of 20 years is not likely sustainable, particularly at the highest harvest intensities. With a target of 35 trees ha^{-1} removed every 20 years, longleaf pine above ground biomass was reduced by 75% of the non-harvested stand. Harwood dominance increases dramatically in this scenario, even with frequent fire management. Increasing the harvest return time to 80 years appears to be sustainable, with most stand characteristics similar to the range found in non-harvested stands.

17. Conclusions and Implications for Future Research/Implementation

The Statement of Need identified the need for basic and applied research that supports the transition of DoD forest management toward an ecological forestry model that will balance military mission support with the maintenance of native biodiversity, sustainable yield of forest products, and enhancement of forest carbon sequestration with a view toward offsetting facility carbon emissions. The overall objective of this project was to develop the research knowledge necessary to create carbon management models that can be used to improve integrated natural resource management of longleaf pine. Specific objectives were to quantify carbon in ecosystem pools in longleaf pine forests located across the species' range and develop longleaf pine carbon models that can be used to evaluate life-cycle carbon balance, forest structure and biodiversity, and yield of forest products in longleaf pine forests. While each chapter focused in great detail on project results, the following discussion highlights the most important results and conclusions, describes the resources developed and enhanced, and concludes with suggested research needs.

Summary of data

Measured ecosystem C stock (all pools except soil C) increased with stand age with a predicted asymptotic maximum of 119 Mg C ha^{-1}. At 100 years, ecosystem C was 69% of the predicted maximum. Ecosystem C was driven by increases in aboveground live tree C related to stand age and basal area. Live root C, the sum of below-stump C, ground penetrating radar measurement of lateral root C and live fine root C, was on average 32% of ecosystem C. Live understory C, forest floor C, down dead wood C and standing dead wood C were a small fraction of ecosystem C. Total soil C stocks At Marine Corps Base Camp Lejeune, US Army Fort Benning and US Army Fort Polk/Kisatchie National Forest ranged from 44.1 to 98.1 ($\bar{x}$ = 77.0) Mg C ha^{-1}, and no effect of stand age, biomass accumulation or geographical location on soil C stocks was detected. Variation in total SOC stocks was largely dependent on depth, though positive associations with clay and extractable Fe content were found. Soil pyrogenic C was a minor component of SOC, comprising 5-7% of the total SOC stock. The majority of pyrogenic C was in the oxidizable fraction, which was found to have a residence time almost a magnitude lower than the resistant fraction. This indicates that pyrogenic C is not contributing substantially to long-term C accumulation in soil within the forest stand where it was produced. There was no enhanced accumulation or deposits of pyrogenic C with depth (to 1 m), pyrogenic C declined in proportion with SOC, conversely the proportion of SOC resistant to oxidation increased with depth. The residence time of SOC in surface soils was hundreds of years and at depths > 50 cm residence time increased to thousands of years. Despite the flow of C from biomass in the form of decay products, litter fall, root turnover and pulses of pyrogenic C, the soils retained little of the new C, which may be rapidly oxidized, lost to the atmosphere from periodic fires or in the case of pyrogenic C may be transported out of the system. Our results indicate that soils are not strong sinks for atmospheric CO_2 compared to C accumulation in live biomass in longleaf pine forests. Our results also indicate that longleaf pine tap root necromass contributes to long-term forest C sequestration.

We developed a novel set of functions to simulate ground cover biomass dynamics in response to timing of prescribed burning longleaf pine stands. The models incorporate the effects of burning frequency, stand age and basal area. Woody understory ground cover was highly reduced as fire

frequency increased, and was also affected by stand basal area when time since the last burn was longer than two years. Herbaceous understory ground cover was little affected by burning frequency, but sensitive to basal area. The set of equations is a useful tool that can be incorporated into fire management models as well as growth and yield and carbon balance models. Coupled with a model that simulates the dynamics of basal area under different thinning schemes, this set of equations allows analysis of the impacts of fire management regimes on ground cover biomass and diversity under varying stand age, basal area and productivity conditions.

We developed and validated the LLM-EA to account for C stock and fluxes in even-aged longleaf pine ecosystems. The model performed accurately when tested against reported C measurements over a wide range of stand ages and site qualities. Using the model to evaluate the effects of silvicultural management systems on C sequestration over a 300 year simulation period, we conclude that: i) site productivity was the major factor driving C sequestration in longleaf pine stands; ii) increasing rotation length increased C storage; iii) prescribed burning had a small effect on C sequestration; and iv) for medium quality sites, C sequestration of thinned 75-year rotation longleaf pine stands was similar than unthinned 25-year rotation slash pine stands. This longleaf pine plantation C model is a useful tool for regional C stock assessments or for C credit verification.

Restoration of longleaf pine forests could assist in reducing the effects of increasing forest disturbance on carbon storage and sequestration, because of resistance of longleaf pine forests to damage from insects, disease, hurricanes and wildfire, when burned regularly, (Johnsen et al. 2009, Mitchell et al. 2014) combined with long rotations and less C loss from harvests associated with long-lived structurally diverse forests (Ryan et al 2010). In longleaf pine forests managed for long rotations with frequent prescribed fire, C dynamics are dominated by biomass accumulation in overstory trees. The understory plant community, while important for compositional and functional diversity, represents a small fraction of ecosystem C, and along with the forest floor and dead wood pools, is moderated and reduced by frequent prescribed fire. Live tree biomass C, however, continues accumulating into the second century, with belowground accumulation of root C, owing to high biomass in lateral coarse roots, apparently playing a larger role than in many other forest types. This time factor potentially balances the more rapid C accumulation associated with intensively managed pine forests, implying that a portfolio of diverse forest types and stand management regimes can contribute to societal climate mitigation objectives, in addition to the myriad of other benefits derived from forests.

We developed a novel set of functions to simulate ground cover biomass dynamics in response to timing of prescribed burning longleaf pine stands. The models incorporate the effects of burning frequency, stand age and basal area. Woody understory ground cover was highly reduced as fire frequency increased, and was also affected by stand basal area when time since the last burn was longer than two years. Herbaceous understory ground cover was little affected by burning frequency, but sensitive to basal area. The set of equations is a useful tool that can be incorporated into fire management models as well as growth and yield and carbon balance models. Coupled with a model that simulates the dynamics of basal area under different thinning schemes, this set

of equations allows analysis of the impacts of fire management regimes on ground cover biomass and diversity under varying stand age, basal area and productivity conditions.

We developed and validated the LLM-EA to account for C stock and fluxes in even-aged longleaf pine ecosystems. The model performed accurately when tested against reported C measurements over a wide range of stand ages and site qualities. Using the model to evaluate the effects of silvicultural management systems on C sequestration over a 300 year simulation period, we conclude that: i) site productivity was the major factor driving C sequestration in longleaf pine stands; ii) increasing rotation length increased C storage; iii) prescribed burning had a small effect on C sequestration; and iv) for medium quality sites, C sequestration of thinned 75-year rotation longleaf pine stands was similar than unthinned 25-year rotation slash pine stands. This longleaf pine plantation C model is a useful tool for regional C stock assessments or for C credit verification.

The LLM-ST model was extended to include carbon dynamics, coarse woody debris, and both single tree and group selection harvesting. Sensitivity analysis was used as a tool to increase understanding of model behavior, evaluate inputs that need higher precision, and provide insight on the limits of model application. In LLM-ST simulations, we found no significant sensitivity to initial placement of trees in the stand lattice after a few decades of simulation. Coefficients of variation for tree biomass were typically less than 10%, and this variation also includes stochastic mortality and recruitment processes. As expected, sensitivity to fire return interval increases with longer simulation periods. Large increases in mean longleaf pine dbh, height, basal area after 250 years with a ten year fire return time reflect a population with poorer recruitment of smaller individuals. Although the mean longleaf tree sizes are larger, the smaller population of trees results in decreased longleaf biomass (carbon). Hardwood biomass increases with the ten year fire return time as a consequence of reduced fire mortality and competition from longleaf pine trees. Simulated harvest scenarios in the LLM-ST were based on an assumption of no damage to the remaining trees and no disruption of recruitment in the gaps left by harvest. We examined a range of harvest intensities for both single tree and group selection harvests. The simulations indicate that a harvest return time of 20 years is not likely sustainable, particularly at the highest harvest intensities. With a target of 35 trees ha^{-1} removed every 20 years, longleaf pine aboveground biomass was reduced by 75% compared to the non-harvested stand. Hardwood dominance increases dramatically in this scenario, even with frequent fire management. Increasing the harvest return time to 80 years appears to be sustainable, with most stand characteristics similar to the range found in non-harvested stands. Our integrated model framework allows simulation of the transition from longleaf pine plantations to old-growth savanna management regimes.

Resources developed/enhanced

This project has provided the most comprehensive, direct assessment of biomass and C stocks in longleaf pine ecosystems on military installations and developed models that can be used to evaluate tradeoffs of different forest management scenarios. The robust allometric equations

developed in this project for longleaf pine allow accurate prediction of longleaf pine C stocks by land managers on military installations located throughout the Southeast. Predictive relationships developed in this project can be used in assessments of C sequestration and to evaluate the effects of forest management on installation C stocks. The plantation model (LLM-EA) is, to our knowledge, the first comprehensive growth and yield system for this species and provides a valuable tool to assess growth and yield and C stocks over time in response to forest management, specifically thinning and planting density, and site index. The single tree model (LLM-ST) highlighted the research needed to better simulate uneven-aged stand development and management. Coupled together and run in long-term simulation mode, this novel simulation system provides the opportunity for forest managers to assess management approaches for converting longleaf pine plantations to uneven aged stands rich in biodiversity and maintain critical habitat for wildlife. The coupled models can be run in an easy-to-use excel interface. The models can be accessed at http://carboncenter.ifas.ufl.edu/models.shtml. A tutorial on LLM-EA model use is also provided.

Future research needs

The linked even aged to single-tree modeling system developed in this project is unique, and is based on the best available data derived from this project, from the literature, and from several large, long-term existing datasets. Regardless, this model system like all models contains uncertainties in parameterization, structure, and assumptions, all of which could benefit from further research. Some of these issues include:

- Because of the long time scales involved, there is no existing information regarding the transition of plantation longleaf pine into mature, "old growth" structure and dynamics managed with frequent fire. One hypothesis is that frequent fire applied to maturing stands is sufficient to facilitate this conversion, and the outputs from our modeling system are consistent with this hypothesis, but this result cannot currently be experimentally verified.
- The equilibrium populations of hardwoods and pines are dependent on patterns of recruitment and rare mortality in both populations, and are dependent primarily on episodic disturbance events at multiple frequencies. All of these factors (recruitment, mortality, and disturbance patterns) require further research and analysis.
- Diameter growth in old trees in the single-tree model is simulated by allowing diameter growth to continue after a specified maximum height is reached. It is not clear what DBH growth rate function should be used for very old trees, but the current structure and parameterization underestimates DBH compared to the few available large diameter trees observed in old stands.
- The current harvesting protocol for the single tree model uses fairly simple rules for choosing harvest trees. For thinning, trees are randomly selected from all longleaf trees greater than 10 cm DBH to reach a specified harvesting intensity. For group selection, a random location is chosen for the specified opening size. In the future, both the group selection and thinning harvest tree selection protocols could be modified to better reflect marking practice for specific silvicultural protocols.

18. Literature Cited

Abrahamson, W.G. 1984. Post-fire recovery of Florida Lake Wales Ridge vegetation. American Journal of Botany 71:9-21.

Abrahamson, W.G., and C.R. Abrahamson. 1996. Effects of fire on long-unburned Florida uplands. Journal of Vegetation Science 7:565-574.

Addo-Danso, S.D., C.E. Prescott, and A.R. Smith. 2016. Methods for estimating root biomass and production in forest woodland ecosystem carbon studies: a review. Forest Ecology and Management 359: 332-351.

Albaugh, T.J., H.L. Allen, and L.W. Kress. 2006. Root and stem partitioning of *Pinus taeda*. Trees 20:176-185.

Albin, L.T. 2014. Restoring the longleaf pine (*Pinus palustris*) forests using pineywoods cattle grazing in conjunction with prescribed burning. PhD dissertation, The University of Southern Mississippi, Hattiesburg, Mississippi, USA.

Alavalapati, J. R., G.A. Stainback, and D.R. Carter, D. R. 2002. Restoration of the longleaf pine ecosystem on private lands in the US South: an ecological economic analysis. Ecological Economics 40: 411-419.

Amateis, R.L., H.E. Burkhart, and T.E. Burk. 1986. A ratio approach to predicting merchantable yields of unthinned loblolly pine plantations. Forest Science 32:287-296.

Andersen, H-E, S.E. Reutebuch, and R.J. McGaughey. 2006. A rigorous assessment of tree height measurements obtained using airborne lidar and conventional field methods. Canadian Journal of Remote Sensing 32:355-366.

Anderson, P.H., K.H. Johnsen, C.A. Gonzalez-Benecke, and L.J. Samuelson. 2014. Predicting taproot decomposition of longleaf pine across the southeastern U.S. 99th ESA Annual Convention Abstract, Sacramento, California, USA.

Arabatzis, A.A., and H.E. Burkhart. 1992. An evaluation of sampling methods and model forms for estimating height-diameter relationships in loblolly pine plantations. Forest Science 38:192-198.

Ascough, P.L., M.I. Bird, F. Brock, T.F.G. Higham, W. Meredith, C.E. Snape, and C.H. Vane 2009. Hydropyrolysis as a new tool for radiocarbon pre-treatment and the quantification of black carbon. Quaternary Geochronology 4: 140-147.

Ascough, P.L., M.I. Bird, S.M. Francis, B. Thornton, A. J. Midwood, A.C. Scott, and D. Apperley 2011. Variability in oxidative degradation of charcoal: Influence of production conditions and environmental exposure. Geochimica Et Cosmochimica Acta 75: 2361-2378.

Augustine, D.J., and D.G. Milchunas. 2009 Vegetation responses to prescribed burning of grazed shortgrass steppe. Rangeland Ecology and Management 62:89-97.

Augustine, D.J., J.D., Derner, and D.G. Milchunas. 2010. Prescribed fire, grazing, and herbaceous plant production in shortgrass steppe. Rangeland Ecology and Management 63:317-323.

Augusto L., D.L. Achat, M.R. Bakker, F. Bernier, D. Bert, F. Danjon, R. Khlifa, C. Meredieu, and P. Trichet. 2015. Biomass and nutrients in tree root systems-sustainable harvesting of an intensively managed *Pinus pinaster* (Ait.) planted forest. Global Change Biology Bioenergy 7: 231-243.

Avery, T.R., and H.E. Burkhart. 2002. Forest Measurements, 5th edition. McGraw-Hill Inc., New York, New York, USA.

Bailey, R.G. 1995. Description of the ecoregions of the United States, second edition. Misc. Publication No. 1391, USDA Forest Service, USA.

Bailey, R.L., B.E. Borders, K.D. Ware, and E.P. Jones. 1985. A compatible model relating slash pine plantation survival to density, age site index, and type and intensity of thinning. Forest Science 31:180–189.

Balboa-Murias, M.A., R. Rodríguez-Soalleiro, A. Merino, and J.G. Álvarez-González. 2006. Temporal variations and distribution of carbon stocks in aboveground biomass of radiata pine and maritime pine pure stands under different silvicultural alternatives. Forest Ecology and Management 237:29-38.

Baldwin Jr., V.C., and J.R. Saucier. 1983. Aboveground weight and volume of unthinned, planted longleaf pine on West Gulf forest sites. Research Paper SO-191. USDA Forest Service, Southern Forest Experiment Station, New Orleans, Louisiana, USA.

Ball, P.N., M.D. MacKenzie, T.H. DeLuca, and W.E. Holben 2010. Wildfire and charcoal enhance nitrification and ammonium-oxidizing bacterial abundance in dry montane forest soils. Journal of Environmental Quality 39: 1243-1253.

Barker, J.R., G.A. Baumgardner, J.J. Lee, and J.C. McFarlane. 1995. Carbon sequestration and forest management at DOD installations: an exploratory study. EPA/600/R-95/037, ERL-COR 826. U.S. Environmental Protection Agency, USA.

Barton, C.V.M., and K.D. Montagu 2004. Detection of tree roots and determination of root diameters by ground penetrating radar under optimal conditions. Tree Physiology 24: 1323-1331.

Baskerville, G.L. 1972. Use of logarithmic regression in the estimation of plant biomass. Canadian Journal of Forest Research 2:49-53.

Batjes, N.H. 1996. Total carbon and nitrogen in the soils of the world. European Journal of Soil Science 47: 151-163.

Beers, B.L, and R.L. Bailey. 1985. Yield stand structure and economic conclusions from a 22-year-old site preparation study with planted loblolly and longleaf pines. General Technical Report SO-54. USDA Forest Service, Southern Research Station, New Orleans, Louisiana, USA.

Bentley, J.W., and R.A. Harper. 2007. Georgia harvest and utilization study, 2004. Resource Bulletin SRS-117. USDA Forest Service, Southern Research Station, Ashville, North Carolina, USA.

Bentley, J.W., and T.G. Johnson. 2004. Eastern Texas harvest and utilization study, 2003. Resource Bulletin SRS-97. USDA Forest Service, Southern Research Station, Ashville, North Carolina, USA.

Berkhout, A.J. 1981. Wave field extrapolation techniques in seismic migration, a tutorial. Geophysics 46: 1638-1656.

Bi, H., J.C. Fox, Y. Li, Y. Lei, and Y. Pang. 2012. Evaluation of nonlinear equations for predicting diameter from tree height. Canadian Journal of Forest Research 42, 789-806. Binkley D., D. Richter, M.B. David, and B. Caldwell. 1992. Soil chemistry in a loblolly/longleaf pine forest with interval burning. Ecological Applications 2: 157-164.

Binford, M.W., H.L. Gholz, G. Starr, and T.A. Martin. 2006. Regional carbon dynamics in the southeastern U.S. coastal plain: Balancing land cover type, timber harvesting, fire, and environmental variation. Journal of Geophysical Research 111:D24S92.

Binkley, D., D. Richter, M. B. David, and B. Caldwell 1992. Soil chemistry in a loblolly/longleaf pine forest with interval burning. Ecological Applications 2: 157-164.

Birdsey, R.A. 1992. Carbon storage and accumulation in United States forest ecosystems. General Technical Report. WO-59. USDA Forest Service, USA.

Birdsey, R.A. 1996. Carbon storage for major forest types and regions in the conterminous United States. Pages 1-25 *in* N. Sampson and D. Hair, editors. Forest management opportunities, forests and global change, volume 2. American Forests, Washington, DC, USA.

Birdsey, R., K. Pregitzer, and A. Lucier. 2006. Forest carbon management in the United States: 1600-2100. Journal of Environmental Quality 35:1461-1469.

Birdsey, R., and Y. Pan. 2015. Trends in management of the world's forests and impacts on carbon stocks. Forest Ecology and Management 355: 83-90.

Bois, C.H., D.T. Janzen, P.T. Sanborn, and A.L. Fredeen. 2009. Contrasting total carbon stocks between ecological site series in a subboreal spruce research forest in central British Columbia. Canadian Journal of Forest Research 39: 897-907.

Boot, C.M., M. Haddix, K. Paustian, and M.F. Cotrufo 2015. Distribution of black carbon in ponderosa pine forest floor and soils following the High Park wildfire. Biogeosciences 12: 3029-3039.

Borchard, P., and D.J. Eldrigde. 2012. Vegetation changes associated with cattle (*Boas taurus*) and wombat (*Vombatus ursinus*) activity in a riparian forest. Applied Vegetation Science 15:62-70.

Borden K.A., M.E. Isaac, N.V. Thevathasan, A.M. Gordon, and S.C. Thomas. 2014. Estimating coarse root biomass with ground penetrating radar in a tree-based intercropping system. Agroforestry Systems 88: 657-669.

Borders, B.E. 1989. Systems of equations in forest stand modeling. Forest Science 35:548–556.

Bouyoucos, G. 1962. Hydrometer method improved for making particle size analyses of soil. Agronomy Journal 54:464-465.

Boyer, W.D. 1980. Interim site-index curves for longleaf pine plantations. Research Note SO-261. USDA Forest Service, Southern Forestry Experiment Station, New Orleans, Louisiana, USA.

Boyer, W.D. 1983. Variations in height-over-age curves for young longleaf pine plantations. Forest Science 29:15-27.

Boyer, W.D. 1990. *Pinus palustris* Mill, longleaf pine. Pages 405-412 *in* R.M. Burns and B.H. Honkala, editors. Silvics of North America, Volume 1, conifers. Agricultural Handbook 654. USDA Forest Service, Washington, D.C. USA.

Boyer, W.D. 1998. Long-term changes in flowering and cone production by longleaf pine. Ninth biennial Southern Silvicultural Research Conference. USDA Forest Service, Southern Research Station, Clemson, South Carolina, USA.

Bracho, R., G. Starr, H.L. Gholz, T.A. Martin, W.P. Cropper Jr., and H.W. Loescher. 2012. Controls on carbon dynamics by ecosystem structure and climate for southeastern U.S. slash pine plantations. Ecological Monographs 82:101-128.

Bragg, D.C. 2002. Reference conditions for old-growth pine forests n the upper west Gulf Coastal Plain. Journal of the Torrey Botanical Society 129: 261-288.

Brockway, D.G. and C.E. Lewis. 1997. Long-term effects of dormant-season prescribed fire on plant community diversity, structure and productivity in a longleaf pine wiregrass ecosystem. Forest Ecology and Management 96:167-183.

Brockway, D.G., and K.W. Outcalt. 2005. Understory vegetation response in longleaf pine

forests to fire and fire surrogate treatments for wildfire hazards reduction and ecological restoration. Pages 38-48 in National Fire and Fire Surrogate Study for Ecosystem Restoration, Fuel Treatments Workshop, Alabama, USA .

Brockway, D.G., K.W. Outcalt, and W.D. Boyer. 2006. Longleaf pine regeneration ecology and methods. Pages 395-133 *in* S. Jose, E.J. Jokela, and D.L. Miller, editors. The longleaf pine ecosystem: ecology, silviculture, and restoration, Springer New York, New York, USA.

Brockway, D.G., E.F. Loewenstein, and K.W. Outcalt. 2014. Proportional basal area method for implementing selection silviculture systems in longleaf pine forests. Canadian Journal of Forest Research 44:977-985.

Brockway, D. G., and K.W. Outcalt. 2015. Influence of selection systems and shelterwood methods on understory plant communities of longleaf pine forests in flatwoods and uplands. Forest Ecology and Management 357: 138-150.

Brooks, J.R., and S.B. Jack. 2006. A whole stand growth and yield system for young longleaf pine plantations in southwest Georgia. General Technical Report SRS-92. USDA Forest Service Southern Research Station, Asheville, North Carolina, USA.

Brown, J.K. 1974. Handbook for inventorying downed woody material. General Technical Report INT-16. USDA Forest Service, USA.

Brown, S., L.R. Iverson, A. Prasda, and D. Liu. 1993. Geographical distributions of carbon in biomass and soils of tropical Asian forests. Geocarto International. 8:45-59.

Burkhart, H.E. 1977. Cubic-foot volume of 1oblolly pine to any merchantable top limit. Southern Journal of Applied Forestry 1:7-9.

Burkhart, H.E., and M. Tomé. 2012. Modeling forest trees and stands. Springer New York, New York, USA.

Butnor, J.R., J.A. Doolittle, L. Kress, S. Cohen, and K.H. Johnsen. 2001. Use of ground-penetrating radar to study tree roots in the southeastern United States. Tree Physiology 21: 1269-1278.

Butnor, J.R., J.A. Doolittle, K.H. Johnsen, L. Samuelson, T. Stokes, and L. Kress. 2003. Utility of ground-penetrating radar as a root biomass survey tool in forest systems. Soil Science Society of America Journal 67: 1607-1615.

Butnor, J.R., K.H. Johnsen, P. Wikstrom, T. Lundmark, and S. Linder. 2006. Imaging tree roots with borehole radar. 11th International Conference on Ground Penetrating Radar, Columbus Ohio, USA.

Butnor, J.R., C. Barton, F.P. Day, K.H. Johnsen, A.N. Mucciardi, R. Schroeder, and D.B. Stover

2012a. Using ground-penetrating radar to detect tree roots and estimate biomass. Pages 213-245 *in* S. Mancuso, editor. Measuring roots, Springer-Verlag Berlin Heidelberg.

Butnor, J.R., K.H. Johnsen, F.G. Sanchez, and C.D. Nelson. 2012b. Impacts of pine species, cultivation and fertilization on soil properties 50 years after planting. Canadian Journal of Forest Research 42: 675-685.

Butnor, J.R., K.H., Johnsen, J.A., Jackson, P.H., Anderson, L.J., Samuelson, and K. Lorenz. 2014. Assessing soil organic carbon stocks in fire-affected *Pinus palustris* forests. American Geophysical Union Fall Meeting, San Francisco, California.

Butnor J.R., L.J. Samuelson, T. Stokes, K. Johnsen, P. Anderson, and C.A. Gonzalez-Benecke. 2016. Surface-based GPR underestimates below-stump root biomass. Plant and Soil 402: 47-62.

Cairns, M.A., S. Brown, E.H. Helmer, and G.A. Baumgardner. 1997. Root biomass allocation in the world's upland forests. Oecologia 111: 1-11.

Campbell, J., D.C. Donato, D. Azuma, and B. Law 2007. Pyrogenic carbon emission from a large wildfire in Oregon, United States. Journal of Geophysical Research-Biogeosciences 112(G4): 11.

Campbell, J., G. Alberti, J. Martin, and B.E. Law. 2009. Carbon dynamics of a ponderosa pine plantation following a thinning treatment in the northern Sierra Nevada. Forest Ecology and Management 257: 453-463.

Canadell, J., R.B. Jackson, J.R. Ehleringer, H.A. Mooney, O.E. Sala, and E.D. Schulze. 1996. Maximum rooting depth of vegetation types at the global scale. Oecologia 108: 583-595.

Canadell, J.G., and M.R. Raupach. 2008. Managing forests for climate change mitigation. Science 320:1456-1457.

Cao, Q.V., and W.D. Pepper. 1986. Predicting inside bark diameter for shortleaf, loblolly, and longleaf pines. Southern Journal of Applied Forestry 10:220-224.

Carter, D.C., J.J Hendricks, R.J. Mitchell, and S.D. Pecot. 2004. Fine root carbon allocation and fates in longleaf pine forests. Forest Science 50:177-187.

Caswell, H. 2001. Matrix population models: construction, analysis, and interpretation. Sinauer Associates, Inc. Sunderland, Massachusetts, USA.

Chapagain, B.P. 2012. Life cycle impact of loblolly pine (*Pinus taeda*) management on carbon sequestration in the southeastern United States. MSc. Thesis, University of Florida, Gainesville, Florida, USA.

Chapman, H.H. 1932. Is the longleaf type a climax? Ecology 13:328-334.

Chen, X, L.B. Hutley, and D. Eamus. 2003. Carbon balance of a tropical savanna of northern Australia. Oecologia, 137:405-416.

Cheng, C.-H., J. Lehmann, J.E. Thies, S.D. Burton, and M.H. Engelhard 2006. Oxidation of black carbon by biotic and abiotic processes. Organic Geochemistry 37: 1477-1488.

Chojnacky, D.C., L.S. Heath, and J.C. Jenkins. 2014. Updated generalized biomass equations for North American tree species. Forestry 87: 129-151.

Churchhill, D.J., A.J. Larson, M.C. Dahlgreen, J.F. Franklin, P.F. Hessburg, and J.A. Lutz. 2013. Restoring forest resilience: from spatial patterns to silvicultural prescriptions and monitoring. Forest Ecology and Management 291: 442-457.

Clark, I.A., R.A. Souter, and B.E. Schlaegel. 1991. Stem profile equations for southern tree species. Research Paper SE-282. USDA Forest Service, Southeastern Forest Experiment Station, Asheville, North Carolina, USA.

Clark, K.L., W.P. Cropper, Jr., and H.L. Gholz. 2001. Evaluation of modeled carbon fluxes for a slash pine ecosystem: SPM2 simulations compared to eddy flux measurements. Forest Science 47:52-59.

Clark, K.L., H.L. Gholz, and M.S. Castro. 2004. Carbon dynamics along a chronosequence of slash pine plantations in north Florida. Ecological Applications 14:1154-1171.

Clary, W.P. 1979. Grazing and overstory effects on rotationally burned slash pine plantation ranges. Journal of Range Management 32:264-266.

Clutter, J.L., J.C. Forston, L.V. Pienaar, G.H. Brister, and R.L. Bailey. 1983. Timber management: a quantitative approach. Krieger Publishing Company, Malabar, Florida, USA.

Clutter, J.L., W.R. Harms, G.H. Brister, and J.W. Rheney. 1984. Stand structure and yields of site-prepared loblolly pine plantations in the lower coastal plain of the Carolinas, Georgia and North Florida. General Technical Report SE-27. USDA Forest Service Southeastern Forest Experiment Station, Asheville, North Carolina, USA.

Conyers, L.B. and D. Goodman. 1997. Ground-penetrating radar: an introduction for archaeologists. AltaMira Press, Walnut Creek, California, USA.

Coulston, J.W., D.N. Wear, and J.M. Vose. 2015. Complex forest dynamics indicate potential for slowing carbon accumulation in the southeastern United States. Scientific Reports 5: 8002.

Cox, K.D., H. Scherm, and N. Serman. 2005. Ground-penetrating radar to detect and quantify residual root fragments following peach orchard clearing. HortTechnology 15:600–607.

Craul, P.J., J.S. Kush, and W.D. Boyer. 2005. Longleaf pine site zones. General Technical Report SRS-89. USDA Forest Service, Southern Research Station, Asheville, North Carolina, USA.

Cropper Jr., W.P., and K.C. Ewel. 1987. A regional carbon storage simulation for large-scale biomass plantations. Ecological Modelling 36:171-180.

Cropper, Jr., W.P., and H.L. Gholz. 1993. Simulation of the carbon dynamics of a Florida slash pine plantation. Ecological Modelling 66:231-249.

Cropper, Jr., W.P. and E.L. Loudermilk. 2006. The interaction of seedling density-dependence and fire in a matrix population model of longleaf pine (*Pinus palustris*). Ecological Modelling 198:487-494.

Cropper, Jr., W.P., K. Peterson, and R.O. Teskey. 1998. MAESTRO simulations of the response of loblolly pine to elevated temperatures and carbon dioxide. Pages. 327-339 *in* S. Fox and R.A. Mickler, editors. The productivity and sustainability of southern forest ecosystems in a changing environment, Springer-Verlag, New York, New York, USA.

Cui, X.H., J. Chen, J.S. Shen, X. Cao, X.H. Chen, and X.L. Zhu. 2011. Modeling tree root diameter and biomass by ground-penetrating radar. Science China Earth Sciences 54: 711-719.

Curtis, R.O. 1967. Height-diameter and height-diameter-age equations for second-growth Douglas-fir. Forest Science 13:365-375.

Cutini, A., F. Chianucci, and M.C. Manetti. 2013. Allometric relationships for volume and biomass for stone pine (*Pinus pinea* L.) in Italian coastal stands. iForest 6: 7.

Dale, V.H., S.C. Beyeler, and B. Jackson. 2002. Understory vegetation indicators of anthropogenic disturbance in longleaf pine forests at Fort Benning, Georgia, USA. Ecological Indicators 1:155-170.

Dalponte, M., L. Bruzzone, and D. Gianelle. 2011. System for the estimation of single-tree stem diameter and volume using multireturn LIDAR data. IEEE Transactions on Geoscience and Remote Sensing 49:2481-2490.

Daniels, D.J. 2004. Ground penetrating radar. Institution of Electrical Engineers, London, England.

Dannoura, M., Y. Hirano, T. Igarashi, M. Ishii, K. Aono, K. Yamase, and Y. Kanazawa. 2008. Detection of Cryptomeria japonica roots with ground penetrating radar. Plant Biosystems 142: 375-380.

Day, F.P., R.E. Schroeder, D.B. Stover, A.L.P. Brown, J.R. Butnor, J. Dilustro, B.A. Hungate, P. Dijkstra, B.D. Duval, T.J. Seiler, B.G. Drake, and C.R. Hinkle. 2013. The effects of 11 years of

CO_2 enrichment on roots in a Florida scrub-oak ecosystem. New Phytologist 200: 778-787.

Dean, T.J. and E.J. Jokela. 1992. A density management diagram for slash pine plantations in the lower Coastal Plain. Southern Journal of Applied Forestry 16:178–185.

Dean, T.J., Q.V. Cao, S.D. Roberts, and D.L. Evans. 2009. Measuring heights to crown base and crown median with LiDAR in a mature, even-aged loblolly pine stand. Forest Ecology and Management 257:126-133.

Deluca, T.H. and G.H. Aplet. 2008. Charcoal and carbon storage in forest soils of the Rocky Mountain West. Frontiers in Ecology and the Environment 6:18-24.

Diéguez-Aranda, U., F. Castedo Dorado, J.G. Álvarez González, and R. Rodriguez Soalleiro. 2005. Modelling mortality of Scots pine (*Pinus sylvestris* L.) plantations in the northwest of Spain. European Journal of Forest Research 124:143–153.

Diéguez-Aranda, U., F. Castedo Dorado, J.G. Álvarez González, and D. Rojo Alboreca. 2006. Dynamic growth model for Scots pine (*Pinus sylvestris* L.) plantations in Galicia (north-western Spain). Ecological Modelling 191:225–242.

Dong, L., L. Zhang, and F. Li. 2015. Developing additive systems of biomass equations for nine hardwood species in northeast China. Trees 29: 1-15.

Doolittle, J.A., F.E. Minzenmayer, S.W. Waltman, E.C. Benham, J.W. Tuttle, and S.D. Peaslee. 2007. Ground-penetrating radar soil suitability map of the conterminous United States. Geoderma 141: 416-421.

Dougherty, P.M., T.C. Hennessey, S.J. Zarnoch, P.T. Stenberg, R.T. Holeman, and R.F. Wittwer. 1995. Effects of stand development and weather on monthly leaf biomass dynamics of a loblolly pine (*Pinus taeda* L.) stand. Forest Ecology and Management 72:213-227.

Drake, J.B., and J.F. Weishampel. 2001. Simulating vertical and horizontal multifractal patterns of a longleaf pine savanna. Ecological Modelling 145:129-142.

Drexhage, M., and F. Colin. 2001. Estimating root system biomass from breast-height diameters. Forestry 74: 491-497.

Eberhardt, T.L., P.M. Sheridan, and J.M. Mahfouz. 2009. Monoterpene persistence in the sapwood and heartwood of longleaf pine stumps: assessment of differences in composition and stability under field conditions. Canadian Journal of Forest Research 39:1357-1365.

Edwards, M.B., and W.H. McNab. 1977. Biomass prediction for young southern pines. Journal of Forestry 7:291-292.

Eusterhues, K., C. Rumpel, and I. Kogel-Knabner 2005. Stabilization of soil organic matter isolated via oxidative degradation. Organic Geochemistry 36(11): 1567-1575.

Fahey, T.J., P.B. Woodbury, J.J. Battles, C.L. Goodale, S.P. Hamburg, S.V. Ollinger, and C.W. Woodall. 2010. Forest carbon storage: ecology, management, and policy. Frontiers in Ecology and the Environment 8:245-252.

Farrar Jr., R.M. 1973. Southern pine site index equations. Journal of Forestry 71:696–697.

Farrar Jr., R.M. 1979. Growth and yield predictions for thinned stands of even-aged natural longleaf pine. Research Paper SO-166, USDA Forest Service Southern Research Station, USA.

Farrar Jr., R.M. 1987. Stem-profile functions for predicting multiple-product volumes in natural longleaf pines. Southern Journal of Applied Forestry 11:161-167.

Farrar Jr., R.M., and T.G Matney. 1994. A dual growth simulator for natural even-aged stands of longleaf pine in the South's East Gulf Region. Southern journal of Applied Forestry 18:147–155.

Farrar Jr., R.M., and W.D. Boyer. 1991. Managing longleaf pine under the selection system—Promises and problems. Pages 357–368 *in* S.S. Coleman and D.G. Neary, editors. Proceedings of the Sixth Biennial Southern Silvicultural Research Conference. USDA Forest Service Southeastern Forest Experiment Station, New Orleans, Louisiana, USA.

Feduccia, D.P., and W.F. Mann, Jr. 1975. Bark thickness of 17-year-old loblolly pine planted at different spacings. Research Note SO-210. USDA Forest Service, Southern Forest Experiment Station, New Orleans, Louisiana, USA.

Fernandes, P., A. Luz, C. Loureiro, P. Ferreira-Godinho, and H. Botelho. 2006. Fuel modelling and fire hazard assessment based on data from the Portuguese National Forest Inventory. Proceedings V International Conference Forest Fire Research. 27-30 D.X. Viegas ed. Figueira da Foz. Coimbra. Portugal.

Foereid, B., J. Lehmann, and J. Major 2011. Modeling black carbon degradation and movement in soil. Plant and Soil 345: 223-236.

Fox, D.G. 1981. Judging air quality model performance. Bulletin of the American Meteorology Society 62:599-609.

Frost, C.C. 1993. Four centuries of changing landscape patterns in the longleaf pine ecosystem. Pages 17-44 *in* S.H. Hermann, editor. The longleaf pine ecosystem: ecology, restoration and management. Proceedings of the 18th Tall Timbers Fire Ecology Conference, Tall Timbers Research Station, Tallahassee, Florida, USA.

Frost, C.C. 2006. History and future of the longleaf pine ecosystem. Pages 9-48 in S. Jose, E.J. Jokela, and D.L. Miller, editors. The longleaf pine ecosystem - ecology, silviculture and

restoration. Springer New York, New York, USA.

Gagnon, J. L., E.J. Jokela, W.K. Moser, and D.A. Huber. 2003. Dynamics of artificial regeneration in gaps within a longleaf pine flatwoods ecosystem. Forest Ecology and Management 172: 133-144.

Gaiser, R.N., 1951. Random sampling within circular plots by means of polar coordinates. Journal of Forestry 49: 916-917.

Garbett, W.S. 1977. Aboveground biomass and nutrient content of a mixed slash-longleaf pine stand in Florida. M.S. Thesis, University of Florida, Gainesville, Florida, USA.

Gardner Jr., F.H. 1989. Wood naval stores. Pages 143-157 *in* D. F. Zinkel and J. Russell, editors. Naval stores: production, chemistry, utilization. Pulp Chemicals Association New York, USA.

Garrett, L.G., G.R. Oliver, S.H. Pearce, and M.R. Davis. 2008. Decomposition of *Pinus radiata* coarse woody debris in New Zealand. Forest Ecology and Management 255:3839–3845.

Garten, C.T. 2002. Soil carbon storage beneath recently established tree plantations in Tennessee and South Carolina, USA. Biomass & Bioenergy 23: 93-102.

Gelinas, Y., K.M. Prentice, J.A. Baldock, and J.I. Hedges. 2001. An improved thermal oxidation method for the quantification of soot/graphitic black carbon in sediments and soils. Environmental Science and Technology 35:3519-3525.

Gholz, H.L., and R.F. Fisher. 1982. Organic matter production and distribution in slash pine (*Pinus elliottii*) plantations. Ecology 63: 1827-1839.

Gholz, H.L., C.S. Perry, W.P. Cropper Jr., and L.C. Hendry. 1985. Litterfall, decomposition and N and P immobilization in a chronosequence of slash pine (*Pinus elliottii*) plantations. Forest Science 31:463-478.

Gholz, H.L., L.C. Hendry, and W.P. Cropper Jr. 1986. Organic matter dynamics of fine roots in plantations of slash pine (*Pinus elliottii*) in north Florida. Canadian Journal of Forest Research 16:529-538.

Gibson, M.D., C.W. McMillin, and E. Shoulders. 1985. Above- and below-ground biomass of four species of southern pine growing on three sites in Louisiana. Report FS-SO-3201-59. USDA Forest Service, USA.

Gibson, M.D., C.W. McMillin, and E. Shoulders. 1986. Moisture content and specific gravity of the four major southern pines under the same age and site conditions. Wood and Fiber Science 18:428-435.

Gilliam, F.S., and W.J. Platt. 1999. Effects of long-term fire exclusion on tree species composition and stand structure in an old-growth *Pinus palustris* (longleaf pine) forest. Plant Ecology 140:15-26.

Gilliam, F.S., W.J. Platt, and R.K. Peet. 2006. Natural disturbances and the physiognomy of pine savannas: a phenomenological model. Applied Vegetation Science 9:83-96.

Glaser, B., L. Haumaier, G. Guggenberger, and W. Zech 1998. Black carbon in soils: the use of benzenecarboxylic acids as specific markers. Organic Geochemistry 29: 811-819.

Glaser, B., L. Haumaier, G. Guggenberger, and W. Zech 2001. The 'Terra Preta' phenomenon: a model for sustainable agriculture in the humid tropics. Naturwissenschaften 88: 37-41.

Glitzenstein, J.S., W.J. Platt, and D.R. Streng. 1995. Effects of fire regime and habitat on tree dynamics in north Florida longleaf pine savannas. Ecological Monographs 65:441-476.

Glitzenstein, J.S., D.D. Wade, and J. Brubaker. 2001. Starting new populations of longleaf pine ground-layer plants in the outer Coastal Plain of South Carolina, USA. Natural Areas Journal 21:89-110.

Glitzenstein, J.S., D.R. Streng, and D.D. Wade. 2003. Fire frequency effects on longleaf pine (*Pinus palustris* P. Miller) vegetation in south carolina and Northeast Florida, USA. Natural Areas Journal 23:22-37.

Goelz, J.C.G. and D.J. Leduc. 2001. Long-term studies on development of longleaf pine plantations. Pages 116–118 *in* J.S. Kush, editor. Forests for our future. Proceedings of the Third Longleaf Alliance Regional Conference, Alexandria, Louisiana, USA.

Goldstein, J.H., G. Caldarone, T.K. Duarte, D. Ennaanay, N. Hannahs, G. Mendoza, S. Polasky, S. Wolny, and G.C. Daily. 2012. Integrating ecosystem-service tradeoffs into land-use decisions. Proceedings of the National Academy of Sciences of the United States of America 109:7565-7570.

Gonzalez-Benecke, C.A., T.A. Martin, W.P. Cropper Jr., and R. Bracho 2010a. Forest management effects on *in situ* and *ex situ* slash pine forest carbon balance. Forest Ecology and Management 260:795-805.

Gonzalez-Benecke, C.A., T.A. Martin, and G.F. Peter. 2010b. Hydraulic architecture and tracheid allometry in mature *Pinus palustris* and *Pinus elliottii* trees. Tree Physiology 30:361-375.

Gonzalez-Benecke, C.A., T.A. Martin, and E.J. Jokela. 2011. A flexible hybrid model of life cycle carbon balance of loblolly pine (*Pinus taeda* L.) management systems. Forests 2:749-776.

Gonzalez-Benecke, C.A., E.J. Jokela and T.A. Martin. 2012a. Modeling the effects of stand development, site quality, and silviculture on leaf area index, litterfall, and forest floor accumulations in loblolly and slash pine plantations. Forest Science 58:457-471.

Gonzalez-Benecke, C.A., S.A. Gezan, D.J. Leduc, T.A. Martin, W.P. Cropper Jr., and L.J. Samuelson. 2012b. Modeling survival, yield, volume partitioning and their response to thinning for longleaf pine (*Pinus palustris* Mill.) plantations. Forests 3:1104-1132.

Gonzalez-Benecke, C.A., S.A. Gezan, T.J. Albaugh, H.L. Allen, H.E. Burkhart, T.R. Fox, E.J. Jokela, C.A. Maier, T.A. Martin, R.A. Rubilar, and L.J. Samuelson. 2014a. Local and general above-stump biomass functions for loblolly pine and slash pine trees. Forest Ecology and Management 334: 254-276.

Gonzalez-Benecke, C.A., S.A. Gezan, T.A. Martin, W.P. Cropper Jr., L.J. Samuelson, and D.J. Leduc. 2014b. Individual tree diameter, height, and volume functions for longleaf pine. Forest Science 60:43-56.

Gonzalez-Benecke, C.A., L.J. Samuelson, T.A. Martin, W.P. Cropper Jr., K.H. Johnsen, T.A. Stokes, J.R. Butnor, P.H. Anderson, and J. Jackson. 2015a. Modeling the effects of forest management on *in situ* and *ex situ* longleaf pine forest carbon stocks. Forest Ecology and Management 355:24-36.

Gonzalez-Benecke C.A., L.J. Samuelson, T.A Stokes, T.A. Martin, W.P. Cropper Jr., K.H. Johnsen. 2015b. Understory plant biomass dynamics of prescribed burned *Pinus palustris* stands. Forest Ecology and Management 344:84-94.

Gonzalez-Benecke, C.A., R.O. Teskey, T.A. Martin, E.J. Jokela, T.R. Fox, M.B. Kane, and A. Noormmets. 2016. Regional validation and improved parameterization of the 3-PG model for *Pinus taeda* stands. Forest Ecology and Management 361: 237-256.

Gough, C.M., C.S. Vogel, K.H. Harrold, K. Georges, and P.S. Curtis. 2007. The legacy of harvest and fire on ecosystem carbon storage in a north temperate forest. Global Change Biology 13:1935-1949.

Greenberg, C.H., and R.W. Simmons. 1999. Age, composition, and stand structure of old-growth oak sites in the Florida high pine landscape: Implications for ecosystem management and restoration. Natural Areas Journal 19:30-40.

Greene, S.W. 1935. Relation between winter grass fires and cattle grazing in the longleaf pine belt. Journal of Forestry 33:339-341.

Gregoire, T.J., O. Schabenberger, and J.P. Barrett. 1995. Linear modelling of irregularly spaced, unbalanced, longitudinal data from permanent-plot measurements. Canadian Journal of Forest Research 25:137-156.

Grissino-Mayer, H.D., H.C. Blount, and A.C. Miller. 2001. Tree-ring dating and the ethnohistory of the naval stores industry in southern Georgia. Tree-Ring Research 57:3-13.

Guldin, J. M. 2006. Uneven-aged silviculture of longleaf pine. Pages 217-249 *in* S. Jose, E.J. Jokela, and D.L. Miller, editors. The longleaf pine ecosystem: ecology, silviculture, and restoration. Springer, New York, USA.

Gundimeda, H. 2001. A framework for assessing carbon flow in Indian wood products. Environment, Development and Sustainability 3:229-251.

Guo, L., J. Chen, X.H. Cui, B.H. Fan, and H. Lin 2013a. Application of ground penetrating radar for coarse root detection and quantification: a review. Plant and Soil 362: 1-23.

Guo, L., J. Chen, X.H. Cui, B.H. Fan, and H. Lin. 2013b. Impact of root water content on root biomass estimation using ground penetrating radar: evidence from forward simulations and field controlled experiments. Plant and Soil 371: 503-520.

Guo, L., Y. Wu, J. Chen, Y. Hirano, T. Tanikawa, W.T. Li, and X.H. Cui. 2015. Calibrating the impact of root orientation on root quantification using ground-penetrating radar. Plant and Soil 395: 289-305.

Hammes, K., M.S. Torn, A.G. Lapenas, and M.W.I. Schmidt. 2008. Centennial black carbon turnover observed in a Russian steppe soil. Biogeosciences 5: 1339-1350.

Han, F.X., M.J. Plodinee, Y. Su, D.L. Monts, and Z`. Li. 2007. Terrestrial carbon pools in southeast and south-central United States. Climatic Change 84:191-202.

Hanula, J.L., M.D. Ulyshen, and D.D. Wade. 2012. Impacts of prescribed fire frequency on coarse woody debris volume, decomposition and termite activity in the longleaf pine flatwoods of Florida. Forests 3: 317-331.

Hardin, E.D., and D.L. White. 1989. Rare vascular plant taxa associated with wiregrass (*Aristida stricta*) in the southeastern United States. Natural Areas Journal 9:234-245.

Harmon, M.E. and J. Sexton. 1996. Guidelines for measurements of woody detritus in forest ecosystems. Publication No. 20. U.S. LTER Network Office University of Washington, Seattle, Washington, USA.

Harmon, M.E., J.M. Harmon, W.K. Ferrell, and D. Brooks. 1996. Modeling carbon stores in Oregon and Washington forest products: 1900-1992. Climatic Change 33:521-550.

Harmon, M.E., J.F. Franklin, F.J. Swanson, P. Sollins, S.V. Gregory, J.D Lattin, N.H. Anderson, S.P. Cline, N.G. Aumen, J.R. Sedell, G.W. Lienkaemper, K. Cromack Jr, K.W. Cummins. 2004. Ecology of coarse woody debris in temperate ecosystems. Advances in Ecological Research 34: 59-234.

Harmon, M.E., W. Christopher, B. Fasth, and J. Sexton. 2008. Woody detritus density and density reduction factors for tree species in the United States: a synthesis. USDA Forest Service, Northern Research Station, Newtown Square, Pennsylvania, USA.

Harrington, C.A., J.C. Brissette, and W.C. Carlson. 1989. Root system structure in planted and seeded loblolly and shortleaf pine. Forest Science 35: 469-480.

Harrington, T.B. 2011. Overstory and understory relationships in longleaf pine plantations 14 years after thinning and woody control. Canadian Journal of Forest Research 41:2301-2314.

Harrison, W.M. and B.E. Borders. 1996. Yield prediction and growth projection for site-prepared loblolly pine plantations in the Carolinas, Georgia, Alabama and Florida. Technical Report 1996-1. Plantation Management Research Cooperative (PMRC) University of Georgia, Athens, Georgia, USA.

Hart, J.H. and D.M. Shrimpton. 1979. Role of stilbenes in resistance of wood to decay. Phytopathology 69:1138-1143.

Hartnett, D.C., and D.M. Krofta. 1989. Fifty-five years of post-fire succession in a southern mixed hardwood forest. Bulletin of the Torrey Botanical Club 116:107-113.

Haywood, T.B. 1995. Prescribed burning and hexazinone herbicide as release treatments in a sapling hardwood-loblolly pine stand. New Forests 10:39-53.

Haywood, J.D. 2005. Effects of herbaceous and woody plant control on *Pinus palustris* growth and foliar nutrients through six growing seasons. Forest Ecology and Management 214:384-397.

Haywood, J.D. 2007. Restoring fire-adapted forested ecosystems-research in longleaf pine on the Kisatchie National Forest. Pages 87-105 *in* General Technical Report PSW-GTR-203.

Haywood, J.D. 2011. Influence of herbicides and felling, fertilization, and prescribed fire on longleaf pine growth and understory vegetation through ten growing seasons and the outcome of an ensuing wildfire. New Forests 41:55-73.

Haywood, J.D. 2012a. Pine straw harvesting, fire, and fertilization affect understory vegetation within a Louisiana longleaf pine stand. Southern Journal of Applied Forestry 36:130-135.

Haywood, J.D. 2012b. Frequency and season of prescribed fire affect understory plant communities in longleaf pine stands. Pages 137-143 in J.R. Butnor, editor. Proceedings of the 16th Biennial Southern Ssilvicultural Research Conference. e-General Technical Report SRS-156. U.S. Department of Agriculture Forest Service, Southern Research Station, Asheville, North Carolina, USA.

Haywood, J.D. 2013. Effects of herbaceous and woody plant control on longleaf pine growth and

understory plant cover. Southern Journal of Applied Forestry 37:108-112.

Haywood, J.D., and H.E. Grelen. 2000. Twenty years of prescribed burning influence the development of direct-seeded longleaf pine on a wet pine site in Louisiana. Southern Journal of Applied Forestry 24:86-92.

Haywood, J.D., and F.L. Harris. 1999. Description of vegetation in several periodically burned longleaf pine forest on the Kisatchie National Forest. Pages 217–224 *in* J.D. Haywood, editor. Proceedings of the 10th Biennial Southern Silviculture Research Conference. General Technical Report SRS-GTR-30. USDA Forest Service, USA.

Haywood, J.D., A.E. Tiarks, M.L. Elliott-Smith, and H.A. Pearson. 1998. Response of direct seeded *Pinus palustris* and herbaceous vegetation to fertilization, burning, and pine straw harvesting. Biomass and Bioenergy 14:157-167.

Haywood, J.D., S.J.S. Sung, and M.A. Sword Sayer. 2012. Copper root pruning and container cavity size influence longleaf pine growth through five growing seasons. Southern Journal of Applied Forestry 36:146-151.

Heath, L.S., R.A. Birdsey, and D.W. Williams. 2001. Methodology for estimating soil carbon for the carbon budget model of the United States, 2001. Environmental Pollution 116: 373-380.

Heath, L.S., J.E. Smith, K.E. Skog, D.J. Nowak, and C.W. Woodall. 2011. Managed forest carbon estimates for the US greenhouse gas inventory, 1990-2008. Journal of Forestry April/May 167-173.

Hendricks, J.J., R.L. Hendrick, C.A. Wilson, R.J. Mitchell, S.D. Pecot, and D. Guo. 2006. Assessing the patterns and controls of fine root dynamics: an empirical test and methodological review. Journal of Ecology 94:40–57.

Heuberger, K.A., and F.E. Putz. 2003. Fire in the suburbs: ecological impacts of prescribed fire in small remnants of longleaf pine (*Pinus palustris*) sandhill. Restoration Ecology 11:72-81.

Heyward, G. 1933. The root system of longleaf pine on the deep sands of western Florida. Ecology 14: 136-148.

Hiers, J.K., S.C. Laine, J.J. Bachant, J.H. Furman, W.W. Greene Jr., and V. Compton. 2003. Simple spatial modeling tool for prioritizing prescribed burning activities at the landscape scale. Conservation Biology 17:1571-1578.

Hiers, J.K., J.J. O'Brien, R.E. Will, and R.J. Mitchell. 2007. Forest floor depth mediates understory vigor in xeric *Pinus palustris* ecosystems. Ecological Applications 17:806-814.

Hiers, J. K., J.R. Walters, R.J. Mitchell, J.M. Varner, L.M. Conner, L.A. Blanc, and J. Stowe.

2014. Ecological value of retaining pyrophytic oaks in longleaf pine ecosystems. The Journal of Wildlife Management 78: 383-393.

Hirano, Y., M. Dannoura, K. Aono, T. Igarashi, M. Ishii, K. Yamase, N. Makita, and Y. Kanazawa. Plant and Soil 319: 15-24.

Hodgkins, E.J., and N.G. Nichols. 1977. Extent of main lateral roots in longleaf pine as related to position and age of the trees. Forest Science 23(2):161-166.

Hoover, C.M., and J.E. Smith. 2012. Site productivity and forest carbon stocks in the United States: analysis and implication for forest offset project planning. Forests 3: 283-299.

Hough, W.A., F.W. Woods, and M.L. McCormack. 1965. Root extension of individual trees in surface soils of a natural longleaf pine-turkey oak stand. Forest Science 11: 223-242.

Hough, W.A. 1982. Phytomass and nutrients in the understory and forest floor of slash/longleaf pine stands. Forest Science 28:359-372.

Howard, E.T. 1973. Physical and chemical properties of slash pine tree parts. Wood Science 5: 312-317.

Hruska, J., J. Cermak, and S. Sustek. 1999. Mapping tree root systems with ground-penetrating radar. Tree Physiology 19: 125-130.

Hu, H. 2011. Restoring longleaf pine (*Pinus palustris*) in loblolly pine (*P. taeda*) stands on the coastal plain of North Carolina. PhD dissertation. Clemson University, Clemson, South Carolina, USA.

Huang, S., and S.J. Titus. 1994. An age-independent individual tree height prediction model for boreal spruce-aspen stands in Alberta. Canadian Journal of Forest Research 24:1295-1301.

Huang, S., S.J. Titus, and D.P. Wiens. 1992. Comparison of nonlinear height-diameter functions for major Alberta tree species. Canadian Journal of Forest Research 22:1297-1304.

Inoue, J., and Y. Inoue. 2009. Comparison of the reflectances of black plant fragments in melanic Andisols with those of fresh charcoal from modern fires. Soil Science and Plant Nutrition 55: 358-362.

Jack, S.B. 2006. The Stoddard-Neel approach-a conservation-oriented approach. Pages 246-249 *in* S. Jose, E.J. Jokela, and D.L. Miller, editors. The longleaf pine ecosystem: ecology, silviculture, and restoration. Springer New York, USA.

Jack, S.B., R.J. Mitchell, and S.D. Pecot. 2006. Silvicultural alternatives in a longleaf pine/wiregrass woodland in Southwest Georgia: understory hardwood response to harvest-created gaps. General Technical Report SRS-92. USDA Forest Service Southern Research Station, Asheville, North Carolina, USA.

Jackson, R.B., J. Canadell, J.R. Ehleringer, H.A. Mooney, O.E. Sala, and E.D. Schulze. 1996. A global analysis of root distributions for terrestrial biomes. Oecologia 108: 389-411.

Jackson, R.B., L.A. Moore, W.A. Hoffmann, W.T. Pockman, and C.R. Linder. 1999. Ecosystem rooting depth determined with caves and DNA. Proceedings of the National Academy of Sciences USA 96: 11387-11392.

Jaffe, R., Y. Ding, J. Niggemann, A.V. Vahatalo, A. Stubbins, R.G.M. Spencer, J. Campbell, and T. Dittmar. 2013. Global charcoal mobilization from soils via dissolution and riverine transport to the oceans. Science 340: 345-347.

Jenkins, J.C., D.C. Chojnacky, L.S. Heath, and R.A. Birdsey. 2003. National-scale biomass estimators for United States tree species. Forest Science 49: 12-30.

Jenny, H. 1941. The factors of soil formation: a system of quantitative pedology. McGraw-Hill, New York, New York, USA.

Johnsen, K.H., D. Wear, R. Oren, R.O. Teskey, F. Sanchez, R. Will, J. Butnor, D. Markewitz, D. Richter, T. Rials, H. L. Allen, J. Seiler, D. Ellsworth, C. Maier, G. Katul, and P.M. Dougherty. 2001. Carbon sequestration and southern pine forests. Journal of Forestry 99: 14-21.

Johnsen, K.H., R. Teskey, L. Samuelson, J. Butnor, C. Maier, D. Sampson, and S. McKeand. 2004. Carbon sequestration in loblolly pine plantations: methods, limitations and research needs for estimating storage pools. *In* M.H.M. Rauscher and K.H. Johnsen, editors. Southern forest science: past, present, and future. General Technical Report SRS-75. USDA Forest Service, Southern Research Station, Asheville, North Carolina, USA.

Johnsen, K.H., J.R. Butnor, J.K. Kush, R.C. Schmidtling, and C.D. Nelson. 2009. Longleaf pine displays less wind damage than loblolly pine. Southern Journal of Applied Forestry 33: 178-181.

Johnsen K.H., L.J. Samuelson, F.G. Sanchez, and R.J. Eaton. 2013. Soil carbon and nitrogen content and stabilization in mid-rotation, intensively managed sweetgum and loblolly pine stands. Forest Ecology and Management 302: 144-153.

Johnsen, K.H., T.L. Keyser, J.R. Butnor, C.A. Gonzalez-Benecke, D.J. Kaczmarek, C.A. Maier, H.R. McCarthy, and G. Sun. 2014. Productivity and Carbon Sequestration of Forests in the Southern United States. Page 193-248 *in* J.M. Vose and K.D. Klepzig, editors. Climate change adaptation and mitigation management options a guide for natural resource managers in southern forest ecosystems. CRC Press, Boca Raton, Florida, USA.

Johnson, D. W., D. E. Todd, and V. R. Tolbert. 2003. Changes in ecosystem carbon and nitrogen in a loblolly pine plantation over the first 18 years. Soil Science Society of America Journal 67: 1594-1601.

Johnson, E.E., and D. Gjerstad. 2006. Restoring the overstory of longleaf pine ecosystems. Pages 271–295 *in* S. Jose, E.J. Jokela, and D.L. Miller, editors. The longleaf pine ecosystem: ecology, silviculture, and restoration. Springer New York, New York, USA.

Johnson, T, S., and G.B. Wood. 1987. Simple linear model reliably predicts bark thickness of radiate pine in the Australian Capital Territory. Forest Ecology and Management 22:173-183.

Jokela, E.J., T.A. Martin, and J.G. Vogel. 2010. Twenty-five years of intensive forest management with southern pines: Important lessons learned. Journal of.Forestry 108:338–347.

Jose, S., S. Merrit, and C.L. Ramsey. 2003. Growth, nutrition, photosynthesis and transpiration responses of longleaf pine seedlings to light, water and nitrogen. Forest Ecology and Management 180:335-344.

Jose S., E. Jokela, and D. Miller. 2006. The longleaf pine ecosystem - an overview. Pages 3-8 *in* S. Jose, E.J. Jokela, and D.L. Miller, editors. The longleaf pine ecosystem: ecology, silviculture, and restoration. Springer New York, New York, USA.

Kaartinen, H, J. Hyyppä, X. Yu, M. Vastaranta, H. Hyyppä, A. Kukko, M. Holo-painen, C. Heipke, M. Hirschmugl, F. Morsdorf, E. Næsset, J. Pitkänen, S. Popescu, S. Solberg, B.M. Wolf, and J.C. Wu. 2012. An international comparison of individual tree detection and extraction using airborne laser scanning. Remote Sensing 4:950-974.

Kalliovirta, J., and T. Tokola. 2005. Functions for estimating stem diameter and tree age using tree height, crown width and existing stand database information. Silvae Fenica 39:227-248.

Kashian, D.M., W.H. Romme, D.B. Tinker, M.G. Turner, and M.G. Ryan. 2013. Postfire changes in forest carbon storage over a 300-year chronosequence of *Pinus contorta*-dominated forests. Ecological Monographs 83: 49-66.

Keely, J.E., and P.H. Zedler. 1998. Evolution of life histories in *Pinus*. Pages 219-250 *in* D.M. Richardson, editor. Ecology and biogeography of *Pinus*. Cambridge University Press, Cambridge, United Kingdom.

Keith, H., B. Mackey, S. Berry, D. Lindenmayer, P. Gibbons. 2010. Estimating carbon carrying capacity in natural forest ecosystems across heterogeneous landscapes: addressing sources of error. Global Change Biology 16: 2971-2989.

Keith, H., D. Lindenmayer, B. Mackey, D. Blair, L. Carter, L. McBurney, S. Okada, and T. Konishi-Nagano. 2014. Managing temperate forests for carbon storage: impacts of logging versus forest protection on carbon stocks. Ecosphere 5: 1-34

King J.S., C.P. Giardina, K.S. Pregitzer, and A.L. Friend. 2007. Biomass partitioning in red pine (*Pinus resinosa*) along a chronosequence in the Upper Peninsula of Michigan. Canadian Journal

of Forest Research 37:93-102.

Kirkman, L.K. 1995. Impacts of fire and hydrological regimes on vegetation in depression wetlands of southeastern USA. Proceedings Tall Timbers Fire Ecology Conference 19:10-20.

Kirkman, L.K., R.J. Mitchell, R.C. Helton, and M.B. Drew. 2001. Productivity and species richness across an Environmental gradient in a fire-dependent ecosystem. American Journal of Botany 88:2119-2128.

Kirkman, L.K., A. Barnett, B.W. Williams, J.K. Hiers, S.M. Pokswinski, and R.J. Mitchell. 2013. A dynamic reference model: a framework for assessing biodiversity restoration goals in a fire-dependent ecosystem. Ecological Applications 23:1574-1587.

Klepzig, K.D., E.B. Smalley, and K.F. Raffa. 1996. Combined chemical defenses against an insect-fungal complex. Journal of Chemical Ecology 22:1367-1388.

Knapp, B.O., G. Wang, and J.L. Walker. 2008. Relating the survival and growth of planted longleaf pine seedlings to microsite conditions altered by site preparation treatments. Forest Ecology and Management 255:3768-3777.

Knapp, B.O., G.G. Wang, H. Hu, J.L. Walker, and C. Tennant. 2011. Restoring longleaf pine (*Pinus palustris* Mill.) in loblolly pine (*Pinus taeda* L.) stands: effects of restoration treatments on natural loblolly pine regenerations. Forest Ecology and Management 262:157-1167.

Knapp, E.E., B.L. Estes, and C.N. Skinner. 2009. Ecological effects of prescribed fire season: a literature review and synthesis for managers. General Technical Report PSW-GTR-224. USDA Forest Service, Pacific Southwest Research Station, Albany, California, USA.

Kobayashi, K., and M.U. Salam. 2000. Comparing simulated and measured values using mean squared deviation and its components. Agronomy Journal 92:345-352.

Kobayashi, K., and M.U. Salam. 2001. Comparing simulated and measured values using mean squared deviation and its components. Agronomy Journal. 92:345–352.

Kuhlbusch, T.A.J., M.O. Andreae, H. Cachier, J.G. Goldammer, J.P. Lacaux, R. Shea, and P.J. Crutzen. 1996. Black carbon formation by savanna fires: Measurements and implications for the global carbon cycle. Journal of Geophysical Research-Atmospheres 101:23651-23665.

Kurth, V.J., M.D. MacKenzie, and T.H. DeLuca. 2006. Estimating charcoal content in forest mineral soils. Geoderma 137: 135-139.

Kush, J.S., R.S. Meldahl, and W.D. Boyer. 1999. Understory plant community response after 23 years of hardwood control treatments in natural longleaf pine (*Pinus palustris*) forests. Canadian Journal of Forest Research 29:1047-1054.

Kush, J.S., J.C.G. Goelz, R.A. Williams, D.R. Carter, and P.E. Linehan. 2006. Longleaf pine growth and yield. IN: The longleaf pine ecosystem: ecology, silviculture, and restoration. S. Jose, E. Jokela and D. Miller eds Springer, New York. pp. 251-267.

Kush, J. S. 2016. The longleaf pines are few and far between. Ecological Restoration 34: 15-16.

Landers, J.L., D.H. Van Lear, and W.D. Boyer. 1995. The longleaf forests of the Southeast: requiem or renaissance? Journal of Forestry 93:39-44.

Larsen, D.R., and D.W. Hann. 1987. Height-diameter equations for seventeen tree species in southwest Oregon. Research Paper 49. Oregon State University Forestry Research Laboratory Oregon, USA.

Lauer, D.K., and J.S. Kush. 2011. A variable density stand level growth and yield model for even-aged natural longleaf pine. Special Report Number 10. Alabama Agricultural Experiment Station, Auburn University, Auburn, Alabama , USA.

Lavoie, M., G. Starr, M.C. Mack, T.A. Martin, and H.L. Gholz. 2010. Effects of a prescribed fire on understory vegetation, carbon pools and soil nutrients in a longleaf pine - slash pine forest in Florida. Natural Areas Journal 30:82-94.

Law, B., T. Arkebauer, J.L. Campbell, J. Chen, O. Sun, M. Shwartz, C. van Ingen, and S. Verma. 2008. Terrestrial carbon observations: protocols for vegetation sampling and data submission. Terrestrial Carbon Observations (TCO) Panel of the Global Terrestrial Observing System (GTOS). Rome, Italy (http://www.fao.org/gtos).

Leduc, D.J., and J.C.G. Goelz. 2009. A height-diameter curve for longleaf pine plantations in the Gulf Coastal Plain. Southern Journal of Applied Forestry 33:164–170.

Leduc, D. J., T.G. Matney, K.L. Belli, and V. Clark Jr. 2001. Predicting diameter distributions of longleaf pine plantations: a comparison between artificial neural networks and other accepted methodologies. USDA Forest Service Research Paper SRS-25.

Leduc, D., and J. Goelz. 2010. Correction: A height-diameter curve for longleaf pine plantations in the Gulf Coastal Plain. Southern Journal of Applied Forestry 33:164-170.

Lee, H., K.C. Slatton, B.E. Roth, and W.P. Cropper Jr. 2009. Prediction of forest canopy light interception using three-dimensional airborne LiDAR data. International Journal of Remote Sensing 30:189-207.

Lee, H., K.C. Slatton, B.E. Roth, and W.P. Cropper Jr. 2010. Adaptive clustering of airborne LiDAR data to segment individual tree crowns in managed pine forests International Journal of Remote Sensing 31:117-139.

Lefsky M.A., W.B. Cohen, G.G. Parker, and D.J. Harding. 2002. Lidar remote sensing for ecosystem studies. Bioscience 52:19-30.

Lewis, C.E., and T.J. Harshbarger. 1976. Shrub and herbaceous vegetation after 20 years of prescribed burning in the South Carolina Coastal Plain. Journal of Range Management 29:13-18.

Li, W., Q. Guo, M.K. Jakubowski, and M. Kelly. 2012. A new method for segmenting individual trees from the Lidar point cloud. Photogrammetric Engineering and Remote Sensing 78:75-84.

Liang, B., J. Lehmann, D. Solomon, J. Kinyangi, J. Grossman, B. O'Neill, J.O. Skjemstad, J. Thies, F.J. Luizao, J. Petersen, and E.G. Neves. 2006. Black carbon increases cation exchange capacity in soils. Soil Science Society of America Journal 70:1719-1730.

Liang, B., J. Lehmann, D. Solomon, S. Sohi, J. E. Thies, J.O. Skjemstad, F.J. Luizao, M.H. Engelhard, E.G. Neves, and S. Wirick. 2008. Stability of biomass-derived black carbon in soils. Geochimica Et Cosmochimica Acta 72: 6069-6078.

Lichstein, J.W., C. Wirth, H.S. Horn, and S.W. Pacala. 2009. Biomass chronosequences of United State forests: implications for carbon storage and forest management. Pages 301-341 *in* C. Wirth, G. Gleixner and M. Heimann, editors. Old-growth forests. Ecological Studies 207, Springer-Verlag Berlin Heidelberg, Germany.

Liski, J., A. Pussinen, K. Pingoud, R. Mäkipää, and T. Karjalainen. 2001. Which rotation length is favorable to carbon sequestration? Canadian Journal of Forest Research 31:2004-2013.

Litton, C.M., M.G. Ryan, D.B. Tinjer, and D.H. Knight. 2003. Belowground and aboveground biomass in young postfire lodgepole pine forests of contrasting tree density. Canadian Journal of Forest Research 33: 351-363.

Loague, K., and R.E. Green. 1991. Statistical and graphical methods for evaluating solute transport models: overview and application. Journal Contaminant Hydrology 7:51-73.

Lohrey, R.E., and R.L. Bailey. 1977. Yield tables and stand structure for unthinned longleaf pine plantations in Louisiana and Texas. Research Paper SO-133. USDA Forest Service Southern Forest Experiment Station, New Orleans, Louisiana, USA.

Loudermilk, E.L., and W.P. Cropper, Jr. 2007. Multi-scale modeling of longleaf pine (*Pinus palustris*). Canadian Journal of Forest Research 37:2080-2089.

Loudermilk E.L., W.P. Cropper Jr., R.J. Mitchel, and H. Lee. 2011. Longleaf pine (*Pinus palustris*) and hardwood dynamics in a fire-maintained ecosystem: A simulation approach. Ecological Modelling 222:2733-2750.

Loveless, R.W., J.A. Pait III, and T. McElwain. 1989. Responses of longleaf pine to varying

intensity of silvicultural treatments. Pages 159-164 *in* General Technical Report SO-74. Proceedings of the Fifth Biennial Southern Silvicultural Research Conference. USDA Forest Service, Southern Forest Experiment Station, New Orleans, Louisiana, USA.

Ludovici, K.H., S.J. Zarnoch, and D.D. Richter. 2002. Modeling in-situ pine root decomposition using data form a 60-year chronosequence. Canadian Journal of Forest Research 32: 1675-1684.

Lutz, D. A., E.A. Burakowski, M.B. Murphy, M.E. Borsuk, R.M. Niemiec, and R.B. Howarth. 2015. Tradeoffs between three forest ecosystem services across the state of New Hampshire, USA: timber, carbon, and albedo. Ecological Applications 26:146-161

Luyssaert, S., E.D. Schulze, A. Boerner, A. Knohl, D. Hessenmoeller, B.E. Law, P. Ciais, and J. Grace. 2008. Old-growth forests as global carbon sinks. Nature 455:213-215.

Maier C.A., K.H. Johnsen, P. Dougherty, D. McInnis, P. Anderson, and S. Patterson. 2012. Effect of harvest residue management on tree productivity and carbon pools during early stand development in a loblolly pine plantation. Forest Science 58: 430-445.

Main, M.B., and M.J. Barry. 2002. Influence of season of fire on flowering of wet prairie grasses in south Florida, USA. Wetlands 22:430-434.

Markewitz, D. 2006. Fossil fuel carbon emissions from silviculture: Impacts on net carbon sequestration in forests. Forest Ecology and Management 236:153-161.

Markewitz, D., F. Sartori, and C. Craft. 2002. Soil change and carbon storage in longleaf pine stands planted on marginal agricultural lands. Ecological Applications 12: 1276-1285.

Martin, K.L., M.D. Hurteau, B.A. Hungate, G.W. Koch, and M.P. North. 2015. Carbon tradeoffs of restoration and provision of endangered species in a fire-maintained forest. Ecosystems 18: 76-88.

Martin, S.W., R.L. Bailey, and E.J. Jokela. 1997. Models for unfertilized and fertilized slash pine plantations: CRIFF B400 and B500 Series. PMRC Technical Report 1997-3.
Masiello, C. A., and E.R.M. Druffel 1998. Black carbon in deep-sea sediments. Science 280: 1911-1913.

Masiello, C. A. 2004. New directions in black carbon organic geochemistry. Marine Chemistry 92: 201-213.

McCarthy, H.R., R. Oren, K.H. Johnsen, A.C. Finzi, S.G. Pritchard, R.B. Jackson, C.W. Cook, and K.K. Treseder. 2009. Reassessment of carbon accumulation at the Duke free air CO_2 enrichment site: Interactions of atmospheric [CO_2] with nitrogen and water availability and stand development. New Phytologist 185: 514-528.

McGarvey, J.C., J.R. Thompson, H.E. Epstein, and H.H. Shugart, Jr. 2015. Carbon storage in

old-growth forests of the mid-Atlantic: toward better understanding of the eastern forest carbon sink. Ecology 96: 311-317.

McKinley, D.C., M.G. Ryan, R.A. Birdsey, C.P. Giardina, M.E. Harmon, L.S. Heath, R.A. Houghton, R.B. Jackson, J.F. Morrison, B.C. Murray, D.E. Pataki, and K.E. Skog. 2011. A synthesis of current knowledge on forests and carbon storage in the United States. Ecological Applications 21:1902-1924.

Means, D.B. 2006. Vertebrate faunal diversity of longleaf pine ecosystems. Pages 157-213 *in* S. Jose, E.J. Jokela, and D.L. Miller, editors. The longleaf pine ecosystem: ecology, silviculture, and restoration. Springer New York, New York, USA.

Means, D.B., and H.W. Campbell. 1982. Effects of prescribed burning on amphibians and reptiles. Pages 89-97 *in* G.W. Wood, editor. Prescribed fire and wildlife in southern forests. Belle W. Baruch Forest Science Institute, Clemson University, Clemson, South Carolina, USA.

Means, D.B., and G. Grow. 1985. The endangered longleaf pine community. ENFO Report 85:1-12.

Means, D.B., C.K. Dodd, Jr., S.A. Johnson, and J.G. Palis. 2004. Amphibians and fire in longleaf pine ecosystems. Conservation Biology 18:1149-1153.

Mehlich, A. 1984. Mehlich-3 soil test extractant - a modification of the Mehlich-2 extractant. Communications in Soil Science and Plant Analysis 15: 1409-1416.

Melin, Y., H. Petersson, and T. Nordfjell. 2009. Decomposition of stump and root systems of Norway spruce in Sweden—a modelling approach. Forest Ecology and Management 257:1445-1451.

Menaut, J.C., and J. Cesar. 1979. Structure and primary productivity of Lamto savannas, Ivory Coast. Ecology 60:1197-1210.

Millikin, C. S., and C. S. Bledsoe. 1999. Biomass and distribution of fine and coarse roots from blue oak (*Quercus douglasii*) trees in the northern Sierra Nevada foothills of California. Plant and Soil. 214: 27-38.

Miller, A.T., H.L. Allen, and C. A. Maier. 2006. Quantifying the coarse-root biomass of intensively managed loblolly pine plantations. Canadian Journal of Forest Research 36: 12-22.

Mitchell, R.J., L.K Kirkman, S.D. Pecot, C.A. Wilson, B.J. Palik, and L.R. Boring. 1999. Patterns and controls of ecosystem function in longleaf pine-wiregrass savannas. I. Aboveground net primary productivity. Canadian Journal of Forest Research 29: 743-751.

Mitchell, R.J., J.K., Hiers, J.J. O'Brien, S.B. Jack, and R.T. Engstrom. 2006. Silviculture that

sustains: the nexus between silviculture, frequent prescribed fire, and conservation of biodiversity in longleaf pine forests of the southeastern United States. Canadian Journal of Forest Research 36:2724-2736.

Mitchell, R.J., Y. Liu, J.J. O'Brien, K.J. Elliott, G. Starr, C.F. Miniat, and J.K. Hiers. 2014. Future climate and fire interactions in the southeastern region of the United States. Forest Ecology and Management 327: 316-326.

Mobley, M. L., D. D. Richter, and P. R. Heine. 2012. Accumulation and decay of woody detritus in a humid subtropical secondary pine forest. Canadian Journal of Forest Research 43:109-118.

Mokany K., R.J. Raison, and A.S. Prokushkin. 2006. Critical analysis of root:shoot ratios in terrestrial biomes. Global Change Biology 12:84–96

Murphy, P.A. and R.M. Farrar Jr. 1988. A new mortality (or survival) function for longleaf pine plantations. U.S. Pages 427-432 *in* General Technical Report SO-74. Department of Agriculture Forest Service Southern Research Station, New Orleans, Louisiana, USA.

Mushinsky, H.R. 1985. Fire and the Florida sandhill herpetofaunal community: with special attention to responses of *Cnemidophorus sexlineatus*. Herpetologica 41:333-342.

Myers, R.L. 1990. Scrub and high pine. Pages 150-193 *in* R.L. Myers and J.J. Ewel, editors. Ecosystems of Florida. University of Central Florida Press, Orlando, Florida, USA.

Myers, R.H. 2000. Classical and modern regression with applications, 2nd edition, Duxbury Press.

Nabuurs, G.J., O. Masera, K. Andrasko, P. Benitez-Ponce, R. Boer, M. Dutschke, E. Elsiddig, J. Ford-Robertson, P. Frumhoff, T. Karjalainen, O. Krankina, W. Kurz, M. Matsumoto,W. Oyhantcabal, N.H. Ravindranath, M.J. Sanz Sanchez, and X. Zhang. 2007. Forestry. *In* B. Metz, O.R. Davidson, P.R. Bosch, R. Dave, and L.A. Meyer, editors. Climate Change 2007: mitigation. Contribution of working group III to the Fourth Assessment Report of the Intergovernmental Panel on Climate Change. Cambridge University Press, Cambridge, United Kingdom and New York, New York, USA.

Naidu, S., E. DeLucia, and R. Thomas. 1998. Contrasting patterns of biomass allocation in dominant and suppressed loblolly pine. Canadian Journal of Forest Research 28: 1116-1124.

Nakai Y., F. Hosoi, and K. Omasa. 2010. Estimation of coniferous standing tree volume using airborne LiDAR and passive optical remote sensing. Journal of Agricultural Meteorology

66:111-116.

Nave L.E., C.W. Swanston, U. Mishra, and K.J. Nadelhoffer. 2013. Afforestation effects on soil carbon storage in the United States: a synthesis. Soil Science Society of America Journal 77: 1035-1047.

Neary, D.G., E.J. Jokela, N.B. Comerford, S.R. Colbert, and T.E. Cooksey. 1990. Understanding competition for soil nutrients - the key to site productivity on southeastern Coastal Plain Spodosols. Pages 432-450 *in* S.P. Gessel, D.S. LaCate, G.F. Weetman and R.F. Powers, editors. Sustained productivity of forest soils." Proceedings of the 7th. North American Forest Soils Conference, University of British Columbia, Vancouver, British Columbia, Canada.

Nelson, L.R., B.R. Zutter, and D.H. Gjerstad. 1985. Planted longleaf pine seedlings respond to herbaceous weed control using herbicides. Southern Journal of Applied Forestry 9:236-240.

Nelson, R., R. Swill, and W. Krabill. 1988. Using airborne lasers to estimate forest canopy and stand characteristics. Journal of Forestry 86:31-38.

Nerg, A.-M., J. Heijari, U. Noldt, H. Viitanen, M. Vuorinen, P. Kainulainen, and J.K. Holopainen. 2004. Significance of wood terpenoids in the resistance of scots pine provenances against the old house borer, *Hylotupes bajulus*, and brown-rot fungus, *Coniophora puteana*. Journal of Chemical Ecology 30:125-141.

Neter, J., M.H. Kutner, C.J. Nachtsheim, and W. Wasserman. 1996. Applied linear statistical models, 4th edition. Irwin Inc., Illinois, USA.

Nguyen, B.T., and J. Lehmann. 2009. Black carbon decomposition under varying water regimes. Organic Geochemistry 40: 846-853.

Nilsson, M. 1996. Estimation of tree heights and stand volume using an airborne lidar system, Remote Sensing of Environment 56:1-7.

Noel, J.M., W.J. Platt, and E.B. Moser. 1998. Structural characteristics of old- and second-growth stands of longleaf pine (*Pinus palustris*) in the Gulf Coastal region of the U.S.A. Conservation Biology 12: 533-548.

Noss, R.F. 1989. Longleaf pine and wiregrass: keystone components of an endangered ecosystem. Natural Areas Journal 9:211-213.

Noss, R.F., E.T. LaRoe, and J.M. Scott. 1995. Endangered ecosystems of the United States: a preliminary assessment of loss and degradation. USDI National Biological Services Biological Report 28. Washington, D.C., USA

Oades, J. M. 1988. The retention of organic-matter in soils. Biogeochemistry 5: 35-70.

Oppenheim, A.V., and R.W. Schafer. 1975. Digital signal processing. Prentice Hall, Englewood Cliffs, New Jersey, USA.

Oswalt, C.M., J.A. Cooper, D.G. Brockway, H.W. Brooks, J.L. Walker, K.F. Connor, S.N. Oswalt, and R.C. Conner. 2012. History and current condition of longleaf pine in the southern United States. General Technical Report SRS-166. USDA Forest Service, Southern Research Station, Asheville, North Carolina, USA.

Ottmar, R.D. and R.E. Vihnanek. 2000. Stereo photo series for quantifying natural fuels. Volume VI: Longleaf pine, pocosin, and marshgrass in the Southeast United States. PMS 835. National Wildfire Coordinating Group, National Interagency Fire Center, Boise, Idaho, USA.

Ottmar, R.D., R.E. Vihnanek, and J.W. Mathey. 2003a. Stereo photo series for quantifying natural fuels. Volume VIa: Sand hill, sand pine scrub, and hardwoods with white pine types in the Southeast United States with supplemental sites for volume VI. PMS 838. National Wildfire Coordinating Group, National Interagency Fire Center, Boise, Idaho, USA.

Ottmar, R.D., R.E. Vihnanek, C.S. Wright, and K.D. Hiers. 2003b. Modification and validation of fuel consumption models for shrub and forested lands in the Southwest, Pacific Northwest, Rockies, Midwest, Southeast, and Alaska. Final Report to the Joint Fire Science Program.

Ottmar, R.D., S.J. Prichard, R.E. Vihnanek, and D.V. Sandberg. 2006. Modification and validation of fuel consumption models for shrub and forested lands in the Southwest, Pacific Northwest, Rockies, Midwest, Southeast and Alaska. Final Report to the Joint Fire Science Program.

Ottmar, R.D., C.S. Wright, and S.J. Prichard. 2009. A suite of fire, fuels, and smoke management tools. Fire Management Today 69:34-39.

Outcalt, K.W. 1994. Seed production of wiregrass in central Florida following growing season prescribed burns. International Journal of Wildland Fire 4:123-125.

Outcalt, K.W., and D.G. Brockway. 2010. Structure and composition changes following restoration treatments of longleaf pine forests on the Gulf Coastal Plain of Alabama. Forest Ecology and Management 259:1615–1623.

Outcalt, K.W., and J.L. Foltz. 2004. Impacts of growing-season prescribed burns in the Florida flatwoods type. Pages 30-34 *in* K.F. Connor, editor. Proceedings of the 12th Biennial Southern Silvicultural Research Conference. General Technical Report SRS-71. USDA Forest Service, USA.

Outcalt, K.W., and P.A. Outcalt. 1994. Response of wiregrass (*Aristida stricta*) to mechanical site preparation. Pages 60-71 *in* L.C. Duever and R.F. Noss, editors. Proceedings of the Symposium on Wiregrass Biology and Management.KBN Engineering and Applied Sciences, Gainesville, Florida, USA.

Palik, B.J., R.J. Mitchell, and J.K. Hiers. 2002. Modeling silviculture after natural disturbance to sustain biodiversity in the longleaf pine (*Pinus palustris*) ecosystem: balancing complexity and implementation. Forest Ecology and Management. 155:347-356.

Palviainen, M., L. Fine´, R. Laiho, E. Shorohova, E. Kapitsa, and I. Vanha-Majamaa. 2010. Carbon and nitrogen release from decomposing Scots pine, Norway spruce and silver birch stumps. Forest Ecology and Management 259:390-398.

Pan, Y., R.A. Birdsey, J. Fang, R. Houghton, P. E. Kauppi, W. A. Kurz, O.L. Phillips, A. Shvidenko, S.L. Lewis, J.G. Canadell, P. Ciais, R.B. Jackson, S.W. Pacala, A. D. McGuire, S. Piao, A. Rautiainen, S. Sitch, and D. Hayes. 2011. A large and persistent carbon sink in the World's forests. Science 333: 988-993.

Parresol, B.R., D. Shea, and R. Ottmar. 2006. Creating a fuels baseline and establishing fire frequency relationships to develop a landscape management strategy at the Savannah River Site. *In* N P.L. Andrews and B.W. Butler, editors. Fuels management: how to measure success. Conference Proceedings RMRS-P-41. USDA Forest Service, Rocky Mountain Research Station, Fort Collins, Colorado, USA.

Parresol B.R., J.I. Blake, and A.J. Thompson. 2012. Effects of overstory composition and prescribed fire on fuel loading across a heterogeneous managed landscape in the southeastern USA. Forest Ecology and Management 273:29-42.

Peet, R.K., and D.J. Allard. 1993. Longleaf pine-dominated vegetation of the southern Atlantic and eastern Gulf Coast region, USA. Tall Timbers Fire Ecology Conference 18:45-82.

Phillips, D.R. 1981. Predicted total-tree biomass of understory hardwoods. USDA Forest Service Research Paper SE-223.

Phillips, M.A., and R.B. Croteau. 1999. Resin-based defenses in conifers. Trends in Plant Science 4:184-190.

Pienaar, L.V. 1979. An approximation of basal area growth after thinning based on growth in unthinned plantations. Forest Science 25:223–232.

Pienaar, L.V. 1995. Results and analysis of a slash pine spacing and thinning study in the southeast Coastal Plain. Technical Report 1995-3. Plantation Management Research Cooperative (PMRC), University of Georgia, Athens, Georgia, USA.

Pienaar, L.V., and J.W. Rheney. 1993. Yield prediction for mechanically site-prepared slash pine plantations in the southeastern Coastal Plain. Southern Journal of Applied Forestry 17:163–173.

Pienaar, L.V., B.D. Shiver, and J.W. Rheney. 1996. Yield prediction for mechanically site-prepared slash pine plantations in the southeastern Coastal Plain. Technical Report 1996-3.

Plantation Management Research Cooperative (PMRC), University of Georgia, Athens, Georgioa, USA.

Platt, W.J., G.W. Evans, and S.L. Rathbun. 1988. The population dynamics of a long-lived conifer (*Pinus palustris*). American Naturalist 131:491-525.

Popescu, S.C. 2007. Estimating biomass of individual pine trees using air-borne LiDAR, Biomass and Bioenergy 31:646-655

Popescu, S.C., and R.H. Wynne. 2004. Seeing the trees in the forest: using LiDAR and multispectral data fusion with local filtering and variable window size for estimating tree height. Photogrammetric Engineering and Remote Sensing 70:589-604.

Popescu, S.C., R.H. Wynne, and R.F. Nelson. 2003. Measuring individual tree crown diameter with lidar and assessing its influence on estimating forest volume and biomass. Canadian Journal of Remote Sensing 29:564-577.

Powell, T.L., H.L. Gholz, K.L. Clark, G. Starr, W.P. Cropper Jr., and T.A. Martin. 2008. Carbon exchange of a mature, naturally-regenerated pine forest in north Florida. Global Change Biology 14:2523-2538.

Powers, M.D., R.K. Kolka, J.B. Bradford, B.J. Palik, S. Fraver, and M.F. Jurgensen. 2012. Carbon stocks across a chronosequence of thinned and unmanaged red pine (*Pinus resinosa*) stands. Ecological Applications 22: 1297-1307.

Pregitzer, K. S. 2002. Fine roots of trees - a new perspective. New Phytologist 154:267-270

Pregitzer, K.S., and E.S. Euskirchen. 2004. Carbon cycling and storage in world forests: biome patterns related to forest age. Global Change Biology 10: 2052-2077.

Preston, C.M., and M.W.I. Schmidt, 2006. Black (pyrogenic) carbon: a synthesis of current knowledge and uncertainties with special consideration of boreal regions. Biogeosciences 3: 397-420.

Prichard, S. J., D.L. Peterson, and R.D. Hammer. 2000. Carbon distribution in subalpine forests and meadows of the Olympic Mountains, Washington. Soil Science Society of America Journal 64:1834-1845.

Prichard, S.J., R.D. Ottmar, and G.K. Anderson. 2007. Consume 3.0 User's Guide. USDA Forest Service Pacific Wildland Fire Sciences Laboratory, Seattle, Washington, USA.

Prowse, T.A.A., C.J.A. Bradshaw, S. Delean, P. Cassey, R.C. Lacy, K. Wells, M.E. Aiello-Lammens, H.R. Akçakaya, and B.W. Brook. 2016. An efficient protocol for the global sensitivity analysis of stochastic ecological models. Ecosphere 7: p.e01238.

Putz, F.E., and K.H. Redford. 2009. Dangers of carbon-based conservation. Global Environmental Change-Human and Policy Dimensions 19:400-401.

Putz, F.E., P.A. Zuidema, M.A. Pinard, R.G.A. Boot, J.A. Sayer, D. Sheil, P. Sist, Elias, and J.K. Vanclay. 2008. Improved tropical forest management for carbon retention. PLOS Biology 6:1368-1369

Quarterman, E., and K. Keever. 1962. Southern mixed hardwood forest: climax in the southeastern coastal plain: U.S.A. Ecological Monographs 32:167-185.

Quicke, H.E., and R.S. Meldahl. 1992. Predicting pole classes for longleaf pine based on diameter breast height. Southern Journal of Applied Forestry 16:79-82.

Quicke, H.E., R.S. Meldahl, and J.S. Kush. 1994. Basal area growth of individual trees: A model derived from a regional longleaf pine growth study. Forest Science 40:528-542.

Radtke, P.J., R.L. Amateis, S.P. Prisley, C.A. Copenheaver, D.C. Chojnacky, J.R. Pittman, and H.E. Burkhart. 2009. Modeling production and decay of coarse woody debris in loblolly pine plantations. Forest Ecology and Management 257:790-799.

Ramsey, C.L., S. Jose, B.J. Brecke, and S. Merritt. 2003. Growth response of longleaf pine (*Pinus palustris* Mill.) seedlings to fertilization and herbaceous weed control in an old field in southern USA. Forest Ecology and Management 172:281-289.

Reinhardt, E.D. 2003. Using FOFEM 5.0 to estimate tree mortality, fuel consumption, smoke production and soil heating from wildland fire. Proceedings of the Second International Wildland Fire Ecology and Fire Management Congress and Fifth Symposium on Fire and Forest Meteorology. American Meteorological Society, Orlando, Florida, USA.

Remucal, J.M., J.D. McGee, M.M. Fehrenbacher, C. Best, and R.J. Mitchell. 2013. Application of the Climate Action Reserve's forest project protocol to a longleaf pine forest under restoration management. Journal of Forestry 111: 59-66.

Retzlaff, W.A., J.A. Handest, D.M. O'Malley, S.E. McKeand, and M.A. Topa. 2001. Whole-tree biomass and carbon allocation of juvenile trees of loblolly pine (*Pinus taeda*): influence of genetics and fertilization. Canadian Journal of Forest Research 31: 960-970.

Richter, D. D., M. Hofmockel, M. A. Callaham, D. S. Powlson, and P. Smith. 2007. Long-term soil experiments: Keys to managing Earth's rapidly changing ecosystems. Soil Science Society of America Journal 71: 266-279.

Richter, D. D., D. Markewitz, S.E. Trumbore. and C.G. Wells. 1999. Rapid accumulation and turnover of soil carbon in a re-establishing forest. Nature 400: 56-58.

Roberts, S.D., T.J. Dean, D.L. Evans, J.W. McCombs, R.L. Harrington, and P.A. Glass. 2005. Estimating individual tree leaf area in loblolly pine plantations using LiDAR-derived measurements of height and crown dimensions. Forest Ecology and Management 213:54-70.

Robertson, K.M., and T.E. Ostertag. 2009. Biomass equations for hardwood resprouts in fire-maintained pinelands in the southeastern United States. Southern Journal of Applied Forestry 33: 121-238.

Robinson, D. 2007. Implications of a large global root biomass for carbon sink estimates and for soil carbon dynamics. Proceedings of the Royal Society B-Biological Sciences 274: 2753-2759.

Row, C., and R.B. Phelps. 1991. Carbon cycle impacts of future forest products utilization and recycling trends. Pages 461-468 *in* Agriculture in a world of change. Proceedings of Outlook '91. USDA, Washington, DC, USA.

Row, C., and R.B. Phelps. 1996. Wood carbon flows and storage after timber harvest. Pages 59-90 *in* R.N. Sampson and D. Hair, editors. Forests and global change, volume 2: Forest management opportunities for mitigating carbon emissions. American Forests, Washington, DC, USA.

Russell, M.B., G.M. Domke, C.W. Woodall, and A.W. D'Amato. 2015. Comparisons of allometric and climate-derived estimates of tree coarse root carbon stocks in forests of the United States. Carbon Balance and Management 10:20.

Ryan, M.G., M.E. Harmon, R.A. Birdsey, C.P. Giardina, L.S. Heat, R.A. Houghton, R.B. Jackson, D.C. McKinley, J.E. Morrison, B.C. Murray, D.E. Pataki, and K.E. Skog. 2010. A synthesis of the science on forests and carbon for U.S. forests. Issues in Ecology Report Number 13.

Samuelson, L.J., K. Johnsen, and T. Stokes. 2004. Production, allocation and stemwood growth efficiency of *Pinus taeda* L. stands in response to 6 years of intensive management. Forest Ecology and Management 192: 59-70.

Samuelson, L.J., J. Butnor, C. Maier, T.A. Stokes, K. Johnsen, and M. Kane. 2008. Growth and physiology of loblolly pine in response to long-term resource management: defining growth potential in the southern United States. Canadian Journal of Forest Research 38:721-732.

Samuelson, L., R. Mathew, T. Stokes, Y. Feng, D.F. Aubrey, and M. Coleman. 2009. Soil and microbial respiration in a loblolly pine plantation in response to seven years of irrigation and fertilization. Forest Ecology and Management 258:2431-2438.

Samuelson, L.J., T.E. Eberhardt, J.R. Butnor, T.A. Stokes, and K.H. Johnsen. 2010. Maximum growth potential in loblolly pine; results from a 47-year-old spacing study in Hawaii. Canadian

Journal of Forest Research 40:1914-1929.

Samuelson, L.J., and T.A. Stokes. 2012. Leaf physiological and morphological responses to shade in grass-stage seedlings and young trees of longleaf pine. Forests 3:684-699.

Samuelson, L.J., and W.B. Whitaker. 2012. Relationships between soil CO_2 efflux and forest structure in 50-year-old longleaf pine. Forest Science 58: 472-484.

Samuelson, L.J., T.A. Stokes, and K. Johnsen. 2012. Ecophysiological comparison of 50-year-old longleaf pine, slash pine and loblolly pine. Forest Ecology and Management 274:108-115.

Samuelson, L.J., T.A. Stokes, J.R. Butnor, K. Johnsen, C.A. Gonzalez-Benecke, P. Anderson, J. Jackson, L. Ferrari, T.A. Martin, and W.P. Cropper Jr. 2014 Ecosystem carbon stocks in *Pinus palustris* Mill. Forests. Canadian Journal of Forest Research 44:476-486.

Samuelson, L.J., T.A. Stokes, J.R Butnor, K.H. Johnsen, C.A. Gonzalez-Benecke, T.A. Martin, W.P. Cropper, Jr., P.H. Anderson, M.R. Ramirez, and J.C. Lewis. 2016. Ecosystem carbon density and allocation across a chronosequence of longleaf pine forests in the southeastern USA. Ecological Applications (in review).

Santin, C., S.H. Doerr, E.S. Kane, C.A. Masiello, M. Ohlson, J.M. de la Rosa, C.M. Preston, and T. Dittmar. 2016. Towards a global assessment of pyrogenic carbon from vegetation fires. Global Change Biology 22: 76-91.

Sartori F., D. Markewitz, and B.E. Borders. 2007. Soil carbon storage and nitrogen and phosphorous availability in loblolly pine plantations over 4 to 16 years of herbicide and fertilizer treatments. Biogeochemistry 84: 13-30.

SAS Software, version 9.3. 2011. SAS Institute Inc. Cary, North Carolina, USA.

SAS Institute Inc. 2013. SAS/STAT 13.1 User's Guide. SAS Institute Inc. Cary, North Carolina, USA.

Satoo, T., and H.A.I. Madwick. 1982. Forest biomass. Martinus Nijhoff, The Hague.

Saucier, J.R., D.R. Phillips, and J.G. Williams Jr. 1981. Green weight, volume, board-foot, and cord tables for the major southern pine species. Georgia Forest Research Paper 19. Georgia Forestry Commission, USA.

Sawadogo, L., P. Savadogo, D. Tiveau, S.D. Dayamba, D. Zida, Y. Nouvellet, P.C. Oden, and S. Guinko. 2010. Allometric prediction of above-ground biomass of eleven woody tree species in Sudanian savanna-woodland of West Africa. Journal of Forestry Research 21:475-481.

Schlesinger, W.H. 1990. Evidence from chronosequence studies for a low carbon-storage potential of soils. Nature 348: 232-234.

Schmid, A.V., C.S. Vogel, E. Liebman, P.S. Curtis, and C.M. Gough. 2016. Coarse woody debris and the carbon balance of a moderately disturbed forest. Forest Ecology and Management, 361: 38-45.

Schmidt, M.W.I., and A.G. Noack. 2000. Black carbon in soils and sediments: analysis, distribution, implications, and current challenges. Global Biogeochemical Cycles 14:777-793.

Schmidt, M.W.I., J.O. Skjemstad, C.I. Czimezik, B. Glaser, K.M. Prentice, Y. Gelinas and T.A.J. Kuhlbusch. 2001. Comparative analysis of black carbon in soils. Global Biogeochemical Cycles 15:163-167.

Schmidtling, R.C. 1973. Intensive culture increases growth without affecting wood quality of young southern pines. Canadian Journal of Forest Research 3: 565-573.

Schmidtling, R.C. 1986. Relative performance of longleaf compared to loblolly and slash pines under different levels of intensive culture. Pages 395-400 *in* General Technical Report. SO-42N. Proceedings of the Fourth Biennial Southern Silviculture Research Conference. USDA Forest Service, USA.

Schmidtling, R. C., and V. Hipkins. 1998. Genetic diversity in longleaf pine (*Pinus palustris*): influence of historical and prehistorical events. Canadian Journal of Forest Research 28: 1135-1145.

Schwenk, W.S., T.M. Donovan, W.S. Keeton, and J.S. Nunery. 2012. Carbon storage, timber production, and biodiversity: comparing ecosystem services with multi-criteria decision analysis. Ecological Applications 22: 1612-1627.

Scott, D.A. 2014. Initial ecosystem restoration in the highly erodible Kisatchie Sandstone Hills. Southeastern Naturalist 13:64-79.
Scott, J.H., and R.E. Burgan. 2005. Standard fire behavior fuel models: a comprehensive set for use with Rothermel's surface fire spread model. General Technical Report RMRS-GTR-153. USDA Forest Service, Rocky Mountain Research Station, Fort Collins, Colorado, USA.

Searle, S.R. 1971. Linear models. Wiley, New York, USA.

Sedjo, R. 1989. Forests to offset the greenhouse effect. Journal of Forestry 87:12-15.

Sedjo, R., N. Sampson, and J. Wisniewski. 1997. Economics of carbon sequestration in forestry. CRC Press, New York, USA.

Seiler T.J., D.P. Rasse, J. Li, P. Dijkstra, H.P. Anderson, D.P. Johnson, T.L. Powell, C.R. Hungate, and B.G. Drake. 2009. Disturbance, rainfall and contrasting species responses mediated aboveground biomass response to 11 years of CO_2 enrichment in a Florida scrub-oak ecosystem. Global Change Biology 15: 356–367.

Seiler W., and P.J. Crutzen. 1980. Estimates of gross and net fluxes of carbon between the biosphere and the atmosphere from biomass burning. Climatic Change. 2:207-247.

Sharma, M., M. Smith, H.E. Burkhart, and R.L. Amateis. 2006. Modeling the impact of thinning on height development of dominant and codominant loblolly pine trees. Annals of Forest Science 63:349-354.

Shaw, J.D., and J.N. Long. 2007. A density management diagram for longleaf pine stands with application to red-cockaded woodpecker habitat. Southern Journal of Applied Forestry 31:28-38. Shorohova, E., E. Kapitsa, and I. Vanha-Majamaa. 2008. Decomposition of stumps in a chronosequence after clear-felling vs. clear-felling with prescribed burning in a southern boreal forest in Finland. Forest Ecology and Management. 255:3606-3612.

Shoemaker, D. A., and W.P. Cropper Jr. 2010. Application of remote sensing, an artificial neural network leaf area model, and a process-based simulation model to estimate carbon storage in Florida slash pine plantations. Journal of Forestry Research 21: 171-176.

Shorohova, E., E. Kapitsa, and I. Vanha-Majamaa. 2008. Decomposition of stumps in a chronosequence after clear-felling vs. clear-felling with prescribed burning in a southern boreal forest in Finland. Forest Ecology and Management. 255:3606-3612.

Silver, E.J., J.E. Leahy, A.R. Weiskittel, C.L. Noblet, and D.B. Kittredge. 2015. An evidence-based review of timber harvesting behavior among private woodland owners. Journal of Forestry 113: 490-499.

Silver, W., and R. Miya. 2001. Global patterns in root decomposition: comparisons of climate and litter quality effects. Oecologia. 129:407-419.

Silvertown, J., S. Holtier, J. Johnson, and P. Dale. 1992. Cellular automaton models of interspecific competition for space--the effect of pattern on process. The Journal of Ecology 80:527-533.

Skog, K.E., and G.A. Nicholson. 1998. Carbon cycling through wood products: the role of wood and paper products in Carbon sequestration. Forest Products Journal 48:75-83.

Smith, J.E., L.S. Heath, and R.A. Birdsey. 2006. Methods for calculating forest ecosystem and harvested carbon with standard estimates for forest types of the United States. General Technical Report NE-343. USDA Forest Service, USA.

Smith, W.B., P.D. Miles, C.H. Perry, and S.A. Pugh. 2009. Forest Resources of the United States, 2007. General Technical Report WO-78. USDA Forest Service, USA.

Smith, J.E., L.S. Heath, and C.M. Hoover. 2013. Carbon factors and models for forest carbon

estimates for the 2005-2011 National Greenhouse Gas Inventories of the United States. Forest Ecology and Management 307: 7-19.

Snowdon, P. 1991. A ratio estimator for bias correction in logarithmic regressions. Canadian Journal of Forest Research 21:720-724.

Soil Survey Staff. 1999. Soil taxonomy: a basic system of soil classification for making and interpreting soil surveys (2nd edition). US Department of Agriculture Soil Conservation Service, Washington, DC, USA.

Soucemarianadin, L.N., S.A. Quideau, M.D. MacKenzie, G.M. Bernard, and R.E. Wasylishen. 2013. Laboratory charring conditions affect black carbon properties: A case study from Quebec black spruce forests. Organic Geochemistry 62: 46-55.

Soucemarianadin, L.N., S.A. Quideau, R.E. Wasylishen, and A.D. Munson. 2015. Early-season fires in boreal black spruce forests produce pyrogenic carbon with low intrinsic recalcitrance. Ecology 96: 1575-1585.

Staudhammer, C., and V. Lemay. 2000. Height prediction equations using diameter and stand density measures. Forest Chronology 76:303-309.
Spokas, K. A. 2010. Review of the stability of biochar in soils: predictability of O:C molar ratios. Carbon Management 1: 289-303.

Stambaugh, M.C., R.P. Guyette, and J.M. Marschall. 2011. Longleaf pine (*Pinus palustris* Mill.) fire scars reveal new details of a frequent fire regime. Journal of Vegetation Science 22: 1094-1104.

Stone, E.L., and P.J. Kalisz. 1991. On the maximum extent of tree roots. Forest Ecology and Management 46: 59-102.

Stout, I.J., and W.R. Marion. 1993. Pine flatwoods and xeric pine forests of the southern lower coastal plain. Pages 373-446 *in* W.H. Martin, S.G. Boyce, and A.C. Echternacht, editors. Biodiversity of the southeastern United States: lowland terrestrial communities. John Wiley, New York, USA.

Stover, D.B., F.P. Day, J.R. Butnor, and B.G. Drake. 2007. Effect of elevated CO_2 on coarse-root biomass in Florida scrub detected by ground-penetrating radar. Ecology 88: 1328–1334.

Streng, D.R., J.S. Glitzenstein, and W.J. Platt. 1993. Evaluating effects of season of burn in longleaf pine forests: a critical literature review and some results from an ongoing long-term study. Pages 227-263 *in* S.M. Hermann, editor. Proceedings 18th Tall Timbers Fire Ecology Conference. Tall Timbers Research, Inc., Tallahassee, Florida, USA.

Stuiver, M., and H.A. Polach. 1977. Reporting of C-14 data - discussion. Radiocarbon 19: 355-363.

Subedi, P., E.J. Jokela, J.G. Vogel, and T.A. Martin. 2014. Inter-rotational effects of fertilization and weed control on juvenile loblolly pine productivity and nutrient dynamics. Soil Science Society of America Journal 78: S152-S167.

Sucre, E.B. and T.R. Fox. 2009. Decomposing stumps influence carbon and nitrogen pools and fine root distribution in soils. Forest Ecology and Management 258:2242-2248.

Sundquist, E.T., R.C. Burruss, S.P. Faulkner, R.A. Gleason, J.W. Harden, Y.K. Kharaka, L.L. Tieszen, and M.P. Waldrop. 2008. Carbon sequestration to mitigate climate change. U.S. Geological Survey Fact Sheet 2008-3097.

Susaeta, A., D.R. Carter, and D.C. Adams. 2014. Sustainability of forest management under changing climatic conditions in the southern United States: Adaption strategies, economic rents and carbon sequestration. Journal of Environmental Management 139: 80-87.

Tallis, H., and S. Polasky. 2009. Mapping and valuing ecosystem services as an approach for conservation and natural-resource management. Annals of the New York Academy of Sciences 1162:265-283.

Tanikawa, T., Y. Hirano, M. Dannoura, K. Yamase, K. Aono, M. Ishii, T. Igarashi, H. Ikeno, and Y. Kanazawa. 2013. Root orientation can affect detection accuracy of ground-penetrating radar. Plant and Soil 373: 317-327.

Taras, M.A., and A. Clark III. 1977. Aboveground biomass of longleaf pine in a natural sawtimber stand in southern Alabama. Research Paper SE-162. USDA Forest Service, Southeastern Forest Experiment Station, Asheville, North Carolina, USA.

Temesgen, H., D.W. Hann, and V.J. Monleon. 2007. Regional height-diameter equations for major tree species of Southwest Oregon. Western Journal of Applied Forestry 22:213-219.

Ter-Mikaelian, M.T., and M.D. Korzukhin. 1997. Biomass equations for sixty-five North American tree species. Forest Ecology and Management 97: 1-24.

Thomas, C.E., B.R. Parresol, K.H.N. Le, and R.E. Lohrey. 1995. Biomass and taper for trees in thinned and unthinned longleaf pine plantations. Southern Journal of Applied Forestry 19:29-35.

Thompson, I.D., K. Okabe, J.M. Tylianakis, P. Kumar, E.G. Brockerhoff, N.A. Schellhorn, J.A. Parrotta, and R. Nasi. 2011. Forest biodiversity and the delivery of ecosystem goods and services: translating science into policy. Bioscience 61:972-981.

Tiarks, A.E., and J.D. Haywood. 1992. Bark yields of 11-year-old loblolly pine as influenced by competition control and fertilization. Pages 525-529 *in* Proceedings of the 7th Biennial Southern Silvicultural Conference, Mobile, Alabama, USA.

Torn, M.S., C.W. Swanston, C. Castanha, and S. Trumbore. 2009. Storage and turnover of organic matter in soil. Pages 219-272 *in* P. M. Huang and N. Senesi, editors. Biophysico-chemical processes involving natural nonliving organic matter in environmental systems. Wiley, Hoboken, New Jersey, USA.

Trumbore, S.E. 1993. Comparison of carbon dynamics in tropical and temperature soils using radiocarbon measurements. Global Biogeochemical Cycles 7: 275-290.

Turner, D.P., G.J. Koerper, M.E. Harmon, and J.J. Lee. 1995. A carbon budget for forests of the conterminous United States. Ecological Applications 5: 421-436.

Ulander, L.M.H., B.G. Patrik, and J.O. Hagberg. 1995. Measuring tree height using ERS-1 SAR Interferometry. Pages 2189-2191 *in* Proceeding of Geoscience and Remote Sensing Symposium IGARSS '95. Florence, Italy.

U.S. Environmental Protection Agency (EPA). 2005. Greenhouse gas mitigation potential in U.S. forestry and agriculture. EPA 430-R-05-006. Washington, DC, USA.

U.S. Geological Survey. 1999. Digital representation of "Atlas of United States Trees" by Elbert L. Little, Jr. http://gec.cr.usgs.gov/data/little.

Van Deusen, P.C., A.D. Sullivan, and T.G. Matney. 1981. A prediction system for cubic foot volume of loblolly pine applicable through much of its range. Southern Journal of Applied Forestry 5:186-189.

Van Lear, D.H., and P.R. Kapeluck. 1995. Above- and below-stump biomass and nutrient content of a mature loblolly plantation. Canadian Journal of Forest Research 25: 361-367.

Van Wagner, C.E. 1968. The line intercept method in forest fuel sampling. Forest Science 14: 20-26.

VanderShaaf, C.L. 2010. LONGLEAF: A diameter-distribution growth and yield model and decision support system for unthinned longleaf pine plantations. Texas Forest Service, College Station, Texas, USA.

Vanninen, P., H. Ylitalo, R. Sievanen, and A. Makela. 1996. Effects of age and site quality on the distribution of biomass in Scots pine (*Pinus sylvestris* L). Trees 10: 231-238.

Varner III, J.M., J.S. Kush, and R.S. Meldahl. 2003. Structural characteristics of frequently-burned old-growth longleaf pine stands in the mountains of Alabama. Castanea 68: 211-221.

Vashum, K.T., and S. Jayakumar. 2012. Methods to estimate above-ground biomass and carbon stock in natural forests- a review. Journal of Ecosystem & Ecography 2:4.

Vaught, C.C. 1989. Evaluation of emission control devices at Waferboard plants. EPA Contract

No. 68-02-4379. Control Technology Center, EPA, Research Triangle Park, North Carolina, USA.

Vikstrom, F., B. Holmbom, and A. Hamunen. 2005. Sterols and triterpenyl alcohols in common pulpwoods and black liquor soaps. E 63:303-308.

Vogel, J.G., L. Suau, T.A. Martin, and E.J. Jokela. 2011. Long term effects of weed control and fertilization on the carbon and nitrogen pools of a slash and loblolly pine forest in north central Florida. Canadian Journal of Forest Research 41:552-567.

Vogel, J.S., J.R. Southon, and D.E. Nelson, 1987. Catalyst and binder effects in the use of filamentous graphite for AMS. Nuclear Instruments & Methods in Physics Research Section B-Beam Interactions with Materials and Atoms 29: 50-56.

Waddell, K.L. 2002. Sampling coarse woody debris for multiple attributes in extensive resource inventories. Ecological Indicators 1:139-153

Wade, D.D., and J.D. Lunsford. 1989. A guide for prescribed fire in southern forests. Technical Publications R8-TP11. USDA Forest Service, Southern Region, Atlanta, Georgia, USA.

Wahlenberg, W.G., S.W. Greene, and H.R. Reed. 1939. Effects of fire and cattle grazing on longleaf pine lands as studied at McNeill, Mississippi. USDA Technical Bulletin 683.

Waldrop, T.A., D.H. Van Lear, E.T. Lloyd, and W.R. Harms. 1987. Long-term studies of prescribed burning in loblolly pine forests of the Southeastern Coastal Plain. General Technical Report SE-45. USDA Forest Service, Southeastern Forest Experiment Station, Asheville, North Carolina, USA.

Walker, J.L. 1993. Rare vascular plant taxa associated with the longleaf pine ecosystem. Proceedings of the Tall Timbers Fire Ecology Conference 18:105-125.

Wang, C.H., and D.W. Hann. 1988. Height-diameter equations for sixteen tree species in the central western Willamette valley of Oregon. Research Paper 51. Oregon State University Forestry Research Laboratory, Oregon, USA.

Wang, G.G., D.H. Van Lear, H. Hu, and P.R. Kapeluck. 2012. Accounting carbon storage in decaying root systems of harvested forests. Ambio 41: 284-291.

Warren, W.G., and P.F. Olsen. 1964. A line transect technique for assessing logging waste. Forest Science 10: 267-276.

Weedon, J.T., W.K. Cornwell, H.C. Johannes, A.E. Zanne, C. Wirth, and D.A. Coomes. 2009. Global meta-analysis of wood decomposition rates: a role for trait variation among tree species? Ecology Letters 12:15-56.

Weiskittel, A.R, D.W. Hann, J.A. Kerhsaw Jr., and J.K. Vanclay. 2011. Forest growth and yield modeling. Wiley, Oxford, United Kingdom.

West, D.C., T.W. Doyle, M.L. Tharp, J.J. Beauchamp, W.J. Platt, and D.J. Downing. 1993. Recent growth increases in old-growth longleaf pine. Canadian Journal of Forest Research 23: 846-853.

West, J.B., J.F. Espeleta, and L.A. Donovan. 2004. Fine root production and turnover across a complex edaphic gradient of a *Pinus palustris–Aristida stricta* savanna ecosystem. Forest Ecology and Management 189:397–406.

Westfall, J.A., and H.E. Burkhart. 2001. Incorporating thinning response into a loblolly pine stand simulator. Southern Journal of Applied Forestry 25:159–164.

White, D.L., T.A. Waldrop, and S.M. Jones. 1991. Forty years of prescribed burning on the Santee fire plots: effects on understory vegetation. Pages 51-59 *in* S.C. Nodvin and T.A. Waldrop, editors. Fire and the environment: ecological and cultural perspectives: proceedings of an international symposium. General Technical Report SE-69. USDA Forest Service, Southeastern Forest Experiment Station. Knoxville, Tennessee, USA.

White M.K., S.T. Gower, and D.E. Ahl. 2005. Life-cycle inventories of roundwood production in Wisconsin – inputs into an industrial forest carbon budget. Forest Ecology and Management 219:13-28.

Wiedemeier, D.B., M.D. Hilf, R.H. Smittenberg, S.G. Haberle, and M.W.I. Schmidt. 2013. Improved assessment of pyrogenic carbon quantity and quality in environmental samples by high-performance liquid chromatography. Journal of Chromatography A 1304: 246-250.

Wiedemeier, D.B., S. Abiven, W.C. Hockaday, M. Keiluweit, M. Kleber, C.A. Masiello, A.V. McBeath, P.S. Nico, L.A. Pyle, M.P.W. Schneider, R.J. Smernik, G.L.B. Wiesenberg, and M.W.I. Schmidt. 2015. Aromaticity and degree of aromatic condensation of char. Organic Geochemistry 78: 135-143.

Williams, C.A., G.J. Collatz, J. Masek, and S.N. Goward. 2012. Carbon consequences of forest disturbance and recovery across the conterminous United States. Global Biogeochemical Cycles 26: GB1005.

Willmott, C., S. Ackleson, R. Davis, J. Feddema, K. Klink, D. Legates, J. O'Donnell, W. Zhao, E.G. Mason, and J. Brown. 2006. Modelling height-diameter relationships of *Pinus radiata* plantations in Canterbury, New Zealand. New Zealand Journal of Forestry 51:23–27.

Woodall, C.W. and V.J. Monleon. 2010. Estimating the quadratic mean diameters of fine woody debris in forests of the United States. Forest Ecology and Management 260: 1088-1093.

Woodall, C.W., L.S. Heath, G. M. Domke, and M.C. Nichols. 2011. Methods and equations for

estimating aboveground volume, biomass, and carbon for trees in the U.S. forest inventory, 2010. General Technical Report NRS-88. USDA Forest Service, USA.

Woodall, C.W., J.W. Coulston, G.M. Domke, B.F. Walters, D.N. Wear, J.E. Smith, H.-E. Andersen, B.J. Clough, W.B. Cohen, D. M. Griffith, S.C. Hagen, I.S. Hanou, M.C. Nichols, C.H. Perry, M.B. Russell, J.A. Westfall, and B.T Wilson. 2015a. The U.S. forest carbon sink accounting framework: stocks and stock change 1990-2016. General Technical Report NRS-154. USDA Forest Service, Northern Research Station, Newton Square, Pennsylvania, USA.

Woodall, C.W., M.B. Russell, B.F. Walters, A.W. D'Amato, S. Fraver and G.M. Domke. 2015b. Net carbon flux of dead wood in forests of the eastern US. Oecologia 177: 861-874.

Woodbury, P.B. 2007. Carbon sequestration in the US forest sector from 1990 to 2010. Forest Ecology and Management 241: 14-27.

Woudenberg, S.W, B.L. Conkling, B.M. O'Connell, E.B. LaPoint, J.A. Turner, and K.L. Waddell. 2010. The forest inventory and analysis database: database description and user's manual version 4.0 for Phase 2. General Technical Report RMRS-GTR-245. USDA Forest Service, USA.

Wright, C.S. 2013. Fuel consumption models for pine flatwoods fuel types in the southeastern United States. Southern Journal of Applied Forestry 37:148-159.

Yavitt, J.B., and T.J. Fahey. 1982. Loss of mass and nutrient changes of decaying woody roots in lodgepole pine forests, southeastern Wyoming. Canadian Journal of Forest Research 12: 745-752.

Yin, R., L.V. Pienaar, and M.E. Aronow. 1998. The productivity and profitability of fiber farming. Journal of Forestry 96:13-18.

Zenone, T., G. Morelli, M. Teobaldelli, F. Fischanger, M. Matteucci, M. Sordini, A. Armani, C. Ferre, T. Chiti, and G. Seufert. 2008. Preliminary use of ground-penetrating radar and electrical resistivity tomography to study tree roots in pine forests and poplar plantations. Functional Plant Biology 35: 1047-1058.

Zhao, D., B. Borders, M. Wang, and M. Kane. 2007. Modeling mortality of second-rotation loblolly pine plantations in the Piedmont/Upper Coastal Plain and Lower Coastal Plain of the southern United States. Forest Ecology and Management 252:132-143.

Zhao, D., M. Kane, D. Markewitz, R. Teskey, and M. Clutter. 2015. Additive tree biomass equations for midrotation loblolly pine plantations. Forest Science 61: 613-623.

Zhao, S., S. Liu, Z. Li, and T. Sohl. 2010. Federal land management, carbon sequestration, and climate change in the southeastern U.S.: A case study with Fort Benning. Environmental Science and Technology 44:992-997.

Zhao, W., E.G. Mason, and J. Brown. 2006. Modelling height-diameter relationships of *Pinus radiata* plantations in Canterbury, New Zealand. New Zealand Journal of Forestry 51:23-27.

Zhang, X. and W. Wang. 2015. The decomposition of fine and coarse roots: Their global patterns and controlling factors. Scientific Reports 5:9940.

Zimmerman, A.R. 2010. Abiotic and microbial oxidation of laboratory-produced black carbon (Biochar). Environmental Science & Technology 44: 1295-1301.

19. Appendices

A. List of Scientific/Technical Publications

Peer-reviewed journal articles (in print)

ArchMiller, A.A. and L.J. Samuelson. 2016. Partitioning longleaf pine soil respiration into its autotrophic and heterotrophic components through root excision. Forests 7: 39.

ArchMiller, A.A., L.J. Samuelson, and Y. Li. 2016. Diurnal and spatial variability of growing season soil respiration in a 64-year-old longleaf pine forest. Plant and Soil 403: 419-435.

Butnor, J.R., L.J. Samuelson, T.A. Stokes, K.H. Johnsen, P.H. Anderson, and C.A. Gonzalez-Benecke. 2016. Surface-based GPR underestimates below-stump root biomass. Plant and Soil 402: 47-62.

ArchMiller, A.A., and L.J Samuelson. 2015. Intra-annual variation of soil respiration across four heterogeneous longleaf pine forests in the southeastern United States. Forest Ecology and Management 359: 370-380.

Gonzalez-Benecke, C.A., L.J. Samuelson, T.A. Martin, W.P. Cropper, K.H. Johnsen, T.A. Stokes, J.R. Butnor, and P. Anderson. 2015. Modeling the effects of forest management on *in situ* and *ex situ* longleaf pine forest carbon stocks. Forest Ecology and Management 355: 24-36.

Gonzalez-Benecke, C.A., L.J. Samuelson, T.A. Stokes, W.P. Cropper, T.A. Martin, and K.H. Johnsen. 2015. Understory plant biomass dynamics of *Pinus palustris* stands. Forest Ecology and Management 344: 84-94.

Gonzalez-Benecke, C.A., S.A. Gezan, L.J. Samuelson, W.P. Cropper Jr., D.J. Leduc, and T.A. Martin. 2014. Estimating *Pinus palustris* tree diameter and stem volume from tree height, crown area and stand-level parameters. Journal of Forestry Research 25:43-52.

Gonzalez-Benecke, C.A., S.A. Gezan, T.A. Martin, W. P. Cropper Jr., L.J. Samuelson, and D.J. Leduc. 2014. Individual tree diameter, height and volume functions for longleaf pine (*Pinus palustris* Mill.). Forest Science 60:43-56.

Samuelson, L.J., T.A. Stokes, J. R. Butnor, K.H. Johnsen, C.A. Gonzalez-Benecke, P. Anderson, J. Jackson, L. Ferrari, T. A. Martin, and W. P. Cropper, Jr. 2014. Ecosystem carbon stocks in *Pinus palustris* Mill. forests. Canadian Journal of Forest Research 44: 476-486.

Gonzalez-Benecke, C.A., S.A. Gezan, D.J. Leduc, T.A. Martin, W. P. Cropper Jr., and L.J. Samuelson. 2012. Modeling survival, yield, volume partitioning and their response to thinning for longleaf pine plantations. Forests 3: 1104-1132.

Peer-reviewed journal articles (submitted for publication)

Samuelson, L.J., T.A. Stokes, J.R Butnor, K.H. Johnsen, C.A. Gonzalez-Benecke, T.A. Martin, W.P. Cropper, Jr., P.H. Anderson, M.R. Ramirez, and J.C. Lewis. 2016. Ecosystem carbon density and allocation across a chronosequence of longleaf pine forests in the southeastern USA. Submitted to Ecological Applications.

Conference or symposium proceedings

Butnor, J., L. Samuelson, T. Stokes, K. Johnsen, and P. Anderson. 2015. Integrating estimates of tree root mass predicted with ground penetrating radar and allometry. Proceedings of the 28th Symposium on the Application of Geophysics to Engineering and Environmental Problems (SAGEEP) Austin, TX.

Abstracts

Cropper, W.P., C.A. Gonzalez-Benecke, D.J. Leduc, D. Atar, S. Gezan, T. A. Martin., L.J. Samuelson. 2016. Simulating the transition form even-aged longleaf plantations to old growth savannas using a multiple model framework. 101th Ecological Society of America Meeting, Fort Lauderdale, FL.

Samuelson, L.J., T. Stokes, J. Butnor, K. Johnsen, C. Gonzalez-Benecke, P. Anderson, T. Martin, W. Cropper. 2016. Ecosystem carbon density across a chronosequence of longleaf pine forests in the southeastern United States. 101th Ecological Society of America Meeting, Fort Lauderdale, FL.

Butnor, J.R., L.J. Samuelson, P. H. Anderson, C. A. González Benecke, C. Boot, F. Cotrufo, K.A. Heckman, J. A. Jackson, K. H. Johnsen, T. A. Stokes, and C. W. Swanston. 2015. Characterizing soil organic carbon recalcitrance in longleaf pine (*Pinus palustris* Mill) stands. American Geophysical Union Annual Meeting, San Francisco, CA.

Anderson, P., K. Johnsen, C. Gonzalez-Benecke, and L. Samuelson. 2014. Predicting taproot decomposition of longleaf pine across the southeastern U.S. 99th Ecological Society of America Meeting, Sacramento, CA.

ArchMiller, A., and L. Samuelson. 2014. Temporal and spatial variability of soil carbon flux in longleaf pine forests in the southeastern United States. International Union of Forest Research Organizations (IUFRO) World Congress/ Society of American Foresters Annual Convention, Salt Lake City, UT.

Butnor, J. K. Johnsen, J. Jackson, P. Anderson, L. Samuelson, and K. Lorenz. 2014. Assessing soil organic carbon stocks in fire-affected *Pinus palustris* forests. American Geophysical Union Annual Meeting, San Francisco, CA.

Gonzalez-Benecke C.A, L.J. Samuelson, T. A. Martin, W. Cropper, T. Stokes, J. Butnor, K. Johnsen, P. Anderson, and J. Jackson. 2014. A flexible hybrid model of fluxes and stock of carbon for planted longleaf pine forests. International Union of Forest Research Organizations (IUFRO) World Congress/ Society of American Foresters Annual Convention, Salt Lake City, UT.

Samuelson, L.J., T. Stokes, T. Martin, K. Johnsen, W. Cropper, C. Gonzalez-Benecke, and J. Butnor. 2014. Forest carbon stocks in longleaf pine forests in the southern United States. International Union of Forest Research Organizations (IUFRO) World Congress/ Society of American Foresters Annual Convention, Salt Lake City, UT.

Stokes, T., L. Samuelson, and C. Gonzalez-Benecke. 2014. Relationships between ground cover biomass and prescribed fire in longleaf pine forests in the southeastern U.S. International Union

of Forest Research Organizations (IUFRO) World Congress/ Society of American Foresters Annual Convention, Salt Lake City, UT.

ArchMiller, A.A., and L.J. Samuelson. 2013. Spatial heterogeneity of soil respiration in a 64-year-old longleaf pine forest at Fort Benning, Georgia. 98th Ecological Society of America Annual Meeting, Minneapolis, MN.

Gonzalez-Benecke C.A., S.A. Gezan, T.A. Martin, L.J. Samuelson, W. Cropper Jr., and E.J. Jokela. 2013. Effect of thinning and prescribed burning on carbon sequestration of *Pinus palustris*. International Conference on Ecology, Ecosystems and Climate Change. Athens, Greece.

Samuelson, L.J., T.A. Stokes, L. Ferrari, K.H. Johnsen, J.R. Butnor, C.A. Gonzalez Benecke, J. Jackson, P. Anderson, T.A. Martin, and W.P Cropper Jr. 2013. Distribution of carbon in longleaf pine ecosystems. 98th Ecological Society of America Annual Meeting, Minneapolis, MN.

Samuelson, L.J., T. Stokes, K. Johnsen, T. Martin, J. Butnor, and C. Gonzalez-Benecke. 2013. Ecosystem carbon pools in longleaf pine forests at Fort Benning, Georgia. 17th Biennial Southern Silviculture Research Conference, Shreveport, LA.

Archer, A.A., and L.J. Samuelson. 2012. Soil respiration in a longleaf pine chronosequence. 97th Ecological Society of America Meeting, Portland, OR.

Ferrari, L., and L.J. Samuelson. 2012. Ground cover in fire-maintained longleaf pine forests varying in age from 5 to 87 years at Fort Benning, GA. 97th Ecological Society of America Meeting, Portland, OR.

Samuelson, L.J., T.A. Martin, K.H. Johnsen, W.P Cropper, C.A. Gonzalez-Benecke, and J.R. Butnor. 2011. Developing tools for ecological forestry and carbon management in longleaf pine. National Workshop on Climate & Forests: Planning Tools and Perspectives in Adaptation and Mitigation Options, Flagstaff, AZ.